THE STRATIGRAPHY AND STRUCTURE OF THE CAMBRIAN AND ORDOVICIAN CHERT-BEARING CARBONATES OF THE WALLKILL RIVER VALLEY: THE STRATIGRAPHIC NATURE OF THE CHERT AND THEIR ARCHAEOLOGICAL POTENTIAL

by

PHILIP CHARLES LAPORTA, JR.

Volume I

A dissertation submitted to the Graduate Faculty in Earth and Environmental Sciences in partial fulfillment of the requirements for the degree of Doctor of Philosophy, The City University of New York

2009

UMI Number: 3485046

All rights reserved

INFORMATION TO ALL USERS
The quality of this reproduction is dependent on the quality of the copy submitted.

In the unlikely event that the author did not send a complete manuscript
and there are missing pages, these will be noted. Also, if material had to be removed,
a note will indicate the deletion.



UMI 3485046

Copyright 2011 by ProQuest LLC.

All rights reserved. This edition of the work is protected against
unauthorized copying under Title 17, United States Code.



ProQuest LLC.
789 East Eisenhower Parkway
P.O. Box 1346
Ann Arbor, MI 48106 - 1346

© 2009

PHILIP CHARLES LAPORTA, JR.

All Rights Reserved

This manuscript has been read and accepted for the
Graduate Faculty in Earth and Environmental Sciences in satisfaction of the
dissertation requirement for the degree of Doctor of Philosophy.

Hannes K. Brueckner

_____ _____
Date Chair of Examining Committee

Yehuda L. Klein

_____ _____
Date Executive Officer

Arthur Langer

Frederick Shaw

Robert M. Finks

James Moore
Supervision Committee

THE CITY UNIVERSITY OF NEW YORK

Abstract

THE STRATIGRAPHY AND STRUCTURE OF THE CAMBRIAN AND ORDOVICIAN CARBONATES OF THE WALLKILL RIVER VALLEY: THE NATURE OF THE DIAGENESIS OF CHERT

by

Philip Charles LaPorta, Jr.

Adviser: Professor Hannes K. Brueckner

The Kittatinny Supergroup in northwestern New Jersey/southeastern New York was correlated to age-equivalent rocks in the Pennsylvania salient (Drake, 1965; Markewicz and Dalton, 1977). Along-strike variations in facies and thickness, from the Pennsylvania salient to the New York recess (Thomas, 1977), are responsible for inconsistencies in stratigraphic assignment between the two depositional settings. Stratigraphic inconsistencies also fostered differing interpretations of the structural history of the area (Gray, 1959; Zen, 1967; Drake, 1969, 1970; Herman and Monteverde, 1989; Herman et al., 1997).

Stratigraphic measurement (1:98 scale) and geologic mapping (1:24,000 scale) conducted for this study recorded diagnostic chert horizons utilizable as mapping aids, in conjunction with previously undocumented faunal assemblages. Therefore, the Kittatinny stratigraphy was redefined; specifically, three new formations and eight new members were created that more accurately illustrated the genetic relationships between adjacent, but different, tectonic depocenters (the Pennsylvania salient vs. the New York recess). The stratigraphic re-organization, and re-mapping of the Hamburg quadrangle,

supported balanced and restored cross sections that clarified the structural evolution of the study area. Finally, the detailed stratigraphic work allowed for sea-level curve construction for this part of the Cambrian-Ordovician passive margin. Bed-by-bed correlation of the chert stratigraphy with sea-level curves suggested that cherts were deposited on unconformities marking regressions on this part of the passive margin.

Inter-disciplinary applications of the revised stratigraphy, and the structural features of the Cambrian-Ordovician rocks, permitted the discovery of greater than 600 prehistoric bedrock chert quarry complexes in the study area. Geologic controls dictate the spatial distribution of the quarries, the success and/or failure of indigenous peoples in mining this ore and the types of tools that were created once mining yielded a utilizable product. A typical quarry plan has been observed in the study area, where quarries have a similar layout based on measureable geological constraints. A new chain-of-operation has been introduced, again based on the geological constraints of mined ore. Previously in lithic studies, tool manufacture began with a blank (Callahan, 1979; Crabtree, 1972). This study redefines stool-tool manufacture as beginning with a microlithon package, a geologically constrained template that controls stone-tool design.

ACKNOWLEDGEMENTS

This dissertation program has been a lesson on endurance and the power of the human spirit. Certainly, for a doctoral program that has been protracted as long as mine has been, considerable debt accumulates. I will do my best to thank as many of my family and friends as possible; but almost certainly, there will be a persons who have not been forgotten, but will be neglected in the mentioning. My apologies to all who may have slipped through these pages, rest assured that you are in my heart always.

First and foremost, I must express my undying gratitude to Professor Yehuda Klein for performing a mitzvah; as without his focused attention on my program, I would not have been given the opportunity to defend this dissertation. Thank you Professor Klein for believing in me and for ensuring that I accomplished my goals and lived up to my dreams. I cannot thank Professor Klein without also thanking Lina McClain. Lina has been with the program through several E.O.'s and she is the safety net of every graduate student in the program. Thank you Lina for everything you have done, including keeping me up to date on deadlines, calling me in on the rug to make sure I kept Fred Shaw, Jeff Osleeb and Professor Klein updated on my progress, and thank you for being a wonderful friend.

My utmost thanks go to a patient and very supportive thesis committee. My dissertation advisor, Hannes K. Brueckner, is not only a dear friend, but a mentor and a colleague. Hannes adopted me during very difficult times in my program and stayed with me through good times and bad. He never gave up on me and this dissertation would not have come to a successful conclusion without his unfailing optimism and support. He was not only a friend to me, but to my wife Margaret and my son Rocco. Hannes rallied

us together and orchestrated the production of the final product. Special thanks must go to Robert M. Finks for shepherding me through the first three levels of my program. Uncle Bob's guidance and advice were desperately needed during the difficult years between 1985 and 1993. Even after I shifted dissertation advisors, Bob stayed the course and continued to be a much valued mentor and friend. I know there was no person happier than Bob on the day I defended this dissertation. Bob believed in Dr. LaPorta long before everyone else did and described me as the "Mozart of this new field of archaeological geology". Fred Shaw steered the ship and provided encouragement and tenured advice during the late 1990's and afterwards. Fred took up the banner for me when he was E.O. of the program and I will always be in debt to him for guiding me through the tough times after Hunter College. To my remaining committee members, Arthur Langer and Jim Moore, thank you both for all of your patience, guidance, advice, collegial relationships and support through this long and enduring program. It was Jim Moore, upon seeing the organization of prehistoric quarries in the Wallkill Valley in 1988, who coined the expression, "folk geology".

I owe a great debt of gratitude to Provost Floyd Moreland, Assistant to the Provost Sharon Lerner and the former president of CUNY, the late Harold Prozanski. Together they fought the tyranny in my program and battled opposing forces to keep me steady in my mission to complete this dissertation. It was Harold Prozanski who first described me as the "diamond of the EES program". My thanks go to Dorothy Pettit, and the late Robert Gillece, for awarding me numerous discretionary academic fellowships. Their attention to my program permitted me to keep my matriculation through the late 1980's and early 1990's. Carl Szkielda assisted in pioneering my investigation of

hammerstones in chert quarries and provided me with much fruitful information on the chain of operation towards the development of quarry tools. Finally, I would also like to thank Joseph Scelsa and the Coalition of Italian American Institutes for all of their support and encouragement in the late 1980's.

The faculty at Brooklyn College must be applauded for standing up to totalitarian rule and for petitioning the then executive officer, Dr. Daniel Habib, on my behalf. That faculty includes Professors Saxena, Friedman, Bhattacharya, Nehru and Chamberlain. These gentlemen came to bat for me, when others at Queens College stood on the sidelines and simply watched the pummeling that I was receiving at the hands of Dr. Habib. Thank you gentlemen for your courage and sense of fairness in what was a very discriminatory setting.

Professor Jeff Osleeb receives my thanks for recruiting me to Hunter College. It was Jeff who took me off the bench, put the ball in my hands, and let me run with it for five years. By his own opinion, he knew I had, "Johnny Rodgers moves". Jeff, and his staff, gave me the opportunity to launch field, lab and lecture courses that graduate students never have the honor of teaching. Jeff gave me the opportunity to hone my skills as a teacher and a researcher, believing that I had something special to offer. Thank you Jeff for your confidence in me, and for believing in my research and its broad, multidisciplinary applicabilities.

Jeff's support in my efforts to rebuild Hunter College's geology program provided me with the opportunity to meet new friends and cultivate students, many of whom assisted me with various scientific projects that pushed the progress of my dissertation, while helping them to learn the art of geology. Many of these students have

gone on to become doctors and professors in geology, in their own right. I am very proud of all of them. Certainly a tremendous debt of gratitude is owed to Anne Kelly-Grogan, Robby Abad, Shimain Rivera, Christine Weiss, Roy Haskell, Albert Latucha, Ruth Reichbart, Seymour Leeds, Danette Tur-Leer, Josephine Amato-Hansen, Dr. Donna Surge, Dr. Linda Sohl, Dr. Margaret Brewer-LaPorta, Sherry Felix, Susan Hollander, Maria Bongiorno-Minunno, Frances Hernandez-Ferraz, Scott Minchak and many, many others. These hard working and dedicated students and scientists helped gather field measurements, packed rock out of the mountains, and enjoyed the atmosphere of the Old Grist Mill. We experienced the coast of Maine, the Adirondacks, and the northern tri-state metropolitan geology together. Those were good times and I will never forget them.

Finally to Dr. Daniel Habib. I want to thank you for teaching me the meaning of racism, discrimination, and anti-Italian sentiment. Your narrow definition of geology and your even narrower perspective on student life eventually led to the early demise of your own program. Your lessons will not soon be forgotten and in the words of Floyd Moreland, “You privileged me to an education money couldn’t buy”.

The “GQ” boys of the New Jersey Geological Survey, especially Richard Dalton, Bob Canace, Rich Volkert, Don Monteverde, Greg Herman and the late Frank Markewicz provided me with friendship and geological support outside of the CUNY system. Whether it was visits to the Mill for a cup of coffee, or a field excursion to look at cherts and carbonates, their presence always brightened up my day. I especially appreciate all the time and effort my mentor, Frank Markewicz, gave to me in the field. It was “Mark” who first introduced me to the cherts of the Great Valley Sequence and showed me their broad application as stratigraphic markers, as well as the potential as a

mapping aid. Also, I want to thank the U.S.G.S. mapping geologists Jack Epstein and Peter Lyttle, who gave me encouragement and provided me with technical support, as well as friendship. Technical and moral support was also given by Dee Breger, manager of the SEM at Lamont Doherty Earth Observatory and Ken Bart, manager of the SEM at Hamilton College.

To the research group at LaPorta and Associates, I want to extend my utmost gratitude for keeping the ship afloat while I finished this dissertation. This includes Margaret Brewer-LaPorta, Scott Minchak, Michael Conrow, and Caleb and Laura Stevenson.

A doctoral dissertation of this capacity is part of a greater life research, which has its roots in my early childhood. I will always have fond memories of my early mentors in the field. I have never forgotten how much they cared about my life. Much of my early research was structured by Adolf Feige, Lewis M. Haggerty, Gustav Grocz, Joseph Civitarese, Carl Ohms and Thomas Fessler. These industrialists of the Newark/Patterson School (whom I fondly refer to as the "Mill School") shaped much of my early thinking. To the Civitarese family, especially to Uncle Joseph, Aunt Loretta, and the "Civit boys" Joseph, Lewis and Thomas, thank you for believing in me and for supporting me during difficult times.

Rare is it that an individual travels half-way through his life and still has a hand-full of his cherished childhood friends along for life's joys and sorrows. For Mark Van Rossen, Ray Canece, Gerrard Lodico and Ken Scarlatelli, thank you for believing in me and for supporting me all these years. For new friends and family that have gathered through the years; Scott Jeffers (and family), Bob and Rose Dunay, Jack and Paula

Webster (and family), Dann and Michelle Jacobus, Richie and Ellie Van Sickle, Scott Minchak (and family), Karen and Bill Antonelli (and family), Tom Boyle, Christine Joyce, and my Brewer in-laws, thank you for seeing me through the waning days of my program and for providing all of the real-world support that helped me finish my dissertation, especially during its last year. Bob Dunay, in particular, would pick me up in Lodi when I didn't have the means to even put gas in the car, so I could drive one hour to my study area and work on my geologic maps. Bob provided me with the support I needed to finish my field maps, make my collections, and also provided me with morale support when everyone else disappeared. I will never forget your kindness Bob, thank you very much. Scott Minchak I will mention again. Scott started out as a student of mine while he was enrolled at Drew University and remained a dear friend through the last 10 years of my program. Scott toughed it out, gave his support, advice and friendship when I needed it most. He assisted with field work, photographic studies and preparation of slabs. Thank you Scott for your perseverance, and for maintaining your unwavering belief in my vision of how this field should unfold. Christine Joyce, Karen Antonelli, and my in-laws gave my son, Rocco, the love and support he needed, while his Dad finished the journey his grandfather set him on. Ladies, your love for my son knows no bounds. Thank you for being there for Rocco, for Margaret, and for me. We would not have been able to wrap this up without you.

For my family, who went through the hell of this program with me, I appreciate their patience and loving support throughout this odyssey. They provided me with a warm home, pocket money to get me where I needed to go, and encouragement through the years. For my brother Robert, my sisters Elaine and Cheryl and their families, thank

you for your love and patience. To my grandparents, Saverio and Josephine Cammarata, I thank for giving me a garden refuge during my earliest years. Cousin John Cammarata and his wife Beth, thank you for assisting me in constructing geological collections in the deserts of Santa Fe back in 1983. My Uncle Dave Cammarata, Aunt Nina, and cousins Paul and David provided me with a refuge at Wildwood Crest each and every summer, one of the few things I had to look forward to in the 80's and 90's. I will never forget those days in the sun. Special thanks go to Paul for all his tutorial help. For my extended family, Philip and Maureen LaPorta (and family), Cousin Anthony LaPorta, and the rest of the LaPorta's, thank you for giving me a home away from home. Your generosity and love gave me strength and shelter from the storm. You were all there when I needed you and I will never forget it. To my calico cat Josephine (Petey), who always sat waiting for me in the window when I was out working in the field. She greeted me home with much love and affection, and provided me with unconditional love for nearly 17 years. I lost her in 2001, she will never be replaced. Finally, my thanks go out to Coach Tom Osborne and the University of Nebraska Cornhusker football program. This team has provided me with nearly 40 years of excitement. Coach Osborne, and his philosophy, put me on solid ground by showing me life in microcosm each and every Saturday afternoon during the autumn months. Whether winning, or rarely losing, I only wish I could learn to leave it on the field, as he did.

This research, which has shaped so much of my past and at the same time is the foundation for my future, was largely engineered by my father, the late Philip LaPorta. Dad not only knew the definition of archaeological geology long before the discipline came together, but he also structured my formal education around his definition of this

new field. Dad is very much alive in memory, as long as this research continues to flourish. To my late mother, Vivian Cammarata LaPorta, I will never be able to thank her enough for providing me with a warm home, with security and love; which when all brought together, resolved itself as the internal strength that provided me with the endurance and the fortitude to persist when all felt lost. Thanks again go to Joseph and Loretta Civitarese, who mentored and guided me through those dangerous years of the 60's and 70's. Rare is it that I travel to a research in this world when I don't take the time to stop and think of all of them.

Finally, I would like to thank my beautiful wife, Margaret Brewer-LaPorta, who has been such a vital part of my life for nearly 20 years. She has been of enormous assistance to me not only as a fellow geologist, but personally as my life mate. Margaret has walked by my side through everything, shared the good and the bad from days even before the Old Grist Mill. She has provided me with an unending fountain of confidence and reassurance all of those days. Margaret's belief in me, and in my abilities, has never waivered and I believe never will. My wife has given me the three greatest gifts of my life: our beautiful son Rocco, who is the absolute joy of our lives; the last year of my mother's life, as Margaret took Mom into our home and gave Mom our family's love as she slipped from the bounds of this life; and the successful pathway out of this dissertation project. No amount of gratitude would ever be sufficient to repay her for her love, dedication and devotion, which knows no bounds.

This dissertation is dedicated to the special people who have had profound impact on my life.

To my beloved parents, Philip and Vivian LaPorta, who placed me on this road as a young child.

To Joseph and Loretta Civitarese, and to my loving wife, Margaret; who have kept me on this path throughout my life, in times of happiness and hardship.

Finally, to my son Rocco, who represents my future, wherever this road may bring me.

TABLE OF CONTENTS

VOLUME I

ACKNOWLEDGEMENTS vi
LIST OF FIGURES xxii
LIST OF PLATES xxxiii

CHAPTER 1: INTRODUCTION 1

STATEMENT OF THE PROBLEM 1
LOCATION OF THE STUDY AREA 3
GOALS OF THE DISSERTATION 3
OUTLINE OF THE DISSERTATION 40

CHAPTER 2: TECTONIC SETTING OF THE HAMBURG 7.5' QUADRANGLE 47

INTRODUCTION 47
TECTONIC SETTING 47
PROTEROZOIC DEFORMATION 48
GREVILLIAN OROGEN 48
IAPETOS RIFT 49
PALEOZOIC DEFORMATION 50
TACONIAN OROGENY 50
ACADIAN OROGENY 51
ALLEGHANIAN OROGENY 52

CHAPTER 3: STRATIGRAPHY OF THE GREAT VALLEY SEQUENCE, HAMBURG 7.5' QUADRANGLE, SUSSEX COUNTY, NEW JERSEY 58

INTRODUCTION 58
FIELD METHODOLOGY AND ORGANIZATION OF REPRESENTATIVE STRATIGRAPHIC SECTIONS 60
PREVIOUS STRATIGRAPHIC WORK 61
CAMBRIAN-ORDOVICIAN LITHOLOGIES OF THE GREAT VALLEY SEQUENCE 64
HARDYSTON FORMATION 64
FAUNAL CONTENT *64*
GENERAL LITHOSTRATIGRAPHIC DESCRIPTION *64*
GENERAL CHERT DESCRIPTION *66*
DISCUSSION OF CHANGES IN STRATIGRAPHIC DEFINITION *66*
LEITHSVILLE FORMATION: CALIFON MEMBER 67
FAUNAL CONTENT *67*
GENERAL LITHOSTRATIGRAPHIC DESCRIPTION *67*
GENERAL CHERT DESCRIPTION *69*
DISCUSSION OF CHANGES IN STRATIGRAPHIC DEFINITION *70*
LEITHSVILLE FORMATION: HAMBURG MEMBER 71

FAUNAL CONTENT *71*
GENERAL LITHOSTRATIGRAPHIC DESCRIPTION *71*
GENERAL CHERT DESCRIPTION *72*
DISCUSSION OF CHANGES IN STRATIGRAPHIC DEFINITION 73
LEITHSVILLE FORMATION: WALLKILL MEMBER 73
FAUNAL CONTENT *73*
GENERAL LITHOSTRATIGRAPHIC DESCRIPTION *74*
GENERAL CHERT DESCRIPTION *75*
DISCUSSION OF CHANGES IN STRATIGRAPHIC DEFINITION *77*
LIMEPORT FORMATION: WILDCAT ROAD MEMBER 78
FAUNAL CONTENT *78*
GENERAL LITHOSTRATIGRAPHIC DESCRIPTION *78*
GENERAL CHERT DESCRIPTION *79*
DISCUSSION OF CHANGES IN STRATIGRAPHIC DEFINITION *81*
LIMEPORT FORMATION: WHEATSWORTH MILLS MEMBER 82
FAUNAL CONTENT *82*
GENERAL LITHOSTRATIGRAPHIC DESCRIPTION *83*
GENERAL CHERT DESCRIPTION *83*
DISCUSSION OF CHANGES IN STRATIGRAPHIC DEFINITION *84*
LIMEPORT FORMATION: GRUENWALD MEMBER 85
FAUNAL CONTENT *85*
GENERAL LITHOSTRATIGRAPHIC DESCRIPTION *85*
GENERAL CHERT DESCRIPTION *86*
DISCUSSION OF CHANGES IN STRATIGRAPHIC DEFINITION *86*
LIMEPORT FORMATION: GLACIAL QUARRY MEMBER 87
FAUNAL CONTENT *87*
GENERAL LITHOSTRATIGRAPHIC DESCRIPTION *87*
GENERAL CHERT DESCRIPTION *88*
DISCUSSION OF CHANGES IN STRATIGRAPHIC DEFINITION *89*
LIMEPORT FORMATION: EDISON MEMBER 90
FAUNAL CONTENT *90*
GENERAL LITHOSTRATIGRAPHIC DESCRIPTION *90*
GENERAL CHERT DESCRIPTION *91*
DISCUSSION OF CHANGES IN STRATIGRAPHIC DEFINITION *92*
LIMEPORT FORMATION: RTE. 94 MEMBER 93
FAUNAL CONTENT *93*
GENERAL LITHOSTRATIGRAPHIC DESCRIPTION *93*
GENERAL CHERT DESCRIPTION *94*
DISCUSSION OF CHANGES IN STRATIGRAPHIC DEFINITION *95*
UPPER ALLENTOWN FORMATION 95
FAUNAL CONTENT *95*
GENERAL LITHOSTRATIGRAPHIC DESCRIPTION *96*
GENERAL CHERT DESCRIPTION *97*
DISCUSSION OF CHANGES IN STRATIGRAPHIC DEFINITION *98*
STONEHENGE FORMATION: CARLTON VILLAGE MEMBER 100
FAUNAL CONTENT *100*
GENERAL LITHOSTRATIGRAPHIC DESCRIPTION *101*
GENERAL CHERT DESCRIPTION *103*
DISCUSSION OF CHANGES IN STRATIGRAPHIC DEFINITION *105*
STONEHENGE FORMATION: CANAL ROAD MEMBER 106
FAUNAL CONTENT *106*

GENERAL LITHOSTRATIGRAPHIC DESCRIPTION *106*
GENERAL CHERT DESCRIPTION *107*
DISCUSSION OF CHANGES IN STRATIGRAPHIC DEFINITION *109*
RICKENBACH FORMATION: HOPE MEMBER 109
FAUNAL CONTENT *109*
GENERAL LITHOSTRATIGRAPHIC DESCRIPTION *110*
GENERAL CHERT DESCRIPTION *111*
DISCUSSION OF CHANGES IN STRATIGRAPHIC DEFINITION *112*
RICKENBACH FORMATION: CROOKED SWAMP MEMBER 113
FAUNAL CONTENT *113*
GENERAL LITHOSTRATIGRAPHIC DESCRIPTION *113*
GENERAL CHERT DESCRIPTION *114*
DISCUSSION OF CHANGES IN STRATIGRAPHIC DEFINITION *115*
EPLER FORMATION: BRANCHVILLE MEMBER 117
FAUNAL CONTENT *117*
GENERAL LITHOSTRATIGRAPHIC DESCRIPTION *117*
GENERAL CHERT DESCRIPTION *118*
DISCUSSION OF CHANGES IN STRATIGRAPHIC DEFINITION *119*
EPLER FORMATION: BIG SPRINGS MEMBER 121
FAUNAL CONTENT *121*
GENERAL LITHOSTRATIGRAPHIC DESCRIPTION *121*
GENERAL CHERT DESCRIPTION *123*
DISCUSSION OF CHANGES IN STRATIGRAPHIC DEFINITION *124*
EPLER FORMATION: LAFAYETTE MEMBER 126
FAUNAL CONTENT *126*
GENERAL LITHOSTRATIGRAPHIC DESCRIPTION *126*
GENERAL CHERT DESCRIPTION *127*
DISCUSSION OF CHANGES IN STRATIGRAPHIC DEFINITION *129*
ONTELAUNEE FORMATION: BEAVER RUN MEMBER 129
FAUNAL CONTENT *129*
GENERAL LITHOSTRATIGRAPHIC DESCRIPTION *130*
GENERAL CHERT DESCRIPTION *131*
DISCUSSION OF CHANGES IN STRATIGRAPHIC DEFINITION *133*
ONTELAUNEE FORMATION: HARMONYVALE MEMBER 134
FAUNAL CONTENT *134*
GENERAL LITHOSTRATIGRAPHIC DESCRIPTION *134*
GENERAL CHERT DESCRIPTION *135*
DISCUSSION OF CHANGES IN STRATIGRAPHIC DEFINITION *137*

CHAPTER 4: DEPOSITIONAL ENVIRONMENT INTERPRETATION OF THE ROCKS OF THE GREAT VALLEY SEQUENCE, SUSSEX COUNTY, NEW JERSEY **175**

INTRODUCTION 175
DESCRIPTION OF PERITIDAL ENVIRONMENTAL SETTINGS 177
SUBTIDAL ENVIRONMENT 177
INTERTIDAL ENVIRONMENT 177
SUPRATIDAL ENVIRONMENT 179
PERITIDAL ENVIRONMENT 180
HARDYSTON FORMATION 180

FACIES DESCRIPTION 180
HARDYSTON FACIES 1 *180*
HARDYSTON FACIES 2 *181*
HARDYSTON FACIES 3 *181*
HARDYSTON FACIES 4 *181*
HARDYSTON FACIES 5 *182*
HARDYSTON FACIES 6 *182*
PALEOENVIRONMENTAL SETTING 182
SEA-LEVEL CURVE INTERPETATION 184
LEITHSVILLE FORMATION: CALIFON MEMBER 185
FACIES DESCRIPTION 185
CALIFON FACIES 1 *185*
CALIFON FACIES 2 *186*
CALIFON FACIES 3 *186*
CALIFON FACIES 4 *186*
PALEOENVIRONMENTAL SETTING 187
SEA-LEVEL CURVE INTERPRETATION 188
LEITHSVILLE FORMATION: HAMBURG MEMBER 189
FACIES DESCRIPTION 189
HAMBURG FACIES 1 *189*
HAMBURG FACIES 2 *190*
HAMBURG FACIES 3 *191*
PALEOENVIRONMENTAL SETTING 191
SEA-LEVEL CURVE INTERPRETATION 194
LEITHSVILLE FORMATION: WALLKILL MEMBER 195
FACIES DESCRIPTION 195
WALLKILL FACIES 1 *196*
WALLKILL FACIES 2 *196*
WALLKILL FACIES 3 *197*
WALLKILL FACIES 4 *197*
PALEOENVIRONMENTAL SETTING 198
SEA-LEVEL CURVE INTERPRETATION 200
LIMEPORT FORMATION: WILDCAT ROAD MEMBER 201
FACIES DESCRIPTION 201
WILDCAT ROAD FACIES 1 *201*
WILDCAT ROAD FACIES 2 *202*
WILDCAT ROAD FACIES 3 *203*
PALEOENVIRONMENTAL SETTING 203
SEA-LEVEL CURVE INTERPRETATION 206
LIMEPORT FORMATION: WHEATSWORTH MILLS MEMBER 207
FACIES DESCRIPTION 207
WHEATSWORTH MILLS FACIES 1 *207*
WHEATSWORTH MILLS FACIES 2 *208*
WHEATSWORTH MILLS FACIES 3 *208*
WHEATSWORTH MILLS FACIES 4 *208*
WHEATSWORTH MILLS FACIES 5 *209*
PALEOENVIRONMENTAL SETTING 209
SEA-LEVEL CURVE INTERPRETATION 211
LIMEPORT FORMATION: GRUENWALD MEMBER 213
FACIES DESCRIPTION 213
GRUENWALD FACIES 1 *213*

PALEOENVIRONMENTAL SETTING 214
SEA-LEVEL CURVE INTERPRETATION 214
LIMEPORT FORMATION: GLACIAL QUARRY MEMBER 216
FACIES DESCRIPTION 216
GLACIAL QUARRY FACIES 1 *216*
PALEOENVIRONMENTAL SETTING 216
SEA-LEVEL CURVE INTERPRETATION 218
LIMEPORT FORMATION: EDISON MEMBER 219
FACIES DESCRIPTION 219
EDISON FACIES 1 *219*
PALEOENVIRONMENTAL SETTING 220
SEA-LEVEL CURVE INTERPRETATION 222
LIMEPORT FORMATION: RTE. 94 MEMBER 223
FACIES DESCRIPTION 223
RTE. 94 FACIES 1 *223*
PALEOENVIRONMENTAL SETTING 224
SEA-LEVEL CURVE INTERPRETATION 225
UPPER ALLENTOWN FORMATION 226
FACIES DESCRIPTION 226
UPPER ALLENTOWN FACIES 1 *226*
UPPER ALLENTOWN FACIES 2 *226*
UPPER ALLENTOWN FACIES 3 *227*
UPPER ALLENTOWN FACIES 4 *227*
PALEOENVIRONMENTAL SETTING 227
SEA-LEVEL CURVE INTERPRETATION 230
STONEHENGE FORMATION: CARLTON VILLAGE MEMBER 231
FACIES DESCRIPTION 231
CARLTON VILLAGE FACIES 1 *231*
CARLTON VILLAGE FACIES 2 *232*
PALEOENVIRONMENTAL SETTING 233
SEA-LEVEL CURVE INTERPRETATION 234
STONEHENGE FORMATION: CANAL ROAD MEMBER 236
FACIES DESCRIPTION 236
CANAL ROAD FACIES 1 *236*
PALEOENVIRONMENTAL SETTING 237
SEA-LEVEL CURVE INTERPRETATION 237
RICKENBACH FORMATION: HOPE MEMBER 238
FACIES DESCRIPTION 238
HOPE FACIES 1 *238*
PALEOENVIRONMENTAL SETTING 239
SEA-LEVEL CURVE INTERPRETATION 240
RICKENBACH FORMATION: CROOKED SWAMP MEMBER 241
FACIES DESCRIPTION 241
CROOKED SWAMP FACIES 1 *241*
PALEOENVIRONMENTAL SETTING 242
SEA-LEVEL CURVE INTERPRETATION 242
EPLER FORMATION: BRANCHVILLE MEMBER 243
FACIES DESCRIPTION 243
BRANCHVILLE FACIES 1 *243*
BRANCHVILLE FACIES 2 *244*
PALEOENVIRONMENTAL SETTING 244

SEA-LEVEL CURVE INTERPRETATION 245
EPLER FORMATION: BIG SPRINGS MEMBER 246
FACIES DESCRIPTION 246
BIG SPRINGS FACIES 1 *246*
PALEOENVIRONMENTAL SETTING 247
SEA-LEVEL CURVE INTERPRETATION 249
EPLER FORMATION: LAFAYETTE MEMBER 251
FACIES DESCRIPTION 251
LAFAYETTE FACIES 1 *251*
LAFAYETTE FACIES 2 *251*
LAFAYETTE FACIES 3 *251*
LAFAYETTE FACIES 4 *252*
PALEOENVIRONMENTAL SETTING 252
SEA-LEVEL CURVE INTERPRETATION 254
ONTELAUNEE FORMATION: BEAVER RUN MEMBER 255
FACIES DESCRIPTION 255
BEAVER RUN FACIES 1 *255*
BEAVER RUN FACIES 2 *256*
BEAVER RUN FACIES 3 *256*
PALEOENVIRONMENTAL SETTING 256
SEA-LEVEL CURVE INTERPRETATION 259
ONTELAUNEE FORMATION: HARMONYVALE MEMBER 260
FACIES DESCRIPTION 260
HARMONVYALE FACIES 1 *260*
HARMONYVALE FACIES 2 *260*
HARMONYVALE FACIES 3 *260*
PALEOENVIRONMENTAL SETTING 261
SEA-LEVEL CURVE INTERPRETATION 263

CHAPTER 5: STRUCTURAL GEOLOGY OF THE HAMURG 7.5' QUADRANGLE, SUSSEX COUNTY, NEW JERSEY 279

INTRODUCTION 279
STRUCTURAL GEOLOGY OF THE HAMBURG 7.5' QUADRANGLE, SUSSEX COUNTY, NEW JERSEY 280
MAP INTERPRETATION OF THE STRUCUTRAL GEOLOGY OF THE HAMBURG 7.5'QUADRANGLE 281
DESCRIPTION OF OUTCROP BLOCK 1 STRUCTURE *282*
DESCRIPTION OF OUTCROP BLOCK 2 STRUCTURE *284*
DESCRIPTION OF OUTCROP BLOCK 3 STRUCTURE *286*
CROSS SECTION INTERPRETATION OF THE STRUCTURAL GEOLOGY IN THE HAMBURG 7.5'QUADRANGLE 291
INTERPRETATION OF CROSS SECTION A-A' *292*
INTERPRETATION OF CROSS SECTION B-B' *294*

REFERENCES CITED 302

VOLUME II

APPENDIX A: TYPE SECTIONS FOR THE KITTATINNY SUPERGROUP, HAMBURG 7.5' QUADRANGLE, SUSSEX COUNTY, NEW JERSEY 331

APPENDIX B: FIELD NOTES AND OBSERVATIONS FROM STRATIGRAPHIC TRAVERSE MEASUREMET IN THE HAMBURG 7.5'AND CONTIGUOUS QUADRANGLES, SUSSEX COUNTY, NEW JERSEY 385

APPENDIX C: THE MAPPING AND CHARACTERIZATION OF PREHISTORIC CHERT BEDROCK QUARRIES IN THE CAMBRIAN AND ORDOVICIAN CARBONATES OF THE HAMBURG 7.5' AND CONTIGUOUS QUADRANGLES, SUSSEX COUNTY, NEW JERSEY 552

LIST OF FIGURES

FIGURE 1.1: LOCATION MAP OF STUDY AREA FOR THE DISSERTATION, THE HAMBURG AND CONTIGUOUS 7.5' QUADRANGLES OF THE WALLKILL RIVER VALLEY OF NORTHWESTERN NEW JERSEY AND SOUTHEASTERN NEW YORK 45

FIGURE 1.2: AERIAL PHOTOGRAPH OF THE CENTRAL AND NORTHERN APPALACHIAN MOUNTAINS. 46

FIGURE 2.1: A REDUCED VERSION OF THE HAMBURG 7.5' QUADRANGLE SHEET. 54

FIGURE 2.2: A REDUCED VERSION OF A GEOLOGIC MAP OF THE HAMBURG 7.5'QUADRANGLE, SHOWING A COMPILATION OF THE MAPPING CONDUCTED FOR THIS DISSERTATION (CAMBRIAN AND ORDOVICIAN) CARBONATES AND MAPPING CONDUCTED BY DALTON ET AL. (1997) FOR THE PROTEROZOIC BASEMENT AND THE ORDOVICIAN MARTINSBURG FORMATION. 55

FIGURE 2.3: SATELLITE IMAGE OF THE NEW YORK-NEW JERSEY-PENNSYLVANIA AREA. 56

FIGURE 2.4: SATELLITE IMAGE OF THE NEW YORK-NEW JERSEY-PENNSYLVANIA AREA. 57

FIGURE 3.1: EVOLUTION OF THE NAMING OF THE KITTATINNY SUPERGROUP, SUSSEX COUNTY, NEW JERSEY. 139

FIGURE 3.2: LOCATION MAP OF STUDY AREA FOR THE DISSERTATION, THE HAMBURG AND CONTIGUOUS 7.5' QUADRANGLES OF THE WALLKILL RIVER VALLEY OF NORTHWESTERN NEW JERSEY AND SOUTHEASTERN NEW YORK, USA. 140

FIGURE 3.3: PROTEROZOIC SAPROLITE IN CONTACT WITH HARDYSTON ARKOSE (CH1), WILDCAT ROAD. 141

FIGURE 3.4: HARDYSTON FORMATION. OUTCROP PHOTOGRAPH OF CROSS BEDDED SAND UNITS, WILDCAT ROAD SECTION. 141

FIGURE 3.5: CALIFON MEMBER. SHALEY DOLOMITE AT RTE. 515 SECTION. 142

FIGURE 3.6: HAMBURG MEMBER. MUDCRACKS ON THE TOP OF THE HAMBURG MEMBER AT THE RTE. 515 SECTION. 142

FIGURE 3.7: CALIFON MEMBER. OUTCROP PHOTOGRAPH OF SPHALERITE CLOT, RTE. 515 SECTION. 143

FIGURE 3.8: CALIFON MEMBER. OUTCROP PHOTOGRAPH OF CALCITE CLOT, RTE. 515 SECTION. 143

FIGURE 3.9: CALIFON MEMBER. THIN SECTION SHOWING OPAQUE LAYERS INFERRED AS CARBONACEOUS LAYERS IN STROMATOLITE. 144

FIGURE 3.10: RTE. 515 SECTION SHOWING CALIFON (CL1)/ HAMBURG (CL2) CONTACT. 144

FIGURE 3.11: HAMBURG MEMBER. OUTCROP OF ARKOSIC SANDSTONE WEATHERING AS PEDESTALS RISING FROM LOW AREAS. 145

FIGURE 3.12: WALLKILL MEMBER. OUTCROP OF SILICIFIED ALGAL STROMATOLITES ALSO SHOWING BLOCKY APPEARANCE AND PITTING (TOWARDS TOP OF OUTCROP) OF WEATHERED PROFILE. 145

FIGURE 3.13: WALLKILL MEMBER. OUTCROP OF ALGAL LAMINATED UNIT SHOWING CLOSE-UP OF THUMB-PRINT WEATHERING PROFILE. 146

FIGURE 3.14: WALLKILL MEMBER. CHERT REPLACED STROMATOLITE IN THE LOWER ALGAL HORIZON, A.K.A. “RUDINSKI POD”, RUDINSKI FARM TRAVERSE. 146

FIGURE 3.15: WALLKILL MEMBER. CHERT REPLACED DOMAL ALGAL WITH LAMINATE BEDDING PLANE EXTENSIONS, UPPER ALGAL HORIZON. 147

FIGURE 3.16: WALLKILL MEMBER. CHERT REPLACING DOMAL ALGAL, SHOWING OUTER CONCENTRIC LAYERS AND CRISS-CROSS RIBBING. 147

FIGURE 3.17: GENERIC PICTURE OF THIN SECTION SHOWING STYLOLITES. 148

FIGURE 3.18: WALLKILL MEMBER. SAWED SLAB SHOWING SILICIFIED OOIDS, PISOIDS AND INTRACLASTS. 148

FIGURE 3.19: WALLKILL MEMBER. SAWED SLAB SHOWING SILICIFIED DOMAL ALGAL. 149

FIGURE 3.20: WALLKILL MEMBER. SAWED SLAB OF CHERT PRESERVING TIGHTLY FOLDED STRUCTURES OF ENTEROLITHIC FORM. 149

FIGURE 3.21: WILDCAT ROAD MEMBER. OUTCROP SHOWS THE REPETITIVE LIGHT GRAY-DARK GRAY-TAN COLOR BANDING THAT IS USEFUL AS A MAPPING AID. 150

FIGURE 3.22: WILDCAT ROAD MEMBER. TYPICAL OUTCROP ILLUSTRATING COLOR BANDING. 150

FIGURE 3.23: WILDCAT ROAD MEMBER. THIN SECTION OF RADIAL OOLITES OF CAMBRIAN AGE. 151

FIGURE 3.24: WILDCAT ROAD MEMBER. SAWED SLAB OF SILICIFIED OOLITE, THE STRATIGRAPHICALLY LOWEST CHERT HORIZON IN THE WILDCAT ROAD MEMBER. 151

FIGURE 3.25: WILDCAT ROAD MEMBER. THIN SECTION SHOWING PRESSURE SOLUTION OF OOIDS. 152

FIGURE 3.26: WILCAT RAOD MEMBER. THIN SECTION SHOWING ANOTHER EXAMPLE OF PRESSURE SOLUTION OF OOIDS. 152

FIGURE 3.27: WHEATSWORTH MILLS MEMBER. SAWED SLAB SHOWING COLONIAL, CAULIFLOWER SHAPED ALGAL. 153

FIGURE 3.28: WHEATSWORTH MILLS MEMBER. ACCUMULATIONS OF DOMAL AGAL BOUNDSTON WITH MUD CRACKED, BAFFLE FILLING MICRITES. 153

FIGURE 3.29: WHEATSWORTH MILLS MEMBER. THIN SECTION SHOWING SILICIFIED OOIDS THAT WERE MICRITIZED AND DOLOMITIZED PRIOR TO SILICIFICATION. 154

FIGURE 3.30: GRUENWALD MEMBER. SILICIFIED OOIDS. 154

FIGURE 3.31: EDISON MEMBER. THIN SECTION SHOWING SELECTIVE SILICIFICATION OF OOIDS. 155

FIGURE 3.32: EDISON MEMBER. THIN SECTION SHOWING PRESSURE SOLUTION HALO IN CLOSE PROXIMITY TO STYLOLITES LINED WITH OPAQUE, INSOLUBLE MATERIALS. 155

FIGURE 3.33: RTE. 94 MEMBER. SAWED SLABS SHOWING SILICIFICATION OF ORGANIC FEATURES, SUCH AS ALGAL LAMINATES AND DOMAL ALGAL. 156

FIGURE 3.34: UPPER ALLENTOWN FORMATION. SAWED SLAB SHOWING CIRCULAR ALGAL STROMATOLITE THAT MAKES A FIRST APPEARANCE IN THE KITTATINNY SUPERGROUP IN THE UPPER ALLENTOWN FORMATION. 156

FIGURE 3.35: UPPER ALLENTOWN FORMATION. SAWED SLAB SHOWING SILICIFIED OOIDS, PISOIDS AND QUARTZ SAND. 157

FIGURE 3.36: UPPER ALLENTOWN FORMATION. SAWED SLAB SHOWING SILICIFIED INTRACLASTS. 157

FIGURE 3.37: CANAL ROAD MEMBER. THIN AND THICK QUARTZ SANDSTONES AT THE BASE OF THE CANAL ROAD MEMBER. 158

FIGURE 3.38: CANAL ROAD MEMBER. LOWER BRECCIATED CHERT REPLACING QUARTZ SADNSTONES. 158

FIGURE 3.39: CARLTON VILLAGE MEMBER (OS1). CHERT BRECCIA AT CONTACT WITH THE UPPER ALLENTOWN FORMATION (CA2). 159

FIGURE 3.40: CARLTON VILLAGE MEMBER. CLOSE-UP OUTCROP PHOTOGRAPH OF THE CHERT BRECCIA AT THE BASE OF THE CARLTON VILLAGE MEMBER. 159

FIGURE 3.41: CANAL ROAD MEMBER. CONTACT BETWEEN THE CANAL ROAD MEMBER (OS2) AND THE HOPE MEMBER OF THE RICKENBACH FORMATION. 160

FIGURE 3.42: HOPE MEMBER. LOWER CONTACT OF THE HOPE MEMBER ON RIPPLE MARKS AND SCOUR-AND-FILL CHANNELS. 160

FIGURE 3.43: HOPE MEMBER. CLOSE-UP OF FIGURE 3.42. 161

FIGURE 3.44: HOPE MEMBER. CHERT REPLACED OOLITE OVERLAIN BY SILICIFIED QUARTZ SAND HORIZONS. 161

FIGURE 3.45: CROOKED SWAMP MEMBER. OUTCROP OF ALGAL LAMINATED DOLOMITE WITH QUARTZ SAND LENSES AND QUARTZ VUGS AT THE BASE OF THE CROOKED SWAMP MEMBER. 162

FIGURE 3.46: HOPE MEMBER. SAWED SLAB SHOWING CHERT BEARING QUARTZ SAND AND OOIDS. 162

FIGURE 3.47: HOPE MEMBER. SAWED SLAB SHOWING BRECCIA INTERPRETED AS BROKEN ENTEROLITHIC STRUCTURES REPRESENTING FORMER EVAPORITES. 163

FIGURE 3.48: CROOKED SWAMP MEMBER. OUTCROP OF INTERBEDDED ALGAL LAMINATED HORIZONS WITH THIN QUARTZ SAND SEQUENCES. 163

FIGURE 3.49: CROOKED SWAMP MEMBER. OUTCROP PHOTOGRAPH OF CHERT BRECCIA AT THE CONTACT BETWEEN THE CROOKED SWAMP MEMBER OF THE RICKENBACH FORMATION AND THE BRANCHVILLE MEMBER OF THE EPLER FORMATION. 164

FIGURE 3.50: CROOKED SWAMP MEMBER. OUTCROP SHOWING CHERT BRECCIA AT THE TOP OF THE MEMBER. 164

FIGURE 3.51: CROOKED SWAMP MEMBER. CHERT BRECCIA OCCURRING ALONG THE TOP OF THE MEMBER. 165

FIGURE 3.52: BRANCHVILLE MEMBER. SILCRETE AT THE TOP OF THE BRANCHVILLE MEMBER. 165

FIGURE 3.53: BRANCHVILLE MEMBER. OUTCROP OF THIN, FLAGGY, SHALY DOLOMITE SHOWING CONTACT BETWEEN THE CROOKED SWAMP MEMBER (OR2) AND THE BRANCHVILLE (OE1). 166

FIGURE 3.54: BRANCHVILLE MEMBER. CONTACT BETWEEN THE BRANCHVILLE MEMBER (OE1) AND THE OVERLYIG BIG SPRINGS MEMBER (OE2), EPLER FORMATION. 166

FIGURE 3.55: BRANCHVILLE MEMBER. SAWED SLAB OF CHERT CONTAINING BLACK, MATTED, LENTIL TO ELONGATE SHAPED PODS. 167

FIGURE 3.56: BIG SPRINGS MEMBER. SAWED SLAB OF PINCH-AND-SWELL, GRAY TO LAVENDER, BRECCIATED CHERT. 167

FIGURE 3.57: BIG SPRINGS MEMBER. SAWED SLAB OF SILICIFIED ALGAL STRUCTURES. 168

FIGURE 3.58: BIG SPRINGS MEMBER. SAWED SLAB OF WHITE TO GRAY CHERT REPLACING ALGAL STRUCTURES. 168

FIGURE 3.59: BIG SPRINGS MEMBER. SAWED SLAB OF WHITE CHERT. 169

FIGURE 3.60: BIG SPRINGS MEMBER. SAWED SLABS REPLACING OOIDS AND ALGAL LAMINATIONS. 169

FIGURE 3.61: LAFAYETTE MEMBER. THIN SECTIONS OF ONCOIDAL AND PISOIDAL GRAINSTONES. 170

FIGURE 3.62: BEAVER RUN MEMBER. STRONGLY BURROWED HORIZONS AND PUNKY CHERT ALONG THE BASE OF THE BEAVER RUN MEMBER. 170

FIGURE 3.63: BEAVER RUN MEMBER. *MACULARITES* GASTROPOD DISCOVERED IN THE BEAVER RUN MEMBER OF THE ONTELAUNEE FORMATION. 171

FIGURE 3.64: BEAVER RUN MEMBER. PUNY, POROUS CHERT REPLACING ALGAL STRUCTURES AT THE BASE OF THE BEAVER RUN MEMBER. 171

FIGURE 3.65: BEAVER RUN MEMBER. CHERT REPLACING CONVEX ALGAL STRUCTURES. 172

FIGURE 3.66: BEAVER RUN MEMBER. SAWED SLABS SHOWING VERTICAL AND HORIZONTAL BURROWS. 172

FIGURE 3.67: BEAVER RUN MEMBER. PINCH-AND-SWELL CHERT BEDS DEVELOPED WITHIN THE TRANSITIONAL FACIES OF THE BEAVER RUN MEMBER. 173

FIGURE 3.68: HARMONYVALE MEMBER. THICK BEDDED, BLUE, BRECCIATED CHERT REPLACING ALGAL LAMINATE AND INFERRED EVAPORITIC HORIZONS. 173

FIGURE 3.69: HARMONYVALE MEMBER. SAWED SLAB OF CHERT BRECCIA IN HARMONYVALE MEMBER. 174

FIGURE 4.1: SKOLITHOS BURROWS IN QUARTZ SAND, EXPOSED ON WEATHERED BEDDING PLANE, HARDYSTON FORMATION, RTE. 515 RAVERSE. 265

FIGURE 4.2: RIPPLE SURFACES ON SHALEY DOLOMITE, UPPER CALIFON MEMBER, LEITHSVILLE FORMATION, RTE. 515 TRAVERSE. 265

FIGURE 4.3: WEATHERED BEDDING PROFILE, HAMBURG MEMBER, LEITHSVILLE FORMATION, RTE. 23N TRAVERSE. 266

FIGURE 4.4: PROFILE OF CROSS BEDS AND RIPPLE SURFACES, NOTE CAVITIES WHERE CARBONATE-RICH SEDIMENTS HAVE WEATHERED OUT, HAMBURG MEMBER, LEITHSVILLE FORMATION. 266

FIGURE 4.5: CHERT REPLACED STROMATOLITES IN THE LOWER ALGAL HORIZONS, A.K.A. “RUDINSKI POD, “ FACIES 1, WALLKILL MEMBER, LEITHSVILLE FORMATION, RUDINSKI FARM TRAVERSE. 267

FIGURE 4.6: CHERT REPLACED DOMAL ALGAL WITH LAMINATE BEDDING PLANE EXTENSIONS, UPPER ALGAL HORIZON, FACIES 1, WALLKILL MEMBER, LEITHSVILLE FORMATION, MARGARET'S ESTATE. 267

FIGURE 4.7: SLAB OF DIGITATE ALGAL LINING LAMINATED ALGAL RUBBER TRAVERSE. 268

FIGURE 4.8: ISOLATED PATCH OF ALGAL COLONIES IN BAFFLE FILLING MICRITE, WHEATSWORTH MILLS MEMBER (CA1-2), LIMEPORT FORMATION, GRUENWALD ESTATE. 268

FIGURE 4.9: GRADED OOLITES WITH MICRITE CAP, UPPER GRUENWALD MEMBER, LIMEPORT FORMATION, GRUENWALD ESTATE. 269

FIGURE 4.10: DIGITATE ALGAL (THROMBILITES), UPPER GRUENWALD MEMBER, LIMEPORT FORMATION, GRUENWALD ESTATE. 269

FIGURE 4.11: CHERT REPLACED FLOWERING ALGAL IN RUBBLE ZONE, BASE OF UPPER ALLENTOWN FORMATION. 270

FIGURE 4.12: LARGE COLONY OF CUP SHAPED CHERT REPLACED ALGAL, BASE OF CARLTON VILLAGE MEMBER, UPPER ALLENTOWN. 270

FIGURE 4.13: SLAB OF OVERTURNED ALGAL COLONY IN RUBBLE OF RE-CEMENTED MICRITE, CARLTON VILLAGE MEMBR, UPPER ALLENTOWN (SCALE NUMBER IN CM). 271

FIGURE 4.14: QUARTZ SAND HORIZONS WITH INTERBEDDED ALGAL STRUCTURES, STONEHENGE FORMATION, HARMONYVALE TRAVERSE. 271

FIGURE 4.15: INTRACLASTIC HORIZON OVER CHERT REPLACED QUARTZ SAND BED, HOPE MEMBER, RICKENBACH FORMATION, HARMONYVALE TRAVERSE. 272

FIGURE 4.16: "SEVEN CHERTS" OF THE HOPE MEMBER, RICKENBACH FORMATION, HARMONYVALE TRAVERSE. 272

FIGURE 4.17: SLAB SHOWING BIRDS-EYE EVAPORITE STRUCTURES AND CHERT REPLACED ENTEROLITHIC GYPSUM, BRANCHVILLE MEMBER, EPLER FORMATION. 273

FIGURE 4.18: CONOCOCHEAGE-LIKE SEQUENCE OF CHERT REPLACED GRADED OOLITE OVERLAIN BY ALGAL COLONY AND ALGAL LAMINATED MICRITE, NOTE CHERT REPLACED INTRACLASTIC HORIZON CAPPING ALGAL, BIG SPRINGS MEMBER, EPLER FORMATION. 273

FIGURE 4.19: ALGAL COLONY IN LOWER SUPRATIDAL ALGAL LAMINATED MICRITIC DOLOMITE, BIG SPRINGS MEMBER, EPLER FORMATION, BEAVER RUN AGGREGATE TRAVERSE. 274

FIGURE 4.20: CALCAREOUS ALGAE, BIG SPRINGS MEMBER, EPLER FORMATION, BEAVER RUN AGGREGATE TRAVERSE. 274

FIGURE 4.21: CALCAREOUS ALGAE IN SUPRATIDAL MICRITE, BIG SPRINGS MEMBER, EPLER FORMATION, BEAVER RUN AGGREGATE TRAVERSE. 275

FIGURE 4.22: CHERT REPLACED EVAPORITES OVERLAIN BY CHERT REPLACED ALGAL STROMATOLITES, BIG SPRINGS MEMBER, EPLER FORMATION, HARMONYVALE TRAVERSE. 275

FIGURE 4.23: CLOSE-UP OF CHERT REPLACED ALGAL OVERLAIN BY CHERT REPLACED EVAPORITE, BIG SPRINGS MEMBER, EPLER FORMATION. 276

FIGURE 4.24: PALEOKARST OF ANGULAR FRAGMENTS OF CHERT IN THE UPPER FACIES OF BIG SPRINGS MEMBER, EPLER FORMATION, BEAVER RUN AGGREGATE TRAVERSE. 276

FIGURE 4.25: BRECCIATED ALGAL IN SILCRETE (LEFT) AND BRECCIATE EVAPORITE IN COARSE DOLOMITE (RIGHT), BIG SPRINGS MEMBER, EPLER FORMATION, BEAVER RUN AGGREGATE TRAVERSE. 277

FIGURE 4.26: CONVEX CHERT REPLACED ALGAL FACIES 2, BEAVER RUN MEMBER, ONTELAUNEE FORMATION, SWARTSWOOD LAKE TRAVERSE. 277

FIGURE 4.27: CLOSE-UP OF STRONGLY BURROWED CHERT REPLACED ALGAL STROMATOLITE HORIZON, BEAVER RUN MEMBER, ONTELAUNEE FORMATION, HOUSTON ROAD TRAVERSE. 278

FIGURE 4.28: CHERT REPLACED EVAPORITE HORIZON WITH PINCH-AND-SWELL BEDS OF MICRITIC ALGAL DOLOMITE, HARMONYVALE MEMBER, ONTELAUNEE FORMATION, HARMONYVALE TRAVERSE. 278

FIGURE 5.1: A REDUCED VERSION OF THE HAMBURG 7.5' QUADRANGLE SHEET. 297

FIGURE 5.2: A REDUCED VERSION OF A GEOLOGIC MAP OF THE HAMBURG 7.5' QUADRANGLE, SHOWING A COMPILATION OF THE MAPPING CONDUCTED FOR THIS DISSERTATION AND MAPPING CONDUCTED BY DALTON ET AL. (1997) FOR THE PROTEROZOIC BASEMENT AND THE ORDOVICIAN MARTINSBURG FORMATION. 298

FIGURE 5.3: SATELLITE IMAGE OF THE NEW YORK-NEW JERSEY-PENNSYLVANIA AREA. THOMAS'(1993) INTERPRETATION OF THE NEW JERSEY TRANSFORM, PLUS HIS DISTINGUISHING BETWEEN THE HUDSON AND NORTHERN BLUE RIDGE RIFT ZONES ON THE NORTH AND SOUTH SIDES OF THE NEW JERSEY TRANSFORM, RESPECTIVELY ARE SHOWN ON THIS FIGURE. 299

FIGURE 5.4: SATELLITE IMAGE OF THE NEW YORK-NEW JERSEY-PENNSYLVANIA AREA. THE STUDY AREA IN THIS DISSERTATION IS IN THE NEW YORK RECESS. 300

FIGURE 5.5: RECRIPROCAL PLOTS FOR STRIKE AND DIP OF BEDDING ORIENTATION IN THE CAMBRIAN AND ORDOVICIAN CARBONATE ROCKS, AS MAPPED WITHIN OUTCROP BLOCKS 1, 2 AND 3 OF THE HAMBURG 7.5' QUADRANGLE. 301

FIGURE A.1: WHEATSWORTH MILLS MEMBER. COLONIES OF TIGHTLY BOUNDED DIGITATE ALGAL STROMATOLITES (THROMBOLITES) AT THE TOP OF THE WHEATSWORTH MILLS MEMBER. GRUENWALD TRAVERSE. 377

FIGURE A.2: COLONIES OF TIGHTLY BOUND DIGITATE ALGAL STROMATOLITES (THROMBOLITES) AT THE TOP OF THE WHEATSWORTH MILLS MEMBER. MICRITE CAPS THE FACIES. GRUENWALD TRAVERSE. 377

FIGURE A.3: WHEATSWORTH MILLS MEMBER. MASSIVE ALGAL BOUNDSTONE COMMUNITIES AT THE UPPER CONTACT OF THE WHEATSWORTH MILLS MEMBER. GRUENWALD TRAVERSE. 378

FIGURE A.4: CARLTON VILLAGE MEMBER. UNIQUE FLOWERING OF CHERT REPLACED ALGAL STROMATOLITES IN MICRITIC RUBBLE ZONE AT THE BASE OF THE MEMBER. 379

FIGURE A.5: UPPER ALLENTOWN FORMATION. PINCH-AND-SWELL CHERT REPLACED LAMINATED ALGAL STRUCTURES AT THE BASE OF THE FORMATION. 379

FIGURE A.6: CARLTON VILLAGE MEMBER. COLONY OF CUP SHAPED CHERT REPLACED ALGAL STROMATOLITES IN RUBBLE ZONE AT THE BASE OF THE MEMBER. 380

FIGURE A.7: CARLTON VILLAGE MEMBER. ASSOCIATION OF FLOWERING, CUP SHAPED AND ROPY INTERTWINED CHERT REPLACED ALGAL STROMATOLITES. 380

FIGURE A.8: CARLTON VILLAGE MEMBER. TIGHTLY BOUND HEMISPHERIC ALGAL STROMATOLITES AT THE TOP OF THE MEMBER. 381

FIGURE A.9: BIG SPRINGS MEMBER. LARGE DOMAL ALGAL SUCCESSIONS, CONOCOCHEAGE-LIKE CYCKES. HARMONYVALE SECTION. 381

FIGURE A.10: BIG SPRINGS MEMBER. LARGE DOMAL ALGAL WITH CHERT REPLACEMENT ALONG THE TOP OF EACH ALGAL SUCCESSION. HARMONYVALE SECTION. 382

FIGURE A.11: BIG SPRINGS MEMBER. WELL DEVELOPED SILCRETE COVERING CREST OF INTRACLASTIC HORIZON AND ALGAL LAMINATED MICRITE. HARMONYVALE SECTION. 382

FIGURE A.12: BIG SPRINGS MEMBER. BLOCKS OF SILCRITIZED, SUPRATIDAL, ALGAL LAMINATED MICRITIC DOLOMITE. HARMONYVALE SECTION. 383

FIGURE A.13: LAFAYETTE MEMBER. SILICIFIED, PUNKY AND POROUS ALGAL STROMATOLITES. HARMONYVALE SECTION. 383

FIGURE A.14: LAFAYETTE MEMBER. OUTCROP PHOTOGRAPH DEPICTING OVERTURNED PALEOKARST COLLAPSE FEATURES INTERRUPTING BEDDING. HARMONYVALE SECTION. 384

FIGURE A.15: IRREGULAR MASSES AND CLOTS OF CHERT INTERPRETED AS REPLACING BURROW STRUCTURES AND INFERRED EVAPORITES. HARMONYVALE SECTION. 384

FIGURE C.1: EVOLUTION OF THE NAMING OF THE KITTATINNY SUPERGROUP, SUSSEX COUNTY, NEW JERSEY. 584

FIGURE C.2: HAMBURG-FRANKLIN METALLOGENIC PROVINCE WITH DISTRICTS, OUTLIERS AND QUARRY CLUSTERS (YELLOW CIRCLES WITH BLACK BORDERS). 585

FIGURE C.3: SCHEMATIC 2-D VIEW OF THE TYPICAL QUARRY PLAN (LAPORTA, 2004), AS ELUCIDATED FROM THE WALLKILL RIVER VALLEY STUDY, DEPICTING ASSOCIATED MINING INSTRUMENTS AND THEIR PETROLOGIES. 586

FIGURE C.4: SCHEMATIC VIEW OF THE TYPICAL QUARRY PLAN, AS ELUCIDATED FROM THE WALLKILL RIVER VALLEY STUDY. PLAN A DEPICTS THE LABOR SUBDIVISIONS, WHILE PLAN B INCLUDES THE ASSOCIATED MINING INSTRUMENTS. 587

FIGURE C.5: CACHE OF HAMMERSTONES AT THE BEAVER RUN STANDARD SECTION. 587

FIGURE C.6: SPALLED HAMMERSTONE IN A PREHISTORIC QUARRY ADIT AT THE BEAVER RUN STANDARD SECTION. 588

FIGURE C.7: INSTRUMENT IN AN ACCENTUATED JOINT, ZONE OF EXTRACTION (ZONE I), HARMONYVALE MEMBER CHERT, HARMONYVALE SECTION. 588

FIGURE C.8: SMALL INSTRUMENT LODGED IN AN ACCENTUATED JOINT, ZONE OF EXTRACTION (ZONE 1), HARMONYVALE MEMBER, HARMONYVALE SECTION. 589

FIGURE C.9: HEAVY SURFACE BATTERING AND PLUG-AND-FEATHER (BY FINGER) ON BEAVER RUN MEMBER CHERT, HARMONYVALE SECTION. 589

FIGURE C.10: CUSPATE AND CASTELLATED SURFACE, HARMONYVALE MEMBER, BEAVER RUN STANDARD SECTION. 590

FIGURE C.11: CONCOIDAL SCARS ON WEATHERED SURFACE OF BIG SPRINGS MEMBER CHERT, HARMONYVALE SECTION. 590

FIGURE C.12: STABLE PLATFORM DIRECTLY IN FRONT OF A ZONE OF EXTRACTION, HARMONYVALE MEMBER CHERT, BEAVER RUN STANDARD SECTION. 591

FIGURE C.13: SCREE OF BEAVER RUN MEMBER CHERT MIDDLING BLOCKS, HARMONYVALE SECTION. 591

FIGURE C.14: CHERT DEBRIS, FLAKES AND SMALL INSTRUMENTS, HARMONYVALE MEMBER CHERT, HARMONYVALE SECTION. 592

VOLUME III

LIST OF PLATES

PLATE 4.1: SEA-LEVEL CURVE FOR THE HARDYSTON AND LEITHSVILLE FORMATIONS (SCALE 1:98).

PLATE 4.2: SEA-LEVEL CURVE FOR THE WILDCAT ROAD MEMBER (SCALE 1:98).

PLATE 4.3: SEA-LEVEL CURVE FOR THE WHEATSWORTH MILLS MEMBER (SCALE 1:98).

PLATE 4.4: SEA-LEVEL CURVE FOR THE GRUENWALD MEMBER (SCALE 1:98).

PLATE 4.5: SEA-LEVEL CURVE FOR THE GLACIAL AND EDISON MEMBERS (SCALE 1:98).

PLATE 4.6: SEA-LEVEL CURVE FOR THE RTE. 94 MEMBER AND UPPER ALLENTOWN FORMATION (SCALE 1:98).

PLATE 4.7: SEA-LEVEL CURVE FOR THE STONEHENGE FORMATION (SCALE 1:98).

PLATE 4.8: SEA-LEVEL CURVE FOR THE RICKENBACH FORMATION (SCALE 1:98).

PLATE 4.9: SEA-LEVEL CURVE FOR THE BIG SPRINGS AND BRANCHVILLE MEMBERS (SCALE 1:98).

PLATE 4.10: SEA-LEVEL CURVE FOR THE LAFAYETTE MEMBER (SCALE 1:98).

PLATE 4.11: SEA-LEVEL CURVE FOR THE BEAVER RUN AND HARMONYVALE MEMBERS (SCALE 1:98).

PLATE 5.1: COMPOSITE GEOLOGIC MAP OF THE HAMBURG 7.5'QUADRANGLE (SCALE 1:24,000).

PLATE 5.2: A-A'CROSS SECTION THROUGH THE HAMBURG 7.5'QUADRANGLE (SCALE 1:24,000).

PLATE 5.3: B-B'CROSS SECTION THROUGH THE HAMBURG 7.5'QUADRANGLE (SCAE 1:24,000).

PLATE A.1: TYPE STRATIGRAPHIC SECTION FOR THE CAMBRIAN HARDYSTON FORMATION (SCALE 1:98).

PLATE A.2: TYPE STRATIGRAPHIC SECTION FOR THE CAMBRIAN CALIFON MEMBER OF THE LEITHSVILLE FORMATION (SCALE 1:98).

PLATE A.3: TYPE STRATIGRAPHIC SECTION FOR THE CAMBRIAN HAMBURG MEMBER OF THE LEITHSVILLE FORMATION (SCALE 1:98).

PLATE A.4: TYPE STRATIGRAPHIC SECTION FOR THE CAMBRIAN WALLKILL MEMBER OF THE LEITHSVILLE FORMATION (SCALE 1:98).

PLATE A.5: TYPE STRATIGRAPHIC SECTION FOR THE CAMBRIAN WILDCAT ROAD MEMBER OF THE LIMEPORT FORMATION (SCALE 1:98).

PLATE A.6: TYPE STRATIGRAPHIC SECTION FOR THE CAMBRIAN WHEATSWORTH MILLS MEMBER OF THE LIMEPORT FORMATION (SCALE 1:98).

PLATE A.7: TYPE STRATIGRAPHIC SECTION FOR THE CAMBRIAN GRUENWALD MEMBER OF THE LIMEPORT FORMATION (SCALE 1:98).

PLATE A.8: TYPE STRATIGRAPHIC SECTION FOR THE CAMBRIAN GLACIAL QUARRY MEMBER OF THE LIMEPORT FORMATION (SCALE 1:98).

PLATE A.9: TYPE STRATIGRAPHIC SECTION FOR THE CAMBRIAN EDISON MEMBER OF THE LIMEPORT FORMATOIN (SCALE 1:98).

PLATE A.10: TYPE STRATIGRAPHIC SECTION FOR THE CAMBRIAN RTE. 94 MEMBER OF THE LIMEPORT FORMATION (SCALE 1:98).

PLATE A.11: TYPE STRATIGRAPHIC SECTION FOR THE CAMBRIAN UPPER ALLENTOWN FORMATION (SCALE 1:98).

PLATE A.12: TYPE STRATIGRAPHIC SECTION FOR THE CARLTON VILLAGE MEMBER OF THE STONEHENGE FORMATION (SCALE 1:98).

PLATE A.13: TYPE STRATIGRAPHIC SECTION FOR THE CANAL ROAD MEMBER OF THE STONEHENGE FORMATION (SCALE 1:98).

PLATE A.14: TYPE STRATIGRAPHIC SECTION FOR THE HOPE MEMBER OF THE RICKENBACH FORMATION (SCALE 1:98).

PLATE A.15: TYPE STRATIGRAPHIC SECTION FOR THE CROOKED SWAMP MEMBER OF THE RICKENBACH FORMATION (SCALE 1:98).

PLATE A.16: TYPE STRATIGRAPHIC SECTION FOR THE BRANCHVILLE MEMBER OF THE EPLER FORMATION (SCALE 1:98).

PLATE A.17: TYPE STRATIGRAPHIC SECTION FOR THE BIG SPRINGS MEMBER OF THE EPLER FORMATION (SCALE 1:98).

PLATE A.18: TYPE STRATIGRAPHIC SECTION FOR THE LAFAYETTE MEMBER OF THE EPLER FORMATION (SCALE 1:98).

PLATE A.19: TYPE STRATIGRAPHIC SECTION FOR THE BEAVER RUN MEMBER OF THE ONTELAUNEE FORMATION (SCALE 1:98).

PLATE A.20: TYPE STRATIGRAPHIC SECTION FOR THE HARMONYVALE MEMBER OF THE ONTELAUNEE FORMATION (SCALE 1:98).

CHAPTER 1: Introduction

1.1 Statement of the Problem

The Cambrian and Ordovician chert bearing rocks of the New Jersey Great Valley sequence have been referred to historically as the undifferentiated Kittatinny Limestone (Rogers, 1840). This general catch-all phrase has served to characterize these rocks for more than a century (Kummel and Weller, 1901; Rogers, 1840; Weller, 1900b). Prior to this time, they were simply known as the blue limestones (Rogers, 1836). A reason for this generalization is that the mixed package of limestone and dolomite had only limited economic value, including furnishing building foundation stone and occasionally for the production of lime and lime products. In addition, as a result of being geographically situated on a the New Jersey structural high (New York promontory) (Thomas, 1977), approximately 707 m of Cambrian-Ordovician carbonates were deposited. Much thicker, less eroded, and more fossiliferous rocks could easily be investigated in the neighboring depocenters occurring in the Pennsylvania salient, just to the south and the Quebec salient, to the north (Thomas, 1977; Walcott, 1898). In general, the area was not seen as being very research worthy, with few exceptions (Brewer and LaPorta, 2006; Dalton et al., 1997; Drake, 1978; Herman and Monteverde, 1989; Herman et al., 1997; LaPorta, 1991, 1992, 1998a, b, 2002). Therefore the Great Valley sequence of northwestern New Jersey played a secondary role in mapping investigations, and was excluded from most correlation studies, except in the broadest sense. Most subsequent investigations shifted to the south where large expansive quarries furnished freshly exposed and continuous stratigraphic sections.

However, during the first half of the 20th century, the region and its mineral rights were the proprietary concern of the New Jersey Zinc Co.; as such, research focus shifted to the Grenvillian basement and associated terrains. An outgrowth of this exploration was a large body of work on the structural geology of the region, especially in the vicinity of the mines at Franklin (Buddington and Baker, 1961; Hague et al., 1956). Unfortunately, this economic focus resulted in the wholesale acceptance of stratigraphic nomenclature, thickness estimates, as well as paleoenvironmental interpretations, translated from the standard sections of neighboring depocenters. Therefore, an accurate and consistent estimate of the thickness of the carbonate succession in the dissertation study area had never been known, and a complete stratigraphic section had yet to be compiled. Furthermore, no explanation had been put forward for the plentiful, nodular and bedded, chert horizons which exhibit lateral continuity along strike. The carbonates deposited on the New York promontory were remapped (scale 1:24,000) for this dissertation in the Hamburg 7.5' Quadrangle employing the chert horizons as mapping aids. A detailed stratigraphic section (scale: 1 in = 250 cm or 1:98) of the Cambrian-Ordovician carbonates was compiled for this dissertation and carbonate depositional environments were interpreted using the compiled data. Finally, the detailed stratigraphic section work permitted stratigraphic, sedimentological and structural data to be collected on the cherts present in the Cambrian-Ordovician carbonates. Models of silica deposition and timing are proposed using the data collected during detailed stratigraphic section measurement. These cherts, which have been ignored until recently (LaPorta, 1986, 1991, 1992, 1998a, b), are the focus of this investigation.

1.2 Location of the Study Area

The study area for this dissertation is the Great Valley sequence of the Hamburg, and contiguous, 7.5' quadrangles in northwestern New Jersey and southeastern New York (Figure 1.1). The stratigraphic section work conducted for this dissertation included parts of the contiguous Branchville, Franklin, and Wawayanda 7.5' quadrangles (Figure 1.1). In addition, specific samples, as well as references, are made to locations occurring within the surrounding quadrangle sheets; including, Pine Island, Unionville, and Newton East (Figure 1.1). The Great Valley sequence, in the Hamburg quadrangle, is a northeast-southwest trending swath of Cambrian and Ordovician carbonates bounded to the east by parautochthonous and allochthonous Proterozoic gneisses, marbles and other metasedimentary rocks and to the west by the Ordovician slate belt (Dale, 1906; Dalton et al., 1997; Drake, 1965, 1969). The study area occurs in the New York recess (Thomas, 1977), representing a pivotal geologic position midway between the two neighboring salients, specifically the Pennsylvania and the Quebec (Thomas, 1977) (Figure 1.2). This strategic geographic locale permits correlation between these two deeper water lithofacies packages which are separated by the New York recess.

1.3 Goals of the Dissertation

This dissertation accomplishes several goals:

1. The first goal was to construct the first complete stratigraphic section of the Cambrian and Ordovician carbonates cropping out in the region of Sussex County, New Jersey. The carbonate stratigraphy was employed to map the bedrock geology of the Hamburg quadrangle. The stratigraphic sections aided correlation studies between the two contiguous salients, adjacent to the recess, where standard stratigraphic sections have

already been constructed (Hobson, 1963; Knopf, 1962). Also, it allowed for a general interpretation of depositional settings, which in turn reflected the paleoenvironments that existed over the study area.

2. The stratigraphic mapping phase of the research included a very detailed chert stratigraphy. The cherts horizons were used as a fine tuned mapping aid, as well as a vehicle for correlation studies, where fossils are rare to absent (Woodward, 1931). The dissertation presents a revised geologic map of the Hamburg 7.5' Quadrangle of northwestern New Jersey. The map was used to delineate the major structures of the region; and used to construct two balanced and palinspastically restored cross sections. As mapping proceeded, it was discovered that different kinds of cherts were useful for the interpretation of facies, repeated sections, regions of overturning, zones of thrusting, and faulting.

3. It was also discovered that the cherts preserve even the most delicate aspects of many of the ancient depositional environments. The fossilized features can be used to reconstruct specific depositional settings, which are otherwise eradicated during diagenesis. The chert-rich parts of each unit helped confirm the varying depositional settings, facies relationships, and even micro-environments which characterize each formation member. In some instances, even microbes are perfectly preserved in chert, especially in the lower Cambrian lithologies.

4. As it has turned out, the chert shared a relationship with sea-level curves which are well established for the region (Mitchum et al., 1977; Vail and Mitchum, 1977; Vail et al., 1977a; Vail et al., 1977b), as well as with new curves produced using the detailed stratigraphy mapped during this study. These curves include those induced by world-

wide, sea-level fluctuations, by thermal subsidence, by glaciation, and by regional tectonics. Each of these processes invoked a different response in chert formation. This in-phase relationship is visible throughout the Great Valley sequence, registered as sequences of carbonate strata, punctuated by chert units.

5. The cherts of the Kittatinny Supergroup were quarried by prehistoric Native Americans for stone tool production. A goal of this part of the study was to locate prehistoric Native American quarries within the Wallkill River Valley. To date, greater than 600 chert quarry complexes have been discovered and mapped within the valley. The quarry extraction process was strongly influenced by geological constraints; such as the attitude of the chert beds, the orientation and placement of master joint sets, as well as the degree to which fracture cleavage, boudinage structures, and pressure solution features were developed. These geological constraints played a significant role in determining the methods employed in developing the quarries, control the types of quarries being engineered, and provide the templates for stone tool design (Brewer and LaPorta, 1999, 2001, 2002; Brewer et al., 2006; Brewer et al., 2000; LaPorta, 1986, 1987, 1989, 1990, 1993a, b, 1994, 1995a, 1996a, b, c, 1997b, 1998c, 1999b, c, d, e, f, 2000a, b, c, 2001, 2004; Sohl et al., 2001).

1.4 Outline of the Dissertation

Chapter 2 of this dissertation presents the tectonic setting of the Hamburg 7.5' Quadrangle. Three orogenic episodes have been interpreted as deforming eastern North America, since the Iapetan break-up of the Rodinian supercontinent in the Neoproterozoic. The evidence for the three Paleozoic orogenies, as they pertain to the Hamburg and surrounding quadrangles, is presented. The purpose of this chapter is to

provide a tectonic framework for the deposition and deformation of the Cambrian-Ordovician carbonates, and the cherts within the carbonates, in the dissertation study area. Review of the tectonic setting also provides a framework for silica deposition and diagenesis in the Cambrian-Ordovician carbonates.

The stratigraphy chapter (Chapter 3) represents the foundation upon which much of the dissertation is constructed. Detailed stratigraphic sections, facies and depositional models were constructed for each member of the Cambrian and Ordovician Kittatinny Supergroup, as cropping out the Hamburg 7.5' Quadrangle. This was largely accomplished through deciphering delicately preserved depositional environments replaced by chert. This dissertation describes the field and diagenetic relations of the cherts in the Wallkill River Valley. Special attention is paid to the outward appearance of the chert, its geologic setting (lithologic description, physical dimensions [width, thickness, height], color, internal structure), as the initial goal of the study was to be able to employ the cherts as geologic mapping aids. As such, the primary contribution of the chert stratigraphy was the development of a revised geologic map for a part of the Hamburg 7.5' Quadrangle, and the accurate determination of the stratigraphic thickness of the Kittatinny Supergroup. It also led to the realization that cherts in different horizons are very different from each other and can be used for more accurate mapping. The associated cherts are now aligned with discrete formations and members, which help characterize rocks where fossils are sparingly found (Woodward, 1931). The results of Chapter 3 propose new standard sections for the members of the Kittatinny Supergroup in Sussex County, New Jersey, breaking some of the connections with the previously constructed sections in Pennsylvania to which they have been forced to fit over the

decades (Willard, 1955, 1958). A very important addition to the stratigraphy has been the discovery of a new formation in the valley (Stonehenge Formation) and the subdivision of the Limeport Formation into six members.

In Chapter 4, the newly constructed stratigraphic sections present their own new sedimentary facies relationships, thereby necessarily filling in a gap in our knowledge of the New York recess. Various facies within each member are described and interpreted, with compilation of each member's facies mosaics into paleoenvironmental interpretations of Laurentia's Iapetan continental margin. Each facies is also presented with a new sea-level curve, created using the 1:98-scale composite stratigraphic column for the Kittatinny Supergroup. As such, a detailed one-to-one relationship is illustrated between facies characteristics indicative of sea-level regression or transgression and the sea-level curve interpretation. Chapter 4 also illustrates how the cherty sequences of each member of the Kittatinny Supergroup correspond with several magnitudes of sea-level curves modeled for this region (Dykstra and Longman, 1995; Mitchum et al., 1977; Vail and Mitchum, 1977; Vail et al., 1977a; Vail et al., 1977b)**,** including a worldwide, sea-level curve, a basin subsidence curve, a curve related to glacio-eustatics, and one relating directly to regional tectonism. These curves and their close correlation to chert horizons clearly illustrate the cherts as occurring in coincidence with punctuations in sea level, all associated with transgression and regression events.

Chapter 5 incorporates the re-interpreted carbonate and chert stratigraphy to elucidate the various structures in the Hamburg 7.5' Quadrangle and to develop a sequence of deformational events. The precise thicknesses and refined mapping that resulted from using chert as a stratigraphic tool led in turn to a viable structural and

tectonic model for the region. Two balanced cross sections were constructed for the quadrangle. In essence, deformed cherts provided a unique record of the various episodes of folding and thrusting events in the quadrangle as they underwent silica diagenesis (Brueckner et al., 1987). Also, the cherts played a significant role in the deformation process. Finally, the catalogue of pressure solution features associated with the chert units clearly contributed to the hypothesis that pressure solution cherts, or stylo-cherts, have formed within the lower Cambrian-Ordovician lithologies. All of the results of the analyses conducted during this investigation lends credence to Bailey Willis' claim that stratigraphy in the Appalachians plays a significant role in determining structure (Willis, 1893).

A cross disciplinary application of the revised chert stratigraphy, sea-level curve models, and structural interpretations of the Hamburg 7.5' Quadrangle is presented in Appendix C. The geological investigation of the prehistoric chert quarries architectured into the landscape of the Cambrian-Ordovician carbonates represents the first logical step towards our understanding of prehistoric lithic based economies, as the prehistoric quarry is where the life cycle of most stone tools begins (Brewer and LaPorta, 2002; LaPorta, 1986, 1987, 1989, 1990, 1991, 1992, 1993b, 1994, 1995b, 1996b, c, 1999a, 2000a). This chapter illustrates how the fine-scale stratigraphic classification of quarries permits the development of a unique quarry predictive model and high resolution provenance tool developed for archaeological investigations. The regional structural controls described in Chapter 5 elucidate a Native American mining engineering (folk geology concept) (Brewer-LaPorta et al., in preparation; Brewer et al., 2006; LaPorta, 1986, 1993a, 1997a, b, 1998c, 1999b, c, d, e, 2000b, c, 2001, 2004). This appendix shows how structural

geology was employed in this investigation to develop a chain of operation (chain du operatoire) that correlations the architecture of quarries to mining instruments and discrete classes of mine tailings. The analyses resulted in the development of a four-part model illustrating task subdivision as occurring within architecturally different styles of quarries. The mines themselves are classified into a hierarchy which permits the researcher to elucidate the pattern of prehistoric land utilization.

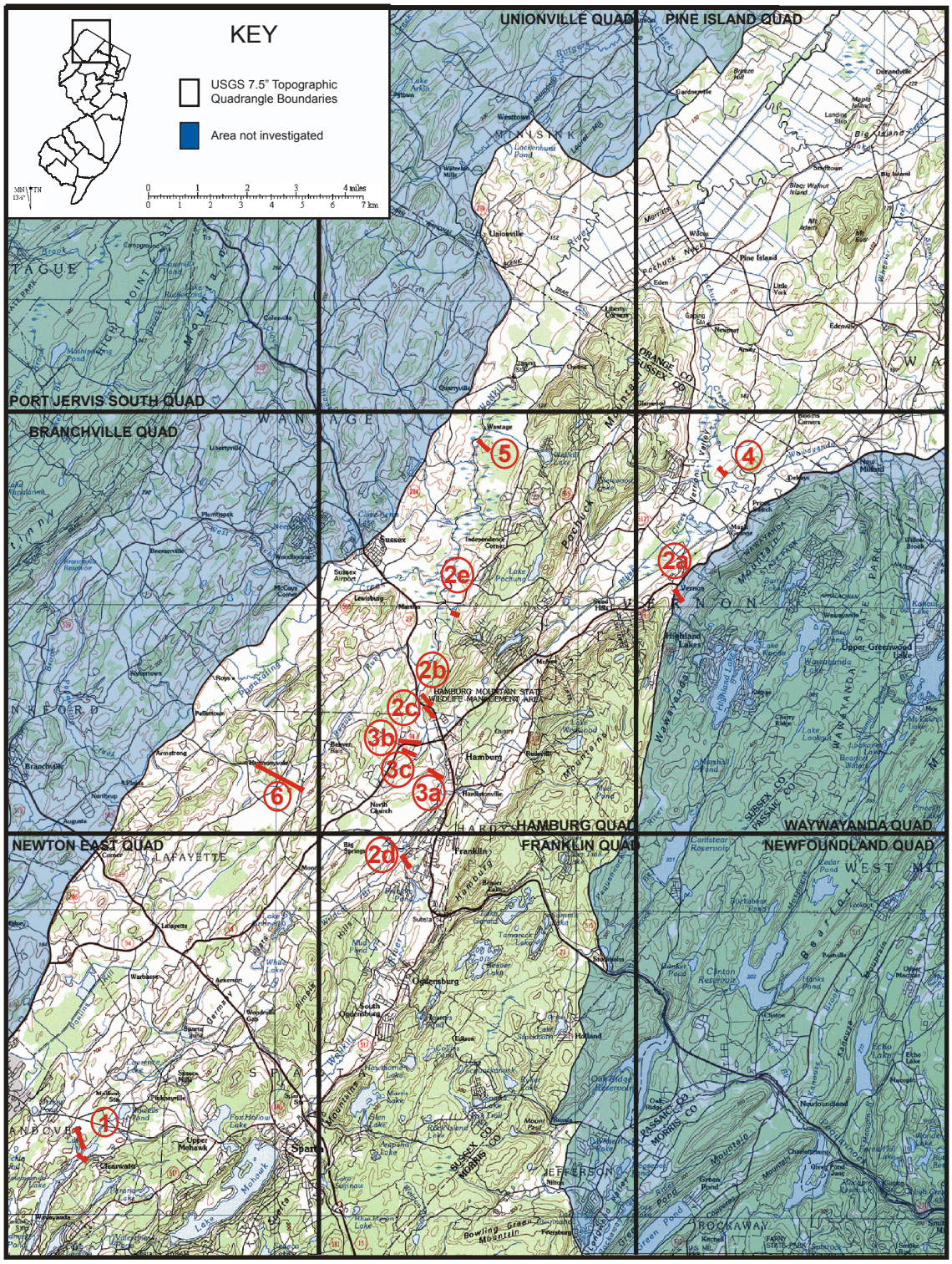


Figure 1.1. Location map of study area for the dissertation, the Hamburg and contiguous 7.5' quadrangles of the Wallkill River Valley of northwestern New Jersey and southeastern New York, U.S.A.

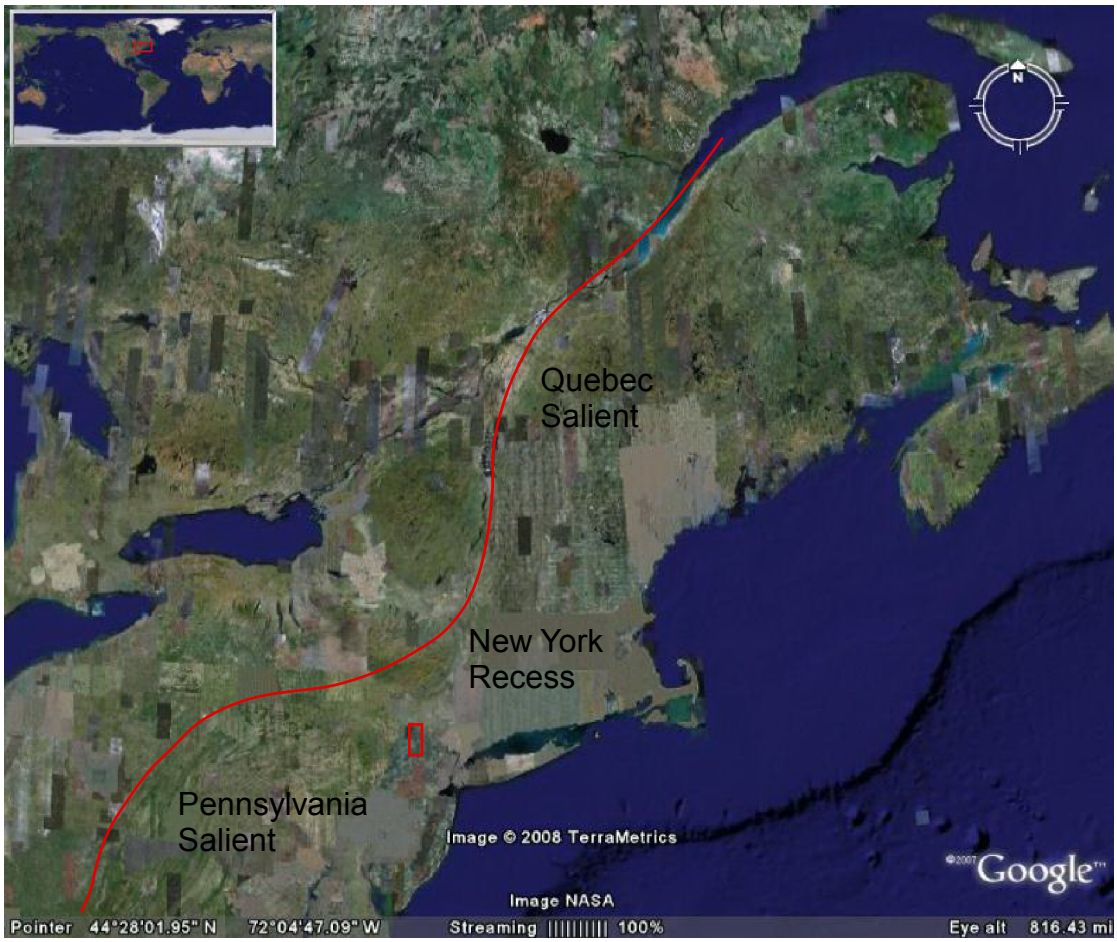


Figure 1.2: Aerial photograph of the central and northern Appalachian mountains. The solid red line marks the cratonward extent of surficial Appalachian structures, which according to Thomas (1977) defines modern day salients and recesses within the Appalachian orocline. The red box marks the location of the Hamburg 7.5' Quadrangle.

CHAPTER 2: Tectonic Setting of the Hamburg 7.5' Quadrangle and Vicinity

2.1 Introduction

As the Hamburg 7.5' Quadrangle, and the surrounding study area, suffered several orogenic episodes in its geological evolution, the tectonic setting of the study area, and its surroundings, is reviewed to provide a framework for the stratigraphic and structural interpretations presented in chapters 3 to 6 of this dissertation. Only the Neoproterozoic and Paleozoic deformational episodes will be presented in this chapter, as they have a bearing on the development of depositional environments discussed in Chapter 4, on silica diagenesis presented in Chapter 7, and on the structural history of the Hamburg quadrangle as discussed in Chapter 6. Development of the passive margin sequences is confined to Chapter 4.

2.2 Tectonic Setting

The Iapetos rift event (1.2 to 0.95 Ga) was the first tectonic event to deform the Laurentian margin of the Rodinian supercontinent after the Grenvillian orogenic event. Continental extension led to the intrusion and extrusion of bimodal igneous rocks and the deposition of thick accumulations of Neoproterozoic sediments into rapidly subsiding rift basins (Brock and Brock, 1999, 2000; Cudzil, 1985; Cudzil and Driese, 1987; Rankin, 1972, 1976; Rast and Kohles, 1986; Schwab, 1971; Simpson and Eriksson, 1989, 1990; Simpson and Sundburg, 1987; Skelly, 1987; Skelly et al., 1987; Thomas, 1977; Walker, 1988, 1990; Walker and Driese, 1991; Walker et al., 1989; Walker et al., 1988; Whisonant, 1974). Culmination of Laurentian rifting resulted in the generation and spreading of the Iapetos (proto-Atlantic) ocean basin, and the deposition of extensive carbonate sediments along a stabilized passive continental margin.

The closing phase of the Iapetos Wilson Cycle was punctuated by the Taconian, Acadian, and Alleghanian orogenies which variously deformed the Grenvillian basement rocks and the succession of Neoproterozoic syn-rift through Cambrian-Ordovician passive-margin rocks, as well as Ordovician through Pennsylvanian syn-orogenic clastic wedge rocks that were deposited on the Cambrian-Ordovician, passive-margin sequence. Most of these events are recorded in the rocks of the New Jersey Reading Prong (Hudson Highlands) and Great Valley provinces in general, and in the Hamburg 7.5' Quadrangle in particular. These events are reviewed briefly below with particular reference to the rocks in the Hamburg 7.5' Quadrangle.

2.2.1 Proterozoic Deformation

Grenvillian Orogen

The Grenvillian orogen extended 13,000 km, from present day Sweden to southern Mexico, and produced amphibolite- to granulite-grade orthogneisses and paragneisses, as well as voluminous granitoids (Gower, 1985; Renne and others, 1989; Ruiz et al., 1988; Woussen et al., 1986). In eastern North America, massifs of Grenvillian rocks (1.1 Ga) are exposed in the cores of later structures along the Blue Ridge, Green, and Long Range mountains (Blue-Green-Long line) from Georgia to Newfoundland (Rankin, 1976). The New Jersey Highlands is a segment of this zone. New Jersey Highland rocks occur in the eastern part of the Hamburg 7.5' Quadrangle (Figure 2.1, Figure 2.2). The Grenville-age crystalline rocks exposed in the New Jersey Highlands are composed of intrusive plutonic rocks, associated migmatites, quartzofeldspathic and calcareous metasedimentary rocks, sodium-rich rocks interpreted

as volcanic-volcaniclastic in origin, and charnockitic rocks of problematic origin (Rankin and others, 1989).

Iapetos Rift

Continental rifting of the southern Laurentian margin (current-day eastern North America) occurred in numerous pulses; from 758 ± 12 Ma (Neoproterozoic-Sturtian) to 525 Ma (Cambrian-Adtabanian) (Hoffman et al., 1974). The trace of the rifted Laurentian continental margin was characteristically zig-zag in map view. Map-view models of continental rifting depict a sub-linear, unidirectional rift that is orthogonally offset by transform faults (Francheteau and LePichon, 1972; Lister et al., 1986, 1991; Scrutton, 1982a, b; Thomas, 1976, 1977, 1983a, 1991). Transform faults and failed rifts project into the craton (Thomas, 1983b). The original map expression of the rifted Laurentian continental margin was expressed as embayments and promontories (concave and convex oceanward bends in the rifted continental margin, respectively). Embayments are modeled as extremely thinned sections of rifted continental crust (Etheridge et al., 1989; Lister et al., 1986, 1991). Promontories bound embayments along strike and are modeled as being topographically positive headlands of Grenvillian basement (Etheridge et al., 1989; Lister et al., 1986, 1991). Thomas proposed that the New York promontory (Hudson rift zone) and the Pennsylvania embayment (Northern Blue Ridge rift zone) formed during Iapetos rifting, offset from each other by the New Jersey transform fault (Thomas, 1993) (Figure 2.3). The Hamburg 7.5' Quadrangle contains rocks that were deposited on the New York promontory (Figure 2.3).

Four rift basins developed in the Hudson and Northern Blue Ridge rift zones; from west to east these are the Rome trough, the Catoctin rift, the Octoraro sea, and the

Iapetos basin (Faill, 1999; Thomas, 1993). Only the Catoctin rift is of consequence in the Hamburg quadrangle (Figure 2.3). The Catoctin rift unconformably overlies Grenville-age rocks and contains a thick sequence of volcanic rocks, the Catoctin volcanics, as well as quartzites, slates and phyllites of the Chilhowee Series (Clark, 1984; Faill, 1999). The craton to the west of the Catoctin rift experienced syn-rift uplift and initiated a source for the eastward transport of sand and mud that largely filled the adjacent rift basin (Faill, 1999). In the dissertation study area, the Hardyston Formation correlates to the youngest beds of the synrift Chilhowee Series (Faill, 1999) and this formation crops out in the Hamburg 7.5' Quadrangle (Plate 1). Catoctin volcanics do not occur in the Hamburg quadrangle.

2.2.2 Paleozoic Deformation

The propagation of stress during the Paleozoic orogenies was controlled by the stratigraphy and structure of the Laurentian rifted margin and the consequent passive margin (Rankin, 1976; Thomas, 1977). The original map expression of the rifted Laurentian continental margin, expressed as embayments and promontories, resulted in synorogenic tectonic structures as salients (convex cratonward bends in the Paleozoic fold and thrust belts) and recesses (concave cratonward bends in the Paleozoic fold and thrust belts) (Rankin, 1976; Thomas, 1977). Thus the Hamburg 7.5' Quadrangle, and contiguous areas, occur in what was the New York promontory, and is now the New York recess (Figure 2.4).

Taconian Orogeny

The Taconian orogeny was the first major compressional event to affect the Laurentian margin after the Grenvillian orogeny (Drake et al., 1989) and involved the

subduction of the Laurentian continental margin beneath an island arc complex that had formed on the Iapetos oceanic plate (Drake et al., 1989; Muller and Chapin, 1984; Rankin, 1975). Most geochronological work indicates that the Taconian orogeny occurred from 483 to 434 Ma. Intrusion of the Cortland complex (470 to 450 Ma) into previously metamorphosed Cambrian and Ordovician rocks provides evidence for Taconian metamorphism in the New York recess (Aleinikoff, 1985; Brueckner et al., 2002; Maxey, 1976; Mose and Nagel, 1982; Ratcliffe et al., 1982). Dallmeyer found no evidence of Taconian metamorphism in the Hudson Highlands southwest of the Hudson River (Dallmeyer et al., 1975; Laird, 1988).

The Taconian orogeny folded rocks of Neoproterozoic through Middle Ordovician age that unconformably lie beneath rocks of Early to Late Silurian age (Drake et al., 1989). The unconformity is called the Taconic unconformity and can be traced southwest from the Hudson Valley, New York to Harrisburg, Pennsylvania. The Taconic unconformity occurs to the west of the Hamburg 7.5' Quadrangle, in the vicinity of Port Jervis, New York and along the Shawangunk ridge.

Acadian Orogeny

The Acadian orogen is widely developed in the northern Appalachians. It is generally considered the result of several collisions between Laurentia, an unknown number of Avalonian microcontinents, and Gondwana (Hutton, 1989; Rast and Skehan, 1993; Soper and Hutton, 1984). Structural evidence for this orogeny is hard to find in the dissertation study area, as the Silurian-Devonian sections that were folded during this orogeny were eroded away. In other areas, and in particular the rocks of the New York City Group, Acadian structural features and retrograde metamorphism, where present,

were superimposed on pre-Silurian rocks that were already deformed and recrystallized (Brock and Brock, 2001).

In addition, there is sedimentological evidence for the Acadian orogeny in the region of the Hamburg 7.5' Quadrangle, if not in the quadrangle itself. A Silurian, post-Taconian, highland that resulted from Acadian collision is interpreted from paleogeographic maps as having extended from southeastern Quebec, through western New England and adjacent New York, into New Jersey; its southward extension is uncertain (Osberg et al., 1989). A large foreland depression, known as the Appalachian basin (Colton, 1970), occurred west of this post-Taconian highland and was the site of nearly continuous sedimentation from Cambrian through Early Permian time to form the Catskill clastic wedge. Silurian detrital rocks in this basin are interpreted as a molasse derived from the Acadian highland.

Alleghanian Orogeny

The Alleghanian orogen was the result of continental collision between Laurentia and Gondwanaland from the Late Mississippian to the Permian (Hatcher, 1989). The Alleghanian is the youngest orogenic event to affect the Appalachians, overprinting previous tectonic structures.

The Alleghanian orogeny in the southern and central Appalachians resulted in the emplacement of the composite crystalline Blue Ridge-Piedmont thrust sheet, which drove the foreland deformation in front of it to form a fold-and-thrust belt. The crystalline rocks of the southern Appalachian Blue Ridge can be traced northward as the New Jersey and Hudson Highlands, and the Berkshire and Green Mountains. If this crystalline unit is allochthonous in the south, then it is reasonable to postulate that it is allochthonous in the

central and northern Appalachians and that it could have been thrust westward during the Alleghanian Orogeny.

In contrast to the Appalachians south of the New York recess, the foreland fold-thrust belt of southern New York has traditionally been thought to be Taconic (Drake et al., 1989; Zen, 1967). However, Bayley hypothesized that large-scale over thrusting of Cambrian and Ordovician rocks in the Kittatinny Valley, a part of which occurs in the Hamburg quadrangle, were the result of the Alleghanian orogeny (Bayley et al., 1914). Sedimentary rocks as young as Devonian are involved in thin skinned deformation as far north as Albany, New York (Hatcher, 1989), consistent with the Bayley hypothesis. Hatcher has suggested that dextral strike-slip faults, sediment-filled fault-bounded basins, metamorphism and plutonism are Alleghanian structures north of the New York recess (Hatcher, 1989). Arguments for Alleghanian deformation, based on mapping in the Hamburg quadrangle, will be presented in Chapter 5 of this dissertation.



Figure 2.1: A reduced version of the Hamburg 7.5' Quadrangle sheet. The varicolored swath of rocks in the central part of the map are the carbonates mapped for this dissertation. The blue swath in the northwestern part, and the gray swath in the southeastern part of the map were not mapped for this dissertation. The blue swath represents the Ordovician Martinsburg siliclastics. The gray swath represents Grenvillian basement (New Jersey highland rocks).

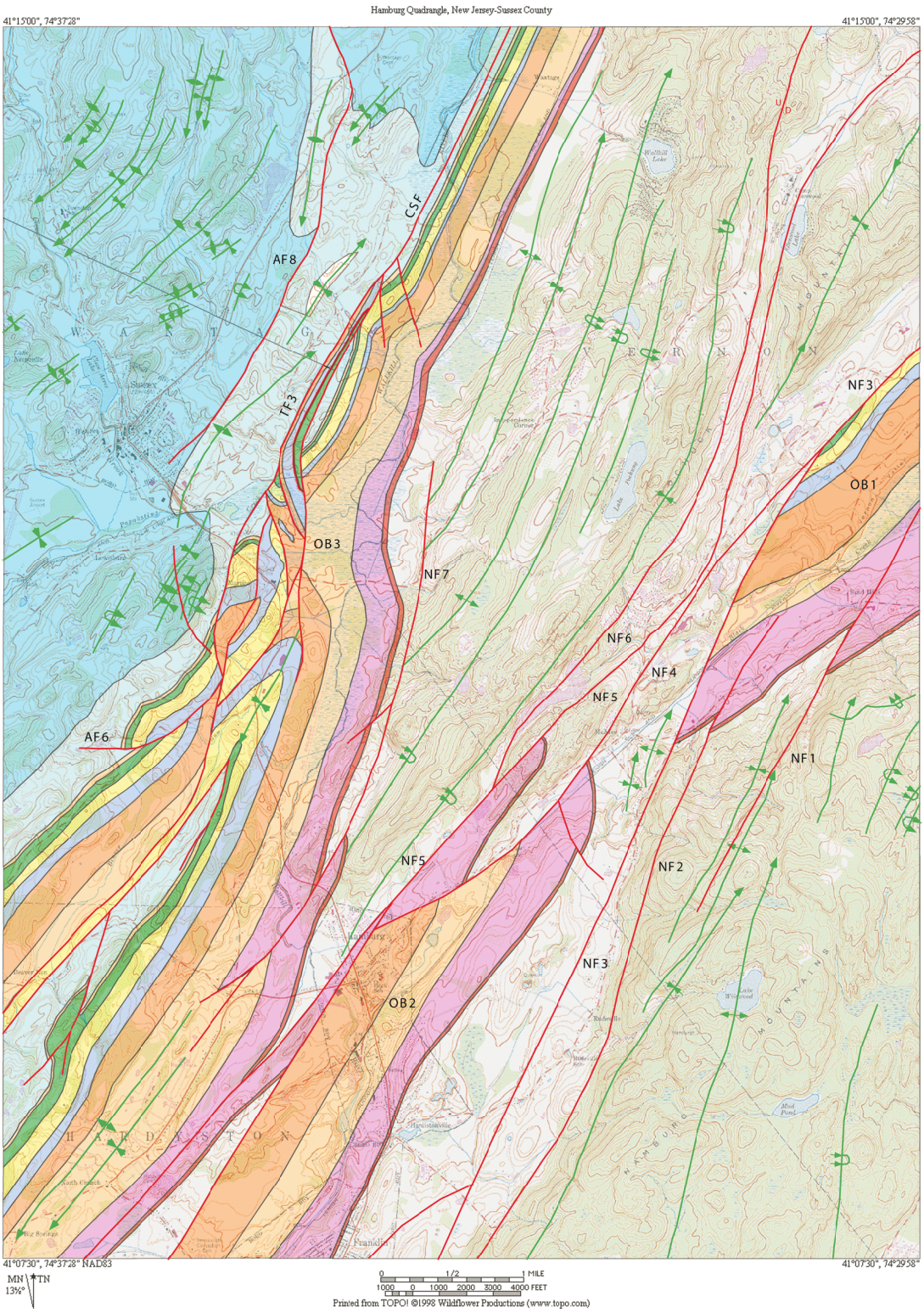


Figure 2.2: A reduced version of a geologic map of the Hamburg 7.5' Quadrangle, showing a compilation of the mapping conducted for this dissertation (Cambrian and Ordovician carbonates) and mapping conducted by Dalton et al. (1997) for the Proterozoic basement and the Ordovician Martinsburg Formation.

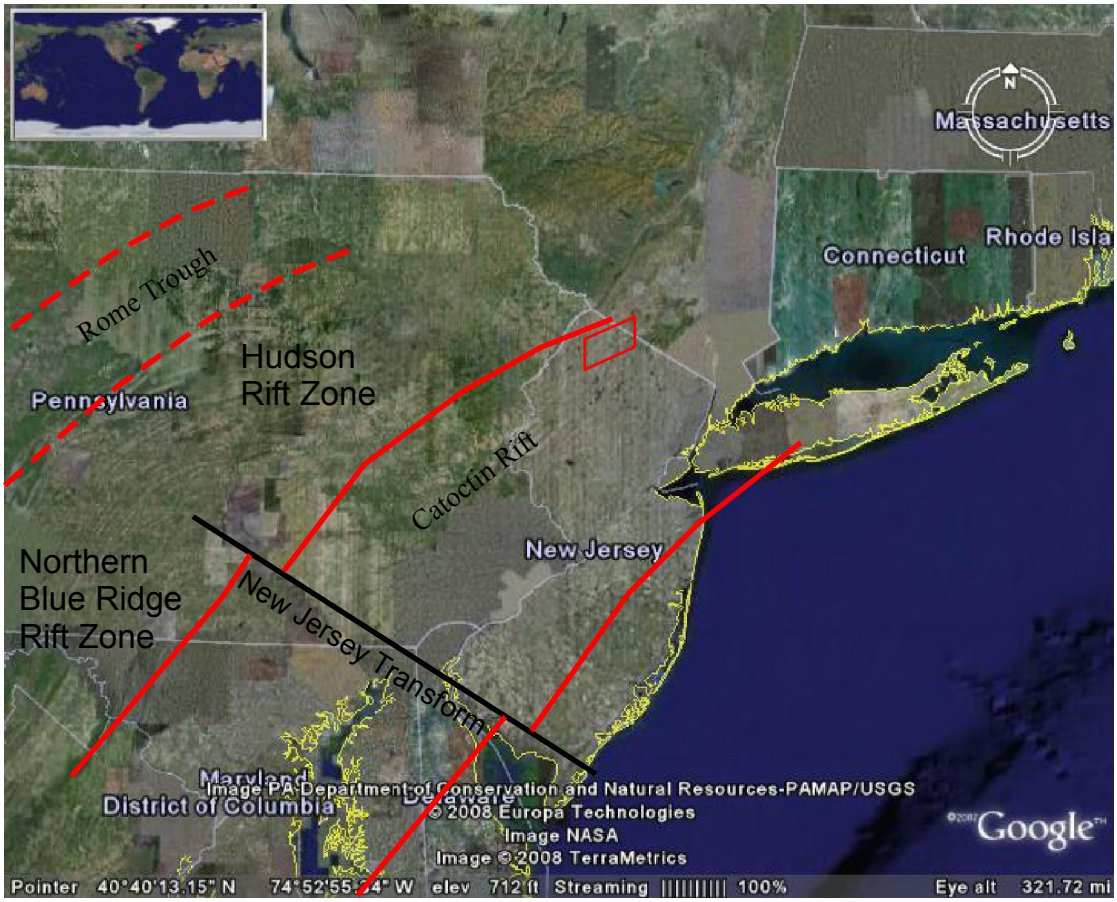


Figure 2.3: Satellite image of the New York-New Jersey-Pennsylvania area. The study area for this dissertation is located in northwestern New Jersey-southeast New York, outlined by the red box. This map incorporates data from this dissertation, Thomas (1993) and Faill (1999).

Thomas' (1993) interpretation of the New Jersey Transform, plus his distinguishing between the Hudson and Northern Blue Ridge rift zones on the north and south sides of the New Jersey Transform, respectively are shown on this figure.

Faill's interpretation of the Catoctin Rift and the Rome Trough are shown on this map.

The offset of the Catoctin Rift by the New Jersey Transform is a postulate of this author. The position of the Rome Trough is well established by Fail (1999); however, it is tentatively placed by the author on this figure (as indicated by dashed red line), due to lack of reliable geographic markers on this satellite image.

The study area for this dissertation is interpreted to be in the Catoctin Rift, near the northwestern (current geographic position) border fault.

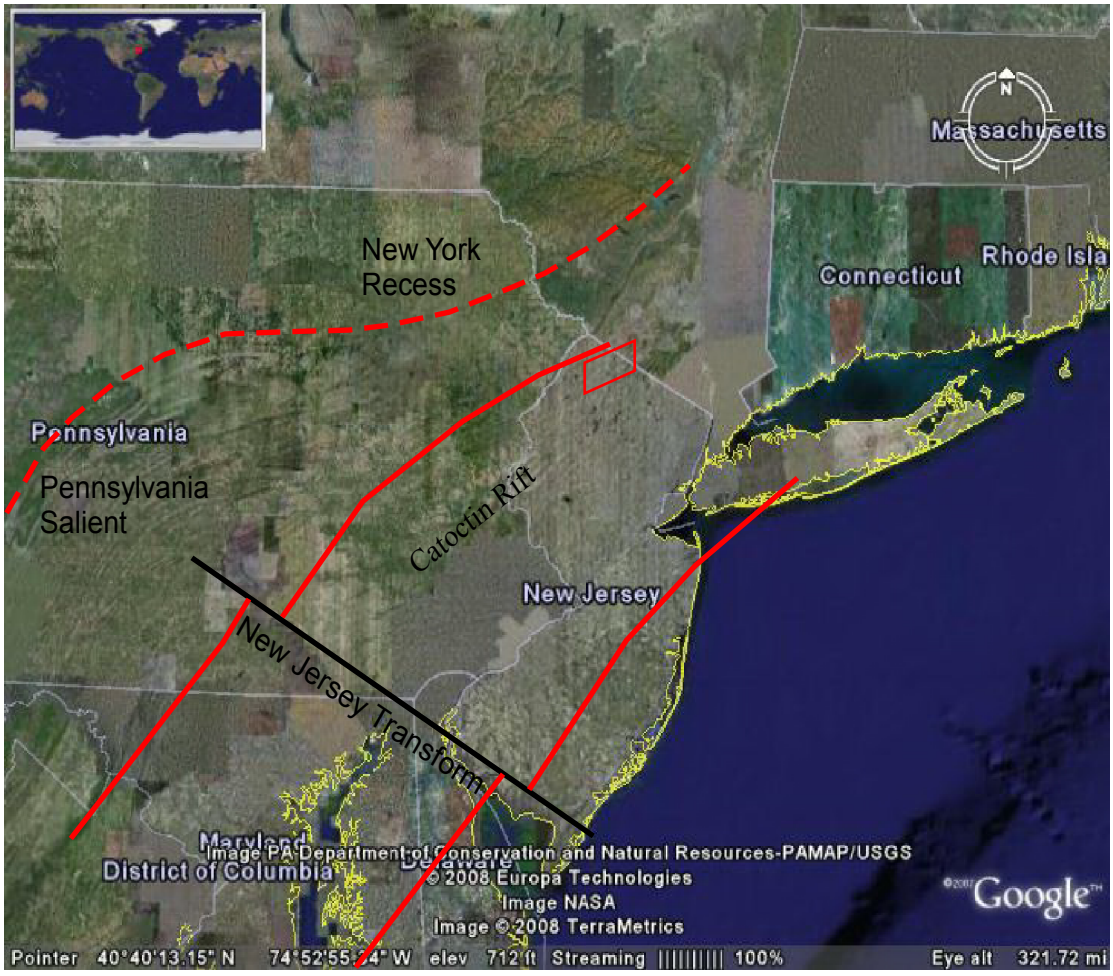


Figure 2.4: Satellite image of the New York-New Jersey-Pennsylvania area. The study area for this dissertation is located in northwestern New Jersey, outlined by the red box. This map incorporates data from this dissertation, Thomas (1993) and Faill (1999).

The study area in this dissertation is in the New York recess. The New York recess and the Pennsylvania salient are best illustrated in this figure by the presence of the dashed red line to the west of the Catoctin rift. The dashed red line illustrates the westernmost extent of Paleozoic orogenic deformation, as exposed on the surface.

CHAPTER 3: Stratigraphy of the Great Valley Sequence, Hamburg 7.5' Quadrangle, Sussex County, New Jersey

3.1 Introduction

This chapter presents a general description of the lithostratigraphy of the Cambrian and Ordovician rocks of the Great Valley sequence, as cropping out in the Hamburg 7.5' and adjacent quadrangles, Sussex County, New Jersey and Orange County, New York. A more detailed description of representative sections, on a bed-by-bed basis, is presented in Appendix A. The stratigraphic descriptions in Appendix A are presented as new stratigraphic type sections for these units in the New York recess. Even more detailed descriptions, based on field notes, are presented in Appendix B for all of the sections that were measured in this study.

The goal of detailed stratigraphic section measurement was to document stratigraphic changes in the Great Valley sequence, with respect to member locations on the New Jersey structural high (New York recess) versus the Pennsylvania and/or Quebec structural lows (salients). Another important aim of this study was the elucidation of a chert stratigraphy through the same detailed stratigraphic section measurement. The Kittatinny Supergroup is divided by this author into eight formations, in order of stratigraphic succession: Cambrian Hardyston, Leithsville, Limeport, Upper Allentown formations; Cambrian-Ordovician Stonehenge Formation; Ordovician Rickenbach, Epler and Ontelaunee formations (Figure 3.1). The eight formations are divided into eighteen members; specifically, the Califon, Hamburg and Wallkill members of the Leithsville Formation; the Wildcat Road, Wheatsworth Mills, Gruenwald, Glacial Quarry, Edison, and Route 94 members of the Limeport Formation; the Carlton Village and Canal Road members of the Stonehenge Formation; the Hope and Crooked Swamp members of the

Rickenbach Formation; the Branchville, Big Springs, and Lafayette members of the Epler Formation; and the Beaver Run and Harmonyvale Members of the Ontelaunee Formation (Figure 3.1).

Seven of the eight formations mapped in the Hamburg quadrangle were defined by previous workers mapping in New Jersey (see section 3.3 for further discussion). However, several major changes were made to the stratigraphy. These changes are discussed in more detail in each of the descriptive sections of this chapter. The most wide sweeping contribution was the development of detailed type sections (1:98 scale) for each member of the Kittatinny Supergroup. Detailed type sections for the Kittatinny Supergroup have never been published for the rocks cropping out in the New York recess. A second contribution was the development of a chert stratigraphy, which prior to this study was non-existent; with the exception of Markewicz and Dalton's (1973) "7 cherts" marker horizon in the Rickenbach Formation. As a result of this stratigraphic work, revisions to the previously published (Markewicz and Dalton, 1973, 1977) stratigraphic nomenclature were made. Markewicz and Dalton (1977) grouped the Limeport and Upper (Allentown) units into the Allentown Formation as members. The Limeport and Upper members of the Allentown Formation were elevated to formation status in this study. Additionally, the creation of six new members in the Limeport Formation is a new contribution of this research and is directly relatable to the detail of the stratigraphic sections measured for this project. The Stonehenge Formation, not previously mapped in New Jersey and/or New York, is a Pennsylvania correlative that has been introduced to the New Jersey/New York nomenclature by this researcher.

3.2 Field Methodology and Organization of Representative Stratigraphic Sections

Parts of the Hamburg, Wawayanda, Franklin, and Branchville quadrangles were investigated for the detailed stratigraphic measurement of the Kittatinny Supergroup (Figure 3.2). Fifteen traverses within the above referenced quadrangles served as ideal locations for stratigraphic section measurement (Figure 3.2; Appendix B); specifically, the outcrops were homoclinally dipping and free from major deformation (faults and folds) and vegetation. Stratigraphic and facies data were collected by measuring stratigraphic sections using the Brunton compass and Abney level technique. Detailed description and illustration of outcrops was made, specifically: rock type; rock color; grain/clast size, orientation, composition, and sorting; bedding characteristics; and faunal identification data was collected and is located in Appendix B.

Laboratory work for this part of the project consisted of stratigraphic column compilation. Representative traverse columnar sections for most of the traverses were digitally drafted using the Deneba Canvas (versions 3 to 11) graphics program at a scale of 1:98 or 1 in = 250 cm (Plates A.1 to A.20 in Appendix A, Appendix B). Primary rock features illustrated were bed thickness, rock type, rock color, bedding characteristics, carbonate and chert sedimentological features and carbonate grain size using the Dunham classification (Dunham, 1962). Standardized U.S.G.S. symbols for stratigraphic columnar sections were used in the stratigraphic columns constructed for this dissertation. In the instance where a U.S.G.S. symbol did not exist for a certain rock characteristic, the author created a symbol that matched, as precisely as possible, the appearance of the characteristic as recognized by geologists actively practicing field geology. The main traverse columnar sections are located in Appendix B.

The intent of this chapter is to introduce a refined stratigraphic section of the Kittatinny Supergroup. The composite section is compiled from the member type sections and represents a complete stratigraphic section of the Cambrian and Ordovician carbonate stratigraphy in this part of the Appalachian orocline (Appendix B). Interpretations of depositional environment and chert diagenesis are addressed in the following chapters.

3.3 Previous Stratigraphic Work

The Kittatinny Supergroup, as it is currently identified in northern New Jersey, has undergone several stratigraphic revisions since H.D. Rogers work in 1840 where the group was called the “Kittatinny Limestone” and broken into three mappable units; specifically the Leithsville and Allentown formations and the Beekmantown Group (Rogers, 1840), (Figure 3.1). Weller and Kummel continued to use the general term "Kittatinny Limestone" for the Cambrian-Ordovician carbonates of northern New Jersey; however, they correlated the Kittatinny Limestone with similar units in Virginia, Maryland, Pennsylvania and New York (Kummel and Weller, 1901; Weller, 1900a). As such, Weller and Kummel termed the Leithsville Formation, the “Tomstown Formation” based on similar units to the south. In Weller’s Annual Report of the State Geologist 1900, page 4, he states, "This limestone formation has a great thickness which is estimated at from 2,700 to 3,000 feet. It is designated the Kittatinny Limestone because it is the great limestone formation of the Kittatinny Valley."

The Kittatinny Limestone was first given supergroup status (Johnson and Willard, 1957) and subdivided into four, memberless formations by Drake during his work in Northampton and Bucks County, Pennsylvania (Drake, 1965), (Figure 3.1). The

Leithsville and Allentown formations retained their status; however, Drake subdivided the Beekmantown Group into the Rickenbach and Epler formations. Drake did not recognize the presence of the Ontelaunee Formation any further north than the Delaware Water Gap, Warren County, New Jersey (Drake, 1969).

Markewicz and Dalton subdivided the formations of Drake's Kittatinny Supergroup into distinct members during their mapping investigations of northwestern New Jersey (Markewicz and Dalton, 1977), (Figure 3.1). They were the first geologists in the region to apply a chert marker horizon to stratigraphic studies, specifically the "7 cherts" of the Hope Member of the Rickenbach Formation.

To the north, in New York State, Knopf classified the Cambrian-Ordovician correlatives of the Kittatinny Supergroup as the Stissing, Pine Plains and Briarcliff formations for the Leithsville, Allentown and part of the Rickenbach formations (Knopf, 1946, 1956, 1962), (Figure 3.1). The upper part of the Rickenbach Formation, the Epler and Ontelaunee formations were correlated with the Halcyon Lake Group (Knopf, 1946, 1956, 1962) (Figure 3.1).

The Kittatinny Supergroup precluded the presence of the basal Hardyston quartzite until the work of Fisher, which included the Hardyston correlative, Poughquag quartzite, with the carbonate rocks of the Wappinger Group of Cambrian and early Ordovician age in New York (Fisher, 1956; Fisher, 1962).

LaPorta (1984 to present) employed the member-level subdivision of the Cambrian-Ordovician carbonates (Markewicz and Dalton, 1973, 1977) during his dissertation studies within the Hamburg and contiguous quadrangles (Brewer and LaPorta, 2006; LaPorta, 1991, 1992, 1998b, 2002). One or more diagnostic varieties of

chert were elucidated for the nineteen members designated by LaPorta, as opposed to the one chert horizon utilized by (Markewicz and Dalton, 1973). Additionally, LaPorta elevated the Markewicz and Dalton (1977) designation of the Limeport and Upper members of the Allentown Formation to formation status and divided the Limeport into six members (Figure 3.1). The upper part of the Upper Allentown Formation, and the Lower Member of the Rickenbach Formation, were reclassified as the Stonehenge Formation based on correlations with rocks in Pennsylvania. As such, LaPorta redefined the Rickenbach Formation as having two members instead of three, as defined by Markewicz and Dalton (1977), (Figure 3.1).

The Stonehenge Limestone was first identified by (Stose, 1908) as the lowest member of the Beekmantown Formation in the village of Stonehenge (now part of Chambersburg), Pennsylvania. Similar strata in the Valley and Ridge were mapped as the Stonehenge Formation by (Ulrich, 1911). Sando followed Ulrich's (1911) lead and mapped correlative rocks in the southern Cumberland Valley as the Stonehenge Formation (Sando, 1957). At the Stonehenge type section in the Chambersburg area, Sando revised Stose's (1908) previous designation to upgrade the member to formation status. Sando also shifted the formation's lower contact by mapping the uppermost 61 m of the underlying Conococheague Formation as the Stoufferstown Member of the Stonehenge Formation, using lithologic similarities and the presence of Lower Ordovician trilobite assemblages. Hobson mapped correlative rocks in western Berks County as the Stonehenge Formation, and extended mapping of the unit through much of the Lebanon Valley (Hobson, 1957, 1958b). LaPorta mapped Stonehenge rocks in the Easton quadrangle during the Queen's College 1986 geologic field school, under the

direction of Dr. Patrick Brock. Examination of the Stonehenge Formation during field school exercises, and subsequent consulting work in the area by the author, permitted correlation between Stonehenge rocks in Easton to similar lithologies in the Hamburg and contiguous quadrangles during this study.

3.4 Cambrian-Ordovician Lithologies of the Great Valley Sequence

3.4.1 Hardyston Formation

Faunal Content

The only fossil found to date by this author within the Hardyston Formation is *Skolithos*. This trace fossil occurs within the upper arenaceous beds and interbedded thin dolomite. There have been reports of the occurrence of *Olenellus thompsoni* with the Hardyston Formation (Bayley et al., 1914; Walcott, 1891; Weller, 1900a). Previous map interpretations of the Hardyston Formation have included rocks now identified as the Califon and Hamburg members of the Leithsville Formation (Spencer et al., 1908). *Olenellus* has been reported in the rocks of the Pine Island 7.5' Quadrangle (Don Monteverde, New Jersey Geological Survey, personal communication, 1994) that this author has mapped as the Hamburg Member. As such, this author suggests that the *Olenellus* finds reported by Bayley, Walcott and Weller as occurring within the Hardyston Formation, may in fact be present in the Hamburg Member (which was mapped by previous workers as Hardyston) (Bayley et al., 1914; Walcott, 1891; Weller, 1900a).

General Lithostratigraphic Description

The Hardyston Formation is thin, discontinuous and laterally extremely variable. The Hardyston Formation is 110 cm thick at the Rte. 515 type section in Vernon

Township, New Jersey (location 2a in Figure 3.2; Plate A.1 in Appendix A). The lower contact with the underlying Proterozoic basement is nonconformable (Figure 3.3). In the northern part of the Hamburg quadrangle, where the Hardyston rests upon Proterozoic crystalline rock, there is a several meter thick zone where ferromagnesian minerals of the crystalline basement are converted to hydrous vermiculite and feldspars are converted to clays. Additionally, the crystalline nature of the basement degrades up section towards the contact with the Hardyston Formation. The texture of the crystalline basement becomes layered; with quartz, weathered feldspars and bleached ferromagnesian minerals incorporated into the layering. This layering suggests that the igneous mineral constituents were mobilized and reorganized into thin lenses and beds. These relations indicate that the contact between the Proterozoic basement and the Hardyston Formation is a saprolite at these locations. At other locations within the quadrangle, the Hardyston directly overlies non-saprolitized, Proterozoic rocks. The upper contact with the overlying Califon Member of the Leithsville Formation is gradational and exhibits facies variations along strike. The presence of continuous beds of shale and/or dolomite indicates that the Hardyston-Califon contact has been crossed.

Hardyston beds are alternating layers of tan to honey brown, conglomeratic, quartzose and arkosic, cross bedded and ripple marked sandstones (Figure 3.4) and orthoquartzites. Arkoses contain graphite, weathered diopside grains and magnetic iron lenses. Franklinite crystals and magnetic iron occurs in the form of euhedral to subhedral iron oxide crystals are present n the local quartz sandstone facies. The conglomeratic sandstones contain basement rock and quartz-cobble clasts. Capping the succession are calcareous sandstones and thin bedded, arenaceous dolomites. Texturally and

compositionally mature, cross bedded orthoquartzites are more common in the southern part of the dissertation area.

General Chert Description

Chert is rare in the Hardyston Formation in the Hamburg quadrangle. Where Hardyston chert is present, it occurs as 1 to 2 cm clots and colloform masses of finely laminated, limonitic, yellow jasper, often in association with large 1 cm length graphite plates, weathered fragments of diopside, and lenses of arkose. Some masses overlie and locally contain magnetic iron deposits and contain interwoven dendrites of pyrolousite and manganosite. The jasper is not restricted to one particular horizon, it is found in the saprolite at the basement-Hardyston contact, as well as within arkoses higher up in the stratigraphic section. The Hardyston is the only unit in the Kittatinny Supergroup to contain jasper.

Discussion of Changes in Stratigraphic Definition

Mapping of the Hardyston Formation for this study has refined Markewicz and Dalton's (1977) thickness of the unit and elaborated on the occurrence of chert in its outcrop exposure. Additionally, general trends of specific facies were spatially outlined during this study and are discussed in Chapter 4 of this document.

Markewicz and Dalton (1977) suggested a 0.3 to 61 m thickness variation in the Hardyston Formation in northern New Jersey. During this study, the Hardyston has been measured as ranging from 1 to 2 m thick in the Unionville and Pine Island quadrangles to the north of the Hamburg; 2 m in the Franklin quadrangle; and 3 m in the central, and 4 to 5 m in the southern, parts of the Hamburg quadrangle. Considering the lateral facies variations and pinch outs in the Hardyston Formation, and the irregularity of the

underlying, rifted Proterozoic basement (Hague et al., 1956), it is not surprising to witness severe differences in thickness estimates along the rifted margin.

The presence of jasper, or silicified limonite colloform masses, in the Hardyston is valuable as a mapping aid in areas where Hardyston outcrops are lean. As jasper is restricted to the Hardyston Formation, its presence as float in the soil profile is a very good indicator of the formation's presence in covered intervals.

3.4.2 Leithsville Formation: Califon Member

Faunal Content

Markewicz (New Jersey Geological Survey, unpublished personal communication, 1964) identified the shelly fossil *Hyolithellus micans* in the Califon, establishing a Lower Cambrian age for the member. *Archaeocyathus* was discovered in this member by Markewicz, and confirmed by John Rodgers, in 1968 and during mapping for this study. In addition, a small colony of *Archaeocyathus* was discovered in the dolomites of the Rte. 515 section by a Hunter College undergraduate student, Josephine Amato, during a summer of 1991 field course offered by the author. *Archaeocyathus* also constrains the age of the Califon Member to the Lower Cambrian (Moore et al., 1952). The trace fossil *Skolithos* was also mapped in the Califon Member during this investigation. Algal stromatolites are also very common in the member, particularly in shale and shaly dolomites in the southern part of the map area.

General Lithostratigraphic Description

The Califon Member of the Leithsville Formation is 300 cm thick at the Rte. 515 type section in Vernon, New Jersey (location 2a in Figure 3.2; Plate A.2 in Appendix A) and varies considerably along strike. The lower contact with the underlying Hardyston

Formation is unconformable. Rocks occurring along the base of the Califon Member are shale and/or dolomite with shale partings (Figure 3.5) and contain irregular clasts of weathered basement and Hardyston rocks, abundant quartz grains and stringers of quartz sandstone. The upper contact with the overlying Hamburg Member contains mudcracks (Figure 3.6) and rip-up clasts in dark gray shale, suggesting an unconformity. Consistent accumulations of light gray and tan, to burgundy and maroon, quartz sandstones are the indication that the Califon beds have terminated and the Hamburg Member is being examined.

At the member type section, Califon beds are dark gray, fine grained, parallel bedded dolomite interbedded with charcoal gray to black shales (Plate 3.2; Plate A.2 in Appendix A). Irregular clots (up to 2 cm diameter) of honey colored sphalerite (Figure 3.7) are associated with 1 cm diameter (or less) quartz lined vugs containing purple fluorite and/or orange calcite crystals (Figure 3.8). The member is stylolitized. The unit also contains mud cracks, rip-up clasts and is sparsely fossiliferous. An unconformity is interpreted from the presence of mud cracks and rip-up clasts occurring at the top of the member.

At other locations (Rte 23 S), the Califon contains thin, evenly bedded, fissile, pyrite bearing, black shales which weather to a bright yellow. Upper and lower bed contacts are sharp, but wavy and undulating. Beds contain horizontal laminae representing flaser beds and are overlain by sparse cross bedded intervals. Locally, the Califon contains thick accumulations of intraclastic horizons composed of ripped up fragments of mud cracks and rolled algal laminates. Dessication features and ripple

surfaces are common throughout the shales and generally, as the shales diminish, so do the occurrences of ripple surfaces.

General Chert Description

There are three types of chert within the Califon Member, though they are not present at the Rte. 515 type section. The stratigraphically lowest chert occurs as irregular, elongate, or columnar masses and irregular nodules that appear to replace the stromatolites present in the shalier facies. The chert is concentrically banded with alternating light- and dark-gray silica. However, the closer to the Hardyston-Califon contact the cherts are stratigraphically, the lighter they become and the gray color takes on a yellow to orange hue. The bands are arranged as en-echelon stripes, concentric layers, and fine filaments. The base of each chert nodule exhibits an open, cellular, coxcomb structure and each nodule contains a thick outer rind of limonitic iron (LaPorta, 1986). Thin sections and slabs reveal amorphous pyrite and euhedral ankerite crystals within the nodules in four different patterns; concentric bands, thin wisps, halos and irregular clots. Many of the sulfide/carbonate horizons are aligned parallel, or subparallel, to the concentric layering of the chert**.** Thin sections and slabs of the chert also reveal opaque bands of dark minerals that are interpreted as accumulations of carbon (Figure 3.9).

The second type of chert in the Califon Member includes chert associated with vugs located in thinly bedded shales, shaly dolomites, and dolomites bounded by shale couplets in the south-central Hamburg and northern Franklin quadrangles. The vugs have a vase-like shape and may represent chert replacing the body parts of *Archaeocyathus.* As such, this chert type can be divided into two sub-types; a filamentous coating of chert

that occurs along the outer parts of the vug, and vacuole filling chert that occurs within the internal parts of the vug**.**

The third chert type within the Califon Member occurs as a siliceous infilling of pores between euhedral dolomite grains, creating a saccharoidal, or sintery, texture to the dolomite. This chert is found solely in dolomites in central-northern Hamburg and western Wawayanda quadrangles. These porosity infillings are closely associated with the occurrence of irregular clots of sphalerite, euhedral fluorite grains and larger vugs, 1 to 2 cm in diameter, which are quartz lined and filled with manganiferous calcite.

Discussion of Changes in Stratigraphic Definition

The descriptions of three chert types within the member is a contribution of this study, as is a refinement of the thickness estimates provided by Markewicz and Dalton (1977).

The stratigraphically lowest chert can occur in such dense concentrations that the unit can be easily mapped by the investigator through the preponderance of chert nodules appearing in topographically low sags and depressions lacking outcrop exposure. The restriction of the pods to the shalier facies of the Califon also allows the researcher to infer which facies is in sub-crop. On a finer scale, the color variation from orange gray to nearly black, with respect to stratigraphic positioning, can allow the researcher to estimate stratigraphic proximity to the Hardyston-Califon contact or can be used as a facing indicator. Because the three cherts of the Califon Member are distinctive in their facies associations and in what they are replacing and/or filling in, they can assist in depositional environment interpretation in that the cherts may preserve fossils and/or occur in certain facies.

Finally, Markewicz and Dalton (1977) estimated that the Califon Member ranges from 3.5 to 14 m thick, but is typically 9 m thick. The Califon Member in the dissertation study area ranges from 1 to 3 m on average, with a maximum of 4 m in the extreme southern part of the study area (Appendices A and B).

3.4.3 Leithsville Formation: Hamburg Member

Faunal Content

The fossil, *Olenellus thompsoni,* was discovered at Wildcat Road in Franklin, New Jersey (location 2d in Figure 3.2) and attributed to the Hardyston Formation (Walcott, 1891). Interestingly, however, the Hardyston Formation, as mapped at the time Walcott discovered *Olenellus thompsoni,* included what is currently defined as the Hamburg Member. As such, it has never been conclusively determined which stratigraphic horizon the fossil hailed from (Hardyston vs. Hamburg) and to date, *Olenellus* has not been re-discovered in either rock unit. Other Cambrian fossil occurrences have not, to date, been attributed to the Hamburg Member. No other age diagnostic fossils have been discovered in the Hamburg Member during mapping for this study.

General Lithostratigraphic Description

The Hamburg Member of the Leithsville Formation is 520 cm thick at the Rte. 515 type section in Vernon, New Jersey (location 2a in Figure 3.2; Plate A.3 in Appendix A). The lower contact with the underlying Califon Member is unconformable (Figure 3.10), and as mentioned in the previous section definitive Hamburg beds are mapped as consistent accumulations of light gray, tan, burgundy and maroon sandstones (Figure 3.10). While dolarenites in the Hamburg Member decrease in abundance towards the top

of the section, fine grained dolomites, micrites and claystones increase towards the top of the section, to be capped by black shale at the upper contact (Figure 3.10). Mudcracks and rip-up clasts in the shale horizon suggest an unconformity at the upper contact. Above the black shale are Wallkill Member dolomites.

The Hamburg Member is a cyclic, light gray, pink to maroon, thin to thick bedded, dolomitic and arkosic arenite with algal stromatolites and shale partings. A very light olive, finely laminated, dolomitic limestone is locally interbedded with the unit, but becomes more predominant and well established towards the top of the section. The characteristic maroon beds are a valuable mapping criterion. The outcrops weather to a lighter slate red and the fissile components exhibit a somewhat flaggy appearance (Figure 3.10). Micrites are strongly fetid when struck and weather to a light cream color. Thick, coarse grained beds are typically arkosic; however, locally developed, thick bedded, coarse grained, dolarenites create pedestals rising from low swampy areas (Figure 3.11). Fabric is present as ribbing through all of the fine grained beds. Three unconformities are interpreted as existing in the Hamburg Member. Other than the two unconformities located at the lower and upper contacts, two unconformities are located mid-member, one was identified due to the presence of mud cracks on ripple marked surfaces, the second was identified due to the presence of scour surfaces truncating underlying beds.

General Chert Description

The cherts of the Hamburg Member are rare and restricted to a succession of charcoal gray, highly siliceous, laminated dolomites occurring towards the top of the member. Chert as nodules does not occur in the Hamburg Member; however, chert is present as thick, homogenous, charcoal gray to black, highly siliceous, yet mildly

dolomitic, claystone beds that break with a splintery to subconchoidal fracture. The chert weathers to a very light gray and has very high clay content. The upper and lower contacts of the beds are sharp and even. The chert replaces a claystone that was deposited on top of the upper unconformity in the Hamburg Member.

Discussion of Changes in Stratigraphic Definition

The upper part of the Hamburg Member contains highly siliceous claystone that is distinctive and unique among the cherts of the Kittatinny Supergroup; however, this chert has not been used as a marker horizon, due to the uniqueness of the Hamburg lithostratigraphy as a whole. The Hamburg red and maroon rocks, and the member's resistant weathering profile (making it a ridge forming lithology), have been used as a mapping criterion for the unit. As such, the presence of the siliceous claystone, while a unique characteristic of this member, was not employed as a mapping aid during this investigation.

A revision in the stratigraphic thickness of this unit is being proposed. Markewicz and Dalton (1977) describe the Hamburg Member as ranging from 8 to 9 m thick in northern New Jersey. The Hamburg Member in the dissertation study area ranges from 3 to 4 m in the Hamburg quadrangle to 5.5 m in the western Wawayanda sheet.

3.4.4 Leithsville Formation: Wallkill Member

Faunal Content

Algal stromatolites and algal laminations have been mapped in the Wallkill Member during this study. No other fossils have been identified in this member in the Hamburg and contiguous quadrangles, to date.

General Lithostratigraphic Description

The Wallkill Member of the Leithsville Formation is 20.75 m thick at the Wildcat Road type section in Franklin, New Jersey (location 2d in Figure 3.2; Plate A.4 in Appendix A). The lower contact with the underlying Hamburg Member is marked by medium gray, chert bearing dolomite overlying an truncated (unconformity) black shale in the Hamburg Member. The lithologic change from black shale to dolomites marks the beginning of the Wallkill Member. The upper contact with the base of the Wildcat Road Member of the Limeport Formation is an abrupt, undulating surface truncating a succession of dark gray, flaggy dolomite containing rip-up clasts and oolitic chert; indicating a surface of unconformity. Three, distinctive chert marker horizons at the contact can be traced throughout the dissertation study area.

The Wallkill Member occurs as thin to thick bedded, medium to coarsely crystalline, light to dark gray, scintillating, algal laminated, stylolitized dolomite. Ooids, pisoids, oncoids, rip-up clasts, quartz-sand grains, euhedral quartz veins in shale and pyrite are all present towards the top of the member. On weathered surfaces, the member is battleship gray, highly pitted, and recessed where shale occurs. Jointing is well developed, as is axial planar cleavage, which penetrates the entire section. The combination of intersecting joints and cleavage render the member blocky in outward appearance (Figures 3.12 and 3.13). There are five unconformities interpreted in the Wallkill Member. One unconformity occurs at the lower contact, the second lowest is in the lower part of the member and three are located near the upper contact (one of the three is interpreted as the upper contact). The lower unconformity is represented by a pronounced irregularity on the upper bed surface. Overlying the undulating surface is a

black slate that exhibits axial planar cleavage. The three upper unconformities are interpreted from the presence of rip-up clasts and incisement of upper bed surfaces.

General Chert Description

Four predominant chert horizons are present in the Wallkill Member with a variety of other cherts that are minor components. The Wallkill Member is the first unit in the Kittatinny Supergroup to contain abundant chert and stromatolites, which are commonly silicified (Figures 3.14 and 3.15). The stratigraphically lowest cherts occur in a thick, rubbly dolomite and are spherical to oblate pods that vary in size, with a maximum width of 91 cm. Internally, the chert pods are translucent, color ranges from black to navy blue to dark gray and they are homogeneous in texture. Individual chert pods bear outer, concentric layers of light to dark gray cherts which are criss-crossed by thinner ribbing (Figure 3.16). Stylolites intersect the chert pods in radial fashion, i.e. there is no preferred spatial orientation of the stylolites. Some of the chert pods contain additional, over thickened rims, many of which are equatorial to the pod; however some lie at oblique or acute angles to the dip angle of the surrounding dolomite beds. The chert pods grade laterally into partially silicified, and completely unsilicified, algal stromatolites. The spherical masses become thinner and smaller and the chert becomes thin and flaggy along strike. The base of the chert pod horizon contains 2 to 5 cm diameter clots of dark gray to black chert associated with fissile shale lenses, some of which are themselves partially to entirely silicified. At the top of the chert pod section is black, silicified shale lining the lowest unconformity in the Wallkill Member.

Volumetrically minor cherts are present in the middle of the Wallkill Member and occur in prolifically algal laminated dolomites. The algal laminations, not the dolomite,

are replaced by dark gray to black chert. There are stylolites which run parallel to the contacts between dolomite and chert. This gives the cherts an appearance of being laminated towards the lower and upper bed contacts. The stylolite surfaces are lined with insolubles (Figure 3.17) and several generations of chalcedony infilling.

The cherts present near the top of the Wallkill Member occur in three, closely spaced horizons bounding the three unconformities at the top of the Wallkill Member. The cherts are 2 to 5 cm thick, pinch-and-swell along strike, and at places assume the form of domal algal, and/or replace ooid horizons instead of laminated algal. The lowest chert is sandwiched between black shales and is located in an algal laminated dolomite, with the chert replacing the algal laminations. Close inspection at the outcrop and with sawed slabs reveals some of the laminations are tightly folded. Freshly broken pieces are dark navy blue, with patches of light blue gray and are highly lustrous.

The second chert horizon in the upper Wallkill cherts is associated with a thick succession of ooid- and pisoid-rich, algal laminated dolomites with zones of rip-up clasts and intraclastic dolomite (Figure 3.18). The black to dark gray, waxy chert completely replaces oolitic lenses in places; while at other locations along strike, it replaces both laminated and domal algal structures. Freshly broken surfaces of silicified oolite scintillate with broken ooid clasts and detrital quartz-sand grains. Domal algal are completely replaced by homogenous chert centers, concentrically wrapped in alternating black and gray chert layers (Figure 3.19).

The third chert horizon at the top of the Wallkill is associated with algal laminated, pyrite-rich dolomite that is thinly bedded and flaggy, and contains rip-up clasts. The lustrous black, to navy blue, to pale gray chert occurs as thick beds that are

up to 36 cm thick and replace oncoids, pisoids, ooids, and algal laminations (Figure 3.20). In places, the chert is tightly folded, with the folds taking on enterolithic form. The chert bearing dolomite section is bound above and below by thin to thick shales and abundant euhedral quartz veins.

Discussion of Changes in Stratigraphic Definition

The Wallkill Member of the Leithsville Formation represents the beginning of the Kittatinny carbonate section; the mapping of which has been problematical through the years due to the similar lithostratigraphic descriptions of the sparsely fossiliferous carbonates. The Wallkill Member has poor outcrop expression, as it underlies sags in the topography (with one exception), and discerning where the upper contact of the Wallkill Member is has always been problematical for previous workers. The similarity in carbonate lithostratigraphy mandated the need for some marker horizon, in this case cherts, to prompt accurate stratigraphic positioning. The three laterally persistent cherts serve as a good marker horizon and in addition, their presence alters the usually subdued Wallkill weathering profile. The spatial closeness of the three upper Wallkill cherts creates a resistant zone that permits a topographic high, which includes the contact between the Wallkill and overlying Limeport Formation. The accurate location of this contact during mapping is impossible without using the three cherts as a guide.

The importance of accurately locating the upper contact can be observed with the change in thickness interpretation of the unit. Markewicz and Dalton (1977) estimated that the Wallkill Member ranged from 152 to 244 m in northern New Jersey. Stratigraphic measurement for this study, using the chert horizons as mapping aids, suggests the thickness is 20 m.

3.4.5 Limeport Formation: Wildcat Road Member

Faunal Content

Algal stromatolites and laminations are the fossils identified in the Wildcat Road Member in the dissertation study area. To date, no other fossils have been found that constrain the age of the formation.

General Lithostratigraphic Description

The Wildcat Road Member of the Limeport Formation is 95.5 m thick at the Wildcat Road type section (location 2d in Figure 3.2; Plate A.5 in Appendix A). The basal contact of the member with the underlying Leithsville Formation is marked by thin, algal laminated dolomites containing rip-up clasts, shale lenses and quartz vugs overlying an unconformity. The chert-marker horizon in the underlying Wallkill Member highlights the contact location. There are three unconformities present mid-member that are indicated by scour surfaces, intraformational conglomerates, rip-up clasts, mudcracks and overturned algal. The upper unconformity is also marked by an orange dolomite, the color of which may suggest subaerial weathering of the carbonate.

The upper contact with the overlying Wheatsworth Mills Member is a succession of intraclastic, algal laminated and stylolitic limestones capped by shale and punctuated by the presence of two distinctive chert horizons underlying an unconformity.

Wildcat Road beds are light to dark gray, thin to thick bedded, dolomite, dolomitic limestone and limestone overlain by very thick, silty shale and very fine grained, fissile, black shale. This shale is different from shales in underlying rocks in that it is very thick (up to 0.5 m) and not the typical shale lenses or infillings found in the underlying carbonates. These shales have sharp contacts with the underlying and

overlying carbonates, indicating a dramatic shift in depositional environment (i.e. as opposed to a gradual facies change from carbonate to shale). This sedimentation pattern (carbonate, shale with abrupt contacts) is repetitive and each repetition is a fining upward sequence. The shales are finely laminated, showing horizontal flaser beds and intermittent cross bedded sequences.

Carbonate beds weather light gray, buff, light tan to pale yellow and possess a rank, fetid odor when struck by a hammer. The repetitive light gray-dark gray-tan color banding of the dolomites and limestones is a useful field indicator for the member (Figures 3.21 and 3.22). The mid to upper parts of the member are interlayered with ooid (Figure 3.23) horizons that are intraclastic. Thick quartz-sand lenses, domal algal boundstones, cross bedded and ripple marked oolites, rip-up clasts, edgewise conglomerates, mudcracks, burrows and stylolites occur throughout the carbonate section. The base, upper mid-section, and top of the member are algal laminated and contain quartz vugs that smell of sulfur when broken. Chicken-wire structures and enterolithic folds are present, suggesting former evaporite horizons. The sulfur smell in the broken clots of quartz in this horizon may preserve sulfate remains.

General Chert Description

Chert is present in the mid-section and at the top of the member. The lowest horizon is a silicified ooid bed (Figure 3.24), which occurs in a cross bedded oolite bearing intraformational conglomerates, thick quartz sandstones, arenaceous limestones, occasional rip-up clasts, breccias and domal algal. Variegated black, charcoal, and light gray chert occurs as nodules and clots at the base and centers of large domal algal. The chert is lustrous and waxy on freshly broken surfaces.

At the top of the Wildcat Road Member are three chert horizons that occur in close spatial proximity to each other (Plate A.5 in Appendix A). The stratigraphically lowest chert replaces olive to black shale which is overlain by quartz sandstone lenses, and underlain by non-graded pisoids and cross bedded rip-up clasts. The second chert horizon is an intraformational chert conglomerate that is underlain by quartz sandstone and laminated siltstone and is overlain by silicified chicken-wire structures and enterolithic folds. The third chert horizon is a silicified, cross bedded, quartz sandstone and oolite underlain and overlain by interbeds of olive shale with intercalations of quartz-sandstone lenses. Bedding parallel cherts with lentil shaped morphology are present in the member. When examined under thin section, the lentil shape is shown to be the suturing of ooid and quartz-sand grains to the degree to which grains lose their individual characteristics and overall outline and a silicification halo penetrates and surrounds the sutured grains (Figures 3.25 and 3.26). Brueckner and others identified similar features in rocks of the Golconda allochthon in Nevada and termed this silicification as a pressure solution phenomenon (Brueckner et al., 1987). The presence of the silica halo around the sutured grains has led this author to refer to this phenomenon as pressure solution halos. In this member, pressure solution halos are seen as mildly translucent phases of silica surrounding ghosts of former ooid grains (Figure 3.25). Locally, the pressure solution halos increase in thickness towards bedding plane contacts. Another type of pressure solution chert has been identified in the member; the concentration of silica is in the center of the bed and is concentrically surrounded by a clay-rich phase of chert, which in turn is followed by an outer rim of cherty dolomite (which forms the lower and upper bed contact).

Discussion of Changes in Stratigraphic Definition

The Wildcat Road Member of the Limeport Formation represents the first major change to the stratigraphy presented by Markewicz and Dalton (1977) for the northern New Jersey area. The Wildcat Road Member is the first of six new member subdivisions of the unit. Additionally, the chert stratigraphy was an aid in defining the lower and upper contacts of this member. Differences in thickness interpretations are also presented; however, as the subdivision of the Limeport Formation into six members is a new contribution, the comparison of thickness interpretations must occur on the scale of the formation as a whole, not as a comparison of individual members.

The distinction of the Wildcat Road Member from the Limeport Formation as a whole was due to the recognition of the distinctive shale beds in the lower Limeport Formation. As mentioned previously, the shale beds were very thick (unlike previous shale occurrences in the Kittatinny Supergroup) and have very sharp contacts. The author recognized that a significant change in depositional environment must have occurred in order to produce thick shales with non-gradational contacts, or a lack of facies gradations. These shales are continuous along strike and were mapped as identifying characteristics of the lower Limeport Formation. The definition of the lower and upper contacts of the member was based on the presence of mappable unconformities at the contacts which were highlighted by distinctive chert occurrences.

The thickness of the Limeport Formation was a factor in the creation of the Wildcat Road Member, as well as the five members lying stratigraphically above it. Markewicz and Dalton (1977) estimated that the Limeport Formation was 121 to 213 m thick through most of New Jersey; however in the northwestern part of the state they

estimated that the formation thickened greatly at the expense of the overlying Upper Allentown Formation; however, they never provided an actual thickness estimate for the rocks in this part of the state. The thickness of the Limeport Formation, as measured during this study, is 326.25 m. A formation of this magnitude of thickness would eventually face subdivision upon closer examination and that was an outcome of this investigation.

A factor that contributed to the thickness estimates of Markewicz and Dalton (1977) was the fact that they considered the upper contact of the Limeport Formation to be gradational with the Upper Allentown. The utilization of the chert stratigraphy to assist in the definition of Limeport vs. Upper Allentown permitted the consistent observation of a chert-lined, unconformable contact between the Limeport and Upper Allentown. The specifics of the chert stratigraphy at the upper Limeport contact will be discussed further in the section of this chapter that describes the Rte. 94 Member section of this chapter.

3.4.6 Limeport Formation: Wheatsworth Mills Member

Faunal Content

Domal algal and algal laminations are the only fossils mapped in the Wheatsworth Mills Member in the dissertation study area. The domal algal are unique, with respect to domal algal present in underlying carbonates. The domal algal are very large, cauliflower shaped, and are found in colonies (Figure 3.27). Their intense concentration and colonial nature permits the formation of mounds within the member. Previous workers noticed similar domal algal in the Allentown Formation and the Conococheague Group to the south and west in Pennsylvania and identified them as LLH-type algal

(MacLachlan, 1967; Miller and others, 1939). Hobson characterized the petrology of similar boundstone units in the overlying Beekmantown Group (Hobson, 1963).

General Lithostratigraphic Description

The Wheatsworth Mills Member of the Limeport Formation is 65 m thick at the Wildcat Road type section in Hamburg, New Jersey (location 3a in Figure 3.2; Plate A.6 in Appendix A). The lower contact with the underlying Wildcat Road Member is dark gray shale overlain by a siliciclastic (shale and sandstone lenses), intraclastic, algal laminated, and strongly stylolitized dolomitic limestone. A silicified, cross bedded sandstone lens is present near the lower contact, approximately 200 cm from the base. The upper contact with the overlying Gruenwald Member is punctuated by mud cracked limestones that contain black to olive shale interbeds.

The Wheatsworth Mills Member contains light to dark gray, thin to thick bedded, limestones and dolomitic limestones. Ooid sequences are cross bedded and graded. Stylolitization is pervasive in the section, as are rip-up clasts and ooid sequences. Intraformational conglomerates are spread through the section at regular intervals. The lower part of the section contains abundant quartz clots, which decrease in abundance up stratigraphic section. Domal algal dominate the lower part of the section (Figure 3.28), while algal laminates hold sway at the top.

General Chert Description

Chert is sparse in the Wheatsworth Mills Member, consisting of two distinctive horizons of chert replaced oolites (Figure 3.29), both of which are bounded by cross bedded and graded oolite lenses and intraclastic limestones. One chert is present near the basal contact and is a marker horizon for lower Wheatsworth Mills rocks. The second

chert occurs mid-way through the member within a zone of strongly stylolitized, thick bedded, dolomitic limestone.

Discussion of Changes in Stratigraphic Definition

The significant stratigraphic change is the subdivision of this member from the Limeport Formation; followed in importance by the creation of a chert stratigraphy. Similar to the underlying Wildcat Road Member, certain facies characteristics were mappable along strike and suggested a significant change in depositional environment. The preponderance of colonizing LLH-type algal (as defined by (Hobson, 1963; MacLachlan, 1967; Miller and others, 1939) in this part of the Limeport Formation marks a change in depositional environment from the carbonate-shale cycles of the underlying Wildcat Road Member. The unconformity truncating the top of the Wildcat Road Member marked a cessation in sedimentation for that member and the represented temporal hiatus in sedimentation allowed for change in depositional environment; hence the deposition of rocks bearing LLH-type algal. As such, the preponderance of LLH-type algal boundstone was the factor that allowed separation of this member from the rest of the Limeport Formation. The top of the Wheatsworth Road Member is marked by an unconformity terminating deposition of this particular environment.

The chert stratigraphy permitted an additional control on stratigraphic correlation that helped to confirm the validity of this member's existence. Markewicz, Dalton and Drake have used faunal assemblages as identifiers of the Kittatinny Supergroup formations; however, the use of faunal assemblages as unit identifiers can be fraught with inconsistency, especially if facies changes occur within that particular stratigraphic unit (Drake, 1969; Markewicz and Dalton, 1977). The lateral persistence of the two chert

horizons in the Wheatsworth Mills Member permitted confirmation that the LLH-algal bearing horizons were indeed within the same stratigraphic horizon and, in this instance, could be used as a stratigraphic identifier.

3.4.7 Limeport Formation: Gruenwald Member

Faunal Content

Algal laminations and stromatolites are the only fossils identified in the Gruenwald Member in this study. LLH-type algal stromatolites are present in this member as well; however they are much larger that the LLH-type algal in the underlying Wheatsworth Mills Member and are found repetitively throughout the member.

General Lithostratigraphic Description

The Gruenwald Member of the Limeport Formation is 92.75 m thick at the Wheatsworth Road type section in Hamburg, New Jersey (location 3a in Figure 3.2; Plate A.7 in Appendix A). The lower contact with the underlying Wheatsworth Mills Member is unconformable and is overlain by a thick, coarse grained, dolomitic limestone that contains intraformational conglomerate in discrete, oolitic horizons. The lower conglomerate horizon bears quartz vugs. Rip-up clasts are present in the carbonate. The upper contact with the overlying Glacial Quarry Member bears a distinctive, mud cracked and intraclastic dolomite which is a thick, domal algal boundstone marked by a sharp unconformity at its base and three distinctive chert horizons overlying the unconformity. These are, in turn, overlain by shale.

The Gruenwald Member is a light to dark gray, fine to coarse grained, dolomitic limestone in the lower section, limestone in the middle-upper parts, and dolomite at the very top. Algal laminations are common in the lower and middle-upper parts of the unit.

Rip-up clasts are common throughout. Stylolites are focused in the mid-upper beds. At other locations along strike, black shales and dolarenites interfinger with the carbonates in the lower part of the member. A fine grained quartz sandstone, siltstone and claystone layer is also present. The fine grain size and quartz-silt composition suggest eolian environments. Mud cracks, rip-up clasts, and overturned algal stromatolites define several unconformities in this member, in addition to the ones located at the lower and upper contacts.

General Chert Description

Gruenwald Member cherts are present only at the top of the member at the type section, overlying the mud crack and rip-up clast horizons indicative of an unconformity. Chert nodules replacing algal laminations sandwich silicified oolites (Figure 3.30) at the upper contact. At other locations in the study area (Ames Rubber Quarry, Glacial Quarry), Gruenwald cherts are not restricted to the upper contact. In ascending stratigraphic order the cherts are: a succession of black shale lenses replaced by chert, with associated clots and nodules of silicified oncoids; partially silicified dolarenites, structureless oolite lenses and domal algal (the base and mid-section of the domal algal are partially silicified); and silicified, strongly stylolitized shales overlying the silicified domal algal. The fine grained quartz sandstone, siltstone and claystone layer, interpreted as an eolian deposit, caps the chert sequence.

Discussion of Changes in Stratigraphic Definition

The Gruenwald Member of the Limeport Formation is distinctive for the large LLH-type algal present in the carbonates. The LLH-type algal are distinctive from those in the underlying Wheatsworth Mills Member in that they are larger and occur

repetitively (cyclically) through the member. The presence of the LLH-type algal alone did not warrant separation of this member from the Limeport in general; however, the distinctive repetitiveness of the algal horizons in the Gruenwald indicated that the environmental setting needed to support LLH-type algal had reached its acme in the member. The presence of unconformities at the base and top of the member helped to define the member's boundaries. The chert present in the Gruenwald Member helped to define the upper contact and the chert present mid-section established a correlation aid that, similar to the Wheatsworth Mills Member, helped to confirm the lateral persistence of faunal assemblages in one stratigraphic zone.

3.4.8 Limeport Formation: Glacial Quarry Member

Faunal Content

Cauliflower shaped algal stromatolites and laminations were mapped in the Glacial Quarry Member during this study. The stromatolites in this member are much smaller than the stromatolites in the underlying Wheatsworth Mills and Gruenwald members and while they still occur cyclically, the cycles are less frequent than those in the underlying member.

General Lithostratigraphic Description

The Glacial Quarry Member of the Limeport Formation is 18 m thick at the Glacial Quarry type section on Rte. 94 in Hamburg, New Jersey (location 3c in Figure 3.2; Plate A.8 in Appendix A). The lower contact with the underlying Gruenwald Member is a dark gray, micritic, mud cracked, dolomite bearing rip-up clasts and shale interbeds overlying an unconformity. The lower contact is marked by three silicified shales. The upper contact with the overlying Edison Member is a very light to medium

gray, algal laminated dolomite with lenses of black, silicified, intraclastic, ooids, pisoids and grainstones. This lithology is truncated by an unconformity.

Glacial Quarry rocks are light to dark gray, micritic to coarse grained, moderately algal laminated dolomites bearing stylolites, abundant ooids, rip-up clasts, intraformational conglomerates, algal stromatolites, and mud cracks with scour-and-fill channels and intraformational conglomerates. The dessication features, scour-and-fill channels and conglomerates are interpreted as unconformities in the section. Shale and quartz sandstone interbeds are common, with shale predominating facies intercalations. Pyrites are associated with cherts in the lower part of the section.

General Chert Description

There are three chert horizons within the Glacial Quarry Member. As mentioned previously, the lower contact of the member is marked by the presence of three black, silicified shales in a micritic, mud cracked and intraclastic dolomite overlying an unconformity.

The second chert horizon contains stylolitized chert pods and/or nodules replacing ooids and algal laminations. Overlying the stylolitized chert nodules in this horizon are two silicified, ooid interbeds, associated with a mud cracked horizon bearing sour-and-fill channels and intraformational conglomerates.

The third chert horizon, as previously indicated, is at the upper contact of the member and is a horizon of chert pods/nodules bearing silicified ooids.

At other locations within the study area, the lower cherts in the Glacial Quarry Member are pyrite-rich and strongly stylolitized. The base of the chert is silicified shale overlain by cut-and-fill channels filled with nodules and clots of silicified oncoids and

pisoids. The oncoid and pisoid nodules are overlain by silicified, sulfide-rich, grainstones. Silicified quartz sandstone overlies the silicified grainstones. Capping the chert succession are two distinctive, structureless, silicified quartz sandstones.

The upper chert horizon of the Glacial Quarry Member is silicified, very fine grained quartz sandstone and siltstone overlain by silicified black shale, cut-and-fill channels filled with silicified clots of pisoidal chert, and thin horizons of silicified ooid and pisoid grainstone. All of the cherts are black, dark gray to olive gray, and translucent only along thin edges. The oolitic cherts, and the silicified siltstone, are saccharoidal and scintillate with quartz sand grains along freshly broken surfaces. The shale lenses are charcoal gray to olive gray and because they are pyrite rich, the entire section weathers yellow. In general, the oolitic and grainstone cherts are more translucent than the algal and shale cherts. The algal structures only reveal selective silicification occurring along the base and internal parts of the domal algal.

Discussion of Changes in Stratigraphic Definition

The Glacial Quarry Member is distinguishable from the underlying Gruenwald Member due to contrasts in size and abundance of the algal stromatolites, their cyclical appearance in the section, and the introduction of greater quantities of intraclastic horizons and ooid sequences. The algal stromatolites in the Glacial Quarry Member are much smaller than those occurring in the underlying members and the population size and density has decreased significantly. While intraclastic horizons and ooid layers are a common feature in carbonates, there is a dramatic increase in their abundance and volume in this member. An identifying characteristic of the underlying Gruenwald Member was the cyclicity of algal stromatolite bearing horizons. This cyclicity is still

present in the Glacial Quarry Member; however, cycle length and frequency has decreased considerably. These observations strongly suggest an environmental change from the LLH-type algal mounds in the Gruenwald Member to the diminishing populations in the Glacial Quarry Member and were the prime reasons for separating the Glacial Quarry Member from surrounding lithologies. Unconformities bound the member at both contacts and the chert marker horizons present at the contacts were utilized to confirm lateral continuity of the member.

3.4.9 Limeport Formation: Edison Member

Faunal Content

Bedding in the Edison Member is controlled by algal laminations and the unit contains abundant cabbage-head domal algal in the upper beds. Other faunal remains were not discovered during this study.

General Lithostratigraphic Description

The Edison Member of the Limeport Formation is 19 m thick at the Rte. 94 type section on Rte. 94 in Hamburg, New Jersey (location 3b in Figure 3.2; Plate A.9 in Appendix A). The lower, unconformable contact with the underlying Glacial Quarry Member is a graded oolite interbedded with algal laminated dolomite capped by 20 cm of tawny yellow, fine grained, quartz sandstone. The quartz sandstone is silicified and grades laterally into dark gray chert nodules or pods and stylolitized shale. The upper, unconformable contact with the overlying Rte. 94 Member is indexed by silicified shale and stylolitized chert interbedded with micrite bearing shale interbeds and domal algal. An unconformity caps the member.

The Edison Member is a light to medium gray, micritic to coarse grained, dolomite interlayered with abundant stylolite bounded mudstones and shales, ooids, intraclasts, mud cracks and quartz sandstones. Quartz sandstones decrease in abundance up stratigraphic section, in correspondence with an increase in micrite and shale. Stylolites and planar cross beds are pervasive in the lower-middle part of the section, while dessication features (interpreted as unconformities) predominate in the top of the member. Quartz vugs and rip-up clasts are sparse in this section.

General Chert Description

There are five chert horizons within the Edison Member of the Limeport Formation. The first (stratigraphically lowest) chert is at the lower member contact and is silicified tawny/yellow sandstone that grades laterally into dark gray, nodular/pod shaped chert replacing sandstone. At other locations, the lowest chert is a partially to completely silicified, thin to thick bedded, fissile, black to dark charcoal-gray shale. The silicified shale is underlain and overlain by well developed stylolite horizons; the shale itself may represent the insoluble residuum of a stylolite.

The second chert is a medium gray, selectively silicified oolite, in which thin sections show only the organic parts of the ooids are replaced by silica (Figure 3.31). The silicified oolite is both underlain and overlain by pressure solution halos. These cherts occur mid-bed, as a fine halo of silica within the matrix of the ooid grainstone and are surrounded by bedding contact stylolites.

The third chert is silicified light gray shale at the type section location. The shale is present in a pervasively stylolitized section in which horizontal and vertical stylolites are present. Along strike, however, the chert selectively replaces filamentous and domal

algal structures. Examination of these cherts in slabs indicates that the silicification is selective in that only organic matter is silicified. Entire lenses of laminated algal are silicified and the bases and mid-sections of some of the domal algal also contain black, dark gray, mildly translucent, chert.

The fourth type is light gray, silicified shale in a stylolitized dolomite. Along strike, however, the chert occurs in intraclastic limestones which possess silicified rip-up clasts, as accumulations of oolite wrapped in silicified algal matter, and as dessication features, the outer edges of which are wrapped in algal filament and are replaced by chert. All of the cherty horizons are strongly stylolitized; however, the pressure solution chert is most visible within the along-strike shales and grainstone facies.

The fifth chert type is also light gray, silicified shale that contains a siliceous halo surrounding radiograph-type and bedding plane stylolites. These often contain, or are lined with, insolubles, clays and shale particles (Figure 3.32).

Discussion of Changes in Stratigraphic Definition

The Edison Member is distinct from the underlying Glacial Quarry Member in that the abundant colonies of LLH-type algal are not present and are not supported in the environment responsible for depositing this member. Domal algal do exist in the upper reaches of the member, but they are smaller, cabbage-head type algal, not the larger, cauliflower shaped, LLH varieties. There is an abundance of micrite and shale lithologies, instead of the grainstone facies that predominated below. The amount of chert in the section increases significantly as well. These lithologic variations are indicative of another significant change in environmental setting in the Limeport Formation and as such, separating this unconformity bounded member from the rest of

the formation was appropriate. The abundance of chert in this member is an identifying criterion, but the presence of chert at both contacts also enabled correlation along strike to confirm the validity of member subdivision.

3.4.10 Limeport Formation: Rte. 94 Member

Faunal Content

Algal in both domal and laminated form is sparse in the Rte. 94 Member, with respect to other carbonates within the Kittatinny Supergroup.

General Lithostratigraphic Description

The Rte. 94 Member of the Limeport Formation is 36 m thick at the Rte. 94 type section in Hamburg, New Jersey (location 3b in Figure 3.2; Plate A.10 in Appendix A). The lower contact with the underlying Edison Member is marked by an unconformity overlain by a stylolitized chert and light gray, coarse grained, structureless dolomite that is stylolitized at the upper contact. The upper contact with the overlying Kingdone Estate Member of the Upper Allentown Formation is also unconformable, with the unconformity truncating dark gray shale sandwiched between ooid and algal (domal and laminated) bearing dolomites. Irregular masses of black, silicified oolite occur just below the top of the member.

The Rte. 94 Member contains light to medium gray, medium to coarse grained, dolomites bearing abundant ooids, oncoids, pisoids and sandstone, and sparse shale, interbeds. Ooids and sandstones are predominantly planar cross bedded and graded. Rip-up clasts are common and the top of the member is pyrite rich. The unit is moderately stylolitized along its expanse. There are two horizons in the Rte. 94 Member that are brecciated and the breccia clasts are rounded along their tops and upper sides.

The clasts do not exhibit rotation; they were split in place, rounded by weathering and re-cemented together suggesting a subaerial weathering that may be karstic. If this weathering is karstic, it is not a sinkhole-type karstification, but a minor weathering of an exposed plane that ceased before any substantial rotation of clasts, or accentuation of joints, could occur. The karstic horizons are also interpreted as unconformities in the member, in addition to those at the lower and upper contacts.

General Chert Description

There are two chert zones in the Rte. 94 Member. The first chert zone is quite thick, spanning the lower 2000 cm of the member. This chert zone contains several varieties of selective silicification occurring as horizons within the chert zone. As mentioned previously, the first chert in the Rte. 94 Member is a silicified stylolite at the basal contact. Overlying the basal chert are silicified sandstones and rip-up clasts. Moving up stratigraphic section, the volume of silicified sandstones decreases and the amount of silicified organics increases. Selective silicification of very delicate organic features, including algal encrusted cortices of oncoids, pisoids and ooids, parts of domal algal and algal laminates occurs in the upper part of the first chert zone (Figure 3.33). The cherts are black to charcoal gray, highly lustrous on fresh surfaces, exhibit conchoidal fracture and some have limonite coatings.

The second chert horizon in the Rte. 94 Member occurs at the top of the member near the upper contact. These cherts are horizons of silicified graded ooids. At other locations, silicification occurring along pressure solution halos is visible at this horizon. The cherts are very clay rich and black with iron staining.

Discussion of Changes in Stratigraphic Definition

The final member of the Limeport Formation is similar to the units underlying the Edison Member. The final member is predominately grainstone, bearing graded ooids and an increased quartz sandstone component. The micrite and shale that predominates the underlying Edison Member are not present in the Rte. 94 Member. Domal algal are present throughout the member, but they do not reach the proportions or density of the LLH-horizons in the lower part of the Limeport. A key feature of the Rte. 94 Member is the existence of two karstic horizons and these karstic plains can be traced through the Hamburg quadrangle. The cherts in the section are unique in that the lower chert horizon is quite thick and is mappable as a concentration of cherts in the lower half of the member. The lower and upper contacts are both silicified. The stylolitic chert at the base of the member, and the ooid chert at the top, helps control the correlation of the unit across the study area.

3.4.11 Upper Allentown Formation

Faunal Content

Algal stromatolites and laminations are the fossils identified in the Upper Allentown Formation in the dissertation study area. Two types of algal structures are present in the Upper Allentown Formation, specifically a circular, concentrically laminated algal stromatolite (Figure 3.34) and a filamentous, algal stromatolite.

The circular algal stromatolites are large and domal; however, they are different in overall outward appearance from the algal stromatolites that occur in the underlying Limeport Formation. The Upper Allentown algal contain very fine, concentric layers that are strongly convex (circular) on their upward surfaces, but are markedly flat along the

lower surface attached to the substrate. The circular algal congregate along bedding planes and possible hard grounds and do not appear to colonize or build mound structures. The filamentous algal stromatolite control bedding, as they do in the lower Limeport Formation; however, in the Upper Allentown Formation, the filamentous algal create a pinch-and-swell effect along stratigraphic strike. In cross section, this variety of algal appears as lenticular shaped, biconvex, structures. Both varieties are associated with grainstone facies and slabs reveal oolite structures, cemented on the surfaces of the algal layers.

General Lithostratigraphic Description

The Upper Allentown Formation is approximately 86 m thick at the Carlton Village type section in Hamburg, New Jersey (location 3d in Figure 3.2; Plate A.11 in Appendix A**)**. The lower contact with the underlying Rte. 94 Member of the Limeport Formation is unconformable and contains a medium gray, medium grained dolomite with shale and planar cross bedded, ooid-pisoid interbeds that yield upward into a thick, graded, and planar cross bedded oolite interbedded with quartz sandstones. Two silicified oolites are present near the lower contact of the member. The upper contact with the overlying Carlton Village Member of the Stonehenge Formation is also unconformable, underlain by a light to medium gray, medium to coarse grained dolomite with rip-up clasts and an intraformational conglomerate at the upper contact. Rip-up clasts, intraformational conglomerates and graded ooids are present at the upper contact.

The Upper Allentown Formation is light to medium gray, medium to coarse grained, thickly bedded dolomite with abundant ooid, shale and sandstone interbeds, in descending order of quantity. The ooid, pisoid and sandstone lithologies are locally

graded and cross bedded. The unit is moderately algal laminated and contains domal algal along the base and top of the member. The member is moderately stylolitized and contains chert at both contacts. At other locations, intraclastic limestones are intercalated with ooid-pisoid horizons. Stylolites are sub-parallel to bedding, mildly castellated to cuspate and generate a concentration of insoluble residue composed largely of clay particles and minor pyrite.

General Chert Description

There are two chert zones in the Upper Allentown Formation, one at the base and the other at the top of the member. The cherts occurring at the base of the Upper Allentown occur as irregularly dispersed clots and fragments of ooids bound together by silicified algal filament, or are all associated with thick dolarenite lenses, cross bedded quartz sandstones containing reworked ooids and pisoids, thin shales and laminated and domal algal (Figure 3.35). Further up in the section, stylolite surfaces are visible in silicified shale and oolites (Figure 3.36). At other locations (Pine Island, Westtown), the intraclastic limestone wedges also suffer chertification. The cherts are highly translucent, lustrous to waxy, black to charcoal to blue gray, and break with a deep conchoidal fracture. Many of the highly translucent fragments are chert replaced edgewise conglomerates, with the clasts composed predominantly of limestone. Generally, silica appears to replace all of these components along the unconformity, which were originally limestone, plus those that were organic rich.

The cherts at the top of the Upper Allentown Formation are strikingly similar to the chert occurring at the base. The cherts are irregular clots and nodules, replacements of both domal and filamentous algal, and chert replaced intraclastic limestone beds. At

other locations, pressure solution phenomena also affect this part of the Upper Allentown Formation. Chert replaced oolitic sequences reveal two types of stylolites. The first is a pressure solution halo occurring within the middle of oolite and algal beds. A second type occurs along bedding plane contacts, also in oolite and algal beds. In this variety, stylolites are parallel, or sub-parallel, to the bedding surface. Close inspection using sawed slabs shows chert replaced limestone clasts occurring within edgewise conglomerates, masses of ooids in a matrix of silicified algal mucilage, and ooids and quartz sandstone horizons. These cherts are highly lustrous, black to dark navy blue, and break with a deep, conchoidal fracture.

Discussion of Changes in Stratigraphic Definition

As indicated previously in the discussion of stratigraphic changes for the Limeport Formation, the boundary between the Limeport and Upper Allentown was considered gradational by Markewicz and Dalton (1977). Additionally, Markewicz and Dalton (1977) placed the Limeport-Upper Allentown contact at the, "…last common appearance of cryptozoa and oolite and the appearance of uniformly textured dolomite." Markewicz and Dalton (1977) also defined the upper contact of the Upper Allentown as, "…at the quartzite conglomerate zone which is about 75 feet above a distinct section of thin bedded, mottled dolomite containing local oolites, cryptozoa, and silt beds."

As discussed previously in this chapter, this study of the Upper Allentown Formation did not locate a gradational lower contact for the formation (an unconformable contact was found instead), nor did it find quartzite conglomerates at the upper contact (quartzite conglomerates were not mapped in the unit at all). Markewicz and Dalton's contact definitions supported wide variations in thickness estimates for both the Limeport

and Upper Allentown; 305 to 366 m in the Hamburg area to less than 152 m in northwestern New Jersey.

The utilization of detailed stratigraphic column measurement and chert stratigraphy during this investigation allowed for the demarcation of consistent, chert lined, unconformable lower and upper contacts. These findings allowed for a laterally consistent thickness for both the Limeport and Upper Allentown formations. The results of this investigation indicate that the Upper Allentown, as a whole, is 86 m thick in the Hamburg and contiguous quadrangles. This thickness is less by one-half of the thickness Markewicz and Dalton (1977) gave for northwestern New Jersey, and by a greater extent when compared with the thickness of the unit in the Hamburg area.

Despite the existence of the unconformable lower contact, the lithologies of the Rte. 94 Member of the Limeport Formation and the Upper Allentown Formation are grainstones and hence very similar. Markewicz and Dalton (1977) indicated that the decrease in faunal concentrations up stratigraphic section was an indicator of the Upper Allentown Formation. This investigation, however, discovered fossil assemblages in the Upper Allentown that are very different from those in the underlying Rte. 94 Member. The faunal assemblages may not have the concentrations present in the Rte. 94 Member, but they are present and laterally persistent. The Upper Allentown preserves the first occurrence of circular and filamentous algal stromatolites in the Kittatinny Supergroup. The occurrence of these fossils is laterally persistent in the carbonates above the Rte. 94-Upper Allentown unconformity. It is apparent that identifying the chert lined unconformity and recognizing the change in faunal content is critical to correctly identifying the Upper Allentown Formation.

Finally, the upper contact of the Upper Allentown Formation was determined by Markewicz and Dalton (1977) as being shared with the Rickenbach Formation; this designation is being changed in favor of inserting a new formation (Stonehenge) within the Kittatinny Supergroup.

3.4.12 Stonehenge Formation: Carlton Village Member

Faunal Content

Three different types of algal stromatolites are present in the Carlton Village Member. At the base of the member are two types that exist in the same stratigraphic interval. The first is a ropy, laminated algal with spiral shaped terminations. The second is a castellated variety about 1 m in length and 1/3 m in height. The final type is a rounded stromatolite that occurs locally.

The ropy, laminated type of algal forms a plexus of algal filament lacing rubbly zones in the carbonate. Weathered surfaces of this type of algal structure are lightly dusted with a stain of hematite. The filaments radiate in different directions; however, the density of the algal filaments varies according to location. Along strike are patches of rubble mounds, or alternatively, pinnacle reefs which bear the convoluted and twisted remains of spiraling algal structures. At some locations, concentric, perfectly preserved, algal structures are found as circular spheres, while others are mildly elongate. The elongation occurs within a fold and is parallel to the fold axis, and as such is interpreted as deformational strain.

The castellated algal also locally contains 1 to 2 cm wide, silicified, anhydrite flowers**,** suggesting the former presence of localized hypersaline conditions. Both types are present in rubble zones deposited on ripple marked and cross bedded grainstone and

quartz sandstone substrates. The middle part of the member contains a circular algal stromatolite that is similar to those found in the underlying Upper Allentown Formation. The difference between the two is that the Upper Allentown circular algal are strataform and stratabound and exist as solitary organisms. The circular algal in the Carlton Village Member are smaller than those in the Upper Allentown, and exist as colonies that form mound structures (up to 3 m in height) within the member.

Rounded algal stromatolites appear in the Carton Village Member as well, developed on top of arenaceous units, and associated oolite sequences.

General Lithostratigraphic Description

The Carlton Village Member of the Stonehenge Formation is 63.75 m thick at the type section in Hardyston Township, New Jersey (Figure 3.2; Plate A.12 in Appendix A). The unconformable lower contact with the underlying Upper Allentown Formation is a thick, cross bedded, siliciclastic and grainstone dolomite containing ropy, laminated algal culminating with spiral shaped terminations (both upright and overturned), with ripple marked surfaces sandwiched between two unconformities. The upper contact with the overlying Canal Road Member is approximately 2 m of medium gray, micritic dolomite that is strongly algal laminated and peppered with quartz vugs. Shale and sandstone interbeds occur intermittently, as do silicified algal laminations underlying the unconformity capping the member.

The unconformity truncating the top of the Carlton Village Member is worthy of special note. The unconformity has been mapped as a zone of rock (typically less than 0.5 m thick) that varies along strike. From south to north, the lithologic transition ranges from:

1-silicified quartz sandstones and intraclastic/edgewise conglomerates to;

2-internally brecciated, domal algal filled with vuggy quartz clots and crystals (up to 2 cm long) to;

3-chert breccias cemented with coarse grained, euhedral dolomite bearing pyrite (the clasts become larger and more tightly welded to the north) to;

4-chert breccias that have smaller clasts, are very tightly welded together and free of matrix to;

5-very thick beds lined with siliceous clay, bearing slightly rounded breccia clasts so tightly welded that boundaries between clasts are difficult to discern and color variations must be used to distinguish between individual clasts to;

6-beds of homogenous, black, highly lustrous cherts to;

7-extremely large (several meter diameter), disjunct blocks of chert bearing dolarenite that are cemented together.

All of these rocks in the unconformity zone are housed in dolarenites. The across-strike transition from sandstones to breccias (with variations in degree of roundness, compaction and cementation), to extremely large breccia blocks, is interpreted by this author as indicating a weathering profile which increases in intensity across strike. The inferred increase in weathering profile may suggest an increase in the severity of unconformity development along the top of the Carlton Village Member.

The Carlton Village Member is a light to dark gray, fine to coarse grained, algal laminated dolomite that contains quartz sandstone and grainstone interbeds, with shale interbeds increasing up stratigraphic section. The grainstones and quartz sandstones are ripple marked near the basal contact, and graded and cross bedded throughout the rest of

the member. Rip-up clasts are common in the lower part of the section. Quartz vugs are present in the middle and upper part of the member and intraformational conglomerates are present in the lower 2000 cm of the unit. At locations other than the type section, pressure solution features are present at the top of the member as radiating, radiograph and mildly cuspate varieties which occur along bedding contacts.

General Chert Description

There are several chert types within the Carlton Village Member of the Stonehenge Formation. Several of these chert varieties occur in the lower 1500 cm of the formation as a silica-rich zone. The stratigraphically lowest chert is a series of thin chert conglomerates overlain by thin horizons of chert replaced, ropy, laminated algal. The cherts are overlain by a substantial accumulation of rubble-zone dolarenites. Sawed slabs of the rubble-zone dolomite reveal a coiled structure spiraling through the rock which represents a variety of types of chert replaced algal structures. At some locations the chert replaced algal is finely dispersed, while at others they are highly concentrated. Where the algal filament is highly concentrated, freshly broken surfaces are light gray, waxy, and mildly translucent. Interbedded with the silicified algal are chert conglomerates that include intraclasts of limestone, which are completely replaced by black, matted chert. The chert clasts are surrounded by fragments of dolomite, rip-up clasts, and edge-wise conglomerates. In general, most of the cherts in the Stonehenge Formation have considerable quartz-sand content. The chert replacing the algal laminations is very similar; black to charcoal gray and matted. The chert units fan out, like an apron, each possessing overlying mounds of rubble-zone dolarenite.

The algal stromatolites, and associated oolitic horizons, all contain cherty lenses. The second chert type occurs as selective silicification of laminated and domal algal types, and as wholesale silicification of mildly convex mounds and a castellated algal. The chert that selectively replaces the laminated and domal algal is a minor constituent of the Carlton Village Member. These cherts occur along the base of the oolite sequences, internally within domal algal, selectively replaces some domal algal filament, and replaces the thin edges of laminated algal accumulations.

The selectively replacive chert has along strike occurrences of wholesale replacement of mildly convex, algal mounds (approximately 6 to 9 m in length, about 5 cm thick) and castellated algal (about 1 m in length and about 1/3 m in height); both types are interbedded with dolarenites. The convex mounds and castellated algal accumulations are wholesale replaced by internally black chert, bearing later generations of blue-gray to light gray chert; giving the algal structures a concentric, layered, outer appearance. The castellated type also contains black to dark and light gray, alternating bands of chert that are mildly translucent on thin edges, and the internal parts of the castellated type sometimes contain a brecciated chert. The chert breccias are composed of desiccated algal fragments wholesale replaced by chert, with the interstices composed of chert replacing coarse grained, euhedral dolomite.

At locations (Blair Rd, Looney, Richter, Majack Farm estates) other than the type section, silicified pressure solution features are present at the top of the Carlton Village Member occurring as the radiating, radiograph type and the mildly cuspate varieties, which occur along bedding contacts.

Discussion of Changes in Stratigraphic Definition

As the Stonehenge Formation was not recognized by previous workers in the New York recess, the rocks of the Carlton Village Member were previously interpreted by Markewicz and Dalton (1977) as being part of the Upper Allentown Formation. Markewicz and Dalton (1977) did not divide the Upper Allentown Formation into members, but they did recognize a change in lithology towards the top of the Upper Allentown, "The upper 100 to 200 feet of the Allentown becomes more siliceous by a greater content of sandy dolomite and local quartzite beds." The inclusion of Carlton Village rocks in the Upper Allentown Formation by Markewicz and Dalton (1977) justifies the vast differences in thickness variation between Markewicz and Dalton (1977) (152 to 366 m) estimates and the thickness provided in this study (86 m).

This investigation found abundant quartz sandstone and grainstone interbeds in the lower part of what was named the Carlton Village Member, with an increase in shale and siltstone interbeds toward the top of the unit. The member also contains three distinctive algal stromatolite types, which were not documented by Markewicz and Dalton (1977) in their description of the uppermost parts of the Upper Allentown Formation. Unconformably overlying the Upper Allentown Formation (as defined in this study) is an algal stromatolite horizon bearing two distinctive types of algal structures; the ropy laminated type and the castellated variety. These are first occurrences of this type of algal structure in the Kittatinny Supergroup. Occurring mid-member is the reoccurrence of the circular type algal stromatolite; however, the difference between the algal occurrences in the Carlton Village Member, compared to the algal in the Upper Allentown, is the smaller size and colonizing nature of the algal. These differences in

faunal content, as documented in this study, permitted segregation of the Carlton Village from the underlying Upper Allentown Formation, and inclusion of the member into the Stonehenge Formation based on lithology and similarity to correlative rocks in Pennsylvania.

Finally, the upper contact of Markewicz and Dalton's (1977) Upper Allentown Formation (which translates to the Carlton Village upper contact) is not located at a quartzite conglomerate, but at a chert lined unconformity truncating micritic, algal laminated dolomites bearing quartz vugs. Establishing the lateral continuity of the unconformable upper contact is aided by the lateral persistence the two silicified algal laminates occurring at the upper contact. This upper contact is significant in the across-strike variation in the lithologic character of the unconformity may be an indicator of fairly significant erosion along this horizon.

3.4.12 Stonehenge Formation: Canal Road Member

Faunal Content

The Canal Road Member only contains algal laminations and one horizon bearing large domal stromatolites.

General Lithostratigraphic Description

The Canal Road Member is 22.50 m thick at the Canal Road type section in Vernon, New Jersey (location 4 in Figure 3.2; Plate A.13 in Appendix A). The lower contact with the underlying Carlton Village Member rests on an inferred major unconformity with gray and black brecciated cherts overlying it. The upper contact with the overlying Hope Member of the Rickenbach Formation is medium gray, thickly bedded, dolomite bearing rip-up clasts, intraformational conglomerates, graded and cross

bedded quartzites, quartz vugs, quartz sandstone and shale interbeds and silicified algal structures. No less than twelve, 2 to 5 cm thick, quartz sandstones occur sporadically along the base of the bed (Figure 3.37) (this occurrence is too fine to depict on the scale of Plate A.13) and cut-and-fill channels occur along the top of the bed. The sandstone is chert replaced (Figure 3.38). As such, this contact is interpreted as an unconformity.

The Canal Road Member is a medium to dark gray, micritic to coarse grained, thick bedded dolomite with algal laminates, quartz sandstone horizons, oolites and sparse shale (Figure 3.39). Quartz vugs are common in the section. Sandstone horizons are predominantly planar cross bedded. Stylolites are sparse in this section, in comparison to underlying beds of the Kittatinny Supergroup, but they do exist. Mud cracks and rip-up clasts are present in the upper part of the member.

General Chert Description

There are four chert types within this formation. The lower breccia unit at the base of the Canal Road Member is the first chert. The chert breccia rests unevenly on the unconformity incised upon the Carlton Village Member. The breccia consists of large, angular fragments of homogeneous black and finely laminated black, navy blue, to light gray chert (Figure 3.40). The chert breccia matrix is sparse, but consists of a coarse grained, light gray dolomite. The chert clasts are either silica replaced algal or fragments of oolite. However, along strike the brecciated units are replaced by three to five, thin to thick, chert replaced, and algal laminated dolomites. Underlying many of the chert breccia lenses are intact to overturned domal algal, which have been replaced by chert. At some locations, the cherty accumulations, although brecciated, are thick, billowy and appear to be algal stromatolite mounds.

The second series of cherts occur mid-section in the formation and are horizons of gray and black, silicified sandstone and quartz vugs. Pressure solution halos occur mid-bed replacing sandstones. At other locations, cherts occurring in the mid-section of the Canal Road Member are located in two dolarenite intervals which contain high concentrations of quartz vugs. In these two horizons are selective and wholesale replaced ooids, laminated, and domal algal structures. The silicification seems to be selective and focused on the organic-rich vacuoles and organic lenses of the algal structures. There are only few pressure solution features in this part of the section; however, pressure solution halos do occur mid-bed.

The two chert horizons at the upper contact of the member replace sandstones in the sub-unconformity beds. At other locations, the third chert horizon is another breccia occurring above a succession of intercalated dolarenites and fine grained algal laminated, dolmicrites. The breccia consists of large angular clasts of black to navy blue and lighter gray chert. Clasts are fragments of laminated or domal algal. Interspersed throughout the breccia and this cherty horizon in general, are silica replaced rip-up clasts, intraclastic dolomites and shale lenses. Quartz sandstones are abundant and chert replaced, graded and cross bedded oolites are common occurrences. Clear phases of chert are present and are associated with quartz-vug horizons.

There is a fourth chert type in the Canal Road Member at locations other than the type section. This chert contains two, mildly translucent, gray chert horizons, which are characterized by selective chertification of quartz sandstones, algal structures and intraclastic grainstones. The translucency of the chert increases toward the centers of the fragments and are surrounded by a lighter, blue gray to lighter gray phase of clay-rich

chert. These "halos" of chert can occupy the entire thickness of a bed; however, along strike they grade gradually into coarse grained, siliceous dolomites and finally dolomite.

Discussion of Changes in Stratigraphic Definition

The segregation of the Canal Road Member in the Stonehenge Formation was based on the presence of the significant unconformity truncating the underlying Carlton Village Member and the change in lithofacies and faunal content, with respect to the Carlton Village Member. As indicated in the discussion of the Carlton Village Member in this chapter, the unconformity truncating the member may be significant in the magnitude of erosion of the Carlton Village Member. The break represented by the Carlton Village unconformity suggests a new cycle of deposition, in the form of the Canal Road Member.

The Canal Road Member differs lithologically from the Carlton Village Member in the abundance of Canal Road arenaceous dolomites, as distinct from Carlton Village shaly dolomites. Also of prime consideration is the faunal change from one member to the other. The presence of algal laminations and sparse domal algal, in lieu of ropy/spiral, cup shaped algal, castellated algal and circular algal stromatolites in the Canal Road member, is a clear indicator of change from the Carlton Village depositional environment.

3.4.13 Rickenbach Formation: Hope Member

Faunal Content

Cryptozoan algal laminations in the Rickenbach Formation replace the diverse algal mounds and colonies characteristic of the Stonehenge Formation. Algal stromatolites are present in the Rickenbach, but not of the diversity or abundance seen in

the underlying Stonehenge. To date, no other fossils have been found that constrain the age of the formation.

General Lithostratigraphic Description

The Hope Member of the Rickenbach Formation is slightly greater than 14 m thick at the Canal Road type section in Vernon, New Jersey (location 4 in Figure 3.2; Plate A.14 in Appendix A). The lower contact with the underlying Stonehenge Formation contains shaly, flaggy, unevenly bedded dolomite (Figure 3.41). The basal Hope dolomites contain pinch-and-swell structures, lenses of quartz sandstone, and ripple marked, hummocky surfaces overlying an unconformable surface (Figures 3.42 and 3.43). The upper contact with the overlying Crooked Swamp Member is a fine grained, dark gray, algal laminated dolomite with cut-and-fill channels, chert breccias and beds, silicified shale partings, and abundant layers of quartz sandstone underlying an unconformity.

The Hope Member is medium to dark gray, micritic to coarse grained, dolomite bearing planar cross bedded quartz sandstone and shale interbeds. The member is characterized by the arenaceous and billowy nature of the dolomite. The Hope Member does not contain the abundance of quartz sandstone lenses that the underlying Canal Road Member bears, but quartz sandstone is present throughout and finer grained. Bedding appears to be controlled by the cryptozoan algal as bedding surfaces are convex upwards (Figures 3.44 and 3.45). Algal stromatolites are present in the member, as are rip-up clasts, ooids, quartz vugs and worm burrows. Stylolites are scarce.

General Chert Description

There are several types of chert in the Hope Member of the Rickenbach Formation. The stratigraphically lowest cherts are lenses or beds replacing dolomite or sandstone horizons.

The second chert horizon occurs mid-way in the Hope Member and contains three to five, closely spaced, thin, chert horizons. The chert is wispy, filamentous or concentrated into thin beds up to 2 to 3 cm in thickness and is located at the top of thick dolarenite beds. Close inspection reveals that these are chert replaced algal filaments bearing occasional quartz sand and ooid grains (Figure 3.46). The close association of these three varieties of chert occurring midway in the Hope Member, has given rise to the notion of the famous "seven cherts" of the Rickenbach Formation (Markewicz, 1976).

The upper chert breccia of the Hope Member is a succession of black, to dark navy blue, mildly to highly translucent, angular chert clasts up to 10 cm in length. The interstices between the chert are filled with lenses of coarse grained, euhedral dolomite; however, along the base and crest of the breccia units, the interstices are a lighter phase of light, blue gray chert and the dolomite matrix is absent. At some locations along strike, the dark angular chert clasts are welded into a lighter gray-blue, blue-gray chert matrix. Close inspection in sawed slabs reveals the preservation of laminated algal and evaporite replacement structures (Figure 3.47). Dolarenites and quartz sandstones abound above and below the breccia horizons, yet detrital quartz sand grains do not occur within the chert clasts. Instead, above the breccia horizons are partially silicified quartz sandstones. The upper chert horizon possesses breccia clasts which are sutured together. It is difficult to locate grain boundaries between angular fragments occurring in the upper

chert breccia horizon. In some cases, marked color differences between the clasts is the only way to differentiate them.

At locations other than the type section, occurring stratigraphically below the upper chert breccia, is another unique variety of chert. Thin section and slab observations of specimens collected from massive accumulations of structureless oolites show that the ooids are entirely replaced by silica, preserving even the concentric nature of the original ooid. Grain boundaries between the chert replaced, and non-silicified, ooids are sharp. Algal structures in the member are also replaced by chert; however, only the top of the algal accumulations is silicified giving the bed outline an overall convexity. The flat, black color of the silicified algal and the associated, mildly convex chert replaced oolites, stand out against the light gray, weathered dolomite.

The final chert in the Hope Member is gray, silicified shale underlying the unconformity truncating the top of the member.

Discussion of Changes in Stratigraphic Definition

The Hope Member is characterized by the presence of unconformable lower and upper contacts. The upper contact bears silicified shale that is mappable along strike and allows for consistent identification of the upper contact. Lithologically, the Hope Member is similar to the underlying Canal Road Member in that both units are arenaceous; however, as indicated previously, the amount of quartz sandstone diminishes significantly with the Hope Member. Additionally, the faunal change from the Stonehenge to the Rickenbach is observable in that the unique faunas of the Stonehenge Formation are not present above the unconformable Stonehenge-Rickenbach contact, and the fauna in the Rickenbach is a cryptozoan species possibly controlling bedding. The

cryptozoan-rich, billowy beds of the Hope Member bear wisps, filaments, and thin beds of chert along their upper bed contacts (the 7 cherts of Markewicz). These cherts are also consistent along strike and utilizable as a mapping aid.

Markewicz and Dalton (1977) estimated that the Hope Member was up to 53 m thick in northern New Jersey. This investigation estimated 14 m of the member in the dissertation study area. The discrepancy between thickness estimates is explained by the introduction of the Stonehenge Formation to the study area. The Canal Road Member of the Stonehenge not only included, as described previously, Markewicz and Dalton's (1977) lower, unnamed member of the Rickenbach; but approximately half of the Hope Member (as defined by Markewicz and Dalton), as well. The presence of Stonehenge fauna in the lower part of Markewicz and Dalton's Hope Member was the criteria used in this study to separate out that part of the Hope Member and include it in the Stonehenge Formation.

3.4.14 Rickenbach Formation: Crooked Swamp Member

Faunal Content

Algal stromatolites and laminations are the fossils identified in the Crooked Swamp Member in the dissertation study area. To date, no other fossils have been found that constrain the age of the member.

General Lithostratigraphic Description

The Crooked Swamp Member of the Rickenbach Formation is 10.5 m thick at the Canal Road type section in Vernon, New Jersey (location 4 in Figure 3.2; Plate A.15 in Appendix A). The lower contact with the underlying Hope Member is unconformable, with light gray, very coarse grained, highly sulfurous, algal laminated dolomite with

shale interbeds, burrow features and quartz vugs overlying the unconformity (Figure 3.45). Chert replaced intraclasts, worm burrows, shale, and pinch-and-swell chert nodules are present at the contact. The upper contact with the overlying Branchville Member of the Epler Formation is truncated by an unconformity that cuts into light gray, coarse grained dolomite with abundant quartz vugs and chert replaced quartz sandstones (Figure 3.48). At locations other than the type section, the cherts at the lower and upper contacts are brecciated (Figure 3.49). Where chert breccia is not present at the member contacts, a thick intraclastic or carbonate conglomerate horizon is.

The Crooked Swamp Member is a light to dark gray, micritic to coarse grained dolomite bearing algal laminations, burrows, sandstone and shale interbeds. Coarse grain size is an identifying characteristic of this unit. Many of the beds have been recrystallized into coarse grained dolomites and/or saddle dolomites. Faunal remains, such as algal stromatolites, present within these recrystallized beds are barely preserved; usually a faint outline of the algal structure is visible. The unit contains domal algal and sparse rip-up clasts and stylolites. An additional unconformity, other than the two present at the lower and upper contacts, is present near the base of the section. Cut-and-fill channels and truncated surfaces permitted this interpretation.

General Chert Description

The Crooked Swamp is a very cherty member, with respect to the underlying members of the Kittatinny Supergroup. There are several horizons of chert replacing shale, rip-up clasts, and burrows in the lower part of the section, just above the unconformity. At both contacts, and in the mid-part of the member, are chert breccias (Figures 3.50 and 3.51). The angular fragments of chert are welded together, especially

the middle part of the member and the upper contact. The dolomite matrix in the breccias decreases in volume in the upper breccias. Also, the chert clasts in the upper contact breccia are so tightly welded that it is difficult to locate the boundaries between the contiguous fragments; as such, variegated colors, ranging from black to navy blue to light blue gray, serve to pinpoint the locations where the chert clasts are fused. The coarse dolomite matrix is replaced in the upper breccia by a late generation of siliceous infilling, which is lighter in color than the clasts in the chert breccia. Intraclastic units, which include sparse mud cracks and edgewise conglomerates, are also replaced by chert. Intraclastic grainstones located at the one unconformity present within the Crooked Swamp Member is partially silicified.

Along strike, the chert breccias evolve into thin and thick layers of laminated and mildly domal algal. Close inspection of the laminated chert in slabs reveal that they are internally brecciated. In most cases, they are filled with a second, or third, generation of silica. Locally, the breccia matrix is a saccharoidal dolomite.

The cherts in the upper part of the member are lenses and/or beds of gray chert replacing sandstone horizons. Silicified sandstone is present underneath the unconformity capping the Crooked Swamp Member.

Discussion of Changes in Stratigraphic Definition

As indicated previously in this chapter, the identifying characteristics of the Crooked Swamp are its coarse grain size, cherty nature, and thick billowy beds. The cherts, in particular the brecciated horizons, are an important factor in identifying the unit. A distinctive chert breccia is present mid-member; however, at locations other than the type section, chert breccias are present at the lower and upper contacts. The presence

of the chert breccias at both contacts is a mapping aid for the unit. Where the chert breccia is not present at the contacts, a thick intraclastic or carbonate conglomerate horizon is.

One major change in the stratigraphic definition of this member is the change from Markewicz and Dalton's (1977) Crooked Swamp facies to this study's designation of a Crooked Swamp Member. Markewicz and Dalton (1977) did not define contacts for the Crooked Swamp, which would be consistent with a facies interpretation for the unit. Instead they describe interbedding of Crooked Swamp facies with rocks of the Hope Member, with a transitional zone occurring where Crooked Swamp lithologies become abundant up stratigraphic section, at the expense of Hope beds. The stratigraphic location where the majority of rocks are coarse grained, recrystallized dolomite is the Crooked Swamp proper. Markewicz and Dalton (1977) do not describe interfingering of the Crooked Swamp with the overlying Branchville Member of the Epler; rather they note the restriction of Crooked Swamp lithologies stratigraphically below a conglomerate, the thickness of which spans from the Crooked Swamp into the lower Branchville.

Markewicz and Dalton describe Crooked Swamp beds as occurring where the majority of the lithology is a coarse grained, recrystallized dolomite. This observation was confirmed during this study; however, brecciated chert zones at both the lower and upper contacts were also mapped during this investigation and hence interpreted as lower and upper contacts. This investigation also does not dispute the interfingering relationships that the Crooked Swamp maintains with the underlying Hope Member;

however, the along-strike interfingering of Hope and Crooked Swamp facies does not preclude a member designation.

Markewicz and Dalton (1977) provide a thickness variation for the Crooked Swamp from 7.5 to 61 m, specifically 46 to 61 m in Lafayette, Sussex County, New Jersey (two quadrangles to the south of the Hamburg quadrangle), with rapid thinning to the north and south. This investigation reported approximately 10 m of Crooked Swamp in the study area, which is consistent with Markewicz and Dalton's estimates.

3.4.15 Epler Formation: Branchville Member

Faunal Content

Algal laminations and small domal algal are the only fauna mapped in the Branchville Member during this study. To date, no other fossils have been found within the member.

General Lithostratigraphic Description

The Branchville Member of the Epler Formation is 6.3 m thick at the Canal Road type section in Vernon, New Jersey (location 4 in Figure 3.2; Plate A.16 in Appendix A) and remarkably persistent along strike. The lower contact is shared with the underlying Crooked Swamp Member as an unconformity bearing a massive, chert breccia composed of welded fragments of highly lustrous, black and dark navy blue to gray, angular fragments of mildly translucent chert replacing algal laminations (Figure 3.52). The interstices between the clasts are filled with light gray, coarse grained, euhedral, saddle dolomite at the type section; however at other locations the clasts are tightly welded together and the dolomite matrix is replaced by silica. The upper contact with the overlying Big Springs Member is a mud cracked horizon interpreted as an unconformity.

The upper surface of the member also contains a finely laminated, ash gray chert. The laminations do not parallel bedding, or the interpreted horizontal depositional surface. The laminations coat all surfaces, horizontal and vertical, fill interstices, and coat all grain surfaces (Figure 3.52). These observations suggest that the laminations may not be algal, but perhaps represent a silcrete.

The Branchville Member is a light to dark gray, micritic to coarse grained and crystallized, extremely pyrite-rich dolomite that is thinly bedded, flaggy and shaly, algal laminated, mud cracked, current ripple marked, quartz-vug and rip-up clast bearing and contains quartz sandstone interbeds in the lower part of the member (Figures 3.53 and 3.54). Algal dolomites are common in the lower part of the member, with stylolites pervasive mid-section. In the mid to upper parts of the section, laminations do not maintain a horizontal orientation, but are also sweeping, diagonal and vertical, wrapping around grains and clasts in the carbonate. As such, the laminations are thought to be silcretes. Cherts are prolific.

General Chert Description

Three chert horizons are present within the Branchville Member of the Epler Formation. The lowest cherts occur in algal laminated dolomites as gray to black breccias of the algal laminates. Overlying the unconformity are lavender chert layers replacing quartz sandstone. At other locations, the chert occurs as homogeneous flat, black, matted, lentil shaped, elongate pods which locally appear to connect (Figure 3.55). The individual chert pods, which range from 1 to 3 cm in thickness, are surrounded by a halo of coarse, saccharoidal dolomite. This in turn is surrounded by a blanket of very shaly, black to dull gray dolomite.

The second chert horizon is a white to lavender chert breccia, silicified rip-up clasts and gray pinch-and-swell beds and nodules. The thin to thick, pinch-and-swell units (up to 10 cm thick); usually terminate in a shaly dolomite. Close inspection of this chert in slabs reveals dark brown venations running throughout a flat, black matted chert matrix. Markewicz and Dalton (1977) did identify a white chert in their mapping of the Epler Formation and called it a porcellainite. The white chert in this horizon correlates to Markewicz and Dalton's description, except that the chert is not a porcellainite. Porcellainite refers to a specific type of chert that was created in certain diagenetic conditions (Isaacs, 1980). It is a common practice among field geologists to term all white cherts as porcellainites, when in fact, that may not be the case (Markewicz and Dalton, 1977).

The third chert occurs at the unconformable upper contact as interbeds between mud-crack intervals and is often associated with intraclasts and edgewise conglomerates. The chert occurs as gray pinch-and-swell that changes along strike to angular and irregular clots (2 to 3 cm in diameter) of deep orchid to pale lavender, highly translucent, waxy chert. Close inspection shows that these cherts can have collections of very minute ooids which have been entirely replaced by chert.

Discussion of Changes in Stratigraphic Definition

The Branchville Member of the Epler Formation is distinguished by the chert breccia shared at the lower contact with the underlying Crooked Swamp Member of the Rickenbach Formation, plus its predominantly dark gray and thin bedded, flaggy appearance. Distinctively colored gray to lavender cherts make a first appearance in the Branchville Member, directly overlying the dark blue to gray brecciated cherts at the

lower contact. These cherts are mappable and allow along-strike correlation of Branchville beds throughout the Hamburg and contiguous quadrangles. The abundance of pyrite in the Branchville Member is also distinctive, as well as the presence of sweeping horizontal to vertical laminations in the upper part of the member.

Markewicz and Dalton (1977) also placed the Rickenbach-Epler contact at, "… a massive chert zone above which the lithic features are different from underlying rock." However, this is as far as they go in describing the chert at the lower contact. No mention is made of the physical characteristics of the chert. As such, this investigation follows Markewicz and Dalton's (1977) definition, to a degree, by placing the contact at a chert breccia separating Crooked Swamp, recrystallized dolomites from dark gray, pyrite-rich, Epler beds bearing gray to lavender chert breccias. Markewicz and Dalton also state that the upper contact between the Branchville and the overlying Big Springs Member is gradational, with the Branchville containing, "thin, siliceous to shaly interbeds similar to the Big Springs." This investigation mapped a mud cracked unconformity truncating ash gray, laminated chert beds as the Branchville-Big Springs contact. The thickness of the Branchville Member ranges from 0 to 76 m by Markewicz and Dalton's estimates. This investigation maps the Branchville Member as a thin, 6.5 m unit that does not vary considerably in thickness along strike. The redefinition of the upper contact as unconformable, and identifiable using a unique chert horizon, may assist in constraining the thickness of the member to a greater degree than the previously interpreted (Markewicz and Dalton, 1977) gradational contact.

3.4.16 Epler Formation: Big Springs Member

Faunal Content

Faunally, the Big Springs Member is diverse with respect to algal types and include laminated varieties (cryptozoan types), digitate (*Epiphyton)* and thrombolitic forms, as well as small and large domal types. The laminated varieties include collections from 1 to 5 cm; however, entire 0.5 m beds may be composed of laminated types. The digitate and thrombolitic varieties are funnel shaped and generally 1 to 2 cm thick along their bases, and are as much as 3 to 4 cm along their tops. Domal forms occur as two types; a smaller variety up to 10 cm in diameter which occurs along the tops of graded and cross bedded oolites, and a large domal form up to 1 m or more in width and height. Hand sample and slab examination of the laminated variety reveal that they are often dissected by polygonal dessication features. The upper surfaces of the laminae are often divided into rounded mound shapes; with the mound shape being constrained by the areal dimensions of dessication features cutting into and dissecting the otherwise continuous laminae. One final variety of algae is visible on bedding plane surfaces and is dendritic in plan view, suggesting that it may be calcareous in composition.

General Lithostratigraphic Description

The Big Springs Member of the Epler Formation is 44 m thick at the Beaver Run Aggregate type section in Hamburg, New Jersey (location 3e in Figure 3.2; Plate A.17 in Appendix A). The lower contact with the underlying Branchville Member is a chert-rich, mud cracked, rubbly, shaly, medium gray, pyrite-rich dolomite interpreted as containing several unconformities. The upper contact with the overlying Lafayette Member is a light gray, micritic, thick bedded, algal laminated dolomite with planar cross bedded,

ripple marked, quartz sandstones containing several, closely spaced mud cracked intervals interpreted as a prominent zone of unconformity. At other locations, a light, pink gray, 30 cm thick, chert-rich, quartz sandstone occurs near the upper contact.

The Big Springs Member is a light to dark gray, micrite to coarse grained, thin to thick bedded, dolomite, dolomitic limestone and limestone bearing interbedded sandstones and shales, ooids, quartz vugs, chicken-wire structures, algal laminations and domal algal. The dolomitic limestones, limestones and dolomites are very similar to the Conococheague-like cycles described in the Limeport Formation (Hobson, 1957, 1958a, b). Several unconformities are present in the member. There is a decrease in the volume of ooids in this section, compared to the previously described members of the Kittatinny Supergroup.

The Big Springs is a repetition of one sedimentary sequence consistently repeated several times throughout the unit. The sequences, start on a base of oolites that are locally graded, are overlain by algal laminates and boundstones, and capped by billowy dolmicrite. The upper surfaces of the billowy dolmicrite capping the sequences contains a thin to thick (1 to 7 cm), finely laminated, light gray to green, argillic coating (as seen in hand samples, slabs and thin sections) containing ripple marks overprinted by mud cracks. The fine laminations could be interpreted as depositional, but locally they look as if they have been sheared. However, the presence of intact ripple surfaces and mud cracks suggests that the former interpretation may be valid. The dolomite occurring immediately underneath the finely laminated layers is locally bright orange in color. This feature, which is common to the Big Springs Member, imparts a rusted color to outcrops, thereby Markewicz (1976) termed the Big Springs Member the, “Big Red”. The

presence of pyrite in the Big Springs Member is a possible source for the orange color in the weathered dolomites. The orange weathered color of some of the dolomites underlying the finely laminated, green argillic coatings bearing ripple marks and mud cracks suggests that these horizons may have been sub-aerial at some point in their development. The orange weathering of some of the dolomites may indicate exposure at a long enough temporal span to create possible paleosol horizons.

General Chert Description

There are several different chert types within the Big Springs Member and they are grouped into four general horizons. The lower succession of cherts at the type section includes thin to thick accumulations of pinch-and-swell, orchid to lavender, to nearly white chert horizons interbedded in thick cross bedded and graded, intraclastic dolomitic limestones (Figure 3.56). At other, along-strike locations, several other types of chert occur within this horizon; specifically cherts replacing algal structures (Figure 3.57) or cherts occurring as irregular clots, wisps, fragments and lenses. Algal structures are either wholesale replaced by chert, or contain clots and lenses of orchid colored chert along their base. The center parts of algal structures locally contain concentric layers of lighter gray, to nearly white, highly translucent chert (Figure 3.58). Irregular clots, wisps, fragments, and lenses of purple chert, where they occur, are masses of small silicified ooids wrapped in a silicified algal filament. White chert present at the base of this series occurs as highly translucent, thick, irregular masses up to 2 to 3 m in length. Sawed slabs of the white chert show it to be a series of concentric linings, or large vacuole fillings (Figure 3.59).

The second chert horizon at the type section contains medium gray to black chert pods, breccias of algal laminates and pinch-and-swell cherts replacing chicken-wire structures and argillic horizons. This horizon changes along strike to contain translucent, pale ash gray, lavender and deep orchid chert pods and brecciated clasts at the base of graded and cross bedded oolites in thick, billowy, algal laminated dolomite. Sawed slabs show the clasts (5 to 7 cm length) replacing oolites, algal laminations, and chicken-wire structures (Figure 3.60). The matrix between the clasts is a coarse grained, saddle dolomite. These porcelain gray to white and lavender cherts change along strike to bright jade green to variegated burgundy to light gray.

The cherts in the upper succession of the member are associated with thick beds of algal laminated, dolomite perforated with quartz vugs and several unconformities. Overlying this thick, quartz-vug horizon at other locations is a succession of domal algal interbedded with intraclastic limestones and overlain by thick, algal laminated dolomite. The cherts occur as mildly brecciated units and silicified laminated and domal algal. A distinctive type of chert occurs within this upper section, a thick series of chert-pebble conglomerates. The chert pebbles are deep purple at the type section, but range from translucent white, to bright orchid, to deep purple in color at other locations. The pebbles occur in a matrix of coarse grained, medium gray dolomite. Gray, chert replaced pods of algal laminations are also present in this horizon, as well as pinch-and-swell structures.

Discussion of Changes in Stratigraphic Definition

The general lithologic description of the Big Springs Member of the Epler Formation has not changed significantly from that of Markewicz and Dalton (1977).

New contributions center on the interpretation of unconformable lower and upper contacts, elucidation of faunal types and a detailed chert stratigraphy.

Markewicz and Dalton (1977) do not elaborate on the nature of the Big Springs contacts in their definition of the unit. This investigation places both contacts at unconformable horizons. The shale at the upper contact of the underlying Branchville Member is silicified at the type section for the Big Springs Member, but this is a local occurrence and is not traceable along strike. Generally, cherts are located near the lower and upper contacts, but not actually on the contact, as with so many other members of the underlying Kittatinny Supergroup. Lithologically, the Big Springs Member is distinct from the underlying Branchville Member. The light gray to pink-gray, thick bedded dolomites, dolomitic limestones and limestones of the Big Springs are easy to distinguish from the dark gray, thin bedded, shaly dolomites of the Branchville Member. A resurgence of distinct varied and large algal fauna mark the Big Springs Member of the Epler as well, providing a first appearance of these fauna in the Ordovician section of the Kittatinny Supergroup. Markewicz and Dalton recognize that the Big Springs Member is siliceous, indicating that, "…siliceous beds weather in strong relief…, giving the rock a ribbed appearance." However, this is the extent of their documentation of chert in the member. The cherts of the Big Springs are unique in their color (gray to lavender, orchid to burgundy, green to white) and have a wide variation in types and forms, with respect to the other cherts of the Kittatinny Supergroup. The four chert horizons mapped in this study are continuous along strike and when used in conjunction with the lithological and faunal characteristics of the Big Springs Member are determinative in defining the member in the field. Finally, Markewicz and Dalton (1977) estimate a 12 to 46 m

thickness for the Big Springs Member. This study documents a 44 m thickness of the Big Springs at the type section, consistent with Markewicz and Dalton's thickness range for this member.

3.4.17 Epler Formation: Lafayette Member

Faunal Content

Burrows are present in the mid-section of the Lafayette Member and punky and perforated, domal algal are common in the upper part of the section. *Ceretopia* and *Schizopea* gastropod fossils mapped in the Lafayette during this study make a first appearance in the Kittatinny Supergroup. The punky and perforated appearance of domal algal in the Lafayette Member is inferred to be a porosity imparted by grazing gastropods. Close inspection of the vacuoles reveals that many of them are six-sided in profile, suggesting the former presence of aragonite needles (Sandberg and Hudson, 1983; Shearman, 1978)**.**

General Lithostratigraphic Description

The Lafayette Member of the Epler Formation is 44 m thick at the Harmonyvale type section in Harmonyvale, New Jersey (location 6 in Figure 3.2; Plate A.18 in Appendix A). The lower contact with the underlying Big Springs Member is unconformable and contains a dark gray, micritic dolomite bearing quartz vugs, intraclastic layers, algal laminates, stylolites and two distinctive chert marker horizons. The lower chert is a black oolite. The upper chert is light gray, silicified algal laminations. The upper contact with the overlying Beaver Run Member of the Ontelaunee Formation is also unconformable and contains a medium gray, medium grained, dolomitic limestone with interspersed algal laminates. Quartz vugs are present

in the midsection and top of this unit. The upper part of this bed is intraclastic and strongly brecciated. The unconformity at the Lafayette-Beaver Run contact has enough topographic expression to allow mapping of conglomerate filled ravines in the Lafayette Member.

The Lafayette Member is light to dark gray, micritic to crystalline dolomite, oncoidal to pisoidal (Figure 3.61) limestone and dolomitic limestone. The dolomite comprises the lower 22 m of the type section; limestone comprises 200 cm mid-section, and the remaining 22 m of the section is a mixture of dolomite and dolomitic limestone. The section is algal laminated with quartz vugs occurring only in the base and top of the section. One bed mid-section contains quartz vugs. The section is not pervasively stylolitized, only the basal bed contains pressure solution deformation. In addition to the unconformities at the lower and upper contacts, a mud cracked and rip-up clast bearing horizon capping the first bed of the member is interpreted as an unconformity.

General Chert Description

There are four chert horizons within the Lafayette Member of the Epler Formation; however, in terms of volume of silica, the Lafayette is considered sparse, with respect to the rest of the Kittatinny Supergroup. The first succession of cherts in the Lafayette Member occurs as two chert-rich horizons within an algal laminated sequence bound above by an unconformity. The cherty horizons are convex, mildly domal, algal structures replaced by light to dark gray, or nearly black, chert. The overlying chert replaced algal structures; however, do not contain any porous intervals.

The second chert interval contains three horizons of light to blue gray, pod-like chert that is punky or replacing ooids. Upon close inspection of the ooids, they are

wholesale replaced by chert and contain another generation of chert within the interstices between the ooids. The chert is black, lustrous and scintillating on broken surfaces. At a few locations, the matrix chert is light gray to blue gray and the ooids appear white and dark navy blue and are peppered through the matrix. Close inspection of these ooids in thin section show that the lighter colored grains are still carbonate, while the dark, nearly black grains are entirely algal encrusted; suggesting a rather selective form of silicification in certain horizons.

The third chert horizon is very similar to the second. The chert is light gray, olive gray to blue, pod-like and is punky or replaces shale and algal laminations. At other locations, the third chert horizon is a siliceous, ash gray to mildly olive green, infilling which occurs throughout the upper parts of the Lafayette Member. It is found filling in accentuated joint surfaces, creating a rubbly exterior texture to overturned and karstic, Lafayette beds. Slabs of this material show that it is actually very dark gray in color and very shaly and yet fills in open joint surfaces. The joint surfaces underlie the brecciated beds of the upper Lafayette Member that are part of the unconformity truncating the unit. The unconformity is hypothesized as extending far enough down stratigraphic section to accentuate joints and weather beds in the mid-upper parts of the Lafayette.

The fourth chert horizon within the Lafayette Member is a thick succession of brecciated, black chert horizons overlain by a dark gray chert and limestone conglomerate which terminates the Lafayette Member of the Epler Formation on an irregular, unconformable surface.

Discussion of Changes in Stratigraphic Definition

The Lafayette Member, as mapped in this study, does not vary considerably from the description presented by Markewicz and Dalton (1977). Chert is said to occur as beds and clots; however, Markewicz and Dalton provide no further explanation of chert characteristics or outcrop trends. The Lafayette Member in the Hamburg quadrangle is considered in this study as the least cherty of all members in the Kittatinny Supergroup; however, chert is still present and a chert stratigraphy was developed to aid in mapping of the unit. The cherts of the Lafayette Member are distinct from the cherts in the lower two members of the Epler Formation in that the exotic coloration of the Branchville and Big Springs chert does not carry over to the Lafayette Member. This characteristic itself makes the cherts in the Lafayette distinguishable from those present in the lower members. The upper contact of the formation is interpreted by Markewicz and Dalton as transitional with the Ontelaunee Formation, despite an intense focus by them towards proving paleokarstification at the upper contact. This study does not dispute the paleokarstification hypothesis put forward by Markewicz and Dalton (1977); however, this author suggests that the upper contact is unconformable, and not gradational as previously suggested. Markewicz and Dalton estimate a 15 to 76 m range in thickness for the Lafayette. This study proposes a more tightly constrained thickness of 44 m for the unit.

3.4.18 Ontelaunee Formation: Beaver Run Member

Faunal Content

Several types of fossils were found by Markewicz and Dalton (1977) in the middle part of the Beaver Run Member; specifically the ever present stromatolitic and

laminated varieties of algal, straight nautiloids, brachiopods, gastropods, corals, bryozoa and conularids. Species identification was not provided in Markewicz and Dalton (1977). In the upper part of the member, Markewicz and Dalton (1977) indicate that fossils occur with an asphalt-like hydrocarbon that occurs as clots or as an interstitial material in the dolomite. The fossils in the upper part of the Beaver Run have not been identified by Markewicz and Dalton (1977). During this study, the author identified burrows and gastropods in the lower half of the member (Figure 3.62). The middle part contains the planispiral gastropod, *Schizopea* and *Macularites* (Figure 3.63).

General Lithostratigraphic Description

The Beaver Run Member of the Ontelaunee Formation is approximately 33 m thick at the Harmonyvale type section in Harmonyvale, New Jersey (location 6 in Figure 3.2; Plate A.19 in Appendix A). The lower contact of the Beaver Run rests on a profound unconformity that severely eroded the underlying Lafayette Member. The lower beds of the Beaver Run Member vary along strike, from locally thick carbonate conglomerates to dark gray, medium to coarse grained, thin bedded, quartz vug and burrow bearing dolomitic limestone. Light gray, punky and porous cherts replacing domal algal are present at the Beaver Run contact (Figures 3.64 and 3.65). The along-strike facies gradations in the lower Beaver Run suggest that topographic relief on the Lafayette was exaggerated enough to support lateral shifts in facies being deposited on the paleokarst surface. The upper contact with the overlying Harmonyvale Member is dark gray, dolmicrite capped by shale. Medium gray to navy blue breccias, overlain by navy blue to robin's egg blue, pod shaped chert, line the unconformity truncating the member.

The Beaver Run Member is a medium to very dark gray, micritic to coarse grained (coarsely crystalline) dolomitic limestone and dolomite. The carbonate is strongly fetid and has a sulfurous and petroleum-rich odor when struck with a hammer. The lower part of the member is coarse grained, thickly bedded and contains quartz vugs in the lowermost part of the section. The section fines upward to micritic beds after a transitional zone of alternating thick beds of light vs. dark dolomites bearing punky and porous chert beds mid-section. Planispiral gastropods, *Schizopea* or some related form, were mapped during this study in the middle part of the member, in association with algal mounds and chicken-wire structures. Truncation of beds, overturned algal stromatolites and localized silcretization suggest the presence of several unconformities in the middle part of the member. The upper micrites are blue to medium gray, stylolitized (radiograph, cuspate and parallel forms) and contain conglomeratic and brecciated chert horizons. Porous and punky carbonates interpreted as being bored by gastropods are interbedded with thick, algal laminated beds that are intact and exhibit no porosity or other evidence of grazing.

General Chert Description

The base of the section is indexed by opaque black, waxy to mildly translucent, punky, porous, mildly convex chert replacing domal algal structures. These are associated with gastropod bearing dolomitic limestones and thin to thick beds of algal laminated, quartz-vug bearing dolomite. The base of the section is also characterized by vertical and horizontal burrow structures (Figure 3.66) and numerous gastropod bearing lenses; however, the burrow structures and gastropodal lenses are partially chert replaced and when silicified appear as irregular clots and stringers of chert. At other locations on

the New York recess, this interval is much thinner and characterized by the presence of alternating layers of silicified burrow and chicken-wire structures.

The burrowed cherts culminate at the second chert horizon, where hummocky, cherty intervals disrupt and control bedding, giving the outcrop an appearance of large, mound-like, structures. The cherts are lustrous black, mildly translucent and are associated with several unconformities. Sawed slabs show that the lower cherts of this horizon are silicified algal laminates, while the intermediate and upper cherts are silicified domal algal structures. Some cherty horizons are porous and punky, with silicified burrowed intervals present between the algal units. At other locations, the algal horizons are predominantly laminated types and the interbeds are silicified chicken-wire structures. The top of this series witnesses a return to silicified algal laminates that are locally interbedded with chicken-wire structures.

As indicated previously, the transitional beds of the Beaver Run are referred to as transitional due to the alternating light and dark color of the carbonates. Correspondingly, the cherts are lighter in color. Clots and wisps of chert, which range in color from black to navy blue, to blue gray are located in thickly bedded dolomite bearing burrows, intraformational conglomerates, and stylolites. Overlying the chert-clot interval are cherts thinly interbedded with horizons bearing chicken-wire structures. Upon close inspection of sawed slabs, the cherts appear finely laminated and replace domal algal and chicken-wire structures. Locally, the silicified domal algal contain an abundance of euhedral quartz crystals, concentric layers and lenses of white quartz, and thick druses of quartz lined vugs. Interestingly, most of the cherts in the transitional horizon are porous

and punky. Close inspection of the porous structures show two types, one hexagonal or geometric in form; the other circular.

The uppermost succession of cherts, in close proximity to the unconformable upper contact, are brecciated and resealed with a later generation of chert. Slabs and thin sections reveal abundant euhedral dolomite grains within this series of cherts. Slabs reveal that the cherts consist largely of algal laminate fragments, which can easily be refitted back together. This succession of cherts is not porous or punky, but more homogeneous than the lower series. The entire section is strongly stylolitized with radiograph stylolites. Many of the chert beds and pods are opaque towards lower and upper bedding contacts and mildly translucent towards the center. Slabs reveal fine laminations, or populations of cuspate and parallel stylolites near bedding contacts. Occasional bedding plane surfaces reveal micaceous clays.

Discussion of Changes in Stratigraphic Definition

The Beaver Run Member, as defined in this study, does not vary significantly from the description provided by Markewicz and Dalton (1977). A consistent theme of this study has been the elucidation of unconformities defining member contacts; this member is no different. Markewicz and Dalton (1977) do not describe the nature of the Beaver Run contacts. A major unconformity exists between the Lafayette and the Beaver Run and along-strike facies changes in Beaver Run beds along that unconformity suggest significant topographic relief imparted upon Lafayette beds. Chert beds are recognized by Markewicz and Dalton, however they only describe them as being, "…as much as ten feet thick". The cherts of the Beaver Run Member are varied in form and very abundant throughout the unit. The chert stratigraphy provided by this study allows observations of

the many different types of structures preserved by silicification (i.e. burrows, stylolites, algal structures, chicken-wire structures, fossils), which contributes to our understanding of depositional environment (Chapter 4 of this dissertation), as well as elucidating cherts unique enough to be used as mapping aids. Finally, Markewicz and Dalton estimate that the Beaver Run Member ranges from 46 to 61 m in thickness. This study estimates a 33 m thickness for this member, which is slightly thinner than previous estimates. Personal communication with Markewicz (1986) at the Beaver Run section at Illif Lake, New Jersey indicated that the Beaver Run rocks at Illif Lake were in a continental shelf setting, whereas the Harmonyvale type section utilized in this study was situated closer to land. Thickness variations highlighted by the two studies would be consistent with a thickening sediment wedge towards the continental shelf edge.

3.4.19 Ontelaunee Formation: Harmonyvale Member

Faunal Content

Fossils identified by Markewicz and Dalton (1977) in the Harmonyvale Member include algal laminations and stromatolites, gastropods, brachiopods and trilobites.

General Lithostratigraphic Description

The Harmonyvale Member of the Ontelaunee Formation is 32.5 m thick at the Harmonyvale type section in Harmonyvale, New Jersey (location 6 in Figure 3; Plate A.20 in Appendix A). The lower contact with the underlying Beaver Run Member is the upper surface of the navy blue, pinch-and-swell chert that caps the underlying member (Figure 3.67). The contact is unconformable, with a number of unconformities occurring in the beds near the contact. The upper contact with the overlying Jacksonburg

Limestone is unconformable and thick, chert replaced algal laminate is sandwiched between blue micritic dolomites which weather white in outcrop (Figure 3.68).

The Harmonyvale Member is easily distinguished from the underlying Beaver Run Member by its chalky white patination and the presence of deeply incised solution cleavage. The member is medium gray to blue, thickly bedded, micritic dolomite that is pervasively stylolitized (radiograph and vertical) and contains abundant chert, brecciated and algal laminated horizons, chicken-wire structures and quartz vugs. The micritic dolomite grades up-section into dolomitic limestone which includes very thick beds of chert, ranging from dark navy blue to bright robin's egg blue, to light blue gray. The member houses several unconformities in addition to the ones at the lower and upper contacts.

General Chert Description

The first succession of cherts at the base of the section is deep blue, bright sky blue, to robin's egg blue, brecciated cherts. Chert clasts within the breccia are tightly welded, leaving very little interstitial space for matrix or cement (Figure 3.69). Fragment edges are welded together and slabs reveal that the clasts are silicified chicken-wire structures and algal laminae. The chert breccias persist along strike for tens of meters then gradually shift facies into fine grained, dolmicrites. The base of the section at other locations is occupied by a succession of silicified domal algal horizons. The silicified algal are overlain by porous, punky, bright blue chert sandwiched between two thick chert breccias. The entire section is penetrated by radiograph stylolites and unconformities.

There are several types of chert in the second series. The basal chert is a billowy, light blue chert underlying an unconformity bound section that is lined with dark blue chert breccias bracketing a punky, porous, light blue chert horizon (Plate A.20 in Appendix A). Another dark blue chert breccia overlies the unconformities in this section; however, the chert clasts differ from the underlying breccias in that they are punky and porous. Brecciated cherts are replaced by a light blue, chert pebble conglomerate overlain by light gray, silicified algal laminates. The next few chert beds are punky and porous and contain sparse algal laminations. The light blue, chert pebbles occur again, sandwiching a silicified algal mound horizon. Chert replaces the algal mounds and forms a chert layer directly underneath the algal mound structures. Overlying the algal mound horizon are silicified algal laminations and burrow structures. The upper part of this series has a repetition of the punky and porous chert and silicified algal laminations. A chert breccia is interbedded with the punky and porous beds, in proximity to another unconformity bearing horizon. Capping this series are chert-pod horizons that exhibit a dark blue center surrounded by a lighter colored, light blue chert rind. This chert horizon is also in close proximity to an unconformable horizon. The entire chert series is stylolitized.

The third succession of chert is present at other locations and includes four closely spaced, mildly convex, chert horizons. The stratigraphic succession is an algal laminated, micritic dolomite that is partially silicified; entire beds of the dolmicrite are silicified, whereas the interbeds escaped silicification. There is one series of chert breccias, the angular fragments are so tightly welded that little or no matrix or cement occurs. Slab inspection of the breccia reveals that clasts are silicified chicken-wire

structures and relict, palmate anhydrite structures, similar to those described by (Shearman and Fuller, 1969). This series of chert replaced algal, with associated chert breccia, is capped by a series of thickly bedded, algal laminated, micritic dolomites containing abundant quartz vugs. The section is laced with strong radiograph stylolites. Vertical pressure solution cleavage creates a vertical ribbing through the beds.

The uppermost cherts are three, thinly developed horizons which occur in order as: a lower, porous, punky, light blue, chert replaced algal laminated unit; a thicker accumulation of chert replaced, punky domal algal structures; and a mildly convex series of dark blue, chert replaced algal units. All of these are couched between strongly siliceous, blue gray, algal laminated, dolmicrite. The entire series is laced with radiograph stylolites and close spaced, vertical ribs of pressure solution features. Sawed slabs of the ribbed section reveal a generation of pressure solution cleavage which is lined with quartz, alternating with cleavage that is somewhat more deficient in quartz, creating the alternating high and low relief pattern seen in the field (i.e., similar to an accordion). At other locations on the New York recess, the Harmonyvale is a very thick succession of dark, navy blue, to robin's egg blue, to highly translucent light blue gray, chert replaced chicken-wire structures.

Discussion of Changes in Stratigraphic Definition

Lithologically, the Harmonyvale Member of the Ontelaunee Formation, as depicted in this study, varies very little from Markewicz and Dalton's (1977) definition of the Harmonyvale Member. Markewicz and Dalton do define the upper contact of the formation as being unconformable, with the unconformity removing the Harmonyvale Member at various locations in northern New Jersey to have the Jacksonburg Limestone

being deposited on the Beaver Run Member. This study agrees with the unconformable upper contact interpretation (and suggests an unconformable lower contact as well), but the unit has escaped severe erosion in the Hamburg quadrangle. Markewicz and Dalton acknowledge the presence of one chert bed in the member; however, this investigation detailed several chert types, which grouped naturally into four horizons that were persistent along strike in the existence of chert, but changed along strike in form and replacive mechanism. Thickness estimates provided by Markewicz and Dalton claim the unit is greater than 67 m thick; however this study suggests a 32 m thickness in the dissertation study area. Discrepancies in thickness can be accounted for by erosion of the member due to the unconformity at the upper contact.

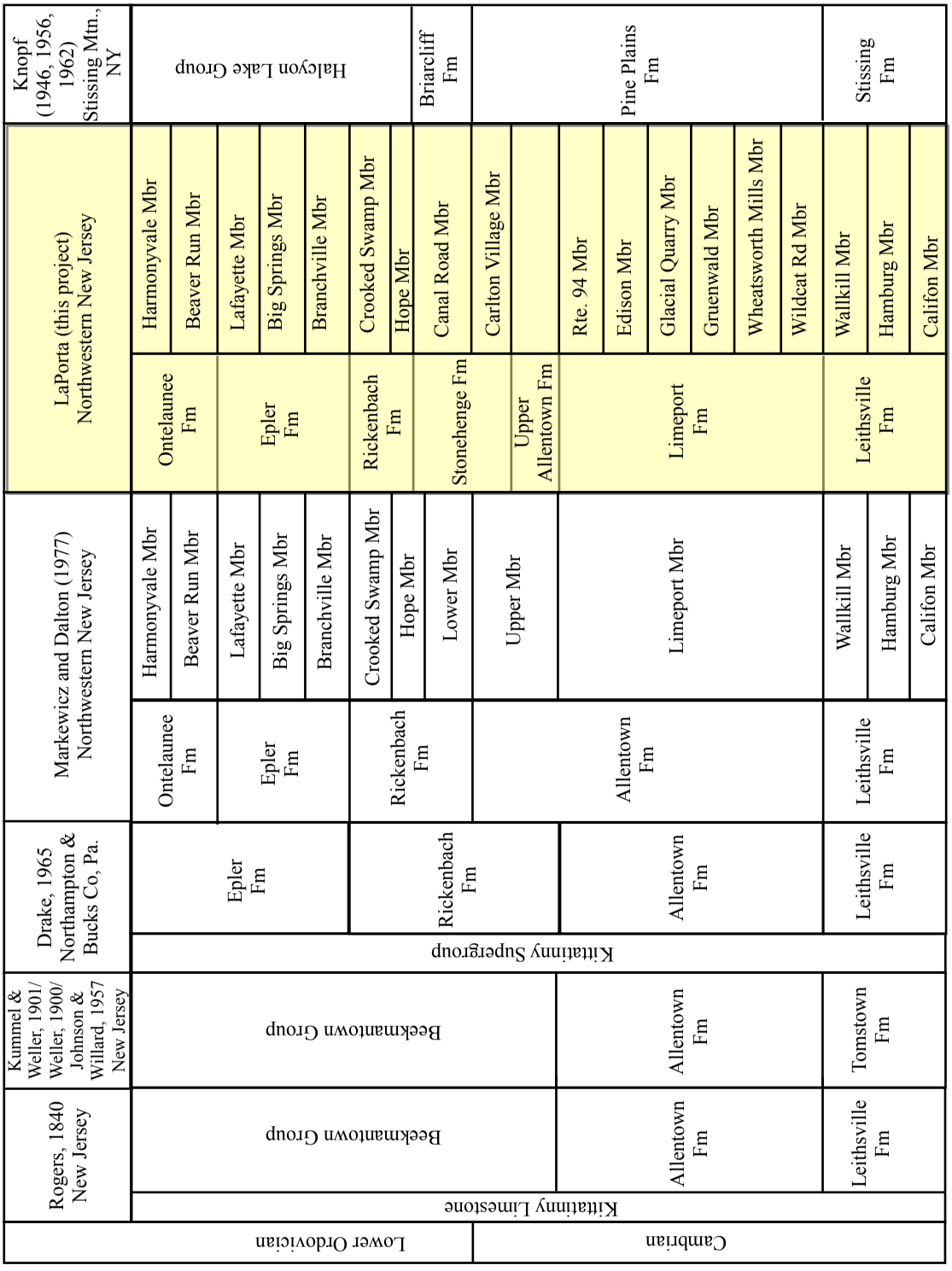


Figure 3.1: Evolution of the naming of the Kittatinny Supergroup, Sussex County, New Jersey.

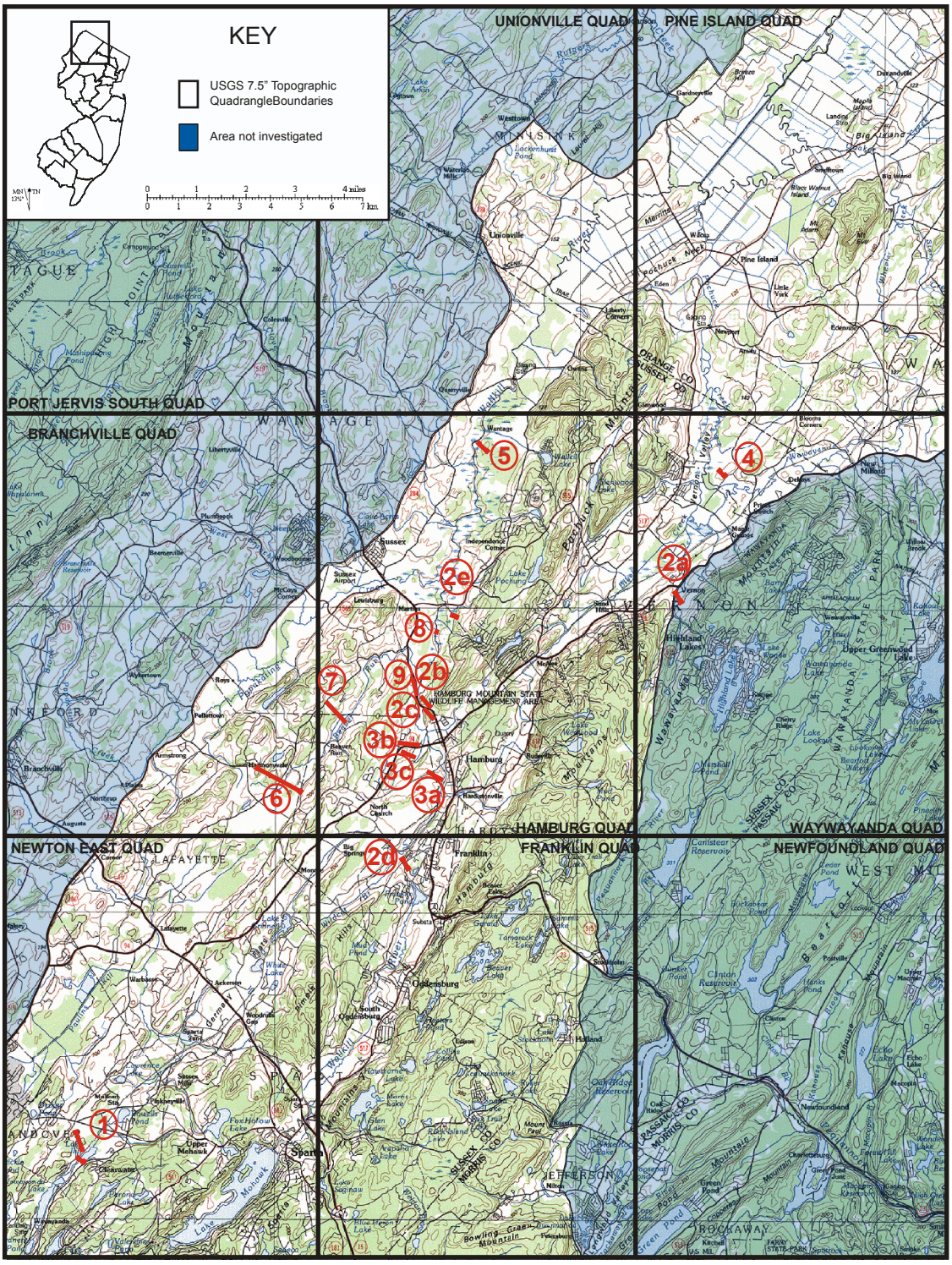


Figure 3.2. Location map of study area for the dissertation, the Hamburg and contiguous 7.5' quadrangles of the Wallkill River Valley of northwestern New Jersey and southeastern New York, USA. Red lines indicate traverses: (1) Lake Iliff; (2a) Vernon Rt. 515; (2b) Raia Quarry; (2c) S. Pochuck Mt; (2d) Wildcat Road; (2e) Chase Farm; (3a) Wheatsworth Road; (3b) Rt. 94; (3c) Glacial Quarry; (4) Canal Road; (5) Rock Island; (6) Harmonyvale; (7) Beaver Run Aggregate; (8) Dump Site; and (9) Rte. 23.

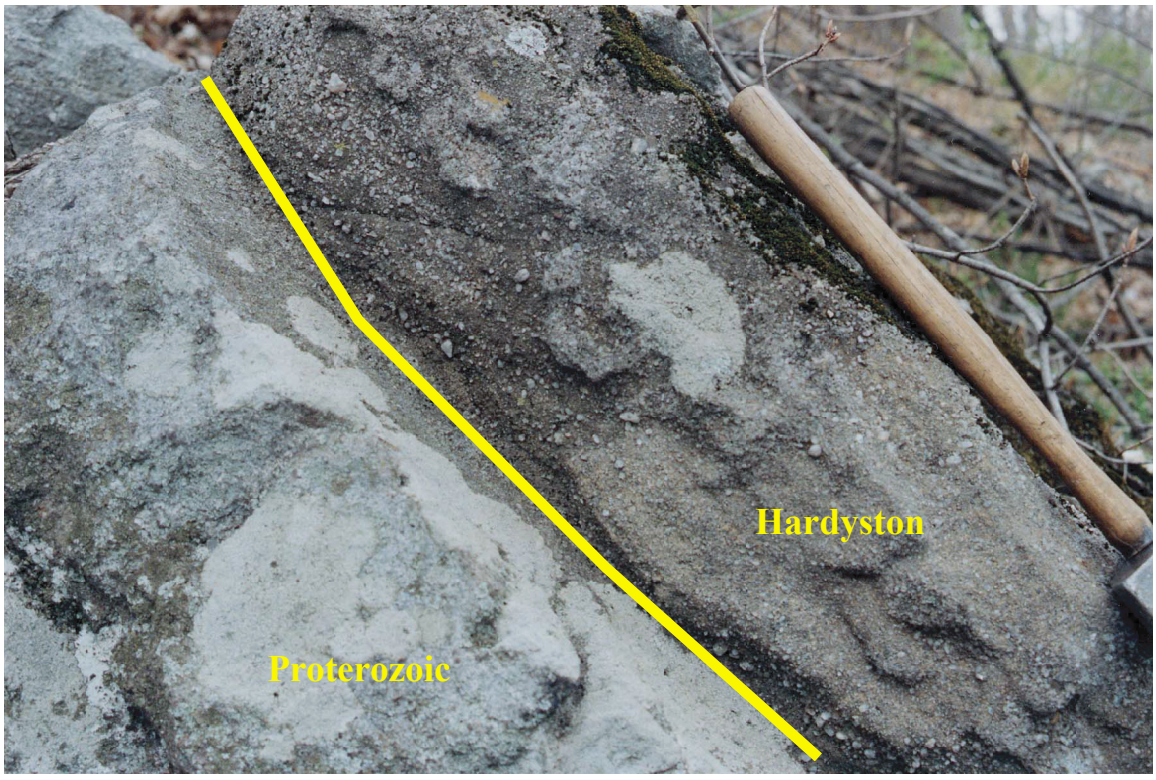


Figure 3.3 - Proterozoic saprolite in contact with Hardyston arkose (Ch_1), Wildcat Road.



Figure 3.4 - Hardyston Formation. Outcrop photograph of cross-bedded sand units, Wildcat Road section.



Figure 3.5 - Califon Member. Shaley dolomite at Rte. 515 section.



Figure 3.6 - Hamburg Member. Mudcracks on the top of the Hamburg Member at the Rte. 515 section.



Figure 3.7 - Califon Member. Outcrop photograph of spahelerite clot, Rte. 515 section.



Figure 3.8 - Califon Member. Outcrop photograph of calcite clot, Rte.515 section.

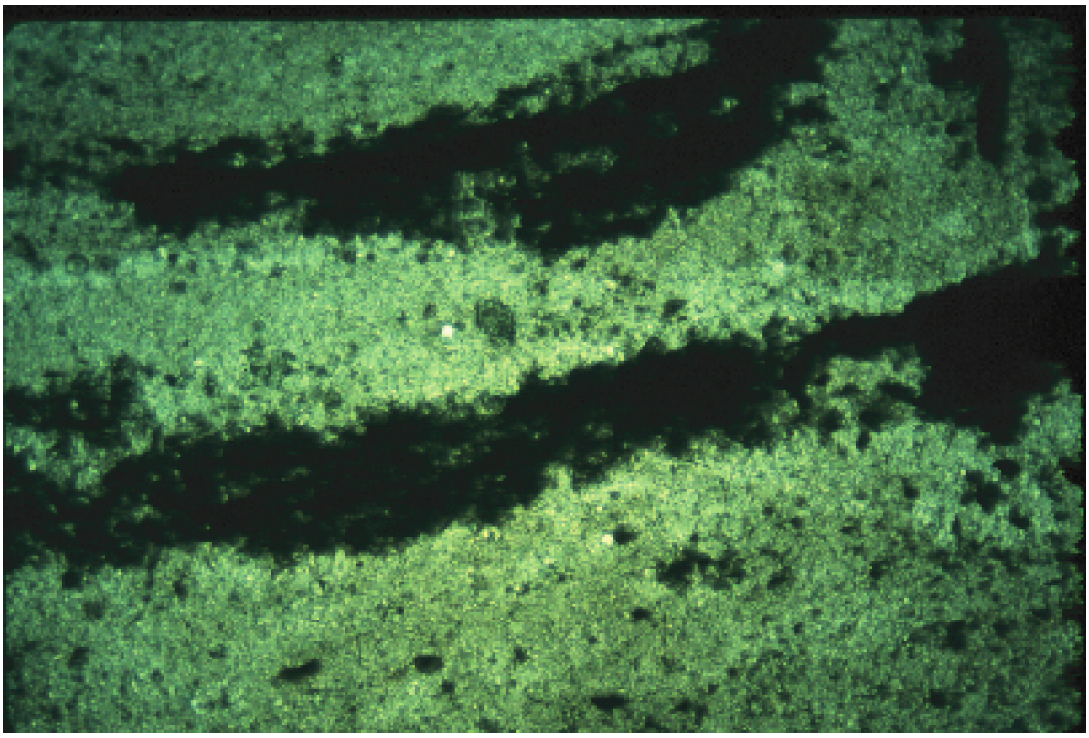


Figure 3.9 - Califon Member. Thin section showing opaque layers inferred as carbonaceous layers in stromatolite.

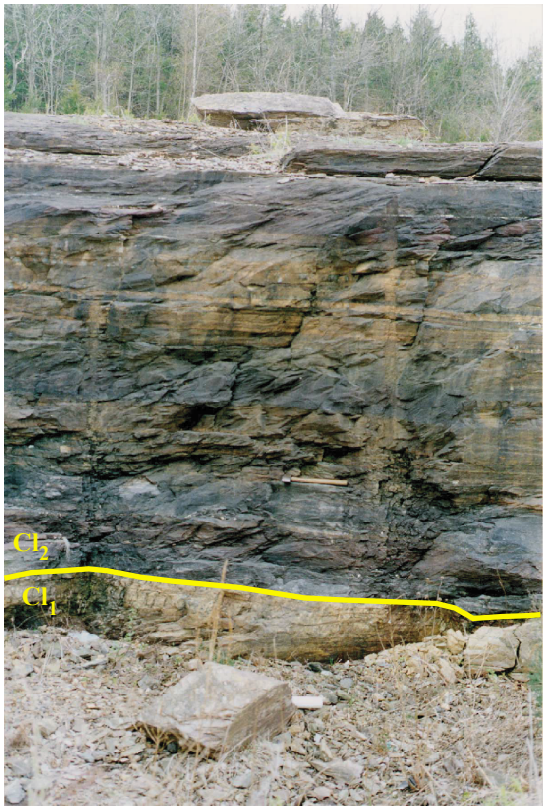


Figure 3.10 - Rte. 515 section showing Califon (Cl_1)/Hamburg (Cl_2) contact.



Figure 3.11 - Hamburg Member. Outcrop of arkosic sandstone weathering as pedestals rising from low areas.

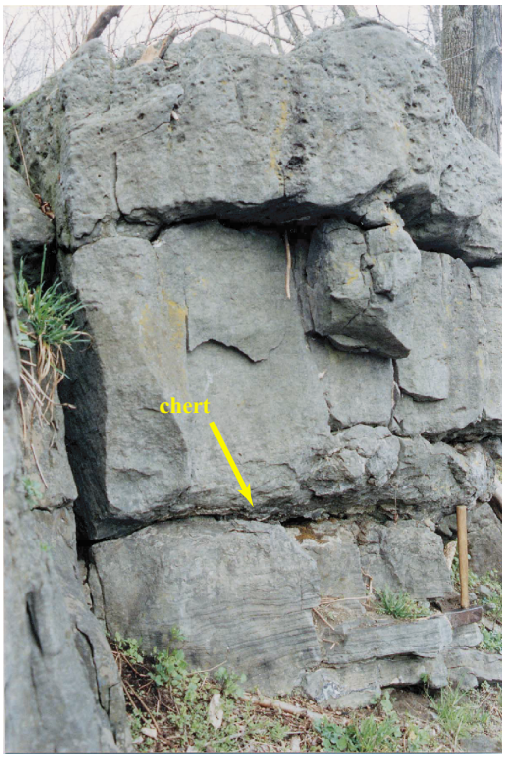


Figure 3.12 - Wallkill Member. Outcrop of silicified algal stromatolites also showing blocky appearance and pitting (towards top of outcrop) of weathered profile. Recessed areas are shale.



Figure 3.13 - Wallkill Member. Outcrop of algal laminated unit showing close-up of thumb-print weathering profile. Margaret's Estate section.

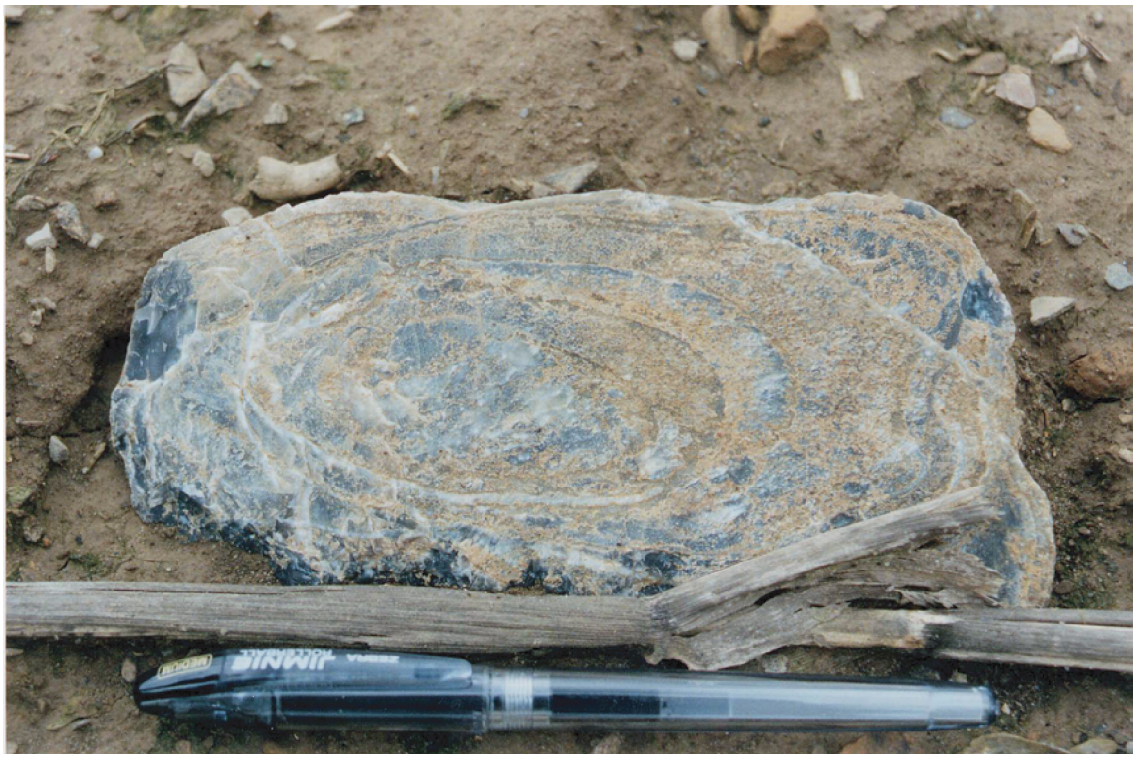


Figure 3.14 - Wallkill Member. Chert replaced stromatolite in the lower algal horizon, a.k.a. "Rudinski Pod", Rudinski Farm traverse.



Figure 3.15 - Wallkill Member. Chert replaced domal algal with laminate bedding plane extensions, upper algal horizon. Margaret's Estate traverse.



Figure 3.16 - Wallkill Member. Chert replacing domal algal, showing outer concentric layers and criss cross ribbing.

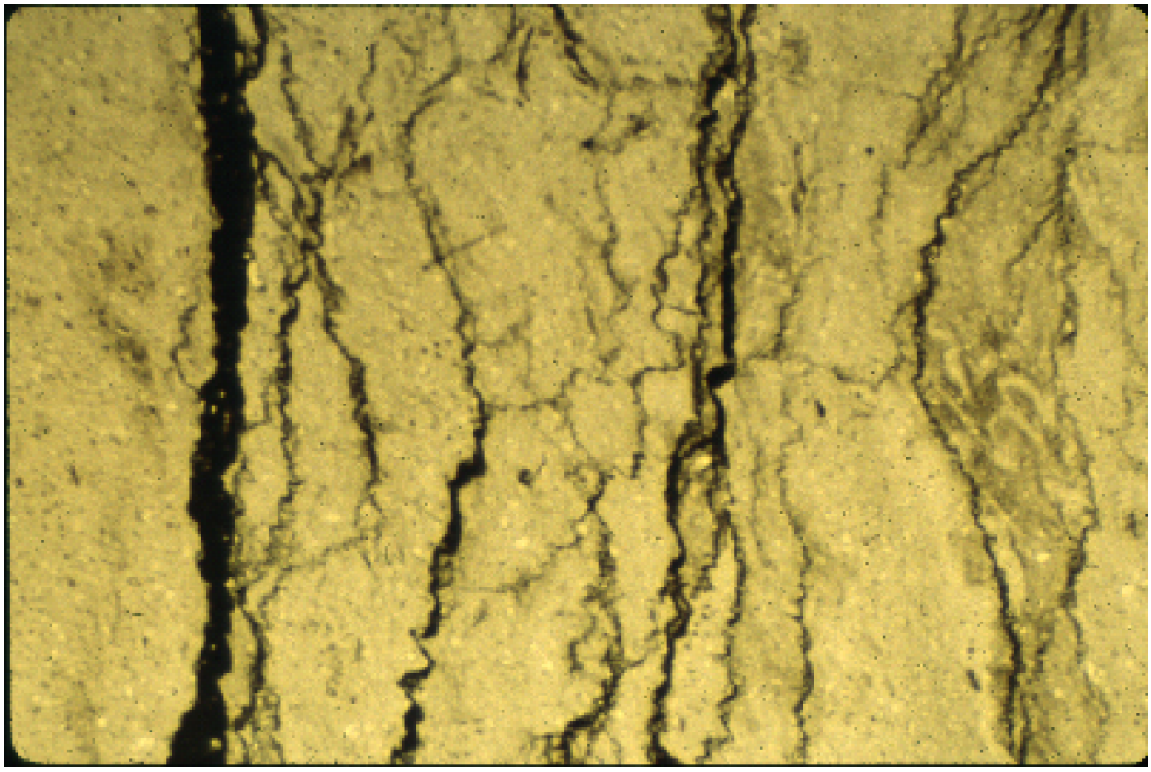


Figure 3.17 - Generic picture of thin section showing stylolites. Dark material in stylolites is inferred to be insoluble residue, such as clay.

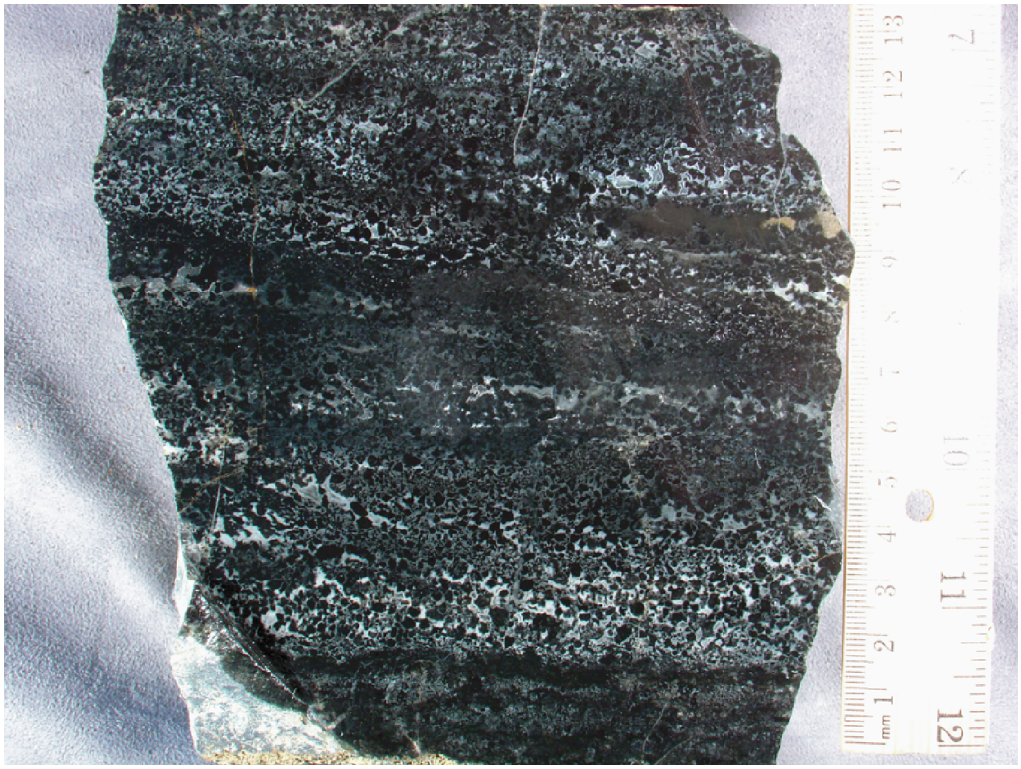


Figure 3.18 - Wallkill Member. Sawed slab showing silicified ooids, pisoids and intraclasts.



Figure 3.19 - Wallkill Member. Sawed slab showing silicified domal algal. The center of the chert pod contains homogenous chert concentrically wrapped in alternating black and gray chert.

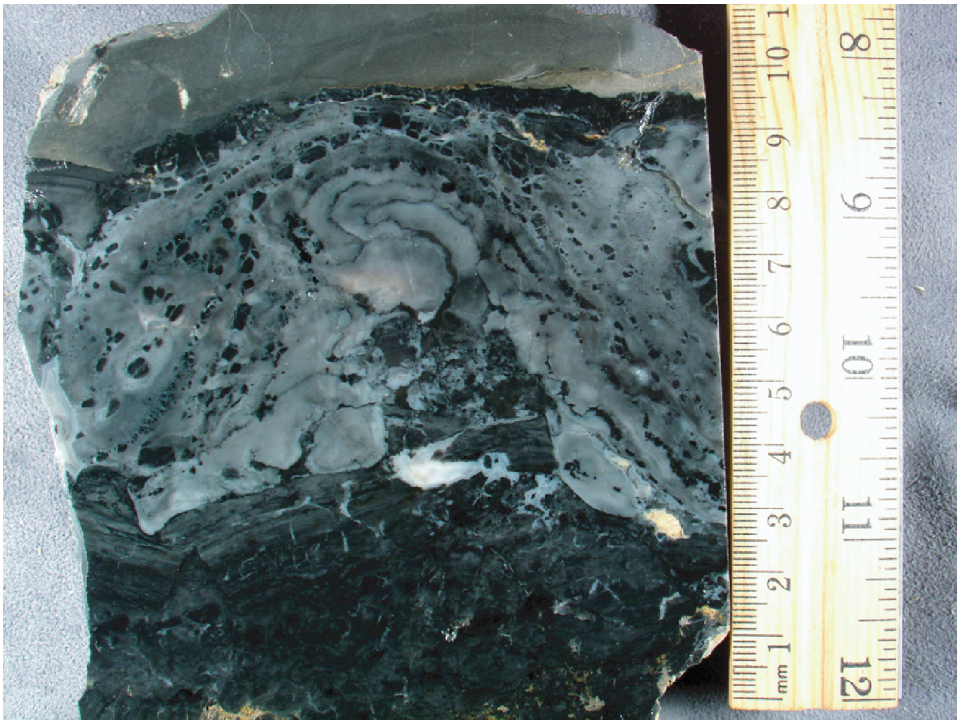


Figure 3.20 - Wallkill Member. Sawed slab of chert preserving tightly folded structures of enterolithic form.

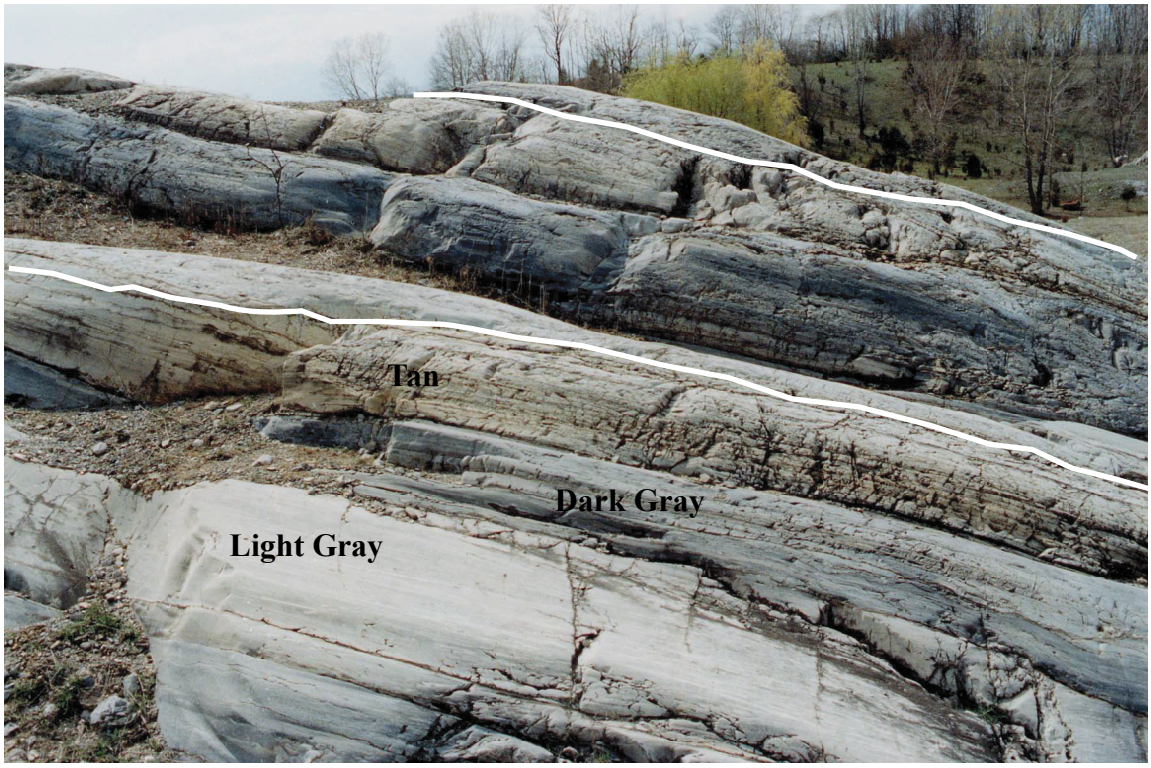


Figure 3.21 - Wildcat Road Member. Outcrop shows the repetitive light gray-dark gray-tan color banding that is useful as a mapping aid.



Figure 3.22- Wildcat Road Member. Typical outcrop illustrating color banding.

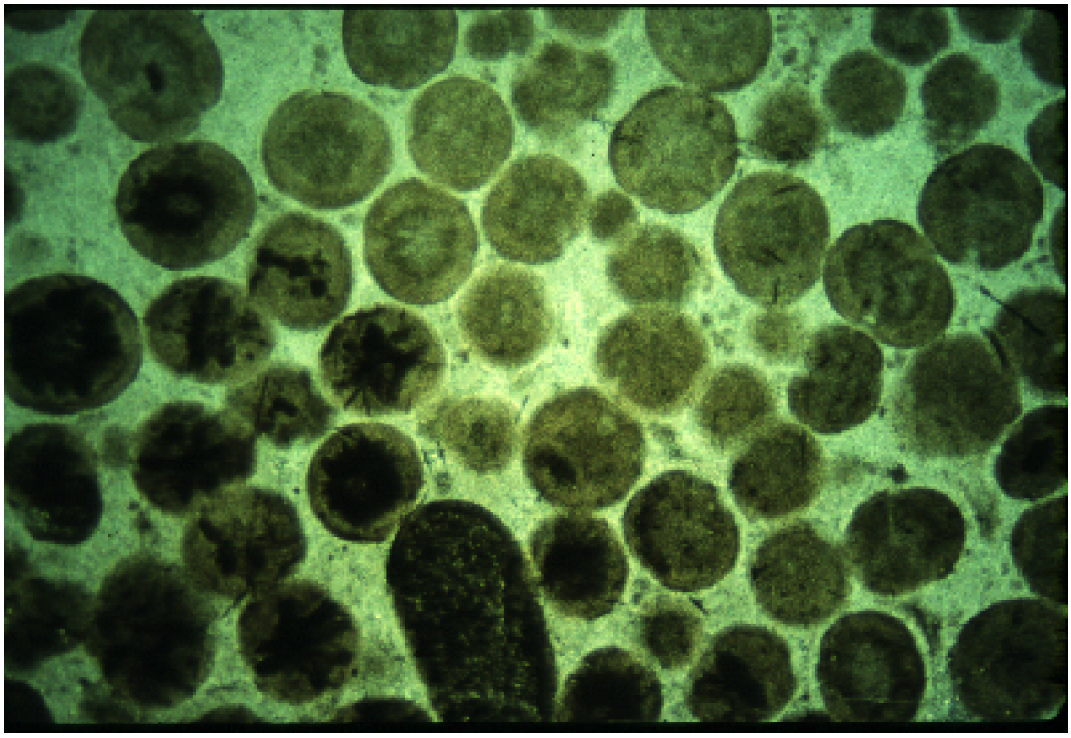


Figure 3.23 - Wildcat Road Member. Thin section of radial oolites of Cambrian age.

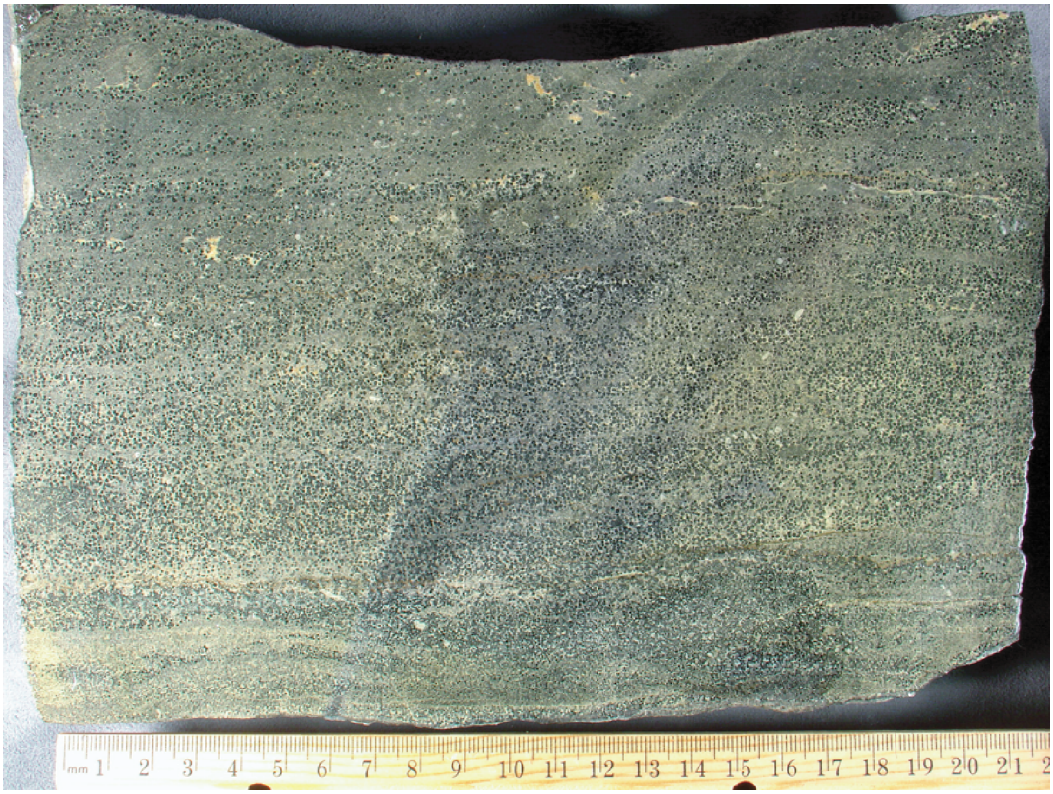


Figure 3.24- Wildcat Road Member. Sawed slab of silicified oolite, the stratigraphically lowest chert horizon in the Wildcat Road Member.

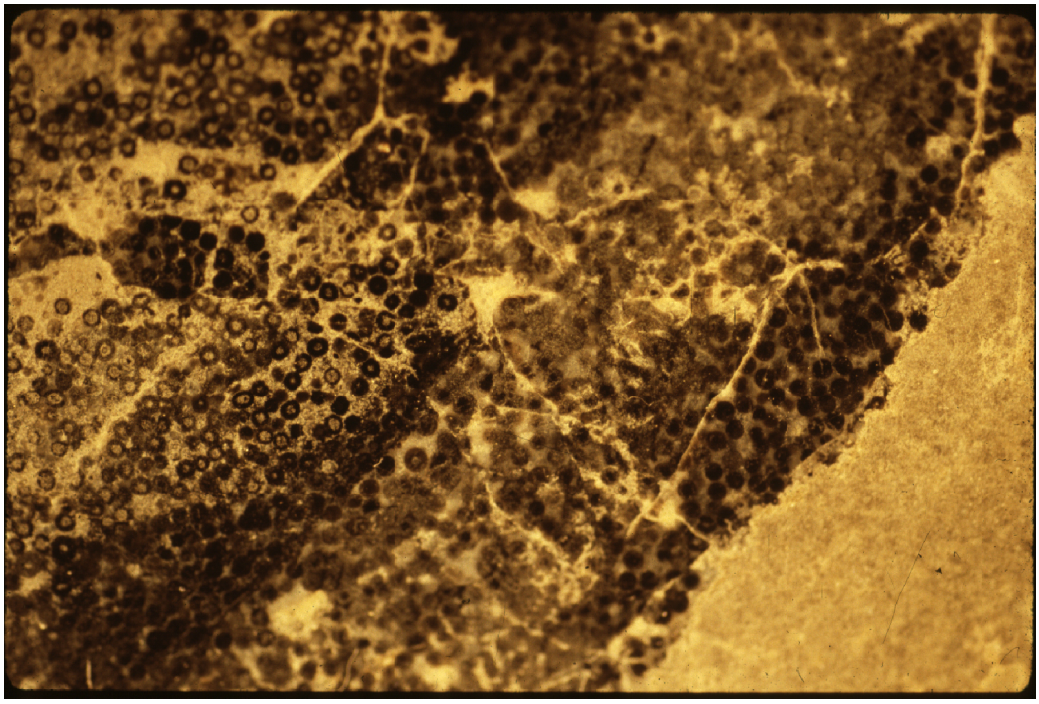


Figure 3.25 - Wildcat Road Member. Thin section showing pressure solution of ooids. Ghosts of dissolved ooids are in light area at bottom right of photograph. Decreasing amount of pressure solution occurs towards upper left corner.

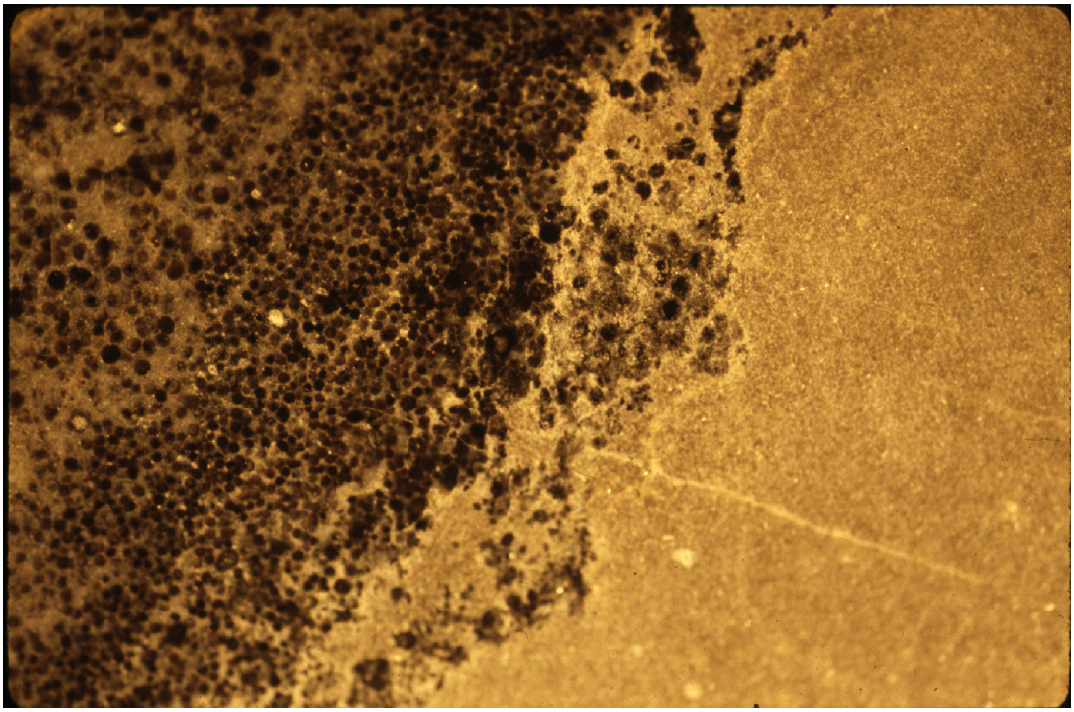


Figure 3.26 - Wildcat Road Member. Thin section showing another example of pressure solution of ooids.

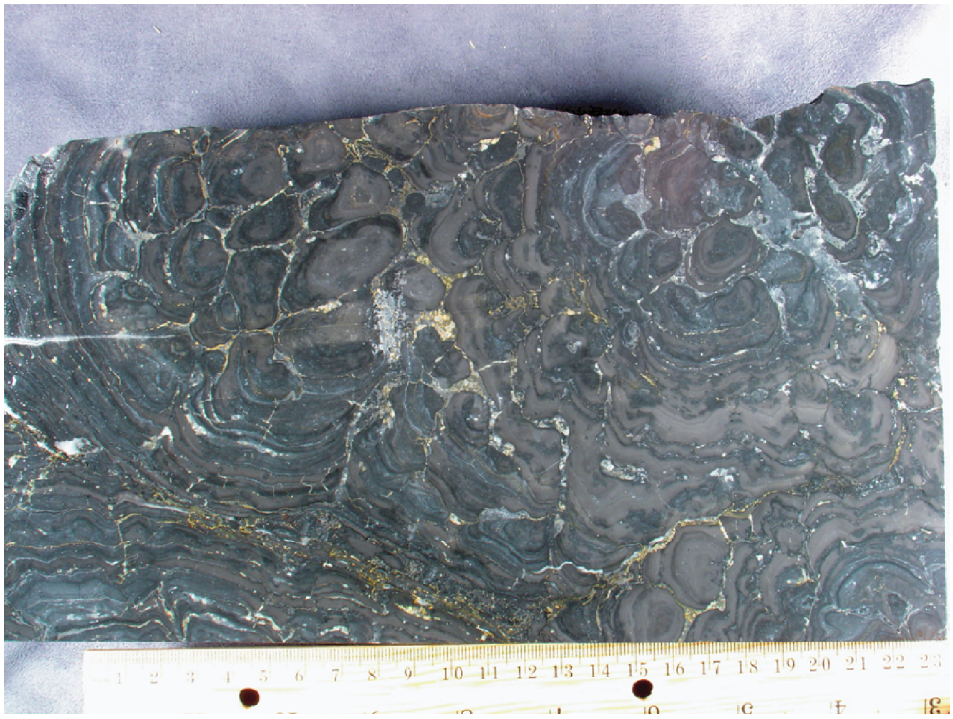


Figure 3.27 - Wheatsworth Mills Member. Sawed slab showing colonial, cauliflower shaped algal.

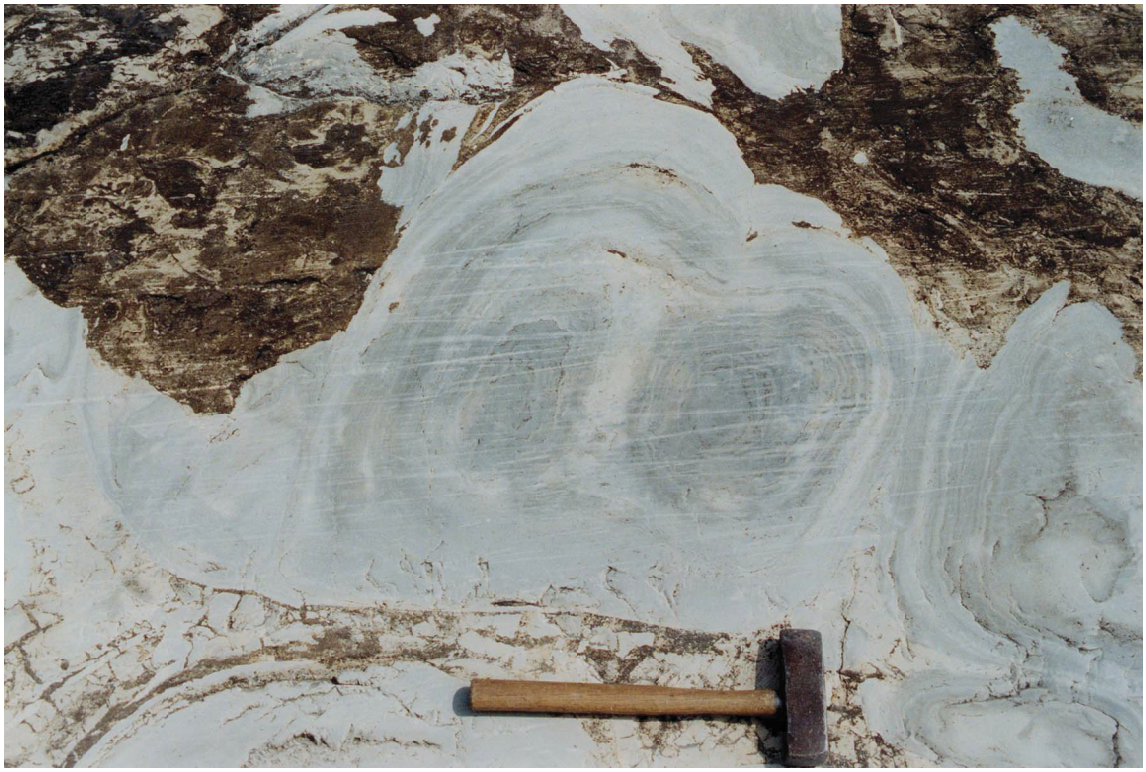


Figure 3.28- Wheatsworth Mills Member. Accumulations of domal algal boundstone with mud cracked, baffle filling micrites.

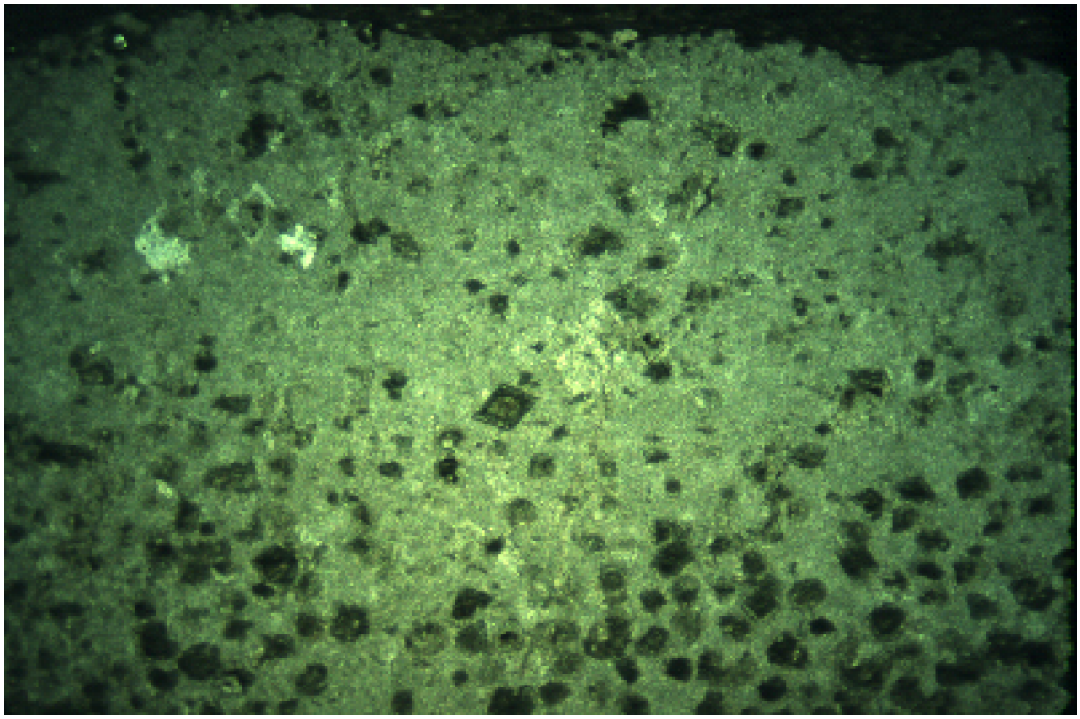


Figure 3.29 - Wheatsworth Mills Member. Thin section showing silicified ooids that were micritized and dolomitized prior to silcification.

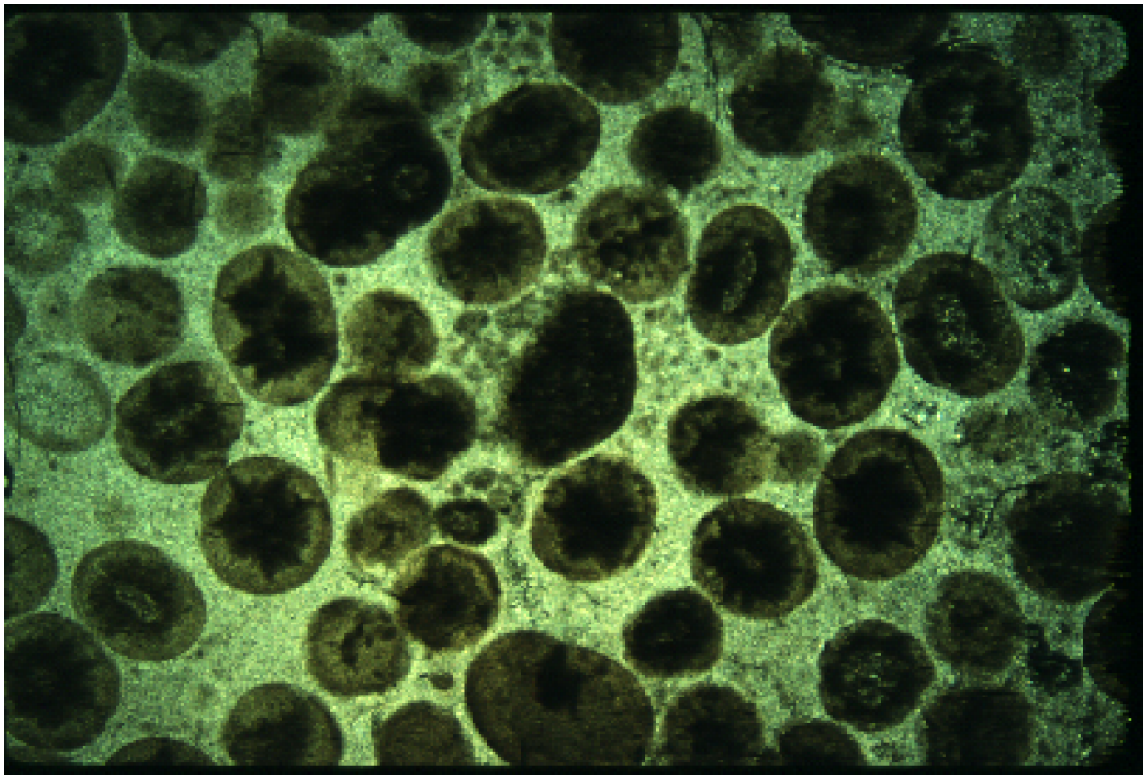


Figure 3.30 - Gruenwald Member. Silicified ooids.

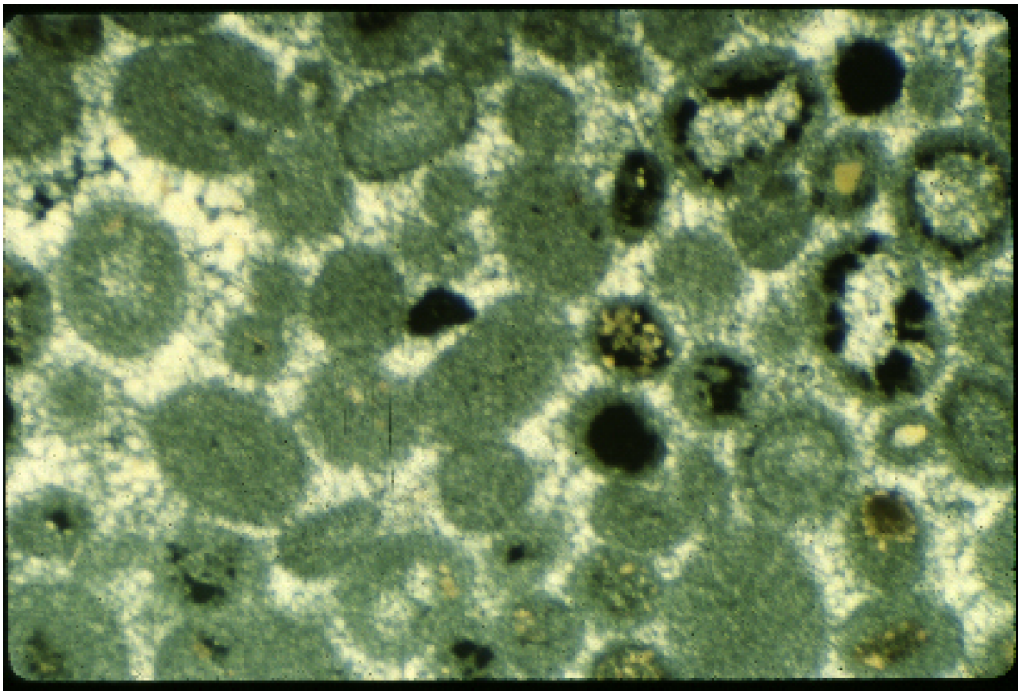


Figure 3.31 - Edison Member. Thin section showing selective silicification of ooids. The outer algal rinds are silicified and the inner core is micritized.

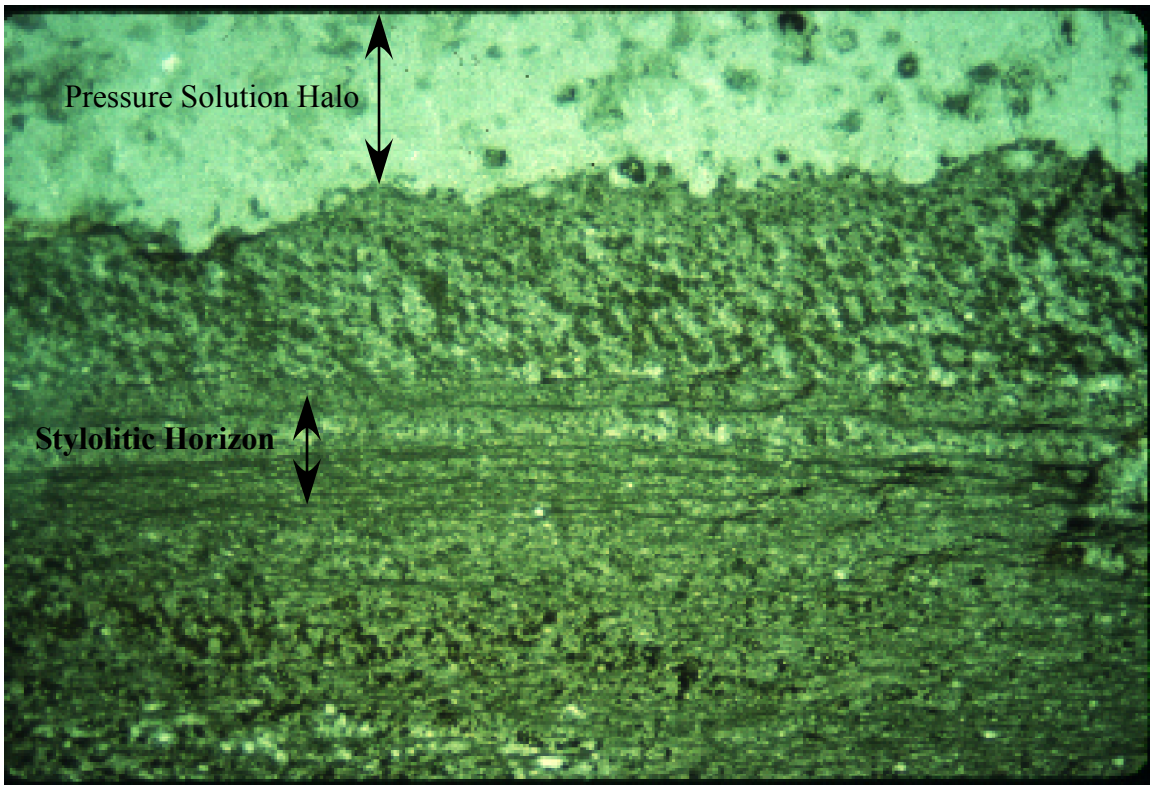


Figure 3.32 - Edison Member. Thin section showing pressure solution halo in close proximity to stylolites lined with opaque, insoluble materials.

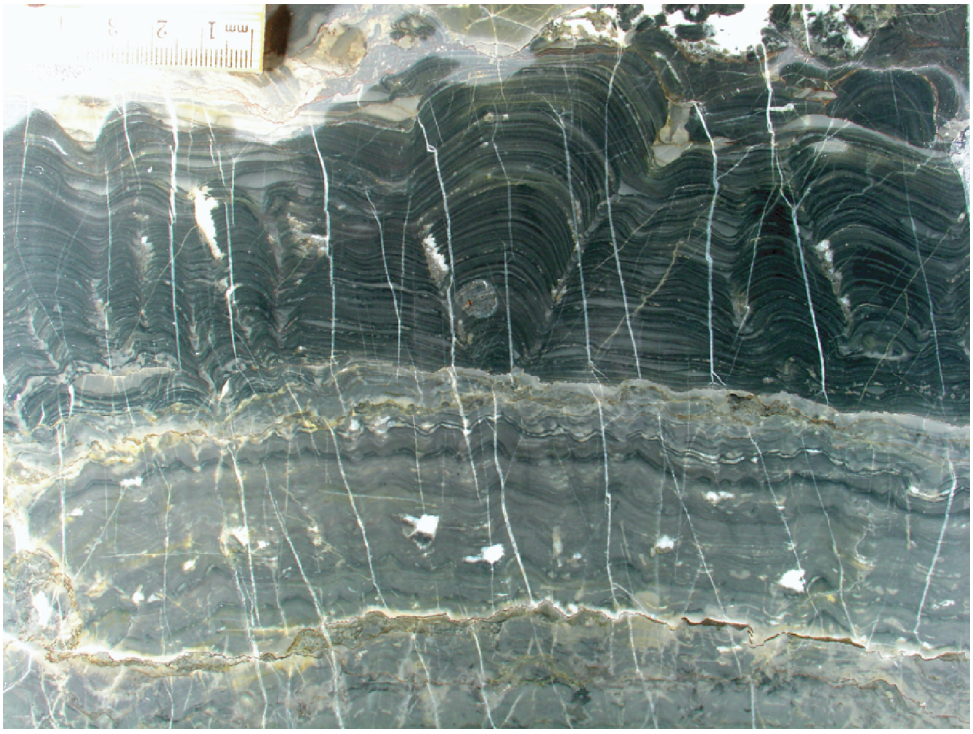


Figure 3.33 - Rte. 94 Member. Sawed slab showing silicification of organic features, such as algal laminatates and domal algal.

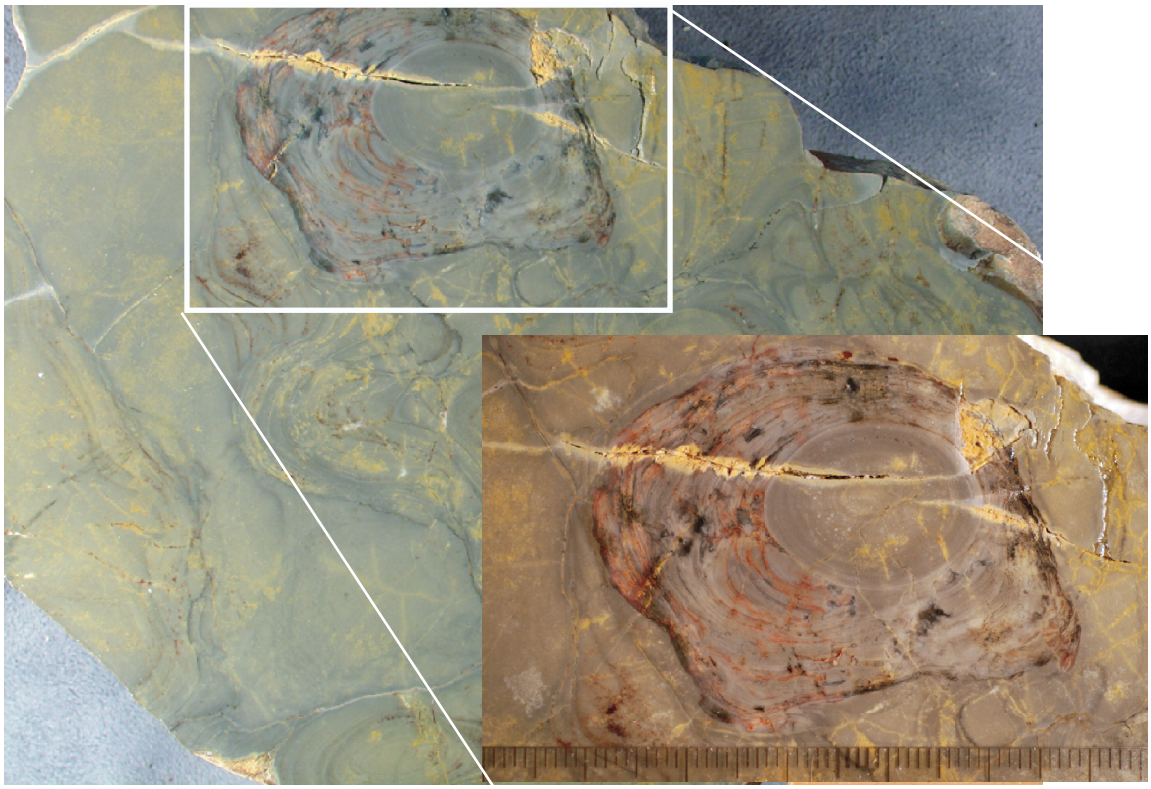


Figure 3.34 - Upper Allentown Formation. Sawed slab showing circular algal stromatolite that makes a first appearance in the Kittatinny Supergroup in the Upper Allentown Formation.

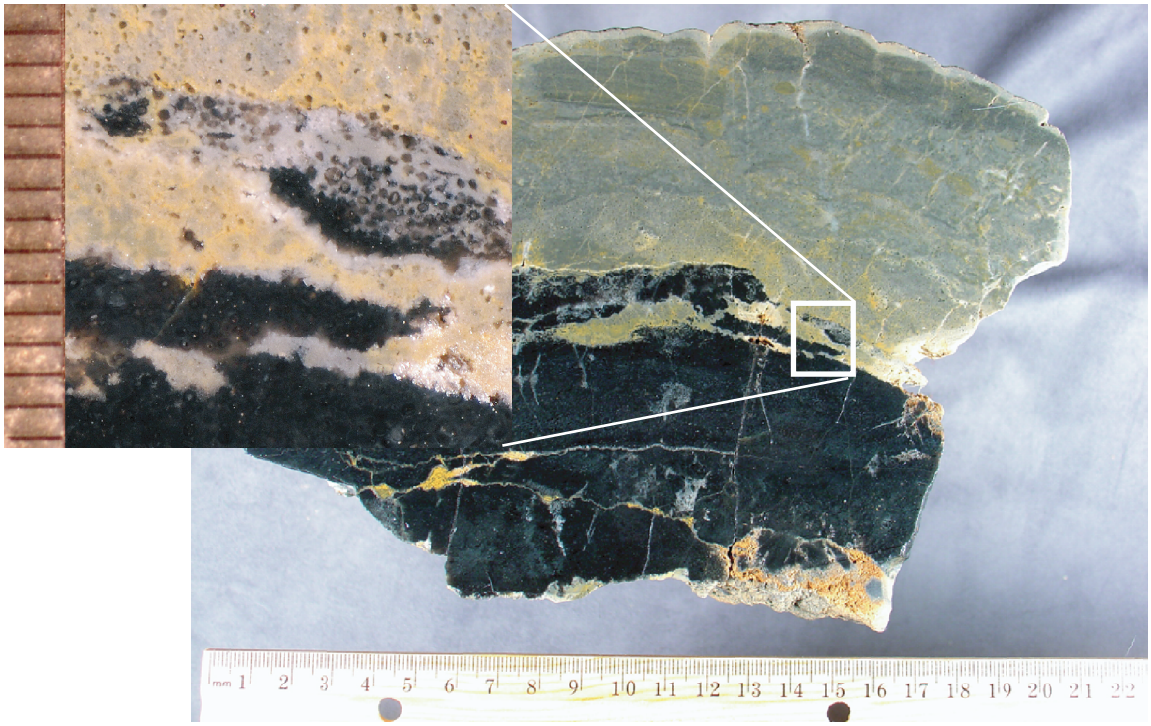


Figure 3.35 - Upper Allentown Formation. Sawed slab showing silicified ooids, pisoids and quartz sand.



Figure 3.36 - Upper Allentown Formation. Sawed slab showing silicified intraclasts.



Figure 3.37 - Canal Road Member. Thin and thick quartz sandstones at the base of the Canal Road Member. Harmonyvale section.

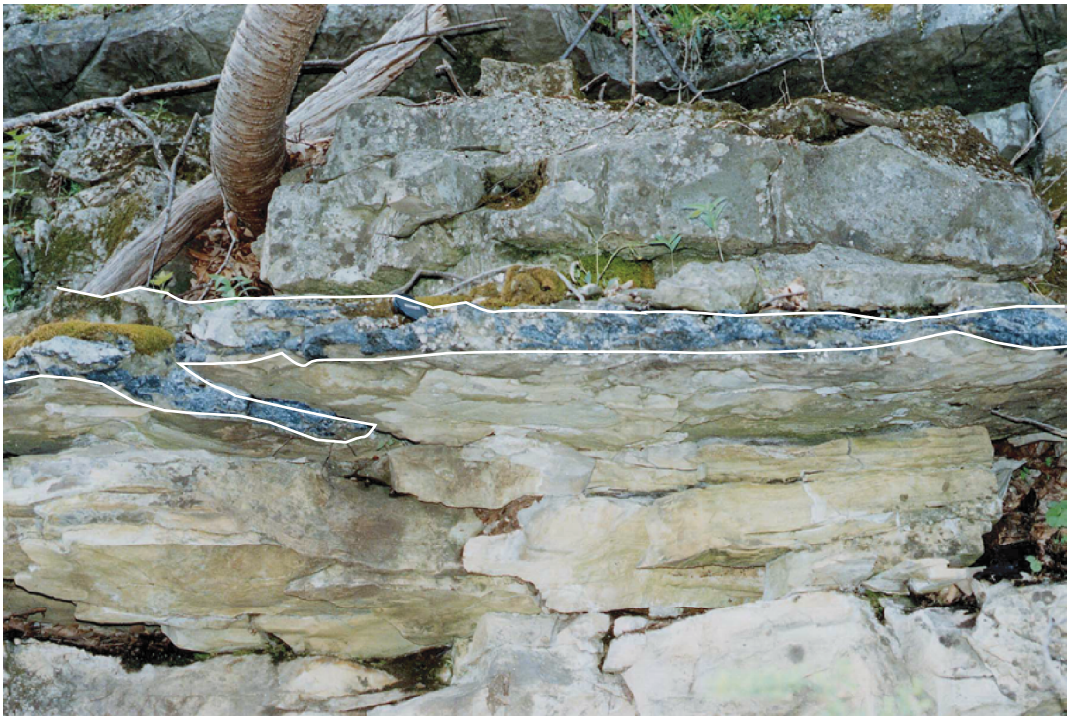


Figure 3.38 - Canal Road Member. Lower brecciated chert replacing quartz sandstones. Harmonyvale section.

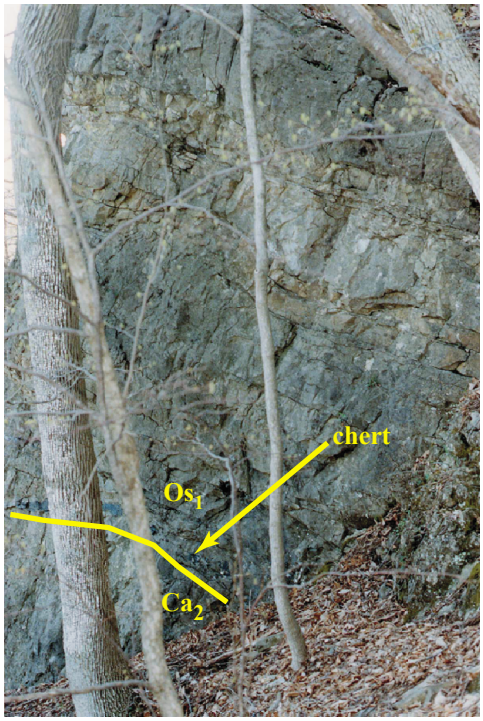


Figure 3.39 - Carlton Village Member (Os_1). Chert breccia at contact with the Upper Allentown Formation (Ca_2). Harmonyvale section.

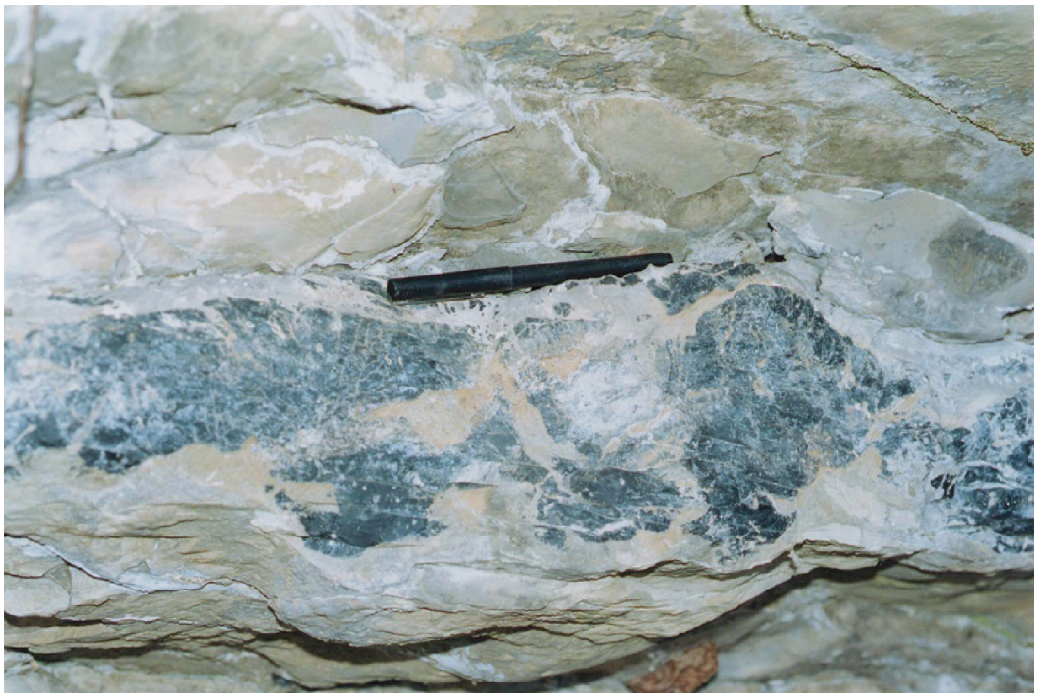


Figure 3.40 - Carlton Village Member. Close-up outcrop photograph of the chert brecciat at the base of the Carlton Village Member. Canal Road section.

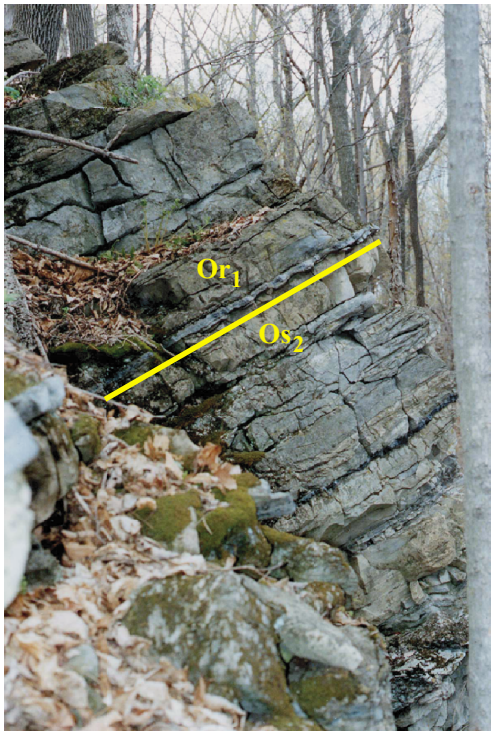


Figure 3.41 - Canal Road Member. Contact between the Canal Road Member (Os2) and the Hope Member (Or1) of the Rickenbach Formation. Harmonyvale section.



Figure 3.42 - Hope Member. Lower contact of the Hope Member on ripple marks and scour-and-fill channels. Chert replaces quartz sandstones. Harmonyvale section.

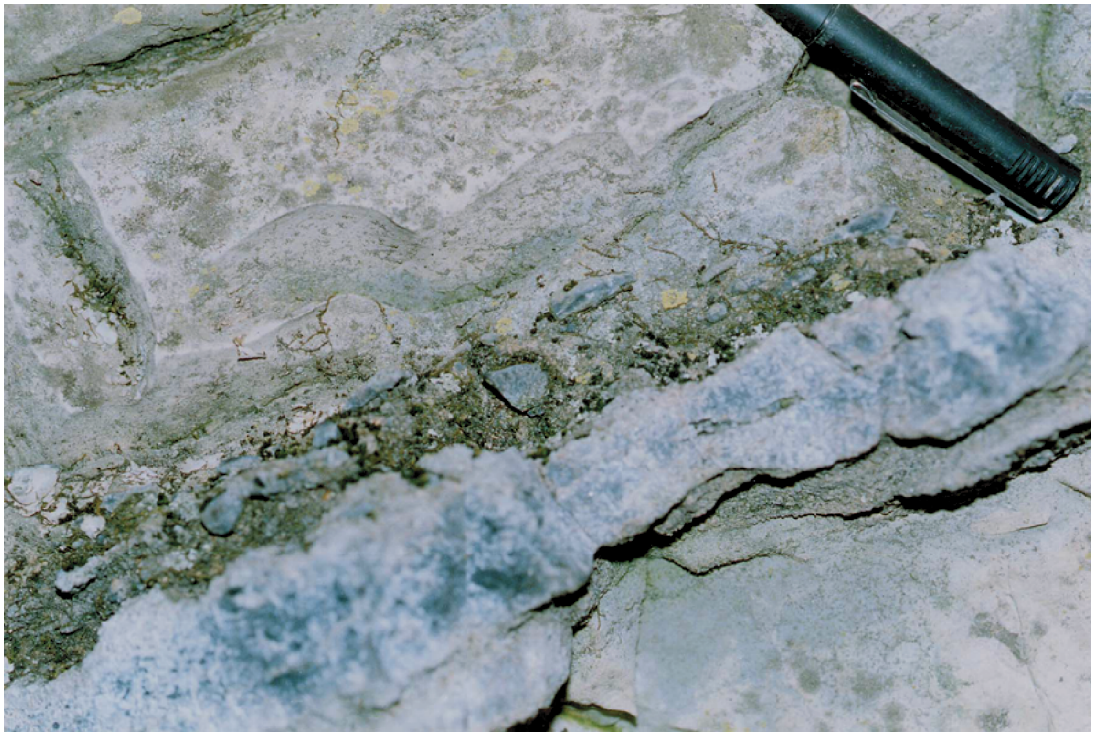


Figure 3.43 - Hope Member. Close-up of Figure 3.42. Outcrop photograph showing chert replaced quartz sand overlain by intraclastic horizons consisting of silicified quartz sand and ooids overlain by algal laminated, ripple marked micrite and another intraclast horizon. Harmonyvale traverse.



Figure 3.44 - Hope Member. Chert replaced oolite overlain by silicified quartz sand horizons. Harmonyvale section.



Figure 3.45 - Crooked Swamp Member. Outcrop of algal laminated dolomite with quartz sand lenses and quartz vugs at the base of the Crooked Swamp Member. Canal Road section.

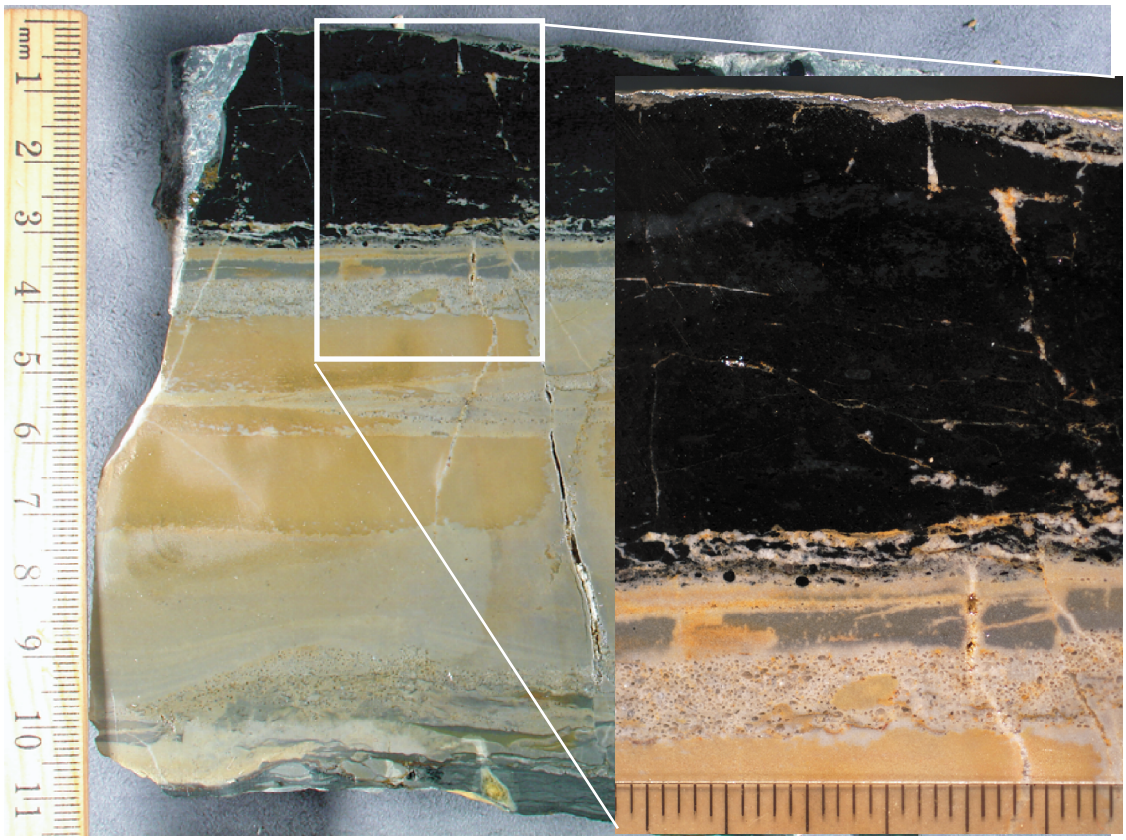


Figure 3.46 - Hope Member. Sawed slab showing chert bearing quartz sand and ooids.



Figure 3.47 - Hope Member. Sawed slab showing breccia interpreted as broken enterolithic structures representing former evaporites. The breccia clasts refit to form folded structure.

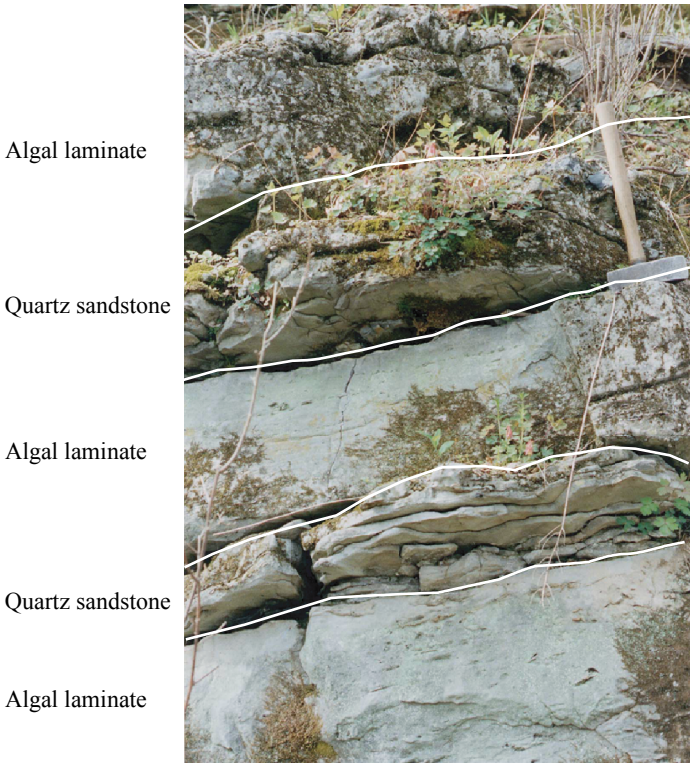


Figure 3.48 - Crooked Swamp Member. Outcrop of interbedded algal laminated horizons with thin quartz sand sequences. Harmonyvale section.



Figure 3.49 - Crooked Swamp Member. Outcrop photograph of chert breccia at the contact between the Crooked Swamp Member of the Rickenbach Formation and the Branchville Member of the Epler Formation.



Figure 3.50 - Crooked Swamp Member. Outcrop showing chert breccia at the top of the member. Note the algal controlled lower contact. Harmonyvale section.



Figure 3.51 - Crooked Swamp Member. Chert breccia occurring along the top of the member. Harmonyvale traverse.



Figure 3.52 - Branchville Member. Silcrete at the top of the Branchville member. Harmonyvale section.

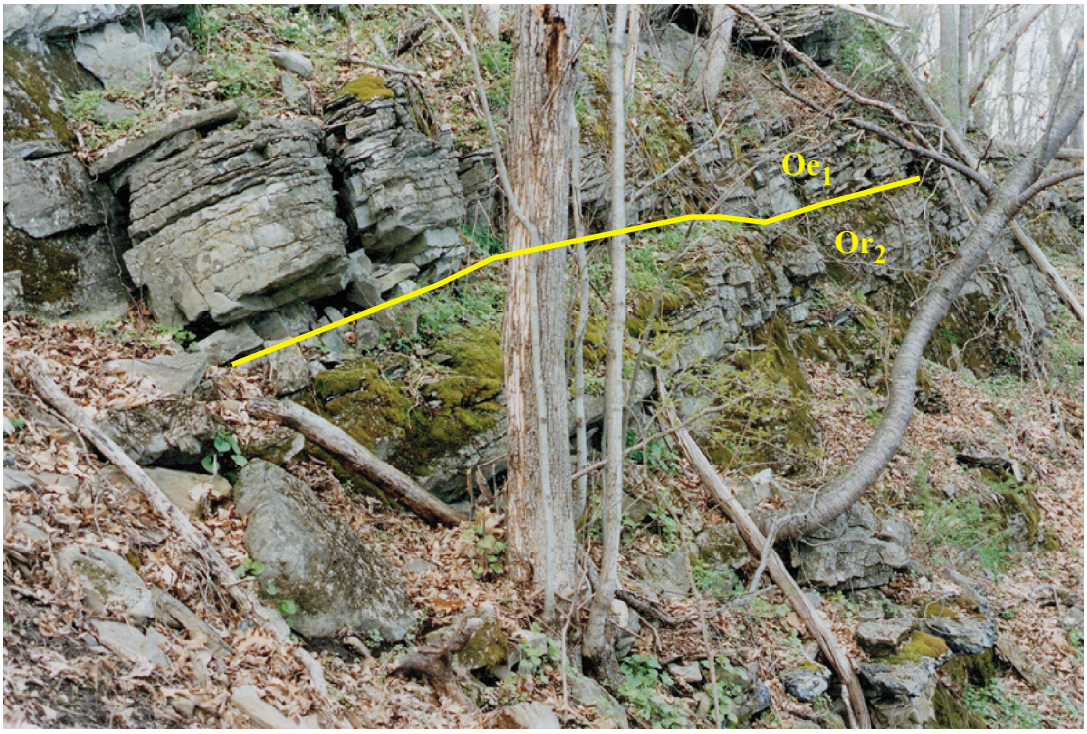


Figure 3.53 - Branchville Member. Outcrop of thin, flaggy, shaly dolomite showing contact between the Crooked Swamp Member (Or2) and the Branchville (Oe1).

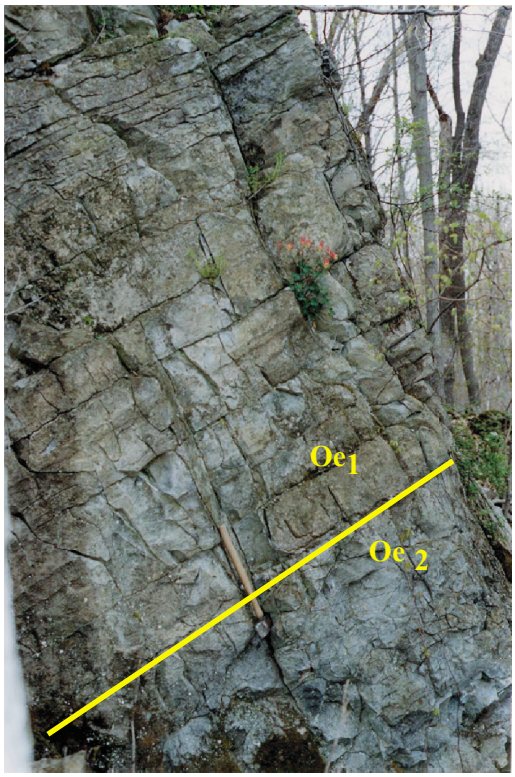


Figure 3.54 - Branchville Member. Contact between the Branchville Member (Oe1) and the overlying Big Springs Member (Oe2), Epler Formation. Harmonyvale section.

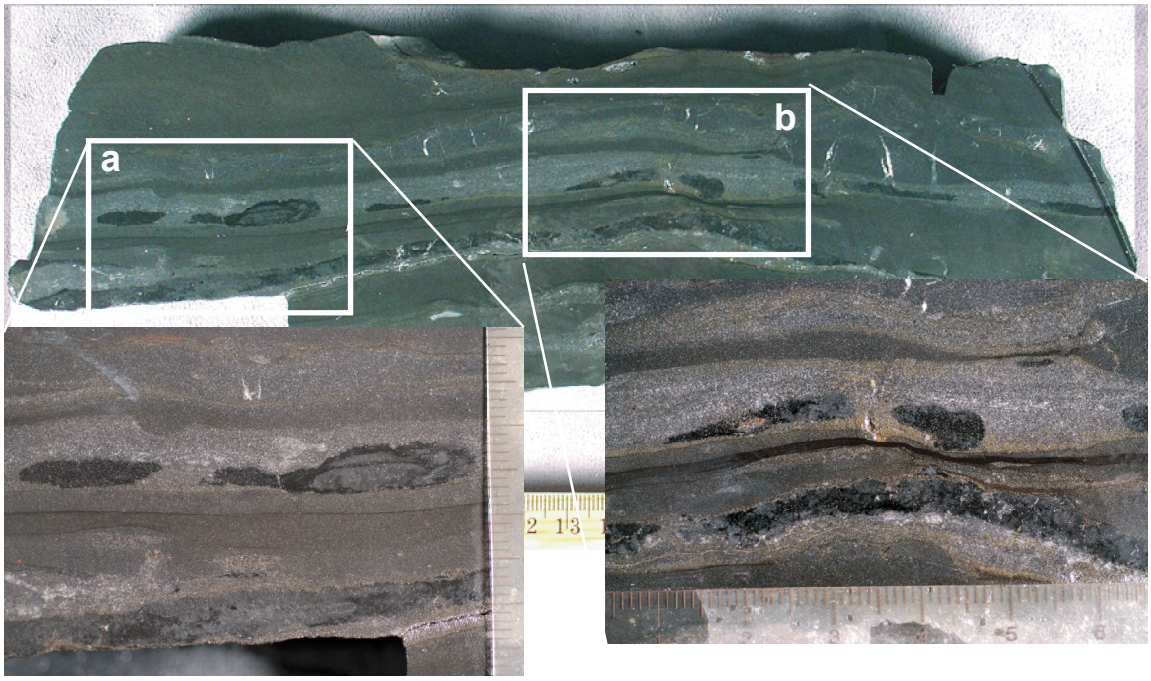


Figure 3.55- Branchville Member. Sawed slab of chert containing black, matted, lentil to elongate shaped pods.

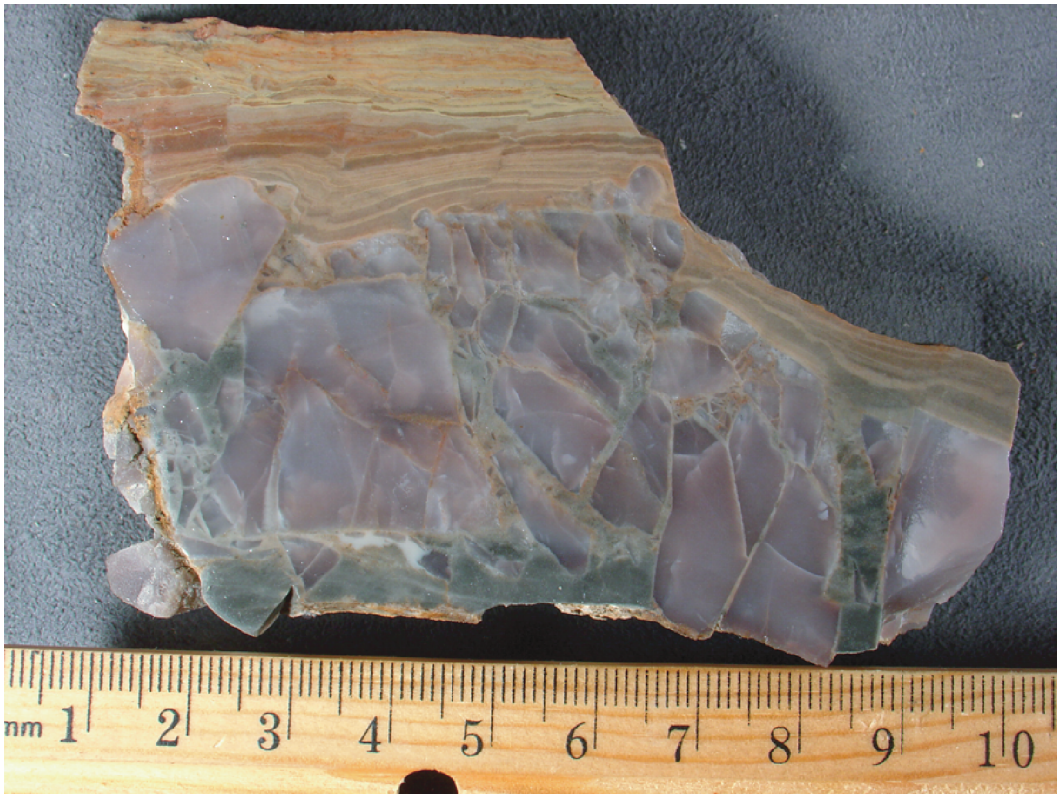


Figure 3.56 - Big Springs Member. Sawed slab of pinch-and-swell, gray to lavender, brecciated chert.

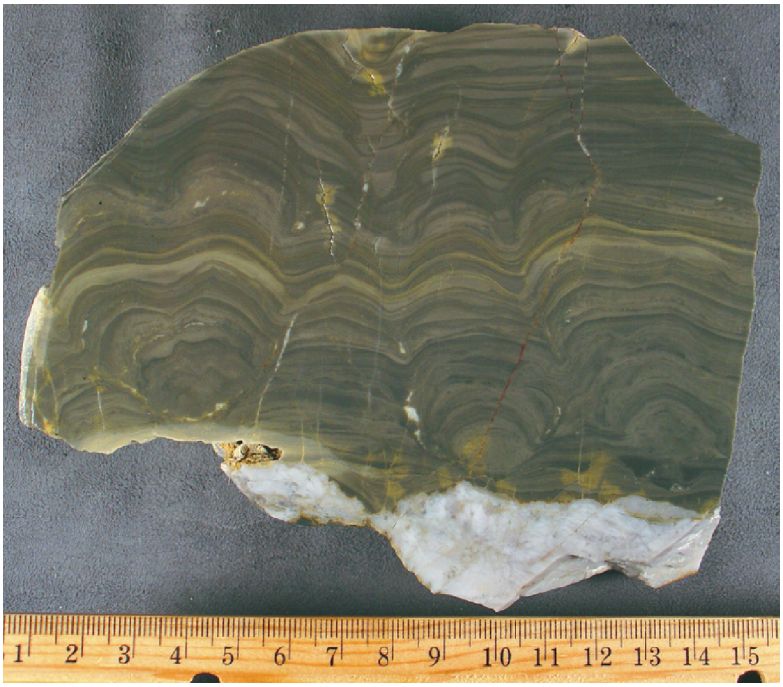


Figure 3.57- Big Springs Member. Sawed slab of silicified algal structures.

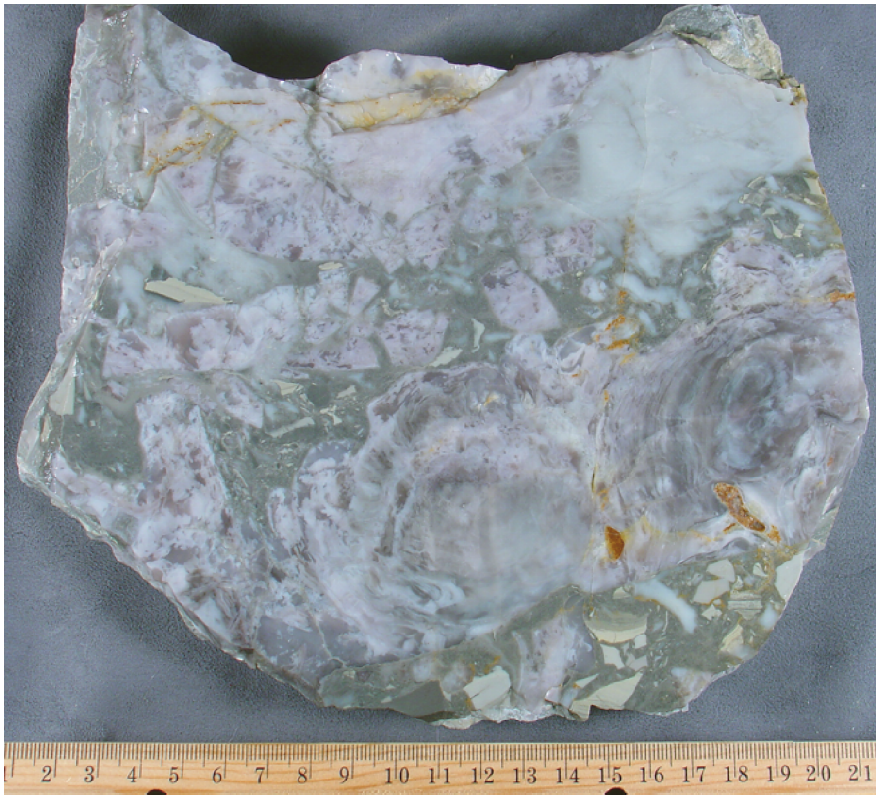


Figure 3.58 - Big Springs Member. Sawed slab of white to gray chert replacing algal structures.

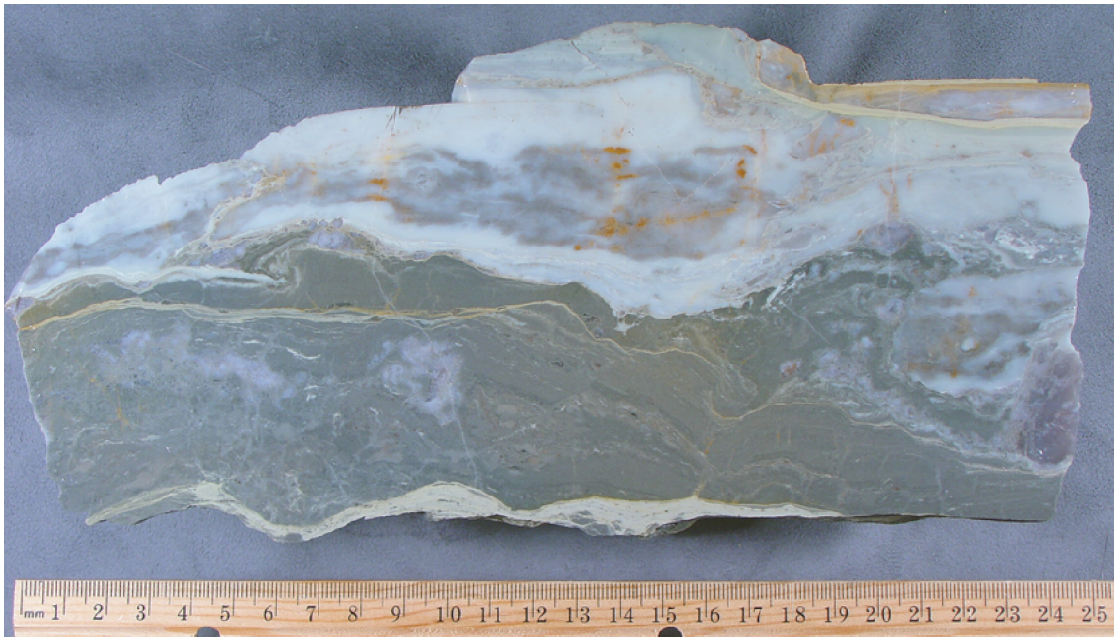


Figure 3.59 - Big Springs Member. Sawed slab of white chert.

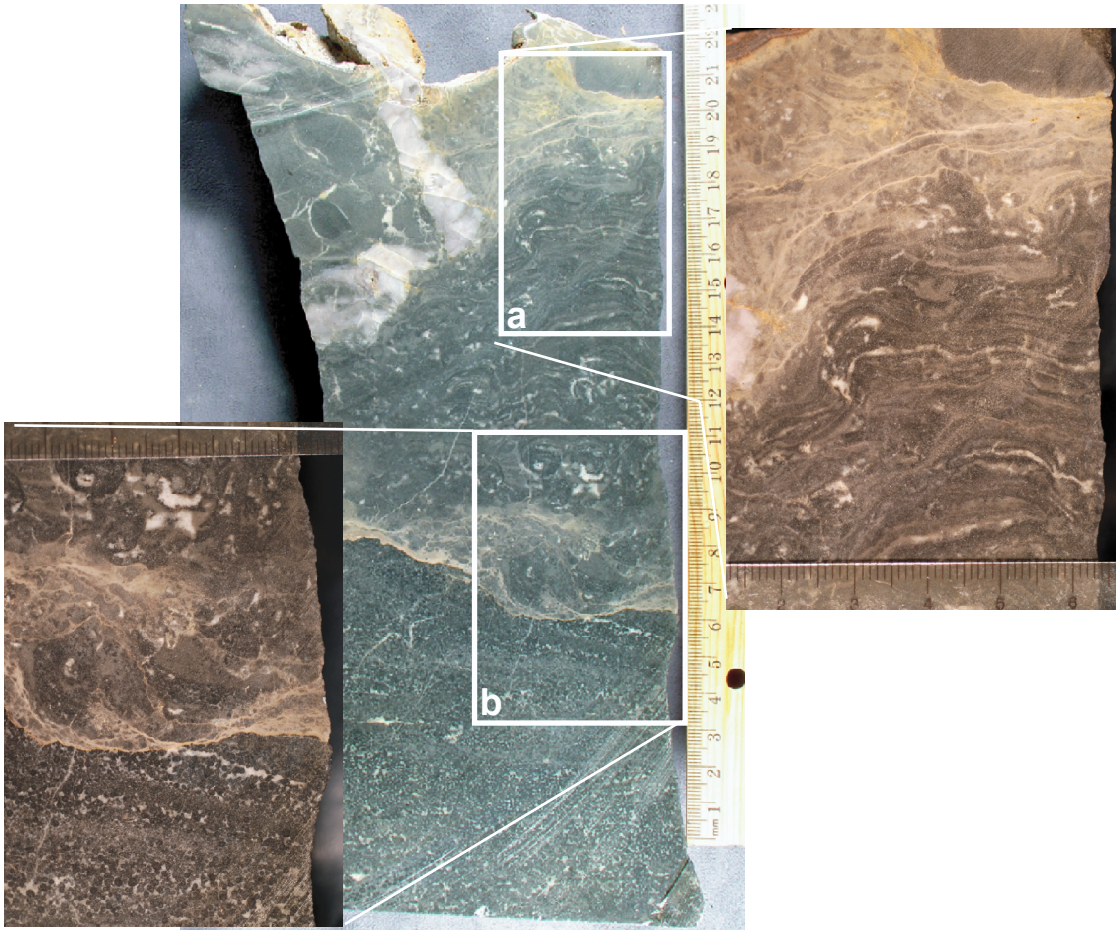


Figure 3.60 - Big Springs Member. Sawed slabs replacing ooids and algal laminations.

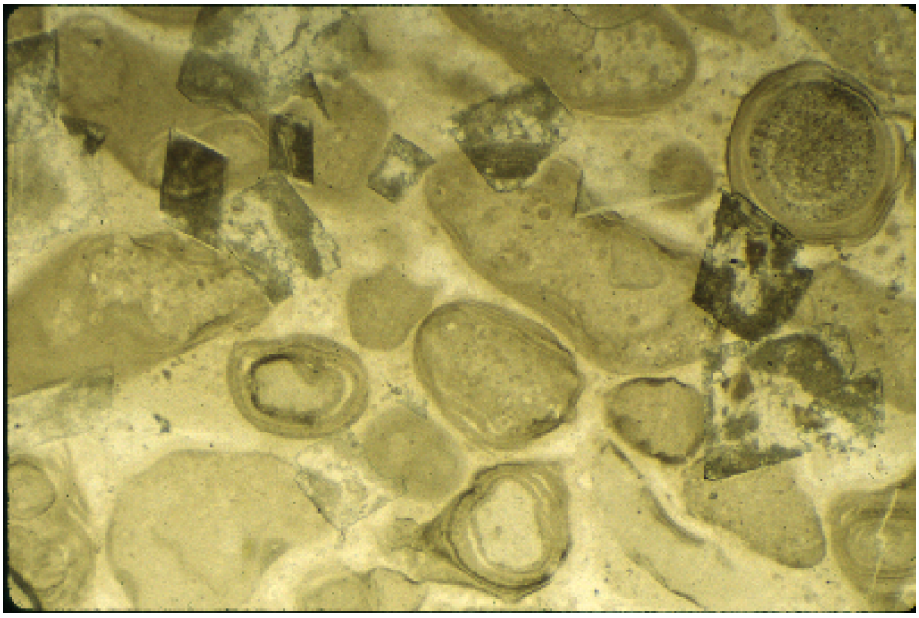


Figure 3.61 - Lafayette Member. Thin section of oncoidal and pisoidal grainstones.



Figure 3.62 - Beaver Run Member. Strongly burrowed horizons and punky chert along the base of the Beaver Run Member. Houston Road traverse.

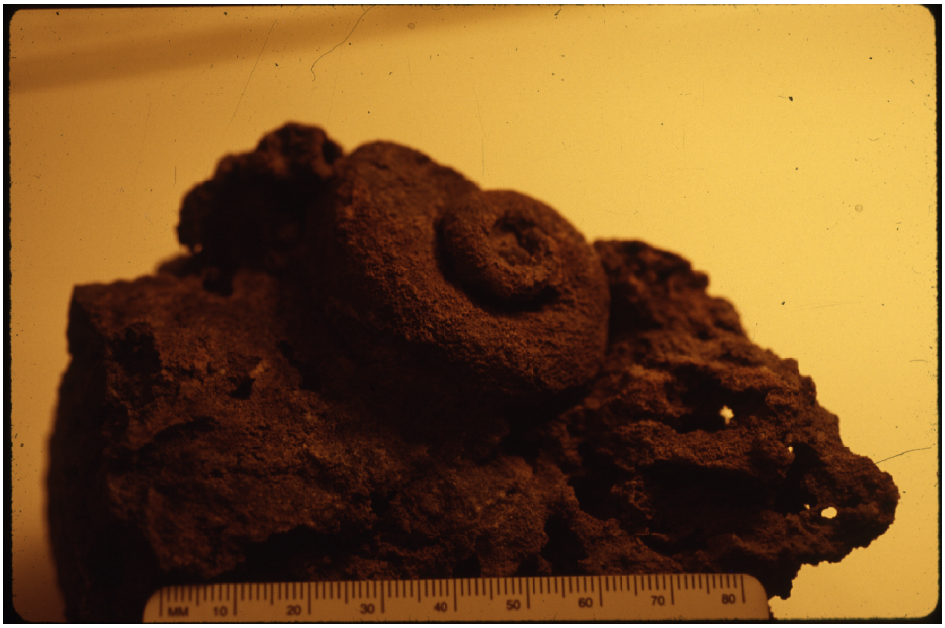


Figure 3.63 - Beaver Run Member. *Macularites* gastropod discovered in the Beaver Run Member of the Ontelaunee Formation.



Figure 3.64 - Beaver Run Member. Punky, porous chert replacing algal structures at the base of the Beaver Run Member.



Figure 3.65 - Beaver Run Member. Chert replacing convex algal structures. Swartswood Lake traverse.

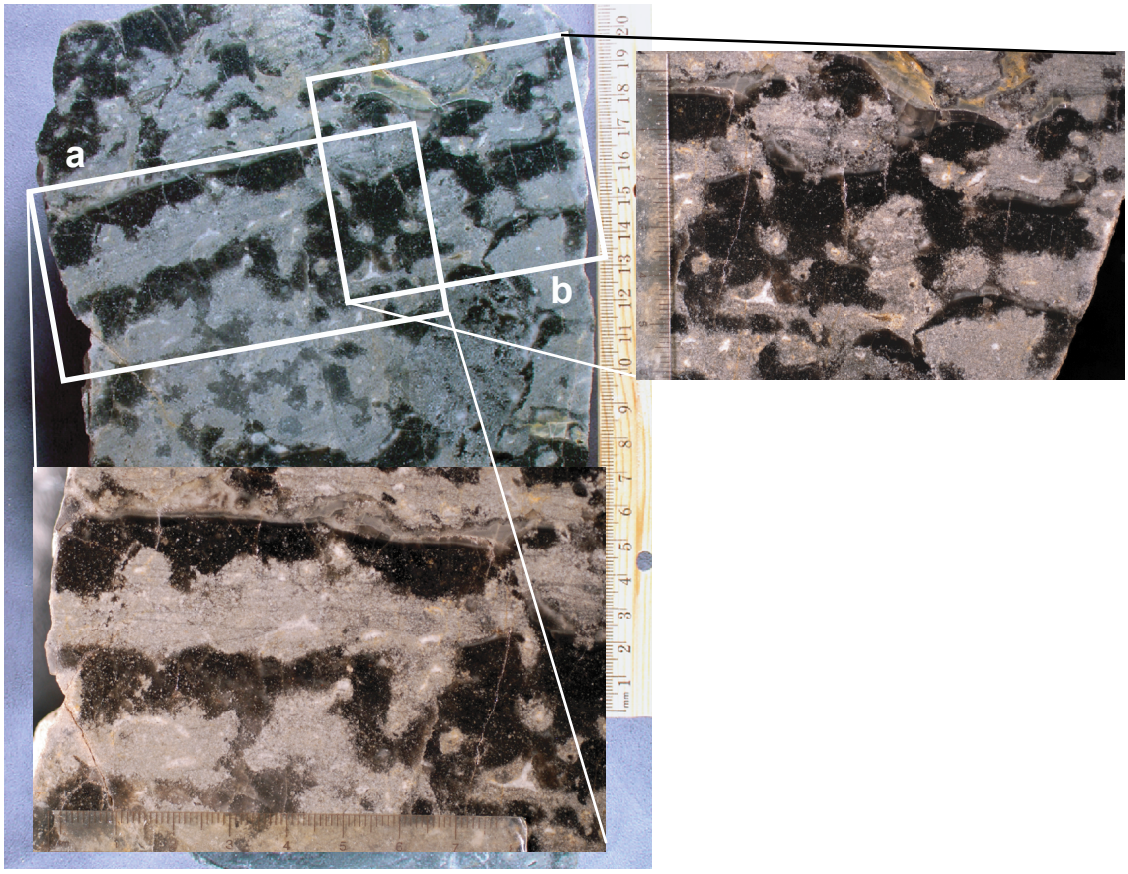


Figure 3.66 - Beaver Run Member. Sawed slabs showing vertical and horizontal burrows.



Figure 3.67 - Beaver Run Member. Pinch-and-swell chert beds developed within the transitional facies of the Beaver Run Member. Beaver Run section.



Figure 3.68 - Harmonyvale Member. Thick bedded, blue, brecciated chert replacing algal laminate and inferred evaporitic horizons. Harmonyvale section.

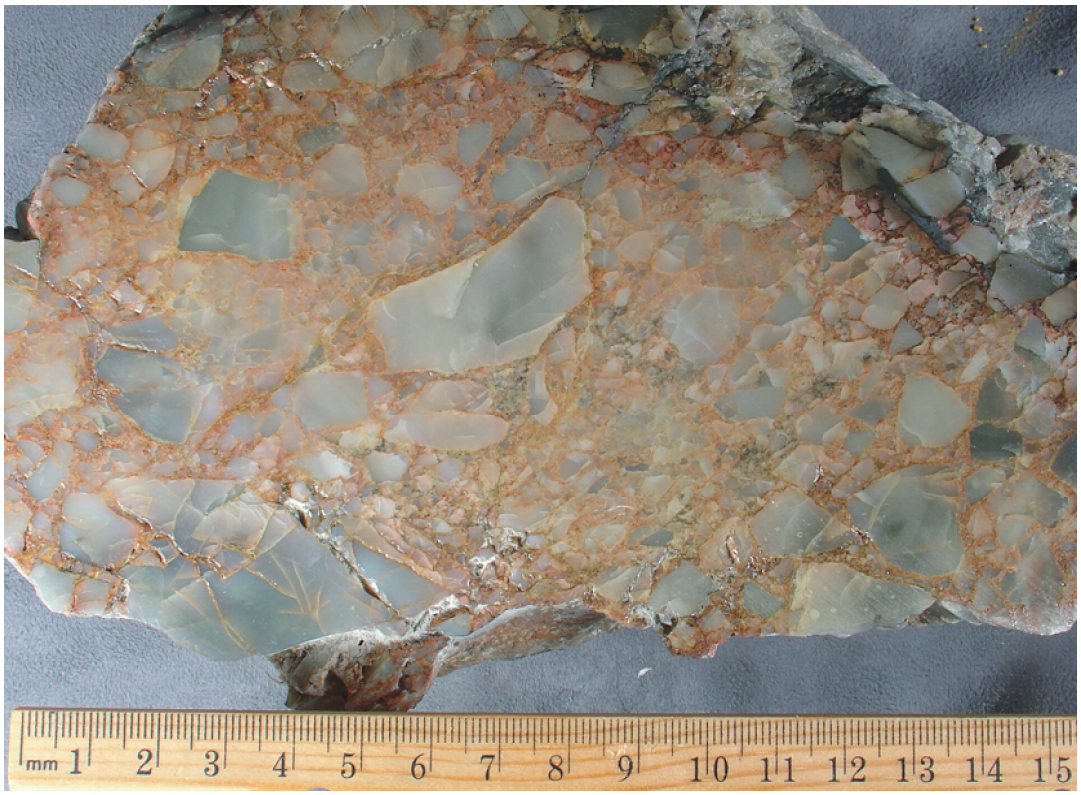


Figure 3.69 - Harmonyvale Member. Sawed slab of chert breccia in Harmonyvale Member.

CHAPTER 4: Depositional Environmental Interpretation of the Rocks of the Great Valley Sequence, Sussex County, New Jersey

4.1 Introduction

This chapter attempts to relate the description of the rocks of the Kittatinny Supergroup, as introduced in Chapter 3 of this dissertation, to the depositional environments responsible for each member (Ahr, 1973). The stratigraphy introduced in Chapter 3, and detailed in this chapter and in Appendix A, illustrates the fine-scale field observations used to infer the environmental conditions responsible for the deposition of the Kittatinny Supergroup (Goldring, 1965).

The carbonates and cherts of the Kittatinny Supergroup record a variety of depositional environments, consistent with a setting on a passive margin continental shelf. They record systematic changes in sea level in a peritidal (around the tides) setting (Folk, 1973) representing a spectrum of environments from shallow subtidal, to intertidal and peritidal (i.e., tidal flat), to supratidal (i.e. sabkhas, marshes and coastal lakes) (Ginsburg, 1975). The evidence for each environment is described below and related to the stratigraphy described in Chapter 3. The environments are described in order of decreasing water depth (i.e. in terms of transgressive-regressive cycles). Each environment is subdivided into lower, medium and upper zones, in correspondence with decreasing bathymetry. The boundaries between the depositional environments are gradational and as such, sedimentological characteristics indicative of each environment can be shared in the transitional zones separating environmental loci.

Sea-level curves for the Kittatinny Supergroup are shown in this chapter. The depositional environment interpretations support sea-level curve interpretations (on the scale of meters) indicative of at least two orders of sea-level fluctuation, specifically

fifth- and fourth-order cycles (Tucker and Wright, 1990). Fifth-order sea-level curves are interpreted directly from sedimentological/stratigraphic data recorded during the construction of 1:98-scale stratigraphic sections measured for this project. Fourth-order curves are statistical interpolations from the fifth-order curves and are also constrained by sedimentological/stratigraphic data. Information used to constrain the inferred sea-level curves were grouped into columns (Plates 4.1 to 4.11) labeled "transgressive and regressive indicators". Transgressive indicators are sparse, being rip-up clasts and grainstone horizons. Regressive indicators included supratidal shales, sandstone horizons, former evaporites replaced by quartz or chert, unconformities, mud cracks, and paleosol horizons.

Analysis of the sea-level curves in this chapter is purely qualitative. Attempts at deciphering water depths go no further than correlation with peritidal environmental settings. Also, the designation of the sea-level curves as fifth- and fourth-order cycles is based purely on the fact that the detailed stratigraphic sections measured for this project permitted an interpretation of relative, not absolute, water depth. The sea-level curves are labeled fifth- and fourth-order cycles because the scale of observation is measured from a minimum of 50 cm to 5 m. The usual genetic connotations associated with terms such as fifth- and fourth-order curves were not applied in this study. This dissertation does not attempt to generate hypotheses on whether or not these cycles were astronomically forced vs. tectonically and/or eustatically forced. Such a level of interpretation goes beyond the scope of this study.

4.1.1 Description of Peritidal Environmental Settings

The term peritidal (Folk, 1973) generally describes a variety of carbonate depositional environments that develop in a variety of settings (i.e. ramps, shelves and platforms) (Tucker and Wright, 1990). Peritidal carbonates may accrete from shorelines of continental margins and islands (Pratt and James, 1985) or they may accumulate on the protected sides of barriers, behind shoals and reefs on ramps or rimmed shelves (Tucker and Wright, 1990).

Subtidal Environment

The subtidal environment is predominantly submerged (exceptions being exposure of the shallowest parts due to semimonthly neap tides) and ranges from low-energy lagoons and restricted bays to high-energy shoals influenced by wave action and tidal currents (Pratt et al., 1992; Tucker and Wright, 1990). Carbonates deposited in a subtidal environment are characterized by bioturbated and pelleted carbonate mud that contain an abundant and diverse fauna depending on geologic age, salinity and water temperature (Tucker and Wright, 1990). Patch reefs may be present in low-energy subtidal environments (Pratt et al., 1992). Low-relief banks of cross bedded oolites are present in higher energy areas of the subtidal, where wave agitation is frequent (Pratt et al., 1992). "Tidal channels and ponds represent extensions of the subtidal zone into the intertidal belt" (Tucker and Wright, 1990, p. 137).

Intertidal Environment

The intertidal environment is constrained to lying between normal low- and high-tide levels and as such is alternatively flooded by marine water and subaerially exposed

on a diurnal or semidiurnal cycle (Pratt et al., 1992; Tucker and Wright, 1990). "Meteorological and climatic effects are very important in these settings and influence the types of features formed" (Tucker and Wright, 1990, p. 137). The intertidal includes a complex assortment of sub-environments; such as intertidal flats, beach ridges, subtidal creeks and brackish ponds (Pratt et al., 1992; Sellwood, 1986).

The lowermost intertidal shares many upper subtidal characteristics, specifically in that the rocks can be bioturbated mud (except where salinities are elevated) (horizontal and U-shaped forms like *Arenicolites* and *Diplocraterion*), pellets and bioclasts (Pratt et al., 1992). Algal laminations may cover the lower intertidal during low tidal; however, if burrowing organisms are present in the environment, the algal laminations may be restricted in aerial distribution due to grazing by gastropods and worms (Garrett, 1970; Pratt et al., 1992). "Wavy, lenticular and flaser bedded peloidal lime mudstone or grainstone… and dolomitized argillaceous lime mudstone (sometimes interbedded with small hemispheroidal stromatolites), arising from the alternation between slack water and sediment transport by both unidirectional currents and waves under low flow regime, are particularly distinctive of Precambrian and lower Paleozoic sequences", (Pratt et al., 1992, p. 309) and commonly contain intraclasts.

In the upper intertidal zone algal laminations are, "more permanent, and form(s) thick, leathery carpets that can be locally shrunken, torn and folded over… These exhibit various surface features such as pustules, blisters, wrinkles, crenulations, or small, domal stromatolites" (Pratt et al., 1992, p. 305). Fenestral porosity can be well developed (Sellwood, 1986). Carbonates underlying the thick algal mats of the upper intertidal are micritized and darker in color due to intense reducing conditions (Sellwood, 1986).

Higher energy intertidal environments may contain bioclastic and/or locally oolitic, cross bedded grainstones inferred by Pratt et al., (1992) as beach deposits.

Supratidal Environment

Pratt et al. (1992) and Tucker and Wright (1990) define the supratidal environment as the area above normal high tide, which is infrequently flooded during storms or semimonthly spring tides. Due to the subaerial nature of the supratidal, evaporitic sediments may be present in the supratidal zone in semiarid and arid climates (Pratt et al., 1992).

The upper intertidal and lower supratidal environments are covered by shrunken and desiccated algal mats that are often disrupted into intraclasts (Pratt et al., 1992). The sediment beneath the algal laminations is usually micritic to fine grained, with local medium to coarse grained sediments that may be deposited from passing storms or winds (Pratt et al., 1992). In Cambrian and Ordovician rocks, a supratidal environment may be interpreted if burrowing is rare or absent, or there is 'evidence for prolonged subaerial exposure such as evaporites, karst horizons or paleosols", (Pratt et al., 1992). Grotzinger suggests that supratidal deposits contain digitate stromatolites ranging from millimeters to centimeters in size (Grotzinger, 1986). Collapse brecciation in supratidal rocks is interpreted by Pratt et al., (1992) as post-depositional leaching of evaporites.

Upper supratidal environments may contain, "eolian deposits, soils, freshwater marshes and lakes, or onlap bedrock surfaces, depending on the region's geography and climate", (Pratt et al., 1992). Stromatolites and algal laminations, interbedded with thin, locally burrowed, micrite, bioclastic and peloidal carbonate sand (deposited during storms) may be present in upper supratidal marshes and lakes (Pratt et al., 1992). Decay

of organic material may create gas-heave vugs (Shinn, 1968, 1983) that are parallel to laminae and have a high preservation potential. Ground water discharge in sub-aerial supratidal environments may cause diagenetic effects such as tepees and cements, as well as the aforementioned leaching of evaporites (Pratt et al., 1992).

Peritidal Environment

Typically in the literature (Pratt et al., 1992; Reading, 1986) the peritidal zone is a catch-all term that includes all environments from the subtidal to the supratidal. In this study, however, the peritidal is referred to as the interface between the intertidal and supratidal environments.

4.2 Hardyston Formation

4.2.1 Facies Description

The variability in composition of the Hardyston Formation from location to location, the thinness (110 cm) of the unit, and the scant outcrop distribution suggest lateral discontinuity in deposition and/or pinch-out of strata along strike. The following facies descriptions of the Hardyston Formation represent lateral, not vertical, facies changes.

Hardyston Facies 1

A well sorted, sub-rounded to well rounded, locally imbricated, quartz-pebble and basement-clast conglomerate is present locally. The conglomerate is clast supported near the bottom and becomes matrix supported up stratigraphic section. The matrix of the conglomerate is coarse grained, quartz sandstone. Locally, the conglomerates are overlain by tan, medium to coarse grained, sub-angular to sub-rounded, trough cross bedded, quartz sandstone that bears rock fragments of Proterozoic basement. The contact

between the conglomerate and the quartz sandstone is sharp, but undulating. Lenses and filaments of magnetite occur in the trough cross beds. The cement in the sandstone varies from silica at the base to carbonate at the top of the facies.

Hardyston Facies 2

Arkosic sandstone locally overlies saprolitized Proterozoic basement or the Hardyston conglomerates described in facies 1. The arkose contains large, 0.5 cm diameter, fragments of kaolinitized feldspar grains, which are still attached to angular quartz. The arkose also contains hydrated ferromagnesian minerals, most of which have been converted to vermiculite/sericite and iron sulfides. Bedding planes in this facies are uneven and scour-and-fill channels are present. Thin wisps and beds of well sorted, coarse grained, quartz sandstone occur within the predominantly arkosic beds.

Hardyston Facies 3

The Hardyston Formation near Franklin, N.J. occurs as thin bedded, dusky yellow to honey colored, quartz sandstone containing weathered feldspar fragments and lenses of euhedral to subhedral magnetite and franklinite crystals. Ripple marks and truncated cross beds occur locally within the sandstone. The lower contact of the Hardyston at Franklin overlies the Franklin iron-zinc-manganese ore deposit located in the Proterozoic Franklin Marble; one of the basement lithologies in the dissertation study area.

Hardyston Facies 4

The upper part of the Hardyston Formation contains relatively clean quartz sandstone in carbonate cement interbedded with thin, fine grained, dolomite. Dolomite bedding surfaces contain mudcracks, oscillation and current ripple marks. Internally, the

dolomites are parallel bedded and contain abundant Skolithos fossils (Figure 4.1). These are the upper transitional beds occurring at the top of the Hardyston Formation.

Hardyston Facies 5

At the rifle club quarry in Franklin, New Jersey, the Hardyston Formation occurs as a clean, white, mildly translucent, orthoquartzite. Vestiges of cross beds are visible. These are relatively thick beds, greater than 1 m thick. Outcrop is poor and the base of the section is not visible.

Hardyston Facies 6

Well to the north, a unique Hardyston occurrence occurs in sags and undulations in the Proterozoic Franklin Marble. At this location, the Hardyston is dark charcoal gray, thick bedded and contains graphic plates, sulfides, decomposed spinels, and other ferromagnesian minerals. Nearby, resting on the basement is a thin horizon of bright yellow to yellow-orange, limonitic iron, with black cortex that occurs as a finely laminated crust, with irregular and concretionary masses, resting directly on the Proterozoic basement.

4.2.2 Paleoenvironmental Setting

The spatial variability in lithologic composition of the Hardyston Formation in the dissertation study area indicates lateral discontinuity in deposition and/or pinch-outs of strata along stratigraphic strike. Saprolitized bedrock grades up stratigraphic section into residuum and arkose. Conglomeratic lags are intercalated with, and/or overlain by, lenses of texturally and compositionally immature arkosic and/or by texturally mature quartz sandstones in thin, cross bedded and ripple marked horizons. The quartz sandstones interfinger with dolomite at the top of the succession.

Well rounded and well sorted conglomerates and pure-quartz sandstones indicate a prolonged weathering and erosion process that was interrupted by the influx of compositionally immature arkosic sandstones. Considering the rifted margin environment of the Laurentian craton (Clark, 1984; Faill, 1999; Hoffman et al., 1974; Thomas, 1976, 1977, 1983a, b, 1991, 1993), it is plausible that localized renewed uplift of Proterozoic basement (possibly along rift-horst shoulders) introduced compositionally immature sediments into a previously existing sedimentary basin.

Quartz sandstones that contain cross-bedded horizons truncated by evenly bedded, horizontal strata may indicate fluvial sediments that are tidally influenced (De Boer et al., 1988). This permits the reworking of insoluble minerals into thin layers and wisps. The presence of thin sandstones interbedded with finely laminated dolomite near the top of the Hardyston marks the inception of marine transgression (McCubben, 1982). The presence of mudcracks, current and oscillation ripple marks in the dolomite indicates short intervals of subaerial exposure in an inferred supratidal setting. The dessication features and ripple marks were buried with progradational pulses of reworked sands. Reworking of arkosic sand into the base of the overlying interdigitate Califon dolomite implies renewed marine transgression. The intermittent fluctuation of sea level permitted quartz sands to prograde over shallow, lower supratidal, dolomite deposited in shallow seas.

Considering the facies relationships described above, the Hardyston Formation is interpreted as a small and thin fan delta (Holmes, 1965; Nemic and Steel, 1988) that was submerged and transgressed over by tidal inlet, marine conditions.

4.2.3 Sea-Level Curve Interpretation

The Hardyston Formation is 110 cm thick and rests on the post-Iapetan rift unconformity. Additionally, one unconformity is present mid-section and the third is located at the formation upper contact (Plate 4.1). Ferruginous chert pods line the lower two unconformities. Fifth-order sea-level curves show three transgressive-regressive cycles in the unit (Plate 4.1). Transgressive maxima-minima for the fifth-order curve are represented in lower and middle peritidal sediments, respectively. The severest regression is interpreted as spanning the peritidal/supratidal transition. The mildest draw down supported an upper peritidal setting. The fifth-order sea level curve shows high periodicity and small wavelengths averaging 50 cm long.

Statistical smoothing of the fifth-order sea-level curve produced a fourth-order curve showing two transgressive-regressive cycles, punctuated by the mid-member unconformity (Plate 4.1). The thinness of the Hardyston Formation and the presence of three unconformities in such a thin stratigraphic package constrain the statistical smoothing of the fourth-order curve. As such, the transgressive-regressive fourth-order cycles have a periodicity and wavelength similar to the corresponding fifth-order curve. Maximum fourth-order transgression occurs in a lower peritidal setting, minimal transgression preserves middle peritidal sediments. The two fourth-order regressions remain in the upper peritidal.

The Hardyston Formation is a regressive unit. Sea-level curves remain in the peritidal realm throughout the deposition of the member, suggesting a relative sea-level low-stand during deposition; however, the high periodicity of both sea-level curves

indicates that sea-level fluctuated repeatedly during the overall low stand. Considering the study area's location on the New York recess, an inherited feature from Iapetus rifting (i.e. promontory, Thomas (1977)), post-rift passive margin subsidence (Bond et al., 1984) would have a different expression on a rifted margin promontory vs. a rifted margin embayment (i.e. the inherited Pennsylvania salient, Thomas (1977)). Essentially, subsidence would be occurring at a slower rate on promontories than embayments, which could cause localized regression on rift-margin promontories despite a regional (or global) sea-level rise that would be marked as a transgressive series tract in rift-margin embayments.

4.3 Leithsville Formation: Califon Member

4.3.1 Facies Description

The Califon, like the Hardyston, is thin (300 cm thick) and varies considerably along strike suggesting lateral facies pinch outs are common. As such, the following facies descriptions represent lateral, as opposed to vertical, transitions in depositional environment.

Califon Facies 1

This facies contains very thin, parallel bedded, shale which reveals flaser-type bedding (Allen and Friend, 1968) upon close inspection. The shale effervesces in hydrochloric acid and is interpreted as having carbonate cement. The base of the facies contains lenses of reworked, coarse grained, quartz sandstones. Large (2 cm diameter) clasts of decomposed rock fragments are present within the sandstone, or float within the shale. Along strike, the facies fluctuate from shale to shaly dolomite to arenaceous dolomite. Thick accumulations of oriented rip-up clasts (up to 13 cm diameter) are

present as edgewise conglomerates in shale. Rubble zones of intraformational conglomerate comprised of reworked dessication features and rolled algal structures occur as thin and thick lenses within the shales (Choi and Ginsburg, 1982; Coates and Jackson, 1987).

Califon Facies 2

This facies is a dark gray, shaly dolomite with shale concentrated along the lower and upper bed contacts. The dolomite is dark battleship gray and mildly pyrite bearing. Algal laminations are sparse, with small algal mounds or stromatolites being replaced by concentrically banded chert.

Califon Facies 3

These are the thickest beds within the Califon Member (12 to 15 cm in thickness). The dolomite is saccharoidal and locally coarsely crystallized; however, lower and upper bed contacts contain up to 1 to 3 cm thick shale couplets. The author identified concentrations of calcite, fluorite, and sphalerite at outcrops and in hand sample in this facies. Chert in the form of porosity infilling is present. Single and small, hand-size colonies of *Archaeocyathus* were observed and collected in this facies (Amato, personal communication, 1991). The lower and upper shale couplets are pyrite rich, exhibiting a bright, yellow weathering profile in outcrop.

Califon Facies 4

The upper arenaceous dolmicrite of the Califon Member differs from the facies 1 arenaceous dolomite in that the siliclastics of facies 4 are medium to coarse grained and compositionally more mature (facies is quartz rich, sparse in feldspar and rock fragments). Facies 4 also contains abundant rip-up clasts; which are mud cracks

occurring as edgewise conglomerates, and fragments of desiccated algal structures. Many of the shales within facies 4 contain oscillation ripples (Figure 4.2) overprinted by mudcracks, or shale shrinkage structures.

4.3.2 Paleoenvironmental Setting

The dolomitic shales of this member are interpreted as being deposited during one of the initial marine incursions of the Iapetos Ocean over the Hardyston Formation. Therefore, it is possible that the marine transgression mixed and reworked the Hardyston siliciclastics with the dolomite. The rubble zones of intraformational conglomerates in facies 1 and 4 are interpreted as subaerially reworked dessication features which were deposited as high-energy sediments within depressions, or sags, in the topography.

The lack of high-energy sediments in this facies (i.e. intraclastic conglomerates, ooids, turbidity grading, cross beds, etc), the presence of sparse algal laminations, silicified algal mounds/stromatolites and shale in facies 2, with a corresponding lack of high-energy features (intraformational conglomerates, ooids, cross beds) is interpreted as a low-energy environment, possibly lagoonal or subtidal.

The presence of pyrite in the shale of facies 3 and the mineral assemblage calcite-fluorite-sphalerite suggests that the Califon was receiving oxygen depleted waters rich resulting in a reducing environment during deposition**.** This inference, together with the interfingering of dolomite and siliciclastics (shale) indicates an upper peritidal environment. However, the delicate morphology of *Archaeocyathus* reportedly found in some shale layers suggests that protected pockets were present that fostered the sparse development of this fauna (Natter, 1967; Palmer and Rozanov, 1976; Zhuravleva, 1970).

The presence of rip-up clasts, and oscillation ripples in facies 4, overprinted by mudcracks and shale shrinkage features in a micrite, indicates a peritidal mudflat that is intermittently wetted and allowed to desiccate. The exposure of mudflats marks the initiation of minor regression during the deposition of this facies. The texturally and compositionally mature quartz sandstone lenses indicate that the sediment fraction was either reworked or has a slightly different provenance from the sandstones in facies 1 of the Califon Member.

The small, fan-delta complex proposed for the Hardyston Formation experienced some inundation to foster deposition of shales into the lower topography and tidal inlets of the Hardyston Formation. The inundation of the Hardyston may have also provided intraclastic debris, which is interbedded with the shaly dolomites (Skelly, 1987; Skelly et al., 1987). Shale facies interbedded and overlain by a coarsely crystalline dolomite indicates continued inundation of the Califon to a level where carbonate production may have repeatedly overrode the siliciclastic influx (Simpson and Eriksson, 1990; Simpson and Sundburg, 1987). The peritidal mud-flat facies can be traced for considerable distances along stratigraphic strike, inferring the establishment of a more even shore face and the topographic smoothing of rifted margin topography.

4.3.3 Sea-Level Curve Interpretation

The 300 cm thick Califon Member shares its basal unconformity with the underlying Hardyston Formation. The Califon has no unconformities mid-member, but is capped by an unconformity at the upper contact. Fifth-order sea-level interpretations indicate five transgressive-regressive cycles for this member (Plate 4.1). Maxima and minima for fifth-order transgression remain static at lower peritidal. Maximum fifth-

order regression permitted sedimentation in the upper peritidal setting, with the minimum draw down supporting lower peritidal environments. Fifth-order periodicity is high and wavelengths are small in the Califon Member. Wavelength average at about 50 cm.

Fourth-order interpretations of sea-level infer one transgressive-regressive cycle for the Califon Member (Plate 4.1). The fourth-order transgression mimicked the fifth-order transgressions in maintaining a lower peritidal setting. Upper peritidal settings were allowed during maximum fourth-order regression. The fourth-order curve has low periodicity and a wavelength of 700 cm.

The Califon Member was a fourth-order transgressive package punctuated by several smaller scale episodes of sea-level draw down. Both orders of sea-level curves in the Califon Member show an intertidal to peritidal range, indicating the discontinuance of relative sea-level low stand prevalent in the underlying Hardyston.

4.4 Leithsville Formation: Hamburg Member

4.4.1 Facies Description

The Hamburg Member is the first member in the Kittatinny Supergroup that shows significant lateral continuity of strata. There are lateral facies gradations in the lower two facies of the member; however, facies 3 shows lateral continuity. While still relatively thin (5 m), with respect to the overlying Kittatinny Supergroup carbonates, the member is thicker than the underlying Hardyston (approximately 1 m) and Califon (approximately 3 m) rocks.

Hamburg Facies 1

The lower facies of the Hamburg Member is a micritic dolomite overlying lenses of coarse grained, quartz sandstone. The amount of dolomite decreases up stratigraphic

section, being replaced by increasing quantities of quartz sandstone and the introduction of siltstone and shale. The color of the unit changes up section from dark gray dolomites at the base to burgundy and finally maroon siliciclastics near the boundary with facies 2.

The dolomite in Hamburg facies 1 is similar to Califon facies 3 dolomite in that both are micritic with arenaceous horizons. A major difference, however, is that the rip-up clasts, oscillation ripples, mudcracks and shale shrinkage features in Califon facies 3 have not been located in the Hamburg. The continuation of micritic dolomite, bearing arenaceous horizons from the Califon into the Hamburg, indicates that the larger scale depositional settings (i.e. lower supratidal mudflat) have not changed, even if smaller details have (i.e., dessication). Additionally, the presence of quartz sandstone lenses in Hamburg facies 1 suggests, as it does with Califon facies 3, the continued reworking of a previously deposited (i.e. Hardyston) siliciclastic fraction or the introduction of siliciclastics from a new provenance. The up-section change in the dolomite/siliciclastic ratio suggests that the minor regression that was interpreted during Califon deposition continued through the deposition of Hamburg facies 1.

Hamburg Facies 2

The second facies contains the first occurrence of 3 m thick, light gray, tan, burgundy and maroon sedimentary rocks. The burgundy to maroon rocks are packaged into repetitive sets of coarse grained sandstones, bearing local edgewise conglomerates, sandwiched between silty shales and sandstones. All of the silty shales are punctuated by ripple marks, overprinted by dessication features. Current ripples, and trough cross beds, are exceptionally common in tan to light gray, thick bedded sandstones at discrete locations, such as the Wildcat Road and Rte. 23 North sections (Figure 4.3). Voids

separate ripple and cross-bed planes in these rocks, as if differential weathering occurred in the form of dissolution at discrete horizons. Siltstones and shales do not cap bedding in the light gray and tan sandstones, but do cap the succession at the lower and uppermost boundaries. At the Rte. 515 section, sandstones are arkosic and contain large granules of weathered feldspar, local lenses of edgewise conglomerates, and insolubles, such as magnetite. Bedding contacts are sharp, but undulatory (Figure 4.4).

Hamburg Facies 3

This facies is the first laterally persistent facies in the Hamburg Member. Arenaceous dolomites are overlain by olive, finely laminated to thick bedded, micritic, dolomitic limestones. Close examination shows that the fine laminations may represent algal filament or are defined by algal filament. Quartz sandstone lenses are present in the micritic dolomitic limestone.

4.4.2 Paleoenvironmental Setting

The dolomite in Hamburg facies 1 is similar to Califon facies 3 dolomite in that both are micritic with arenaceous horizons. A major difference, however, is that the rip-up clasts, oscillation ripples, mudcracks and shale shrinkage features in Califon facies 3 have not been located in the Hamburg. The continuation of micritic dolomite, bearing arenaceous horizons from the Califon into the Hamburg, indicates that the larger scale depositional settings (i.e. lower supratidal mudflat) have not changed, even if smaller details have (i.e., dessication). Additionally, the presence of quartz sandstone lenses in Hamburg facies 1 suggests, as it does with Califon facies 3, the continued reworking of a previously deposited (i.e. Hardyston) siliciclastic fraction or the introduction of siliciclastics from a new provenance. The up-section change in the dolomite/siliciclastic

ratio suggests that the minor regression that was interpreted during Califon deposition continued through the deposition of Hamburg facies 1.

The presence of siltstones, shales and sandstones in Hamburg facies 2 indicates that the small scale, regressive cycle that started in Califon facies 3, and continued through Hamburg facies 1, have reached its acme in Hamburg facies 2. The burgundy to maroon siliciclastics in Hamburg facies 2 are organized into cyclic deposits of coarse grained sandstones, with local edgewise conglomerates, sandwiched between siltstones and shales. This distinctive packaging suggests that the coarse grained siliciclastics were deposited in pulses of sedimentation, with enough of a time lag to allow for the gravitational settling of siltstones and shales. However, the presence of ripple marks and dessication features in the associated siltstones and shales also suggests that water depth was shallow enough to permit repetitive dessication of these sediments. The presence of edgewise conglomerates in the sandstones indicates that during coarse grained sedimentation, the flow regime contained enough energy to imbricate the conglomerate clasts; however a lowering of flow regime was needed to permit the formation of current ripples and trough cross beds (Cudzil, 1985). Additionally, the presence of gaps between cross bedded and ripple marked horizons in this facies is interpreted as dissolution of thin laminations of sediment, such as carbonate (Figure 4.4). This interpretation or inference has two implications: that sedimentation of the lighter colored siliciclastics also occurred in pulses that allowed the deposition of thin carbonate lamellae in a siliciclastic regime; and if carbonate was present as thin lamellae encrusting cross bedded and ripple marked beds, the siliciclastics might have been deposited in shallow water at a shore face. Finally, the presence of local arkoses bearing large weathered feldspars and insoluble

minerals (magnetite) suggests that a nearby igneous rock terrane might have been exposed to provide a source for these sediments.

The presence of dolomites, overlain by dolomitic limestones in facies 3, indicates that the siliciclastic influx of Hamburg facies 2 dwindled to a point where carbonate production could resume. However, the lower dolomites in this facies are arenaceous and the upper dolomitic limestones contain sandstone lenses, indicating that while siliciclastic influx was severely reduced, it either did not cease all together or the underlying siliciclastics were being reworked by water action. Fine laminations in the carbonate may be algal controlled, suggesting local quiet water conditions, possibly tidal pools or inlets. The presence of carbonates in facies 3 indicates marine inundation of the local shelf.

The regressive cycle that was started with the deposition of Califon facies 3 may represent the local introduction of siliciclastic sediments at a rate greater than that of sea-level rise, in effect producing a localized regression. An alternative hypothesis may be the introduction of siliciclastics coincident with lowering of sea-level. The presence of current ripples in the sandstone and siltstone/shale horizons, the possible presence of carbonate lamellae, as well as the packaging of the sandstones in siltstone facies, indicates that the siliciclastics may have been debouched into a shallow body of water. This scenario would support localized regression during sea-level rise (Budd and Harris, 1990).

The increasing siliciclastic content from the base to the middle of the Hamburg Member, with the re-introduction of carbonates in the upper part provides clear evidence of localized regression followed by marine transgression in this part of the New York recess. The siliciclastic mineral composition, with the presence of magnetite, indicates

an igneous provenance, possibly from renewed uplift of rift blocks created during Iapetan rifting, or from other sources outboard of the rifted margin (Thomas, 1991, 1993) Tectonic models of Iapetan rifting show evidence for a spreading center jump from the mid-ocean rift created during Iaptan rifting to a transient inboard rift, locally called the Rome Trough (Southworth et al., 2007; Thomas, 1991). Thermal activity from the creation of an inboard rift would have caused uplift of the riften margin, possibly exposing Proterozoic basement. Such tectonic activity would provide source terrain for the siliciclastics in the lower and middle Hamburg. Carbonate deposition in the upper Hamburg marks retardation in siliciclastic influx and the resumption of marine transgression onto the rifted margin. However, the presence of an unconformity at the upper contact indicates the marine transgression was short lived, or locally replaced by a renewed siliciclastic pulse.

Modern-day analogs from the Trucial coast at Abu Dhabi (Kinsman and Park, 1976) show that the most proximal facies of wadi systems include red bed sequences (facies 1 and 2) which grade into anastomatic (facies 2) and braided channel deposits that diminish prior to reaching shoreline settings. However, in tectonically active areas, red siliciclastics could be transported to a peritidal setting and be intercalated with a more rapidly subsiding carbonate margin. Facies 3 is laterally persistent throughout the dissertation study area, unlike facies 1 and 2. As such, the geometry of facies 3 is suggestive of a peritidal setting, rather than a tidal inlet or lagoon channel.

4.4.3 Sea-Level Curve Interpretation

The 520 cm thick Hamburg Member unconformably overlies the Califon Member, contains two unconformities in the mid-section and one chert-lined

unconformity at the upper contact. Fifth-order sea-level interpretations depict four transgressive-regressive cycles during Hamburg deposition (Plate 4.1). Maxima-minima for fifth-order transgression ranged from lower peritidal to upper peritidal, respectively. The severest draw down in the fifth-order fostered a supratidal environmental. The mildest draw down supported the lowest reaches of the upper peritidal. Fifth-order periodicity is high, with wavelengths ranging from 50 to 100 cm in length.

Fourth-order sea-level curves show two transgressive-regressive pulses in the Hamburg (Plate 4.1). Lower fourth-order periodicity supports larger wavelengths, which measure at approximately 250 cm in length. Maximum transgression preserved lower peritidal sediments. Minimum transgression supported middle peritidal settings. Extremes in regressional pulses range from lower-middle supratidal to upper peritidal, respectively.

The Hamburg Member is deposited in a setting where transgression and regression occur almost equally, with transgression having a slight advantage. The continued restriction of both fifth- and fourth-order curves to the peritidal setting suggests renewed local sea-level low stand, with periodic fluctuations in sea level. The periodicity of the Hamburg is lower than the periodicities in the underlying Califon and Hardyston units, indicating a lessening of the number of sea-level fluctuations in the Hamburg, with respect to the underlying stratigraphy.

4.5 Leithsville Formation: Wallkill Member

4.5.1 Facies Description

The Wallkill Member is the thickest member described to date (20.7 m) and as such is divided into four facies that stack vertically. The facies are laterally persistent

sediment packages correlated along strike during stratigraphic mapping and section construction.

Wallkill Facies 1

The base of the Wallkill Member is marked by the presence of blocky, homogeneous, matted black shale overlying an unconformity. Overlying this marker horizon are algal laminated dolomites interspersed up section with thick, shaly dolomites. Chert couplets occur along the upper surfaces of many of the shale beds. Silicified algal structures occur as discrete, oblate spheres, flattened along the base and ranging in size from 5 to 40 cm. The algae are strata-bound deposits and are usually separated by as much as 1 to 2 m of finely algal laminated dolomite (Figure 4.5) (Aitken, 1967, 1988). They are not closely associated colonies, but are essentially isolated structures, occurring in isolated patches up to 75 to 100 m apart. Large, linear, domal algal stromatolites are also replaced by chert within this facies (Cummings, 1932).

Wallkill Facies 2

The base of Wallkill facies 2 consists of alternating thin and thick sequences of fine to coarse grained, parallel and cross bedded, pisoidal (pea sized) dolomite interbedded with algal laminated dolomite bearing abundant rip-up clasts, intraclasts, mud cracks and extensive, convex upward algal stromatolites. The upper part of the facies includes, in upward stratigraphic succession; intraformational conglomerates, graded oolites, laminated algal and a zone of structureless pisoids. Partial to complete, silicification of these structures is common. Black shale underlying an unconformity is present near the top of the facies. Algal structures in facies 2 are markedly different from those occurring in facies 1. The algal range in size from 1 to 5 m in length, are flat along

the bottom and convex along upper surfaces. They are locally elongate, rilled and striated. Volutions occur locally along the crests and between successions of domal algal. The algal lie side by side, almost like ribs. The domal algal also bear projections which radiate outward from their flattened, equatorial regions. At other locations, the domal algal contain large, circular, puckered masses 10 to 15 cm in diameter that are interpreted as areas of renewed growth occurring along upper re-wetted surfaces of desiccated algal.

Wallkill Facies 3

The basal part of facies 3 is a succession of coarse grained, thickly bedded, mildly oolitic, algal laminated dolomites. Algal laminations are particularly concentrated along the base and crest of the beds and impart a control to the bedding surfaces, including a mild convexity in places. Mildly convex, domal algal stromatolites are present in the upper part of the facies. Capping the domal algal are algal laminated dolomites and intraclastic horizons.

Wallkill Facies 4

This facies contains medium to coarse grained, alternating thin to thick, undulating beds of shaly dolomite. Quartz vugs that emit a sulfurous odor when broken are present in the mid-lower part of the facies and are interbedded with abundant algal laminations. These are capped by olive-gray shale overlain by three intraclastic horizons that include 10 cm thick beds of intraclasts, intraformational conglomerates and irregular masses of oolite. The intraclastic horizons are overlain by finely algal laminated dolomite at locations other than the type section that include cross bedded and structureless oolites interbedded with the thin to thick algal laminates. The upper beds of

this facies contain several unconformities. Many of the beds pinch-and-swell along strike and continue to be flaggy locally. The facies is capped by another intraclastic horizon with includes structureless masses of ooids, pisoids and cross bedded oncoids. Silicified enterolithic and cauliflower shaped structures are visible in cut slabs of this facies and are interpreted as being chert replaced anhydrites. Chert replaced algal laminates sandwich the silicified anhydrite at locations other than the type section. The silicified anhydrite is thinnest where underlying and overlying algal laminates are silicified. Conversely, the chert replaced evaporite units are thickest (up to 0.5 m) where they replace large, radiating, masses of cauliflower anhydrite. This is overlain by a mildly burrowed horizon that is partially silicified. Thin to thick accumulations of silicified ooids and pisoids are capped by a thick bed of chert replaced, graded and cross bedded oncoids at the type section.

4.5.2 Paleoenvironmental Setting

The presence of shale at the base of the Wallkill Member implies sediment settling in a low-energy environment. The presence of siliciclastics in the system may have restricted the carbonate production mechanism (Tucker and Wright, 1990). The presence of algal laminations and domal algal stromatolites, interbedded with shaly horizons, suggests a restricted environment (i.e. lagoon) that permitted the development of laminations; however, the presence of oblate spheres and linear domal algal indicates that the setting changed from a restrictive to a more open system. The linearity of the domal algal suggests that wave action may have influenced the system (Gebelein and Hoffman, 1973) (Figure 4.6).

The parallel and cross bedded, pisoidal facies indicates deposition above wave base in the peritidal zone. Parallel and cross bedding suggests ebb-and-flow wave action. The presence of reworked, edgewise conglomerates composed of rolled dolomite, and rounded clasts of mudcracks, indicates sub-areal exposure, followed by marine-water encroachment reworking previously deposited carbonates. Facies 2 represents the continuation of the peritidal environment interpreted for the upper part of facies 1, but restricted to the seaward reaches of a lagoon, or a bight. The regrowth positions on desiccated algal surfaces and the presence of an unconformity near the top of the facies suggests that the area is occasionally subaerial, with intermittent periods of submergence permitting renewed growth. The large size of the algal structures, and their elongate, preferred orientation, suggests tidal conditions. A bight setting would provide the necessary environments for the growth of such algal. As such, facies 2 algal are interpreted as a forming in a higher energy environment than what is represented in facies 1. Regardless, both facies 1 and 2 remain peritidal, lower supratidal conditions. The shale near the top of the series would support a supratidal interpretation for facies 2.

Coarse grained, thick bedded, mildly oolitic, algal laminated dolomites indicate a restrictive setting, such as a tidal flat/lagoon. Domal algal stromatolites in the upper facies, and the presence of rip-up clasts, indicates the establishment of a more open subaqueous setting that would support the development of the domal algal and serve as a depocenters for rip-up clasts gouged from a nearby shoreline. This facies suggests fluctuations in sea level, alternately flooding and exposing the carbonate platform.

Sulfurous quartz vugs are interpreted as evaporites that have been replaced by quartz. If this interpretation is correct, the evaporites, interbedded with shaly dolomite,

algal laminates and overlain by shales, strongly suggest a supratidal setting. The intraclastic horizons containing structureless masses of ooids, pisoids, and cross bedded oncoids interbedded with algal laminations indicates exposure of the supratidal setting to a more energetic environment, either a slight inundation of the supratidal or occasional storm surges. The inundation is replaced by a more subaerial setting, as indicated by the three unconformities present near the upper contact.

The deposition of the Wallkill Member marks the appearance of the first laterally persistent Cambrian carbonate on the New York recess, which developed in accordance with thermal subsidence occurring along the margin (Bond et al., 1984). The facies range from lagoon inlet and bight (lower supratidal), to near shore face (lower supratidal), to algal dominated (peritidal), to evaporitic (lower supratidal), to shoaling/flanking/draping oolite, pisoid and oncoid (lower peritidal) setting, in accordance with mild punctuations in sea level.

4.5.3 Sea-Level Curve Interpretations

The 20.75 m thick Wallkill Member contains four unconformities, not including the erosional surface at the lower contact. Cherts line all unconformities within the member; specifically black siliceous claystones and algal laminated cherts at the lower unconformity and silicified ooids at the three unconformities at the upper contact. Fifth-order sea-level interpretations based on facies and unconformity data indicate eleven transgressive-regressive cycles during Wallkill deposition (Plate 4.1). Maximum transgression supported upper intertidal settings. Minimum transgression preserved upper peritidal conditions. The severest fifth-order draw down promoted supratidal settings; with the mildest draw down having supported mid-upper peritidal conditions.

Fifth-order periodicity and wavelength vary up stratigraphic section. Periodicity is low and wavelength is long (600 cm to 1.5 m) in the lower 3 m of the member. Periodicity increases and wavelength decreases (50 to 100 cm) in the upper meter or so of the unit.

Fourth-order sea-level interpretations infer four transgressive-regressive cycles in the Wallkill Member (Plate 4.1). Maxima-minima settings for fourth-order transgressions in the Wallkill range from upper intertidal to the lower peritidal, respectively. Extremes in regression vary from lower supratidal conditions under maximum regression to upper peritidal during minimum regression. Periodicity and wavelength patterns documented in the fifth-order curve are inherited by the fourth-order curve, i.e. periodicity increases and wavelength decreases up stratigraphic section (Plate 4.3).

The Wallkill Member is inferred as having been deposited in slightly more transgressive, than regressive, setting with sea-level fluctuation becoming more of a factor in the upper parts of the member. The fifth- and fourth-order sea-level curves are not restricted to one depositional setting. The major transgression in the lower part of the member deepens the continental margin into the intertidal setting, suggesting that local sea-level may be leaving a low-stand position.

4.6 Limeport Formation: Wildcat Road Member

4.6.1 Facies Description

Wildcat Road Facies 1

Sulfurous quartz vugs in dolomite are present at the base, mid-section and top of the facies. The first facies is punctuated by repeated successions of black shale overlain by thick beds of massive, structureless to graded and cross bedded ooids and pisoids

capped by algal boundstones. Generally, algal structures in the boundstones become larger up section. The entire series contains algal laminates; however, the thickest accumulations of laminated algal directly overlie the quartz-vug horizons within the base, mid-section and crest of this facies. Algal laminations are also interbedded with burrowed horizons. Intraclastic horizons increase in the upper half of this facies, in accordance with the increase in numbers of boundstones. The top of the facies contains intraclastic limestone and cross bedded oolites, ripple marks, black shales, overturned algal structures and is pervasively mud cracked. Micrites are more common in the upper half of the section.

Wildcat Road Facies 2

Wildcat Road facies 2 is distinguished from facies 1 by the lack of shale and includes repetitive sedimentation of intraclastic limestones overlain by oolitic and peloidal grainstones, capped by coarse grained limestones and/or large accumulations of algal boundstone. The boundstone horizons are overlain by draping and cross bedded oolites interbedded with intraclastic limestones. The upper part of the facies witnessed an increased influx of quartz sandstone. Boundstone horizons were established wherever the quartz sandstone was overlain by intraclastic limestones, graded and cross bedded oolites and algal laminated limestones. Intraclastic units are more common where cross bedded oolites and quartz sandstones occur. Locally, the convex algal are overturned and ripple marks are present. The section is capped by the recurrence of thin and thick black shale overlain by intraformational conglomerates and intraclastic limestones.

Wildcat Road Facies 3

The third facies is distinguished from facies 2 by the lack of massive grainstones and the re-introduction of black shale. Facies 3 contains a thick accumulation of micritic, algal laminated limestone capped by black shale that is overlain by alternating thin and thick beds of algal laminated dolomitic limestone bearing graded oolite. Intraclastic horizons predominantly comprised of rip-up clasts of algal laminates and digital algal successions occur towards the top of the section, which is capped by shales (Figure 4.7). Quartz vugs occur in the mid-upper part of the facies and the facies is strongly algal laminated at its base and crest. Black shale is common in the upper half of the section. Intraformational conglomerates and shales are partially to completely silicified. There is a thick accumulation of angular fragments of chert in dolomitic limestone which is underlain by chicken-wire evaporite structures.

4.6.2 Paleoenvironmental Setting

The shale overlain by grainstone is indicative of either a lagoonal, inlet setting inundated by a higher energy subaqueous regime suggesting deepening, or a subtidal shale sequence overlain by grainstone; suggesting subsequent shallowing. Very thick accumulations of black shale in the base of the Limeport Formation extend towards the Pennsylvania depocenter (Greg Herman, New Jersey Geological Society, personal communication, 1998). Thick wedges of correlative black shales support a subtidal interpretation for this microfacies. However, the lack of algal laminations associated with the shale indicates that the latter scenario. Also, as mentioned in the underlying Califon Member, quartz vugs bearing the odor of sulfates are interpreted as gypsum and/or anhydrite flowers that have been replaced by quartz. This interpretation of anhydrites

indicates hypersalinity and restricted conditions at the base, mid-section and crest of facies 1. Overlying the shale/grainstone is an association of interlayered algal laminates and burrowed horizons, which is capped by intraclastic grainstones, shales and mud cracked horizons.

The interbedded nature of the algal laminations and burrowed horizons indicates fluctuating environmental settings. Shallow-water conditions may have prevailed to facilitate the presence of algal and burrow structures; however, salinity fluctuations can also explain alternating algal/burrow horizons (i.e., the flourishing of algal laminates due to possible declines in predating burrowing organisms) (Tucker and Wright, 1990). The presence of intraclastic limestone and cross bedded oolites, ripple marks, overturned algal, black shales and mud cracks at the crest of the facies characterizes agitated water conditions with occasional subaerial exposure. The intraclasts are interpreted as the gouging of subaerial sediments by flooding.

The intraclastic horizons are deposited in the peritidal and serve as a substrate for the large algal structures capping the facies. The large algal boundstones, and overturned algal, index a return to higher energy subaqueous environment, with the increasing size of domal algal suggesting encroachment of open-marine conditions.

Finally, the presence of micritic limestones, black shales, quartz vugs, ripple marks, and mud cracks at the top of the facies indicates subaerial exposure and the re-establishment of quiet-water conditions in a near shoreline/shoreline environment, such as a tidal flat or lagoon.

The presence of intraclastic limestones, overlain by grainstones, capped by coarse grained limestones and/or boundstones suggests marine transgression initiating the

deposition of Wildcat Road facies 2. The presence of intraclastic limestones indicates that the inundation of the shoreline transported rip-up clasts seaward, to be overlain by grainstones deposited in a high-energy environment. The intraclastic and grainstone carbonates are the substrate for algal laminations, which are overlain by patchwork domal algal. The repetitive nature of this association in Wildcat Road facies 2 suggests fluctuation of sea-level between the extremes of exposure and submergence deep enough to support boundstone accumulations becoming inundated with intraclastic debris.

The quartz sandstone in the upper part of facies 2 indicates renewed siliciclastic influx from a provenance that is, to date, uncertain. Still eroding highlands on the Laurentian craton, or land masses off shore, may have been providing sand into the depositional environment. The presence of black shales at the top of the section, overlain by intraformational conglomerates and intraclastic limestones, suggests the reworking of beach sediments and strandline deposits and the progradation of the beach line, and associated lagoon, over the boundstone accumulations.

Facies 3 contains micritic, algal laminated limestone capped by black shale indicates a supratidal setting at the base of this facies. Algal laminated, dolomitic limestone bearing graded oolite indicates an increase in water energy, suggesting submergence of the lower supratidal environment. Rip-up clasts of algal laminate at the top of the section are inferred as near shore face facies where wave action scoured exposed algal laminate and redeposited the ripped clasts into the peritidal realm. The shale capping the rip-up clast horizons, and the increasing shale content towards the top of the section indicates a renewed influx of siliciclastics into the section. The co-occurrence of quartz vugs, interpreted as replaced anhydrite and gypsum structures,

suggests exposure in a supratidal setting. An alternative hypothesis suggests that the numerous shale horizons in the top of the section represent aspects of a renewed or rejuvenated lagoon or tidal flat setting.

4.6.3 Sea-Level Curve Interpretations

The Wildcat Road Member is 95.5 m thick at the stratigraphic type section. The basal contact shares an unconformity with the underlying Wallkill Member. Five additional unconformities mark the member, with the unconformities at the basal and upper contacts of the member being lined with chert. The upper unconformable contact contains tan, silicified shale and/or claystone. Fifty-seven fifth-order transgressive-regressive cycles are interpreted from facies characteristics of the member (Plate 4.2). Extremes in transgression range from a lower subtidal maximum to an upper peritidal minimum. The maximum drop in sea level promoted supratidal environments, with the minimum draw down breaching the upper intertidal-lower peritidal. There are two cycles of periodicity and wavelength variation in the fifth-order curve. Both cycles start with long wavelength curves that experience wavelength attenuation up stratigraphic section. The long wavelength sections of the fifth-order curve represent severe marine inundation (lower intertidal/lower subtidal, respectively), while the shorter wavelength sections show shallower ranges of sea-level fluctuation (lower intertidal to upper peritidal). The larger wavelengths range from 250 cm to 1.5 m. The shorter wavelengths range from 50 to 150 cm.

Fourth-order sea-level curve interpretations, from statistical smoothing of the fifth-order curve, propose the presence of seven transgressive-regressive pulses (Plate 4.2). The maximum level of transgression supported lower subtidal environments.

Peritidal sedimentation was supported by the minimum level of fourth-order transgression. Maxima/minima settings for regression range from the lower supratidal-upper peritidal transition to upper intertidal, respectively. Predictably, the lower periodicity and larger wavelengths of the fourth-order curves are of the same magnitude as the larger fifth-order wavelengths. Periodicity decreases and wavelength increases up stratigraphic section, from approximately 1 to 3 meters.

The sea-level curves for the Wildcat Road Member show the sedimentation range expanding out of the peritidal and in this case, into the subtidal to the supratidal. The lower half of the Wildcat Road Member is deposited in predominantly peritidal conditions, with one incursion into the intertidal for 800 cm of section. However, a 3.5 m section of the upper half of the member is deposited under intertidal conditions, with a major transgression into the subtidal. Deeper marine conditions do not last, however. The upper 800 cm of the Wildcat Road Member document a return to peritidal conditions, indicating a return to low-stand sea level in the region.

4.7 Limeport Formation: Wheatsworth Mills Member

4.7.1 Facies Descriptions

Wheatsworth Mills Facies 1

The basal Wheatsworth Mills facies is a blanket of structureless, to graded, to cross bedded oolite overlain by a thick, algal laminated, dolomite containing massive chicken-wire evaporites and mud cracks. The algal laminate in turn is overlain by thick beds of oncoidal grainstone, supporting LLH-type, domal algal structures (Davies et al., 1985; Davies and Montaggioni, 1985; Dill et al., 1986). The domal algal are overlain by

quartz sandstone and intraformational conglomerates. Oncoids, ooids and rip-up clasts terminate the facies (Figure 4.8).

Wheatsworth Mills Facies 2

Facies 2 begins with thick beds of cross bedded oolite and overturned algal interbedded with quartz sandstone. Thrombolitic domal algal overlie the cross bedded oolite, and in turn are overlain by massive, cross bedded, oncoidal beds capped by fine algal laminated dolomites. Thick, intraformational conglomerate caps the algal laminations.

Wheatsworth Mills Facies 3

Facies 3 starts with a basal grainstone sequence of mixed ooids and pisoids and shallows to a boundstone of LLH-type stromatolites. The stromatolite horizons are overlain by an olive to black, silty shale which in turn is capped by thick dolomitic limestone bearing chicken-wire evaporite structures. This is capped by a thick sequence of cross bedded, coarse grained, quartzitic siltstone and thick, compositionally and texturally mature, fine to medium grained, quartz sandstone capped by mud cracked, micritic dolomitic limestone (Geister, 1980). The quartz sandstone in this facies is unlike others mapped in the Kittatinny Supergroup in that it occurs as individual beds of cross bedded sediments, as opposed to thin wisps and layers of sandstone interbedded with carbonate.

Wheatsworth Mills Facies 4

Facies 4 is an accumulation of upright and overturned algal boundstones succeeded by a thick accumulation of dark gray, micritic, strongly algal laminated dolomitic limestone. Facies 4 is the acme of development of the large domal algal

sequences. The algal occur interbedded between thick intraclastic limestones and intraformational limestone conglomerates (Geister, 1980; Ginsburg and Schroeder, 1973; Graus and Macintyre, 1989). The base of facies 4 is strongly brecciated. This breccia is different from edgewise conglomerate and intraclastic horizons in that the breccia clasts have not been transported, but can be refit back together given small amounts of rotation and the reconstruction of rounded edges. The upper part of the facies includes a succession of intraclastic limestones and graded oolites.

Wheatsworth Mills Facies 5

This facies begins with a thick accumulation of alternating thin and thick beds of arenaceous limestone which yields to graded oolite. The lower part of the facies contains intraformational conglomerates and intraclastic horizons, which are peppered with quartz vugs and thin horizons of cross bedded oolite. The upper section contains strongly cross bedded (tangential and trough) sandstones. This series yields to alternating thin and thick bedded, intraclastic, micritic limestones bearing thick accumulations of graded and cross bedded oolite, sparse domal algal structures and mud cracked intervals.

4.7.2 Paleoenvironmental Setting

The basal blanket of structureless, graded and cross bedded oolite of the Wheatsworth Mills Member represents rapid inundation of the underlying supratidal facies of the Wildcat Road Member. These features indicate high-energy subaqueous environments. The algal laminated beds in the upper part of this facies bear chicken-wire evaporite structures and mud cracks indicating a supratidal/tidal flat setting associated with a draw down in sea level. The second grainstone succession bearing large, LLH-type, domal, indicates the re-establishment of a more open-marine environment where

wave action fostered the growth of the large algal (Dunham, 1970). Many of the domal algal are truncated, convoluted and even overturned, probably by storm and wave surge, suggesting that the algal grew vertically toward the photic zone and experienced shearing or growth retardation as the water-air interface was approached. Eventually, the domal algal were smothered by interbeds of intraformational conglomerates, rip-up clasts, desiccated algal and thin and thick quartz sandstones indicating another draw down in sea level within the Wheatsworth Mills Member.

The presence of cross bedded oolite, overturned algal and quartz sandstone in facies 2, capped by fine algal laminates and intraformational conglomerates, indicates inundation and the creation of an open-marine environment, followed by sea-level draw down and the re-establishment of a supratidal environment. Open, epeiric conditions permits the flourishing of the LLH-type domal algals (Dunham, 1970; Graus and Macintyre, 1989). However, the reef system is overridden with intraclastic deposits derived from gouging of exposed sections of the platform, possibly as the result of marine inundation or shorter term storm events. The appearance of thick beds of oolite overlain by thrombolites, with the draping of contiguous oncoidal and cross bedded oolite sequences suggests the continual progradation of the shelf margin.

Facies 3 is another example of grainstone serving as the substrate for LLH-type algals and boundstones presumably in an epeiric setting. The capping of the algals by shales overlain by evaporite structures, siliciclastics and mud cracked, micrite indicate progradation of supratidal sediments and exposure of the unit. The thick, bedded arenite contains compositionally and texturally mature quartz sandstones that are silt to medium-grain size and very well sorted. The silt grain size, cross bedding and high degree of

sorting and compositional maturity suggests that the quartz arenites may be eolian dune deposits encroaching the shore face and being reworked.

The breccia in facies 4 that contain weathered and slightly rotated clasts that can be refit are interpreted as being the result of karst development on an exposed carbonate platform. Overlying the inferred karstic plain are domal algal interbedded with intraclastic limestones and intraformational limestone conglomerates suggesting marine transgression in which a high-energy subaqueous environment is responsible for the creation of intraclasts, conglomerates and overturned algal, but quiet enough to permit settling of these clasts in the water column (Kennard and James, 1986). The large domal algal are best developed in open, marine conditions where waves move through the environment (Longman, 1981). The accumulation of micritic, strongly algal laminated dolomitic limestone at the top of the facies indicates a shift in environments to lower supratidal (algal laminated micrite).

Arenaceous limestone in facies 5 indicates additional siliciclastic influx into the system, with the intraclasts, quartz vugs and cross bedded oolites suggesting an upper intertidal/lower supratidal setting. However, the tangential and trough cross bedded sandstones are typical of beach deposits indicating possible deposition at the shore face within the upper reaches of the peritidal. Mud cracked, micritic limestones at the top of the facies require subaerial exposure and a shifting of the peritidal setting to a supratidal setting (Grotzinger, 1989; James and Gravestock, 1990).

4.7.3 Sea-Level Curve Interpretation

The Wheatsworth Mills Member is 65 m thick at the type section and contains twelve mud cracked unconformities. Fifth-order sea-level curves infer the documentation

of forty-seven transgressive-regressive pulses in sea level (Plate 4.3). Extremes in fifth-order transgressions supported middle subtidal and lower peritidal conditions, respectively. The maximum amount of regression supported lower supratidal conditions, while the minimum regressive episode permitted lower peritidal environments. Large periodicity and small wavelengths (100 to 600 cm) of the fifth-order sea-level curve indicate that sea level fluctuated frequently in the lower 4.8 m of the member. One transgressive pulse in the upper third of the member exhibits the greatest wavelength of this curve, standing at 1.4 m. The remaining 1.5 m of the member returns to a small wavelength curve inferring rapidly fluctuating sea-level.

Fourth-order curves infer thirteen episodes of sea-level rise and fall (Plate 4.3). The maximum amount of sea-level transgression is documented by lower subtidal sediments. Minimal sea-level transgression supported middle peritidal settings. Extremes in regressions range from upper peritidal maximums to lower peritidal minimums. The periodicity and wavelengths of the fourth-order curve in the lower 1 m of the member are of the same magnitudes as the corresponding fifth-order curve. The remainder of the Wheatsworth Mills Member has a fourth-order curve exhibiting wavelengths of greater magnitude than the corresponding fifth-order curve.

The Wheatsworth Mills Member, for the most part, was deposited under peritidal conditions; although, restricted incursions into middle and upper intertidal settings in the lower part of the member and one pulse into the lower subtidal in the upper half of the unit are exceptions. This member is interpreted as having been deposited in continuing low-stand conditions carrying over from the underlying Wildcat Road Member.

4.8 Limeport Formation: Gruenwald Member

4.8.1 Facies Description

Gruenwald Facies 1

Generally, mud cracked and desiccated micritic limestones, and associated intraformational conglomerates, comprise the base and crest of the Gruenwald Member. Encapsulated in this section are no less than fourteen, thick accumulations of intraformational conglomerates, including alternating thin and thick lenses of oncoids, pisoids and graded oolites, intraclastic limestones comprised of rolled algal laminate, and ooids wrapped in algal laminate (Figure 4.9). The base of each grainstone sequence is peppered with quartz vugs. All eleven boundstone occurrences are overlain by intraclastic limestones and capped with mud cracked intervals (Kennard and James, 1986). The baffles of the boundstone accumulations are filled with micrite, which is desiccated on its surface. Overlying these successions are dark, micritic, algal laminated, dolomitic limestones. The intraclastic units and overlying micritic limestones serve as the foundation for eleven accumulations of domal algal structures, some of which are very closely spaced; while others are truncated along their upper surfaces (Figure 4.10) (Longman, 1981).

Two tangentially and trough cross bedded sandstone and siltstone occurrences are located in the midsection, and at the crest, of the section. This recurrent theme of basal intraclastic horizons, overlain by draping facies of cross bedded, peloidal grainstones and packestones, succeeded by boundstone accumulations is strongly reminiscent of the Conococheague Cycles occurring to the south and west of the dissertation study area

(Hobson, 1963; Valentin et al., 1964; Zadnik, 1960), with the exception that Conococheague Cycles are not capped by fine grained, mudcracked micrites and shales along their crests (James and Ginsburg, 1979; James and Gravestock, 1990).

4.8.2 Paleoenvironmental Setting

The pattern of grainstone-algal laminated micrite-truncated boundstone in this facies indicates a shallowing upward section reaching for the air-water interface, being eroded and subsequently inundated in a repetitive fashion. The baffle filling micrites and upper mud cracked surfaces preclude the determination that these massive boundstones are located along the edge of a shelf. In fact, the micrite cappings and mud cracked intervals indicate that the environment for the Gruenwald Member is not the shelf margin, or shelf edge, but instead the boundstone accumulations may have occurred on stabilized shoals of intraclastic debris derived from the inundation of the land surface and encroachment of the shoreline (Chappell and Polach, 1976; Davies and Hopley, 1983; Dill et al., 1986). The repeated boundstone sequence may represent a barrier environment, which would represent the intertidal parts of what is, overall, a lower peritidal sequence (Kennard and James, 1986; Kobluk and Crawford, 1990; Neumann and Macintyre, 1985). If this is the case, subsequent marine drawdown would permit the progradation of the tidal flat facies, lagoonal sequences, and shoreline facies over the boundstone horizons; which appears to be the case for the Gruenwald Member (Dunham, 1970; Graus and Macintyre, 1989; Longman, 1981).

4.8.3 Sea-Level Curve Interpretation

The 92.75 m thick Gruenwald Member contains seven mud cracked unconformities. Fifty-one episodes of sea-level fluctuation are documented by the fifth-

order sea level curves created for the member (Plate 4.4). Transgressions reach a maximum represented by middle subtidal sediments and a minimum preserved by upper peritidal settings. Lower supratidal environments represent the greatest magnitude regression and middle intertidal settings were supported by the lowest magnitude draw downs. The lower 2.8 m is a fairly large wavelength transgression curve, with minor fluctuations representing minor regressions. The remainder of the member contains a fifth-order curve that has wavelengths ranging from 100 to 400 cm and a greater periodicity.

The fourth-order cycle documents fourteen pulses of transgressive-regressive cyclicity (Plate 4.4). Transgressive maxima and minima range from lower subtidal to middle peritidal, respectively. Regressive extremes span a lower supratidal maximum to a middle intertidal minimum. The fourth-order curve in the lower 2.8 m of the section has a wavelength of similar magnitude to the corresponding fifth-order curve. The wavelengths of the fourth-order curve range from 200 to 800 cm in the mid-section of the member and experience the corresponding periodicity increase. Fourth-order wavelength increases again towards the top of the section to a range of 2 to 2.5 m. Twenty-seven smaller scale sea-level draw downs punctuate the fourth-order curve in the upper Gruenwald Member.

The lower 2.8 m of the Gruenwald Member experience a departure from peritidal depositional settings and exhibit sedimentological features indicative of intertidal deposition. The remainder of the member fluctuates from deposition in the intertidal to deposition in the peritidal. The unit as a whole was deposited in a primarily intertidal environment, indicating that regional low-stand sea-level conditions were changing to

deeper water environments at this point in the evolution of the passive margin of eastern Laurentia.

4.9 Limeport Formation: Glacial Quarry Member

4.9.1 Facies Description

Glacial Quarry Facies 1

This facies contains four complete Conococheague-like cycles (Hobson, 1963), all of which are markedly similar in that they overlie grainstone facies which were interpreted for the Gruenwald member as representing stationary shoals. These repetitive sedimentation patterns contain interbeds of parallel and cross bedded ooids, pisoids and algal fragments. Each succession is, in turn, overlain by beds of carbonate edgewise conglomerates, cut-and-fill channels, rip-up clasts and ooid sequences. The cut-n-fill channels contain a carbonate lag. Generally, the lower and upper parts of the sequence are similar in that they are finer grained, contain more mud cracked intervals, while the intermediate part of the sequence is more thickly bedded, bears more intraclastic horizons and is very coarse grained. Quartz sandstone is present at the top of the facies, containing cut-and-fill channels, and is sandwiched between strongly algal laminated, mud cracked, micrites bearing thin shale horizons.

4.9.2 Paleoenvironmental Setting

The interbeds of parallel and cross bedded ooids, pisoids and algal fragments imply high-energy, subaqueous environments (Pratt, 1982a, b; Pratt and James, 1982; Rees et al., 1989). The overlying successions of edgewise conglomerates, rip-up clasts and ooids indicate currents either debouching into an open body of water, or tidal channels moving sediments between open, epeiric and back-barrier environments. The

presence of cut-and-fill channels marks the appearance of the cycles at sea level. Due to the lack of siliciclastics in the conglomeratic/cut-and-fill series, the latter hypothesis is preferred, as terrestrial fluvial channels debouching into a delta would have provided siliciclastics into the system (Neumann and Macintyre, 1985). As such, these interbeds of parallel and cross bedded ooids, pisoids and algal fragments are interpreted as shallow subtidal, high-energy, shoaling grainstone facies, which become stabilized by the first appearance of algal laminates capped by colonizing boundstones, which coarsen upward towards sea level. The cut-and-fill channels may represent the lateral migration of prograding, lower and intermediate peritidal, lagoonal outlet facies (Sheehan, 1985; Stearn, 1982). The truncation of the grainstone/boundstone sequences along their crests infers that they are not located on a shelf edge, but instead shoreward, on raised platforms (possibly the remnants of karstic pedestals developed in the underlying Gruenwald Member). The presence of strongly cross bedded grainstones, and the lack of sandstones and micrites in the Conococheague-like cycles, indicates that the small patches of reef-like structures were established on a part of the barrier, possibly exposed on the oceanward side (Tudhope, 1989).

The medial part of the facies witnesses an increase in the number and thickness of intraclastic horizons consisting of graded and non-graded ooids, draping cross bedded oolite sequences, capped with domal algal structures. Cut-and-fill channels are still present, but are fewer in number and the incisement is upon the boundstones, not on micrites. There are no siliciclastics in the form of shales, sandstones and there are only a few micritic facies in the mid-part of the member (Rowland and Gangloff, 1988; Schlager, 1989). This is interpreted as possibly the furthest advancement seaward of the

small boundstone accumulations. The paucity of quartz sandstones in the lower and middle part of the facies may suggest the establishment of a lagoon-margin barrier, which may be protecting a large quantity of terrestrially derived quartz sandstone on the landward side. Therefore, the thick blankets of intraclastic debris can be interpreted as pass-through grainstone facies and intraclastic horizons, which are channeled through raised pedestals of stabilized boundstones. This minor pass-through resides under storm base, in the shallow subtidal, along the edge of the carbonate platform (Dill et al., 1986; Dunham, 1970).

The upper part of the facies witnesses the appearance of quartz sandstones, cut-and-fill channels superimposed on black shales, and algal laminated micrites. Boundstones are generally larger in dimension than those occurring in the lower parts of the facies; however, they are fewer in number.

The abundance of quartz sandstone lenses, black shales, and mud cracked micrites in the upper part of the facies suggest that progradation of the lagoonal facies over the underlying boundstones. Progradation and lateral migration of fine grained, lagoon sequences is associated with sea-level draw down and the associated progradation eventually drowns the small patches of boundstone and micritic muds. The reintroduction of abundant quartz sandstones suggests a lagoon-margin barrier may have been breached, or overridden, providing an outlet for the reservoir for detrital quartz sandstone.

4.9.3 Sea-Level Curve Interpretation

The Glacial Quarry Member is 18 m thick in the type section and bears three unconformities, not including the unconformity the unit shares with the underlying

Gruenwald Member. Chert lines the upper two unconformities in the member. The middle unconformity is lined with silicified grainstones, sandstones and stylolites. The sandstone and grainstone cherts are pods underneath the unconformity and beds above the unconformity. The uppermost unconformity contains silicified sandstone beds. Ten fifth-order scale regressions are interpreted from facies relationships in the member (Plate 4.5). Extremes in fifth-order transgression range from the transition between upper subtidal and lower intertidal to upper peritidal, respectively. Maximum regression supported supratidal sedimentation, whereas minimal regressive episodes permitted upper intertidal conditions. Wavelengths of the fifth-order curve range from 50 to 400 cm.

The fourth-order curve interpolated from the fifth-order interpretation contains four transgressive pulses of a 600 to 800 cm wavelength (Plate 4.5). Maximum transgression approaches the lower intertidal-upper subtidal transition, minimum transgression supports medium peritidal sedimentation. Regressions range from an upper peritidal maximum to a lower peritidal minimum.

The Glacial Quarry Member is deposited equally in transgressive and regressive settings. The sea-level curves extend from the subtidal-intertidal transition to the lower supratidal, indicating that while regressions are common, the passive margin is experiencing rising regional seas that are commonly punctuated by local regressions.

4.10 Limeport Formation: Edison Member

4.10.1 Facies Description

Edison Facies 1

Facies 1 of the Edison Member contains seven repeated sedimentation patterns of algal laminated, micritic limestone and dolomitic limestone, interbedded with thin and

thick accumulations of quartz sandstone capped with algal boundstone (Friedman et al., 1973; Frost, 1974). Grainstone facies are not as abundant in the Edison Member as they are in the underlying members of the Limeport Formation; however, the grainstones that do occur in the facies are alternating beds of graded oolite and cross bedded quartz sandstone. Boundstones capping the micrites are of two types, large domal successions that occur towards the base of the member; and smaller colonies of convex domal algal in the mid and upper parts of the facies that contain a great number of truncated (i.e. thinner beds and smaller algal) boundstone horizons. Intraclastic limestone or shales blanket the boundstone colonies at the top of the member. Chicken-wire structures occur near the base of the section, overlying shale and underlying algal laminated dolomite. Quartz vugs become more common in the upper half of the facies and are associated with algal laminated horizons. The crest of the facies contains black shales and mud cracked intervals, indicating the presence of an unconformity (Friedman, 1969).

4.10.2 Paleoenvironmental Setting

Algal laminated, micritic limestone, and dolomitic limestone bearing chicken-wire and/or quartz vugs indicate supratidal environments. There are three shallowing cycles within the facies indicating sea level lowered enough to at least three progradational pulses. The presence of quartz sandstones and shales interbedded with, or sandwiching, these supratidal sediments indicates siliciclastic influx. In contrast, the presence of truncated boundstones indicates several episodes of low amplitude, sea-level transgression. Large domal algal in the lower part of the facies indicates that sea-level transgression had a greater magnitude than towards the top of the facies; where beds are

thinner and bear smaller domal algal colonies (Garrett, 1970; Gebelein, 1969; Gebelein and Hoffman, 1973).

The interbedded siliciclastics are interpreted as being derived from the sandstone reservoirs that were hypothesized as accumulating behind grainstone/boundstone barriers in the underlying Wheatsworth Mills, Gruenwald and Glacial Quarry members. A breach in such quartz sandstone reservoirs would provide a unique substrate for the smaller-scale algal boundstone sequences in the mid and upper part of this facies. The shoaling sandstones could be stabilized by algal laminations with the algae serving to stabilize the surface for further colonization by domal algal communities (Hoffman, 1973a; Hoffman, 1973b; Howe, 1966). Each colony of algal was subsequently terminated by algal laminated micrites and shales, which cap the upper cycles in the facies. The convex algal structures are also surrounded by algal laminated and quartz vug bearing micrites and shales, indicating that the upper half of the facies experienced the re-establishment of shaly, outer lagoonal, facies (Kumar, 1973). Outcrop profiles of the section show that the channels between the grainstone/boundstones are filled to an equal elevation with the raised carbonate platform. This type of micritic channel infilling indicates that any hypothesized pre-existing karstic undulations in the carbonate platform were being smoothed over. Cross bedded, quartz sandstones and intraclastic limestone conglomerates override the smoothed carbonate platform, overlying (and smothering) the large algal boundstone colonies of the underlying members. As such, these colonies are starved, desiccated, or completely buried and the only living colonies of algal boundstone are represented by the re-establishment of small, patch mounds occurring along the distal

end of the re-established tidal flat (Heckel, 1972, 1974; Klein, 1967, 1970a, 1971; Lucia, 1972).

4.10.3 Sea-Level Curve Interpretation

The Edison Member is 19 m thick at the type section and contains two unconformities (not including the basal contact), one mid-member and one at the upper contact. The upper unconformity is underlain by silicified shale and overlain by silicified stylolites. Six fifth-order transgressive-regressive episodes mark the member (Plate 4.5). Maximum transgression is documented by upper intertidal sediments. Minimum transgression preserved upper peritidal sediments. The regressive curves stay constant in the upper peritidal-lower supratidal transition. Periodicity increases and curve wavelength decreases up stratigraphic section, ranging from 500 to 600 cm lengths in the lower 2 m of the member to 150 to 200 cm in the upper parts of the unit.

Fourth-order sea-level interpretations show one transgressive-regressive pulse of large magnitude, i.e. 2 m wavelength (Plate 4.5), with transgression in the upper intertidal. Maximum regression remained constant as upper peritidal sedimentation in the unit.

The sea-level curves for the Edison Member span upper intertidal to transitional upper peritidal/lower supratidal settings. As a whole, the Edison Member is interpreted as being a regressional stratigraphy, with one major transgressive pulse located in the lower mid-member. The constriction of the sea-level curves to intertidal-peritidal settings suggests that regional sea level may have dropped with respect to the underlying Glacial Quarry Member, but one transgressive pulse did occur during Edison deposition.

4.11 Limeport Formation: Rte. 94 Member

4.11.1 Facies Description

Rte. 94 Facies 1

The Rte. 94 facies contains twelve repetitions in sedimentation pattern that are similar to the Conococheague-like cycles described in the underlying members of the Limeport Formation. As with the underlying Glacial Quarry Member, these cyclic occurrences are truncated; eight of the twelve repetitions are tightly constrained into two, thinly developed stratigraphic horizons. The remaining four cycles occur towards the top of the facies and are somewhat larger scale, Conococheague-like cycles, founded on blankets of graded ooids, pisoids and intraclastic limestones (Logan, 1961; Logan et al., 1964).

The base of the Rte. 94 facies is brecciated, with the clasts showing solution weathering and being close enough to re-fit to each other. Directly overlying the brecciated horizon are fine to medium grained, well sorted, compositionally mature, cross bedded, quartz sandstones. The Conococheague boundstone occurrences in the lower cycles are smaller than their predecessors and each is covered by intraclastic limestones (Logan et al., 1969). The truncated cycles overlie sulfurous quartz vug, algal laminated, dolomitic limestones and are blanketed by draping, cross bedded, pisoid and ooid sequences. The upper half of the facies is different from the lower half in that grainstone horizons increase in abundance and thickness. Cross bedded varieties and lenses of quartz sandstone decrease significantly. The boundstones occurring in the upper half of the member are based on thicker blankets of intraclastic limestones and graded to cross

bedded oolites and oncolites. Cross bedded sandstones, in close association with mud cracked intervals, intraclastic limestones, and shales cap each boundstone sequence.

4.11.2 Paleoenvironmental Setting

As discussed previously in the Edison Member, the brecciated base of the facies is interpreted as a subaerially exposed, karstic horizon. Texturally and compositionally mature, cross bedded quartz sandstones directly overlying the karstic plain suggest that the lower half of the member is deposited in association with exhumed siliciclastics or possible dune structures which may have collapsed along the shore face. The sulfurous quartz vugs are interpreted as silica replaced gypsum and anhydrite.

The presence of cross bedded quartz sandstones, evaporitic structures, in combination with the algal laminated dolomitic limestone suggests a supratidal, near shoreline setting. The compressed nature of the boundstone horizons indicates that each accumulation of laminates, and overlying convex algal, occurs close to sea level. However, the graded oolites and cross bedded sandstones buttressing the boundstone horizons indicate that the environment is of a higher energy. The quartz sandstone lenses may represent stabilized, migrating sand shoals (Martinsson, 1974).

The upper half of the facies witnesses the reintroduction of graded, grainstone facies and intraclastic rip-up clast horizons overlain by mud cracked, algal laminated micrite, capped by black shale. As such, the upper half of the facies may be a shoaling upward succession deposited at peritidal mean wave base. The subsequent covering of the grainstone/intraclast horizons and algal laminated sediments may suggest lateral migration of lower shoreline, lagoonal setting over the peritidal sequence.

As both the lower and upper part of this facies occur in the lower supratidal/peritidal regime (at or within mean wave base), the author infers that the upper part of the member represents a lateral facies relationship to the lower part of the member. Perhaps stabilized sand shoals resulting from the progradation of dunes seaward (Osleger, 1991; Otvos, 1966; Palmer, 1971; Purdy, 1963a, 1963b, 1974).

4.11.3 Sea-Level Curve Interpretation

The 36 m of the Rte. 94 Member contain three unconformities in the section, not including the basal unconformity. There are 28 fifth-order regressions in this member, ranging from 100 to about 600 m in wavelength (Plate 4.6). Periodicity remains fairly constant in this section. Transgression maxima/minima range from upper subtidal to mid-upper intertidal, respectively. Maximum regression allowed supratidal depositional conditions while minimum regression allowed middle intertidal sediments to be deposited.

Fourth order sea-level curves in the Rte. 94 Member are of a large wavelength (approximately 1 m) and constant periodicity (Plate 4.6). There are four, fourth-order, transgressive pulses. Maximum transgression supports lower intertidal, while minimum conditions permitted upper intertidal sedimentation. Maximum fourth-order regression supported upper intertidal conditions. On average, seven to nine fifth-order regressions punctuate the fourth-order transgressions in the Rte. 94 Member.

The Rte. 94 Member sea-level curves show equal amounts of transgressive vs. regressive episodes, with periodicity of the curves showing regular transitioning between sea-level rises vs. sea-level falls. The curves span from upper subtidal to lower

supratidal, indicating and overall departure from sea-level low stand, with regressive punctuations being commonplace.

4.12 Upper Allentown Formation

4.12.1 Facies Description

Upper Allentown Facies 1

The lowermost facies in the Upper Allentown Member overlies the unconformities occurring along the crest of the Limeport Formation (discussed in Chapter 3). The lower facies is an interbedded, thin to thick, hummocky grainstone which includes interbedded pisoid and ooid lenses, graded and cross bedded oolites and fine grained, algal laminated dolomitic limestones. This facies is typified by thin to thick, cross bedded, quartz sandstones.

Intraclastic and dolomitic limestones cap the quartz sandstone lenses. Domal algal occur in two discrete zones and are strongly convex, but not thrombolitic. The domal algal occur directly over the cross bedded quartz sandstones and associated grainstone facies. The top of this facies contains a thick sequence of graded oolite and pisoid (Lohmann, 1976).

Upper Allentown Facies 2

The second facies is a thick bedded, graded, quartz sandstone bearing intraclasts or clots of quartz sand wrapped in algal filament (quartz grains are visible in thin section and slabs). Directly overlying this marker horizon is a thick succession of graded oncoid, pisoid and ooid beds, each capped by a quartz sandstone bearing intraclasts of algal filament coated quartz sand. Concentrations of chert along the base of the facies primarily replace grainstone, with sparse amounts of algal structures, quartz sandstone

lenses, irregular clots, and rip-up fragments of algal being selectively silicified.

Upper Allentown Facies 3

The third facies contains cross bedded, quartz sandstones interbedded with thick accumulations of ooids, pisoids, and oncoids. The base and crest of this facies contains algal laminated dolomitic limestones.

Upper Allentown Facies 4

The fourth facies preserves cross bedded, ripple marked, quartz sandstones occurring as thin to thick, hummocky beds, the bases of which are scour-and-fill channels. The base of the facies also contains algal laminated, fine grained dolomitic limestone with abundant intraclastic grainstones. The upper half contains a minimum of five intraformational conglomerates. Each limestone conglomerate overlies quartz sandstone and is, in turn, overlain by large convex, domal algal. The quartz sandstones are lined with shale at their bases. This succession is repeated six times in the upper half of the fourth facies. Many of the delicate depositional features associated with the upper half of the fourth facies are replaced by silica. These include intraformational conglomerates, laminated and convex algal structures, quartz sandstones and grainstones. The top of the fourth facies and the uppermost part of the Upper Allentown Member is capped by an intraformational limestone conglomerate with algal laminated horizons and intraclastic facies. An unconformity truncates this facies of the Upper Allentown Member.

4.12.2 Paleoenvironmental Setting

The presence of hummocky, interbedded, pisoid and ooid grainstones in facies 1 overlying unconformable surfaces in the underlying Rte. 94 Member of the Limeport

Formation, indicate marine inundation of a subaerially exposed surface by a high-energy subaqueous system. The presence of algal laminates in facies 1 of the Upper Allentown is not interpreted as representing a supratidal setting, as there are no dessication and/or evaporite features in the laminates to confirm that environment. Cross bedded, quartz sandstones overlain by intraclastic carbonates indicates that the sediments may be obtained from scouring and reworking of a shore face (Schlager, 1981, 1990), with deposition of the intraclasts in the peritidal realm. Hummocky beds support this interpretation indicating the re-establishment of near shore-face conditions, possibly well within the peritidal zone. The quartz sandstone also indicates that the shoreline is receiving siliciclastic influx from some subaerial setting. The textural and compositional maturity of the sandstone indicates that the sediment is far travelled from it source terrane. The domal algal capping the quartz sandstone and grainstone units suggest that the depositional setting was open to wave action (Sellwood, 1986).

Graded and cross bedded quartz sandstones in facies 2 and 3 bearing quartz sand wrapped in algal filament, and the presence of graded oncoid, pisoid and ooid grainstones, suggests that open, epeiric conditions continued from the first facies, into the second facies, and into the third. Algal laminates at the base and crest of the third facies do not occur with evaporite or dessication features and this lack of association challenges a supratidal interpretation. The presence of algal laminates in the third facies may suggest a quieter setting than the sandstones and grainstones in facies 2 represents; however, both facies are still interpreted as being higher energy, open systems, not restricted lagoons, as was suggested for the underlying Limeport Member. Therefore,

facies 3 may represent a lower intertidal/shallow subtidal setting below mean wave and storm base (Frost, 1974).

Scour-and-fill channels in the quartz sandstones of the fourth facies indicate channel flow. Algal laminated, fine grained, dolomitic limestones with hummocky, intraclastic grainstones and intraformational conglomerates indicate deposition in the lower peritidal, but perhaps in a lower energy setting than interpreted for the lower facies of this member. Shale lining the bases of quartz sandstones supports this interpretation. The scour-and-fill channels, in combination with the influx of siliclastics into the facies, and the lower energy peritidal setting suggest a possible subaqueous carbonate fan deposit, or a tidal setting where the channelized deposits are tidal inlets. The presence of algal laminations lends support to the tidal setting interpretation, in which the siliciclastic influx would stem from reworking of a nearby shore face.

The Upper Allentown Formation represents inundation of the carbonate platform and is associated with the rapid influx of massive quantities of detrital quartz sand and rip-up intraformational limestone conglomerates. The mid part of the member (facies 2) may represent the deepest depositional environment (subtidal) achieved during this time, possibly that of a subtidal shelf where thick deposits of grainstone may have created fans or drapes along the shelf. However, the subtidal regime still manifests itself through the influx of reworked quartz sand. Shallowing occurs from facies 2 to facies 3 (shift from subtidal to peritidal setting), with the reappearance of abundant intraclastic limestone deposits and cross bedded quartz sandstones (Halley, 1969; Hardie et al., 1991; Lohmann, 1976; Markello and Read, 1981, 1982; Otvos, 1966; Owen, 1973). Re-established near shore-face conditions are suggested by the reappearance of abundant

laminated and domal algal accumulations each founded on a blanket of intraclastic carbonate including limestone, cross bedded quartz sandstones and sparse shale.

4.12.3 Sea-Level Curve Information

The 86 m Upper Allentown Formation houses two unconformities, one each at both formational contacts. As the basal unconformity was described previously in this chapter, the unconformity at the upper contact will be discussed here. The unconformity at the upper contact with the overlying Carlton Village Member of the Stonehenge Formation is lined with silicified grainstones, chert breccias and rip-up clasts. Fifty-three fifth-order transgressions-regressions are present in the Upper Allentown, with the maximum regression reaching the upper peritidal-lower supratidal transition and minimum regressions permitting lower intertidal sedimentation (Plate 4.6). Intervening transgression curves show maximums allowing middle subtidal sedimentation and minimums reaching middle peritidal conditions. Wavelengths are attenuated in the Upper Allentown Formation, ranging from 100 cm to 1 m in maximum length. Periodicity is fairly constant in the formation, with the exception of a wavelength lengthening in the lower half of the formation, indicating a reduction in the periodicity of sea-level fluctuations.

Fourth-order sea-level change shows seven transgressive-regressive cycles (Plate 4.6). Wavelength of the fourth-order curve is of a different magnitude than the corresponding fifth-order curve, with fourth-order wavelengths ranging from 1 to 2 m. One extended period of fourth-order sea-level transgression is present along the 5 to 7 m formation thickness markers. This maximum transgression permits middle subtidal sedimentation and is punctuated by thirteen fifth-order regressive pulses. The minimum

transgression allowed lower peritidal conditions to prevail. Extremes of fourth-order regressions range from upper peritidal maximums to upper intertidal minimums.

The Upper Allentown sea-level curves generally stay within the peritidal range, with one pronounced transgression into the subtidal and two slides across the intertidal-peritidal transition. Generally, the Upper Allentown was deposited in a sea-level low stand, with one major and a few minor exceptions.

4.13 Stonehenge Formation: Carlton Village Member

4.13.1 Facies Description

Carlton Village Facies 1

The lower facies of the Carlton Village Member is known for its diversity of algal stromatolite structures. The facies rests on an unconformity incised into the top the Upper Allentown Formation (see Chapter 3). Bedding is hummocky and uneven. Cross bedded grainstones and sandstones, overlain by intraformational conglomerates, rip-up clasts, and ripple marked surfaces mark the base of the member. Thin to thick shale occurs along the base; however, the shales also occur as thin wisps throughout the facies. Overlying the intraformational conglomerates are rubble zones, or pinnacle mounds, penetrated by a ropy and intertwined form of algal stromatolite binding the rubble/pinnacles together (Figure 4.11). The structures are finely laminated and range from large concentric masses to open vase shape. The algal structures become crenulated, and develop open, apron shaped mounds along stratigraphic strike. The pinnacle structures and mounds represent only two types of algal structures in this facies. Approximately ten intraformational conglomerates mark the mid-section of the facies. Each conglomerate is overlain by thin to thick, quartz sandstone and algal laminated, fine

grained dolomite. Intraformational conglomerates cap the sandstone/dolomite succession in turn. The facies is capped by algal laminated, dolomitic limestone.

Carlton Village Facies 2

The second facies of the Carlton Village Member contains two, coarse grained, intraclastic horizons occurring at the base and crest of the facies. Each horizon contains well sorted oncoid, pisoid and ooid grainstones interbedded with quartz sandstones. The facies are algal laminated and shale occurs intermittently towards the top of the facies. The base of facies 2 contains several horizons of chicken-wire evaporite structures interbedded with quartz-vug horizons. The mid-section of the facies includes algal laminated, dolomitic limestones, interbeds of pisoids, ooids and quartz sandstone. Shales increase towards the top of the facies. The upper part of the facies includes greater quantities of cross bedded quartz sandstone and associated cross bedded dolarenites. These are overlain by structureless to graded oolites. The upper surfaces of the oolite are truncated. Upon these flat plains are algal stromatolite boundstones. The algal are different from those discussed previously; they are spherical and highly concentric. The algal occur as closely associated boundstone colonies where the edges or perimeters of each boundstone connect to the adjacent stromatolite. The colonies occur grouped on top of each other, creating a large convex mound. Sparse overturned algal are present and the upper surfaces of the stromatolites are convex, not truncated or incised with volutions. The algal colonies are covered by cross bedded dolarenite, capped with wisps and thin layers of black shale, which in turn draws closure to the Carlton Village Member.

4.13.2 Paleoenvironmental Setting

Quartz sandstone and interbedded intraclastic limestones (facies 1) overlying the unconformity at the top of the underlying Upper Allentown Formation suggests that the subaerially exposed Upper Allentown was the source for the intraclastic carbonate debris in the lower Carlton Village beds. The Upper Allentown unconformity would have generated aprons of mudcracks and rip-up clasts of algal laminated limestone. Subsequent submergence of the coastline during deposition of the Carlton Village Member would have transported this debris oceanward, depositing it in the peritidal and intertidal realm and resorting it into the shallow subtidal. Possible irregular topography generated during Upper Allentown subaerial exposure would have permitted the colonization of unique algal stromatolite forms of varied morphotypes. The domal and open-vase shape of the algal indicates that they grew in an open, epeiric environment (Figure 4.12). However, this environment yielded to an inundation of intraformational conglomerates, quartz sandstones and graded, intraclastic limestone horizons which blanketed the pinnacle structures and mounds (Figure 4.13). As the pinnacle structure algal are restricted to the basal part of the facies and are not observed in higher stratigraphic positions, the author infers that the grainstone/sandstone influx lead to the demise of the organisms. However, the upper part of the member witnesses the efflorescence of eight boundstone accumulations of a different algal fauna. The boundstones overlie thick beds of cross bedded, quartz sandstone and interbedded grainstone indicating a continuation of the shallow subtidal-lower peritidal environment. The algal colonies are capped by finely algal laminated dolomites, intraclastic debris and quartz sandstone. The grainstone/sandstone is interpreted as being derived from the

shoreward side of the mound structures (Hoffman, 1973b; Howell, 1945). As such, the mound structures may serve as a barrier to land derived sediments until it is overridden by the accumulation of aprons of intraclastic debris occurring behind the barrier face (Garrett, 1970; Gebelein, 1969; Hoffman, 1973b).

The presence of chicken-wire structure and quartz vugs, both of which are interpreted as evidence for the previous existence of evaporites, are present and infer the establishment of lower supratidal conditions over the boundstone horizons of facies 1. However, the presence of interbedded and cross bedded grainstones (ooids, pisoids, and oncoids) suggests that the lower supratidal setting was succeeded by a deepening to peritidal conditions. Highly concentrated, algal laminated dolomites mark the facies at no less than six locations, where fine grained sediments cap the grainstone facies. The algal laminates mark the deepest phase of subtidal development during this period and occur over and distal to the grainstone sequences in a slightly more oceanward direction. The upper half of the member witnesses the influx of quartz sandstone interbedded with graded and cross bedded grainstone facies. Stabilization of these proposed quartz sandstone shoals by algal laminated units provides the substrate for the colonization of the most prolific algal boundstone colonies witnessed in the upper part of the Carlton Village Member (Halley, 1969; Howe, 1966).

4.13.3 Sea-Level Curve Interpretation

The Carlton Village Member is 63.75 m thick and contains two unconformities (not including the basal contact), both of which are lined with chert. The lower unconformity contains light gray chert breccias, while the upper unconformity is a mixture of light gray to black, silicified algal laminations, algal stromatolites and

breccias. Fifth-order sea-level curves show thirty-nine pulses of sea-level transgression-regression cycles (Plate 4.7). Maximum and minimum regressions permitted deposition in upper peritidal and lower peritidal, respectively. Upper subtidal and upper peritidal are the environments supported by maximum and minimum transgressions, respectively. Wavelengths of transgressive-regressive pulses on the fifth-order curve are attenuated in the lower 2 m of the member and become longer in the remainder of the section, ranging from 100 cm to 800 cm along the entire curve.

The corresponding fourth-order curve exhibits wavelengths of a different order of magnitude to the fifth-order curve (Plate 4.7). Fourth-order wavelengths range from 200 cm at the very base of the member to 2.75 m towards the top. Four transgressive and regressive pulses mark the fourth-order curve, with several fifth-order regressions punctuating the fourth-order curve. Maximum and minimum fourth order transgressions permit upper subtidal and middle peritidal conditions, respectively. Corresponding maximum and minimum fourth-order regressions range from upper to lower peritidal, respectively.

Generally, the Carlton Village Member represents a predominantly transgressive unit that experiences smaller scale pulses of sea-level down draws throughout its deposition. The sea-level curves exhibit an environmental range from subtidal to peritidal, indicating regional rising sea levels and a transition away from sea-level low stands.

4.14 Stonehenge Formation: Canal Road Member

4.14.1 Facies Description

Canal Road Facies 1

The facies was deposited on an unconformity marked by a thick, chert breccia (Beales and Oldershaw, 1969). The breccia fragments are tightly welded and the remains of the original laminated and domal algal structures are visible in the clasts, the clasts break up layers of silicified enterolithic quartz (interpreted as former evaporites) interbedded with silicified algal laminate. The first succession of Stonehenge rock deposited on this unconformity is a fine to coarse grained, algal laminated dolomite. The upper parts of the algal laminated dolomite contain sulfurous quartz vugs and burrow structures. Overlying this series are three successions of algal laminated, dolmicrites and dolarenites capped by quartz-vug dolarenites and cross bedded quartz sandstones. The quartz sandstones locally fill in open joint surfaces in the algal laminated dolomites, especially towards the base of the facies. Generally, the succession starts with a micritic facies and coarsens upward to coarse grained, arenaceous horizons. The base and mid-sections of the sequences are punctuated with burrowed horizons, while the tops of each section are perforated with quartz vugs, cross bedded dolarenites and quartz sandstones. Chert occurring as thin wisps and filaments, and breccias line the crests of each succession. Quartz sandstones lining the succession crests are also partially silicified. Laminated algal structures and mildly convex algal are common; however domal algal only occur in the upper mid-part of the facies.

4.14.2 Paleoenvironmental Setting

The deposition of algal laminated dolomite on the Carlton Village unconformity indicates marine transgression; with the algal laminated dolomite grading up stratigraphic section into dolomite bearing sulfurous quartz vugs and burrows indicating the environment may have started in the shallow subtidal, but shallowed to the supratidal (Chowns and Elkins, 1979). Each of the repetitive sequences is floored in this subtidal to supratidal dolomite. The third sequence, however, contains algal laminated dolomite capped by burrows and domal algal, the quartz vugs are fewer in number. As such, the floor of the third sequence is interpreted as being deposited in a slightly deeper subtidal than the underlying two.

The repetitive sequences in the Stonehenge Formation change up stratigraphic section from fine grained algal laminated dolmicrites to coarse grained, cross bedded dolarenites (Figure 4.14). This succession infers that the sequences are coarsening and shallowing upward cycles (Calvert and Tucker, 1988). Possible dune sequences near the coastline may have provided a source of sediment for the quartz sandstones present in the facies (Friedman et al., 1973; Hobson, 1957) or the sandstone may have sourced from sources further from the shore face.

4.14.3 Sea-Level Curve Interpretation

The Canal Road Member is 22.5 m thick at the type section and contains one chert lined unconformity at the upper contact. Chert occurs as silicified sandstones lenses and layers underlying the unconformity. Twenty sea-level draw downs are represented in the fifth-order curve for the Canal Road Member (Plate 4.7). Sea-level fall in the fifth-

order cycle remains consistent at upper peritidal. Twenty corresponding transgressions document a maximum fifth-order flooding allowing for upper subtidal conditions and a minimum condition permitting lower peritidal sedimentation. Wavelength exhibits a fairly constant periodicity with lengths ranging from 100 cm to 600 cm along the entire length of the Canal Road curve.

Fourth-order sea-level fluctuations are of a lower periodicity and longer wavelength (Plate 4.7). Wavelengths range from 600 cm to 1.5 m. Maximum and minimum transgressions range from upper subtidal to lower peritidal, respectively. Corresponding maxima and minima for fourth-order regressions range from upper to middle peritidal, respectively.

The Canal Road Member starts with a large wavelength transgressive pulse, followed by an even longer wavelength regression. The following two transgressions, and intermediate regression, at the top of the member are of smaller wavelengths. Fifth-order regressions punctuate the entire fourth-order curve; however, the lower fifth-order punctuations are of a larger wavelength than the remaining three-fourths of the member. The member is inferred as having been deposited equally in transgressive and regressive systems. Overall sea-level range ranges from subtidal to peritidal, continuing the regional sea-level rise indicated in the underlying Carlton Village Member.

4.15 Rickenbach Formation: Hope Member

4.15.1 Facies Description

Hope Facies 1

The basal Hope Member of the Rickenbach Fm is a thickly bedded dolomite intercalated with cross bedded dolarenite bearing shale wisps, burrow structures,

sulfurous quartz vugs, and chert breccias. The chert breccias contain angular fragments and clasts of algal laminated chert, silicified former evaporites, and silicified silcrete in a matrix of coarsely, recrystallized dolomite. The basal beds are overlain by a thin succession of thick bedded, algal laminated dolarenites, intraclastic and algal laminated dolomites (Figure 4.15). The upper surfaces of beds are usually truncated and contain brecciated chert horizons. Dolarenites, quartz sandstones, and algal (both domal and laminated varieties) are more common at the base and crest of the facies. Burrow horizons are more common in the upper half of the member. Many of the burrow horizons are interbedded with sulfurous quartz vugs. Chert marks many of the coarse grained beds; replacing algal laminations, quartz sandstones, oolites, or chert breccias. Shale is also common in the upper half of the unit (Natter, 1967; Pratt and James, 1985).

4.15.2 Paleoenvironmental Interpretation

Thickly bedded dolomite intercalated with cross bedded dolarenite bearing shale wisps, burrow structures and sulfurous quartz vugs indicate that the base of the Hope Member was deposited in the uppermost reaches of the peritidal/lower supratidal setting. The presence of overlying quartz vugs, burrows and shale wisps in dolomite suggests a supratidal setting, indicating the onset of regression. The upper half of the member preserves lesser quantities of intraclastic units and domal algal, although never in great quantities (Sando, 1957). Intraclastic units indicate eventual deepening to an upper peritidal environment where intraclasts winnowed from the shoreline could be deposited in water. Algal laminates suggest that the water column was restricted and shallow enough to support lamination formation, instead of domal algal build up. The upper surfaces of these beds; however, are truncated and bear brecciated chert horizons.

Truncation of beds could indicate wave action, possibly from intermittent storm sequences agitating a restricted environment or subaerial exposure. Two distinctive chert breccias cap the section; they are inferred to represent a period of subaerial weathering or prolonged exposure of a mixture of domal and algal laminated units and evaporitic horizons (Figure 4.16) as was found by Mazzullo and Friedman (1974).

4.15.3 Sea-Level Curve Interpretation

The Hope Member of the Ontelaunee Formation is about 14 m thick and contains one unconformity at the upper contact. The unconformity is lined with silicified shale. Twelve fifth-order transgression-regression cycles are interpreted for the member (Plate 4.8). Maximum-minimum regressions were fairly constant in supporting upper peritidal conditions throughout Hope deposition. Transgression extremes ranged from upper subtidal to upper peritidal. Fifth-order wavelengths range from 100 to 400 cm, with periodicity being relatively uniform in the member.

Fourth-order sea-level cyclicity ranged from 400 cm to approximately 1 m wavelengths (Plate 4.8). The longest wavelength is represented by a regressive curve in the mid-part of the member. Three regressive-transgressive cycles are present on the fourth-order curve. Maxima-minima values for fourth order transgression range from upper subtidal to upper peritidal, respectively. Maximum regression supports upper peritidal conditions and minimum regression preserved lower-middle peritidal sedimentation.

The Hope Member is interpreted as having been deposited under slightly more regressive fourth-order conditions, with several fifth-order pulses punctuating the larger scale cycles. Sea-level curve environmental range continues from what was established

in the Carlton Village Member, subtidal to peritidal conditions indicating regional sea-level rise onto the continental platform.

4.16 Rickenbach Formation: Crooked Swamp

4.16.1 Facies Description

Crooked Swamp Facies 1

The Crooked Swamp Member is made up of nearly one dozen, short, repetitive sedimentation sequences. Each sequence bears a distinctive chert breccia at its base and is abruptly overlain by coarse grained, quartz sandstones, intraclastic rip-up dolomites, mudstone facies, and occasional sweeping ooids (Blount and Moore, 1969; Demille et al., 1964). At other locations, the base includes shale couplets, burrowed units, algal laminated structures and dolomites peppered with quartz vugs (possible silicified anhydrite flowers) and cut-n-fill channels. However, these are quickly overlain by micritic, algal laminated dolomite that is burrowed. The burrowed horizons continue through the mid-section of the member and have along their base, thick intraclastic deposits. Five thick, chert breccias mark the mid-section of the member and they occur overlain by a thick, black shaly dolomite (Chowns and Elkins, 1979; Clifton, 1967). Above this horizon is a succession of small, domal algal colonies interbedded with convex, laminated algal sequences. Much of the Crooked Swamp is coarsely recrystallized to a saddle dolomite and contains finely dispersed sulfides and sulfurous quartz vugs. Quartz sand lenses are more common towards the crest of the member, which is in turn capped by yet another distinctive, thick, chert breccia (Beales and Oldershaw, 1969; Blount and Moore, 1969). This breccia is comprised of angular fragments of silicified algal, silcrete, and silicified anhydrite clasts. The difference

between the Crooked Swamp facies and the underlying Hope and Canal Road members is the presence of large, domal algal structures that appear near the base of each cycle. The algal structures are interpreted as boundstone and framestone structures, with occasional cross bedded oolite and coarse sand units and draping oolites (Cuffey, 1985).

4.16.2 Paleoenvironmental Setting

The Crooked Swamp was deposited in the lower reaches of the peritidal and built up rapidly to the sea surface, where each of the twelve sequences was truncated (Beales and Oldershaw, 1969). In summary, the Hope and the Crooked Swamp appear to represent the progradation of shoreline during periods of submergence, followed by episodes of subaerial weathering associated with sea-level drawdown. These punctuations in sea level permitted the development of strongly burrowed horizons and the colonizations of algal mound structures. However, the sequences appear to be short termed and markedly truncated. All of the Crooked Swamp, from the lower supratidal to the shallow/intermediate/lower peritidal seems to have been deposited in an environment of hypersalinity. The Hope and the Crooked Swamp, although lithologically very different in appearance, may represent the contiguous, along strike, near shoreline configurations. Therefore, the Hope and the Crooked Swamp represent a facies mosaic of shoreline environments.

4.16.3 Sea-Level Curve Interpretation

The Crooked Swamp Member is 10.5 m thick and contains chert lined unconformities only at the contacts. The upper contact contains several chert varieties, including silicified former evaporite sequences, silicified sandstones and brecciated algal laminations. Seven fifth-order transgressive-regressive cycles are present for this

member (Plate 4.8). Curve periodicity is fairly uniform, with wavelengths ranging from 100 to 400 cm. Regression on the fifth-order curve remains in the upper peritidal. Transgression ranges from the upper subtidal-lower intertidal transition maximum to upper peritidal minimum.

The fourth-order curve contains four transgression-regression cycles (Plate 4.8). Maximum transgression occurs in the upper subtidal and minimum transgression is reflected in the upper intertidal. Maximum and minimum regressive series range from the upper peritidal to the lower-middle intertidal, respectively. Periodicity in the fourth-order curve is regular, with curve wavelengths ranging from 100 to 600 cm. The overall environmental range for the Crooked Swamp sea-level curves extends from the subtidal to the peritidal. Generally, the Crooked Swamp is interpreted as being a transgression unit.

4.17 Epler Formation: Branchville Member

4.17.1 Facies Description

Branchville Facies 1

The base of the facies rests on the chert breccia capping the underlying Crooked Swamp Member (Demille et al., 1964). The lower facies contains sulfide-rich, shaly dolomite bearing oscillation ripple marks, mud-crack intervals, and intraclastic horizons. The intraclasts are reworked rip-up clasts composed of fragments of mud cracks wrapped in algal filament. Slab examination reveals elongate and rounded lenses of shale, 5 to 7 cm in length, which are rolled together as an intraformational conglomerate. The shale lenses are commonly wrapped in algal filament and replaced by chert. Glauconite is present in the lower facies as thin layers capping shales (Friedman et al., 1973).

Branchville Facies 2

Sparse, small, domal algal structures were discovered within facies 2; however, they were never persistent. Glauconite is present as burrow infillings. Locally, facies 2 preserves layers of bird's eye, chicken-wire and enterolithic evaporitic structures. The bird's eye structures are overlain by burrow features. The evaporitic structures are commonly replaced by chert. Locally, the upper surfaces of beds bear cut-and-fill channels containing quartz sandstone.

4.17.2 Paleoenvironmental Setting

A shaly dolomite bearing oscillation ripple marks, intraclastic horizons, and mud crack intervals suggests an environment that was near shoreline with water of a high enough energy to transport and deposit intraclastic horizons; however, as evidenced from the presence of mud cracks, was also intermittently subaerially exposed. Oscillation ripples and the presence of rip-up clasts wrapped in algal filament attest to the swash and backwash of waves at a shoreline. However, the presence of pyritic sulfide in the shaly dolomite of facies 1 indicates that at some points in the depositional history of this member, the environment was anoxic and was intermittently cut-off from the circulation of open marine waters. Glauconite in the lower facies occurs as sheets capping the shale horizons, not as pellets which are commonly observed in younger Paleozoic rocks. Glauconite is usually interpreted as being authigenic, precipitated from waters that were anoxic, as opposed to being deposited as fecal matter (Frost, 1974).

The sparse, small domal algal, in combination with bird's eye, chicken-wire, and enterolithic evaporitic structures indicate a supratidal setting (Figure 4.17). However, burrow structures (some filled with glauconite) overlying the evaporitic series indicates

that a shift from supratidal to peritidal occurred. Cut-and-fill channels bearing quartz sandstone indicate that current water flow was introduced to the environment, possibly as tidal channels, possible distributary outlets, or migrating beach barrier bars. Quartz sandstone in the talwegs of some of the cut-and-fill channels suggests siliciclastic influx from a possible cratonic source or from reworking of quartz-sand reservoirs that possibly existed in the underlying Crooked Swamp Member, or are migrating parallel to the shoreline as a barrier system (Pratt and James, 1985).

The persistent thickness of the Branchville Member along strike indicates that the member was deposited on an essentially flat, planar surface. In summary, it is possible, that the inferred supratidal dolomites, and their lower shale facies represent a protected lagoon located behind a off-shore barrier. The upper facies is lower supratidal and strongly contains features suggesting evaporitic conditions, with intermittent shifts to peritidal conditions (Enos, 1977; Hobson, 1958a, b).

4.17.3 Sea-Level Curve Interpretation

The Branchville Formation is 6.3 m thick at the type section and contains two unconformities at the upper contact. The lower unconformity is chert lined and the upper unconformity is along a green argillite. The fifth-order sea-level curve for the member contains four transgressive-regressive cycles (Plate 4.9). Regressions remain constant in the upper peritidal, transgressions range from a maximum in the upper intertidal to minimums in the middle peritidal. Periodicity in the curve is uniform, with wavelengths ranging from 100 to 400 cm.

The fourth-order curve contains one transgressional and two regressional pulses (Plate 4.9). The transgression permits upper intertidal sedimentation and the regressions

range from a maximum in the upper peritidal-lower supratidal realm to a minimum in the middle-upper peritidal.

The Branchville Member is predominantly transgressional in nature, with fourth-order regressive pulses located at the lower and upper reaches of the unit. Fifth-order regressive pulses punctuate the fourth-order curve. Environmental settings in the Branchville Member are slightly more restricted, with respect to the underlying Rickenbach and Stonehenge Formations. The Branchville sea-level curve is restricted to intertidal and peritidal settings, allowing inferral of a slight lowering of regional sea-level on the continental platform.

4.18 Epler Formation: Big Springs Member

4.18.1 Facies Description

Big Springs Facies 1

The Big Springs carbonates are thin to thick bedded, worm burrowed and contain wisps of intercalated shales overlain by oolite grainstones, algal laminates and moderate amounts of domal algal. The grainstone/boundstone succession is overlain by a thin series of intraclastic limestones overlain by thick, algal laminated dolmicrites. The intraclasts are predominantly irregular masses of fine grained ooids grown inside large vacuoles or pore spaces, much like cave pearls, indicating hypersaline conditions (Neumann and Land, 1975). In a few cases, large accumulations of oncoids and rolled glauconite pellets occur, also wrapped in algal filament. Thick, light gray to translucent white chert horizons, occur at the base of, and are intercalated with, the algal laminated, dolmicrite. Many of these cherts are strongly contorted (as if drawn out plastically), elongate, somewhat rounded lenses, some of which are broken apart but still retain a

linear continuity with the intact sections. Polished slabs of these cherts reveal a fine coating of light brown, quartz siltstone occurring around the edges. As discussed in Chapter 3, the dolmicrites contain silcretized upper surfaces. The green silcretes are superimposed by oscillation ripple marks and mud cracks. Bright orange dolomite is commonly present below the green silcretes. Additionally, the algal laminates housing the silcretes contain thin strands of euhedral garnets and other insolubles, that were not identifiable in hand sample. At several horizons where the orange dolomite occurs there are distinctive features worth noting. The first is a local occurrence of elongate, vertical and diagonal fractures which are filled with quartz sandstone. The second is a breccia, in which the clasts are closely refitted and the interstices between clasts are filled with quartz sandstone and chert pebble conglomerates (Beales and Oldershaw, 1969; Demille et al., 1964).

4.18.2 Paleoenvironmental Setting

The thin to thick, worm burrowed dolomites and intercalated shales of the Big Springs Member, as well as the absence of evaporitic structures and algal laminations in the worm burrowed dolomites, supports a subtidal, rather than a supratidal, interpretation for these sedimentary units. Thick oolite grainstones (also bearing oncoids and rolled glauconite in algal filament), domal algal and algal laminated dolomites overlie the burrowed horizons and infer the establishment of higher energy environments, possibly due to marine shallowing and the lowering of mean wave base (Figure 4.18). Ooids, oncoids and glauconite suggest that these sediments were deposited between mean and storm wave bases and were continuously rolled. Intraclasts with authigenic ooids,; thick, algal laminated dolmicrites bearing weathered orange dolomite, and silcretized upper

surfaces are indicative of minor regressive intervals capping the peritidal units, forming a lower supratidal environment (Figure 4.19). The overprint of oscillation ripple marks and mudcracks on the upper surfaces of the dolmicrite and/or silcretes indicates that subaerial surfaces were exposed and periodically re-wetted. Elongate, contorted, quartz-sandstone lined, sometimes brecciated, chert horizons at the base of the supratidal dolomites have an enterolithic form and are interpreted as a silicified evaporitic unit, which would support the interpreted supratidal facies shift (Figures 4.20-4.21). Algal laminated dolmicrites housing the silcretes contain thin lenses and stringers composed of garnet and other insolubles parallel to bedding. These heavy minerals are interpreted as small placer occurrences deposited along the shoreline.

To summarize, the Big Springs facies contains twelve cyclical shallowing upwards series which are gradually overlain by a prograding, lower supratidal, fining upward sequence. The cycles within the Epler Formation represent a near shore-face configuration, which is the response to an initial transgressive pulse with ensuing shallow subtidal environment overlain by a prolonged period of progradation and sea-level draw down. When the peritidal setting is established for long periods of time, algal communities accumulate, which are reminiscent of older Conococheague cycles (McNeill, 1988; Pratt and James, 1982). However, these episodes are short lived and followed by the progradation of lower supratidal, micritic dolomites which cap each cycle. The presence of silcretes, authigenic ooids, and associated evaporitic units of the lower supratidal suggest the presence of a broad, flat, arid plain; one which is only intermittently wetted and is exposed to meteoric conditions that promoted growth of

calcareous algae (Figures 4.20-4.21) (Kobluk and Crawford, 1990; Neumann and Land, 1975).

The regressive units capping each cycle within the Big Springs Member might be sabkha-like in their appearance; however, the flat landscape is incipiently drowned, submerging a broad expanse of flat coastline (Figures 4.22-4.23). Therefore, the sabkha system and lower supratidal facies are established only for time periods long enough to weather in meteoric conditions with subsequent inundation. Therefore, this is not a true sabkha setting. The upper part of the Big Springs Member bears vertical and diagenetic fractures filled with sandstone, as well as a breccia, the matrix of which is sandstone and conglomerate. These are the imprints of karstification and solution topography developed at the top of the Big Springs, at the same stratigraphic horizon as the Sauk interval (Figures 4.24-4.25) (McNeill, 1988; Pratt, 1982a, b; Pratt and James, 1982).

4.18.3 Sea-Level Curve Interpretation

The Big Springs Member of the Epler Formation is 44 m thick and contains twenty-six unconformities, eleven of which are lined with chert beds, pods, silicified evaporitic structures, breccias and algal structures. The fifth-order sea-level curve interpreted for this member contains fifty-three transgressive-regressive cycles (Plate 4.9). Maximum regression supported lower supratidal sedimentation in the unit; minimum regression preserved upper peritidal settings. Maxima-minima for transgressions in the Big Springs Member range from upper subtidal to upper peritidal, respectively. Periodicity decreases up stratigraphic section, with wavelengths on the fifth-order curve increasing towards the top of the unit. Wavelengths near the base of the

unit range from 50 to 200 cm. Fifth-order wavelengths in the middle and upper parts of the member range from 100 to 500 cm.

Fourth-order sea-level regressions show twenty-two transgression-regression cycles that mimic the fifth-order cycles in decreasing periodicity and increasing curve wavelength up stratigraphic section (Plate 4.9). Fourth-order wavelengths in the lower part of the member are of the same order of magnitude as fifth-order wave lengths, ranging from 50 to 200 cm. Up section in the Big Springs, the wavelength of the fourth-order curve increases to ranges varying from 600 to 1 m in length. The abundance of unconformities in the lower 1.25 m of the member controls the interpretation of the fourth-order curve, prohibiting smoothing of the line where unconformities are numerous. Up stratigraphic section, however, unconformities lessen in number, permitting smoothing of the fourth-order curve and increasing the interpreted wavelengths represented by the line. Maxima and minima of the fourth-order transgressions range from upper subtidal to upper peritidal, respectively. Extremes for fourth-order regressions range from lower supratidal to upper peritidal, respectively.

As a whole, the Big Springs Member is shows much fluctuation of sea level through time. The large number of unconformities in the member, plus the restriction of sea-level to intertidal and peritidal settings, permit a regressive general interpretation for the member.

4.19 Epler Formation: Lafayette Member

4.19.1 Facies Description

Lafayette Facies 1

This facies is a unique, dark gray, coarse grained, calcarenite comprised of numerous successions of alternating dark and medium gray, parallel bedded, dolomite interbedded with cross bedded, dark gray, dolomite. The dolomites are marked by the appearance of graded and cross bedded ooids and the establishment of algal laminates overlain by large domal algal. Many of the upper surfaces are truncated by incisement, or scour surfaces. Gradually, the succession becomes more oolitic, beginning with wisps of graded and cross bedded oolites, finally with the appearance of algal laminates overlain by domal algal structures (Bridges and Chapman, 1988).

Lafayette Facies 2

Across strike on the New York recess, the base of the Lafayette, as represented in facies 2 is a long succession of thin and thick beds of intraclastic limestone. Each bed is marked by abundant quartz-sand grains occurring as wisps and thin lenses, rip-up clasts and reworked mudcracks. Overlying the intraclastic limestone are thin oolite sequences intercalated with rip-up clasts and intraformational conglomerates, capped by a fine grained, micritic limestone. The fine grained micritic units are finely algal laminated.

Lafayette Facies 3

The base of this facies, similar to the two underlying facies, is a long series of dolarenites and intraclastic limestones, which are overlain by thin, oolitic lenses and capped by algal laminates. However, unlike the lower two facies, this unit is burrowed

and domal algal are established along the oolite and algal laminated sequences at a lower comparative stratigraphic interval than in the other two facies. This observation possibly indicates that the domal algal were established much more quickly in this facies.

Lafayette Facies 4

This facies is similar to the other three facies, with one major exception. The unit includes largely silicified oolites, overlain by perforated and punky domal algal. These domal algal fossils persist towards the top of the section. Quartz sandstone and intraclastic limestones comprised of reworked algal, mud cracks, ooids and pisoids occur near the top. The domal algal disappear at the top of the section and are replaced by algal laminates. The entire section is truncated by an uneven unconformity capped by a limestone-chert conglomerate.

4.19.2 Paleoenvironmental Setting

A coarse grained, calcarenite interbedded with parallel bedded and cross bedded dolomite bearing cross bedded ooids, algal laminates and domal algal indicates a peritidal environment in facies 1. Parallel bedded dolomites interbedded with cross bedded facies suggests deposition along a shore face, where the swash and backwash of wave action would produce parallel beds, while cross beds would form from storm surges, flow through distributaries debouching into the shore face,, or flow through tidal inlets. The appearance of algal laminates overlain by large domal algal indicates either a shallow laminate-rich environment deepening to a domal faunal environment or a subtidal realm where either fauna could thrive.

The presence of intraclastic limestone (facies 2) bearing thin lenses of quartz sandstone, rip-up clasts and reworked mudcracks indicates an environment where the

shore face was reworked by encroaching water either from tidal forces or storm surge. The reworked clasts from the shore face were transported to depositional sites within the peritidal realm. Thin oolite sequences intercalated with rip-up clasts and intraformational conglomerates indicate a higher energy environment. The peritidal setting may have deepened slightly to accommodate this high energy regime, or continued as a peritidal environment with occasional storm surge providing the energy needed to form oolitic shoals. Algal laminated micrites overlying the oolitic beds in this facies are suggestive of either a deepening to subtidal or a shallowing to a supratidal setting. Burrow structures, domal algal and/or evaporites have not been observed and as such cannot support one hypothesis or the other.

Burrowed dolarenites and intraclastic limestones in facies 3 indicate shore face environments that support burrowing organisms. Siliciclastic influx into the basal dolomites also suggests a near shoreline environment where the siliciclastic source could range from the craton, to migrating barrier bars, to offshore subaerial island or microcontinents. Intraclastic facies represent reworking of a shoreline with transport and deposition of the intraclasts in the peritidal (McNeill, 1988). As with the previous two facies, upward transition to algal laminated sequences bearing domal algal indicates mild deepening where domal algal can flourish in open, epeiric conditions (Tudhope, 1989; Wanless and Tagett, 1989). The onset of domal algal lower in the stratigraphic level of the facies indicates that facies 3 was submerged sooner than its lower counterparts and may represent a more offshore facies, therefore representing a deeper water regime. Facies are entirely within the lower peritidal/upper subtidal, where the domal algal are well established.

The depositional settings for facies 1 through 3 hold for facies 4, with the exception of the presence of punky and perforated domal algal. Burrows were present in facies 3, indicating the former existence of burrowing organisms. It is plausible to conclude that such organisms existed in facies 4 as well and could be responsible for the porosity imparted onto the domal algal (Tedesco and Wanless, 1989; Toomey and Nitecki, 1979). This development would suggest a continuation of an upper supratidal/lower peritidal environment capable of supporting domal algal colonization and the introduction of burrowing organisms. As the presence of burrowing organisms usually destroys algal laminations and as such can leave a rock with the appearance of sparse, or no, algal laminations; it is plausible to conclude that burrowing organisms invaded the facies 4 ecosystem after the domal algal had been permitted the time to develop.

4.19.3 Sea-Level Curve Interpretation

The Lafayette Member of the Epler Formation is 44 m thick at the type section and distinct from the underlying Big Springs Member in that only two unconformities are present in the section, not including the basal unconformable contact. Both unconformities are lined with chert, either as silicified algal laminations or chert breccias. Fourteen fifth-order transgression-regression cycles are interpreted for the Epler Formation (Plate 4.10). Periodicity of the fifth-order curve is lower than what has previously been shown as typical for the Kittatinny Supergroup. Wavelengths range from 100 to 200 cm in the lower 600 cm of the section to 1.5 m in the mid-section, to 400 to 800 cm in the upper third of the unit. Maximum transgressions permitted middle subtidal settings, whereas minimal transgressions preserved middle peritidal

environments. Maxima-minima calculations for regressions show lower supratidal and lower peritidal settings, respectively.

Fourth-order cycles in the Lafayette Member have larger wavelengths than the fifth-order curve, with the exception of the 1.5 m mid-section where the fifth-order transgression is has a large wavelength and as such the fourth-order extrapolation mimics the amplitude and wavelength of the corresponding smaller scale cycle (Plate 4.10). Wavelengths for the outstanding fourth-order curve range from 400 to 600 cm. Five transgression-regression cycles are represented in the fourth-order curve. Extremes of transgression include middle subtidal maxima to middle peritidal. Regression maxima/minima range from upper peritidal to the lower-middle intertidal transition, respectively.

Generally, the Lafayette Member is a transgressive unit that is punctuated by four mild fourth-order regressions and several more severe, fifth-order regressions. Sea-level is no longer constrained to intertidal-peritidal settings, but reaches the subtidal. The general decrease in periodicity and increase in curve wavelengths in this member indicate that sea-level cycles were long-lived and that flooding of the passive margin was more prevalent during the deposition of this member.

4.20 Ontelaunee Formation: Beaver Run Member

4.20.1 Facies Description

Beaver Run Facies 1

This facies is predominantly worm burrowed, thick bedded, dark gray dolomite, the lower units of which are peppered with sulfurous quartz clots. This succession of quartz vugs is overlain by a thick horizon of finely algal laminated dolomite containing

intermittent worm burrow horizons. This horizon in turn is overlain by a very dark, thickly bedded dolomite, containing interbeds of algal laminate and domal algal, all of which are punky, perforated and porous. Close inspection of the porosity occurring within the algal structures and burrow features shows that many of the burrow features are filled with quartz sandstone and in turn are partially replaced by chert. Also, the outer parts of the perforated algal structures sometimes contain openings that are rhombic, instead of circular. Many reveal a geometric opening (Bathurst, 1982).

Beaver Run Facies 2

This facies is a succession of thick, algal laminated dolomites interbedded with chicken-wire evaporite structures and sequences of domal algal, all of which are silicified. Punky and porous, thick bedded, algal laminated dolomite and domal algal overlie the evaporitic horizons. Intercalated with the algal structures are broken and intact shells of small, spiraled gastropods.

Beaver Run Facies 3

This unit is referred to as the transitional facies because the beds lighten in color. The base of the third facies is a succession of thick dolomites, peppered with sulfurous quartz vugs. Worm burrowed horizons occur sparingly. This succession grades to thick, algal laminated, domal algal and evaporitic units, which are brecciated and recemented by a generation of coarse grained, saccharoidal dolomite. As with the underlying Beaver Run Facies, the dolomites are punky and porous.

4.20.2 Paleoenvironmental Setting

As indicated earlier in this chapter, quartz clots that emit a sulfurous odor upon breakage are interpreted as replacing evaporite structures. The presence of sulfurous

quartz clots, algal laminates, and worm burrows, in a thickly bedded dolomite, indicate a stratigraphic position just below sea level, possibly in a protected inlet or quiet embayment setting. Evaporite structures suggest episodes of hypersalinity through time. The domal algal are thin and probably accumulated in very shallow water conditions, possibly in the furthest inland reaches of the tidal setting. The punky and porous nature of the domal algal, and algal laminate, is interpreted as gastropodal burrows. Certain gastropod types, in this case possibly *Ceretopia*, posses an extremely high tolerance to hypersaline conditions (Moore et al., 1952). These environments, which are not conducive to the proliferation of other marine fauna, posses a niche space for the accumulation of abundant gastropods. These gastropod fauna appear to have predated upon both algal mats, and mildly convex domal algal mats, cropping them and rendering them porous.

The algal laminated dolomite, interbedded with evaporite and domal algal sequences, is indicative of shallow peritidal settings. These sediments in modern settings are thought to accumulate in the mouths of protected, shallow embayments debouching into open marine conditions, yet protected by some type of barrier (Mesolella et al., 1970; Pratt, 1982a, b; Pratt and James, 1982; Stearn, 1982; Talent, 1988). The punkiness of the algal structures, and the presence of spiral gastropodal shells, suggests that grazing gastropods could have produced the punkiness and the perforated outer texture present in both domal and laminated algal forms (Figure 4.27). The morphology of the gastropod shell, and the Lower Middle Ordovician age of the rock, suggests that *Ceretopia* may have been the organism responsible for the predation of the Beaver Run algal structures (Yochelson and Barnett, 1972).

Thick dolomites bearing sulfurous quartz vugs, sparse worm burrows, laminated and domal algal represents the lower supratidal. The algal structures, and associated gastropodal facies, accumulated in small protected embayments and lagoonal features. However, they prograded over the more distal, lower supratidal conditions.

Facies 1 represents the progradation of the lowermost supratidal/peritidal conditions seaward into a shallow, restricted, subtidal setting possibly one protected by oceanward spits, bars, and possibly migrating barriers of coarser grainstone facies. The establishment of this facies included, in succession, severely worm burrowed horizons overlain by both horizontal and vertical burrowed sequences, which are indexed by the introduction of small gastropods. These gastropods are able to tolerate hypersaline conditions where other predating fauna could not thrive (Tedesco and Wanless, 1989). The volume of burrowed, often thickly bedded, dolomites interbedded with an equally impressive volume of severely perforated and predated upon domal and algal laminated structures, suggest that these organisms thrived with limited or no competition. The thick, billowy dolomites contain quartz-vug horizons at their base; however, the vestiges of thick, enterolithic gypsum horizons are not present in this basal facies.

Facies 3 represents the final period of progradation of the middle and lower supratidal units out over the peritidal to a position where they were subaerial and perhaps in very close proximity to an offshore barrier that may have provided it with protection. However, its subaerial nature led to the internal brecciation of both the evaporitic units and desiccated algal structures. Eventually, erosion reduced the distal parts of this facies to a collection of brecciated horizons, which are in turn replaced by chert.

4.20.3 Sea-Level Curve Interpretation

The Beaver Run Member of the Ontelaunee Formation is approximately 33 m thick and contains six, chert lined unconformities. The cherts replace gastropodal algal pods, beds and hemispheres, as well as chert breccias near the top of the member. Fifth-order sea-level curves contain twenty-three transgression-regression cycles (Plate 4.11). Maximum fifth-order transgression established upper subtidal-lower intertidal settings, with upper peritidal minimums. Regression extremes range from the upper peritidal-lower supratidal transition maximas to middle peritidal minimas. Fifth-order periodicity is large, with wavelengths staying relatively steady at 200 to 400 cm, inferring rapid sea-level fluctuation at this scale.

Fourth-order interpolation shows six transgression-regression cycles of a very low periodicity and very large wavelength, except for the region in the upper third of the member where five of the six unconformities in the unit are grouped in close stratigraphic proximity (Plate 4.11). The presence of these unconformities constrains the interpolation of the fourth-order curve, increasing periodicity and lowering wavelengths to 200 to 300 cm ranges. For the upper 1.5 m of the unit, fourth-order wavelength increases again to 1.5 m. Extremes of transgressional effects range from lower intertidal to lower peritidal. Regression maxima-minima remain constant in the upper peritidal.

Generally, the Beaver Run Member is a transgressive unit that experiences a significant regressional pulse in one restricted area of the stratigraphic section. The fourth-order transgressional setting is punctuated by several smaller scale regressions of

fifth order. The sea-level curve spans subtidal to peritidal settings, indicating rising regional sea level on the continental platform.

4.21 Ontelaunee Formation: Harmonyvale Member

4.21.1 Facies Description

Harmonyvale Facies 1

Facies 1 is very similar to facies 3 in the Beaver Run Member of the Ontelaunee Formation. It is a light blue-gray, micritic dolomite that is thickly bedded. The dolomite contains interbeds of evaporitic, chicken-wire structure, dolomite; thin gastropodal facies; and successions of layers of algal laminated dolomite. Many of the algal laminated sections are strongly brecciated (Figure 4.28) (Beales and Oldershaw, 1969).

Harmonyvale Facies 2

This facies is a succession of very thick, homogeneous, dolmicrites which are mildly algal laminated. This facies is characterized by an abundance of quartz vugs, also interpreted as quartz replacements of anhydrite flowers. It is laced with thin and thick, algal laminates, some of which are punky, porous and perforated. The upper parts of this facies contain domal algal and worm burrow structures. This is capped by thick algal laminated sequences, many of which are porous, punky, and perforated (Ahr, 1973; Hardie and Shinn, 1986; Knoll and Swett, 1990).

Harmonyvale Facies 3

This facies is a long succession of thick, billowy, algal laminated, and dolomite units punctuated mid-section by perforated and porous algal laminated units and capped towards the crest by a succession of domal algals and thick, billowy, chert replaced, evaporitic sequences (Grotzinger, 1986; Logan, 1961; Wilkinson, 1982).

4.21.2 Paleoenvironmental Setting

The preservation of former evaporites suggests a lower supratidal, possibly even a protected shoreline condition. Some units contain a peppering of quartz vugs, which have been interpreted as quartz replaced, anhydrite flowers (Demille et al., 1964). In general, this is in the lower supratidal, mid-reach, section (Harris, 1983).

Facies 2 represents a mild progradation of the middle supratidal over the lower supratidal and the inundation of the tidal flat. This permitted the establishment of protected, worm burrowed, units and enough deepening to permit the development of domal algal over algal laminates (Coates and Jackson, 1987; Logan et al., 1964). The section progrades upwards to include laminated algal, evaporitic units and finally a strongly brecciated upper chert surface (Beales and Oldershaw, 1969; Middleton, 1961; Mossop, 1979). Each succession has at its base burrowed sequences which overlie quartz vug units. They are in turn interbedded with gastropod bearing horizons and strongly algal laminated successions (Bova and Read, 1987). The section culminates with the development of thickly bedded algal laminates interbedded with anhydrite and finally domal algal structures (Friedman et al., 1973). However, the cycles are continually prograded over by mud-flat micrites and middle supratidal, thickly bedded, micrites and chicken-wire evaporite structures (Brown and Dodd, 1990; Kendall and Schlager, 1981; Sarg, 1988). Prolonged subaerial erosion and collapse of the evaporitic horizons into the more plastic algal laminated sequences permits the generation of the strongly brecciated horizons visible at three intervals within the Harmonyvale section. Ultimately, the sequence is overridden by thick beds of lower supratidal micrite interbedded with algal laminates which are most strongly developed along the base and cap of each bed

(Bosellini and Hardie, 1973). Gastropod fauna become progressively less common up section in the Harmonyvale, this is in part due to the fact that the lower and middle supratidal evaporitic facies has prograded over the lower supratidal/peritidal algal laminated and domal algal sequences (Rhoads, 1967). However, it should be noted that mid-way in the Harmonyvale Member there is a different group of gastropod fauna. These gastropod fauna are slightly larger than those that occur in the Beaver Run Member and more planispiral. They may represent a hypersaline tolerant successor to the *Ceretopia*. Therefore, it is very possible that these later generations of gastropod fauna represent *Macularites*. Close inspection of the chert horizons which are up to a half meter thick, reveal ghosts of former palmate structures, which are characteristic of certain massive evaporitic sequences, especially those that occur within the middle supratidal. Therefore, the sequence terminates prograding, possibly towards an offshore barrier; however, witnessing prolonged periods of subaerial erosion (Fisher, 1977; Pratt and James, 1982; Riding et al., 1991; Twenhofel and others, 1954).

The porous, punky nature of the algal structures in facies 3 suggests that gastropod fauna were still abundant, therefore the succession may still have been a restricted basin. The domal algal appear to have built toward sea level and were overlain again by lower supratidal micrite mudflats (Gebelein, 1969; Rooney and Perkins, 1972; Schlager, 1989). Alternatively, the last sequence could also represent the onset of transgression due to the foundering of the prograding lower supratidal sabkha sequence. The Beaver Run and Harmonyvale members of the Ontelaunee Formation are the closest associations to modern-day sabkha (i.e. Abu Dhabi-type) sequences in the Cambrian and

Ordovician successions (Belperio et al., 1988; Hardie, 1977; Monty, 1967; Schlager, 1989).

The Harmonyvale base and midsection appear to represent the preservation of the upper part of the lower supratidal section of a sabkha environment, which had reached its acme of development. The Beaver Run Member and the lower parts of the Harmonyvale Member at Rock Island represent the lower-middle, supratidal. It is possible, that the most proximal facies of this sabkha set included deep ravines, or possibly a wadi system that produced red beds, or terra rosa soils, which were reworked towards the shoreline. Environments like this are present along the Dead Sea, the Red Sea and the Trucial coastline (Amiel and Friedman, 1971; Beyth, 1980; Colter and Reed, 1980; Crawford and Dunham, 1982; Garber et al., 1987; Strasser, 1988; Zenger, 1972).

4.21.3 Sea-Level Curve Interpretation

The Harmonyvale Member is 32.5 m thick at the stratigraphic type section and contains nine chert lined unconformities. The chert ranges from breccias and pods near the base of the member to elongate pods near the top. The cherts replace algal laminated sections, gastropodal sections and quartz vug horizons. The fifth-order sea-level curve in the member contain twenty-three transgression-regression cycles (Plate 4.11). Maxima-minima values for fifth-order transgression include upper intertidal and upper peritidal settings, respectively. Regression extremes range from upper peritidal to middle peritidal, respectively. Periodicity decreases and wavelength increases up stratigraphic section. Wavelengths at the base of the member range from 100 to 200 cm and increase in the upper half of the member from 600 cm to 1 m.

Fourth-order cycles contain five transgression-regression cycles (Plate 4.11). The largest transgression permitted middle-upper intertidal deposition, while the smallest transgression preserved upper peritidal sediments. Maxima-minima for regressions stay constant in the upper peritidal. Periodicity is low in the fourth-order curve and correspondingly curve wavelength is large, ranging from 400 cm in the lower part of the member to 1.5 m in the upper part. The lower 1.6 m of the Harmonyvale Member, cyclicity in transgression-regression fluctuations is evident. The remainder of the Harmonyvale Member is predominantly transgressive in nature, with the exception of 600 cm of the section where unconformities show regression producing peritidal conditions. Fifth-order sea-level fluctuations punctuate the fourth-order transgressions more in the lower part of the Harmonyvale than in the upper part of the member.

The sea-level curve for the Harmonyvale Member is restricted to the peritidal, with minor transgressions into the intertidal. Generally, the Harmonyvale Member is regressive in nature. The restriction of the sea-level curve to one environmental setting indicates that regional sea level may have lowered toward a low stand during deposition of the Harmonyvale Member, inferring exposure of much of the continental platform.



Figure 4.1 - Skolithos burrows. in quartz sand, exposed on weathered bedding plane, Hardyston Fm (Ch_1), Route 515 traverse.



Figure 4.2 - Ripple surfaces on shaley dolomite, upper Califon Mbr (Cl_1), Letihsville Fm, Route 515 traverse.



Figure 4.3 - Weathered bedding profile, Hamburg Mbr (Cl_2), Leithsville Fm, Route 23N traverse.



Figure 4.4 - Profile of cross beds and ripple surfaces, note cavities where carbonate-rich sediments have weathered out, Hamburg Mbr (Cl_2), Letihsville Fm.

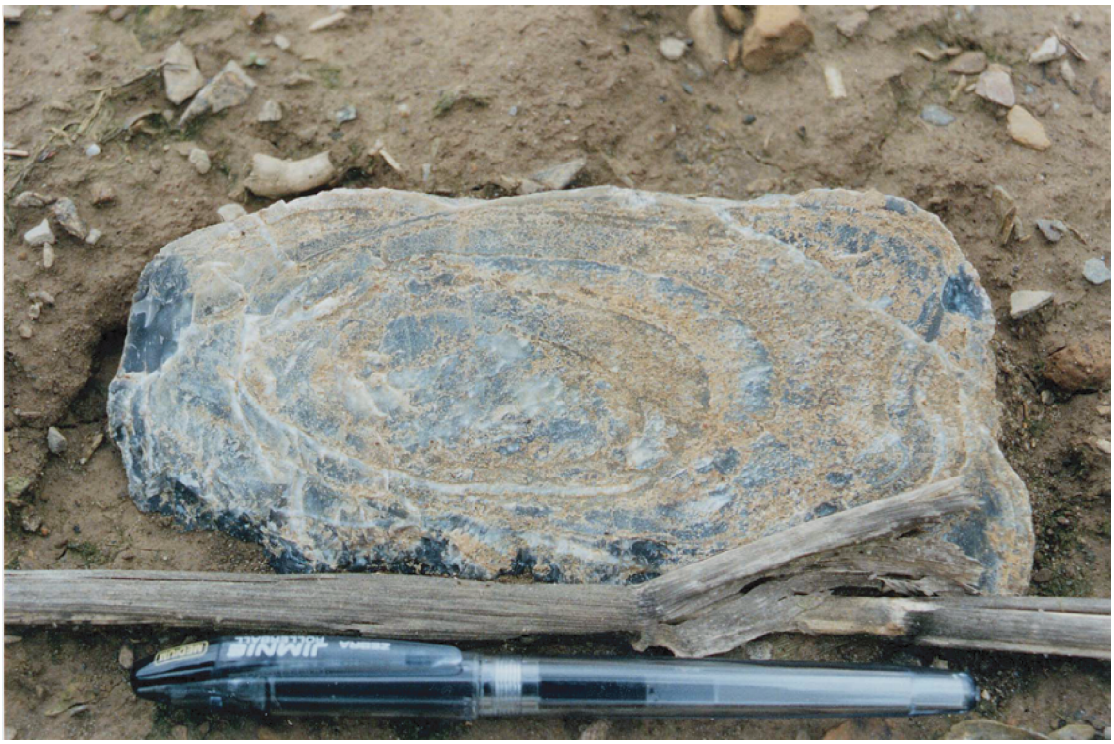


Figure 4.5 - Chert replaced stromatolite in the lower algal horizon, a.k.a. "Rudinski Pod," Facies 1, Wallkill Mbr (Cl_3). Leithsville Fm, Rudinski Farm traverse.



Figure 4.6 - Chert replaced domal algal with laminate bedding plane extensions, upper algal horizon, Facies 1, Wallkill Mbr (Cl_3), Letihsville Fm, Margaret's Est.



Figure 4.7 - Slab of digitate algal lining laminated algal horizon, Wildcat Road Mbr (Ca_{1-1}), Limeport Fm, Ames Rubber traverse.

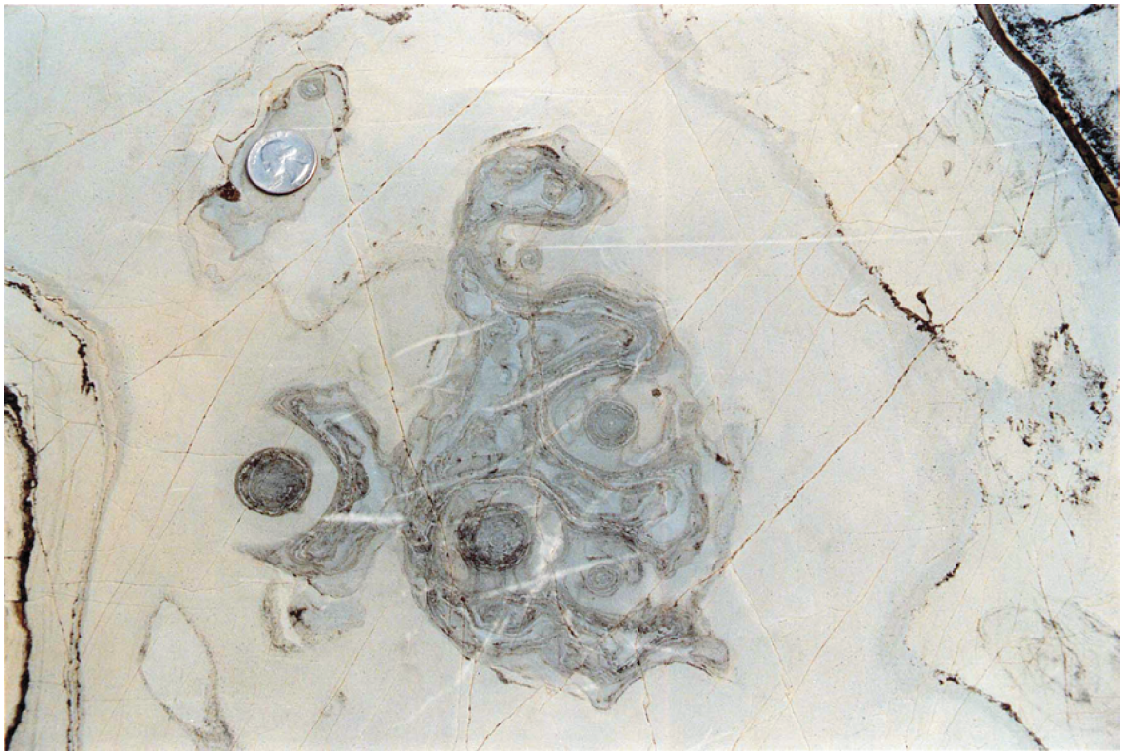


Figure 4.8 - Isolated patch of algal colonies in baffle filling micrite, Wheatsworth Mills Mbr (Ca_{1-2}), Limeport Fm, Greunewald Est.

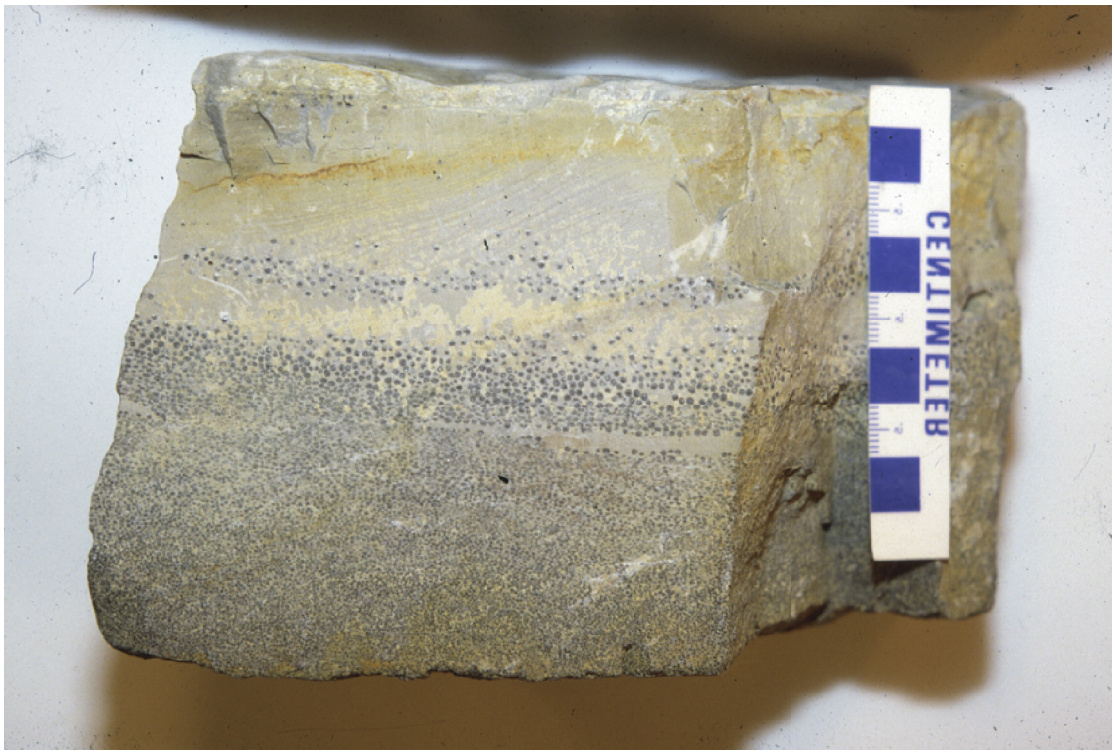


Figure 4.9 - Graded oolites with micrite cap, Upper Greunewald Mbr (Ca_{2-3}), Limeport Fm, Greunewald Est.



Figure 4.10 - Digitate algal (thrombolites), Upper Greunewald Mbr (Ca_{2-3}), Limeport Fm, Greunewald Est.



Figure 4.11 - Chert replaced flowering algal in rubble zone, base of Carlton Village Mbr (Ca_{2-2}), Upper Allentown.



Figure 4.12 - Large colony of cup shaped chert replaced algal, base of Carlton Village Mbr (Ca_{2-2}), Upper Allentown.



Figure 4.13 -Slab of overturned algal colony in rubble of re-cemented micrite, Carlton Village Mbr ($Ca_{2\text{-}2}$), Upper Allentown (scale numbers in cm).

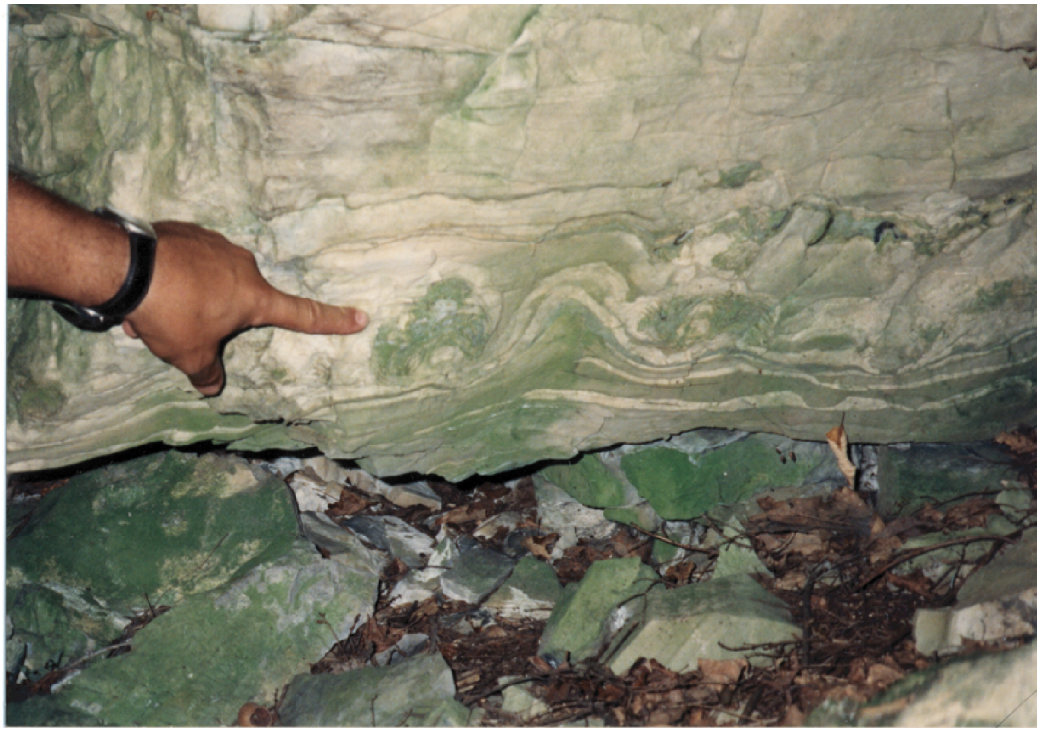


Figure 4.14 - Quartz sand horizons with interbedded algal structures, Stonehenge Fm (Or_1), Harmonyvale traverse.



Figure 4.15 - Intraclastic horizon over chert replaced quartz sand bed, Hope Mbr (Or_2), Rickenbach Fm, Harmonyvale traverse.



Figure 4.16 - "Seven inch cherts" of the Hope Mbr (Or_2), Rickenbach Fm, Harmonyvale traverse.



Figure 4.17 - Slab showing birds-eye evaporite structures and chert replaced interolithic gypsum, Branchville Mbr (Oe_1), Epler Fm.



Figure 4.18 - Conococheague-like sequence of chert replaced graded oolite overlain by algal colony and overlain by algal laminated micrite, note chert replaced intraclastic horizon capping algal, Big Springs Mbr (Oe_2), Epler Fm.

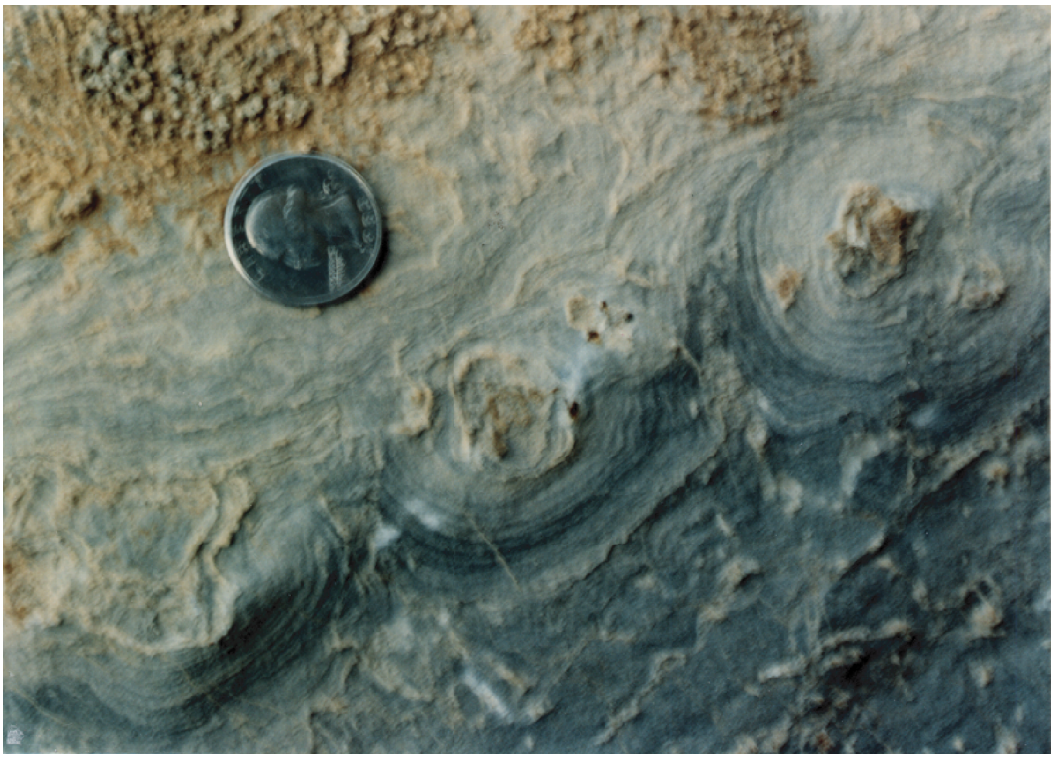


Figure 4.19 - Algal colony in lower supratidal algal laminated micritic dolomite, Big Springs Mbr (Oe_1), Epler Fm, Beaver Run Aggregate traverse.



Figure 4.20 - Calcareous algae, Big Springs Mbr (Oe_2), Epler Fm, Beaver Run Aggregate traverse.



Figure 4.21 - Calcareous algae in supratidal micrite, Big Springs Mbr (Oe_2), Epler Fm, Beaver Run Aggregate traverse.



Figure 4.22 - Chert replaced evapoites overlain by chert replaced algal stromatolites, Big Springs Mbr (Oe_2), Epler Fm, Harmonyvale traverse.



Figure 4.23 - Close-up of chert replaced algal overlain by chert replaced evaporite, Big Springs Mbr (Oe_2), Epler Fm.



Figure 4.24 - Paleokarst of angular fragments of chert in the upper facies of the Big Springs Mbr (Oe_2), Epler Fm, Beaver Run Aggregate traverse.



Figure 4.25 - brecciated algal in silcrete (left) and brecciated evaporite in coarse dolomite (right), Big Springs Mbr (Oe_2), Epler Fm, Beaver Run Aggregate traverse.



Figure 4.26 - Convex chert replaced algal facies 2, Beaver Run Mbr (Oo_1), Ontelaunee Fm, Swartswood Lake traverse.



Figure 4.27 - Close-up of strongly burrowed chert replaced algal stromatolite horizon, Beaver Run Mbr (Oo_1), Ontelaunee Fm, Houston Road.



Figure 4.28 - Chert replaced evaporite horizon with pinch and swell beds of micritic algal dolomite, Harmonyvale Mbr (Oo_2), Ontelaunee Fm, Harmonyvale traverse.

CHAPTER 5: Structural Geology of the Hamburg 7.5' Quadrangle, Sussex County, New Jersey

5.1 Introduction

This chapter focus' on the bedrock structural geology of the Hamburg 7.5' Quadrangle, as re-interpreted from previous work (Dalton et al., 1997) in the quadrangle, using the revised Cambrian-Ordovician stratigraphy presented in Chapters 3, 4 and Appendix B of this dissertation. As the area suffered several orogenic episodes in its geological evolution, the tectonic setting of the study area, and its surroundings, was reviewed in Chapter 2 to provide a framework for the structural reinterpretations. The author was responsible for mapping only the carbonate rocks in the Hamburg 7.5' Quadrangle and this mapping will be discussed in this chapter (Figure 5.1). The Proterozoic basement and the Ordovician Martinsburg Formation also crop out in the quadrangle, but these units were mapped by Dalton et al. (1997).

Balanced and restored structure cross sections were produced. To produce a deformed state cross section of the quadrangle, several sets of data were used. In addition to the carbonate rocks mapped by the author, data mapped by previous workers for the Proterozoic basement and the Martinsburg Formation were also used (Dalton et al., 1997). This is reflected in a compilation map that combines the mapping efforts made for this dissertation, with the efforts of previous workers in the basement and the slate (Figure 5.2). Additionally, Herman and Monteverde and Herman et al. published a series of cross sections (1:7,632 scale and 1:196,850 scale, respectively) for the Kittatinny Valley of New Jersey (of which the Hamburg quadrangle is a small part) and provided seismic profiles to support their interpretations (Herman and Monteverde, 1989; Herman et al., 1997). This author reinterpreted the published seismic profiles that were

closest to the Hamburg quadrangle to provide at depth data for the 1:24,000 scale cross sections constructed for this dissertation. Additionally, the stratigraphic description of several deep wells were published (Fletcher and Woodrow, 1970; Saunders, 1983) describing the stratigraphy at depth in the study area. This well data was used to further constrain the elevations of stratigraphic contacts at depth, again using the revised stratigraphy presented in Chapters 2 and 3 as guides for reinterpreting the stratigraphic interpretations provided in the wells.

5.2 Structural Geology of the Hamburg 7.5' Quadrangle, Sussex County, New Jersey

The large scale structures of the carbonate rocks of the Hamburg 7.5' Quadrangle were mapped by this investigator over five field seasons and are shown in detail in Plate 1. The maps were then used to construct the balanced cross sections. In many respects, interpretive problems rising from investigation of structural geology in the Hamburg 7.5' Quadrangle are similar to the stratigraphic issues described in Chapter 3 of this dissertation. Previous structural interpretations for this region, like the previous stratigraphic thicknesses for the sections, were extrapolated from other areas where fold-nappe theory, and large-scale overturning, was considered the rule (i.e. (Drake, 1970; Drake et al., 1969; Gray, 1959; MacLachlan, 1979; Zen, 1967)). This study, following the previous work of Herman and Monteverde (1989) and Herman et al. (1997), has revealed that large-scale folds, overturning and fold-nappe structures are not present within this region. Imbricate thrust slices and duplexes, as mapped for this project, represent the dominant structural style in the Hamburg 7.5' Quadrangle. Thrust geometries were elucidated when the contact mapping for this dissertation utilized the revised stratigraphy, as presented in chapters 3 and Appendix B of this document.

Regionally, the Hamburg quadrangle occurs within what Herman and Monteverde (1989) and Herman et al. (1997) refers to the Ridge and Valley Thrust System, which was subdivided into two thrust belts; one of which, the Jenny Jump-Crooked Swamp thrust belt, crops out in the southwestern part of the Hamburg 7.5' Quadrangle and was remapped for this investigation (Plate 1).

5.2.1 Map Interpretation of the Structural Geology of the Hamburg 7.5' Quadrangle

As indicated in the introduction to the chapter, the outcrop distribution in the Hamburg 7.5' Quadrangle consists of Proterozoic basement cropping out in the east, Ordovician Martinsburg siliciclastics cropping out in the west and Cambrian-Ordovician carbonates underlying the central part of the quadrangle (Figure 5.1). The mapped northeast-southwest trending Cambrian-Ordovician swath of carbonates and the structures deforming them are located in the core of the quadrangle. The carbonates are labeled on the geologic map produced for this dissertation as OB1 (the easternmost carbonate outcrops), OB2 (the medial carbonate outcrops in the south-central part of the quadrangle) and OB3 (the westernmost carbonate outcrops) (Plate 1). The carbonate rocks range from the Cambrian Hardyston to the Ordovician Jacksonburg formations (Plate 1; see Chapters 3 and Appendix B).

A first-order observation of the outcrop pattern in the Hamburg 7.5' Quadrangle is the repetition of the carbonate section. OB1 and OB2 are exposed in an en-echelon fashion with respect to each other; the different carbonate swaths separated by a series of northeast-southwest striking, southeast dipping, faults that were originally mapped by Dalton et al. (1997) (and confirmed during mapping for this dissertation) as normal faults (Plate 1). Several of the normal faults were formally named by Dalton et al. (1997) as,

from east to west; the East fault, the Hamburg fault, the Pochuck fault, the Lake Panorama fault, and the Quarry fault. The Lake Panorama fault will not be discussed in this section, as it does not cut through Paleozoic lithologies. However, the fault is included in the composite geologic map presented in this chapter (Plate 1) because it crosses the line of cross-section A-A'. As such, the fault will be discussed with the cross-section interpretations later in this chapter. Two faults mapped by Dalton et al. (1997) were not named and as such, these faults are informally labeled NF1 and NF2 in this dissertation. OB3, the western most belt, extends diagonally through the quadrangle, and is dissected by synthetic and antithetic faults (labeled TF1 through TF3, and AF1 through AF4, respectively). The northern part of OB3 is a panel of steeply dipping rocks (dip to the northwest), separated from the Martinsburg section by a fault labeled as TF1. The central western part of OB3 is dominated by duplex structures repeating the carbonate stratigraphy in a series of thrust fault-bound horses involved faults labeled TF2 and TF3, and a few as yet unnamed faults. The southwestern part of OB3 is dominated by a southwest plunging, Martinsburg cored, syncline, the limbs of which are cut by a series of antithetic faults.

5.2.2 Description of Outcrop Block 1 Structure

OB1 contains rocks of the Hardyston through Ontelaunee formations (Plate 1). The carbonates dip shallowly to the northwest at angles of 4° to 14° (Figure 5.5). The dip angle of the carbonates steepens to the northwest, in conjunction with the cropping out of younger rocks proximal to the bounding fault (specifically, the Hamburg fault) (Plate 1). This observation infers tilting of OB1 towards the Hamburg fault, with preservation of

younger rocks proximal to the fault plane where the degree of fault block rotation would be the greatest, and the rate of erosion the least.

Proterozoic basement, and the Paleozoic carbonates in OB1, are dissected by four faults; NF1, NF2, the East fault, and the Hamburg fault. Dalton et al. (1997) did not exhibit much curvature in the map interpretations of these faults, nor was fault-plain attitude data available; the lack of curvature suggests that the four faults are steeply dipping.

NF1 and NF2 offset the basement-Hardyston and Hardyston-Leithsville contacts in an en-echelon fashion (Plate 1). The faults do not offset the Leithsville-Limeport contact. There is a slight fold in the Leithsville-Limeport contact where the NF2 tip line occurs on the map, indicating that displacement on the normal fault may have been transferred into a buckle fold in the overlying stratigraphy (Plate 1). As NF1 and NF2 offset the basement-Hardyston and Hardyston-Leithsville contacts, the last movements on the faults are inferred to be Paleozoic. It is not clear from map relations if the faults are re-activated Neoproterozoic basement faults initiated during Iapetos rifting. As NF1 and NF2 are not folded, there is a strong possibility that they are Alleghanian in age, instead of Taconian or Acadian-age faults folded by Alleghanian deformation.

The northwestern part of the outcrop belt is separated from the Proterozoic basement by the East fault, which cuts across the Cambrian and Ordovician stratigraphy in a hanging wall ramp (i.e. the fault cuts across the Cambrian and Ordovician stratigraphy in the hanging wall of the fault). The East fault is mapped as a diverging splay that has a branch point with the Hamburg fault near the hanging wall location of the Ontelaunee Formation in OB1. The Hamburg fault continues to the southwest of OB1

and truncates the northern part of OB2 in the southern half of the Hamburg 7.5' Quadrangle (Plate 1).

5.2.3 Description of Outcrop Block 2 Structure

OB2 is located to the southwest of OB1, in the southern part of the Hamburg quadrangle. Only four mappable units crop out in this outcrop block; Hardyston Formation through the Upper Allentown Formation (Plate 1). Strike and dips are steeper in OB2 than in OB1, ranging from 22° to 50° to the northwest (Figure 5.5) (Plate 1). OB2 fishtails in the north, with the Hamburg fault hanging wall comprising the western part, and the Pochuck fault hanging wall forming the eastern part of the outcrop block (Plate 1). The attitude of the Hamburg fault, as discussed in the previous section, is interpreted as being steep. Dalton et al. (1997) mapped the Pochuck fault as cutting a moderately sinuous trace through the basement rocks in the northern part of their version of the Hamburg geologic map (see Plate 1 for presentation of Dalton et al. (1997) data). Dalton et al. (1997), and this author, map the fault trace as losing its sinusoidal curvature and becoming more linear as OB2 is approached. As such, this author infers that the Pochuck fault dips more gently in the basement rocks in the northern part of the quadrangle and steepens as it cuts Paleozoic rocks in the southern part of the quadrangle. There may be rheological reasons for the along-strike change in dip of the Pochuck fault; i.e. Franklin marble is present in the basement rocks mapped by Dalton et al. (1997).

The displacement relationships of faults in the Hamburg 7.5' Quadrangle are described in this chapter in terms of hanging wall and footwall ramps (Boyer and Elliot, 1982; Brewer, 2004; Butler, 1982; Dahlstrom, 1970; Rich, 1934; Thomas, 1990). Flats are faults that cut parallel to stratigraphic bedding at the time of displacement. Ramps cut

obliquely through the stratigraphic succession in the direction of displacement. The adjectival modifier, hanging wall or footwall, serves to indicate where the ramp exists (Thomas, 1990). If the fault cuts obliquely through the stratigraphic succession in the hanging wall, then the fault is a hanging wall ramp. The same fault may also cut parallel to stratigraphic bedding at the time of displacement; as such the fault may also be a footwall flat. Any number of combinations of ramps and flats could be described according to the relationships any particular fault exhibits with the stratigraphy it cuts. As geologic maps and cross sections are geometric projections of rock onto planar surfaces, the concept of hanging wall and footwall ramps and flats can be used equally with either projection method (Brewer, 2004).

The Hamburg fault forms a hanging wall ramp in the northern part of the outcrop belt, cutting through basement, Hardyston, Leithsville, Limeport and Upper Allentown formations in the hanging wall. The Hamburg fault changes to a hanging wall flat in the Upper Allentown Formation in the central and southern parts of OB2. The Hamburg fault is also a footwall ramp in OB2, cutting up section from the Proterozoic basement through the Hardyston and Leithsville formations in the northwestern part of OB2. The fault then cuts back down section again, into basement rocks, in the southwestern part of OB2 near the southern quadrangle boundary (Plate 2).

The Pochuck fault cuts across basement, Hardyston and Leithsville rocks in the northern tip of its hanging wall; however, the fault becomes a hanging wall flat in the Leithsville Formation a short distance south of the Hardyston-Leithsville contact. Trending north-south, the fault separates OB2 from the southeastern boundary of OB3. Previous mapping by Dalton et al. (1997) mapped this boundary between the two outcrop

blocks as Leithsville rocks in the Pochuck hanging wall being down dropped against a Limeport footwall in OB3. This author re-interprets the Pochuck footwall as containing Leithsville rocks; as the lithostratigraphy, and chert marker horizons, present in the footwall did not permit a Limeport interpretation. As such, this author infers the presence of the Pochuck fault separating rocks of the same lithology to explain the repetition of the Cambrian sections exhibited in outcrop blocks 2 and 3.

The Hamburg and Pochuck faults are also considered Paleozoic structures. The faults cuts through Cambrian and Ordovician lithologies and are not folded by Paleozoic orogenesis. As such, they are interpreted as Alleghanian features or alternatively Iapetan-age basement faults that were reactivated during the Alleghanian.

5.2.4 Description of Outcrop Block 3 Structure

OB 3 is the largest of the carbonate outcrop belts and the most complicated structurally. A southwest plunging, Martinsburg-cored, syncline is the most prominent feature of OB3 (Plate 1). Dalton et al. (1997) do not interpret this structure as a syncline, but as a northwest dipping panel of rock. Mapping for this dissertation, however, provided data that confirmed the presence of the fold in the quadrangle and will be presented below. Dips range from 20° to 50°, northeast and northwest depending on which limb of the syncline is being examined (Figure 5.5). A few outlier measurements do exist in the 60° and 70° dip range.

The eastern limb of the syncline contains rocks from the Hardyston Formation to the Bushkill Member of the Martinsburg Formation. The only fault interrupting the succession is the Quarry fault, which duplicates the Hardyston and Leithsville formations in that part of the eastern limb (Plate 1). The western limb of the syncline is truncated by

faulting and is visible in the up-plunge termination of the syncline; specifically, where the stratigraphic section wraps around the nose of the fold, and continues on the opposing limb as a thin sliver of Epler Formation that is truncated at both contacts by faults (Plate 1). This up-plunge termination of the fold is tightly constrained with stratigraphic contact and strike-and-dip data; thereby allowing much confidence in the map interpretation of a synclinal structure (Plate 1). Outside of the up-plunge termination section of the fold and the thin sliver of fault bounded Epler, the western limb is missing. It is replaced by a panel of northwest dipping rocks that are facing stratigraphically up; specifically the section extends from the Limeport Formation, in fault contact with the "underlying" Epler Formation, up to the Ramseyburg Member of the Martinsburg Formation (Plate 1).

The fault separating the Epler Formation from the Bushkill Member in the core of the syncline is a hypothetical construct to explain the presence of the Epler Formation proximal to the Bushkill Member. No data was found during mapping of this dissertation to directly support the attitude, or displacement, interpretations for this fault. A fault was mapped in the Bushkill Member in the core of the syncline, as AF1. The presence of AF1 was supported by the presence of mappable offsets in the Ontelaunee-Jacksonburg and Jacksonburg-Bushkill contacts (Plate 1). The fault separating the Epler Formation from the Limeport Formation in the northwest dipping panel and taking the place of the "missing western limb" is labeled AF2.

The syncline is dissected by a number of synthetic and antithetic faults. The Quarry fault is interpreted by Dalton et al. (1997) as being a normal fault that dips to the southeast. Mapping for this dissertation indicates that the fault cuts northwest dipping beds of the eastern limb of the Martinsburg cored syncline. The map trace of the Quarry

fault is curved enough to permit a moderate-angle, northwest dip interpretation for the attitude of the fault plane (Plate 1). Outcrop patterns of the offset Leithsville-Limeport contact in the hanging wall of the fault show that the contact migrated in the direction of bedding dip after erosion. Basic geologic mapping theory predicts that it is the up thrown block of a fault that will exhibit down-dip contact migration due to fault-scarp erosion. Thus, the Quarry fault is re-interpreted as an antithetic, reverse fault, i.e. back-thrust, that dips to the northwest. The fault is also mapped as terminating along strike to the southwest, but not before it splays into another small, unnamed fault (Plate 1). Two small folds (southwest plunging anticline-syncline pair) were mapped at the termination of the Quarry fault, and its unnamed splay, and both are inferred as transferring displacement along-strike into the southwest plunging folds.

Fault AF1 is evident from the offsets mapped in the Ontelaunee-Jacksonburg and Jacksonburg-Bushkill contacts. The fault was mapped by Dalton et al. (1997) and its presence and orientation were confirmed by this author. Reasoning similar to that described above for the Quarry fault is used to describe the orientation of this fault. Both Dalton et al. (1997) and this author interpret the map trace of AF1 as representing a moderate dip to the northwest. Migration of offset contacts in the direction of bedding dip, in the hanging wall of AF1, indicate that the hanging wall is the up thrown block and is therefore an antithetic, reverse fault, i.e. back thrust. This author took license to branch AF1 with the unnamed, theoretical fault separating the Martinsburg synclinal core from the Epler Formation, in what was supposed to be the syncline's western limb. Reasoning for this interpretation stems from the recognition that the unnamed, theoretical fault most likely accommodates tightening in the synclinal core. Therefore, it is not unreasonable to

assume that AF1 is also an accommodation structure and may be related to the unnamed, theoretical fault.

AF2 is the fault that separates the northwest dipping panel on the western side of the Martinsburg syncline from the fault bounded Epler Formation, also cropping out on the western side of the Martinsburg syncline (Plate 1). The slightly curved outcrop pattern of AF2 indicates that the fault dips moderately to the west. Kinematic indicators were not forthcoming for AF2 during mapping; however, considering the inferred attitude of the fault and its relationship with the synclinal structure, it is likely that it too is an antithetic reverse fault, similar to the Quarry fault and AF1. AF2 is a hanging wall flat in the Limeport Formation for most of its outcrop length, but along strike, to the northeast, becomes a hanging wall ramp where it cuts across stratigraphic section from the Limeport to the Upper Allentown Formation. The fault is interpreted as branching with AF3 near the duplex zone of OB3 (Plate 1). AF2 is also a footwall ramp in the Epler Formation, cutting down section from the Epler into the Rickenbach Formation. The footwall ramp of AF2 truncates the preserved western limb of the Martinsburg-cored syncline. These outcrop relationships between AF2, and the Martinsburg-cored syncline, may indicate that the AF2 thrust sheet is stacked on top of the western limb of the syncline.

The fault labeled AF3 is present on the northwestern boundary of the AF2 hanging wall (Plate 1). AF3 is curved and is interpreted as being a shallowly dipping fault. Contact migration of offset contacts in the AF3 hanging wall indicates that the hanging wall is the up thrown block; as such AF3 is a back thrust. AF3 is a hanging wall flat in the Rickenbach Formation and changes along strike to a hanging wall ramp,

moving up stratigraphic section from the Rickenbach through the Bushkill Member of the Martinsburg Formation. AF3 is also a footwall ramp, cutting up section in the AF2 hanging wall from the Upper Allentown through the Bushkill Member.

Both limbs of the Martinsburg-cored syncline are dissected by the antithetic reverse faults discussed in this section of the chapter. The antithetic faults also do not exhibit any folding from tectonic events and therefore are interpreted as being Alleghanian in age. The Martinsburg-cored syncline is interpreted as being older than the antithetic faults that dissect it.

In the west-central part of OB3 are four horses that belong to a duplex structure in this outcrop belt. Moving northward from the Martinsburg-cored syncline, the first horse is bound by unnamed faults that encompass rocks from the Upper Allentown to the Bushkill Member (Plate 1). Directly to the east and sharing a fault is a second horse that contains slightly folded rocks of the Upper Allentown, Rickenbach and Epler formations. The third horse to the north of horses one and two is a fault bounded block composed on Upper Allentown through Rickenbach rocks. The northern border fault of horse three is labeled TF3. The fourth horse in this system shares TF3 with the third horse and is bound on the other side of the block by TF2. The fourth horse contains the Upper Allentown and Rickenbach formations.

A northwest dipping panel of Cambrian-Ordovician rocks, extending from the Proterozoic basement into the Ordovician Martinsburg Formation, comprises OB3 north of the up-plunge termination of the Martinsburg-cored syncline (Plate 1). In order to structurally explain the presence of this panel, a hypothetical fault is interpreted as occurring in the transition zone between the up-plunge termination of the Martinsburg-

cored syncline and the panel as it extends north of the fold-plunge termination. The syncline in OB3 is mapped as having an up-plunge termination in the Hamburg quadrangle. The eastern limb of the syncline cannot extend northward of the up-plunge termination. As such, a mechanism must be proposed to accommodate the transition from terminated syncline to homoclinal panel of rock.

The rocks in this homoclinal panel vary in dip angle towards the northern part of the quadrangle sheet. Proximal to the synclinal termination, the beds in the homocline dip an average of 20°. Along strike, towards the northern boundary of the quadrangle sheet, the beds dip on average 75°.

The homoclinal panel is bound on its western boundary by TF1, a fault that varies in its map trace along strike. Near the termination of the syncline, the fault is curved, suggesting a shallow to moderate dip. Along strike to the north, the fault map traces becomes linear, indicating a steepening of dip. This change in fault dip corresponds with the increase in bedding dip in the rocks of the homoclinal panel. The outcrop trace of the fault near the synclinal termination indicates that the fault dips to the east-southeast, placing the homoclinal panel in the hanging wall of TF1. The presence of the Bushkill Member in both the hanging wall and footwall of TF1, in the northern part of the outcrop belt indicates that displacement along this fault is not large.

5.3 Cross-Section Interpretation of the Structural Geology in the Hamburg 7.5' Quadrangle

Two cross sections were constructed for the Hamburg 7.5' Quadrangle. The northernmost cross section is A-A' and the southernmost cross section is B-B' (Plates 2 and 3). The cross sections were constructed using the conservation of line length and cut-

off angles**.** Stratigraphic thickness is kept constant in the cross sections, except where there is geologic field evidence to show that stratigraphic thickness variations did occur along the line of section, in which case the variation in stratigraphic thickness was interpreted as varying in a smooth, linear fashion between the locations of the two data points. Four seismic lines and three oil exploration wells, published in the Herman et al. (1997) manuscript, were reinterpreted in this dissertation to constrain subsurface interpretations. The seismic data includes 4- to 5-second (s), two-way travel times. According to Herman et al., (1997) the lines are un-migrated, 60-fold, common-depth-point stacked sections with no vertical exaggeration. This author's interpretation of the substructure is based on the correlation of acoustic boundaries with up-dip outcrops in contiguous quadrangles of the Hamburg, and tracing of those structures along strike into the Hamburg 7.5' Quadrangle. The revised stratigraphic thicknesses (Chapter 3) were also used. Subsurface stratigraphic depth is interpreted from deep wells published by Fletcher and Woodrow (1970) and Saunders (1983), and from detailed stratigraphic sections (Appendix E) measured during fieldwork conducted for this dissertation (Chapter 3 and Appendix B).

5.3.1 Interpretation of Cross-Section A-A'

The A-A' cross section extends along a northwest-southeast trend (Plate 1). The A location is studded in the Martinsburg Slate and the A' location is in the Proterozoic basement**.** The cross section extends through the Cambrian-Ordovician section that spans the interval between the Martinsburg slate and the Proterozoic basement (Plate 1) (Figure 5.6).

The seismic profiles (Herman et al., 1997) and well data (Fletcher and Woodrow, 1970; and Saunders, 1983) indicate the subsurface elevation of the basement-Hardyston contact is approximately 5,000 ft (1,524 m) below sea level (Plate 2). Additionally, the basal decollement is interpreted at approximately 5,500 ft (1,676 m) (Plate 2).

The first fault that crosses the line of cross section, from the starting point at A, is AF4, which is interpreted as moderately dipping to the northwest based on the fault outcrop trace near the line of section. The displacement of the older Bushkill Member (Omb) in the AF4 hanging wall against the younger Ramseyburg Member (Omr) in the AF8 footwall infers that the hanging wall moved upwards relative to the footwall, making AF4 a thrust fault interpreted as a back thrust (Plate 1). The fault is interpreted as containing a hanging wall flat and a footwall ramp as the fault remains in the Bushkill Member in the hanging wall and cuts across the stratigraphic succession in the footwall.

An unnamed synclinal structure forms the footwall of AF4 (Figure 5.6). Truncating the unnamed syncline to the east is the steep fault identified on Plate 1 as TF1 (Plate 1). The stratigraphic separation of the fault along this line of cross section is small, as the Bushkill Member in the hanging wall is displaced against the Bushkill Member in the footwall. The thinness of the Bushkill Member in the hanging wall; however, suggests structural thinning of the unit. Additionally, the Cambrian-Ordovician rocks in the TF1 hanging wall can be interpreted in cross section as representing a large fault propagation fold cut by TF1 or inferred as a pre-existing fold cut by TF1 with possible steepening of dips due to deformation along the fault zone. The two hypotheses are best fitted to a thrust fault interpretation for TF1.

Two additional faults (Lake Panorama and Pochuck) cross the line of cross-section A-A'. As Proterozoic basement was mapped by Dalton et al. (1997) on both sides of the Pochuck fault and the Lake Panorama fault, this author infers that stratigraphic displacement on these faults is small along the line of cross-section A-A'; however, along strike to the southwest, the faults are mapped as having younger Cambrian lithologies in the hanging wall juxtaposed against older Proterozoic lithologies in the footwall, permitting a normal kinematic interpretation for these faults (Plate 1).

The dissection of fold limbs by faults in section A-A' permits an interpretation that folds formed prior to faulting. A partial retrofit for cross-section A-A', where the faults in cross-section A-A' were palinspastically restored to a pre-faulting state representing deformation due to faulting alone (Plate 2). This stage of folding is interpreted as F_1 or Taconic folding.

5.3.2 Interpretation of Cross-Section B-B'

Cross-section B-B' trends northwest-southeast with the Martinsburg Formation (Bushkill Member) in the northwest (point B) and the Proterozoic basement in the southeast (point B'). The entire Cambrian and Ordovician succession is transected by this cross-section (Plate 1). The top of the basement varies from exposure at the ground surface in the east, to depths of approximately 4,000 ft (1,219.2 m) below mean sea level in the west. The basal decollement is interpreted from seismic lines (Herman et al., 1997) as having an elevation of approximately 5,500 ft deep (1,676.4 m). The eastern limb of the Martinsburg-cored syncline is transected by cross-section B-B' (Plate 1) (Plate 3). There are two faults that cross the line of the section on the geologic map; the Pochuck fault and an unnamed diverging splay from the Pochuck fault. Fault AF1 has a tip line

just north of the line of B-B' section. However, a blind expression of AF1 is interpreted as being on the B-B' section, as fault displacement is usually modeled as being transferred into accommodations folds as fault propagation diminishes to zero (Dahlstrom, 1969).

Viewing the cross section from west to east, the first structure represented on the line of the cross section is the eastern limb of the Martinsburg cored syncline, with attendant parasitic folds (southwest plunging anticline-syncline pair) in the surficial expression of the Limeport Formation.

Two small-scale, southwest plunging, folds are mapped on the quadrangle sheet where it intersects the line of section (Plate 1) (Figure 5.7). Both structures, an antiform and a synform, are shown on the map as extending from the tip lines of the Quarry fault and an unnamed, diverging splay. The faults are interpreted as being present in the subsurface as along-strike, blind, extensions of the surficial expression of the faults.

The next structure intersected on cross-section B-B' is the Pochuck fault. This steep fault curves to the northwest which suggests that dip shallows in that direction. The dip direction changes along strike, from northwest in the south to southeast in the north (Plate 1). The previous interpretation of a normal fault separation for the Pochuck fault appears to be valid. Cross-section B-B' depicts the Pochuck fault as cross cutting the eastern limb of the Martinsburg-cored syncline. The fault cuts across stratigraphy in both the hanging wall and footwall in cross-section B-B'.

Palinspastic restoration of the B-B' cross section was, again, accomplished in two stages; a restoration to the pre-faulting/post-folding stage (Plate 3) and then a restoration to the pre-folding stage (Plate 3). Figure 5.7a shows the core of the Martinsburg syncline

and its eastern limb. The eastern limb is the predominant structure with smaller scale folds deforming the limb.



Figure 5.1: A reduced version of the Hamburg 7.5' Quadrangle sheet. The varicolored swath of rocks in the central part of the map are the carbonates mapped for this dissertation. The blue swath in the northwestern part, and the gray swath in the southeastern part of the map were not mapped for this dissertation.

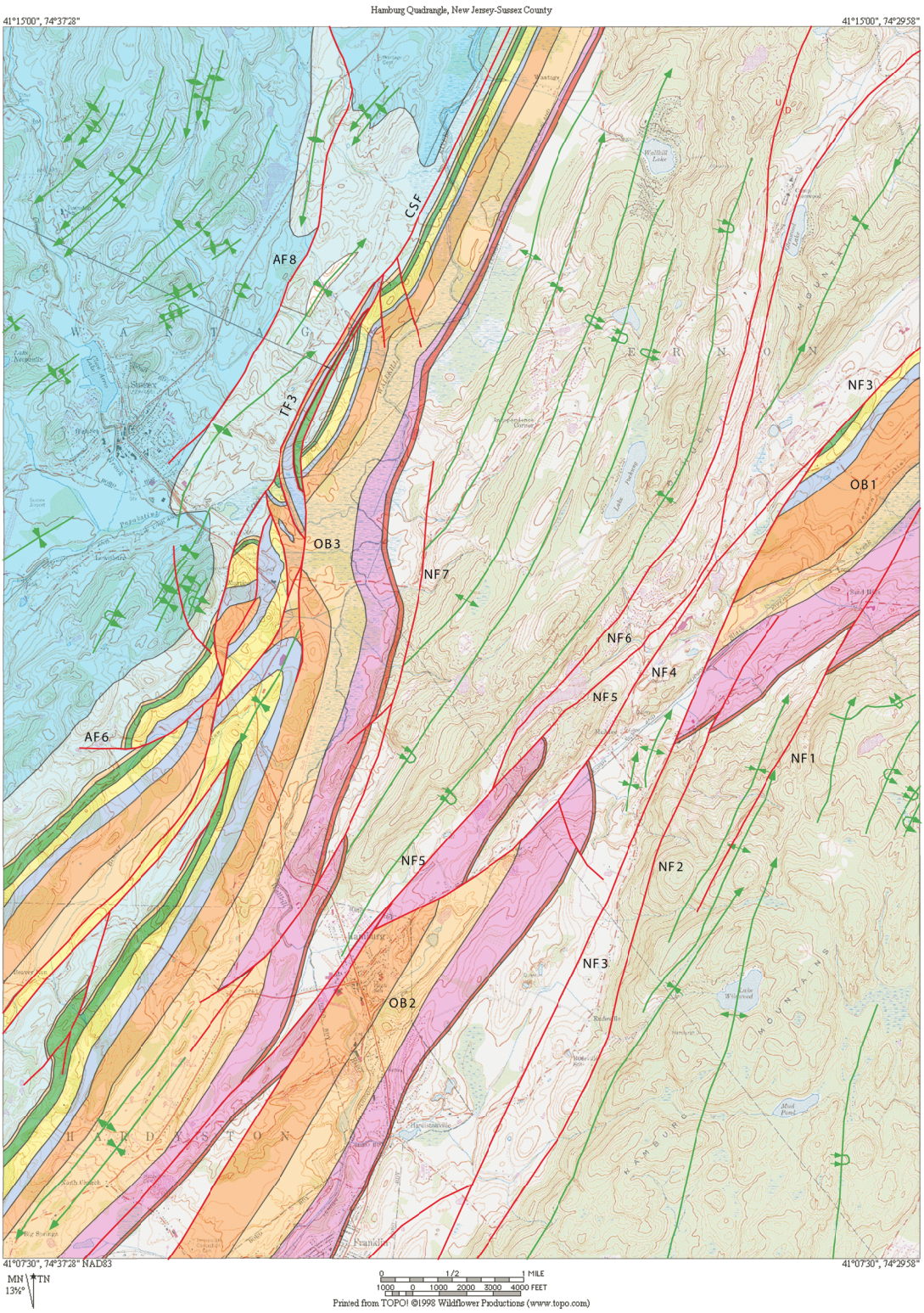


Figure 5.2: A reduced version of a geologic map of the Hamburg 7.5' Quadrangle, showing a compilation of the mapping conducted for this dissertation and mapping conducted by Dalton et al. (1997) for the Proterozoic basement and the Ordovician Martinsburg Formation.

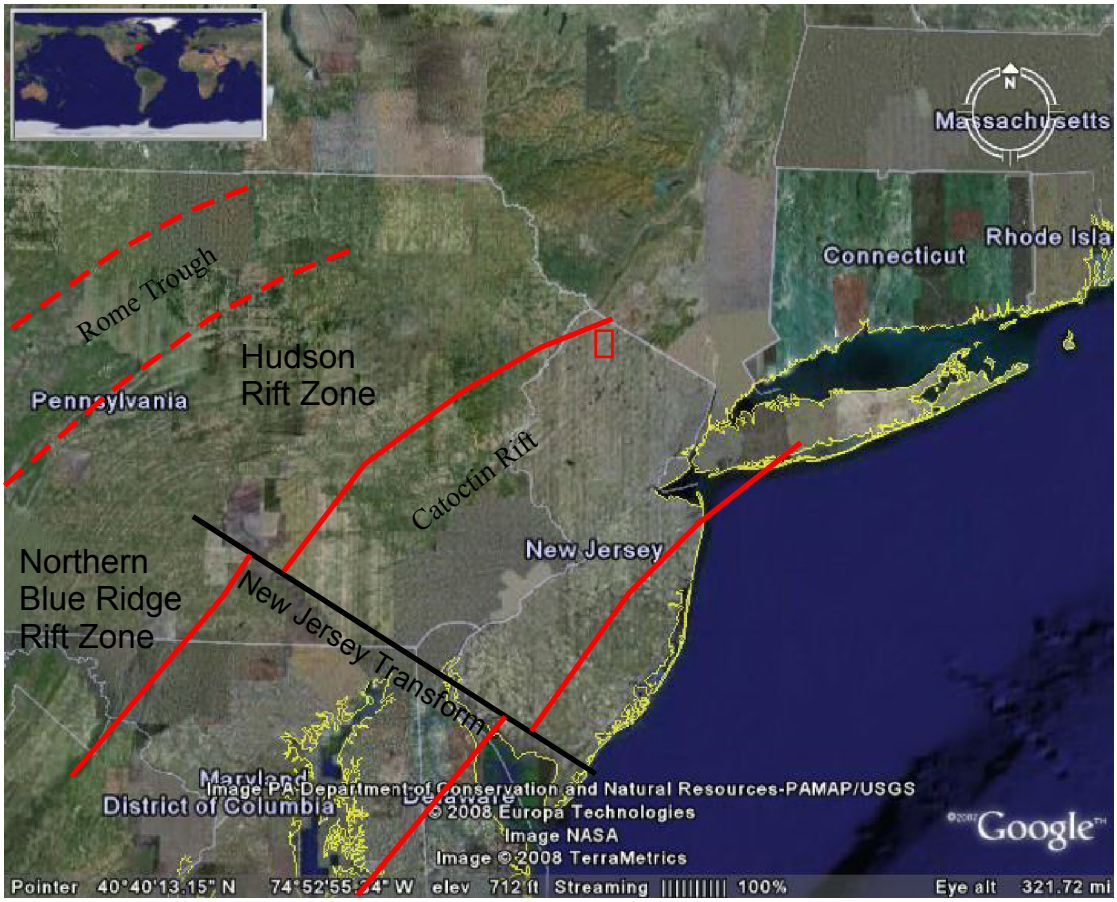


Figure 5.3: Satellite image of the New York-New Jersey-Pennsylvania area. The study area for this dissertation is located in northwestern New Jersey, outlined by the red box. This map incorporates data from this dissertation, Thomas (1993) and Faill (1999).

Thomas' (1993) interpretation of the New Jersey Transform, plus his distinguishing between the Hudson and Northern Blue Ridge rift zones on the north and south sides of the New Jersey Transform, respectively are shown on this figure.

Faill's interpretation of the Catoctin Rift and the Rome Trough are shown on this map.

The offset of the Catoctin Rift by the New Jersey Transform is an interpretation of this author. The position of the Rome Trough is well established by Fail (1999); however, it is tentatively placed by the author on this figure (as indicated by dashed red line), due to lack of reliable geographic markers.

The study area for this dissertation is interpreted to be in the Catoctin Rift, near the northwestern (current geographic position) border fault.

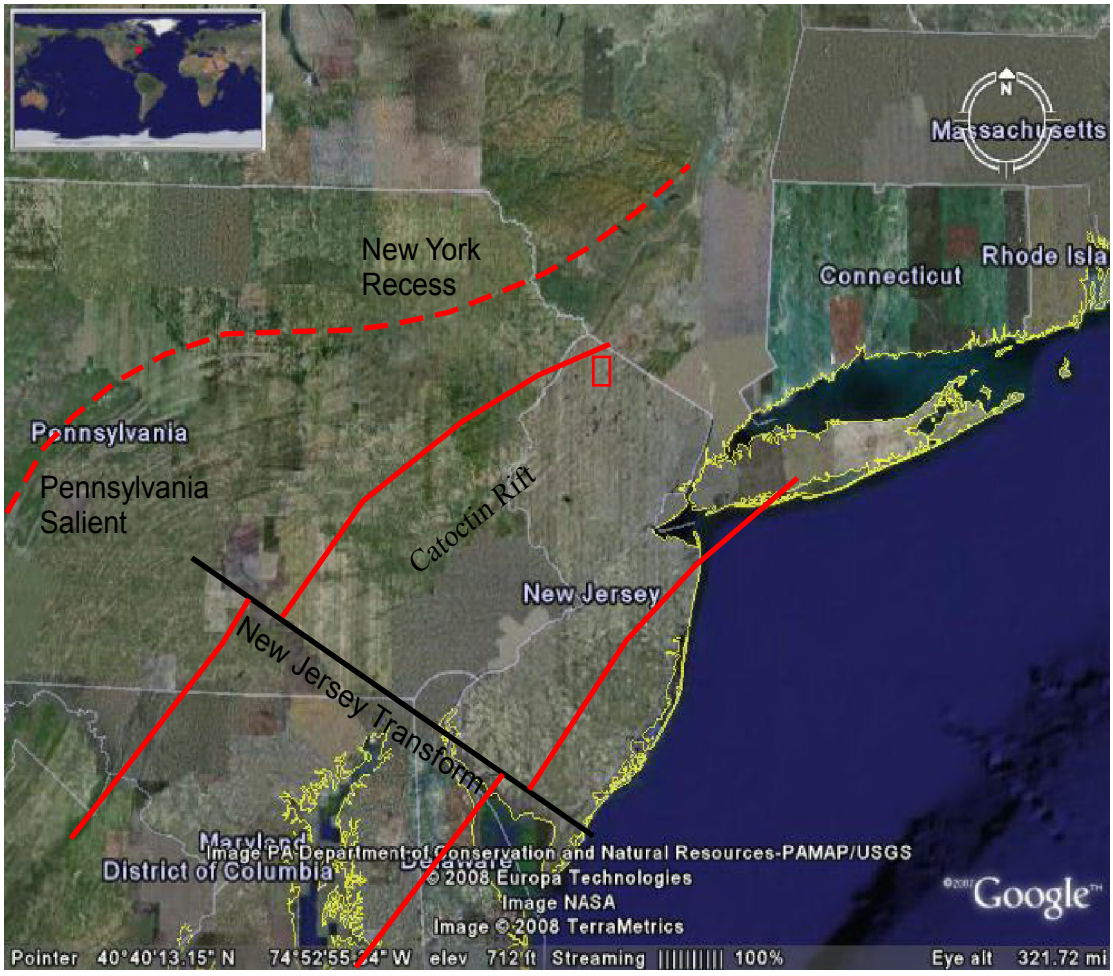
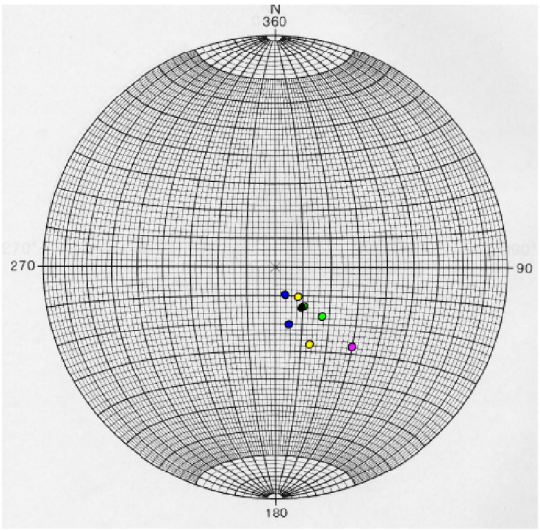
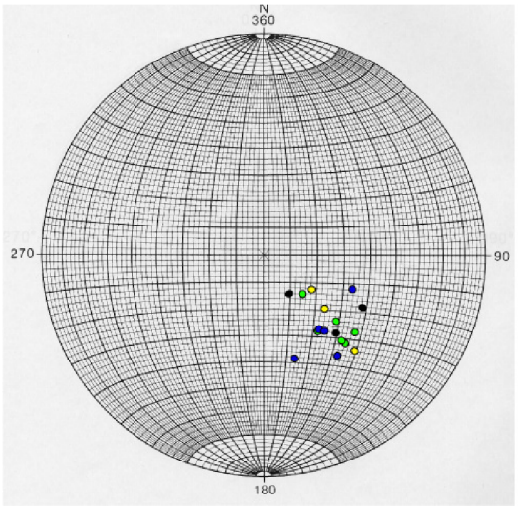


Figure 5.4: Satellite image of the New York-New Jersey-Pennsylvania area. The study area for this dissertation is located in northwestern New Jersey, outlined by the red box. This map incorporates data from this dissertation, Thomas (1993) and Faill (1999).

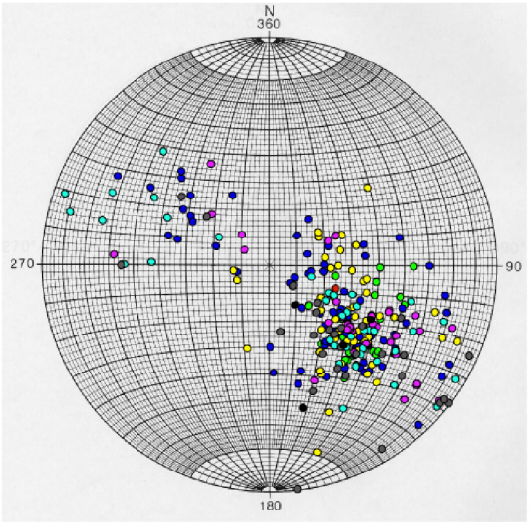
The study area in this dissertation is in the New York recess. The New York recess and the Pennsylvania salient are best illustrated in this figure by the presence of the dashed red line to the west of the Catoctin rift. The dashed red line illustrates the westernmost extent of Paleozoic orogenic deformation, as exposed on the surface.



Outcrop Block 1



Outcrop Block 2



Outcrop Block 3

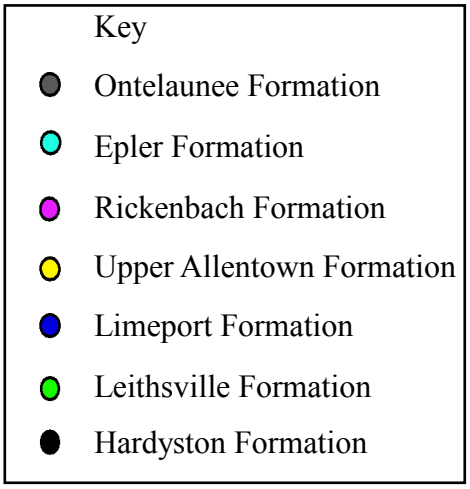


Figure 5.5: Reciprocal plots for strike and dip of bedding orientation in the Cambrian and Ordovician carbonate rocks, as mapped within outcrops blocks 1, 2, and 3 of the Hamburg 7.5' Quadrangle (Plate 1).

REFERENCES CITED

Ahr, W., 1973, The carbonate ramp: an alternative to the shelf model: Transactions of Gulf Coast Association of Geological Societies, v. 23, p. 221-225.

Aitken, J., 1967, Classification and environmental significance of cryptalgal limestones and dolomites, with illustrations from the Cambrian and Ordovician of southwestern Alberta: Journal of Sedimentary Petrology, p. 1163-1178.

-, 1988, Giant "algal reefs", Middle/Upper Proterozoic, Little Dal Group (>1200 Ma), Mackenzie Mountains, N.W.T., Canada, *in* Geldsetzer, H., James, N., and Tebbutt, G., eds., Reefs, Canada and Adjacent Areas, Canadian Society of Petroleum Geologists, p. 13-23.

Aleinikoff, J., 1985, Isotopic and morphologic evidence for the age of the Fordham Gneiss: American Journal of Science, v. 285, p. 459-479.

Allen, J., and Friend, P., 1968, Deposition of the Catskill facies, Appalachian region: With notes on some other Old Red Sandstone basins, *in* Klein, G., ed., Paleozoic and Mesozoic Continental Sedimentation, Northeastern North America, Special Paper 106, Geological Society of America, p. 21-72.

Amiel, A., and Friedman, G., 1971, Continental sabka in Arava Valley between Dead Sea and Red Sea: Significance for origin of evaporites American Association of Petroleum Geologists Bulletin, v. 55, p. 581-592.

Bathurst, R., 1982, Genesis of stromatactic cavities between submarine crusts of Paleozoic carbonate mud buildups: Journal of the Geological Society of London, v. 139, p. 165-181.

Bayley, W., Salisbury, R., and Kummel, H., 1914, Description of the Raritan quadrangle [New Jersey], United States Geological Survey Geologic Atlas, Folio 191, 32 p.

Beales, F., and Oldershaw, A., 1969, Evaporite-solution brecciation and Devonian carbonate reservoir porosity in western Canada: American Association of Petroleum Geologists Bulletin, v. 53, p. 503-512.

Belperio, A., Gostin, V., Cann, J., and Murray-Wallace, C., 1988, Sediment-organism zonation and the evolution of Holocene tidal sequences in southern Australia, *in* de Boer, P., van Gelder, A., and Nio, S., eds., Tide-Influenced Sedimentary Environments and Facies: Dordrecht, Reidel Publishing Company, p. 475-497.

Beyth, M., 1980, Recent evolution and present stage of Dead Sea brines *in* Neissenbaum, A., ed., Hypersaline Brines and Evaporitic Environments.

Blount, D., and Moore, C., 1969, Depositional and non-depositional carbonate breccias, Chianta Quadrangle, Guatamala: Geological Society of America Bulletin, v. 80, p. 429-442.

Bond, G., Nickeson, P., and Kominz, M., 1984, Breakup of a super-continent between 625 Ma and 555 Ma: New evidence and implications for continental histories: Earth and Planetary Science Letters, v. 70, p. 325-345.

Bosellini, A., and Hardie, L., 1973, Depositional theme of a marginal marine evaporite: Sedimentology, v. 20, p. 5-27.

Bova, J., and Read, J., 1987, Incipiently drowned facies within a cyclic peritidal ramp sequence, Early Ordovician Chepultepec interval, Virginia Appalachians: Geological Society of America Bulletin, v. 98, p. 714-727.

Boyer, S., and Elliot, D., 1982, Thrust systems: American Association of Patroleum Geologists Bulletin, v. 66, p. 1196-1230.

Brewer-LaPorta, M., LaPorta, P., and Minchak, S., in preparation, Petrofabric constraints on quarry development and stone tool design: North-central Appalachians, *in* Brewer-LaPorta, M., Burke, A., and Field, D., eds., Prehistoric Mines and Quarries: A Transatlantic Perspective: Oxford, U.K., Oxbow Press.

Brewer, M., 2004, Geometric and Kinematic Controls of the Bessemer Transverse Zone, Alabama Alleghanian Thrust Belt: University of Kentucky, Department of Geological Sciences, 235 p.

Brewer, M., and LaPorta, P., 1999, The prehistoric quarry landscape in the eastern Appalachians: Society for American Archaeology, Annual Meeting Abstracts, v. 64, p. 58.

-, 2001, Prehistoric lithic resource utilization in New Jersey: Society for American Archaeology, Annual Meeting Abstracts, v. 66, p. 101.

-, 2002, Petrofabric and microfossil characteristics of chert as a provenance tool: Society for American Archaeology, Annual Meeting Abstracts, v. 67, p. 56.

-, 2006, Cross-sectional Interpretation of the Tectonic History of the Hamburg 7.5' Quadrangle, Sussex County, New Jersey: Geological Society of America, Annual Meeting Abstracts

Brewer, M., LaPorta, P., and Minchak, S., 2006, Petrofabric Constraints on Quarry Development and Stone Tool Design: North-Central Appalachians: Society for American Archaeology, Annual Meeting Abstracts, v. 71, p. 80.

Brewer, M., Minchak, S., and LaPorta, P., 2000, A mineral resource approach to raw material analysis and quarry investigations: Examples from the Central Appalachians: Society for American Archaeology, Annual Meeting Abstracts, v. 65, p. 64.

Bridges, P., and Chapman, A., 1988, The anatomy of a deep water mud-mound complex to the southwest of the Dinantian platform in Derbyshire, UK: Sedimentology, v. 35, p. 139-162.

Brock, P., and Brock, P., 1999, The birth of Iapetus: Geochemical evidence for late Neoproterozoic rifting form the metaigneous rocks of the Ned Mountain Formation, Manhattan Prong, Geology of Long Island and Metropolitan New York Stony Brook, Department of Geosciences, SUNY Stony Brook.

-, 2000, Chemistry and stratigraphy of the rift-related late-Proterozoic metaigneous rocks of the Ned Mountain Formation, Manhattan Prong: Geological Society of America, Abstracts with Programs, v. 32, p. A-7.

-, 2001, Bedrock geology of New York City: More than 600 m.y. of geological history, Field Guide for Long Island Geologists Field Trip, p. 11.

Brown, M., and Dodd, J., 1990, Carbonate mud bodies in Middle Mississippian strata of southern Indiana and northern Kentucky: end members of a Middle Mississippian mud-mound spectrum: Palaios, v. 5, p. 236-243.

Brueckner, H., Brock, P., and Brock, P., 2002, Taconian delamination in the Manhattan Prong? Zircon ages of mafic complexes with alkali basalt affinity, and the timing of peak granulite-facies (Opx-Sill) metamorphism, Geological Society of American, Abstracts with Programs.

Brueckner, H., Snyder, W., and Boudreau, M., 1987, Diageneitic controls on the structural and tectonic evolution of siliceous sediments, Golconda Allochthon, Nevada.

Budd, D., and Harris, P., 1990, Carbonate-siliciclastic mixtures: Society of Economic Paleontologists and Mineralogists, v. Reprint Series 14, p. 272 pages.

Buddington, A., and Baker, D., 1961, Geology of the Franklin and part of the Hamburg quadrangles, New Jersey, U.S.G.S. Professional Paper 638, United States Geological Survey, 73 p.

Butler, R., 1982, The terminology of structures in thrust belts: Journal of Structural Geology, v. 4, p. 239-245.

Callahan, E., 1979, The Basics of Biface Knapping in the Eastern Fluted Point Tradition: A Manuel for Flintknappers and Lithic Analysts: Archaeology of Eastern North America, v. 7, p. 180.

Calvert, F., and Tucker, M., 1988, Outer ramp cycles in the Upper Muschelkalk of the Catalan Basin, northern Spain: Sedimentary Geology, v. 57, p. 185-198.

Chappell, J., and Polach, H., 1976, Holocoene sea-level change and coral-reef growth at Huon Peninsula, Papua, New Guinea: Geological Society of America Bulletin, v. 87, p. 235-239.

Choi, D., and Ginsburg, R., 1982, Siliciclastic foundations of Quaternary reefs in the southernmost Belize Lagoon, British Honduras: Geological Society of America Bulletin, v. 93, p. 116-126.

Chowns, T., and Elkins, J., 1979, The origin of quartz geodes and cauliflower cherts through the silicification of anhydrite nodules, *in* McBride, E. F., ed., Silica in Sediments: Nodular and Bedded Chert: Oklahoma, Society of Economic Paleontologists and Mineralogists p. 129-147.

Clark, J., 1984, The core of the Blue Ridge anticlinorium in northern Virginia, *in* Bartholomew, M. J., ed., The Grenville event in the Appalachians and related topics, p. 155-160.

Clifton, H., 1967, Solution-collapse and cavity filling in the Windsor Group, Nova Scotia, Canada: Geological Society of America Bulletin, v. 75, p. 819-832.

Coates, A., and Jackson, J., 1987, Clonal growth, algal symbiosis, and reef formation by corals: Paleobiology, v. 13, p. 363-378.

Colter, V., and Reed, A., 1980, Zechstein 2 Forden Evaporites of the Atwick No. 1 borehole, surrounding areas of N.N. England and the adjacent southern North Sea, *in* Fuchtbauer, H., and Peryt, T., eds., The Zechstein Basin with Emphasis on carbonate sequences.

Colton, G., 1970, The Appalachian basin-its depositional sequences and their geologic relationships, *in* G.W.Fisher, and et al., eds., Studies of Appalachian geology, central and southern, New York, Interscience Publishers, p. 5-47.

Crabtree, D., 1972, An Introduction to Flintworking, Occasional Papers of the Idaho State University Museum, Idaho State University, 98 p.

Crawford, G., and Dunham, J., 1982, Evaporite sedimentation in the Permian Yates Formation, Central Basin Platform, Andrews County, West Texas, *in* Handford, C., Loucks, R., and Davies, G., eds., Depositional and diagenetic spectra of evaporites, Society of Economic Paleontologists and Mineralogists.

Cudzil, M., 1985, Fluvial, tidal and storm sedimentation in the Chilhowee Group (lower Cambrian), northeastern Tennessee [M.S. thesis], 164 p.

Cudzil, M., and Driese, S., 1987, Fluvial, tidal and storm sedimentation in the Chilhowee Group (lower Cambrian), northeastern Tennessee, Sedimentology, p. 861-883.

Cuffey, R., 1985, Expanded reef-rock textural classification and the geologic history of bryozoan reefs: Geology, v. 13, p. 307-310.

Cummings, E., 1932, Reefs or bioherms?: Geological Society of America Bulletin, v. 43, p. 331-352.

Dahlstrom, C., 1969, Balanced cross sections: Canadian Journal of Earth Sciences, v. 6, p. 743-757.

-, 1970, Structural geology in the eastern margin of the Canadian Rocky Mountains: Bulletin of Canadian Petroleum Geology, v. 18, p. 322-406.

Dale, N., 1906, Slate deposits and slate industry of the United States: U.S. Geological Survey Bulletin, v. 275, p. 154.

Dallmeyer, R., Sutter, J., and Baker, D., 1975, Incremental 40Ar/39Ar ages of biotite and hornblende from the northeastern Reading Prong: Their bearing on late Proterozoic thermal and tectonic history, Geological Society of America Bulletin, p. 1436-1443.

Dalton, R., Canace, R., Volkert, R., Monteverde, D., and Herman, G., 1997, Bedrock Geologic Map of the Hamburg Quadrangle, Sussex County, New Jersey (scale 1:24,000): New Jersey Geological Survey, Open File Report.

Davies, G., and Hopley, D., 1983, Growth facies and growth rates of Holocene reefs in the Great Barrier Reef: BMR Journal of Australian Geology and Geophysics, v. 8, p. 237-252.

Davies, P., Marshall, J., and Hopley, D., 1985, Relationships between reef growth and sea level in the Great Barrier Reef, Proceedings of the Fifth International Coral Reef Congress: Tahiti, p. 95-103.

Davies, P., and Montaggioni, L., 1985, Reef growth and sea level change: the environmental signature, Proceedings of the Fifth International Coral Reef Symposium: Tahiti, p. 477-511.

De Boer, P., van Gelder, A., and Nio, S., 1988, Tide-influenced sedimentary environments and facies: Dordrecht, D. Reidel, p. 530.

Demille, G., Shouldice, J., and Nelson, H., 1964, Collapse structures related to evaporates of the Prairie Formation, Saskatchewan: Geological Society of America Bulletin, v. 75, p. 307-316.

Dill, R., Shinn, E., Jones, A., Kelly, K., and Steinen, R., 1986, Giant subtidal stromatolites forming in normal salinity waters: Nature, v. 324, p. 55-58.

Drake, A., 1970, Structural geology of the Reading Prong, *in* Fisher, G. W., ed., Studies in Appalachian Geology-The Central and Southern Appalachians of New York, John Wiley and Sons, p. 271-291.

-, 1978, The Lyon Station-Paulins Kill nappe-the frontal structure of the Musconetcong nappe system in eastern Pennsylvania and New Jersey, U.S. Geological Survey, Professional Paper 1023, p. 20.

Drake, A., Sinha, A., Laird, J., and Guy, R., 1989, The Taconic orogen, *in* R.D. Hatcher Jr, W. A. T., and Viele, G. W., eds., The Appalachian-Ouachita Orogen in the United States, Geological Society of America, Decade of North American Geology Series, p. 101-177.

Drake, A. J., 1965, Carbonate rocks of Cambrian and Ordovician age, Northampton and Bucks Counties, eastern Pennsylvania, and Warren and Hunterdon Counties, western New Jersey: United States Geological Survey Bulletin, v. 1194-B, p. 7 pages.

-, 1969, Precambrian and Lower Paleozoic geology of the Delaware Valley, New Jersey-Pennsylvania, *in* Subitzky, S., ed., Geology of selected areas in New Jersey and eastern Pennsylvania and guidebook of excursions: New Brunswick, New Jersey, Rutgers University Press p. 51-132.

Drake, A. J., Epstein, J., and Aaron, J., 1969, Geologic map and sections of parts of the Portland and Belvidere quadrangles, New Jersey-Pennsylvania: United States Geological Survey Inv. Map, v. I-552.

Dunham, R., 1962, Classification of carbonate rocks according to depositional texture, Classification of Carbonate Rocks: AAPG Memoir 1, American Association of Petroleum Geologists, 108-121 p.

-, 1970, Stratigraphic reefs versus ecologic reefs: American Association of Petroleum Geologists Bulletin, v. 54, p. 1931-1932.

Dykstra, J., and Longman, M., 1995, Gas Reservoir Potential of the Lower Ordovician Beekmantown Group, Quebec Lowlands, Canada: American Association of Petroleum Geologists Bulletin, v. 79, no. 4, p. 513-530.

Enos, P., 1977, Holocene sediment accumulation of the South Florida shelf margin, *in* Enos, P., and Perkins, R., eds., Quaternary sedimentation in South Florida, Geological Society of America, p. 1-130.

Etheridge, M., Symonds, P., and Lister, G., 1989, Application of the detachment model to reconstruction of conjugate passive margins, American Associations of Petroleum Geologists Memoir 46, p. 23-40.

Faill, R., 1999, Paleozoic history, *in* Schultz, C. H., ed., The Geology of Pennsylvania, Special Publication 1, Pennsylvania Geological Survey and Pittsburg Geological Society, p. 418-433.

Fisher, D., 1956, The Cambrian System of New York State, *in* Rodgers, J., ed., El Sistema Cambrico, Su Paleogeografia y el Problema de su Base-Symposium International Geological Congress: Mexico City p. 321-352.

-, 1962, Correlation of the Cambrian rocks in New York State: New York State Museum and Science Service Map and Chart, v. Series 2.

-, 1977, Correlation of the Hadrynian, Cambrian, and Ordovician rocks in New York State: New York State Museum Map and Chart Series No. 25, p. 75 pages.

Fletcher, F., and Woodrow, D., 1970, Geology and economic resources of the Pennsylvania portion of the Milford and Port Jervis 15-minute quadrangles, Department of Environmental Resources Atlas 223, Commonwealth of Pennsylvania Topographic and Geological Survey, p. 64.

Folk, R., 1973, Evidence for peritidal deposition of Devonian Coballos Novaculite, Marathon Basin, Texas: American Association of Petroleum Geologists Bulletin, v. 57, p. 702-725.

Francheteau, J., and LePichon, X., 1972, Marginal fracture zones as structural framework of continental margins in South Atlantic Ocean: American Association of Petroleum Geologists Bulletin, v. 56, p. 991-1007.

Friedman, G., 1969, Recognizing tidal environments in carbonate rocks with particular reference to those of the Lower Paleozoics in the northern Appalachiens: Abstracts with Programs, pt. 1, Northeastern Section, p. 20-21.

Friedman, G., Amiel, A., Braun, M., and Miller, D., 1973, Generation of carbonate particles and laminites in algal mats - example from sea-marginal hypersaline pool, Gulf of Aqaba, Red Sea: American Association of Petroleum Geologists Bulletin, v. 57, p. 541-557.

Frost, J., 1974, Subtidal algal stromatolites from the Florida backreef environment Journal of Sedimentary Petrology, v. 44, p. 532-537.

Garber, R., Levy, Y., and Friedman, G., 1987, The sedimentology of the Dead Sea: Carbonates and Evaporites, v. 2, p. 43-57.

Garrett, P., 1970, Phanerozoic stromatolites: non-competitive ecological restriction by grazing and burrowing animals: Science, v. 169, p. 171-173.

Gebelein, C., 1969, Distribution, morphology, and accretion rate of Recent subtidal algal stromatolites, Bermuda: Journal of Sedimentary Petrology, v. 39, p. 49-69.

Gebelein, C., and Hoffman, P., 1973, Algal origin of dolomite laminations in stromatolitic limestone: Journal of Sedimentary Petrology, v. 43, p. 603-613.

Geister, J., 1980, Calm water reefs and rough water reefs of the Caribbean Pleistocene: Acta Paleontologica Polonica, v. 25, p. 541-556.

Ginsburg, R., 1975, Tidal deposits: a casebook of Recent examples and fossil counterparts: New York, Springer-Verlag.

Ginsburg, R., and Schroeder, J., 1973, Growth and submarine fossilization of algal cup reefs, Bermuda: Sedimentology, v. 20, p. 575-614.

Goldring, R., 1965, Sediments into Rock: New Scientist, v. 26, p. 863-865.

Gower, C., 1985, Correlations between the Grenville province and Sveconorwegian orogenic belt; Implications for Proterozoic evolution of the southern margins of the Canadian and Baltic shields, *in* Tovi, A. C., and Touret, J. L. R., eds., The deep Proterozoic crust in the Nrth Atlantic provinces Dordrecht, D. Reidel Publishing Company, p. 247-257.

Graus, R., and Macintyre, I., 1989, The zonation patterns of Caribbean coral reefs as controlled by wave and light energy input, bathymetric setting and reef morphology: computer simulation experiments: Coral Reefs, v. 8, p. 9-18.

Gray, C., 1959, Nappe structures in Pennsylvania: Geological Society of America Bulletin, v. 70, p. 1611.

Grotzinger, J., 1986, Cyclicity and paleoenvironmental dynamics, Rocknest platform, northwest Canada: Geological Society of America Bulletin, v. 97, p. 1208-1231.

-, 1989, Facies and evolution of Precambrian carbonate depositional systems: emergence of the modern platform architype, *in* Crevello, P., Wilson, J., Sarg, J., and Read, J., eds., Controls on carbonate platform development, Society of Economic Paleontologists and Mineralogists, p. 79-106.

Hague, J., Baum, J., Hermann, L., and Pickering, J., 1956, Geology and structure of the Franklin-Sterling area, New Jersey: Geological Society of America Bulletin, v. 67, no. 4, p. 435-474.

Halley, R., 1969, Paleo-environmental interpretations of the Upper Cambrian cryptalgal limestones of New York State [M.S. thesis]: Brown University, 93 p.

Hardie, L., 1977, Sedimentation on the modern carbonate tidal flats of northwest Andros Island, Bahamas: John Hopkins University, p. 202 pages.

Hardie, L., Dunn, P., and Goldhammer, R., 1991, Field and modelling studies of Cambrian carbonate cycles, Virginia Appalachians-Discussion: Journal of Sedimentary Petrology, v. 61, p. 636-646.

Hardie, L., and Shinn, E., 1986, Carbonate depositional environments: modern and ancient. Part 3: Tidal Flats: Colorado School of Mines, Quaterly, v. 81, p. 74 pages.

Harris, P., 1983, Carbonate buildups: a core workshop, Society of Economic Paleontologists and Mineralogists, p. 593 pages.

Hatcher, R., 1989, Appalachians introduction, *in* Hatcher, R., Thomas, W., and Viele, G., eds., The Appalachian-Ouachita orogen in the United States: The Geology of North America, Geological Society of America, p. 1-6.

Heckel, P., 1972, Recognition of ancient shallow marine environments, *in* Rigby, J., and Hamblin, W., eds., Recognition of Ancient Sedimentary Environments, Society of Economic Paleontologists and Mineralogists, p. 226-286.

-, 1974, Carbonate buildups in the geologic record: a review, *in* Laporte, L., ed., Reefs in time and space, Society of Economic Paleontologists and Mineralogists, p. 90-155.

Herman, G., and Monteverde, D., 1989, Tectonic framework of Paleozoic rocks of northwestern New Jersey; Bedrock structure and balanced cross sections of the Valley and Ridge Province and southwest Highlands area, *in* Grossman, I. G., ed., Paleozoic Geology of the Kittatinny Valley and Southwest Highlands Area, New Jersey: Field Guide and Proceedings, Geological Association of New Jersey, 6th Annual Meeting, p. 1-5.

Herman, G., Monteverde, D., Schlische, R., and Pitcher, D., 1997, Foreland crustal structure of the New York recess, northeastern United States: GSA Bulletin, v. 109, p. 955-977.

Hobson, J., 1963, Stratigraphy of the Beekmantown Group in southeastern Pennsylvania, General Geological Report 37, Pennsylvania Geological Survey, 331 p.

Hobson, J., Jr., 1957, Lower Ordovician (Beekmantown) succession in Berks County, Pennsylvania: American Association Petroleum Geologists Bulletin, v. 41, p. 2710-2722.

-, 1958a, Stratigraphy and petrology of Lower Ordovician dolomites, southeastern Pennsylvania: Geological Society America Bulletin, v. 69, p. 1583-1584.

-, 1958b, Stratigraphy of the northern belt of the Beekmantown Group in southeastern Pennsylvania [Ph.D. thesis]: The Pennsylvania State University.

Hoffman, P., 1973a, Evolution of an early Proterozic continental margin: the Coronation Geosyncline and associated aulacogens of the NW Canadian Shield Roy Soc. London Phil. Trans, v. A273, p. 547-581.

-, 1973b, Recent and ancient algal stromatolites: Seventy years of pedagogic cross-pollination, *in* Ginsburg, R., ed., Evolving Concepts in Sedimentology: Baltimore, John Hopkins University Press.

Hoffman, P., Dewey, J., and Burke, K., 1974, Aulacogens and their genetic relations to geosynclines, with a Proterozoic example from Great Slave Lake, Canada, Society of Economic Paleontologists and Mineralogists Special Publication 19, 38-55 p.

Holmes, A., 1965, Principles of Physical Geology: London, Thomas Nelson, 1288 p.

Howe, W., 1966, Digitate algal stromatolite structures from the Cambrian and Ordovician of Missouri: Journal of Paleontology, v. 40, p. 64-77.

Howell, B., 1945, Revision of the Upper Cambrian faunas of New Jersey: Geologic Society of America Memoir, v. 12, p. 46 pages.

Hutton, D., 1989, Strike-slip terranes and a model for the evolution of the British and Irish Caledonides: Geological Magazine, v. 124, p. 405-425.

Isaacs, C., 1980, Diagenesis in the Monterey Formation Examined Laterally along the Coast Near Santa Barbara, California [Doctoral thesis]: Stanford University, 329 p.

James, N., and Ginsburg, R., 1979, The seaward margin of Belize barrier and atoll reefs, International Assocation of Sedimentologists, p. 191 pages.

James, N., and Gravestock, D., 1990, Lower Cambrian shelf and shelf margin buildups, Flinders Ranges, South Australia: Sedimentology, v. 37, p. 455-480.

Johnson, M., and Willard, B., 1957, Delaware Valley Paleozoics [N.J.-Pa.] Geological Society of America, Annual Meeting Guidebook for Field Trips, Field Trip No. 2, Geological Society of America, 125-131 p.

Kendall, C., and Schlager, W., 1981, Carbonates and relative changes in sea-level: Marine Geology, v. 44, p. 181-212.

Kennard, J., and James, N., 1986, Thrombolites and stromatolites: two distinct types of microbial structures: Palaios, v. 1, p. 492-503.

Kinsman, D., and Park, R., 1976, Algal belt and coastal sabkha evolution, Trucial Coast, Persian Gulf, *in* Walter, M., ed., Stromatolites: Amsterdam, Elsevier, p. 421-433.

Klein, G., 1967, Comparison of Recent and ancient tidal flat and estuarine sediments, *in* Laruff, G., ed., Estuaries, American Association of Advanced Science, p. 207-218.

-, 1970a, Depositional and dispersal dynamics of inter-tidal sand bars: Journal of Sedimentary Petrology, v. 40, p. 1095-1127.

-, 1971, A sedimentary model for determining paleo-tidal range: Geological Society of America Bulletin, v. 82, p. 2585-2592.

Knoll, H., and Swett, K., 1990, Carbonate deposition during the Late Proterozoic era: an ecample from Spitzbergen: American Journal of Science, v. 290A, p. 104-132.

Knopf, E., 1946, Stratigraphy of the Lower Paleozoic rocks surrounding Stissing Mountain, Dutchess County, New York: Geologic Society of America Bulletin, v. 57, p. 1211.

-, 1956, Stratigraphy and structure of the Stissing area, Dutchess County, New York: Geologic Society of America Bulletin, v. 67, no. 1817.

-, 1962, Stratigraphy and structure of the Stissing Mountain area, Dutchess County, New York [Masters thesis], 55 p.

Kobluk, D., and Crawford, D., 1990, A modern hypersaline organic mud and gypsum-dominated basin and associated microbialites: Palaios, v. 5, p. 134-149.

Kumar, N., 1973, Modern and ancient barrier sediments: New interpretation based on stratal sequence in inlet-filling sands and on recognition of nearshore storm deposits: New York Academy of Science Annals, v. 220, p. 245-340.

Kummel, H., and Weller, S., 1901, Paleozic limestones of Kittatinny Valley, New Jersey: Geologic Society of America Bulletin, v. 12, p. 147-164.

Laird, J., 1988, Arenig to Wenlock age metamorphism in the Appalachians, *in* Harris, A. L., and Fettes, J. J., eds., The Caledonian-Appalachian Orogen: Oxford,U.K., Blackwell Scientific Press, p. 581-615.

LaPorta, P., 1986, The archaeological potential of the Leithsville Formation: A Lower Cambrian chert-bearing carbonate in New Jersey: Geological Society of America, Abstracts with Programs, v. 18, p. 28-29.

-, 1987, Prehistoric resource analysis: Field observations and petrographic characteristics of Cambrian-Ordovician chert: Geological Society of America, Abstracts with Programs, v. 19, p. 24-25.

-, 1989, The stratigraphic relevance and archaeological potential of the chert-bearing carbonates within the Kittatinny Supergroup: New York State Geological Association Field Trip Guidebook, 61st Annual Meeting

-, 1990, The Stratigraphic Relevance and Archaeological Potential of the Cambro-Ordovician Kittatinny Supergroup of the Wallkill River Valley of Northern New Jersey [Masters thesis]: Queens College of the City University of New York, 50 p.

-, 1991, A chert stratigraphy for the Cambro-Ordovician carbonates of the Kittatinny Supergroup: Their geological and human geographic potential: Association of American Geographers, Middle States Division, Annual Meeting Abstracts.
.

-, 1992, Nodular cherts of the Cambro-Ordovician Kittatinny Supergroup: Their diagenesis, stratigraphic relevance and archaeological potential: Materials Research Society, Annual Meeting Abstracts

-, 1993a, The application of cognitive models for lithic resource exploitation: Folk geology within the Wallkill River Valley: New York State Archaeological Association, Annual Meeting Program and Abstracts, p. 11.

-, 1993b, Prehistoric chert exploitation in the Cambro-Ordovician lithologies of the Wallkill River Valley: Society of American Archaeology, Annual Meeting Abstracts, p. 81.

-, 1994, Lithostratigraphic models and the geographic distribution of prehistoric chert quarries within the Cambro-Ordovician lithologies of the Great Valley Sequence, Sussex County, New Jersey: Recent Research into the Prehistory of the Delaware Valley, v. 10, p. 47-66.

-, 1995a, Chert resource exploitation in the New York Metropolitan Area: The idea of a shared mining technology: Professional Archaeologists of New York City, Annual Meeting Abstracts

-, 1995b, Petrographic identification of lithic sources: Geological Society of America, Abstracts with Programs, v. 27, p. 62.

-, 1996a, A geological approach to lithic provenance studies: Society for American Anthropology Annual Meeting Abstracts, v. 61, p. 161.

-, 1996b, Lithostratigraphic models and the geographic distribution of prehistoric chert quarries within the Cambro-Ordovician lithologies of the Great Valley Sequence, Sussex County, New Jersey and Orange County, New York: Annual Field Conference - Geological Association of New Jersey, v. 13, p. 47-70.

-, 1996c, Lithostratigraphy as a predictive tool for prehistoric quarry investigations: Examples from the Dutchess Quarry Site, Orange County, New York, *in* Lindner, C., ed., p. 73-84.

-, 1997a, Geologic controls on lithic resource distribution and the development of prehistoric quarries.

-, 1997b, The prehistoric mining technology of the Cambro-Ordovician carbonates of the Wallkill River Valley of northwestern New Jersey: Geological Society of America, Abstracts with Programs, v. 29, p. A-146.

-, 1998a, Chertification processes and silica sources: Examples from the Central Appalachians: Geological Society of America, Abstracts with Programs, v. 30, p. A-333.

-, 1998b, Diagenesis of Cambro-Ordovician cherts: Geological Society of America, Abstracts with Programs, v. 30, p. 31.

-, 1998c, The prehistoric mining landscape and evolution of ore exploitation: Eastern States Archaeological Federation, Annual Meeting Abstracts

-, 1999a, Chert formation mechanisms and lithic raw material selection.

-, 1999b, Criteria for prehistoric quarry development in the eastern Appalachians: New York State Archaeological Association Annual Meeting

-, 1999c, Diagenesis, stratigraphic, and structural relationships and their role in quarry location and raw material selection through time: Middle Atlantic Archaeological Conference, Annual Meeting Abstracts, p. 28.

-, 1999d, The organization of prehistoric mining technology in the Wallkill River Valley of northwestern New Jersey: Geological Society of America, Abstracts with Programs, v. 31, p. A-29.

-, 1999e, Prehistoric mining technology in the Central Appalachians: Geological Society of America, Abstracts with Programs, v. 31, p. A-343.

-, 1999f, Recent approaches to provenance studies and raw material analysis, from classical methods to modern technology.

-, 2000a, The employment of geological techniques for archaeological provenance studies: Geological Society of America, Abstracts with Programs.

-, 2000b, Geologic constraints on prehistoric quarry development, *in* Rammlmair, D., Mederer, T., Oberthur, T., and Himann, R., eds.: Rotterdam, A.A. Balkema, p. 1013-1015.

-, 2000c, The organization of prehistoric mining technology in the Wallkill River Valley of northwestern New Jersey: Field and petrographic evidence: Geological Society of America, Abstracts with Programs, v. 32, p. A-275.

-, 2001, The stratigraphic and structural relations of prehistoric chert quarries in the Wallkill River Valley, New York and New Jersey: Society for American Archaeology, Annual Meting Abstracts, v. 66, p. 54.

-, 2002, Inorganic silica sources contributing to the formation of nodular cherts within the Kittatinny Supergroup carbonates, northwestern New Jersey: Geological Society of America Abstracts with Programs, v. 34, no. 6, p. 17.

-, 2004, A geological model for the development of bedrock quarries, with an ethnoarchaeological application, *in* Topping, P., and Lynott, M., eds.: U.K., Oxbow Books.

Lister, G., Etheridge, M., and Symonds, P., 1986, Detachment faulting and the evolution of passive continental margins, Geology, p. 246-250.

-, 1991, Detachment models for the formation of passive continental margins, Tectonics, p. 1038-1064.

Logan, B., 1961, Cryptozoon and associated stromatolites from the Recent, Shark Bay, Western Australia: Journal of Geology, v. 69, p. 517-534.

Logan, B., Harding, J., Ahr, W., Williams, J., and Snead, R., 1969, Carbonate sediments and reefs, Yucatan shelf, Mexico, Pt. 1, American Association of Petroleum Geologists Bulletin, Memoir 11, 5-128 p.

Logan, B., Rezak, R., and Ginsburg, R., 1964, Classification and environmental significance of algal stromatolites: Journal of Geology, v. 72, p. 68-83.

Lohmann, K., 1976, Lower Dresbachian (upper Cambrian) platform to deep-shelf transition in eastern Nevada and western Utah: an evalution through lithologic cycle orrelation, Geological Studies, Brigham Young University, p. 860-878.

Longman, M., 1981, A process approach to recognizing facies of reef complexes, *in* Toomey, D., ed., European fossil reef models, Society of Economic Paleontologists and Mineralogists, p. 9-40.

Lucia, F., 1972, Recognition of evaporite-carbonate shoreline sedimentation, *in* Rigby, J., and Hamblin, W., eds., Recognition of Ancient Sedimentary Environments, Society of Economic Paleontologists and Mineralogists, p. 160-191.

MacLachlan, D., 1967, Structure and stratigraphy of the limestones and dolomites od Daupin County, Pennsylvania: Pennsylvania Geological Survey, v. 4th series, Bulletin G44, p. 168 pages.

-, 1979, Geology and mineral resources of the Temple and Fleetwood quadrangles, Berks county, Pennsylvania, Pennsylvania Geological Survey, 4th. Ser. Atlas 187ab, p. 71.

Markello, J., and Read, J., 1981, Carbonate ramp to deeper shale shelf transitions of an upper ambrian intrashelf basin, Nolichucky Formation, southwest Virginia Appalachians: Sedimentology, v. 28, p. 573-597.

-, 1982, Upper Cambrian intrashelf basin, Nolichuckt Formation, southwestern Virginia Appalachians: American Association of Petroleum Geologists Bulletin, v. 66, p. 860-878.

Markewicz, F., 1976, Lower Ordovician Ontelaunee Formation in New Jersey: Arlington, Va., Geological Society of America.

Markewicz, F., and Dalton, R., 1973, Stratigraphy and structure of the Branchville, Franklin, Hamburg, Newton East, Newton West, Pine Island, Stanhope, Tranquility, Unionville, and Wawayanda quadrangles, Geologic Overlay Sheet 22, N.J. Dept. of Enivomental Protection.

-, 1977, Stratigraphcy and applied geology of the lower Paleozoic carbonates in northwestern New Jersey, *in* Markewicz, F., Dalton, R., Spink, W., Metsger, R., and Lucey, C., eds., Stratigraphy and Applied Goelogy of the Lower Paleozoic Carbonates in Northwestern New Jersey: Guidebook for the 42nd Annual Field Conference of Pennsylvania Geologists, p. 1-47.

Martinsson, A., 1974, The Cambrian of Norden, Cambrian of the British Isles, Norden and Spitsbergen, Wiley Interscience, 185-283 p.

Maxey, L., 1976, Petrology and geochemistry of the Beemerville carbonatite-alkalic rock complex, New Jersey, Geological Society of America Bulletin, p. 1551-1559.

McCubben, D., 1982, Barrier-island and strand-plain facies, *in* Scholle, P., and Spearing, D., eds., Sandstone depositional environments, American Association of Petroleum Geologists Memoir 31, p. 247-279.

McNeill, D., 1988, Initiation and development of tidal-inlet reef mounds, South Florida, Proceedings of the Sixth International Coral Reef Symposium: Australia, p. 513-518.

Mesolella, K., Sealy, H., and Matthews, R., 1970, Facies geometries within Pleistocene reefs of Barbados, West Indies: American Association of Petroleum Geologists Bulletin, v. 54, p. 1899-1917.

Middleton, G., 1961, Evaporite solution breccias from the Mississippian of soutwest Montana: Journal of Sedimentary Petrology, v. 31, p. 189-195.

Miller, B., and others, 1939, Northampton County, Pennsylvania: Pennsylvania Geological Survey, County Report 48, no. 4, p. 496 pages.

Mitchum, R., Vail, P., and Thompson, S., 1977, Seismic stratigraphy and global changes of sea level, part two: the depositional sequence of a basic unit for stratigraphic analysis: Association Petrol. Geol. Mem., v. 26, p. 53-62.

Monty, C., 1967, Distribution and structure of Recent stromatolitic algal mats, East Andros Island, Bahamas: Annual Society of Geologists de Belgique, v. T. 90, no. Bulletin 3, p. 55-99.

Moore, R., Lalicker, C., and Fischer, A., 1952, Invertebrate Fossils: New York, McGraw-Hill Book Company, Inc., 766 p.

Mose, D., and Nagel, M., 1982, Chronology of metamorphism in western Connecticut: Rb-Sr ages, *in* Joesten, R., and Quarrier, S. S., eds., Guidebook for field trips in Connecticut and south-central Massachusetts, p. 247-262.

Mossop, G., 1979, The evaporites of the Ordovician Baumann Fiord Formation, Ellesmere Island, Arctic Canada: Geological Survey of Canada Bulletin, v. 298, p. 52 pages.

Muller, P., and Chapin, D., 1984, Tectonic evolution of the Baltimore Gneiss anticlines Maryland, *in* Bartholomew, M. J., ed., The Grenville event in the Appalachians and related topics, p. 127-148.

Natter, A., 1967, Tidal flat deposits in the Ordovician of western Maryland: Journal of Sedimentary Petrology, v. 37, p. 601-609.

Nemic, W., and Steel, R., 1988, Fan Deltas: Sedimentology and Tectonic Settings: Glasgow and London, Blackie, 444 p.

Neumann, A., and Land, L., 1975, Lime mud deposition and calareous algae in the Bight of Abaco, Bahamas: a budget: Journal of Sedimentary Petrology, v. 45, p. 763-786.

Neumann, A., and Macintyre, I., 1985, Reef response to sea level rise: keep-up, catch-up or give-up, Proceedings of the Fifth International Coral Reef Congress: Tahiti, p. 105-110.

Osberg, P., James, F., Robinson, P., Hon, R., and Butler, J., 1989, The Acadian orogen, *in* R.D. Hatcher, W. A. T., and Viele, G. W., eds., The Appalachian-Ouachita Orogen in the United States in the United States $I Geological Society of America, p. 179-232.

Osleger, D., 1991, Subtidal carbonate cycles: implications for allocyclic versus autocyclic controls: Geology, v. 19, p. 917-920.

Otvos, E., 1966, Sedimentary structures and depositional environments, Potsdam Formation, Upper Cambrian: American Association of Petroleum Geologists Bulletin, v. 50, p. 159-165.

Owen, R., 1973, Red Sea algal sediments and the Hoyt Limestone of New York: a comparison of Recent and Cambrian algal deposition [M.S. thesis]: Rensselaer Polytechnic Institute, 121 p.

Palmer, A., 1971, The Cambrian of the Appalachian and eastern New England region, eastern United States, *in* Holland, C., ed., Cambrian of the New World, Wiley Interscience, p. 169-211.

Palmer, A., and Rozanov, A., 1976, Archeocyatha from New Jersey: Evidence for an intra-Cambrian in the north-central Appalachian: Geology, v. 4, p. 773-774.

Pratt, B., 1982a, Stromatolite decline-a reconsideration: Geology, v. 10, p. 812-815.

-, 1982b, Stromatolitic framework for carbonate mudmounds: Journal of Sedimentary Petrology, v. 52, p. 1203-1227.

Pratt, B., and James, N., 1982, Cryptalgal-metazoan bioherms of Early Ordovician age in the St. George Group, western Newfoundland: Sedimentology, v. 29, p. 543-569.

-, 1985, The St. George Group (Lower Ordovician) of western Newfoundland: tidal flat island model for carbonate sedimentation in shallow epeiric seas: Sedimentology, v. 33, p. 313-343.

Pratt, B., James, N., and Cowan, C., 1992, Peritidal Carbonates, *in* Walker, R., and James, N., eds., Facies Models: Response to Sea Level Change, Geological Association of Canada, p. 303-322.

Purdy, E., 1963a, Recent calcium carbonate facies of the Bahama Banks, Pt. 1: Journal of Geology, v. 71, p. 334-355.

-, 1963b, Recent calcium carbonate facies of the Bahama Banks, Pt. 2: Journal of Geology, v. 71, p. 472-497.

-, 1974, Karst-determined facies in British Honduras: Holocene carbonate sedimentation model: American Association of Petroleum Geologists Bulletin, v. 58, p. 825-855.

Rankin, D., 1972, Late Precambrian rifting in the Appalachians: Evidence from the Crossnore plutonic-volcanic group of the Blue Ridge anticlinorium, American Geophysical Union Transactions, p. 525.

-, 1975, The continental margin of eastern North America in the southern Appalachians: The opening and closing of the Proto-Atlantic Ocean, American Journal of Science, p. 298-336.

-, 1976, Journal of Geophysical Research, v. 81, p. 5605-5619.

Rankin, D., and others, 1989, Proterozoic rocks east and southeast of the Grenville front, *in* Reed, J. C., and others, eds., Precambrian: Conterminous U.S.: The Geology of North America, Geological Society of America.

Rast, N., and Kohles, K., 1986, The origin of the Ocoee Supergroup, American Journal of Science, p. 593-616.

Rast, N., and Skehan, J., 1993, Mid-Paleozoic orogenesis in the North Atlantic, *in* D.C. Roy, D. C., and Skehan, J. W., eds., The Acadian orogeny: Recent studies in New England, maritime Canada, and the autochthonous foreland, p. 1-26.

Ratcliffe, N., Armstrong, R., Mose, D., Seneschal, R., and Baiamonte, M., 1982, Emplacement history and tectonic significance of the Cortlandt complex, related plutons, an dike swarms in the Taconide zone of southeastern New York based on K-Ar and Rb-Sr investigations, American Journal of Science, p. 358-390.

Reading, H., 1986, Sedimentary Environments and Facies, Blackwell Scientific, p. 615.

Rees, M., Pratt, B., and Rowell, A., 1989, Early Cambrian reefs, reef complexes, and associated lithofacies of the Shakleton Limestone, Transantarctic Mountains: Sedimentology, v. 36, p. 341-361.

Renne, P., and others, 1989, 40Ar/39Ar and U-Pb evidence for Late Proterozoic (Grenville age) continental crust in north-central Cuba and regional tectonic implications, Precambrian Research.

Rhoads, D., 1967, Biogenic reworking of intertidal and subtidal sediments in Barnstable Harbor and Buzzards Bay, Massachusetts: Journal of Geology, v. 75, p. 461-476.

Rich, J., 1934, Mechanics of low-angle overthrust faulting as illustrated by Cumberland thrust block, Virginia, Kentucky and Tennessee, American Association of Petroleum Geologists Bulletin, p. 1584-1596.

Riding, R., Martin, J., and Braga, J., 1991, Coral-stromatolite reef framework, Upper Miocene, Almeria, Spain: Sedimentology, v. 38, p. 799-819.

Rogers, H., 1836, Report on the geological survey of the State of New Jersey, N. J. Geol. Survey, p. 157 pages.

-, 1840, Description of the geology of the State of New Jersey, being a final report, New Jersey Geological Survey, 301 p.

Rooney, W., and Perkins, R., 1972, Distribution and geologic significance of microboring organisms within sediments of the Arlington Reef Complex, Australia: Geological Society of America Bulletin, v. 83, p. 1139-1150.

Rowland, S., and Gangloff, R., 1988, Structure and paleoecology of Lower Cambrian reefs Palaios, v. 3, p. 111-135.

Ruiz, J., Patchett, P., and Ortega-Gutierrez, F., 1988, Proterozoic and Phanerozoic basement terranes of Mexico from Nd isotopic studies, Geological Society of America Bulletin, p. 274-281.

Sandberg, P. A., and Hudson, J. D., 1983, Aragonite relic preservation in Jurassic calcite-replaced bivalves: Sedimentology, v. 30, p. 879-892.

Sando, W., 1957, Beekmantown Group (lower Ordovician) of Maryland: Geological Society America Memoir, v. 68, p. 161.

Sarg, J., 1988, Carbonate sequence stratigraphy, *in* Wilgus, C., ed., Sea-level changes: an integrated approach, Society of Economic Paleontologists and Mineralogists, p. 155-182.

Saunders, J., 1983, Reinterpretation of the subsurface structure of the Middletown gas well 1 (Crom-Wells, Inc. 1 Fee) in light of concept of large-scale bedding thrusts, Northeastern Geology, p. 172-182.

Schlager, W., 1981, The paradox of drowned reefs and carbonate platforms: Geologic Society of America Bulletin, v. 92, p. 197-211.

-, 1989, Drowning unconformities on carbonate platforms, *in* Wilgus, C., ed., Sea level changes- an integrated approach, Society of Economic Paleontologists and mineralogists p. 15-25.

-, 1990, Depositional bias and environmental change-important factors in sequence stratigraphy: Sedimentary Geology, v. 69, p. 109-130.

Schwab, F., 1971, Harpers Formation, central Virginia: A sedimentary model, Journal of Sedimentary Petrology, p. 139-149.

Scrutton, R., 1982a, Crustal structure and development of sheared passive continental margins, American Geophysical Union Geodynamics Series, p. 133-140.

-, 1982b, Passive continental margins: A review of observations and mechanism, American Geophysical Union Geodaynamics Series, p. 5-11.

Sellwood, B., 1986, Shallow-marine carbonate environments, *in* Reading, H., ed., Sedimentary environments and facies: Oxford, Blackwell Scientific Publications.

Shearman, D., and Fuller, J., 1969, Anhydrite diagenesis, calcitization, and organic laminites, Winnipegosis Formation, Middle Devonian, Saskatchewan: Bulletin of Canadian Petroleum Geology, v. 17, p. 469-525.

Shearman, D. J., 1978, Evaporites of coastal sabkhas, *in* Dean, W. E., and Schreiber, B. C., eds., Marine Evaporites, Society of Economic Paleontologists and Mineralogists, p. 6-42.

Sheehan, P., 1985, Reefs are not so different-They follow the evolutionary pattern of level bottom communities: Geology, v. 13, p. 46-49.

Shinn, E., 1968, Practical significance of birdseye structures in carbonate rocks: Journal of Sedimentary Petrology, v. 38, p. 612-616.

-, 1983, Tidal flats, *in* Scholle, P., Bebout, D., and Moore, C., eds., Carbonate depositional environments, American Association of Petroleum Geologists, p. 171-210.

Simpson, E., and Eriksson, K., 1989, Sedimentology of the Unicoi Formation in southern and central Virginia: Evidence for late Proterozoic to early Cambrian rift-to-passive margin transition, Geological Society of America Bulletin, p. 42-54.

-, 1990, Early Cambrian progradational and transgressive sedimentation patterns in Virginia: An example of the early history of a passive margin, Journal of Sedimentary Petrology, p. 84-100.

Simpson, E., and Sundburg, F., 1987, Early Cambrian age for synrift deposits of the Chilhowee Group of southwestern Virginia, Geology, p. 123-126.

Skelly, R., 1987, Sedimentology of a fluvial-to-marine transition: The Chilhowee Group (lower Cambrian), southeast Tennessee, 211 p.

Skelly, R., Driese, S., and Cudzil, M., 1987, Facies variability within a fluvial-to-marine transition; examples from the Lower Cambrian Chilhowee Group, East Tennessee, Society of Economic Paleontologists and Mineralogists Abstracts, p. 78.

Sohl, L., LaPorta, P., and Brewer, M., 2001, Prehistoric quarry landscapes and cultural resource management, p. 58.

Soper, N., and Hutton, D., 1984, Late Caledonian sinistral displacement in Britain: Implications for a three-plate collision model, Tectonics, p. 161-170.

Southworth, S., Aleinikoff, J., Bailey, C., Rankin, D., and Tollo, R., 2007, Neoproterozoic to Cambrian rift architecture of eastern Laurentia: A prolonged record of extension before and after development of the Iapetus Ocean: Geological Society of America Abstracts with Programs, v. 39, no. 6, p. 614.

Spencer, A., Kummel, H., Wolff, J., Salisbury, R., and Palache, C., 1908, Franklin Furnace, N.J.: U.S. Geological Survey Geol. Atlas, v. Folio 161.

Stearn, C., 1982, The shapes of Paleozoic and modern reef-builders: a critical review: Paleobiology, v. 8, p. 228-241.

Stose, G., 1908, The Cambro-Ordovician limestones of the Appalachian Valley in southern Pennsylvania: Journal of Geology, v. 16, p. 698-714.

Strasser, A., 1988, Shallowing-upward sequences in Purbeckian peritidal carbonates (lowermost Cretaceous, Swill and French Jura Mountains): Sedimentology, v. 35, p. 369-383.

Talent, J., 1988, Organic reef-building episodes of eztnction and symbiosis?: Senckenbergiana lethaea, v. 69, p. 315-368.

Tedesco, L., and Wanless, H., 1989, Role of burrow excavation and infilling in creating the preserved depositional favric of Pennsylvanian phylloid mounds of foutheastern Kansas, *in* Watney, W., French, J., and Franseen, E., eds., Guidebook for sequence stratigraphic interpretations and modelling cyclothms, Kansas Geological Society p. 179-191.

Thomas, W., 1976, Evolution of the Ouachita-Appalachian margin, Journal of Geology, p. 323-342.

-, 1977, Evolution of Appalachian-Ouachita salients from reentrants and promontories in the continental margin, American Journal of Science, p. 1233-1278.

-, 1983a, Basement-cover relations in the Appalachian fold and thrust belt, Geological Journal, p. 267-276.

-, 1983b, Continental margins, orogenic belts and intracratonic structures, Geology, p. 270-272.

-, 1990, Controls on locations of transverse zones in thrust belts: Eclogae Geologicae Helvetiae, v. 3, p. 727-744.

-, 1991, The Appalachian-Ouachita rifted margin of southeastern North America, Geological Society of America Bulletin, p. 415-431.

-, 1993, Low-angle detachment geometry of the late Precambrian-Cambrian Appalachian-Ouachita rifted margin of southeastern North America, Geology, p. 921-924.

Toomey, D., and Nitecki, M., 1979, Organic buildups in the Lower Ordovician (Canadian) of Texas and Oklahoma: Fieldiana, New Series, v. 2, p. 181 pages.

Tucker, M., and Wright, V., 1990, Carbonate sedimentology: Oxford, Blackwell Scienific Publications, p. 482 pages.

Tudhope, A., 1989, Shallowing-upwatds sedimentation in a coral reef lagoon, Great Barrier Reef of Australia: Journal of Sedimentary Petrology, v. 59, p. 1036-1051.

Twenhofel, W., and others, 1954, Correlation of the Ordovician formations of North America: Geological Society of America Bulletin, v. 65, p. 247-298.

Ulrich, E., 1911, Revision of the Paleozoic systems, parts 1-3: Geologic Society of America Bulletin, v. 22, no. part 3.

Vail, P., and Mitchum, R., 1977, Seismic stratigraphy and global changes of sea level, Part I, *in* Payton, C., ed., Seismic Stratigraphy-Applications to Hydrocarbon Exploration: AAPG Memoir, American Association of Petroleum Geologists, p. 51-52.

Vail, P., Mitchum, R., and Thompson, S., 1977a, Seismic stratgraphy and global changes of sea level, part three: relative changes of sea level from coastal onlap: American Association of Petrol. Geol. Mem. 26, p. 83-98.

Vail, P., Todd, R., and Sangree, J., 1977b, Seismic stratigraphy and global changes of sea level, part five: chronostratigraphic significance of seismic reflections: American Association of Petroleum Geology Memoir 26.

Valentin, E., Zadnick, and Carozzi, A., 1964, Cyclic Sedimentation in the Upper Cambrian Dolomites of Warren County, New Jersey, USA: Bulletin d'Institut National Genevois, v. 62, p. 3-55.

Walcott, C., 1891, Correlation papers; Cambrian: U.S. Geological Survey Bulletin, v. 81, p. 360.

-, 1898, Fossil Medusae, United States Geological Survey Monograph 30: Washington, D.C., p. 201.

Walker, J., 1988, Tectono-stratigraphic evolution of the North American-Iapetos continental margin, southern Appalachians: Review and Speculation, *in* Driese, S. G., and Walker, D., eds., Depositional history of Paleozoic sequences, southern Appalachians, University of Tennessee, p. 4-29.

-, 1990, The sedimentology and stratigraphy of the Chilhowee Group (uppermost Proterozoic to lower Cambrian) of Eastern Tennessee and Western North Carolina: The evolution of the Laurentian-Iapetos Margin, p. 274.

Walker, J., and Driese, S., 1991, Constraints on the position of the Precambrian-Cambrian Boundary in the southern Appalachians, American Journal of Science, p. 258-283.

Walker, J., Driese, S., and Hatcher, R., 1989, Paleotectonic significance of the quartzite of the Sauratown Mountains window, North Carolina, Geology, p. 913-917.

Walker, J., Skelly, R., Cudzil, M., and Driese, S., 1988, The Chilhowee Group of east Tennessee: Sedimentology of the lower Cambrian fluvial-to-marine transition, *in* Driese, S. G., and Walker, D., eds., Depositional history of Paleozoic sequences, southern Appalachians, University of Tennessee, p. 30-61.

Wanless, H., and Tagett, R., 1989, Origin and dynamic evolution of carbonate mudbanks in Florida Bay Bulletin of Marine Science, v. 44, p. 454-489.

Weller, S., 1900a, Description of Cambrian Trilobites from New Jersey, New Jersey Geological Survey Annual Report for 1899, New Jersey Geological Survey 47-53 p.

-, 1900b, A preliminary report on the Paleozoic formations of the Kittatinny Valley in New Jersey: Annual Report of the State Geologist for 1900, p. 3.

Whisonant, R., 1974, Petrology of the Chilhowee Group (Cambrian and Cambrian (?) in central eastern and southern Tennessee, Journal of Sedimentary Petrology, p. 228-241.

Wilkinson, B., 1982, Cyclic cratonic carbonates and phanerozoic calcite seas: Journal of Geological Education, v. 30, p. 189-203.

Willard, B., 1955, Cambrian contacts in eastern Pennsylvania: Geological Society of America Bulletin, v. 66, p. 819-833.

-, 1958, Lower Ordovician, Lehigh and Delaware valleys: Pennsylvania Academy of Science Proceedings, v. 32, p. 177-183.

Willis, B., 1893, The mechanics of Appalachian structure, Annual Report, U.S. Geological Survey, 211-281 p.

Woodward, H., 1931, Paleozoic cherts of west-central Virginia: Journal of the Geological Society of America, v. 29, p. 277-287.

Woussen, G., Roy, D., Dimroth, E., and Chown, E., 1986, Mid-Proterozoic extensional tectonics in the core zone of the Grenville province, *in* J.M. Moore, A. D., and Baer, A. J., eds., The Grenville province, p. 297-326.

Yochelson, E., and Barnett, S., 1972, The Early Ordovician gastropod Ceratopea and the Plattsburg, New York area: Journal of Paleontology, v. 46, p. 685-687.

Zadnik, V., 1960, Petrography of the Upper Cambrian dolomites of Warren County, New Jersey [Ph.D. thesis]: University of Illinois, 96 p.

Zen, E., 1967, Time and space relationships of the Taconic allocthon and autochthon, Geologic Society of America Special Paper 97, p. 107.

Zenger, D., 1972, Significance of supratidal dolomitization in the geologic record: Geologic Society of America Bulletin, v. 83, p. 1-12.

Zhuravleva, I., 1970, Marine faunas and Lower Cambrian stratigraphy: American Journal of Science, v. 269, p. 417-445.

Volume II

Appendix A: Type Sections for the Kittatinny Supergroup, Hamburg 7.5' Quadrangle, Sussex County, New Jersey

A.1 Hardyston Formation

The Rte. 515 type section in Vernon, New Jersey (location 2a in Figure 3.2; Plate A.1) contains the most representative section of the Hardyston Formation in the dissertation study area. The Hardyston Formation at this location is divided into two beds. Bed 1 is approximately 20 cm of dolomitic sandstone. Bed 2 is approximately 90 cm thick, consists of eight, 10 to 15 cm thick, layers of light gray to light brown, quartz sandstones bearing angular quartz sand grains and re-worked lenses of dark minerals which have been altered to vermiculite. The beds coarsen upward, starting with fine grained siltstone and sandstone and grading up section into coarse grained, quartz sandstone. The quartz sandstone is poorly sorted into parallel layers and there is considerable clay content in the matrix. Skolithos burrows, despite being common at other locations where the Hardyston crops out are not present at this location.

A.2 Leithsville Formation: Califon Member

The Rte. 515 type section in Vernon, New Jersey (location 2a in Figure 3.2; Plate A.2) contains the most representative section of the Califon Member of the Leithsville Formation in the Hamburg quadrangle study area. The member contains six beds at the type section location.

The Califon Member is dark gray, weathers to a medium gray or can be iron stained yellow, and is fine grained (Figure 3.5). Upper and lower bed surfaces are lined with olive to black shales, which are enhanced by stylolites (beds 1 to 6). At other

stratigraphic sections, such as Rte. 23 (Figure 3.2), the lower beds are dolomitic and sulfide rich; however, the section is predominantly shale. Shaly dolomite present in the upper parts of the member is thin and parallel bedded. Mudcracks, dolomite rip-up clasts, and ripple marks are common in bed 6 (Figure 3.6). Vugs containing purple fluorite, orange calcite, and yellow sphalerite are common throughout the member (beds 1 to 6) (Figures 3.7 and 3.8). The fossil *Archaeocyathus* was discovered in this section of the Califon during mapping for this dissertation. John Rodgers of Yale University and Frank Markewicz of the New Jersey Geological Survey also discovered the fossil in the shale beds at the Wildcat Road section (Figure 3.2) during Robert Fink's 1968 NYSGA field trip.

A.3 Leithsville Formation: Hamburg Member

The Rte. 515 type section in Vernon Township (location 2a in Figure 3.2; Plate A.3) contains the most representative section of the Hamburg Member of the Leithsville Formation in the Hamburg quadrangle study area (Figure 3.10). Nine beds of the Hamburg Member are present at the type section (Plate A.3).

Bed 1 of the Hamburg Member include homogenous dark to ash gray, coarse grained dolomite that grades up section into thick beds of quartz sandstone in a matrix of drab, olive-gray, silty dolomite (Plate A.3). The quartz sand grains are sub-angular to sub-rounded and blue gray in color. Bed 1 is pervasively stylolitized. Bed 2 is a drab, olive dolarenite that includes thick, quartz sandstones, capped by black shale. Dark maroon beds are present in bed 3 of the section (Plate A.3). These are burgundy siltstones and fine grained sandstones, alternating with quartz sandstone lenses (Figure 3.10). Massive, light gray, dolarenites (bed 4) intercalate with the underlying sediments.

The upper part of the bed includes distinctive dolarenites, each lined with thick lenses of quartz sandstone. The lower part of bed 5 is an intercalated olive and maroon, phyllitic, coarse grained, quartz sandstone overlain by maroon siltstone (Plate A.3). The upper part of the bed is maroon and drab olive, quartz sandstone and arkose that fines upward to a gradational upper contact. Olive to ash gray dolomite is present in bed 6, but the lower 15 cm contain thinly bedded, maroon siltstones. These horizons are largely dolarenites; however, some upper beds are almost completely free of quartz sand grains. Bed 7 contains maroon sedimentary rocks that gradationally shift to olive and buff colored layers (Plate A.3). The lower 15 cm are bright maroon siltstones, interbedded with thin lenses of coarse grained, quartz sandstone. Finely laminated, dolostones overlie the quartz sandstones. A repetition of this sedimentation pattern is present in bed 8, beginning with burgundy siltstone overlain by finely laminated, evenly bedded, ash-gray, micritic dolomite. Burgundy to maroon siltstones overlies the dolomite in bed 9 (Plate A.3). This upper surface, and all the individual bed surfaces within the maroon series, contain mud cracks, rip-up clasts, and ripple marks.

A.4 Leithsville Formation: Wallkill Member

The Wildcat Road type section in Franklin, New Jersey (location 2d in Figure 3.2; Plate A.4) contains thirty-nine beds in the Wallkill Member of the Leithsville Formation. The member is divided into three general series based on gross lithologic characteristics: beds 1 through 12 are the algal laminated and lower chert rich series; beds 13 to 22 are the massive and structureless dolomite series; and beds 23 to 39 are the algal laminated, intraclastic dolomite series bearing the upper chert horizons of the member.

The base (bed 1) is a thin, strongly fetid, medium-gray dolomite carrying abundant, lustrous black and gray, chert clots and nodules (Plate A.4). The next eleven beds (beds 2 to 12) are 550 cm thick and are light to medium gray, medium to coarse grained, fetid, algal dolomites interbedded with sparse, thin, black shale and shaly dolomite. The shale occurs lining beds or as intrabed laminations. Beds 2 and 3 contain chert nodules and pods. The chert in bed 3 replaces algal structures in pod form (Figure 3.14). Bed 5 contains dark gray chert lenses. Algal stromatolites and rip-up clasts are present in beds 9 and 10. Upright and overturned domal algal stromatolites are replaced by chert in these beds (Figure 3.15). Bed 11 is distinctive black shale which weathers bright yellow and is silicified. This bed contains an unconformity that is lined above and below by silicified algal laminates. Bed 12 is a thick, algal laminated, coarse grained, medium-gray dolomite containing silicified algal laminations.

The overlying succession of beds (13 through 22) are 775 cm thick, medium to dark gray, coarse grained to crystalline, scintillating, sparsely algal laminated dolomites bearing porous, punky, weathered outer surface rinds (Plate A.4). Cherts are sparse in this section of the Wallkill Member and sedimentary structures, other than bedding, are lacking. The upper surface of bed 22 is capped by silicified algal laminates.

The third and final series of beds (23 through 39) comprises approximately 675 cm of thin to thickly bedded, strongly algal laminated, light to dark gray dolomites, with sparse thin bedded shale (Plate A.4). Two distinctive shales (beds 28 and 30) serve as the base and crest of a very thick, algal laminated quartz vug-rich bed (bed 29). Beds 31 through 33 are strongly stylolitized and abundant rip-up clasts occur in beds 31, 35, and 37 to 39 of this interval. Bed 35 contains intraformational conglomerates and the upper

three beds (37 to 39) contain abundant parallel and cross bedded ooids in association with rip-up clasts, marking unconformities. Three distinctive chert sets are present at the crest of the Wallkill Member. The lower chert set contains cauliflower shaped structures that are interpreted as silica replaced evaporites. Stylolite surfaces occur within cherts of this lower set. The intermediate set contains chert as pods and the silica replaces ooids and algal laminations. The upper chert set varies along strike. At the Wildcat Road stratigraphic section the upper Wallkill chert contains ooids. Along strike, however, the ooids grade into parallel and cross bedded, silica replaced, oncoids and pisoids. The upper Wallkill chert can also appear elongate and globular in profile view, with the elongate axis of the chert oriented perpendicular to bedding. This chert occurrence is interpreted as a burrow structure. Additionally, the upper Wallkill Member chert set exhibits pinch-and-swell and enterolithic forms (Figure 3.20). This upper chert horizon at bed 39 caps the Wallkill Member and is shared with the base of the overlying Limeport Formation, Wildcat Road Member. As such, the chert at bed 39 will not be described again in the following paragraphs introducing the Wildcat Road Member.

A.5 Limeport Formation: Wildcat Road Member

Wildcat Road in Franklin, New Jersey (location 2d in Figure 3.2; Plate A.5) contains the most representative section of the Wildcat Road Member of the Limeport Formation in the Franklin 7.5' Quadrangle. The Wildcat Road Member is divided into eighty-seven beds and five series based on lithologic differences. Series 1 (beds 1 to 40) is 26.5 m thick and is an algal laminated, quartz vug, burrow, intraclastic dolomite series. Beds 41 to 49 are a 500 cm thick transitional zone in which dolomite, dolomitic limestone and shale facies in and out of the line of section. Series 3 (beds 50 to 76) is a

42 m thick limestone section bearing algal laminations at the base and crest, with an intermediate position bearing abundant oolites. The fourth series (bed 77) is a 14.5 m thick dolomitic limestone succession containing interbeds of quartz sandstones. The final series of the section (beds 78 to 87) is a 700 cm thick limestone that is pervasively stylolitized, intraclast bearing, algal laminated and contains shale interbeds.

In series 1, beds 1 through 10 (600 cm) are alternating light to dark gray, fine to coarse grained, mildly algal laminated dolomite with the algal laminations concentrated at bedding contacts (Plate A.5). The lower five beds also contain shale partings and couplets along the upper and lower bed contacts. This lower section is overlain by a 300 cm thick, fine grained, very dark gray, strongly algal laminated dolomite (bed 11). Thin to thick bedded, light to dark gray, fetid, algal laminated dolomites comprise beds 12 through 22 (850 cm thick). Quartz vugs pepper bed 12, as well as multiple horizons of burrow structures. The bed is pervasively stylolitized. Beds 13 through 17 are algal laminated with burrow structures present at the top of bed 17. Beds 18 through 22 exhibit no sedimentological features, other than bedding and stylolites at the base of bed 19. Beds 22 to 40 (850cm) are marked by the appearance of six horizons indexed by intraclastic conglomerates/breccias and rip-up clasts. This succession is algal laminated, interbedded with silty shale. Stylolites are present in beds 22, 25, 31 and 32. Algal stromatolites and overturned algal were documented in bed 28. Several distinctive, thick, shale horizons mark the section, especially at beds 27, 32, 38 and 40. This part of the section, in general, contains rubbly bed surfaces and the bottoms of beds bear scour-and-fill structures and flute casts.

Series 2 is 500 cm thick and is transitional in that medium to dark gray, micritic to coarse grained, thin to medium bedded, dolomite, dolomitic limestone, shale and quartz sandstone are intercalated (Plate A.5). Beds 41 to 43 mark the first dolomitic limestones that are intraclastic, contain domal and laminated algal and planar cross beds. Dolomite is present in beds 44 to 49, as are algal laminations, shale interbeds and rip-up clasts. The crest of bed 49 contains quartz sandstone.

Light to dark gray, micritic to coarse grained, thin to thickly bedded, limestones are present in series 3 (beds 50 to 76) (42 m) (Plate A.5). The section is characterized by the presence of algal laminations (beds 50, 56, 61, 66, 72 to 76), graded ooids (beds 50, 53, 58, 60, 66, 69, 71 to 74) and stylolites (beds 53 to 62, 68 to 70, 73 to 76). Quartz sandstone lenses are present in beds 50, 64/64, 67 to 70. Mud cracks associated with overlying and underlying intraclastic limestones are in beds 64 and 65. Large domal algal occur with associated quartz vugs in beds 51, 52. Domal algal minus the quartz-vug association, but associated with sandstone lenses or ooids are present near the upper mid-part of the section in beds 68 and 74. Overturned domal algal occur within the quartz sandstones (bed 64), in close association with mud cracks and in intraclastic horizons (bed 74). Beds 55 and 56 contain evaporite structures. Chert is present in this series as light gray, nodular silica replacing algal in bed 68. A silicified oolite is present in stylolitized bed 74 and is underlain by intraformational conglomerate and overlain by ooids.

Bed 66 in series 3 is a 1200 cm covered interval (Plate A.5). Scattered outcroppings within the covered interval, as well as examination of outcrops above and below the covered section, were used to infer that dark gray, thickly bedded, oolitic

limestone was present in the section. The presence of intraformational conglomerates, rip-up clasts, mud cracks, ooid and pisoid accumulations wrapped in algal, and edgewise conglomerates in the rocks adjacent to the covered interval infers their presence in the covered interval.

The second covered interval of the member is represented as bed 76 of the type stratigraphic section (Plate A.5). The covered interval is 1480 cm thick. The rock, as inferred from immediately adjacent outcrops, is thin to thick, medium to dark gray, algal laminated, dolomitic limestone. The third covered interval is represented as bed 77, which is 1419 cm thick. Adjacent outcrops allow extrapolation of alternating thin and thick, medium-light gray, arenaceous dolomitic limestone as existing in the covered interval. The series is inferred as containing intraformational conglomerates, rip-up clasts, and graded and cross bedded ooids, as observed in adjacent outcrops.

Series 4 is represented by one bed (bed 77), a 14.5 m thick, medium gray and dolomitic limestone containing abundant quartz sandstone horizons (Plate A.5). The base and crest of the series is stylolitized. The upper contact of the series contains rip-up clasts and cross bedded sandstones.

Beds 78 to 87 (series 5) represents the crest of the Wildcat Road Member and are 725 cm thick (Plate A.5). Light to dark gray, micritic to coarse grained, thin to thick bedded limestone caps the member with interbeds of dolomitic limestone (bed 79), dolomite (bed 81) and shale (beds 82, 83 and 87). Three thick horizons of intraclastic limestone are also present, including graded and cross bedded ooids (beds 78, 80, 84 to 86), abundant rip-up clasts, pisoids, and intraformational conglomerates. Bed 79 is burrowed. Evaporite structures occur in bed 86. Associated with the lower shale (beds

82 and 83) is a silicified shale lens. A silicified intraformational conglomerate occurs in bed 85. Shale (bed 87) marks the end of the Wildcat Road Member.

A.6 Limeport Formation: Wheatsworth Mills Member

Wheatsworth Road in Hamburg, New Jersey (location 3a in Figure 3.2; Plate A.6) contains the most representative section of the Wheatsworth Mills Member of the Limeport Formation in the Hamburg 7.5' Quadrangle. The section can be divided into 106 beds and seven general series based on gross lithologic characteristics: beds 1 to 7 are the transitional series; beds 8 to 19 are the intraclastic, domal algal series; beds 20 to 49 are the quartz vug, intraclastic limestone series; beds 50 to 71 is the arenaceous series; beds 72 to 77 are the algal stromatolite series; beds 78 to 88 are the algal laminated, intraclast series; and beds 89 to 106 are the arenaceous and shaly limestone series.

Series 1 is 10.75 m thick. The base of the section (bed 1) is a black to olive shale that weathers bright yellow (Figure 3.5). Overlying the shale are thinly bedded, algal laminated, alternating dolomites and dolomitic limestones bearing rip-up clasts (beds 2 to 7). The first seven beds are arenaceous. Even the shales in this part of the section contain quartz sandstone laminations. This section is also pervasively stylolitized. Bed 7 contains cross bedded quartz sandstone replaced by chert.

Thickly bedded, light to medium gray, algal laminated, oolitic, stylolitized limestone is present in beds 8 to 19 (Plate A.6). Two distinctive domal algal series occur within beds 9 and 19. Bed 19 possesses enormous LLH-type domal algal associated with mud cracks (Figure 3.28). The interstices of the domal algal are filled with micritic limestone. There are four planar cross bedded, quartz sandstones present at the upper and lower contacts of bed 8, and in beds 9 and 16. The quartz sandstones are underlain or

overlain by graded ooids. Thick, intraformational conglomerates occur within beds 12 and 15. Quartz vugs cap limestones in beds 9, 16, 18, and 19. Dessication features and rip-up clasts are present within beds 9, 11, 13, the base of 16, and 19.

Beds 20 through 49 are 18.75 m thick and are made diagnostic by the presence of no less than fourteen intraclastic beds including abundant graded and cross bedded ooids and pisoids (beds 22, 24, 27, 29, 30, 32, 35, 38, 40, 41, 44 to 47) (Plate A.6). A distinctively colored, thick, cross bedded oolite is present in bed 28; however, beds 24, 29, 35, 43/44, 47 and 49 are arenaceous and contain both graded and cross bedded sandstones. The surrounding intraclastic limestones contain abundant quartz vugs (beds 24, 26, 28, 30, 38, 45, and 46). The base of bed 46, near the crest of this series, is a thick intraclastic limestone comprised of intraformational, limestone clasts, conglomerates and thick ooid sequences. The base of this bed contains thick, coarse grained, silicified sandstone. Domal algal occur sparingly (bed 30).

The overlying series (beds 50 to 71) is 950 cm thick and includes thin to thick bedded, intraclastic limestones characterized by the presence of abundant graded and cross bedded quartz sandstones and intraclastic ooids and pisoids (Plate A.6). Beds 63, 65 and 68 are distinct, mud cracked, micritic limestones. These beds are finely algal laminated; however, algal laminations and domal algal are sparse in the remainder of this series. Bed 62 contains tangentially cross bedded, quartz sandstone and siltstone capped by minor, intraclastic, ooids. Above the quartz sandstone are three intraclastic, fine grained, mud cracked limestones. Generally, beds 50 to 71 of this series show a stratigraphically upward increasing content of quartz sandstone and ooids. Stylolitization decreases up stratigraphic section in this series.

Beds 72 through 77 are 620 cm thick and mark the appearance of very dark gray, boundstones including seven distinctive domal algal horizons (beds 72 to 75) (Plate A.6). The algal are 1 to 2 m in length, up to 1 m in height, and are upright and overturned. The algal rest upon a thick blanket of graded, arenaceous oolite (beds 70 (of the previous section) to 72). A mud cracked horizon occurs at the crest of bed 74 and is severely brecciated. Beds 73 to 75 contain abundant quartz vugs. Beds 73 through 77 contain thick accumulations of edgewise conglomerates, graded ooids, rip-up clasts and overturned algal structures. Edgewise conglomerates are up to 70 cm thick.

Beds 78 through 88 are approximately 10.25 m thick and witness a return to thick bedded, dark gray, algal laminated, dolomitic limestones (Plate A.6). The dolomitic limestones contain shale partings along their upper and lower contacts. Bed 79 contains large, circular algal colonies comprised of countless numbers of small algal structures (Figures A.1 and A.2). Beds 81 through 86 are thin to thick bedded, stylolitized, dolomitic limestones containing abundant algal laminations. Beds 87 and 88 cap the series and are thin to thick bedded, arenaceous limestones containing graded ooids capped with an intraformational limestone conglomerate.

Beds 89 through 106 are 925 cm thick and are characterized by the presence of interbedded, graded ooids and cross bedded, quartz sandstones (Plate A.6). Bed 89 contains 130 cm of tangentially cross bedded, quartz sandstone, rip-up clasts and intraformational edgewise conglomerates along its base. The crest of the bed is truncated and overlain by thick, non-graded, ooids. Beds 90 through 93, 95, 98, 101 and 102, the mid-section of 103, 105 and 106 contain graded and cross bedded ooids. The section also contains thick, intraclastic limestones occurring at beds 88, 97, 98, 99, 100, 103, 104 and

106. The intraclastic limestones are capped with thick intraformational, edgewise conglomerates (bed 88, 97 and 106). Mud cracked intervals, and distinctive hummocky surfaces occur in beds 99, 100 and the crest of 105. Domal algal are only present in bed 104. The top of the section is marked by an increase in the quantity of shale, with respect to the underlying stratigraphy.

A.7 Limeport Formation: Gruenwald Member

Wheatsworth Road in Hamburg, New Jersey (location 3a in Figure 3.2; Plate A.7) is the most representative section of the Gruenwald Member of the Limeport Formation in the Hamburg 7.5' Quadrangle. The section can be divided into eighty-one beds and seven general series based on gross lithologic characteristics.

The first series include beds 1 to 12 and is 23 m thick. Beds 1 to 12 are medium to thick bedded, medium to dark gray, fine to coarse grained, algal laminated dolomitic limestone with interbeds of limestone (Plate A.7). The base of the series (bed 1) includes two distinctive edgewise conglomerates and is peppered with quartz vugs and rip-up clasts. Beds 2 through 4 occur largely in a covered section and the interpretation of rock underlying this section comes from adjacent outcrops and float within the covered interval. A small outcrop is present in the middle of the covered interval, at approximately 640 cm from the covered section base. This permitted refinement of the covered interval stratigraphy into a lower section (identified on the stratigraphic profile as bed 2) and an upper section (divided into beds 3 and 4). Bed 2 is 700 cm thick and is interpreted as containing very fine grained, medium to dark gray, micritic limestone with interbeds of algal laminate and non-graded oolite. Beds 3 and 4 include 775 cm of medium grained, medium gray, algal laminated, rip-up clast, dolomitic limestone. Beds 5

through 11 are medium to thick beds of light to dark gray, very fine to medium grained, algal laminated, dolomitic limestone. The series is capped (bed 12) with a bed bearing rip-up clasts, stylolites and a thick, intraformational conglomerate.

Thirteen beds (spanning almost 14 m) comprise series two, which begin at bed 13; a stylolitized, rip-up clast bearing dolomitic limestone and terminates at bed 25 with a very fine grained, dark gray, micritic, algal laminated, dolomitic limestone containing abundant intraclasts, rip-ups, mud cracks, and edgewise conglomerates composed of algal wrapped ooids (Plate A.7). This series is highlighted by two thick, domal algal successions in bed 24. The large 1 m wide x 1m tall domal algal are present in approximately 300 cm of carbonate, the base and the crest of which contains thin arenite or quartz rose lenses and the crest of which is algal laminated (Figures A-3 and A-4). Beds 14 and 15 contain 170 cm of very fine grained, light gray, micritic, laminated and domal algal limestone. The algal laminated limestone is overlain by 200 cm of evenly bedded, interbedded, coarse grained, dolomitic limestone and layers of structureless oolite (bed 16). Overlying bed 17 is approximately 100 cm of intraclastic, oolitic limestone bearing edgewise conglomerates overlain by algal laminate. Beds 18 and 19 are mud cracked, oolitic limestones, approximately 200 cm thick and peppered with quartz vugs. Bed 20 is a dolomitic limestone approximately 150 cm thick, capped by approximately 50 cm of intraformational, edgewise, limestone conglomerate (bed 21) with occasional rip-up clasts of algal laminate. Beds 22 and 23 are medium gray, medium grained, algal laminated, stylolitic, dolomitic limestone. Micritic, medium gray, stylolitic, dolomitic limestone (bed 24) is approximately 300 cm thick and serves as the base for the succession of large domal algal described earlier in this paragraph. Stylolites

are present at the same interval as shale in bed 24. Quartz vugs are very common in bed 25, in close association with mud cracks, rip-up clasts and edgewise conglomerates composed of algal laminated pisoids and oncoids.

The third series includes beds 26 through 49 and is approximately 975 cm thick (Plate A.7). This series includes numerous thin beds of medium to dark gray, dolomitic limestones and limestones. No less than fourteen rip-up clast beds occur within this series (beds 26, 29, 30, 32, 33, 34, 39, 41, 42, 43, 44, 46, 47 and 49). The intraclasts are pisoids and ooids wrapped in algal filament, and rolled filamentous algal structures. Domal algal occur sporadically (beds 31, 32, 44, 45). The domal algal are underlain by carbonate which is peppered with quartz vugs (beds 29, 30 and 43). Quartz sandstone lenses are uncommon, bed 32 being the exception.

Beds 50 through 54 comprise the fourth series in the Gruenwald Member (Plate A.7). This series is approximately 16 m thick. The base of the series contains thin, but distinctive, planar cross bedded, quartz sandstones intercalated with intraclastic limestones containing a coarse limestone matrix with fragments of oolite. The base of bed 50 includes 125 cm of algal laminated, dark gray, coarse grained limestone. The lower 125 cm of bed 50 are overlain by 250 cm of interbedded, dark gray, coarse grained, algal laminated limestone. The upper 150 cm includes thin interbeds of structureless oolite. Bed 51 is approximately 600 cm thick. The base is peppered with quartz vugs and the lower 125 cm is an algal laminate interbedded and overlain by thin, intraformational conglomerates. These in turn are overlain by 230 cm of interbedded, dark gray, coarse grained limestones with interbeds of structureless oolites. A second horizon of quartz vug, and intraformational conglomerate bearing, algal laminate is

present in the lower-upper part of bed 51. The top of the bed is composed of limestone with interbeds of structureless oolites. Bed 52 is approximately 675 cm of thick, medium gray, medium grained limestone bearing ungraded oolites midway, and along the upper part, of the series. Most noticeable in bed 52 are four distinctive intraformational conglomerates that occur within the limestone are sandwiched between the oolites. Domal algal occur sporadically throughout the series and the bed is pervasively stylolitized. Bed 53 is approximately 100 cm thick and is very similar to the underlying bed 52 in that it is a medium gray, medium grained limestone bearing thin beds of structureless oolite and stylolites. Domal algal occur in the limestone at three distinctive horizons. Bed 53 is capped with thin, black shale, which is overlain by approximately 100 cm of micritic, stylolitized, rip-up clast limestones.

The fifth series in the Gruenwald Member extends from beds 55 to 64 and has a thickness of approximately 1450 cm (Plate A.7). This series of beds includes sixteen intraclastic horizons comprised predominantly of oolite rip-up clasts wrapped in algal laminate, and sparse peloids. Numerous thin, medium gray, coarse grained, stylolitized limestones, interbedded with thin beds of intraclastic oolite, comprise beds 55 through 58. Bed 58 has a thick intraformational conglomerate. Above this conglomerate, the overlying beds are pervasively algal laminated for approximately 800 cm. Interbeds of structureless oolite are present in beds 63 to 64, with domal algal capping both beds. Rip-up clasts and quartz vugs are present in beds 63 and 64 as well.

Series six includes five beds that extend for a little less than 500 cm in thickness (Plate A.7). Beds 65, 66, 67, and 68 are characterized by interbeds of medium gray, medium to coarse grained, strongly algal laminated limestone, with thin interbeds of

structureless oolite. Stylolites are present in beds 65 and 66. Bed 69 is approximately 300 cm thick and is a medium to dark gray, micritic limestone with six thin, shales occurring in the lower and upper parts of the section. The top of bed 69 is a thin, dark gray, micrite which possesses a mud cracked surface. Bed 69 is stylolite bound.

Series seven, which contains beds 70 to 81, indexes the reappearance of thick, intraclastic, cross bedded, oolitic limestones, cross bedded quartz sandstones, and large domal algal (Plate A.7). The series is approximately 750 cm thick and includes 100 cm of interbedded, medium gray, medium grained, algal laminated limestone which yields upward to interbeds of oolites, rip-up clasts and intraclastic limestones. The intraclasts are primarily peloids and ooids. Shale is present at the base of bed 73 and quartz sandstone is present at the crest of bed 74. Bed 77 includes quartz vugs within intraclastic, algal laminated, micrite overlain by cross bedded oolite and thick accumulations of large domal algal measuring greater than 1 m in diameter. Beds 77 and 78 are the transition from limestone to dolomitic limestone. Two shales occur just above the first domal algal succession (crest of bed 79/base of bed 80). Bed 80, which is 150 cm thick, contains shale at its base, overlain by rip-up clasts, mudcracks and a thick concentration of domal algal, which in turn is overlain by structureless oolite. Bed 81, which caps the Gruenwald Member, is thick shale. Three chert horizons are present within the uppermost succession of beds. The upper and lower chert horizons are silicified algal stromatolites. The intermediate chert is a silicified oolite. The cherts are present in the thick, intraclastic, dolomitic limestone of bed 80.

A.8 Limeport Formation: Glacial Quarry Member

The Glacial Quarry stratigraphic section on Rte 94 in Hamburg, New Jersey (location 3c in Figure 3.2; Plate A.8) contains the most representative section of the Glacial Quarry Member in the Hamburg 7.5' Quadrangle. The member can be divided into thirty-four beds and three general series based on gross lithologic characteristics: beds 1 through 9 are the algal laminated series with associated arenaceous, ooid and rip-up clast horizons; beds 10 to 17 are the ooid-intraclastic series; and beds 18 to 34 are the boundstone-intraclastic-oolite series.

The lower series (beds 1 to 9) is approximately 500 cm thick and rests on a mud crack and rip-up clast bearing, micritic, dolomite (Plate A.8). Bed 2 is tawny colored shale and beds 1 and 2 contain distinctive silicified shale lenses. Beds 3 to 6 are light to medium gray, micritic to coarse grained, medium bedded, dolomite containing structureless ooid horizons and rip-up clasts. The rip-up clasts are predominantly fragments of dolomite, and clots of oolite, surrounded in layers of algal laminae. A cross bedded, stylolitized, arenaceous horizon occurs in bed 4. Bed 7 is a medium gray, medium grained, stylolitized dolomite containing layers of quartz sandstone capped by medium gray shale. Bed 8 contains large domal algal measuring 1 m wide by 40 cm tall. Bed 9 is quartz sandstone with rip-up clasts of algal laminates and oolite, and it is stylolitized at its base. Generally, this lower series is arenaceous and the arenites are closely associated with rip-ups and stylolites.

The second series (beds 10 to 17) are almost 525 cm thick and represent the ooid-intraclastic series and exhibit a sharp decline in the quantity of quartz sandstone (Plate A.8). This is associated with an increase in algal laminates and a general coarsening in

dolomite grain size. Noteworthy within this series is the presence of three distinctive, intraclastic, edgewise conglomerates occurring within the base and crest of beds 14 and 17. Bed 14 contains coarse grained, light gray, dolomite, graded ooid horizons, rip-up clasts and stylolites. The series contains abundant algal laminated horizons at the base, mid-section, and along the crest within beds 10, 13 and 15. Quartz vugs occur along the base of bed 15. Bed 17 marks the top of the series and is a 40 cm thick bed of edgewise conglomerates, rip-up clasts and clots of algal encrusted oolite and mud cracks. The top of bed 17 contains a thick, black shale overlying cut-and-fill channels present within the grainstone horizon. The mud cracks, rip-up clasts, and conglomerates of bed 17 allow interpretation of an unconformity present within this horizon.

The third series (beds 18 through 34) represents approximately 800 cm of thin to thick, fine to coarse grained, intraclastic, dolomites with shale interbeds increasing in abundance towards the top of the section (Plate A.8). The base of the series (beds 18 through 20) is marked by the reappearance of LLH-type domal algal. The algal structures are established on blankets of black shale (beds 18 and 28). Shales are common in this series (beds 18, 22, 25 28, 30 through 32). Generally, the lower beds (20 through 24) are thick, rip-up clast bearing, dolomites containing abundant graded oolite horizons and stylolites. Beds 21 thorough 24 all contain silicified pods and nodules of graded oolite and algal laminations and are surrounded by chert replaced stylolites. Beds 24 to 34 mark a change in the carbonate constituents, as the beds become thinner, darker and finer grained. Shale increases in abundance towards the top of this series. Bed 24 contains a cut-and-fill channel. Intraformational, edgewise conglomerates occur in beds 26 and 27. Chert replaced graded and structureless oolite also occurs within beds 25, 27 and 33.

A.9 Limeport Formation: Edison Member

The Rte 94 type section in Hardyston Township, Sussex County, New Jersey (location 3b in Figure 3.2; Plate A.9) contains the most representative section of the Edison Member of the Limeport Formation in the Hamburg 7.5' Quadrangle. The member can be divided into fifty-four beds and three general series based on gross lithologic characteristics: beds 1 through 9 are the shaly series; beds 10 to 31 are the shale and quartz sandstone interbed series bearing cross bedded sandstones and abundant stylolites; beds 32 to 54 are the domal algal series with thin shale interbeds.

Series 1 is just shy of 400 cm thick and is marked by the presence of two distinctive cherts (Plate A.9). The first (bed 1) occurs as dark gray to black, irregular masses of silicified ooids in a coarse gray, dolomite. The second chert (bed 2) partially replaces a 25 cm thick, tawny yellow, quartz sandstone. Beds 3 to 9 are predominately medium gray, fine to medium grained, shales with dolomite interbeds. Bed 4 is a coarse grained dolomite bearing chicken-wire structures and ooids. Beds 5 and 8 are medium gray, micrite to medium grained, respectively, algal laminated dolomite. Stylolites are present in bed 5. Bed 9 is shale with several quartz sandstone interbeds.

Series 2 is approximately 750 cm thick. The base of series 2 is a series of thin beds bearing graded and planar cross bedded oolites (Plate A.9). Beds 12 through 21 are light to medium gray, fine to medium grained dolomites bearing shale and cross bedded oolite and algal laminates Intraclast horizons (rip-up clasts) are common in these beds. Domal algal are present in beds 15, 18, 19, 21, and 22. The domal algal in beds 15-16 and 22 are bound by stylolite features. The upper parts of this series are dolomites peppered with quartz vugs (beds 25, 29, and 30), stylolites and shale interbeds (beds 28 to

31). These are overlain by internally brecciated, rip-up clast bearing dolomite interpreted as containing an unconformity. Noteworthy are two chert horizons, one a graded oolite sequence in beds 15 and 16. The second chert is silicified shale occurring in the base of bed 27.

Beds 32 to 54 are approximately 775 cm thick and in general are finer grained, darker, dolomites punctuated by thin, shale and quartz sandstone interbeds (Plate A.9). There are five vertical successions of grainstone/algal boundstone in this series, each separated by shale horizons and minor arenaceous units (beds 36, 40, 44, 46, 51). Thick accumulations of algal laminates occur in beds 34, 36, 45 to 47, and 53 and 54. Domal algal in this series are up to 1 m in diameter and occur in beds 41, 45, 47 to 48, 51 to 53. The series is marked by two silicified silty shales and partially chert replaced algals (beds 53 and 54).

A.10 Limeport Formation: Rte. 94 Member

The Rte. 94 type section in Hamburg, New Jersey (location 3b in Figure 3.2) contains the most representative section of the Rte. 94 Member of the Limeport Formation in the Hamburg 7.5' Quadrangle. The member can be divided into eighty-four beds and four general series based on gross lithologic characteristics: beds 1 through 26 are the cross bedded oolite, algal laminated and intraclastic dolomite series; beds 27 to 45 are the cross bedded and graded oolite series, with intraclasts and burrowed horizons; beds 46 to 59 are the intraclastic dolomite series bearing abundant horizons of graded and cross bedded oolites; and beds 60 to 84 are the shaly, dolomite series associated with intraclastic, cross bedded and graded oolites and mud cracks.

Above the structureless dolomite horizon (bed 1), and the associated zone of chert replaced stylolites, is a 825 cm thick succession of thin, intraclastic dolomites featuring rip-up clasts and graded and cross bedded ooids (Plate A.10). Algal laminations (beds 4, 8, 15, 17 to 19) and quartz sandstone (beds 3, 4, and 6) interbeds are present in the lower part of the series. Ooids (beds 9, 11, 12, 14, 19, 24), shale (beds 2, 13, 21, 25) and domal algal (beds 15, 19, 21, 22, and 26) horizons replace algal laminations and sandstone beds as predominant bed forms in the upper part of the series. Cross bedded horizons include beds 3 to 8, 12, 16 and 19. Intraclastic horizons occur in beds 3, 7, 14, 18 and 21. Beds 1, 8, 15, 16, and 22 contain stylolites. Bed 7 contains quartz vugs. At two horizons (bed 5 and 17), quartz sandstone and ooids are replaced by chert, respectively. Chert replaced intraclasts occur within beds 7, 15, 17, 18 and 26 and irregular masses and a light gray, chert bed occurs in bed 21.

Series two occurs between beds 27 and 45, is 10 m thick, and is indexed by an increased volume of oolite as graded and structureless beds; although planar cross bedded horizons do occur (beds 27, 33 and 39) (Plate A.10). The base and mid-section of the series are peppered with quartz vugs (beds 29, 33 and 39). Burrows are present in bed 30. As in the case of other described sections, beds 32, 35, 42, 43 and 45 contain domal algal structures. Stylolites are present in beds 28, 29, 34, 35, 40, and 41. Several chert horizons are present in series two. Silicified rip-up clasts are present in bed 29. Oolite horizons replaced by chert are present in beds 30, 37, and 41. A light gray chert bed is present in bed 42.

Beds 46 through 59 comprise series three, which is approximately 775 cm thick, and contains graded and planar cross bedded oolite sequences, all occurring within thick,

medium to coarse grained, dolomite (Plate A.10). The unit is sparsely algal laminated and domal algal are present only in beds 47, 50 and 58. Stylolites are concentrated in the lower part of the series, particularly in beds 51 to 54. Quartz vugs are only present in bed 56. Shale is present in bed 48 and at the interface (represented as thin black line on the section) of beds 56 to 59. Quartz sandstone is present in bed 53.

The fourth series includes beds 60 to 84, is approximately 10 m thick, and contains interbedded, planar cross bedded sandstone, algal laminations and intraclastic dolomite along the base (beds 60 to 63) (Plate A.10). The abundant rip-up clasts and intraclastic nature of bed 60 permit interpretation of an unconformity at this horizon. Bed 60 contains graded and cross bedded ooids capped with algal laminations. The top of bed 63, all of 64 and 65 contain algal laminated dolomite with shale interbeds. Rip-up clasts and mud cracks are present at the top of bed 64. Beds 65 through 73 are thin to medium bedded, fine to coarse grained, sparsely algal laminated, dolomites bearing sparse oolites and sandstone interbeds, shale interbeds and domal algal in beds 69 and 70. Quartz sandstones lenses are present in beds 72 and 73. Beds 74 through 84 cap the section and the series contains graded and cross bedded pisoid and ooid horizons (beds 74, 76, 80 to 82). Bed 82 is stylolitized. Thin, fine grained, algal laminate caps the oolite series. Gray to black, calcareous shales are abundant (beds 60 and 62 (depicted as thin black lines on the section), 65, 67, 69 to 71 and the top of bed 83). Most of the black shale horizons occur in association with algal laminate horizons. Near the crest of the section (top of bed 81) and towards the base of bed 82, occur irregular masses of chert replaced oolites.

A.11 Upper Allentown Formation

The Carlton Village type section in Hardyston Township, Sussex County, New Jersey (location 3d in Figure 3.2; Plate A.11) contains the most representative section of the Upper Allentown Formation in the Hamburg 7.5' Quadrangle. The formation can be divided into seventy-six beds and eight general series based on gross lithologic characteristics: beds 1 through 5 are the graded and cross bedded oolite series that contain abundant quartz sandstones; beds 6 to 11 is the shaly algal laminate series containing abundant graded oolites towards the base and domal algal structures towards the crest of the series; beds 12 to 16 are the oolite, intraclastic series with very coarse grained dolomites; beds 17 to 36 are the oncoid, pisoid and graded oolite with quartz rose sandstone series; beds 37 to 48 are the algal laminate, oolitic, quartz rose series; beds 49 to 54 are the cross bedded, oolite series; beds 55 to 66 are the intraclastic, quartz rose, cross bedded oolite series; and beds 67 to 76 are the intraclastic, domal algal series.

Series one contains four quartz sandstone horizons occurring in beds 3 to 5 and is slightly greater than 600 cm thick. Cross bedded oolites are present in beds 1 and 3 to 5 (Plate A.11). Intraclasts occur between these horizons midway in bed 3 and along the crest of bed 5. Strongly algal laminated horizons (Figure A-5) (upper part of bed 3) occur above the graded oolite sequences and domal algal structures occur in between graded oolites and quartz sandstones within bed 3. Thick shale is found along the base of bed 2 and is sandwiched between thick accumulations of chert replaced oolites.

The second series starts on black shale (basal contact of six and upper contact of seven; seen as thick lines on the section) which is overlain by a thick accumulation of algal laminated, dolomitic limestone (Plate A.11). These in turn are overlain by no less

than eight, graded oolitic sequences. The series is approximately 650 cm thick. Domal algal occur in beds 10 and 11. Generally, the stratigraphic succession includes the following; a base of black shale overlain by graded oolite. The domal algal rests on the upper surfaces of the oolite horizons and the dense accumulation of laminated algal occur over the domal structures. This sequencing occurs three times in the upper part of the second series. This series is capped by black shale (seen as thick line in section).

The third series includes beds 12 through 16 and is approximately 500 cm thick. Accumulations of ooids are found in beds 12, 13, and 15 (Plate A.11). The ooid succession in bed 12 is planar cross bedded. The domal algal occur between graded oolite in bed 12. Beds 12 and 16 are intraclastic (rip-up clasts). The upper part of the series is algal laminated (bed 13). Shales are located in the mid-section of bed 12 and in bed 16 at the crest of the series. Algal laminations are present in beds 13, sandwiched between two ooid horizons. Stylolites are present in bed 12, at the base of the section and in bed 16, at the top of the section. Near the crest of the third series, silicified stylolites are present in bed 13.

Beds 17 through 36 in the fourth series are 23.5 m thick. Beds 21, 22, 27 to 29, and 31 are characterized by the presence of thick beds of oncoid, pisoid, oolite and graded oolite successions; many of which are capped by thick lenses of cross bedded oolite. Thick, quartz sandstones are in beds 19, 20, 26, 29 to 31. Many of these beds contain intraclasts of rip-ups of quartz sand wrapped in laminated algal. The base of the beds is scoured locally. Graded ooids occur in beds 17 and 18 and shale is abundant in the upper part of bed 28 to the top of the series. The shale couplets occur along the upper and lower contacts of each bed and are stylolitized. Algal laminates appear throughout

the series; however, they increase in abundance from bed 29 to 36. Generally, algal laminates increase in concentration at the stratigraphic position where oncoids and pisoids diminish in occurrence. The series is capped by graded quartz sandstone with intraclasts of quartz sand wrapped in algal laminations (bed 36).

Series 5 contains beds 37 to 48 and is 18 m thick. Beds 37 through 43 witness a continuation of strongly algal laminated, thickly bedded, oolitic dolomite; however, beds 39 to 43 also contain mid-bed quartz sandstone. The concentrations of algal structures diminish from beds 37 to the crest of 39. Algal structures appear again along the upper half of bed 44 and 45 to 48, overlying oncoid, pisoid and graded oolite sequences. The upper part of this series, form bed 44 to 48, is similar to the mid-section of series 4 (beds 20 to 23 and beds 27 to 32). Generally, the lower and upper parts of this series are strongly algal laminated, thickly bedded, medium gray, medium grained, quartz rose, oolitic dolomites. The mid-section of the series witnesses and increase in quartz rose units. The series culminates within beds 47 and 48 with the reappearance of oncoids, pisoids and graded oolites, with occasional shale lenses.

Beds 49 through 54 comprise series 6 and are 850 cm thick. The series contains thickly bedded, medium gray, medium grained, light gray to tan or cream colored, algal laminated dolomite. The series is characterized by the presence of abundant, cross bedded oolite sequences occurring in the upper parts of beds 49 to 54. In most cases, beds 49 to 53, the cross bedded oolites overlie graded oolite sequences. Generally, each bed is bounded along its base and crest by dense concentrations of algal laminate and occurring mid-bed are graded oolites overlain by cross bedded oolites. The overlying algal successions are founded on the crests of the cross bedded oolites. Bed 54, which

terminates the series, represents approximately 250 cm of the below mentioned succession, the bed is bounded along its base and crest by algal laminate and contains two distinct, mid-bed oolite sequences which start at their base graded and terminate at strongly cross bedded.

Beds 55 through 66 comprise series 7 and are 10 m thick. The series is a thickly bedded, medium to coarse grained, medium to dark gray to cream/tan, nearly white, interbeds of quartz rose, algal laminates, and oolitic dolomite. This series of dolarenites is indexed by the increased abundance of quartz sandstone occurring along the crest, mid-bed and base of most beds. Intraclastic lenses occur at the base of bed 59 to 62; while cross bedded oolites occupy beds 63 and 64 and shale horizons punctuate the base and crest of the series.

Series 8 includes beds 67 through 76 and is 880 cm thick. The series is indexed by the reappearance of large domal algal; each overlying thick accumulations of intraclastic and edgewise conglomerates. The beds in general are hummocky in appearance, possessing more uneven lower and upper bed contacts. Shale horizons cap the series within beds 75 and 76. Domal algal rest upon blankets of graded quartz sand within beds 68 to 73, excluding bed 70. The lower algal horizons rest on intraclastic and intraformational and edgewise conglomerates; while the upper algal horizons are interbedded between structureless and cross bedded oolite sequences. Ripple marks are abundant towards the top of the series and the entire series witnesses a steady influx of quartz sand. The base of the series rests on a thick horizon of graded quartz sandstone. Chert becomes abundant in the member only in this series. Chert replaced intraclastic

units occur in beds 67, 70, 73, 74 and 76. Silicified ooids occur in beds 72 and 75 and partially chert replaced algal structures occur in beds 68, 69, 72 and 73.

A.12 Stonehenge Formation: Carlton Village Member

The Carlton Village stratigraphic section Hardyston Township, Sussex County, New Jersey (Plate A.12) contains the most representative section of the Carlton Village Member of the Stonehenge Formation in the Hamburg 7.5' Quadrangle. The member can be divided into seventy-five beds and five general series based on gross lithologic characteristics: beds 1 through 24 are the intraclastic, rubble mound, domal algal series; beds 25 through 34 are the intraclastic and graded oolite series; beds 35 to 47 are the quartz rose, cross bedded, algal mound series; beds 48 to 61 are the algal laminated, dolarenite series; and beds 62 to 75 are the shaly, quartz vug, algal dolomite series.

Beds 1 to 24 represent the first series at 13.5 m thick. There are twenty-four beds which comprise the first series above the unconformity capping the crest of the underlying Upper Allentown Formation. The lower two beds are thin to thick accumulations of graded and cross bedded oolites and dolarenites. The cross bedded series is capped by a thick algal laminated, dark shale horizon, in turn overlain by beds 3 to 9 representing greater than 400 cm of a rather unique occurrence of algal stromatolites. The base of this succession is silicified shale overlain by a chert replaced edgewise conglomerate. These give way to thin to thick horizons of chert replaced algal laminates, which are overlain by thick beds (3 to 9) of micritic, medium to dark gray, dolomite bearing thick intraclastic horizons. The beds have a rubbly appearance, mound-like structures are present and in places the beds are nearly structureless. Occurring throughout this part of the series are countless occurrences of spiral shaped, concentric,

almost pin-wheel like forms of algal stromatolite. The stromatolites also occur in ropy forms, twisting and turning through the rubbly beds (Figures A-6 and A-7). In many cases their concentric nature outlines tilted or overturned horizons. These have been interpreted as pinnacle-reef mounds all based in thick horizons of intraclastic dolarenite and graded oolite beds. The mound-like structures occur sporadically along strike and the forms range from finely laminated to tall, spiraling varieties. Isolated, chert replaced stromatolites are revealed in diamond cut slabs and are up to 3 ft (1 m) in diameter. Close inspection of both hand samples and slabs reveal that the algal structures are cementing irregular masses of dolomite, which have accumulated and then fallen into a final resting place, and then stromatolites grow through the interstices of the recemented fragments of dolomite and then grow upward toward sunlight. The pinnacle mounds, or reefal structures, terminate rather abruptly at the crest of bed 9, giving way to laminated algal forms and finally a succession of dolarenites interbedded with graded and cross bedded oolites. The mound structures are overlain by no less than six intraclastic horizons (beds 10, 12, 13, 17 to 19, 21 and 23). Interbedded between the intraclastic horizons are oolites occurring in beds 11, 16, 18, 20, 22, and 24. Generally, the succession overlying the pinnacle reefs, or mounds from beds 10 through 24 include intraclastic, oolitic dolomites overlain by thick accumulations of algal laminate, overlain by structureless oolite, which is overlain by graded oolite, overlain by cross bedded oolite, capped by strongly algal laminated, shaly dolomite. Cherts occur throughout the series from beds 1 to 21, replacing edgewise conglomerates of limestone clasts, rolled algal structures, irregular masses of quartz sand and oolite wrapped in algal mucilage, as well as algal structures. In particular, the algal structures occurring within the reefs, or

pinnacle structures and mounds, represent some of the best examples of selective silicification of stromatolites.

Series 2 consists of beds 25 through 34 and is approximately 900 cm. The series is characterized by the presence of thin to thick bedded, coarse grained, alternating light to medium gray, strongly algal laminated dolarenites. Intraclastic horizons occur along beds 25, 28, 30, 32 and along the crest of 34. Graded units include beds 26 through 29. In general, the series witnesses an increase in concentration of laminated algal.

Series 3 includes beds 35 through 47 and is 15 m thick. Series 3, as series 1, is characterized by beautifully developed algal mound structures (Figure A.8); however, these algal mounds are markedly different than those that occur in series 1. In many ways, the mounds are vaguely similar to the LLH-type algal present in the Wheatsworth Mills, Gruenwald, and Glacial Quarry members of the Limeport Formation. However, with several marked exceptions. The algal mounds themselves rest on 250 cm of thickly bedded, strongly cross bedded, dolarenites containing thick quartz rose sequences and intermittent lenses of graded and cross bedded oolite. This thick blanket of dolarenite serves as the base of the accumulation of no less than 400 cm of domal algal structures. The algal rest directly upon the upper part of the dolarenites and are up to 12 to 15 m in length and 300 to 400 cm high. They are tightly concentrated, one adjacent to the other, and occur stacked upon themselves. The concentric nature of the stromatolite is such that they appear to be more tightly bound than the LLH-types and more tightly concentrated into large, mound-like structures. The mounds within this part of the Carlton Village Member are up to 10 to 15 m in length; whereas the pinnacle mounds occurring in series 1 of the Carlton Village Member appear to disperse gradually (or fan out) along strike,

giving way to laminated forms and finally rubble zones and conglomerates. The matrix beds are thick bedded, hummocky, strongly algal laminated, coarse grained, medium to light gray, dolarenites. This series of mound structures is overlain by draping beds (40 to 42) of strongly algal laminated dolarenites. Occasional graded sequences and wisps and bands of oolite occur mid-bed. The dolarenites are overlain by 350 cm of micritic dolomite with abundant quartz vugs, shale seams and chert replaced evaporitic structures (bed 43). The upper part of the series is marked by interbeds of thick and thin, fine to coarse grained, shaly, algal laminated dolomite. Occasional clots and masses or nodules of chert replaced oolite and quartz sandstone occur with overturned algal structures. The series is capped by the reappearance of domal algal structures partially replaced by chert. Thick shale occurs along beds 44, 45, and 47.

Series 4 contains beds 48 to 61 and is 1360 cm thick. The series is punctuated by the presence of quartz vugs occurring along the base and mid-section of bed 48 and within bed 62. In general, the lower and upper parts of the series are strongly algal laminated; this includes beds 48 to 51 and 56 to 59. Chert occurs replacing algal structures in beds 52, 53 and 57. Chert replaced oolites occurring as irregular masses and convex mounds occur in bed 54. The series is terminated with the appearance of a thick dolarenite, peppered with quartz vugs.

Series 5 contains beds 62 through 75 and is 11 m thick. The series is indexed by the presence and reappearance of thick bedded, very coarse grained, light to medium gray, dolomites peppered with numerous quartz-vug horizons. The horizons occur in beds 63, 69 to 73 and 75. Algal laminae are sparse, occurring within beds 68 and 75 and shale

horizons punctuate the series along beds 64, 65, 67, 69, and 74. Chert replaced algal structures occur in abundance along the mid-section and upper part of bed
75.

A.13 Stonehenge Formation: Canal Road Member

The Canal Road type section, Vernon, New Jersey (location 4 in Figure 3.2: Plate A.13) contains the most representative section of the Canal Road Member in the Hamburg 7.5' Quadrangle. The member can be divided into thirty-one beds and four general series based on gross lithologic characteristics: beds 1 through 9 are the chert breccia, algal laminated series; beds 10 through 17 are the quartz rose series; beds 18 through 24 are the nodular chert and quartz-vug series; and beds 25 through 31 are the burrowed, domal algal series.

Series 1 is just shy of 600 cm thick (Plate A.13). Bed 1 is a thick, medium gray, highly sulfurous, algal laminated dolomite containing wisps and clots of black, highly translucent chert. The upper part of the bed contains tightly welded, angular fragments of algal laminated chert (Figure 3.40). This marker horizon is overlain by light to dark gray, thick bedded, micritic to coarse grained, strongly algal laminated dolomite (beds 2 through 9). Bed 5 contains a horizon of light gray, nodular chert. Beds 5 and 8 contain high concentrations of quartz vugs.

Beds 10 through 17 (approximately 450 cm thick) contain increased quantities of detrital quartz sand (Plate A.13). Much of the quartz sandstone is silicified. The dolomites range from strongly to mildly algal laminated (beds 11, 15, and 16). Bed 16 reveals cross bedded, thick quartz sandstones partially replaced by chert. Shale interbeds

overlie the silicified sandstones in bed 16. Bed 17 contains nodular black and gray chert. Much of the series (beds 11 to 15 and 17) is peppered with quartz vugs.

Series 3 is approximately 400 cm thick (Plate A.13). Beds 18 through 24 are a series of medium to very dark gray, thick bedded, micritic to coarse grained, algal laminated, dolomite. Quartz vugs are ubiquitous in this section, occurring in beds 18 through 20, 23 to 25. Planar cross bedded, quartz sandstone interbeds are present in beds 23 and 24. Three chert horizons are present within this series. The basal cherts (bed 18) are gray to black pods of chert containing quartz vugs. Bed 19 contains nodular black chert and beds 23 and 24 contain silicified sandstones.

Comprising the upper 800 cm of the section, series 4 contains light to dark gray, micritic to coarse grained, thick bedded dolomites (Plate A.13). The series is sparsely algal laminated and contains quartz sandstone and shale interbeds in the upper part of the section. Burrows occur in beds 25, 27 and 30; while large domal algal highlight bed 27. Quartz vugs occur in beds 25, 27, 29 and 31. Domal algal occur mid-way in bed 27, overlying laminated algal and burrow horizons. Thick, cross bedded, quartz sandstone is present at the top of the series at beds 29 and 30. These distinctive cross bedded sandstones are capped by a thick, lighter colored, algal laminated, dolomite containing quartz vugs and silicified sandstones. Silicified black shale is present along the bottom and top of bed 31. Thick accumulations of algal laminations are also present in bed 31, and the unit is capped by cut-and-fill channels incised into quartz sandstone layers. There are two chert horizons in the section. A basal chert in bed 26 is black, nodular chert. The top of the member is capped by quartz sandstones replaced by chert.

A.14 Rickenbach Formation: Hope Member

The Canal Road type section in Vernon, New Jersey (location 4 in Figure 3.2; Plate A.14) contains the most representative section of the Hope Member of the Rickenbach Formation in the Hamburg 7.5' Quadrangle. The member can be divided into twenty-five beds and three general series based on gross lithologic characteristics: beds 1 through 7 are the algal laminated-quartz sandstone interbed series; beds 8 through 16 are the quartz vug, burrowed, shaly, algal laminated series; and beds 17 through 25 are the algal laminated, arenaceous chert breccia series.

Series 1 is approximately 450 cm thick and includes dark gray, thickly bedded, micritic, laminated and domal algal dolomite alternating with light gray, coarse grained, algal laminated, arenaceous beds (Plate A.14). Beds 2, 4 and 7 are strongly algal laminated. Beds 3, 5, 6 and the top of 7 contain quartz sandstone horizons. The coarsening upward sequences characterize the series and upright and overturned domal algal occur towards the base of the section. Cherts occur sporadically as discontinuous black lenses and layers (bed 2) and chert replaced quartz sandstones (bed 6) (Figure 3.44).

Series 2 is approximately 500 cm of medium to dark gray, micritic to coarse grained and algal laminated, quartz-vug rich, dolomite (Plate A.14). The quartz-vug horizons include beds 8 and 11; while the burrowed horizons include the base and crest of bed 11 and bed 16. Intraclastic dolomites occur in beds 13 and 16 and are associated with algal laminated and shaly dolomite. Intermittent quartz sandstones and rip-up clasts are replaced by silica.

In series 3 (approximately 480 cm thick), the dolomites are algal lamination (beds 17, 20, 22, 24), quartz sandstone (beds 17, 23 to 25), and shale (bed 25) bearing (Plate A.14). Quartz vugs are present in bed 17. Burrows were examined in bed 23. Bed 22 contains convex domal algal (50 x 10 cm dimensions) occurring in the upper 40 cm of the bed. Two very distinctive chert breccia horizons occur along the crests of beds 22 and 24. Both of the chert breccia horizons occur in very coarse grained, light gray, algal laminated, arenaceous dolomites. Bed 25 is a fine grained, dark gray, algal laminated dolmicrite with cut-and-fill channels, shale partings and abundant layers of quartz sandstone. Silicified shale is present in the bed and caps the member.

A.15 Rickenbach Formation: Crooked Swamp Member

The Canal Road type section in Vernon, New Jersey (location 4 in Figure 3.2; Plate A.15) contains the most representative section of the Crooked Swamp Member of the Rickenbach Formation in the Hamburg 7.5' Quadrangle. The member can be divided into twenty-one beds and three general series based on gross lithologic characteristics: beds 1 through 5 are the chert-rich, arenaceous, algal laminated series; beds 6 through 12 are algal laminated, burrowed, intraclastic, chert breccia series; and beds 13 through 21 are the quartz vug, domal algal series.

Series 1 (beds 1 through 5) contains 300 cm of light to dark gray, micritic to coarse grained, algal laminated, arenaceous and shaly dolomite (Plate A.15). Bed 1 contains algal laminations, quartz vugs, rip-up clasts and burrows. Beds 2 and 3 contain abundant quartz vugs and shale and sandstone interbeds. Bed 5 is approximately 150 cm thick and can be divided into a lower, micritic, algal laminate interlayered with burrows; and an upper section of quartz sandstone interbeds. Rip-up clasts, shale lenses, burrows

and quartz sandstone horizons are all chert replaced (beds 1 to 3). Silicified shale sits astride the contact between beds 5 and 6 of the section.

Series 2 is 325 cm thick and includes medium to dark gray, coarse grained, algal laminates with abundant burrow features (beds 8 to 10) (Plate A.15). Bed 6 contains silicified shale in close proximity to stylolites. Intraclasts occur in beds 10 and 11 and the series is capped by an arenaceous dolomite overlain by two, silicified shales. The cherts occurring in the upper part of the series occur as two distinct breccia horizons separated by chert replaced shale and sand lenses (Figures 3.50 and 3.51). The interstices between the angular fragments of chert are filled with very coarse grained, light colored dolomite. Clasts range up to 3 to 5 cm in length and show fine laminations. Some of the chert fragments are highly translucent, medium to dark gray to navy blue; while other fragments are nearly opaque and black.

Series 3 is 400 cm thick (Plate A.15). The series coarsens and lightens in color up stratigraphic section. Beds 13 through 15, 19, and 20 are algal laminated. Domal algal occur at the base of beds 15 and 18 with overturned algal present in bed 15. Quartz vugs are present in beds 16, 19, and 21. Stylolites are pervasive in bed 20. Chert replaces the algal structures in bed 15, as well as the quartz sandstone of beds 15, 16, and 21. Bed 21 is terminated along its upper contact by thick, black, chert seams.

A.16 Epler Formation: Branchville Member

The Canal Road type section in Vernon, New Jersey (location 4 in Figure 3.2; Plate A.16) contains the most representative section of the Branchville Member of the Epler Formation in the Hamburg 7.5' Quadrangle. The member can be divided into ten beds and two general series based on gross lithologic characteristics: beds 1 through 6 are

the chert-rich, domal algal series and beds 7 to 10 are the dark gray, algal laminated dolomite series.

In general, the first series is 250 cm thick (Plate A.16). Bed 1 is 40 cm of dark gray, rubbly, argillic dolomite and is a prominent feature at all Branchville outcrops. The bed is overlain by micritic, finely algal laminated, dolomite with quartz sandstone interbeds. Domal algal overlies the sandstone (beds 2 and 3). The upper beds in the first series (beds 4 and 6) are algal laminated, arenaceous, and peppered with quartz vugs. The top of bed 6 contains colonies of domal algal. The base of the section is a thick chert breccia; however, intraclasts of chert clots, irregular masses, and silicified shale does occur. The most unique occurrence of chert in the lower series occurs within the base of beds 4 and 6, where thick quartz sandstones are composed of coarse and medium grained, purple chert clasts. The lavender to purple quartz sandstones are specific to the Branchville Member.

Series two is 400 cm thick and is composed of light to dark gray, thick bedded, micrite to coarse grained, dolomites (Plate A.16). Bed 7, 8, and 10 contain abundant algal laminations. Bed 8 is pervasively stylolitized and bed 9 contains quartz clots. The upper surface of bed 10 contains mudcracks and rip-up clasts and is interpreted as an unconformity. Clots, nodules and irregular intraclasts of bright lavender, to orchid to white chert are present in bed 9.

A.17 Epler Formation: Big Springs Member

The Beaver Run Aggregate type section in Hamburg, New Jersey (location 3e in Figure 3.2; Plate A.17) contains the most representative section of the Big Springs Member of the Epler Formation in the Hamburg 7.5' Quadrangle. The member can be

divided into forty-one beds and three general series based on gross lithologic characteristics. Beds 1 through 19 contain laminations which are parallel to bedding and fill in interstices. Many of the beds are arenaceous, contain ripple marks and mud cracked dessication surfaces. Beds 20 to 30 are the thickly bedded, quartz vug and chert breccia, dolomite series. Beds 31 to 41 represent the strongly algal laminated, intraclastic, dolomitic limestone series.

Series 1 is approximately 16 m thick (Plate A.17). The base of bed 1 contains finely laminated, bright green, silty shale which is strongly foliated. The foliations parallel bedding, but also wrap around and fill in interstices within the rock. As such, this green silty shale is interpreted as a silcrete. The silcrete is overlain by a bright orange, dolomitic limestone, which is overlain by a second green silcrete enveloped in two thin shales (one shale depicted as black line between the beds 1 and 2 contact). The upper shale is capped by mud cracks and algal laminations. Bed 3 contains graded ooids which transition upward to cross bedded oolites. Purple quartz sandstones are present in bed 3. Domal algal are present in bed 4 covered by a blanket of structureless quartz sandstone (Figures A.9 and A.10). Beds 5 to 7, 9, 10, 12, 13, 16, and 17 are algal laminated. Beds 5, 9, 12, 18, and 19 contain quartz vugs. Beds 1, 7, 9, 14, 16, 18 and 19 contain severely weathered, orange dolomite interpreted as saprolite deposits (i.e. paleosols), which are overlain by strongly foliated, sweeping bands of silcrete (Figures A.11 and A.12); inferring the presence of unconformities. Burrows are present in beds 8, 14, and 15. Mud cracks occur in beds 2 and 16. Quartz sandstone interbeds occur in beds 4, 8 to 13, and 17 to 19. Bed 19 is approximately 300 cm thick. The base of this bed contains two distinctive, bright orange, weathered dolomites overlain by structureless quartz sand. The

mid and upper parts of the bed contain two (50 cm thick) chicken-wire horizons and are peppered with quartz vugs. The chicken-wire horizons are interlayered with structureless quartz sandstone and overlain by a thick, domal algal horizon. This series contains several chert horizons (Plate A.17). Six distinctive, nodular and lenticular chert horizons occur in beds 1 to 5 and 8. These cherts range in color from light gray, porcellainous to lavender. The algal structures in bed 19 are 50 to 70 cm wide x 15 to 20 cm tall and are chert replaced and brecciated. Both evaporitic horizons in bed 19 contain thin beds, lenses, nodules and clots of highly lustrous, opaque, black chert.

Beds 20 through 30 are 17 m thick and contain thickly bedded, light to dark gray, fine to coarse grained, dolomite with abundant quartz vug-rich horizons (Plate A.17). Four distinctive silcrete lenses occur within beds 20, 26, and 27 and they mark the positions of closely spaced unconformities. Bed 20 is mud cracked and contains bright orange staining and thin lenses of green silcrete. Quartz vugs are present in beds 22, 24, and 29. Stylolites are sparse in this series, only occurring at the lower and upper contacts of bed 22. Algal laminations are also sparse, only occurring in bed 24, in association with a distinctive intraformational breccia made of silcrete clasts. Chicken-wire horizons occur in the mid-sections of beds 26, 27 and 29. The chicken-wire horizons are sandwiched by quartz vugs in quartz sandstones or between silcretes. Both the base and the crest of this series contain thick, bright purple, lavender and white chert breccia horizons. Nodular and pod shaped, black chert is present in bed 23, just above the stylolite horizon and below cross bedded quartz sandstones. Bed 29 contains light gray, pod shaped chert above and below the chicken-wire horizon. A 60 cm thick, purple,

white to light gray chert, breccia occurs along the crest of the series. The surrounding dolomite is also brecciated and contains siliceous infillings.

Series 3, which is 11 m thick is marked by the reappearance of large successions of domal algal (bed 32), occurs over a base of intraformational conglomerates (Plate A.17). The series witnesses the reappearance of numerous evaporitic horizons located midway through beds 31, 33, and 35 through 37. The lower two evaporitic horizons (beds 31 and 33) occur in close spatial association with intraformational conglomerates. Algal laminations are common in this series, occurring in beds 32 through 35, and 37 through 41. One thick, green silcrete occurs in bed 34. The upper part of the series (beds 39 through 41) are a 300 cm thick succession of light to medium gray, micritic, algal laminated, dolomite bearing numerous ripple mark surfaces with overprinted mud cracked intervals. Mud cracks are interpreted as representing surfaces of unconformity. The upper section is brecciated in its entirety. In general, beds 38 to 41 see the reappearance of quartz rose sandstone horizons, included cross bedded sandstone (bed 41). Distinctive lavender to purple, chert-pebble conglomerates occur midsection in bed 35. Algal laminated chert pods are present in bed 38 that are light gray in color. There is selective replacement of the lower quartz sandstone horizons with light gray chert in bed 39.

A.18 Epler Formation: Lafayette Member

The Harmonyvale type section in Harmonyvale, New Jersey (location 6 in Figure 3.2; Plate A.18) contains the most representative section of the Lafayette Member of the Epler Formation in the Hamburg 7.5' Quadrangle. The member can be divided into thirty-four beds and three general series based on gross lithologic characteristics: beds 1

through 13 represent the strongly algal laminated series; beds 14 through 28 are the algal laminated and burrowed series; and beds 29 to 34 are the quartz vug-rich series.

Series 1 is 20.75 m thick (Plate A.18). Bed 1 of the member is 375 cm of dark gray, micritic, thick bedded, dolomite with quartz vugs occurring in the mid-section and algal laminations towards the crest. The upper 100 cm of bed 1 contain abundant rip-up clasts of desiccated algal. The upper surface of bed 1 contains dessication features and is interpreted as an unconformity. Beds 2 through 13 are medium to dark gray, fine to coarse grained, medium to thick bedded, strongly algal laminated, dolomite. In particular, beds 3 to 8 and 10 to 13 contain great concentrations of algal laminations. The upper half of bed 1 contains two distinctive chert horizons; the lower of which is a black, lustrous, translucent, silicified oolite and the upper is a lighter gray, silicified algal laminate horizon.

Series 2 is 1400 cm thick and contains the transition from dolomite (beds 14 to 18), to limestone (bed 19), to dolomitic limestone (beds 20 to 23), back to dolomite (beds 27 ad 28) (Plate A.18). Three distinctive burrowed horizons are present in this series: the first of which occurs along the base of the series (bed 14); the second in bed 20; and the third in bed 24. Beds 18 to 20, 22 to 25, 27, and 28 contain abundant algal laminations. In bed 19, bedding is hummocky from the algal but even, and two cross bedded horizons occur mid-bed. Large domal algal are present in bed 24. The top of the series (bed 28) is approximately 300 cm of extremely dark gray, micritic, algal laminated, dolomite. Several chert horizons are present within series 2. The base of the series is lined with elongate pods of light gray chert that are porous and punky (bed 14) (Figure A.13). Bed 19 contains lenses and irregular masses of silicified oolite. Mid-series, light gray cherts

replacing algal laminations and shale interbeds are present, as well as porous and punky chert. The series is capped with a bright blue-gray, porous, punky, algal laminated chert that pinches-and-swells along strike.

Beds 29 through 34 are the last series of this member and include approximately 900 cm of light to medium gray, medium to coarse grained, algal laminated, dolomite and dolomitic limestone (Plate A.18). Bed 29 is an algal laminated, dolomitic limestone overlain by algal laminated dolomite in bed 30. Bed 31 reverts back to a dolomitic limestone and contains large domal structures, which are porous and punky. Beds 32 to 34 are all dolomitic limestone. Beds 33 and 34 contain quartz vugs and algal laminations. The crest of bed 34 is 150 cm of rip-up clast breccia and is interpreted as an unconformity. Many of the beds in the last series are juxtaposed and out of place. They are recemented with dark green, micritic infilling. This has been interpreted as paleokarst (Figure A.14). Chert occurs only at the crest of this series. Bed 34 contains scattered, dark gray to black, clots of chert and chert nodules, some up to 10 cm in diameter. Chert replaced algal structures occur, along with silicified rip-up clasts of algal laminate.

A.19: Ontelaunee Formation: Beaver Run Member

The Beaver Run Aggregate type section in Hardyston Township, Sussex County, New Jersey (location 6 in Figure 3.2; Plate A.19) contains the most representative section of the Beaver Run Member of the Ontelaunee Formation in the Hamburg 7.5' Quadrangle. The member can be divided into ten beds and four general series based on gross lithologic characteristics: beds 1 and 2 are the quartz vug, burrowed and gastropodal, dolomitic limestone series; bed 3 is the burrowed, gastropodal dolomite

series; beds 4 through 7 are the punky, algal (domal and laminated) series; and beds 8 to 10 are the chert breccia series.

Series 1 is 875 cm of dark gray, coarse grained, moderate to thick bedded, dolomitic limestone (Plate A.19). The series features alternating layers of horizontal and vertical, quartz sand lined, burrows. The burrows are spatially associated with quartz vugs. The Beaver Run Member is indexed by the appearance of gastropod fauna occurring in this series in thin lenses. Field and laboratory inspection has determined the gastropods to be *Ceretopea or Schizopea* (Moore et al., 1952; Yochelson and Barnett, 1972). Freshly broken hand samples of the dolomitic limestone reveal a crystalline texture of carbonate grains and possess a petroleum odor. Close inspection shows that parts of the burrows are partially silicified; however, the chert is a minor occurrence within this series. Along the base of the series, at 50 cm, is a silicified, punky and porous, algal stromatolite horizon.

Series 2 is 770 cm of medium to dark gray, thick bedded, coarse grained, dolomite (Plate A.19). Vertical and horizontal, quartz sand filled, burrow structures are present in bed 3, as are thin lenses of gastropods. As in the lower series, chert selectively replaces aspects of the burrow structures.

Series 3 is approximately 950 cm thick and the beds are porous and punky (Plate A.19). Beds 4 and 5 are medium to dark gray, coarse grained, burrowed dolomite bearing lenses of gastropods and an increasing concentration of chert replaced algal structures up section. Bed 4 contains irregular clots and masses of silicified burrow structures overlain by punky and porous, chert replaced algal laminates. Bed 5 contains large, domal algal which control bedding, creating an uneven, hummocky bed form.

Three, 20 cm thick, black, homogenous, chert replaced algal horizons overlie the domal algal. Bed 6 contains abundant algal, bearing eight, silicified, algal horizons in vertical succession. The lowest chert is highly lustrous, black, algal laminated and pinches-and-swells along the base of the bed. Punky, porous, domal algal horizons overlie the basal chert. A thin, 40 cm thick, dark gray, algal laminated dolomite overlies the domal algal horizon. This general theme repeats itself twice in bed 6, where mid-section are two domal algal horizons overlain by algal laminates. All of the algal horizons are porous, punky and replaced with chert. In outward appearance, the algal structures contort bedding, creating sweeping, undulating beds, hummocky surfaces and mound structures. The silicified mound structures are visible for great distances along stratigraphic strike. Bed 7, the algal laminate, caps the series.

Series 4 is 700 cm thick (Plate A.19). Bed 8 witnesses a marked transition in color, texture, and composition and can be inferred as a transitional series within the Beaver Run Member. The beds are micritic, bright blue-gray, and possess a chalky, white, weathering profile. Solution cleavage and stylolitization create a vertical, ribbing-like appearance to the weathered, outer surfaces of outcrops. Scattered throughout bed 8 are horizons of bright robin's egg blue to navy blue, clots of chert. The clots represent selective, chert replaced horizontal burrow fillings. There are horizons of silicified intraformational, edge-wise conglomerates. Bed 9 is fine grained, micritic, but returns to the dark gray dolomite color of the lower part of the Beaver Run Member. The mid-section of bed 9 contains thin lenses and horizons of clots and masses of dark gray chert. These have been interpreted as edgewise conglomerates, rip-up clasts, and burrow features. The mid-part of the bed contains a chert breccia overlain by a second horizon of

dark, navy blue, brecciated chert. This is overlain by 20 cm of thick, navy blue, homogeneous, pinch-and-swell chert beds. The upper chert bed contains fine, light colored, shale partings along the upper and lower surfaces of the bed. The entire upper part of the series is strongly undulating and pinches-and-swells along strike.

A.20: Ontelaunee Formation: Harmonyvale Member

The Harmonyvale type section in Harmonyvale, New Jersey (location 6 in Figure 3.2; Plate A.20) contains the most representative section of the Harmonyvale Member of the Ontelaunee Formation in the Hamburg 7.5' Quadrangle. The member can be divided into eleven beds and three general series based on gross lithologic characteristics: beds 1 and 2 mark the upper transitional series; beds 3 to 6 are the algal laminated, chert breccia series; beds 7 to 11 are the domal and laminated algal series.

Series 1 is 475 cm thick and bed 1 includes 170 cm of alternating, convex, chert replaced algal and breccia horizons (Plate A.20). No less than four chert breccia horizons occur in bed 1, of which the upper two retain the outlines of the former domal algal structures which the chert replaced. Some of the chert masses are as large as 100 cm in diameter, reflecting the size of the domal algal that was silicified. The cherts in this bed are also stylolitized. This distinctive, lower marker horizon is overlain by bed 2, which is 300 cm of dark gray, micritic dolomite and represents the final appearance of Beaver Run-like beds.

Series 2 is 1120 cm of blue-gray, micritic dolomite (Plate A.20). The base and crest of this series are marked by chert replaced algal horizons which pinch-and-swell along strike. In many cases, following them along strike, they gradually transition into micritic dolomite. Bed 3 is convex and its base contains 50 cm of blue-gray, micritic

dolomite, overlain by two chert breccia horizons interbedded with a punky, blue-gray, algal laminated dolomite. These beds are billowy and undulating for considerable distances along strike. Bed 4 is 150 cm of algal laminated, micritic, dolomite. The mid-section of the bed contains chert breccias overlain by horizons of irregular clots and masses of robin's egg blue chert (Figure A.15). The clots are in turn overlain by three distinctive, chert replaced, algal laminated horizons. The base of bed 5 is 100 cm of alternating, chert replaced, algal laminates in thin, micritic dolomites. The top of bed 5 contains abundant quartz vugs, and convex chert masses within this bed can be 102 cm in diameter or more. Bed 6 is 625 cm of blue-gray, micritic, thick bedded, algal laminated dolomite. The base of the bed is marked by a chert replaced, punky, algal laminate and mid-bed are three, silicified algal laminate horizons, of which the upper and lower are punky and perforated. Large, punky, domal algal are present mid-series at 1180 cm. These are overlain by silicified intraformational conglomerates. These are also overlain by thinner horizons of chert replaced, punky, algal laminates and silicified burrow structures. All of the chert beds are internally brecciated and re-sealed with later generations of silica. The series is capped by a 50 cm thick, hummocky, silicified, punky, algal laminate where the cherts are continuous for meters along strike.

Series 3 is 1660 cm of algal laminated, micritic dolomite (Plate A.20). The base, mid-section, and crest are indexed by chert-rich horizons. Bed 7 witnesses the final appearance of Beaver Run-like beds. The 60 cm thick, dark gray, fine grained, shaly dolomite is directly overlain by a chert breccia in bed 8. The overlying 250 cm includes a chert breccia overlain by two distinctive silicified algal laminates, overlain by a final horizon of irregular clots, masses and nodules of concentric cherts. These cherts have

dark, navy blue centers, overlain by an outer rind of light blue chert. Bed 8 is a continuous, algal laminated, micritic dolomite. This dolomite weathers white in outcrop and possesses vertical solution cleavage, giving a corrugated outward appearance to outcrops. A punky, chert replaced algal horizon occurs at 2460 cm (bed 8) and bed 8 terminates at 2670 cm. Beds 9 to 11 represent the upper part of series 3 and possess a punky, porous, large domal algal structures just above the base of the bed at 27 m. These are overlain by thick bedded, algal laminated, micritic dolomite. The series is capped by a thick, dark blue, convex, algal laminated chert horizon. The entire series is strongly stylolitized and contains abundant pressure solution features.

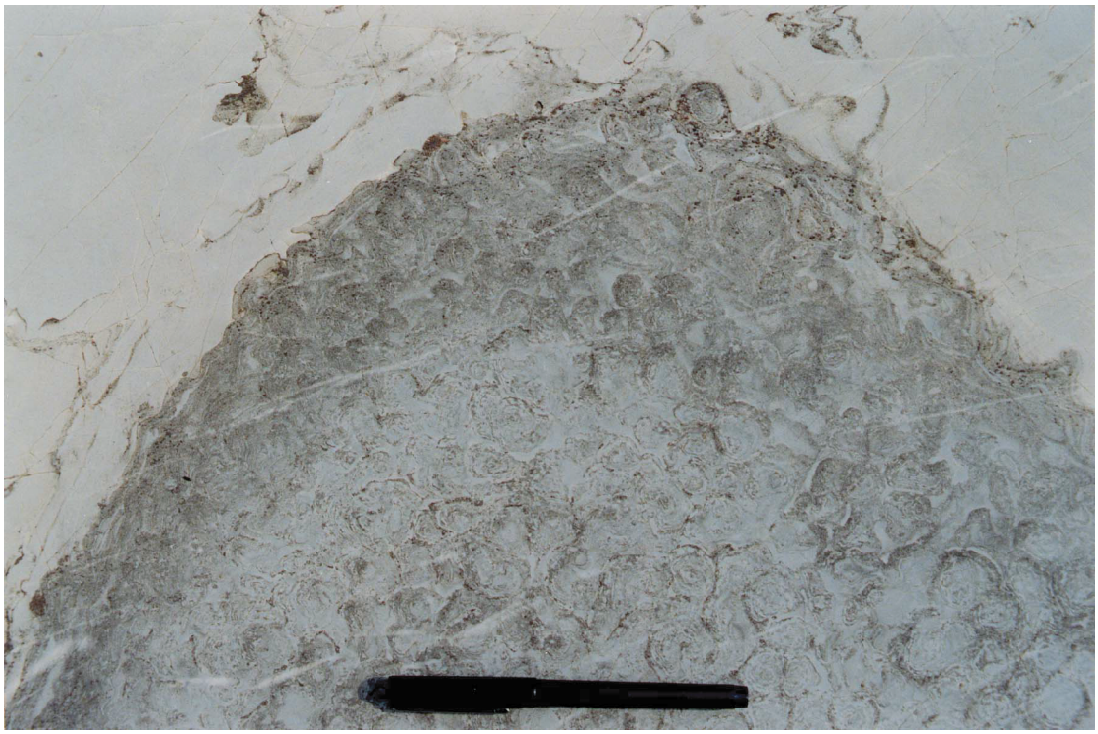


Figure A.1 - Wheatsworth Mills Member. Colonies of tightly bound digitate algal stromatolites (thrombolites) at the top of the Wheatsworth Mills Member. Gruenwald traverse.



Figure A.2- Colonies of tightly bound digitate algal stromatolites (thrombolites) at the top of the Wheatsworth Mills Member. Micrite caps the facies. Gruenwald traverse.

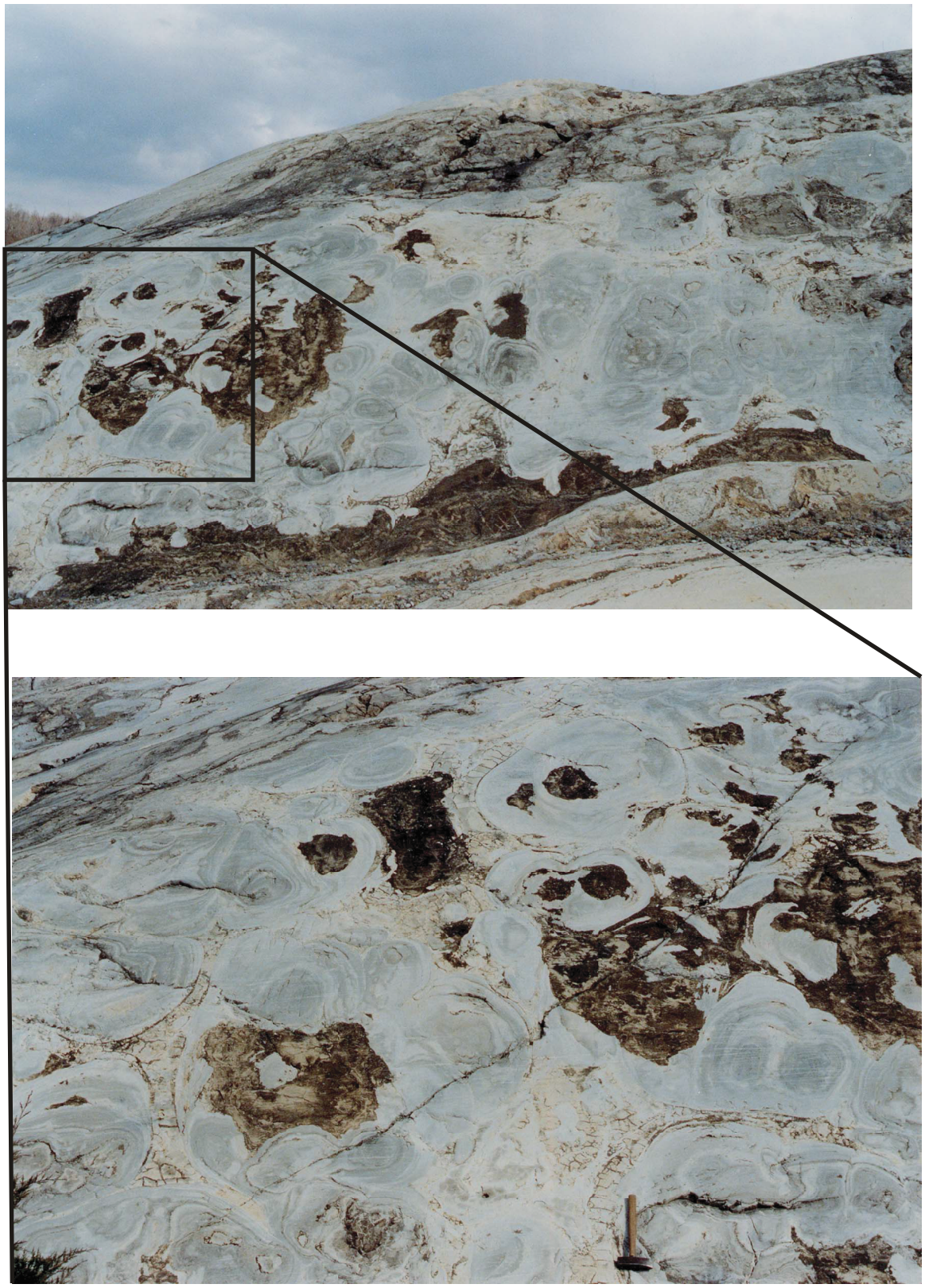


Figure A.3 - Wheatsworth Mills Member. Massive algal boundstone communities at the upper contact of the Wheatsworth Mills Member. Gruenwald traverse.



Figure A.4 - Carlton Village Member. Unique flowering of chert replaced algal stromatolite in micritic rubble zone at the base of the member.

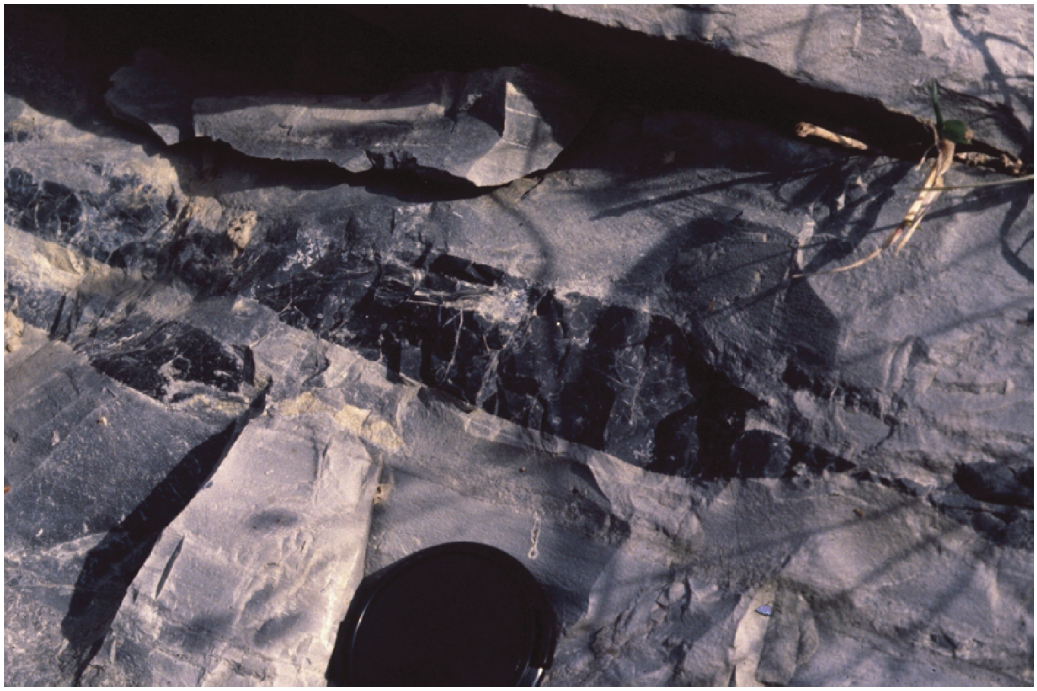


Figure A.5 - Upper Allentown Formation. Pinch-and-swell chert replaced laminated algal structures at the base of the formation.

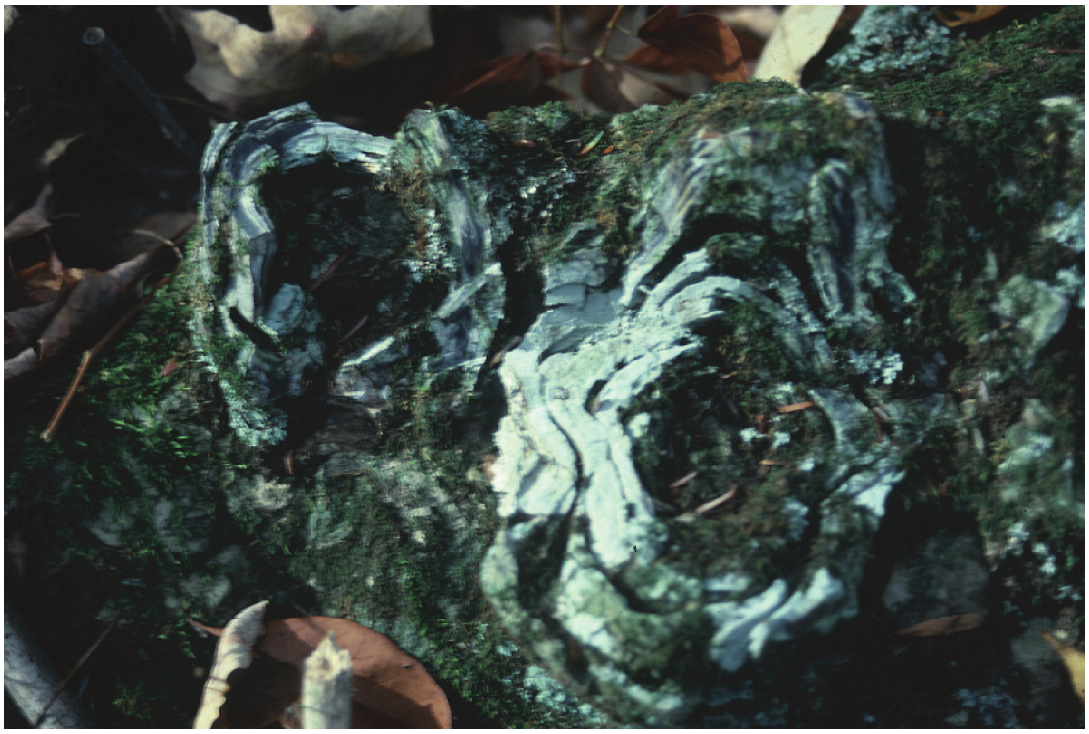


Figure A.6 - Carlton Village Member. Colony of cup shaped chert replaced algal stromatolites in rubble zone at the base of the member.



Figure A.7 - Carlton Village Member. Association of flowering, cup shaped, and ropy intertwined chert replaced algal stromatolites.

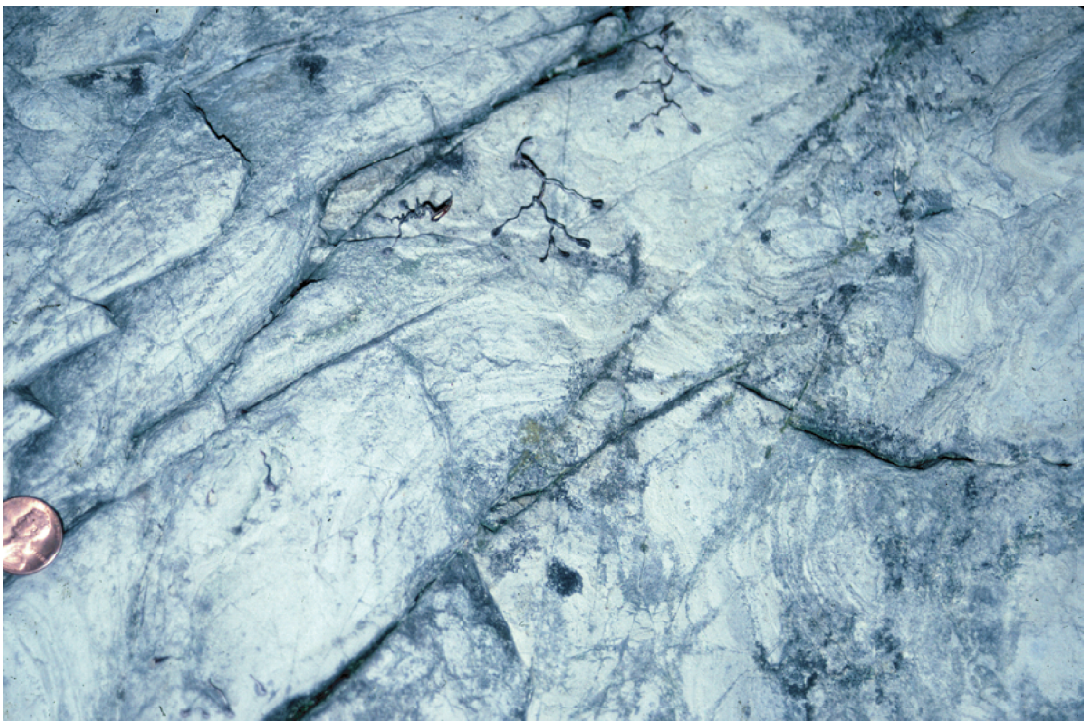


Figure A.8 - Carlton Village Member. Tightly bound hemispheric algal stromatolites at the top of the member.



Figure A.9 - Big Springs Member. Large domal algal successions, Conococheague-like cycles. Harmonyvale section.



Figure A.10 - Big Springs Member. Large domal algal with chert replacement along the top of each algal succession. Harmonyvale section.

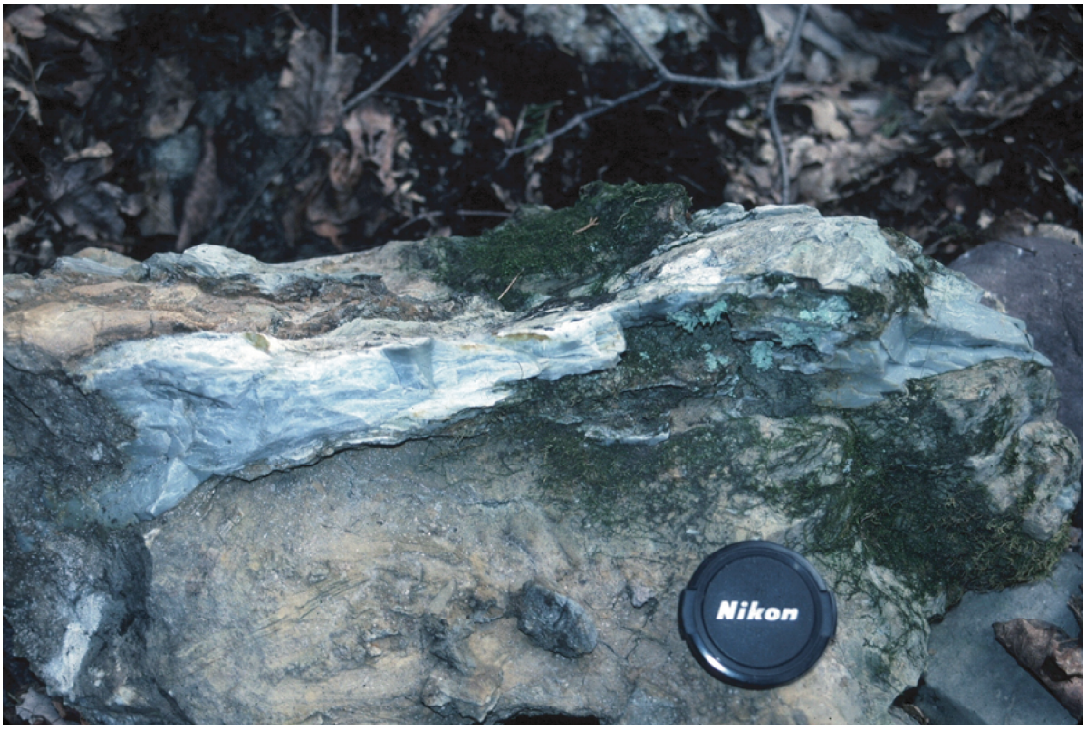


Figure A.11 - Big Springs Member. Well developed silcrete covering crest of intraclastic horizon and algal laminated micrite. Harmonyvale section.



Figure A.12 - Big Springs Member. Blocks of silcritized, supratidal, algal laminated micritic dolomite. Harmonyvale section.



Figure A.13 - Lafayette Member. Silicified, punky, and porous alagal stromatolites. Harmonyvale section.



Figure A.14 - Lafayette Member. Outcrop photograph depicting overturned paleokarst collapse features interrupting bedding. Harmonyvale section.



Figure A.15 - Irregular masses and clots of chert interpreted as replacing burrow structures and inferred evaporites. Harmonyvale section.

APPENDIX B – SECTION NOTES

B.1 – RTE. 94 SECTION

Rte. 94 Section, Sussex County, New Jersey								
Bed	**Thickness**	**Color**	**Grain Size**	**Bedding**	**Lithology**	**Chert**	**Member**	**Formation**
1	41	medium gray		no stylolites or ooids, upper 11 cm: scattered sulfides	dolomite	none	Limeport	Allentown
2	24	light gray	fine	bounded at both contacts by stylolite surface (shale partings, clay seams), structureless	dolomite	none	Limeport	Allentown
3	26	dark gray		stylolite-bounded with sulfides and clay partings at both contacts, cross-bedded, sweeping beds and bands,	dolomite	none	Limeport	Allentown
4	32	medium gray		oolitic, graded bedding, stylolite-bounded contacts	dolomite	none	Limeport	Allentown
5	13	medium gray		stylolite-bounded contacts with clay and sulfides	dolomite	chert replacing ooids	Limeport	Allentown
6	41	light gray		stylolite-bounded contacts, clay seams in upper 8 cm, lower 32 cm: arenaceous, cross-bedding, upper 8-9 cm: clay filaments (at least 8), slightly more fine-grained, fining-upward sequence	dolomite	none	Limeport	Allentown
7	45	medium gray	variable	lower 24 cm: arenaceous, algal stromatolites (25-34 cm diameter), convex upward, bedding created by algal filaments and clasts of calcite within algal horizon, upper 14-15 cm: almost medium gray, micritic	dolomite	none	Limeport	Allentown

8	27	dark gray	fine	muddy shales, fissile to micritic, lower 15 cm: very shaly dolomite, thin fissile layers, upper 13 cm: slightly more thickly bedded, higher lime content, almost looks like a slump breccia	shaly dolomite	none	Limeport	Allentown
9	8	light gray	micrite	sparse algal laminations, may be top of a parasequence	dolomite	none	Limeport	Allentown
10	138	variable	variable	lower 23 cm: medium gray, very coarse-grained, calcite clots, next 83 cm: light gray, fine-grained, strong stylolite at upper surface, strong convexity, may be algal controlled, next 51-52 cm: dark gray, coarse-grained, strong stylolites	dolomite	none	Limeport	Allentown
11	20	light gray	fine	stylolite-bounded	shale	none	Limeport	Allentown
12	30	medium gray	fine	sulfide rich, lots of calcite clots	dolomite	none	Limeport	Allentown
13	41	very light gray	micrite	sulfide rich in upper half of unit	dolomite	none	Limeport	Allentown
14	11	dark gray	fine	Marker Horizon: stylolite-bounded, numerous shale partings, undulating surface: may be a wave cut terrace	dolomite	high silica content, looks like it is very cherty	Limeport	Allentown
15	22	medium gray	very fine	vertical stylolites, cross-bedding, dark gray shale partings starting at 22 cm, 3 cm thick	dolomite	none	Limeport	Allentown
16	14	light gray	very fine	shale partings and sulfides in upper section, calcite clots replaced by quartz	dolomite	none	Limeport	Allentown
17	19	dark gray	very fine	shale partings every cm or so, quartz clots, upper 3 cm are black, laminated shale or algal stromatolites, probably undulating	dolomite	none	Limeport	Allentown

				algal				
18	64	light gray	very fine	upper 34 cm: very fine grained, lower 30 cm: algal laminations, shale partings/ horizontal and vertical stylolites, quartz clots, 26-30 cm: imbricate rip-up clasts, an unconformable surface, 30-34 cm: light gray micrite horizon	dolomite	none	Limeport	Allentown
19	11		micrite	shaly, upper 2 cm: extremely shaly, quartz clots interrupting bedding	dolomite	none	Limeport	Allentown
20	34	medium gray	micrite	very finely laminated, laminations are very dark, lower 10 cm: high concentration of quartz clots	dolomite	none	Limeport	Allentown
21	28	light gray	micrite	upper 15 cm: rather dense concentration of very fine ooids, no sign of bedding in oolite zone	dolomite	none	Limeport	Allentown
22	34	very dark gray		lower 16 cm: dense concentration of very small ooids, no bedding, 16-28 cm: more finely dispersed ooids	dolomite	none	Limeport	Allentown
23	52	medium gray		26-40 cm: good cross-bedding, upper 10 cm: very concentrated zone of arenite	dolomite	none	Limeport	Allentown
24	20	very light gray	micrite	algal laminated	dolomite	none	Limeport	Allentown
25	18	dark gray	fine	shaly, billowy	dolomite	none	Limeport	Allentown
26	28	very dark gray	fine	thinly bedded, shaly	dolomite	none	Limeport	Allentown
27	46	variable	variable	lower 12 cm: very light gray, micrite, very finely bedded, next 1 cm: black	dolomite	none	Limeport	Allentown

				algal shale, next 6 cm: medium gray, arenaceous, next 1 cm: black shale, algal stromatolites, next 25 cm: more thickly bedded micrite, occasional sand lenses (storm deposits)				
28	16	very dark gray		finely bedded, rip-up clasts	dolomite	none	Limeport	Allentown
29	7	very dark gray	micrite	finely laminated	dolomite	none	Limeport	Allentown
30	89	very dark gray	fine	lower 13 cm: finely laminated, shaly, next 33 cm: shaly, more thickly bedded, billowy, next 37 cm: very finely laminated, shale, upper 6 cm: very fine black laminated shale partings	dolomite	none	Limeport	Allentown
31	42	medium gray	medium	lower 8 cm: coarsely bedded, arenaceous, rest of unit: coarsely bedded	dolomite	none	Limeport	Allentown
32	34	light gray	micrite	lower contact: convex upward, upper contact: convex upward, good algal stromatolite mounds	dolomite	none	Limeport	Allentown
33	29	medium gray		coarsely bedded, arenaceous	dolomite	none	Limeport	Allentown
34	14	medium gray		arenaceous, intermediate algal laminations	dolomite	none	Limeport	Allentown
35	34	light gray	micrite	algal stromatolites, lower 9 cm: laminated, upper 5 cm of 9 cm: digitate algal, convex upper surface, upper 13 cm: laminated, algal stromatolites, convex upward	dolomite	none	Limeport	Allentown
36	32	medium gray	micrite	finely laminated, algal stromatolites, upper section, digitate stromatolites,	dolomite	none	Limeport	Allentown

				stromatolites have convex upper and lower surfaces				
37	17	dark gray	fine	finely laminated, calcareous, very fissile	shale	none	Limeport	Allentown
38	6	light gray	fine	rip-up clasts	dolomite	none	Limeport	Allentown
39	11	light gray	coarse	arenaceous, coarsely bedded	dolomite	none	Limeport	Allentown
40	2	black	fine	finely laminated, black, shaly, algal stromatolites	dolomite	upper surface of shale has turned to chert	Limeport	Allentown
41	115	light gray	micrite	convex contacts, six mound surfaces at 13, 19, 46, 70, 97, and 115 cm, one half to one cm of shale on top of all mound surfaces, upper 9 cm: light gray micrite, lower 5 cm of upper 9 cm: digitate algal, upper 4 cm: laminated algal, upper 5cm: rip-up clast	dolomite	shale on mound 6 has turned to chert	Limeport	Allentown
42	17	dark gray	fine	thinly bedded, shaly	dolomite	none	Limeport	Allentown
43	4	light gray	micrite	unconformity	dolomite	none	Limeport	Allentown
44	57	variable	medium	lower 30 cm: light gray, thickly bedded, solution breccia, upper 2-3 cm: dark gray, karstic	dolomite	1 cm thick stylolite on upper part of lower 30 cm is replaced by chert	Limeport	Allentown
45	4		fine	calcareous	shale	none	Limeport	Allentown
46	4			arenaceous, uneven, karstic	dolomite	none	Limeport	Allentown
47	3	medium gray	coarse	karstic	dolomite	none	Limeport	Allentown
48	19	medium gray	coarse	cross-bedded, large rip-up clasts on bottom	dolomite	none	Limeport	Allentown
49	10	dark gray	medium	finely algal laminated	dolomite	none	Limeport	Allentown
50	34	medium gray	medium	structureless	dolomite	none	Limeport	Allentown
51	13	medium gray	variable	lower 5 cm: finely laminated, medium-grained, next 3 cm: calcareous shale, upper 3 cm: quartz rich, arenaceous,	dolomite	none	Limeport	Allentown

				coarse-grained				
52	14	medium gray	coarse	steeply cross-bedded, arenaceous	dolomite	upper contact, undulatory stylolite (<1/2 cm), looks like shale or chert	Limeport	Allentown
53	35	medium gray	coarse	lower 20 cm: cross-bedded, quartz present, but unit is not a sandstone, upper 15 cm: rip-up clasts on top, evenly bedded	dolomite	none	Limeport	Allentown
54	40	dark gray	medium		dolomite	very cherty, occasional shards of black chert	Limeport	Allentown
55	29	medium gray	variable	lower 5 cm: very coarse-grained, cross-bedded, upper 2 cm of 5 cm: occasional large ooids, upper 7-13 cm: medium-grained, stylolites and algal (4 cm) evenly bedded	dolomite	none	Limeport	Allentown
56	48	medium gray	coarse	lower 7 cm: structureless, homogenous, 7-22 cm: very small ooids (storm deposit), 22-31 cm: thick accumulation of very large ooids, 31-48 cm: fine-grained, sporadic ooids	dolomite	none	Limeport	Allentown
57	57	medium gray		lower 15 cm: graded oolite, upper 42 cm: sporadic ooids, rather structureless	dolomite	none	Limeport	Allentown
58	22	medium gray	coarse	Recess Center: sporadic ooids	dolomite	none	Limeport	Allentown
59	21	medium gray	coarse	cross-bedded	dolomite	none	Limeport	Allentown
60	11	medium gray	coarse	oolitic, no structure (storm deposit)	dolomite	none	Limeport	Allentown
61	6	medium gray		sporadic ooids	dolomite	none	Limeport	Allentown
62	9		fine	very thinly bedded, fissile, calcareous	dolomite	none	Limeport	Allentown
63	17	very dark gray	fine	slightly more thickly bedded	shaly dolomite	none	Limeport	Allentown
64	13	dark	very	rip-up clasts, edge-	dolomite	none	Limeport	Allentown

		gray	coarse	wise conglomerates, some ooids				
65	23	medium gray	very coarse	very small and fine ooids, thinly bedded	dolomite	none	Limeport	Allentown
66	14	light gray	fine	algal laminated, slightly convex upward	dolomite	occasional clasts of chert	Limeport	Allentown
67	23	very light gray		stromatolitic, large convex mounds, 60 cm in diameter	dolomite	none	Limeport	Allentown
68	10	dark gray	coarse	Cross bedded, thinly bedded	dolomite	black, oolitic chert	Limeport	Allentown
69	29	light gray	fine	algal laminated, top bed is convex upward	dolomite	occasional clasts of chert	Limeport	Allentown
70	17	medium gray	medium	abundant rip-up clasts, algal structure	dolomite	none	Limeport	Allentown
71	16	medium gray	fine	laminated, algal stromatolite	dolomite	none	Limeport	Allentown
72	13	dark gray	coarse	cross-bedded, oolitic	dolomite	none	Limeport	Allentown
73	16	light gray	fine	large algal stromatolites, truncated upper surface	dolomite	thin beds of chert	Limeport	Allentown
74	17	dark gray	very fine	thin to thickly bedded, very shaly, calcareous shale on bottom of unit	dolomite	none	Limeport	Allentown
75	5	light gray	very fine	rip-up clasts	dolomite	none	Limeport	Allentown
76	43	medium gray	medium	stromatolitic, stylolite-bounded, convex surfaces within unit, upper surface truncated with abundant sulfides	dolomite	none	Limeport	Allentown
77	8	light gray	micrite	stromatolitic and convex upward	dolomite	none	Limeport	Allentown
78	32	dark gray	medium	oolitic, ooids increase in size towards top of unit, reverse grading, abundant sulfides	dolomite	none	Limeport	Allentown
79	14	dark gray	medium	oolitic, structureless	dolomite	none	Limeport	Allentown
80	10	dark gray	fine	algal laminated, sulfides	dolomite	none	Limeport	Allentown
81	22	medium gray		algal laminated, sulfides abundant at both contacts, rounded quartz clots	dolomite	none	Limeport	Allentown

				at bottom of unit, undulating scour surface at upper contact, enriched in sulfides				
82	21	light gray	micrite	algal stromatolites, 30 cm in diameter	dolomite	occasional chert clasts on upper contact	Limeport	Allentown
83	9	light gray	micrite	thinly bedded, laminated, stromatolites, upper contact enriched in sulfides	dolomite	none	Limeport	Allentown
84	41	medium gray	coarse	lower 3 cm: dolarenite, some cross-bedding, next 29 cm: medium grained, occasional ooids and sand grains, upper 9 cm: abundant ooids	dolomite	none	Limeport	Allentown
85	33	light gray	very coarse	lower 14 cm: evenly bedded, small ooids in layers, essentially horizontal, next 10 cm: evenly bedded, very large ooids, upper 7-9 cm: scattered large ooids, mostly very small ooids on top, stylolite and sulfide-bound, convex upward	dolomite	none	Limeport	Allentown
86	51	medium gray	coarse	oolitic, abundant stylolites, quartz clots, and sulfides at top of unit, horizontal bedding, no grading, upper 6 cm: much finer grained, truncated upper surface of bed (uneven)	dolomite	none	Limeport	Allentown
87	15	medium gray	coarse	coarse bedding, very large ooids, 6 cm from bottom, 1 cm thick algal lamination	dolomite	none	Limeport	Allentown
88	18	dark gray	coarse	ooids increase in abundance towards top of unit, scattered quartz clots	dolomite	none	Limeport	Allentown
89	27	dark gray	coarse	oolitic, scattered quartz clots,	dolomite	none	Limeport	Allentown

				abundant sulfides towards top of unit				
90	15	medium gray	coarse	oolitic, abundant rip-up clasts, sulfides, rhomb-shaped features that seem to have grown around ooids, evaporite clasts, quartz clots may be anhydrites	dolomite	none	Limeport	Allentown
91	28	dark gray	very coarse	oolitic, abundant sulfides, occasional rip-up clasts, upper contact is stylolite-bound and sulfide rich, occasional thin laminations	dolomite	scattered chert	Limeport	Allentown
92	25	light gray	coarse	storm surface, could also be a scour channel, possibly gastropod burrows, very oolitic, rip-up clasts, especially towards top of unit, sulfides very abundant towards top	dolomite	none	Limeport	Allentown
93	51		coarse	evenly bedded, oolitic with quartz clasts, stylolites and sulfides abundant, upper surface is stylolite-bound	dolomite	none	Limeport	Allentown
94	9	light gray	coarse	lower 4 cm: oolitic, evenly bedded, next 4 cm: oncolitic, upper 1 cm: pisoid-rich, gently undulating surface, upper surface a stylolite	dolomite	mid-4 cm: chert layer, oncoids are silicified	Limeport	Allentown
95	26	medium gray	medium	sparsely oolitic, some quartz clasts	dolomite	none	Limeport	Allentown
96	22	light gray	fine	algal laminated, convex upper surfaces 20 cm in diameter, occasional rip-up clasts, some hopper shaped structures, very finely laminated, shale partings at top	dolomite	none	Limeport	Allentown
97	25	light gray	micrite	algal stromatolites abundant towards lower 6 cm, stylolites and sulfides are	dolomite	none	Limeport	Allentown

				abundant				
98	30	variable	coarse	lower 12 cm: dark gray, remainder, light gray, very oolitic, some cross-beds, abundant sulfides on upper contact	dolomite	none	Limeport	Allentown
99	31	medium gray	coarse	very oolitic at base, actually oncolitic the whole bed, evaporite clasts abundant on upper surface, convex (60 cm diameter)	dolomite	none	Limeport	Allentown
100	15	medium gray	medium	stylolite-bounded, oncoid rich, abundant sulfides	dolomite	none	Limeport	Allentown
101	16	medium gray	fine	algal stromatolitic, domal variety (45 cm diameter)	dolomite	none	Limeport	Allentown
102	17	dark gray	very coarse	oolitic, quartz clots at base, sulfides common towards top of unit	dolomite	none	Limeport	Allentown
103	25	dark gray	coarse	oolitic, lower 10 cm: very oolitic, graded, thickly bedded, sulfide horizon on top, smaller and less abundant ooids towards top	dolomite	none	Limeport	Allentown
104	19	dark gray	coarse	lower 4 cm: fine-grained ooids, remainder: very large ooids and oncoids, coarsely bedded in places	dolomite	none	Limeport	Allentown
105	18	variable	variable	lower 5 cm: light gray, micritic, algal laminated, next 12 cm: medium gray, fine-grained, oolitic, abundant rip-up clasts	dolomite	upper 1 cm: oncolitic black chert	Limeport	Allentown
106	2	black	micrite		dolomite	none	Limeport	Allentown
107	14	dark gray	micrite	laminated, ooids at base (approximately 1 cm), no algal, grades upward	dolomite	none	Limeport	Allentown
108	7	dark gray	micrite	pinches and swells, finely laminated	dolomite	none	Limeport	Allentown

109	5	black	fine	fissile, very finely laminated	shaly dolomite	none	Limeport	Allentown
110	20	dark gray	micrite	finely laminated, grades upward	dolomite	none	Limeport	Allentown
111	5	medium gray	fine	laminated, grades upward	dolomite	none	Limeport	Allentown
112	5	medium gray		finely laminated, some cross-bedding and truncation	dolomite	none	Limeport	Allentown
113	50	dark gray	coarse	oolitic, lower 30 cm: oncoids, upper 20 cm: ooids, stylolite-bounded, fining-upward sequence, very sulfide rich	dolomite	none	Limeport	Allentown
114	39	dark gray	coarse	oolitic, lower 7 cm: rip-up clasts, upper 10 cm: fragments achieve pisoid-size	dolomite	upper 32 cm: scattered oncoids turned to chert, ooids still chert, upper 5 cm: oncolitic black chert, pinches and swells	Limeport	Allentown
115	15	light gray	medium	large, convex, algal stromatolites (45 cm diameter), oolitic, abundant sulfides	dolomite	scattered chert at top	Limeport	Allentown
116	28	light gray	micrite	stylolites and sulfides throughout	dolomite	none	Limeport	Allentown
117	13	medium gray	very coarse	upper 5 cm: pisoid-size	dolomite	oncolitic chert	Limeport	Allentown
118	51	light gray	coarse	oolitic with large domal algal stromatolites (70 cm diameter)	dolomite	chert seams at top of bed	Limeport	Allentown
119	32	dark gray	fine	oolitic, large domal algal stromatolites (50 cm diameter)	dolomite	none	Limeport	Allentown
120	24	dark gray	medium	oolitic, upper surface very fine shaly partings	dolomite	none	Limeport	Allentown
121	75	light gray	fine	stromatolitic, convex mounds (50 cm diameter)	dolomite	none	Limeport	Allentown
122	17	dark gray	coarse	oolitic	dolomite	none	Limeport	Allentown
123	19	light gray	micrite	stromatolitic (30 cm diameter)	dolomite	none	Limeport	Allentown
124	33	medium gray	medium	finely oolitic, upper 1 cm, black shaly partings at top, convex upward	dolomite	none	Limeport	Allentown
125	15	medium gray	medium	ooltic, convex upward	dolomite	none	Limeport	Allentown

126	8	medium gray	very fine	algal laminated	dolomite	none	Limeport	Allentown
127	9	medium gray	medium	oolitic with laminated algal stromatolites	dolomite	none	Limeport	Allentown
128	25	dark gray	medium	oolitic	dolomite	none	Limeport	Allentown
129	12	dark gray	medium	oolitic	dolomite	none	Limeport	Allentown
130	6	medium gray	very coarse	oncolitic, top bed: stylolitized surface, abundant sulfides	dolomite	none	Limeport	Allentown
131	28	medium gray	micrite	finely algal laminated, upper surface has stylolites and sulfides	dolomite	none	Limeport	Allentown
132	18	dark gray	very coarse	sulfides and stylolites abundant towards top	dolarenite	none	Limeport	Allentown
133	13	light gray	very coarse	rip-up clasts	dolomite	none	Limeport	Allentown
134	60	variable	variable	lower 25 cm: medium gray, coarse-grained, cross-bedded, oolitic; 5 cm: light gray, very coarse-grained, oolitic; 10 cm: medium gray, coarse-grained, oolitic, coarsely bedded; 9 cm: medium gray, medium-grained, oolitic, abundant rip-up clasts	dolomite	next 7 cm: medium gray, medium-grained, oolitic, rip-up clasts, coarsely bedded, upper 4 cm: medium gray, coarse-grained, oolitic, rip-up clasts, quartz clots, stylolite-bounded on top surface.	Limeport	Allentown
135	42	medium gray	medium	oolitic, coarsely bedded	dolomite	none	Limeport	Allentown
136	5	light gray	very fine	algal laminated	dolomite	none	Limeport	Allentown
137	65	medium gray	medium	oolitic, lower 10-15 cm: lenses of micrite (may be algal), clots of quartz, lower 7 cm: rip-up clasts made of micrite	dolomite	none	Limeport	Allentown
138	10	medium gray	coarse	rip-up clasts and fine algal laminations	dolomite	lower 2 cm: chert	Limeport	Allentown
139	47	medium gray	coarse	oolitic, graded bedding, fining-upward sequence	dolomite	none	Limeport	Allentown
140	12	medium gray	coarse	oolitic, rip-up clasts	dolomite	none	Limeport	Allentown
141	25	medium	coarse	oolitic	dolomite	none	Limeport	Allentown

		gray						
142	57	medium gray	medium	oolitic, occasional algal stromatolites	dolomite	none	Limeport	Allentown
143	20	medium gray	medium	oolitic	dolomite	none	Limeport	Allentown
144	6	dark gray	medium	oolitic with algal stromatolites	dolomite	none	Limeport	Allentown
145	23	medium gray	medium	oolitic	dolomite	none	Limeport	Allentown
146	19	medium gray	medium	oolitic	dolomite	none	Limeport	Allentown
147	55	medium gray	medium	lower 10 cm: large rip-up clasts made of micrite, oolitic	dolomite	none	Limeport	Allentown
148	17	medium gray	coarse	lower 10 cm: very small, abundant ooids, upper 1 cm: algal stromatolites, still micritic	dolomite	none	Limeport	Allentown
149	6	medium gray	medium	abundant ooids and rip-up clasts	dolomite	none	Limeport	Allentown
150	56	variable	variable	lower 6 cm: medium gray, oolitic, next 11 cm: light gray, very micritic, algal laminated, next 7 cm: medium gray, coarse-grained, arenaceous, evenly bedded, next 13 cm: medium gray, coarse-grained, abundant rip-up clasts and quartz grains	dolomite	upper 19 cm: medium gray, very coarse-grained, mildly cross-bedded, algal laminated, may have overturned algal, unconformable upper surface	Limeport	Allentown
151	19	very dark gray	very coarse	no visible structures, stylolite-bound lower contact	dolomite	none	Limeport	Allentown
152	6	medium gray	coarse	rip-up clasts	dolomite	none	Limeport	Allentown
153	8	dark gray	coarse	structureless, may be some fine parallel bedding	dolomite	none	Limeport	Allentown
154	7	light gray	fine	finely algal laminated, some rip-up clasts, very close to sea level	dolomite	none	Limeport	Allentown
155	74	medium gray	medium	evenly bedded	dolomite	none	Limeport	Allentown
156	32	medium gray	medium	upper 8 cm: cross-bedded	dolomite	none	Limeport	Allentown
157	10	medium gray	fine	algal laminated	dolomite	none	Limeport	Allentown

158	14	dark gray	micrite	algal laminated	dolomite	none	Limeport	Allentown
159	10	black	micrite	calcareous, algal laminations	shaly dolomite	none	Limeport	Allentown
160	7	black	fine	calcareous, extremely fissile	shale	none	Limeport	Allentown
161	49	light gray	very fine	algal laminated, birds-eye structures (possible evaporite structures), abundant mud cracks, has a ridge-like structure (more resistant, may be a sand layer)	dolomite	none	Limeport	Allentown
162	40	variable	variable	lower unit: medium gray, medium-grained, abundant fine-grained quartz sand grains, ooids and intraclasts at upper contact of lower unit; upper unit: light gray, fine-grained, algal laminated	dolomite	none	Limeport	Allentown
163	26	dark gray	fine	algal laminated, convoluted round surface, like a micrite with a high shale content, bubbly unit	dolomite	none	Limeport	Allentown
164	46	light gray	very fine	algal laminated	dolomite	none	Limeport	Allentown
165	4	dark gray	coarse	arenaceous	dolarenite	none	Limeport	Allentown
166	13	medium gray	medium	algal stromatolite rich, lower 5 cm: small domes (15 cm diameter)	dolomite	none	Limeport	Allentown
167	11	black	fine	calcareous, very fissile	shale	none	Limeport	Allentown
168	26	medium gray	very fine	laminated	shaly dolomite	none	Limeport	Allentown
169	40	variable	variable	lower 13 cm: medium gray, medium-grained, finely laminated, abundant quartz grains, upper 1 cm: pure quartz lens; upper unit: light gray, micritic	dolomite	none	Limeport	Allentown

170	51	light gray	very coarse	cross-bedded, few rip-up clasts, quartz clots and sulfides, lower 28 cm: extremely cross-bedded, more quartz grains, upper unit: oolitic, no cross-bedding, may be storm deposit	dolomite	none	Limeport	Allentown
171	15	medium gray	micrite		dolomite	none	Limeport	Allentown
172	48	medium gray	coarse	lower 9 cm: graded ooids, next 4 cm: algal laminated, micrite; remainder: structureless oolite, towards upper contact, pure sand lens (2-3 cm)	dolomite	none	Limeport	Allentown
173	25	variable	variable	lower 9 cm: medium gray, coarse-grained, rubbly, next 11 cm: micritic, upper 5 cm: medium gray, very coarse-grained, arenaceous	dolomite	none	Limeport	Allentown
174	33	dark gray	medium	oolitic	dolomite	none	Limeport	Allentown
175	75	medium gray	coarse	oolitic, lower 20 cm: oncoid zone	dolomite	lower 20 cm: cherty	Limeport	Allentown
176	90	medium gray	medium	mildly cross-bedded, coarsely bedded, oolitic, abundant sulfides at base and stylolites mid-unit, upper 19 cm: oncoidal and pisoidal, coarsening upward sequence	dolomite	none	Limeport	Allentown
177	53	medium gray	medium	oolitic, upper 14 cm: algal stromatolite-rich, at base, 1 cm: shale seem and stylolite surface	dolomite	none	Limeport	Allentown
178	8	dark gray	fine	algal laminated	dolomite	none	Limeport	Allentown
179	14	black	fine	upper 4 cm: calcareous	shaly dolomite	none	Limeport	Allentown
180	61	medium gray	medium	oolitic, lower 12 cm: finely bedded, next 3 cm: black shale partings, next 18 cm: very small ooids,	dolomite	none	Limeport	Allentown

				finely bedded, remainder: large ooids, color darkens, cross-bedding				
181	41	medium gray	coarse	oolitic, graded, upper contact: sulfides and stylolites	dolomite	ooids partially replaced by chert	Limeport	Allentown
182	40	dark gray	medium	oolitic, coarsening upward sequence, especially upper 15 cm	dolomite	none	Limeport	Allentown
183	22	medium gray	medium	abundant floating sand-grains, bands of ooids running through unit, ripped up algal stromatolites and clasts, upper 4 cm: very shaly, dark gray	dolomite	occasional ooids replaced by chert	Limeport	Allentown
184	105	medium gray	medium	quartz clots mid-section, abundant stylolites, lower 24 cm: cross-bedding, coarsely-grained, arenaceous	dolomite	none	Limeport	Allentown
185	95	dark gray	medium	ooids and sand grains, upper 35 cm: domal algal stromatolites (20 cm diameter), abundant ooids and sand grains	dolomite	none	Limeport	Allentown
186	28	medium gray	medium	oolitic, upper 35 cm: domal algal stromatolites (20 cm diameter), abundant ooids and sand grains	dolomite	none	Limeport	Allentown
187	63	medium gray	medium	lower 15 cm: algal laminated, upper 15 cm: rip-up clasts and graded ooids	dolomite	none	Limeport	Allentown
188	39	medium gray	coarse	lower 3 cm: pure oolite, next 6 cm: algal laminated, micrite, abundant quartz sand grains, mildly cross-bedded, upper 13 cm: micritic, capped by stylolite seam and 1 cm thick black quartz grain unit	dolomite	none	Limeport	Allentown
189	18	medium gray	medium	oolite with abundant quartz grains	dolomite	none	Limeport	Allentown

190	40	medium gray	medium	lower surface: stylolite-bound with sulfides, cross-bedded, lower 20 cm: mildly cross-bedded, abundant quartz grains, next 13 cm: slightly lighter gray, upper 5 cm: abundant quartz grains and ooids	dolomite	none	Limeport	Allentown
191	7		very coarse	abundant rip-up clasts and quartz grains	dolomite	none	Limeport	Allentown
192	6	dark gray	coarse	very coarsely bedded, oolitic with abundant sand grains	dolomite	none	Limeport	Allentown
193	38	medium gray	medium	oolitic	dolomite	none	Limeport	Allentown
194	51	dark gray	very coarse	graded oolite, 20-35 cm: becomes oncoidal, 35-45 cm: pisoidal, upper 11 cm: scattered pisoids in ooid bed	dolomite	none	Limeport	Allentown
195	10	medium gray	coarse	oolitic	dolomite	none	Limeport	Allentown
196	13	medium gray	coarse	oolitic	dolomite	none	Limeport	Allentown
197	34	medium gray	medium	coarsely bedded, upper 12 cm: algal laminated	dolomite	none	Limeport	Allentown
198	65	dark gray	medium	oolitic, mildly cross-bedded towards top of bed, ooids increase in size and abundance towards top of bed	dolomite	none	Limeport	Allentown
199	45	medium gray	medium	very oolitic towards top, upper 10 cm: very oolitic	dolomite	none	Limeport	Allentown
200	9	medium gray	medium	oolitic	dolomite	none	Limeport	Allentown
201	31	light gray	medium	oolitic	dolomite	none	Limeport	Allentown
202	50	dark gray	medium	cross-bedded, oolitic	dolomite	none	Limeport	Allentown
203	31	medium gray	medium	graded bedding, oolitic, could be fossil?	dolomite	none	Limeport	Allentown
204	36	dark gray		very oolitic	dolomite	none	Limeport	Allentown
205	33	medium gray	coarse	coarsely bedded, oolitic, lower 10 cm:	dolomite	none	Limeport	Allentown

				very large oncoids and intermediate algal stromatolites				
206	30	medium gray	coarse	oolitic, intermittent algal	dolomite	none	Limeport	Allentown
207	22	medium gray	coarse	oolitic with intermittent algal stromatolites	dolomite	none	Limeport	Allentown
208	22	medium gray	coarse	oolitic with intermittent algal stromatolites	dolomite	none	Limeport	Allentown
209	35	medium gray	coarse	oolitic with large algal stromatolites (20 cm diameter)	dolomite	none	Limeport	Allentown
210	18	medium gray	medium	scattered ooids, occasional algal stromatolites	dolomite	none	Limeport	Allentown
211	31	medium gray	medium	scattered ooids, algal laminations	dolomite	none	Limeport	Allentown
212	13	medium gray	medium	oolitic	dolomite	none	Limeport	Allentown
213	56	medium gray	coarse	lower 9 cm: oolitic, occasional rip-up clasts, abundant stylolites; remainder of unit: abundant shale partings and stylolites	dolomite	none	Limeport	Allentown
214	53	medium gray	coarse	oolitic with cross-bedding, lower 10 cm: oncoid rich	dolomite	none	Limeport	Allentown
215	84	light gray	coarse	oolitic, graded throughout, upper 30 cm: domal algal stromatolites	dolomite	none	Limeport	Allentown
216	68	medium gray	medium	lower 16 cm: lower 4 cm are oncoid rich, next 12 cm: very fine, algal laminated, next 1 cm: bedded ooids, next 5 cm: algal laminations, remainder of unit: graded ooids, static	dolomite	none	Limeport	Allentown
217	83	medium gray	medium	lower 50 cm: evenly bedded, 50-66 cm: light gray, slightly finer grained, abundant algal and large ooids, remainder of unit: extremely fine-grained, algal laminated, cross-	dolomite	at 50 cm: chert clasts in stylolites seams	Limeport	Allentown

				bedded, ooids				
218	28	medium gray	medium	occasional quartz grains	dolomite	none	Limeport	Allentown
219	17	medium gray	very fine	laminated, algal-rich, occasional ooids	dolomite	none	Limeport	Allentown
220	35	medium gray	coarse	oolitic with large intraclasts of micrite, ooids coarsen upwards, upper 10 cm: rip-up clasts extremely abundant	dolomite	none	Limeport	Allentown
221	52	light gray	medium	lower 9 cm: very shaly, very micritic, remainder of unit: evenly bedded, fine laminations, abundant stylolites, sulfides abundant toward top of unit.	dolomite	none	Limeport	Allentown

B.2 – CANAL ROAD SECTION

Canal Road Section, Sussex County, New Jersey								
Bed	**Thickness (cm)**	**Color**	**Grain Size**	**Bedding**	**Lithology**	**Chert**	**Member**	**Formation**
Bucky Lane Traverse								
1	70	dark gray	micrite	algal laminated, domal algal (150 cm. diameter), several very thin shaly dolomite units (1-5 cm thick) toward top of unit, very sulfurous	dolomite	5 chert layers are within algal structures, black, homogeneous, opaque, occurs as nodules, clots, and beds		Upper Allentown
2	35	medium gray	fine	algal laminated, upper 8 cm: very finely spaced, abundant algal laminations, sand lenses, flaggy, upper contact very sharp, appears to be disconformity	dolomite	upper 20 cm: abundant chert, occurs as biconvex lentils and pods, black centers with white rinds, some become entirely light gray, chert pods (up to 40 cm diameter)		Upper Allentown
3	50	very dark gray	micrite	algal laminated, upper contact sharp, but uneven, could be disconformity	dolomite	none		Upper Allentown
4	70	dark gray	micrite	lower 20 cm: contains abundant quartz vugs up to 3 cm. wide, upper bed surface uneven, sharp and convex/concave (undulations), each concavity up to 60 cm wide, upper contact very sharp	dolomite	none		Upper Allentown
5	30	dark gray	medium	algal laminated, uneven but sharp contacts	dolomite	25 cm from base: thin, gray chert seam, also occurs as thin clasts, nodules and wisps		Upper Allentown
6	12	medium gray	medium	finely algal laminated, uneven but sharp contacts	dolomite	none		Upper Allentown
7	5	light gray	medium	algal laminated	dolomite	none		Upper Allentown

8	15	dark gray	micrite	algal laminated, lower contact hummocky	dolomite	none		Upper Allentown
9	20	dark gray	micrite	very finely algal laminated	dolomite	upper 10 cm: chert occurs as nodules (5-20 cm diameter).		Upper Allentown
10	65	very dark gray	micrite	algal laminated, lower 20 cm: quartz vugs (2 cm diameter), upper 20 cm: quartz vugs (up to 5 cm diameter)	dolomite	chert lenses and pods, chert occurs as fracture infillings (5-30 cm diameter, 5-20 cm thick).		Upper Allentown
11	50	medium gray	micrite	highly sulfurous, algal laminated, upper 10 cm: fairly continuous seams of quartz, above seam, quartz vugs (2-3 cm diameter), all are hollow	dolomite	chert occurs as thin lenses and pods (30-40 cm in diameter) about 20 up from base, chert is black and charcoal gray		Upper Allentown
12	60	light gray	very coarse	highly sulfurous, swamp-like facies, lower 12 cm: discontinuous and continuous quartz vugs (1-50 cm diameter), above vugs, bed becomes porous, burrow marked, especially upper 20 cm, algal laminations uncommon	dolomite	none		Upper Allentown
13	140	variable	variable	lower 40 cm: algal laminated, upper 20 cm: great concentration of quartz vugs (up to 20 cm. diameter), upper 100 cm: dark gray, micritic, few algal laminations, sharp upper bed contact, mid 30 cm of 100: medium gray, micrite, upper contact sharp	dolomite	none		Upper Allentown
14	100	variable	variable	lower unit: dark gray, micrite, algal laminated, creates convex surface (40 cm diameter), upper unit, medium gray, coarse-	dolomite	none		Upper Allentown

				grained, lower 70 cm: very heavily algal laminated with convex algal, upper 30 cm: more swamp-like facies				
15	50	medium gray	medium	occasional algal laminations, castilated upper bed surface	dolomite	none		Upper Allentown
16	45	variable	variable	algal laminated, lower 20 cm: light gray, coarse-grained, upper section, fine-grained, dark gray, occasional sand lenses toward top.	dolomite	none		Upper Allentown
17	45	very dark gray	micrite	algal laminated, sharp, uneven upper contact	dolomite	none		Upper Allentown
18	65	medium gray	fine	finely algal laminated, upper 20 cm: more concentrated in algal, upper contact castilated	dolomite	40 cm from base: 2 very thin chert horizons, chert occurs as clots and thin wisps (1-5 cm thick) up to 20 cm of diameter		Upper Allentown
19	60	medium gray	coarse	sulfurous, algal laminated	dolomite	lower 40 cm: 4 distinct chert beds (2-4 cm thickness, 1-40 cm width), convex upward and surrounded by wisps, clots and spider webs of chert. Chert is homogenous, black, opaque to gray or translucent black, 25 cm of broken angular chert fragments		Upper Allentown
20	60	very dark gray	micrite	algal laminated, very sulfurous	dolomite	none		Upper Allentown
21	20	medium gray	medium	algal laminated	dolomite	none		Upper Allentown
22	80	medium gray	coarse	sulfurous, occasional algal laminations	dolomite	none		Upper Allentown

23	75	dark gray	micrite	algal laminated, sulfurous, mid-unit (40 cm thick): filled with quartz vugs up to 20 cm in diameter, extremely coarse-grained, unit above mid-portion is medium gray, fine-grained, and very algal laminated	dolomite	at base of unit: thin wisps of chert (1-5 cm thick, 50 cm diameter)		Upper Allentown
24	70	medium gray	medium	highly sulfurous, algal laminated	dolomite	none		Upper Allentown
25	45	light gray	medium /coarse	algal laminated	dolomite	none		Upper Allentown
26	90	medium gray	micrite	sulfurous, upper 40 cm: extremely algal laminated, contains abundant quartz vugs	dolomite	none		Upper Allentown
Total (cm):	1427							
Total (m):	14.27							
Total (ft):	46.8							
Appalachian Trail Outcrop								
27	30	dark gray	micrite	finely algal laminated, sharp upper contact	dolomite	none		Upper Allentown
28	25	dark gray	micrite	finely algal laminated, sharp upper contact	dolomite	none		Upper Allentown
29	20	dark gray	micrite	finely algal laminated, sharp upper contact	dolomite	none		Upper Allentown
30	15	dark gray	micrite	finely algal laminated, sharp upper contact	dolomite	none		Upper Allentown
31	50	medium /dark gray	micrite	2.5-3 cm thick sand layers running throughout, mid-unit, 7 cm thick sand unit, upper 2 cm: 5 cm thick sand layer, upper 5 cm: algal laminations	dolomite	none		Upper Allentown
32	50	very dark gray	micrite	laced with countless numbers of sand layers, bedding controlled by algal laminations	dolomite	none		Upper Allentown
33	50	dark gray	micrite	algal laminated, 2-3 cm thick sand layers, evidence of cross-	dolomite	base of unit: chert seam (1 cm thick),		Upper Allentown

				beds, quartz vugs throughout		seam has floating quartz grains		
34	20	dark gray	micrite	algal laminated, 2-3 cm thick sand layers, evidence of cross-beds, quartz vugs throughout	dolomite	none		Upper Allentown
35	50	dark gray	micrite	floating quartz sand throughout	dolomite	at base: occasional chert seams replacing quartz grains		Upper Allentown
36	30	medium gray	coarse	arenaceous, quartz sand throughout, no sense of structures, upper beds convex, no sign of algal	dolomite	none		Upper Allentown
37	45	medium gray	coarse	arenaceous, quartz sand throughout, no sense of structures, upper beds convex, no sign of algal, upper 20 cm: abundant quartz vugs up to 5 cm diameter	dolomite	none		Upper Allentown
38	45	dark gray	micrite	abundant wisp of quartz sand, lower 20 cm: quartz vugs up to 2 cm diameter, upper 20 cm: quartz vugs and stringers up to 30 cm diameter	dolomite	none		Upper Allentown
39	100	dark gray	micrite	algal laminated, occasional sand lenses, upper beds flaggy, divided into 10 9 cm beds, extremely medium dark gray/blue, coarse-grained, saccharoidal, sulfurous (could be Baby Swamp or Markist beds), abundant tangential cross beds throughout unit.	dolomite	none		Upper Allentown
40	75	dark gray	micrite	lower 25 cm: abundant quartz sand layers, upper 50 cm: abundant algal laminations, very thin sand lenses, quartz vugs (5 cm diameter)	dolomite	upper 10 cm: chert occurs as clots and fracture-infillings (1 cm thick), gray, pinches out after 40		Upper Allentown

						cm, also occurs as occasional pods (3cmX20cm), dark gray to black, abundant quartz sand grains		
41	100	dark gray	micrite	algal laminated, sharp uneven contacts, lower 60 cm: abundant algal laminations, upper 15 cm of lower 60 cm: abundant quartz vugs (1 cm. diameter)	dolomite	abundant chert as clots and fracture-infillings on lines with quartz stringers (15-20 cm diameter)		Upper Allentown
42	55	very dark gray	micrite	algal laminated, abundant quartz vugs and clots (10 cm diameter)	dolomite	top of unit: black chert (5 cm thick), homogenous, opaque, seams up to 100 cm wide		Upper Allentown
43	70	medium gray	coarse	occasional algal laminations, scattered quartz vugs (1 cm diameter)	dolomite	none		Upper Allentown
44	30	very dark gray	micrite		dolomite	none		Upper Allentown
45	55	dark gray	micrite	abundant algal laminations	dolomite	none		Upper Allentown
46	25	medium gray	medium	floating quartz sand, cross-bedding, vugs (up to 10 cm. diameter) filled with large euhedral quartz crystals	dolomite	none		Upper Allentown
47	35	medium gray	medium	arenaceous, floating quartz sand, cross-bedding	dolomite	none		Upper Allentown
48	15	medium gray	medium	arenaceous, floating quartz sand, 20 cm vugs filled with quartz crystals, weathers a distinct dark gray	dolomite	top of unit: chert seams (10 cm diameter), dark gray with lighter colored rind, seems to replace quartz sand		Upper Allentown
49	38	very dark	micrite	algal laminated, occasional floating	dolomite	none		Upper Allentown

		gray		quartz grains, quartz sand lenses at top of unit, quartz vugs and stringers				
50	80	dark gray	fine	highly sulfurous, upper 50 cm: contains quartz vugs, weathers to a punky, worm burrowed look, some algal laminations at bottom of unit	dolomite	none		Upper Allentown
51	125	very light gray	micrite	upper 40 cm: algal laminated	dolomite	at base of algal laminations: discontinuous seam of black chert (40X5 cm), opaque, in some places looks folded		Upper Allentown
52	170	variable	variable	lower 20 cm: dark gray, micrite, finely algal laminated, highly sulfurous, 21-45 cm: very dark gray, micrite,algal laminations, convex upward, punky, worm-burrowed weathering, next 80 cm: extremely dark gray, micrite, occasional quartz vugs throughout,	dolomite	none		Upper Allentown
Appalachian Trail # 2: Cross Bed Location								
53	80	dark gray	micrite	abundant sand lenses and algal laminations, sharp upper contact	dolomite	none		Upper Allentown
54	85	very dark gray	fine	abundant algal laminations and quartz sand lenses, layers	dolomite	none		Upper Allentown
55	90	dark gray	very coarse	8 or 9 10 cm beds: fetid, algal laminations, signs of cross-bedding, hummocky upper contact, upper 10 cm: abundant quartz seams	dolomite	none		Upper Allentown
56	80	dark gray	coarse	sulfurous, arenaceous, abundant cross-beds throughout, upper 25 cm: cross-beds diminish and burrows increase in frequency	dolomite	none		Upper Allentown

57	85	variable	micrite	fetid, lower 20 cm: 4 beds, dk gray, 2 cm quartz sand layers, next 10 cm: very dk gray, algal, uneven, sharp upper contact with black shale partings, next 35-40 cm: very dk gray, algal lams, shale partings, 8 quartz sand layers (2 cm thick), cut-n-fill	dolomite	none		Upper Allentown
58	20	charcoal gray/ black	fine	very thinly bedded, flaggy, uneven bedding surfaces (pinch and swell), may even have some sandy units	shaly dolomite	none		Upper Allentown
59	130	dark gray	variable	lower 70 cm: fetid, micrite, abundant algal laminations, upper 60 cm: medium-grained, sulfurous, flat algal laminations, top 30 cm: convex/concave algal	dolomite	unit topped by black, homogenous, opaque to translucent chert that follows contact of upper algal surface.		Upper Allentown
60	55	medium gray	coarse	fetid, uneven upper surface, almost castilated, sparse algal laminations, occasional floating quartz sand grains	dolomite	none		Upper Allentown
61	40	dark gray	micrite	finely algal laminated, sharp upper bed contact	dolomite	none		Upper Allentown
62	25	dark gray	micrite	finely algal laminated, sharp upper bed contact	dolomite	none		Upper Allentown
63	40	medium gray	coarse	arenaceous, abundant algal laminations in lower half of unit, floating sand grains, 5 cm. thick quartz sand lenses at top of unit.	dolomite	none		Upper Allentown
64	45	light gray	coarse	highly sulfurous, abundant quartz sand lenses in lower half of unit	dolomite	chert seams (50 cm diameter), possibly replacing quartz sand, pinch and swell.		Upper Allentown

65	100	very dark gray	medium to fine	upper 20 cm: quartz sand lenses, occasional algal laminations throughout	dolomite	none		Upper Allentown
66	70	very dark gray	micrite	finely algal lamination throughout, quartz vugs scattered throughout lower half of unit, concentrated into seam mid-unit (5 cm thick).	dolomite	none		Upper Allentown
67	30	medium gray	medium	fetid	dolomite	top of unit: (5X50cm) chert seam		Upper Allentown
68	20	very dark gray	micrite	fetid, wisps of quartz sand lenses and abundant algal laminations (restricted to top of unit)	dolomite	none		Upper Allentown
69	180	medium gray	medium	burrow structures and occasional quartz vugs, upper half of unit: concentration of quartz vugs (5 cm thick) and burrows.	dolomite	none		Upper Allentown
Canal Road Quarry Section								
70	25	medium gray	fine	some algal partings	dolomite	none		Upper Allentown
71	25	dark gray	micrite		dolomite	none		Upper Allentown
72	17	medium gray	micrite		dolomite	none		Upper Allentown
73	10	dark gray	micrite	flaggy, signs of discontinuities or rip-up clasts	shaly dolomite	none		Upper Allentown
74	15	battleship gray	micrite		dolomite	none		Rickenbach Formation
75	45	dark gray	medium	algal laminated, sharp upper contact	dolomite	none		Rickenbach Formation
76	30	medium gray	micrite	occasional algal partings, 1 cm. thick shale unit at base of bed	dolomite	none		Rickenbach Formation
77	50	dark gray	micrite	lower 15 cm: Crooked Swamp like: brecciated, burrowed/ripped-up, stylolite surface in middle, lower 5 cm: quartz sand lenses followed by intermediate quartz sand lenses between dolomite, next 22	dolomite	upper 5 cm: quartz sand and shale partings which are replaced by chert along strike		Rickenbach Formation

				cm: thick quartz sand lenses, upper 20 cm: algal lam				
78	70	medium gray	coarse	upper 25 cm: wisps and layers of quartz sand and occasional algal and quartz vugs	dolomite	none		Rickenbach Formation
79	25	dark gray	medium	sulfurous	dolomite	none		Rickenbach Formation
80	50	medium gray	coarse		dolomite	none		Rickenbach Formation
81	115	variable	variable	lower 40 cm: dark gray, micrite, algal laminated, next 17 cm: medium gray, micrite, fetid, next 40 cm: medium gray, medium-grained, finely algal laminated, upper 5 cm: very closely spaced algal, domal algal (10X50 cm) convex/concave contact	dolomite	none		Rickenbach Formation
82	30	very dark gray	micrite	finely algal laminated, lower 10 cm: floating quartz sand, upper 10 cm: abundant quartz sand lenses, horizontal burrows	dolomite	none		Rickenbach Formation
83	20	very dark gray	micrite	convex upward surface, fine algal laminations	dolomite	abundant, very small, angular chert fragments (1 cm. diameter)		Rickenbach Formation
84	70	medium gray	coarse	fetid, lower 20 cm: fine algal laminations and wisps of quarts sand, Crooked Swamp-type: extremely coarse-grained, medium gray, fetid	dolomite	upper 50 cm: broken clots of translucent, opaque, navy blue/black chert, lower 2 or 3 beds, largely intact, chert replaced algal, very thick chert unit, brecciated, overturned, upper part of bed: 25 cm of		Rickenbach Formation

						broken chert lenses and beds: dilation breccia		
85	15	dark charcoal gray	micrite	abundant quartz sand layers	dolomite	none		Rickenbach Formation
86	15	dark gray	micrite	occasional algal laminations	dolomite	none		Rickenbach Formation
87	20	nearly black	micrite	fetid, sharp contacts, abundant algal laminations, floating quartz sand grains	dolomite	none		Rickenbach Formation
88	30	blue/gray	micrite	abundant algal laminations, lower bedding contact sharp and appears to have shale partings	dolomite	upper contact: 5 cm chert bed containing abundant quartz sand grains, grades into quartz sand at lower contact, convex upward, fills cut-n-fill channels at lower portion		Rickenbach Formation
89	30	light gray	very coarse	Crooked Swamp-like, fetid, lower surface, abundant rip-up clasts for 10 cm of lower portion of bed, burrow infillings, shale partings	dolomite	wispy, gray, laminated chert, seems to replace rip-up clasts and burrows, (5X10 cm), 10 cm above base of wispy chert is another wispy chert (3X5cm)		Rickenbach Formation
90	30	blue/gray	very coarse	fetid, algal laminated, lower 10 cm: Crooked Swamp dolomite, quartz sand lenses abundant, upper 20 cm: finely algal laminated, micrite, abundant quartz vugs up to 10 cm in diameter, sharp upper contact	dolomite	pinch and swell chert pods (10X5cm)		Rickenbach Formation
81	50	dark gray	medium /fine	fetid, lower 10 cm: quartz sand lenses, upper 20-30 cm: abundant quartz	dolomite	scattered chert wisps		Rickenbach Formation

				vugs (2cm diameter), top: large open vugs with euhedral quartz crystals, bottom of bed has black shale partings				
Sunshower Location								
92	15	charcoal gray	micrite		dolomite	none		Rickenbach Formation
93	40	medium gray	medium	algal laminated, concave/convex upper bedding	dolomite	none		Rickenbach Formation
94	35	dark gray	micrite	algal laminated, concave/convex upper bedding, burrowing in upper surface (10 cm wide)	dolomite	none		Rickenbach Formation
95	10	dark gray	micrite	algal laminated, concave/convex contacts	dolomite	none		Rickenbach Formation
96	25	very dark gray	micrite	occasional algal laminations, upper surface has shale partings, 3 cm cut-n-fill quartz sand lenses.				Rickenbach Formation
97	60	variable	micrite	lower 15 cm: dark charcoal gray, algal laminated, next 20 cm: medium/dark gray, upper 25 cm: abundant stylolite surfaces, occasional quartz vugs, algal filament, and abundant quartz sand stringers	dolomite	none		Rickenbach Formation
98	15	variable	micrite	lower 15 cm: dark charcoal gray, algal laminated, next 20 cm: medium/dark gray, upper 25 cm: abundant stylolite surfaces, occasional quartz vugs, algal filament, and abundant quartz sand stringers	dolomite	none		Rickenbach Formation
99	40	medium gray	medium /coarse	lower 20 cm: abundant quartz vugs (1 cm diameter), upper 20	dolomite	upper shale lenses; 2 cm thick chert		Rickenbach Formation

				cm: abundant sand lenses, upper 8 cm: sand lenses, quartz sand floats, lenses, rip-up clasts, top of unit: shale lenses				
100	105	variable	variable	lower 20 cm: medium gray, medium-grained, next 40 cm: interbedded algal laminations and burrow horizons, next 45 cm: dark gray, very coarse-grained, burrowed dolomite, upper 10 cm: extensive burrowing, also lined with shale partings.	dolomite	none		Rickenbach Formation
101	90	dark gray	medium	extremely sulfurous, algal laminated, upper 10 cm: deeply burrowed	dolomite	upper surface: shale partings replaced by chert		Rickenbach Formation
102	40	medium gray	medium /fine	fetid, lower 20 cm: rip-up clasts, burrows, 5 cm or more of floating quartz sand lenses, remainder, finely laminated, micrite with algal laminations	dolomite	lower 20 cm: between 5-10 cm in bed, great concentrations of chert fragments (>1 cm diameter)		Rickenbach Formation
103	40	medium gray	medium	lower 10 cm: algal laminated, floating quartz sand lenses, next 20 cm: algal laminated dolomite, lower 10 cm of 20 cm: floating sandstone grains and lenses, above 10 cm: coarse-grained, fetid, abundant algal laminations	dolomite	lower 10 cm of 20 cm interval: occasional algal replaced by chert (1-2 cm thickX10 cm wide)		Rickenbach Formation
104	20	medium gray	very coarse	Crooked Swamp-like, sharp upper bed contact	dolomite	brecciated chert: lower 10 cm: 2 distinct cherts replacing algal (5 cm thick), continuous, remaining 10 cm: black and		Rickenbach Formation

						gray, opaque to translucent, angular chert fragments		
105	40	dark gray	micrite	algal laminated	dolomite	none		Rickenbach Formation
106	30	light gray	micrite	thin algal laminations	dolomite	none		Rickenbach Formation
107	35			completely algal laminated, some convex algal (30 cm diameter), interbedded between algal laminations are quartz lenses and seams up to 3-4 cm thick, lower sand lenses are large clots and vugs of quartz in channel bottoms (5 cm. diameter)	dolomite	capping unit: 5cm thick chert replacing quartz sandstone, chert has abundant quartz and pods are convex down, chert is associated with 5 cm thick quartz sand lenses, chert and sand in cut-n-fill channels at top of algal structures,		Rickenbach Formation
108	50	medium gray	medium	fetid, abundant floating quartz sand grains, occasional quartz vugs	dolomite	top of unit: 2-3 cm chert bed, stretches across entire bed surface, goes from wisps to 2-3 cm thick.		Rickenbach Formation
109	25	very dark gray	very fine	finely algal laminated, sharp contacts, fetid	dolomite	none		Rickenbach Formation
110	70	dark gray	medium /coarse	very fetid, lower 20 cm: abundant floating quartz sand and algal stromatolites (laminated and some convexity), upper 30 cm: abundant quartz vugs (1-2 cm diameter).	dolomite	none		Rickenbach Formation
111	35	dark gray	medium	fetid, abundant algal laminations in lower 10 cm	dolomite	none		Rickenbach Formation
112	90	light gray	medium	algal laminated, abundant stylolites through out	dolomite	none		Rickenbach Formation

				sequence				
113	30	light gray	very coarse	fetid, Crooked Swamp-like, abundant quartz-vugs along base	dolomite	abundant chert along base, chert as clots and seams in middle, chert occurs at upper contact, chert seams 2-3 cm thick, 30-40 cm long, convex upward		Rickenbach Formation
Epler Traverse								
114	100	dark gray	micrite	algal laminated	dolomite	none	Big Springs Member	Epler Formation
115	40	dark gray	micrite	algal laminated	dolomite	none	Big Springs Member	Epler Formation
116	90	dark gray	micrite	algal laminated	dolomite	none	Big Springs Member	Epler Formation
Epler 2 Traverse								
117	150	light blue gray	medium	slightly fetid, algal laminations throughout, concentrated at top 50 cm	dolomite	none	Big Springs Member	Epler Formation
118	50	dark gray	micrite	algal laminated, occasional quartz vugs, convex upward	dolomite	none	Big Springs Member	Epler Formation
119	60	variable	variable	fetid, lower 20 cm: light gray, very coarse-grained, floating quartz grains and lenses, cut-n-fill channel, next 20 cm: dark gray, micrite, algal laminated, weathers orange, upper 20 cm: medium gray, micrite, finely algal laminated	dolomite	none	Big Springs Member	Epler Formation
120	50	medium gray	micrite	algal laminated toward top, floating sand grains	dolomite	none	Big Springs Member	Epler Formation
121	30	medium gray	micrite	fetid, occasional algal laminations, sporadic layers and lenses of quartz grains, upper	dolomite	none	Big Springs Member	Epler Formation

				surface concave/convex				
122	40	light gray	coarse	fetid, occasional algal laminations, floating quartz grains	dolomite	none	Big Springs Member	Epler Formation
123	40	medium gray	coarse	fetid, concentration of algal stromatolites, algal concentrated at top, weathers orange	dolomite	none	Big Springs Member	Epler Formation
124	25	dark charcoal gray	micrite	fetid, algal laminated	dolomite	none	Big Springs Member	Epler Formation
125	30	dark charcoal gray	micrite	fetid, algal laminated	dolomite	none	Big Springs Member	Epler Formation
126	40	dark charcoal gray	micrite	fetid, abundant algal laminations, thick sand lenses and shale partings, some of the quartz grains are in dessication surfaces and cut-n-fill channels	dolomite	none	Big Springs Member	Epler Formation

B.3 – BEAVER RUN AGGREGATE TRAVERSE

Beaver Run Aggregate Traverse, Epler Formation, Sussex County, New Jersey								
Bed	**Thickness (cm)**	**Color**	**Grain Size**	**Bedding Description**	**Lithology**	**Chert**	**Member**	**Formation**
1	260	dark gray	medium	thickly bedded, finely algal laminated, upper 20 cm: rip-up clasts, intermittent sand lenses up to 4 cm. thick, pure white, gray, purple quartz sand, very well rounded and sorted, towards base, concentration of clots of white quartz, 2 cm in diameter,	dolomite	occasional lenses and clots of purple chert	Branchville	Epler
2	110	very dark gray	fine	finely laminated, algal rich, unconformity, mud cracks and soilized dolomite at top of bed	dolomite	porcellainite zones may be interface of Branchville and Big Springs	Branchville	Epler
3	30	light gray	very fine	unconformity at upper contact, green argillic surface and bright orange iron staining	dolomite	none	Big Springs	Epler
4	40	light gray	very fine	finely laminated	dolomite	none	Big Springs	Epler
5	40	medium gray	medium	lower 30 cm: thickly algal laminated, green argillic coating, mudcracks, unconformity	dolomite	none	Big Springs	Epler
		medium gray	medium	upper 10 cm: thickly laminated, unconformity, green and orange beds	dolomite	2-3 cm: gray, finely laminated chert on top of unconformity, porcellainite	Big Springs	Epler
6	50	dark gray	coarse	thinly bedded, abundant cross-bedded ooids, pattern: graded ooids/digitate algal stroms/purple chert/quartz grain lenses	dolomite	at 50 cm mark: 2 cm of dark purple chert on an irregular surface	Big Springs	Epler
7	60	medium	very	30 cm thick lenses	arenaceous	gray/white chert	Big	Epler

		gray	coarse	of sand, unconformity at 30 cm	dolomite	on unconformity	Springs	
8	88	dark gray	coarse	lower 20 cm: very rich in large quartz vugs	dolomite	none	Big Springs	Epler
		dark gray	coarse	upper 30 cm: finely laminated, algal rich, upper contact unconformable	dolomite	3 cm of gray chert	Big Springs	Epler
9	30	dark gray	micrite	finely laminated, upper 8 cm: rip-up clasts, upper contact unconformable, 1-2 cm of bright green/yellow argillite and orange iron staining	dolomite	none	Big Springs	Epler
10	40	dark gray	coarse	finely laminated, upper contact unconformable, 1 cm green argillaceous mud and orange staining	dolomite	none	Big Springs	Epler
11	47	dark gray	coarse	lower 20 cm: rich in quartz vugs, upper surface unconformable, 1 cm of green and orange argillite, upper 8-10 cm: dolarenite	dolomite	none	Big Springs	Epler
12	34	medium gray	coarse	lower 10 cm: burrowed, remainder of unit, dolarenite, very thick quartz-grained beds, upper 7 cm: purple sand	dolomite	interspersed chert lenses in purple sand of upper 7 cm.	Big Springs	Epler
13	35	dark gray	medium	floating sand lenses	dolomite	none	Big Springs	Epler
14	68	dark gray	medium	lower 30 cm: very rich in quartz vugs, intermittent or finely laminated	dolomite	none	Big Springs	Epler
15	25	very dark gray	micrite	finely laminated, unconformable upper and lower contacts	dolomite	none	Big Springs	Epler
16	17	dark gray	micrite	finely laminated, upper contact unconformable	dolomite	none	Big Springs	Epler
17	26	very dark	micrite	finely laminated, upper contact	dolomite	none	Big Springs	Epler

		gray		unconformable				
18	22	medium gray	micrite	finely laminated on weathered surfaces, sand lenses, stylolites, upper contact unconformable with 5 cm of bright orange, soilized dolomite	dolomite	none	Big Springs	Epler
19	32	medium gray	micrite	sand lenses, possible unconformity on upper contact	dolomite	none	Big Springs	Epler
20	85	dark gray	coarse	thinly bedded, sand lenses, upper contact stylolitized	dolomite	none	Big Springs	Epler
21	90	medium gray	coarse	very thin sand lenses, upper 15 cm: large quartz clots, hint of fine algal laminations and stylolites	dolomite	none	Big Springs	Epler
22	130	medium gray	medium	intermittent sand lenses, upper 15 cm: finely laminated with sand lenses	dolomite	none	Big Springs	Epler
23	60	medium gray	medium	thinly bedded, upper 15 cm: distinct laminations, sand lenses, bioturbated, upper contact unconformable with very thin bright orange sand	dolomite	none	Big Springs	Epler
24	25	medium gray	fine	numerous sand lenses, upper 10 cm: numerous sand lenses, upper 5 cm: deeply weathered, bright orange/green argillic clay, upper contact mud-cracked	dolomite	none	Big Springs	Epler
25	40	medium gray	medium	finely laminated	dolomite	none	Big Springs	Epler
26	110	medium gray	coarse	upper 30 cm: light gray and finely laminated, interspersed fine quartz sand lenses, unconformable upper contact with very thin brown	dolomite	none	Big Springs	Epler

				soilized bed.				
27	85	medium gray	medium	occasional clots of quartz	dolomite	none	Big Springs	Epler
28	30	medium gray	medium	finely bedded, arenaceous, thick bands of quartz sand, within upper quartz zone, bright orange/green, deeply weathered profile	dolomite	none	Big Springs	Epler
29	17			arenaceous, thinly bedded, numerous quartz grains, entire unit deeply weathered bright orange, upper contact unconformable	dolomite	none	Big Springs	Epler
30	175	very dark gray	coarse	upper portions of bed, interspersed with quartz, chicken wire patterns, upper 20 cm: thin beds	dolomite	upper 20 cm: thin nodules of black chert	Big Springs	Epler
31	85	dark gray	coarse	thickly bedded, chicken wire pattern throughout, upper 25 cm: thin beds, subtidal environment	dolomite	upper 25 cm: black chert nodules, top of unit, silicified algal structures (50-70 cm diameter, 15-20 cm high) completely overturned and brecciated	Big Springs	Epler
32	25	dark olive gray	medium	finely laminated, upper contact unconformable with mud cracks, bright orange stains and green argillaceous soil	dolomite	none	Big Springs	Epler
33	22	light gray	fine	stylolite surface at top of unit	dolomite	none	Big Springs	Epler
34	250	light ash gray	medium	structureless, numerous quartz clots, capped by stylolites, may be mylonitized	dolomite	none	Big Springs	Epler
35	80	charcoal gray	medium	lower 30 cm: chicken wire structures of quartz, thinly bedded,	dolomite	interspersed thin beds, seams, clots, and nodules of black	Big Springs	Epler

				cross-bedded in places		chert		
36	170	medium gray	medium	interspersed quartz clots, brecciation of green argillite (25x20 cm in diameter), finely laminated, infillings of a sort	dolomite	none	Big Springs	Epler
37	90	medium gray	coarse	structureless dolomite with quartz clots, upper contact unconformable	dolomite	none	Big Springs	Epler
38	30	medium gray	coarse	structureless dolomite with quartz clots, upper contact unconformable	dolomite	none	Big Springs	Epler
39	120	very light gray	micrite	algal laminated	dolomite	none	Big Springs	Epler
40	140	light gray	medium	intermittent argillic spider webs, upper surface unconformable with weathered orange profile, 3 cm of green argillite	dolomite	none	Big Springs	Epler
41	220	light gray	very coarse	structureless dolomite with quartz vugs	dolomite	none	Big Springs	Epler
42	350	light gray	coarse	quartz, vuggy structureless, upper 50 cm: continuous argillite beds	dolomite	upper 50 cm: light gray chert nodules	Big Springs	Epler
43	90	light gray	coarse	quartz, vuggy structureless, upper 50 cm: continuous argillite beds, intermittent green spider webs throughout	dolomite	upper 50 cm: light gray chert nodules	Big Springs	Epler
44	150	light gray	coarse	structureless with quartz vugs	dolomite	upper 50 cm: brecciated chert (karstic), clasts are micritic, siliceous infillings	Big Springs	Epler
45	80	dark gray	fine	finely laminated, intensely brecciated, green argillic spider webs throughout, convex upward	dolomite	none	Big Springs	Epler

				upper contact				
46	15	dark gray	fine	algal laminated, convex upward	dolomite	none	Big Springs	Epler
47	95	medium gray	very fine	algal laminated, very intensely brecciated in places, green spider webs throughout	dolomite	none	Big Springs	Epler
48	40	charcoal gray	very fine	finely laminated, totally brecciated, green argillic infillings	dolomite	none	Big Springs	Epler
49	160	medium gray	medium	structureless, finely laminated, occasional spider webs	dolomite	occasional clasts of purple chert	Big Springs	Epler
50	60	light gray	coarse	structureless, spider webs, possible unconformity	dolomite	none	Big Springs	Epler
51	115	medium gray	medium	finely algal laminated, occasional spider webs and quartz clots	dolomite	none	Big Springs	Epler
52	75	medium gray	medium	lower 15 cm: rip-up clasts, 3,4,and 5 cm of quartz bands running throughout, green spider webs throughout, upper contact possible unconformable	dolomite	intermittent clots of chert replaced algal structures above 15 cm, micrite turned to chert	Big Springs	Epler
53	85	light gray	micrite	lower 30 cm: finely bedded quartz sand	dolomite	none	Big Springs	Epler
54	30	light pink gray	micrite	finely laminated	dolomite	aphanitic chert	Big Springs	Epler
55	20	ash gray	micrite	finely laminated, upper contact unconformable	dolomite	none	Big Springs	Epler
56	20	light brown	micrite	finely laminated, upper contact unconformable	dolomite	none	Big Springs	Epler
57	15	light brown	micrite	upper contact unconformable	dolomite	occasional clots of chert	Big Springs	Epler
58	10	light brown	micrite		dolomite	none	Big Springs	Epler
59	10	very light brown	micrite		dolomite	none	Big Springs	Epler
60	15	light gray	micrite	upper contact unconformable	dolomite	none	Big Springs	Epler
61	20	light	micrite	upper contact	dolomite	none	Big	Epler

		gray		unconformable, finely laminated			Springs	
62	25	light gray	micrite	upper contact unconformable	dolomite	none	Big Springs	Epler
63	20	light gray	micrite	laminated	dolomite	none	Big Springs	Epler
64	20	light gray	micrite	algal laminated, upper contact desiccated, contains ripple marks, and one of larger unconformities	dolomite	none	Big Springs	Epler

B.4 – GLACIAL QUARRY SECTION

Glacial Quarry, Rte. 94, Sussex County, New Jersey								
Bed	**Thickness**	**Color**	**Grain Size**	**Bedding Description**	**Lithology**	**Chert**	**Member**	**Formation**
1	41	dark gray	coarse	oolitic grainstone, numerous zones of rip-up clasts, some sense of cross-bedding	dolomite	none		Allentown
2	114	dark gray	medium	algal laminated, 76-89 cm: large concentration of convex algal (13 cm diameter), upper contact, very sharply truncated	dolomite	none		Allentown
	15			above unconformity: domal algal stromatolites, unconformity coated with shale in places above and below the algal				
3	152	dark gray	fine	algal laminated, lower 51 cm: large convoluted masses of rip-up clasts in a dessication surface filled with debris, convex algal (6-10 cm long), upper-unit: larger-grained facies: pisoids and ooids	dolomite	at 76 cm: concentrated algal laminations and chert horizon, black wisps, knots and clots, opaque and contains ooids, 76-127 cm: interspersed layers of algal laminations, grainstone and boundstone, wisps and seams of chert replacing algal and ooids		Allentown
4	30	light ash gray to black	very coarse	gritty, may be algal controlled	shale	none		Allentown
5	46	dark gray	micrite	domal algal stromatolites (30X38 cm), diapirs of desiccated features filled with angular fragments of algal and rip-up clasts between algal domes	dolomite	at base of some algal: discontinuous layers of black, opaque chert		Allentown

6	28	dark gray	micrite	entirely composed of large algal stromatolites (46cm diameter)	dolomite	occasional wisps of chert		Allentown
7	30	variable	variable	lower 1 cm: brown shale, next 4 cm: dark gray, micritic, finely laminated, dolomite, next 13 cm: pinch and swell unit: very sandy, signs of algal in sand, upper 13 cm: shale, pinch and swell, hummocky, algal controlled	variable	chert nodules, translucent, black (5X10cm) at 18 cm		Allentown
8	46	medium gray	medium	lower part of unit: strongly stylolitized, somewhat arenaceous for 5 to 8 cm, breaks into a cross-bedded unit with scattered ooids	dolomite	none		Allentown
9	10	medium gray	coarse	occasional rip-up clasts, ooid zone, upper 5 cm: graded	dolomite	none		Allentown
10	96	variable	variable	algal laminated, lower 36 cm: medium gray, medium-grained medium thrombolitic algal, next 33 cm: light gray, coarse-grained, grainstone facies, angular and rolled carbonate fragments, remainder: very dark gray, medium/coarse-grained, finely algal laminated	dolomite	none		Allentown
11	122	variable	variable	lower 5 cm: dark gray, fine-grained, argillite, next 13 cm: dark gray, coarse-grained, ooid grainstone, broken, rounded debris fragments, next 46 cm: strongly stylolitized, next 10 cm: numerous angular rip-up, upper 5 cm: black shale, large rip-up clasts	dolomite	none		Allentown
12	81	variable	variable	lower 5 cm: pinch and swell shale, next 10 cm: recemented boundstone, next 33 cm: washed oolite, no sense of grading, wisps of fine-grained micrite between grains, upper-unit: non-	dolomite	none		Allentown

				graded, 1/2 cm shale sequence, large domal algal (61-81cm diameter), stylolites				
13	30	variable	variable	interbedded quartz sand lenses (no signs of cross-bedding) and rip-up clasts of dolomite and a finely laminated algal sequence.	dolomite	none		Allentown
14	61	variable	variable	lower 10 cm: dark gray/black, medium-grained, numerous large rip-up clasts and broken fragments of shale lenses, occasional micritic algal, next 13 cm: massive, non-graded, oolite, dark gray to black, coarse-grained, upper portion: algal laminated	dolomite	none		Allentown
15	41	medium gray	coarse	oolitic grainstone, cut-n-fill channels at top of bed (15X10cm)	dolomite	none		Allentown
16	66	medium gray	coarse	grainstone, hint of graded bedding, cut-n-fill channel at upper part of unit, filled with large amount of debris	dolomite	none		Allentown
17	41	medium gray	coarse	grainstone, rip-up clasts, ooids, pisoids, occasional algal structures (5-7X10-12 cm), sense of graded bedding, occasional stylolite surfaces (sulfide-bound), base: large amounts of rip-up clasts	dolomite	none		Allentown
18	91	medium gray	coarse	graded ooid and pisoid grainstone, occasional rip-up clasts of algal, cut-n-fill channel with broken, angular clasts of dolomite, occasional sulfide-bound stylolites, intraformational conglomerate	dolomite	none		Allentown
19	36	medium gray	coarse	graded ooid and pisoid grainstone, abundant sulfide-bound stylolites, upper surface: 1/2 cm of black shale, occasional	dolomite	none		Allentown

				overturned and ripped-up algal, intraformational conglomerate				
20	28	medium gray	coarse	graded oolite sequence, lower 8 cm: pisoid grainstone with shale lenses (5X38 cm), interbedded with sand lenses, abundant quartz vugs (3 cm diameter), patches of intraformational conglomerate (4 cm diameter).	dolomite	none		Allentown
21	127	medium gray	coarse	pisoid/ooid grainstone, graded, upper 18 cm: darker gray, finer grained, algal laminated, abundant sulfide-bound stylolites	dolomite	none		Allentown
22	30	very dark gray	very coarse	large scale intraformational conglomerate (shale lenses, ooids), lower 15 cm: shale units, finely laminated, algal controlled, sand lenses in places	dolomite	very sandy chert wisps (15X2.5 cm) occur above shale and within sand, chert at interface with sand and shale		Allentown
23	30	dark gray to black		finely laminated, algal controlled, convex/concave in places	shale	none		Allentown
24	41	dark gray	micrite	domal algal (76X2.5 cm), occasional sulfide-bound stylolites, upper 10 -15 cm: ooid/pisoid grainstone surface	dolomite	none		Allentown
25	76			grainstone deposits, large rounded pisoids, ooids, and algal rip-up clasts	dolomite	none		Allentown
26	76			grainstone deposits, large rounded pisoids, ooids, and algal rip-up clasts, signs of graded bedding	dolomite	none		Allentown
27	76			5-9 cm: sulfide rich shale, next 13 cm: oolite, next 61 cm: convex upward algal, laminated (15X15cm), very tightly bound (reefal?), stylolites throughout, seem to refract around algal, zones of intraformational conglomerates (56X40	dolomite	at base: chert nodules (10X5cm) in cut-n-fill channel, chert replacing grainstone, 61 cm interval: chert replacing algal near stylolite		Allentown

				cm), overturned algal		surfaces, overturned algal sequences, chert seems to be at base or in core of algal.		
28	61			algal boundstone, abundant stylolites, signs of current orientation or overturning, cut-n-fill channelization cutting into algal sequences, shaly debris in channels, sand lenses grade laterally into stylolites in one direction and chert in the other	dolomite	43-61 cm: ooid grainstone with fragments of overturned algal, chert replacing ooids, especially at base, intraformational conglomerates of cherts		Allentown
29	122			lower 8 cm: intraformational conglomerate/grainstone, yields to algal laminated micrite, sharp contact, 20 cm: very fine-grained oolitic grainstone, 64 cm: algal laminated, shale partings, 33 cm: ooid grainstone, 13 cm: intraformational conglomerate	dolomite	20 cm interval: mid and top parts of grainstone, chert replacing ooids (8X2.5 cm), upper 33 cm: four oolitic chert seams		Allentown
30	53	black	fine	very iron rich, some coarse units, some siltier units	shale	none		Allentown
31	68	dark gray	medium	domal algal unit with strong stylolites, structures present that may be boudins, algal controlled, or ball-n-pillow structures	dolomite	none		Allentown
32	23	black	fine	sulfide rich	shale	none		Allentown
33	36	very dark gray	micrite	shale partings throughout, algal controlled, cut-n-fill channels of ooids and pisoids	dolomite	none		Allentown
34	5	black	fine	silty, very sulfide rich	shale	none		Allentown
35	6	light gray	coarse	oolitic grainstone	dolomite	none		Allentown
36	5	black	fine	sulfide rich	shale	none		Allentown
37	10	medium gray	coarse	ooid/pisoid grainstone	dolomite	none		Allentown
38	7	very dark gray	coarse	sandy, silty grainstone, coarse-pebble conglomerate, rounded	dolomite	none		Allentown
39	13			graded, ooid/pisoid	dolomite	chert fragments,		Allentown

				grainstone		rounded		
40	76	medium gray	micrite	algal laminated, coarse ooid/pisoid grainstone (51-76 cm diameter) intermixed with micrite	dolomite	none		Allentown
41	43	variable	variable	lower 13 cm: cut-n-fill channels (on top of last bed), very sandy, sags in channel, very sandy, tops of channels silty, tan sand above shales, upper 30 cm: very flaggy, light gray, very fine-grained, silty shale, looks like wind blown loess	dolomite	chert replacing sand units above channels (8X38 cm), opaque, black chert with sandy dolomite matrix as cement		Allentown
42	30	medium gray	medium	grainstone, large pisoid fragments, white calcite venation, looks almost like chicken wire structure, capped by 2.5 cm of dark gray, fine-grained, strongly laminated silt	dolomite	none		Allentown
43	15	medium gray	fine	algal laminated	dolomite	none		Allentown
44	1	dark gray	fine	fissile	siltstone	none		Allentown
45	23	medium gray	fine	algal laminated, severely stylolitized	dolomite	none		Allentown
46	2.5	gray	fine		siltstone	none		Allentown
47	50	medium gray	medium	severely stylolitized, algal laminated, abundant calcite veins, zones of rip-up clasts throughout	dolomite	none		Allentown
48	8	gray	fine		siltstone	none		Allentown
49	43	black	fine	finely laminated, sulfide-rich	shale	none		Allentown
50	33	medium gray	medium	algal laminated, chicken wire calcite infillings, grainstone fragments in calcite infillings, unit not homogeneous, internally cracked	dolomite	none		Allentown
51	2.5		coarse	ferruginous, quartz rich	sandstone	none		Allentown
52	102	variable	fine	interbedded black silty shale and gray/olive sandy silt lenses, very fissile and very thinly bedded	siltstone	none		Allentown
54	43	olive gray		algal laminated, convex domes of algal (53X15 cm), lower 28 cm: more finely algal laminated,	dolomite	none		Allentown

				upper 23 cm: algal becomes domal, upper 8 cm: finely laminated and very shaly				
	2588 ft							

B.5 – GRUENWALD SECTION

Gruenwald Section, Sussex County, New Jersey								
Bed	**Thickness (cm)**	**Color**	**Grain Size**	**Bedding Description**	**Lithology**	**Chert**	**Member**	**Formation**
1	20	very dark gray	coarse	billowy beds, alternating layers of micrite and oolite	dolomite	none		Allentown Formation
2	15	dark gray	fine	oolitic	dolomite	none		Allentown Formation
3	10	dark gray	fine	algal laminated	dolomite	none		Allentown Formation
4	2.54		coarse	arenaceous	dolomitic limestone	none		Allentown Formation
5	36	dark gray	medium	occasional algal laminations, 2.5 to 5 cm thick pisoid/ooid beds	limestone	none		Allentown Formation
6	18	very dark gray	medium	large algal structures comprising unit (36-38 cm high x 35-38 wide), rip-ups at upper contact, arenaceous units, sulfide concentrations around algal	limestone	none		Allentown Formation
7	46	dark gray	fine	upper 13 cm: large algal structures (38 cm diameter), surrounded by rip-ups, quartz/calcite clots.	limestone	none		Allentown Formation
8	800			Covered interval				Allentown Formation
9	23	very dark gray	coarse	oolitic, stylolite-bounded contacts	limestone	none		Allentown Formation
10	10	dark gray	micrite	chicken-wire structure, stylolite-bounded contacts	dolomite	none		Allentown Formation
11	20	dark gray	fine	strongly algal laminated, 23 cm diameter convexity to beds, stylolite-bounded contacts	limestone	none		Allentown Formation
12	13	dark gray	medium	algal laminated, upper 2.5 cm: rip-up clasts, stylolite-bounded contacts	limestone	none		Allentown Formation
13	10	medium gray	coarse	oolitic, lower 5 cm: coarser than rest of unit	limestone	none		Allentown Formation
14	38	dark gray	very coarse	oncoidal grainstone composed of black, rounded pieces of organic matter, interstices; light-colored, finer-grained carbonate	limestone	none		Allentown Formation
15	15	dark	fine	algal laminated, large	limestone	none		Allentown

		gray		convex upper surface 30 cm in diameter, floating ooids, stylolite-bounded contacts				Formation
16	8	dark gray	coarse	entirely rip-up clasts and intraformational conglomerates, stylolite-bounded contacts, oncoid grainstone	limestone	none		Allentown Formation
17	15	light gray	medium-fine	algal laminated, stylolite-bounded contacts	limestone	none		Allentown Formation
18	15	medium gray	fine	algal laminated, upper surface contains rip-up clasts, current orientation to rip-up clasts	dolomitic limestone	none		Allentown Formation
19	10	brown	coarse	finely laminated, mudcracked, overturned algal	dolomitic limestone	none		Allentown Formation
20	10	light gray	fine	algal laminated, broken up into patchworks of oncoids, discreet patches of micrite filling in between algal (Light tan, micritic, desiccated and broken, interstices filled with arenaceous limestone, called a brecciola), some of algal (1 meter diameter).	limestone	none		Allentown Formation
21	15	dark gray	coarse	(In 6 meter sag): oolitic, upper 7 cm: rip-up clasts and intraformational conglomerate.	limestone	none		Allentown Formation
22	18	dark gray	coarse	graded ooids, some sense of algal throughout, top of bed: 2.5 cm of arenaceous limestone.	limestone	none		Allentown Formation
23	23	dark gray	fine	cabbage head algal comprising entire bed (25.4 cm diameter)	limestone	Chatoyant, nodular chert in center of algal.		Allentown Formation
24	10	light gray	fine	mildly convoluted, cut-n-fill channel at top of unit, channel contains intraformational conglomerate and quartz sand, stylolite-bounded.	limestone	none		Allentown Formation
25	20	dark gray	coarse	oolitic, signs of graded-bedding, stylolite-bounded surfaces	limestone	none		Allentown Formation

26	8	light gray	micrite	algal laminated, stylolite-bounded contacts	limestone	none		Allentown Formation
27	10		coarse	arenaceous, upper 5 cm: non-graded ooids, rip-ups, and intraformational conglomerate, strong radiographic stylolite-bounded contacts.	limestone	none		Allentown Formation
28	30	light gray	fine	algal laminated with lenses of cross-bedded ooids, upper 8 cm: massive ooids	limestone	none		Allentown Formation
29	51	dark gray	coarse	large ooids, strong stylolite-bounded contacts, upper 15 cm: numerous quartz vugs (2 cm in diameter)	limestone	none		Allentown Formation
30	28	dark gray	coarse	graded ooids, lower 8 cm: abundant algal laminations, coarse to fine ooids above, upper 8 cm: massive, dark gray ooids.	limestone	none		Allentown Formation
31	25	dark gray	coarse	graded ooids, upper few cm, light gray, algal laminated, intraformational conglomerates, rip-up clasts, overturned algal, brecciola.	limestone	none		Allentown Formation
32	5		coarse	arenite, quartz sand lenses, rip-up clasts, brecciola, filling in of baffle zone	limestone	none		Allentown Formation
33	10	dark gray	coarse	ooid grainstone, fragments of ooids, broken and brecciated, filled with 2nd generation of carbonate	limestone	none		Allentown Formation
34	33		coarse	graded oncoid to ooid grainstone, ooid on top of unit, stylolite-bounded contact.	limestone	none		Allentown Formation
35	30		coarse	oncoid to ooid grainstone, stylolite-bounded contacts, contains occasional algal stromatolites, upper 10 cm: much more fine-grained, algal laminated, convex upward	limestone	none		Allentown Formation
36	41	dark gray	coarse	ooid grainstone, strong grading, strong stylolite-bound contacts, 30-35 cm: strong pisoid unit,	limestone	from 35-40 cm: ooid		Allentown Formation

				occasional rip-up clasts.		unit selectively replaced by chert.		
37	8			finely laminated, algal laminated	limestone	none		Allentown Formation
38	30	light gray	medium-fine	algal laminated	limestone	none		Allentown Formation
39	23	light gray	medium-fine	algal laminated, entirely internally brecciated	limestone	none		Allentown Formation
40	30	medium-dark gray	fine	algal laminated	limestone	none		Allentown Formation
	1400			Covered interval				Allentown Formation
41	15		coarse	arenaceous, quartz arenite, upper 7 cm: rip-up clasts, intraformational conglomerates, made of algal clasts	dolomitic limestone	none		Allentown Formation
42	13		coarse	mildly graded to cross-bedded, arenaceous	dolomite	none		Allentown Formation
43	48		coarse	slightly graded, oolitic, mid-unit to top: rip-up clasts, bed pinches and swells				Allentown Formation
44	20	medium-dark gray	coarse	oolitic grainstone, signs of cross-bedding in upper 7 cm: rip-up clasts in upper 2.5 cm: quartz vugs, 1 cm diameter in lower part of unit				Allentown Formation
45	18	medium-dark gray	micrite	mottled, completely algal laminated	dolomitic limestone	none		Allentown Formation
46	76	medium gray	medium	signs of cross-bedding, scattered ooids throughout, when wet: pisoid-grainstone, lower 15 cm: non-graded oolite with rip-ups.	limestone	none		Allentown Formation
47	15	medium gray	fine	algal laminated, stylolite-bounded shale partings at contacts	dolomite	none		Allentown Formation
48	20	olive/black	fine	silty	shale	upper shale units cherty		Allentown Formation
49	36	dark gray	fine	algal laminated, occasional silty/sandy lenses	limestone	none		Allentown Formation
50	30	medium	fine	algal laminated, pervasive	limestone	mid-		Allentown

		gray		stylolite boundaries, mid-unit: 5 cm sequences of rip-up clasts and intraformational conglomerate.		unit: black, homogenous, shardy chert		Formation
51	23	medium gray	fine	algal laminated, stylolite-bounded, mid-unit: compact oolite and intraformational conglomerate, quartz vugs, remainder of unit: very finely algal laminated.	limestone	none		Allentown Formation
52	2.5	black/olive	fine	silty	shale	none		Allentown Formation
53	51	medium gray	coarse	lower 13 cm: graded oolite, next 15 cm: severe stylolite-bounded, thin wisps of chicken-wire algal, remainder of unit, micrite, algal laminated.	limestone	none		Allentown Formation
54	20	black/olive	fine	silty, extremely thin-bedded	shale	none		Allentown Formation
55	48	medium gray	fine	algal laminated, lower 18 cm: numerous shale partings, stylolite surfaces, sandy lenses, next 7 cm: algal laminated micrite, upper part of unit: algal laminated, pisoid boundstone with numerous rip-up clasts.	limestone	none		Allentown Formation
56	51	medium gray	fine	thinly bedded, lower 15 cm: finely algal laminated, numerous shale partings, next 7 cm: very fine-grained, algal laminated, upper 20 cm: 2.5 cm: olive shale, 2.5 cm micrite, 2.5 cm: olive-drab, silty shale, next 10 cm: intraformational conglomerate	limestone/shale	2.5 cm: cross-bedded quartz sand that is silicified		Allentown Formation
57	28	medium gray	coarse	ooid/pisoid packstone, slightly arenaceous, upper 12 cm: arenaceous, algal laminated, thick sulfides, stylolite surfaces, mildly cross-bedded.	limestone	none		Allentown Formation
58	25	medium gray	coarse	ooid/arenaceous packstone, severe radiographic stylolites	limestone	none		Allentown Formation
59	20		coarse	oolitic grainstone, both	limestone	none		Allentown

				contacts convex/concave, cut-n-fill with quartz sand, cross-bedded				Formation
60	28	medium gray	coarse	graded oolitic grainstone, lower 2.5 cm, arenaceous and rip-up clast zone	limestone	none		Allentown Formation
61	33		coarse	oolitic grainstone, graded, mid-unit: abundant algal laminations, upper portion: arenaceous, quartz vugs, strong stylolite-bound contacts, upper contact: iron sulfide rich	limestone	none		Allentown Formation
62	23		coarse	oolitic grainstone, rip-up clasts scattered throughout, some evidence of channelization, upper 2.5 cm: abundant rip-up clasts, but also algal laminated, upper contact: stylolite bound, iron sulfide rich, hummocky	limestone	none		Allentown Formation
63	13	medium gray	micrite	occasional algal filaments, stylolite-bound contacts lined with iron sulfides	limestone	none		Allentown Formation
64	15	medium	micrite	finely algal laminated, local rip-up clasts	limestone	none		Allentown Formation
65	13	light gray	coarse	quartz-sand rich, rip-up clasts throughout unit	limestone	none		Allentown Formation
66	13	light gray	very coarse	extremely uneven and hummocky, stylolite-bound, ooid/pisoid boundstone	limestone	none		Allentown Formation
67	18	medium gray	very coarse	ooid/pisoid packstone, zones of intraformational conglomerates, stylolite-bounded contacts.	limestone	none		Allentown Formation
68	13	dark gray	coarse	oolitic grainstone, moderately graded	limestone	none		Allentown Formation
69	58	medium -light gray	fine	stylolite-bounded, hummocky upper surface, large concentration of iron sulfides on upper contact, shale partings at upper contact, numerous rip-up clasts, upper 7 cm: intraformational conglomerate	limestone	none		Allentown Formation
70	25	dark gray	coarse	lower 13 cm: ooid grainstone, rip-up clasts at base of bed, mid 7 cm:	limestone	none		Allentown Formation

				graded ooids, numerous rip-up clasts, remainder of unit: oolitic grainstone, cross-bedded, rip-up clasts.				
71	30	dark gray	coarse	ooid grainstone, abundant stylolites, cross-bedded, oriented rip-up clasts and ooids, lower 15-18 cm: graded, numerous quartz vugs at base.	limestone	none		Allentown Formation
72	36	light gray	coarse	gradational out of underlying unit: stylolite-bounded, lower 18 cm: coarsening upward sequence, ooids to large pisoids, 5 cm thick pisoid unit, next 7 cm: graded, very large pisoids, fining upward sequence to very fine oolite, rest of unit: homogenous	limestone	none		Allentown Formation
73	23	light gray		fairly homogenous, quartz vugs throughout, very finely algal laminated	limestone	none		Allentown Formation
74	25	light gray	fine	hummocky bedding, cabbage-head algals (23X10 cm), centers of algal filled with calcite and quartz crystals, upper unit: algal unit, mudcracked, baffle infillings.	limestone	none		Allentown Formation
75	28	very light gray	micrite	weathers light brown, occasional algal laminations, floating ooids, very sharp shale partings at top.	limestone	none		Allentown Formation
76	10	light gray	very coarse	arenaceous, capped with shale partings, grades upward into ooid sequence	limestone	none		Allentown Formation
77	36		coarse	lower 13 cm: ooid packstone, numerous intraclasts, next 23 cm: graded oolite, pervasive stylolites at top of unit	limestone	none		Allentown Formation
78	15		very coarse	ooid/pisoid grainstone	limestone	none		Allentown Formation
79	20	light gray	very coarse	arenaceous, oolitic, graded, 2 cm quartz vugs at base and middle, top: occasional rip-up clasts	limestone	none		Allentown Formation
80	36	dark	coarse	oolite, numerous rip-up	limestone	none		Allentown

		gray		clasts composed of ooid with micrite matrix, 2-3 cm beds of saddle dolomite and quartz, slightly fetid				Formation
81	18		coarse	very hummocky, stylolite-bounded, alternating layers of micrite and graded oolite, occasional vugs filled with calcite and quartz, upper surface rich in sulfides.	limestone	none		Allentown Formation
82	81	medium gray	medium	lower 35 cm: occasional rip-up clasts, stylolites throughout, next 20 cm: cross-bedded oolite, fragments of ooid intraclasts, next 13 cm: non-graded oolite, next 13 cm: medium-coarse grained, intraformational conglomerate, upper contact: sulfide-stylolites	limestone	none		Allentown Formation
83	33	variable	coarse	lower 13 cm: black/olive gray, graded to cross-bedded oolite grainstone, occasional rip-up clasts, stylolite-bounded with iron sulfides, upper unit: light gray, hummocky contacts, occasional quartz vugs (2 cm. diameter), ooid rip-ups from lower unit	limestone	none		Allentown Formation
84	10	medium gray	coarse	very uneven bedding, arenaceous, numerous sulfide-bounded stylolites and rip-up clasts, hummocky upper contact, ribbon-like, arenaceous	limestone	none		Allentown Formation
85	30		coarse	graded oolite, very hummocky bedding, wave ripples? ranges from 20-33 cm, some velocity, occasional quartz vugs	limestone	none		Allentown Formation
86	13		coarse	non-graded oolite with numerous rip-up clasts, pinches and swells, numerous quartz vugs	limestone	none		Allentown Formation
87	46	medium gray	micrite	lower 15 cm: graded oolite with occasional quartz vugs (2.5 cm. diameter), next 15 cm: somewhat graded ooids with numerous rip-up	limestone	none		Allentown Formation

				clasts, upper 15 cm: large cabbage head algal (5X38 cm).				
88	23	very dark gray	micrite	algal laminated	dolomitic limestone	none		Allentown Formation
89	36	dark gray	fine	ooid grainstone, no signs of bedding	dolomitic limestone	none		Allentown Formation
90	7	dark gray	coarse	intraformational conglomerate fills in hummocky lower contact, cut-n-fill or algal controlled	limestone	none		Allentown Formation
91	5	dark gray	fine	oolitic grainstone	limestone	none		Allentown Formation
92	5			intraformational conglomerate, clasts of algal and oolite	limestone	none		Allentown Formation
93	25	medium -dark gray	medium	graded ooid packstone	limestone	none		Allentown Formation
94	15	dark gray	coarse	graded ooid wackestone, clay rich, strong iron sulfides, stylolite-bound upper contact	limestone	none		Allentown Formation
95	33	medium gray	coarse	graded ooid packstone, arenaceous and rip-up clasts upper 7 cm, upper contact uneven	limestone	none		Allentown Formation
96	25	medium gray	coarse	non-graded oolite, strong stylolite-bounded upper contact, strong iron sulfide, numerous arenaceous sand lenses at base	dolomitic limestone	none		Allentown Formation
97	30	medium gray	coarse	graded ooid wackestone, strong stylolites with iron sulfide surfaces, very uneven upper contact	dolomitic limestone	none		Allentown Formation
98	10	medium gray	coarse	intraformational conglomerates, numerous rip-up clasts of algal and ooids, numerous quartz vugs of 2.5 cm diameter	dolomitic limestone	none		Allentown Formation
99	8	dark gray	micrite	some algal laminations	limestone	none		Allentown Formation
100	8			ooid/pisoid packstone with large intraclasts of ripped-up ooid in fine-grained matrix	dolomitic limestone	none		Allentown Formation
101	8			graded ooid packstone with occasional vugs of saddle dolomite, strong stylolites with iron sulfide	dolomitic limestone	none		Allentown Formation

				surfaces				
102	30	medium gray	very coarse	lower 18 cm: coarsening upward oolite, rip-up clasts increase toward upper portion of unit, upper 13 cm: large pisoids, reverse grading	dolomitic limestone	none		Allentown Formation
103	28			lower 10 cm: cross-bedded ooids and pisoids, upper 20 cm: mostly oolite and somewhat graded, fining-upward sequence	dolomitic limestone	none		Allentown Formation
104	36	dark gray	fine	algal laminated, occasional quartz silt lenses throughout	limestone	none		Allentown Formation
105	15	medium -light gray	very coarse	massive ooid grainstone	limestone	none		Allentown Formation
106	10			arenaceous limestone, pinch and swell throughout, rip-up clasts of algal and ooids	limestone	none		Allentown Formation
107	40	medium gray	coarse	graded oolite, coarsening upward sequence, lower 13 cm: cross-bedded, oolitic grainstone, next 20 cm: graded bedding and cross-bedding, oolitic packstone with large intraclasts, upper 7 cm: pisoids	limestone	none		Allentown Formation
108	35.5	dark gray	coarse	lower 20 cm: graded oolite, fining upward sequence, upper 15 cm: graded oolite that fines upward, both sections stylolite-bound, occasional rip-up clasts	dolomitic limestone	bottom of unit, chert replaci ng ooid lenses (61X5 cm)		Allentown Formation
109	53	dark gray	coarse	oolite, coarsening upward sequence, numerous quartz vugs in lower part of unit, top of unit: abundant stylolites, iron sulfides, and rip-up clasts, unit bounded by stylolites.	limestone	none		Allentown Formation
110	35.5	very dark gray	coarse	arenaceous, graded oolite, 15 cm arenaceous unit, scattered ooids, stylolites, and occasional rip-up clasts, signs of cross-bedding throughout unit,	dolomite	none		Allentown Formation

				sharp iron-sulfide line stylolites at upper contact.				
111	30.5	variable	variable	lower 12.7 cm: very dark to light gray, graded oolite, abundant rip-up clasts, scattered ooids, next 18 cm: very light to dark gray, micrite with sand units, abundant quartz vugs, upper 7 cm: dark gray, very coarse-grained, arenaceous, rip-ups, stylolites	limestone	none		Allentown Formation
112	23	light gray	variable	lower 5 cm: micrite, upper 18 cm: occasional rip-up clasts, circular to cauliflower algal colonies (5-40 cm diameter), algals ripped-up at top	limestone	none		Allentown Formation
113	61	variable	variable	lower 20 cm: micrite bounded by stylolites, next 15 cm: light gray, fine-grained, oolitic, top 25.5 cm: dark gray, fine-grained, oolitic, upper 10 cm: cross-bedded	limestone	none		Allentown Formation
114	15	light gray	coarse	graded oolite, arenaceous, stylolites, 2 cm wide calcite vugs, occasional rip-up clasts in upper 5 cm, stylolite-bounded contacts.	limestone	none		Allentown Formation
115	10	light gray	coarse	arenaceous, cross-bedded, stylolite-bounded contact lined with iron sulfide	limestone	none		Allentown Formation
116	76	light gray	medium	arenaceous, cross-bedded, stylolite-bounded contact lined with iron sulfide	limestone	none		Allentown Formation
117	61	variable	variable	oolitic, lower 15 cm: very dark gray, abundant ooids, rip-up clasts, middle 15 cm: very light gray, very fine-grained, homogenous, upper 30 cm: medium gray, ripped-up algal stromatolite lower 10 cm, graded oolite, very coarse at base, abundant stylolites.	limestone	none		Allentown Formation
118	56	light gray	fine	eolian loess, tangential cross-beds, possible dune ripples, finely laminated, possible quartz silt component, top seams	loess	none		Allentown Formation

				truncated, filled with rip-up clasts, intraformational and edgewise conglomerates of algal fragments.				
119	10	medium gray	fine	eolian loess, tangential cross-beds, thin-bedded, laminated	loess	none		Allentown Formation
120	8	medium gray	micrite	algal laminated, desiccated bed that passes laterally into channels with edgewise conglomerates of broken algal structures, becomes 20 cm thick laterally, stylolite-bound	limestone	none		Allentown Formation
121	5	medium gray	fine	eolian loess, thinly bedded, beautifully sorted	loess	none		Allentown Formation
122	15		micrite	abundant floating quartz silt especially in lower 10 cm, the whole unit is mud-cracked, in places infillings between cracks filled with intraformational conglomerate, stylolite-bound contacts.	limestone	none		Allentown Formation
123	10		coarse	arenaceous, lower 5 cm: abundant coarse-grained quartz sand and heavy minerals that grade upward into a clean quartz sand bed with carbonate cement, radiographic-stylolite-bound contacts with iron sulfide linings	sand	none		Allentown Formation
124	18	variable	variable	lower 8 cm: gradational from lower unit: dark gray, micrite, algal structures, next 10 cm: oolite, very thick, coarse-grained, graded, projecting out of micrite into and through oolite are abundant circular algal colonies (2.5-61 cm).	limestone	none		Allentown Formation
125	13	dark gray	coarse	oolitic	limestone	none		Allentown Formation
126	33	black	fine	finely laminated, very thinly bedded, truncated upper surface	shaly limestone	none		Allentown Formation
127	33	dark gray	fine	very thinly bedded, lower 7 cm: algal laminations,	limestone	none		Allentown Formation

				convex bedding (possible ripple or algal control), upper portion of unit lines with 0.6 cm of shale				
128	25.5			very thin bedded, poorly sorted oolite, becomes large domal algal, which are 1 foot in diameter and constitute entire thickness of bed	limestone	none		Allentown Formation
129	73.5	dark gray	fine	algal boundstone, convex/concave contacts (91cm diameter), intervals of algal are brecciated and some quartz filled	limestone	none		Allentown Formation
130	61	dark gray	fine	fine algal laminations, continuation of lower algal unit, convexities in bedding conform to those of bed below, cauliflower shaped algal, baffles between algal filled with dark gray micrite, stylolites conform to shape of algal, micrite desiccated	limestone	none		Allentown Formation
131	86	dark gray	micrite	thoroughly stylolitized, bed thickens and thins along strike, numerous 1 cm wide calcite and quartz vugs, small cauliflower algal laminations comprise entire unit like lacework (2.5 cm wide algal), upper 40 cm of unit, ripped-up algal fragments, edgewise	limestone	none		Allentown Formation
132	30.5	dark gray	coarse	sandy/silty oolite, looks like top of storm deposit, large algal floating as edgewise conglomerate, baffles between algals filled with micrite, unit thoroughly stylolitized, in places algal project up through oolitic sequence from beds below.	limestone	none		Allentown Formation
133	35.5	medium gray	coarse	graded oolite, abundant rip-up clasts	limestone	none		Allentown Formation
134	71	dark gray	micrite	algal laminated, very thinly bedded, finely laminated, algal control to bedding, stylolite-bounded, sulfide-rich contacts, occasional	limestone	none		Allentown Formation

				patches of circular cabbage algal (7.5-10 cm diameter) occur as colonies, upper 15 cm: very dark gray, algal lam, micrite				
135	40.5	dark gray	medium	occasional algal, top of unit (few cm) are small algal (2.5-5 cm diameter), perfectly circular algal colonies	dolomitic limestone	none		Allentown Formation
136	40.5	dark gray	medium	no algal	dolomitic limestone	none		Allentown Formation
137	15	dark gray	micrite	abundant, enormous algal colonies, several meters in diameter, between colonies, dark gray, desiccated micrite	limestone	none		Allentown Formation
138	15	very dark gray/black	fine	finely laminated, fissile	shale grades into dolomitic limestone	none		Allentown Formation
139	23	light gray	micrite	finely algal laminated, stylolite-bound contacts, black shale partings throughout	limestone	none		Allentown Formation
140	48	dark gray	micrite	stylolite-bound contacts, weathers brown on upper surface, upper 7 cm: looks like eolian loess	dolomitic limestone	none		Allentown Formation
141	254			Covered interval				Allentown Formation
142	51		coarse	arenaceous, oolitic, lower 7.6-10 cm: algal laminated, micrite, surface is truncated by a thin lens of intraformational conglomerate, next 43 cm: arenaceous, windblown loess, tangential, truncated cross-beds of fine silt quartz with carbonate cement.	limestone	none		Allentown Formation
143	8		fine	arenaceous carbonate cemented loess, few remaining tangential beds, finely laminated, lower surface rests on dune ripples?, upper contact is stylolitized.	loess	none		Allentown Formation
144	30.5		coarse	oolitic, series of graded beds, fining-upward	limestone	none		Allentown Formation

				sequence, lower 13 cm: fining-upward oolite, upper 18 cm: another fining-upward oolite.				
145	38	dark gray	coarse	oolite packstone, abundant quartz silt component, coarsening-upward unit, oolites become larger up section, lower part of unit has 2 cm diameter quartz vugs	limestone	none		Allentown Formation
146	7.5	light gray	very coarse	very large ooids, intraformational conglomerates, upper 5 cm: filled with quartz sand.	limestone	none		Allentown Formation
147	30.5	medium gray	medium	arenaceous, looks like loess unit: windblown, scattered ooids, fragments of quartz silt, few signs of cross-beds, stylolite-bounded contacts.	limestone	none		Allentown Formation
148	18	medium gray	medium/ coarse	arenaceous, coarsening-upward sequence, ooids scattered throughout, sulfide-replacement of ooids, mid-unit: 5-7 cm wide calcite vugs, upper 7.5 cm: intraformational conglomerate, ooids not graded, stylolite-bound contacts.	limestone	none		Allentown Formation
149	18	medium gray	coarse	non-graded oolite, occasional rip-up clasts, occasional intraformational conglomerate with algal and rip-up clasts, stylolite-bounded contacts	limestone	none		Allentown Formation
150	20	medium gray	coarse	non-graded oolite, occasional intraformational conglomerate, some quartz silt, stylolite-bound contacts	limestone	none		Allentown Formation
151	20	medium gray	micrite	algal laminated, lower 20 cm: thoroughly mud-cracked with quartz silt infillings, upper 10 cm: finely laminated, some signs of dessication, but not many.	limestone	none		Allentown Formation
152	8	dark gray	coarse	intraformational conglomerates, rip-up clasts	limestone	none		Allentown Formation

153	15	medium gray	coarse	Arenaceous, lower 7.5 cm: graded -bedding, fining-upward sequence, hummocky upper and lower surfaces: upper 7.5 cm: intraformational conglomerate, large rip-up clasts, edgewise conglomerates, lower portion of upper 7.5 cm sits in a cut-n-fill channel.	limestone	none		Allentown Formation
154	10	medium gray	coarse	non-graded oolite, upper surface is rippled (25.4 cm long ripples).	limestone	none		Allentown Formation
155	13	medium gray	medium	scattered ooids and quartz silt grains	limestone	none		Allentown Formation
156	15	dark gray	medium	occasional floating ooids, some black shale partings, very thinly bedded	limestone	none		Allentown Formation
157	30.5	variable	variable	lower 7.6 cm: dark gray, medium-grained, interbedded shale partings, middle 15 cm: thinly bedding with occasional quartz silt lenses, next 2.5 cm: shaly limestone, upper 5 cm: intraformational conglomerates and rip-up clasts	limestone	none		Allentown Formation
158	30.5	variable	coarse	lower 7.5 cm: medium gray, scattered ooid patches, quartz vugs up to 1 cm. diameter, next 18 cm: medium gray, possibly algal laminated, upper 5 cm: dark gray, algal controlled	limestone	none		Allentown Formation
159	40.5	dark gray/olive	fine	lower 15 cm: shaly, fissile, next 5 cm: floating intraclasts and intraformational conglomerate with floating quartz silt, upper 15 cm: algal laminated, quartz silt seams throughout, laterally breaks out into a large cabbage (66X 30 cm) algal.	limestone	none		Allentown Formation
160	10	medium gray	micrite	algal laminated, oncoidal algal (5-13 cm diameter) colonies, hummocky contacts	limestone	none		Allentown Formation
161	33	light	micrite	algal laminated, micrite	limestone	none		Allentown

		ash gray		seems to be a baffle filling for an oncoidal zone below, oncoid colonies are 76 cm in diameter, micrite is mud-cracked in places and filled with a fine quartz silt, quartz vugs in cores of algal colonies				Formation
162	30.5	black/olive	micrite	shaly, fissile, mid-unit: zone of rounded, very coarse (sand size) fragments, two zones of them, many look like feldspars weathered to clay, lower zone not well-defined, upper zone well-defined, may be volcanic glass fragments turned into shardy clay.	limestone	none		Allentown Formation
163	35.6	medium gray	coarse	peloidal, pinches and swells, made entirely of intraclasts, intraformational and edgewise conglomerates (7-25 cm diameter), may be storm deposit, lower 10 cm: thinly bedded, large vugs with 10 cm dolomite crystals.	dolomitic limestone	none		Allentown Formation
164	43	dark gray	coarse	peloidal, entire unit composed of intraclasts and intraformational conglomerate	dolomitic limestone	none		Allentown Formation
165	15		micrite	algal laminated, baffle infilling between oncoid patches, 18 cm pockets of medium gray, medium grained, oncoidal patches 152 cm in diameter (oncoids 5 cm diameter).	limestone	none		Allentown Formation
166	660			Covered interval				Allentown Formation
167	66	dark gray	fine	interbedded with layers of rip-up clasts, very finely laminated	dolomitic limestone	none		Allentown Formation
168	30.5	light gray	micrite	algal laminated, stylolite-bounded contacts	dolomitic limestone	none		Allentown Formation
169	30.5	medium gray	medium	mildly algal laminated, stylolite-bounded contacts	dolomitic limestone	none		Allentown Formation
170	61	medium gray	micrite	algal laminated, thin bedded	dolomitic limestone	none		Allentown Formation
171	35.5	dark gray	fine	algal laminated	dolomitic limestone	none		Allentown Formation

172	56	dark gray	micrite	more thickly bedded unit, upper 15 cm: algal laminated	dolomitic limestone	none		Allentown Formation
173	127			Covered interval				Allentown Formation
174	12.5	dark gray	coarse	intraformational conglomerates, stylolite-bounded contacts	dolomitic limestone	none		Allentown Formation
175	10	light gray	micrite	algal laminated	dolomitic limestone	none		Allentown Formation
176	152.5			Covered interval				Allentown Formation
177	28	medium gray	coarse	algal colonies up to 28 cm diameter, micrite in bathyl zone between colonies, intraformational conglomerates on top, non-graded ooid blanket covering entire unit	dolomitic limestone	none		Allentown Formation
178	23	dark gray	coarse	graded oolite, two fining-upward sequences, calcite vugs up to 10 cm in diameter at top of unit, infillings of micrite on top, a veneer of mud-cracked micrite	dolomitic limestone	none		Allentown Formation
179	152			Covered interval				Allentown Formation
180	30.5	dark gray	coarse	lower 18 cm: predominantly rip-up clasts, intraformational and edgewise conglomerate, upper 13 cm: extremely dark gray	dolomitic limestone	none		Allentown Formation
181	18	medium gray	medium	algal laminated, stylolitized contacts	dolomitic limestone	none		Allentown Formation
182	10	medium gray	fine	algal laminated	dolomitic limestone	none		Allentown Formation
183	56	medium gray	micrite	thinly bedded, stylolites throughout unit	dolomitic limestone	none		Allentown Formation
184	18	medium gray	micrite	shale partings and stylolites at both contacts, flat lower bed surface, upper surface is concave/convex and algal controlled	dolomitic limestone	none		Allentown Formation
185	38	light gray	micrite	domal algal up to 101 cm diameter (18-51 cm thick), concave/convex bedding	dolomitic limestone	none		Allentown Formation
186	40.5	medium gray	micrite	strong algal laminations, stylolite-bounded contacts	dolomitic limestone	none		Allentown Formation
187	71	dark gray	coarse	lower 7.5 cm: algal laminated, pelletal mud,	dolomitic limestone	none		Allentown Formation

				pellets, ooids, oncoids, silver dollar size algals, intraformational conglomerates, upper 63.5 cm: intraformational conglomerates, rip-up clasts, non-graded ooid blankets, micrite fills baffle zones of top				
188	18	dark gray	micrite	algal laminated	dolomitic limestone	none		Allentown Formation
189	20	dark gray	coarse	intraformational conglomerate, rip-up clasts, edgewise conglomerate, sporadic algals up 20-25 cm diameter, occasional patches of micrite	dolomitic limestone	none		Allentown Formation
190	18	dark gray	fine	entire unit filled with dendritic algals, branching and digitate, look like worm burrows but are not.	dolomitic limestone	none		Allentown Formation
191	30.5	dark gray	coarse	non-graded oolite, projecting through oolite to upper 30.5 cm is a large algal colony, small circular oncoids drawn into large colonies up to 1 meter in diameter, ooids are baffle infilling, very little micrite.	dolomitic limestone	none		Allentown Formation
192	101			Covered interval				Allentown Formation
193	38	dark gray	coarse	oolite, intermittent oncoidal algal through entire unit, oolite at 13 cm breaks into 7cm of intraformational conglomerate, stylolites with iron sulfide encrustations throughout, upper surface irregular, quartz vugs un upper 10 cm.	dolomitic limestone	none		Allentown Formation
194	10	light gray	micrite	algal laminated	dolomitic limestone	none		Allentown Formation
195	13	dark gray	coarse	peloidal/ooid packstone, no signs of grading, upper 7.5 cm: spider webs of quartz that marks presence of large algal (15 cm diameter) and entirely infilled with sometimes recrystallized	dolomitic limestone	none		Allentown Formation

				quartz, upper 15 cm: intraformational conglomerate and rip-up clasts.				
196	23	variable	variable	lower 7.5 cm: charcoal/black, very finely bedded, shaly, next 5 cm: very compact, non-graded ooids, next 10.2 cm: light gray, micrite, algal laminated.	limestone	none		Allentown Formation
197	8	medium gray	medium	entire unit is rip-up clasts and intraformational conglomerate	limestone	none		Allentown Formation
198	10	medium gray	medium	thinly bedded, peloidal/ooidal, non-graded, shale partings, capped by 5 cm dark gray, fine grained limestone, all rip-up clasts and intraformational conglomerate	limestone	none		Allentown Formation
199	18	ash gray	fine	algal laminated, stylolite-bound contacts, iron sulfides on top	limestone	none		Allentown Formation
200	15	medium gray	coarse	algal rich, some digitate type algal that stand up to 5 cm tall, abundant compacted pellets and ooids, stylolite-bound contacts with calcite vugs up to 5 cm in diameter.	limestone	none		Allentown Formation
201	15	dark gray	fine	oolite, non-graded	limestone	none		Allentown Formation
202	25.5	medium gray	medium	oolite with occasional rip-up clasts, thoroughly stylolitized, strong concentration of iron sulfides, lenses of ooids throughout.	limestone	none		Allentown Formation
203	7.5	medium ash gray	micrite	algal laminated, stylolite-bounded contacts	limestone	none		Allentown Formation
204	20	dark gray	coarse	oolite, 2 graded cycles, both fining-upward, scattered intraclasts	limestone	none		Allentown Formation
205	18	medium gray	fine	lower 5 cm: peloid/ooid grainstone, intraclasts, quartz vugs (1 cm diameter), next 8 cm: coarser grained, ooids/pellets/oncoids rolled together, medium-grained, upper 5 cm: peloid/ooid grainstone,	limestone	none		Allentown Formation

				stylolite-bound contacts				
206	10.5	medium gray	medium	ooid/peloid packstone, stylolite-bounded contacts	limestone	none		Allentown Formation
207	15	medium gray	medium	lower 10 cm: non-graded oolite with rip-up clasts, upper 5 cm: graded oolite sequence, numerous rip-ups clasts, intraclasts upper 10 cm, moldic porosity	limestone	none		Allentown Formation
208	18	medium gray	medium	oolite, stylolite-bounded contacts	limestone	none		Allentown Formation
209	23	medium gray	coarse	oolite with occasional rip-ups clasts, pelletal mud, looks like bed below was ripped up	limestone	none		Allentown Formation
210	10	light gray	micrite	occasional lenses of pellets and occasional intraclasts, algal stromatolites up to 30 cm in diameter, and 10 cm in thickness	limestone	none		Allentown Formation
211	13	dark gray/black	coarse	graded oolite, occasional pellets and rip-up clasts	limestone	none		Allentown Formation
212	15			Covered interval				Allentown Formation
213	15	medium gray	fine	lower 5 cm: oolite, rip-up clasts, algal fragments, upper 10 cm: graded oolite, dark gray, coarse-grained	limestone	none		Allentown Formation
214	30.5	dark gray	coarse	graded oolite, lower 13 cm: oolites, intraclasts, rip-up clasts, upper part: graded oolite, cross-bedded quartz sand in lower 10 cm, lower part: abundant quartz silt, arenaceous	limestone	none		Allentown Formation
215	18	dark gray	coarse	non-graded oolite	limestone	none		Allentown Formation
216	18	dark gray	coarse	non-graded oolite, moldic porosity, stylolite-bounded contacts	limestone	none		Allentown Formation
217	18	dark gray	coarse	non-graded oolite, moldic porosity, stylolite-bounded contacts	limestone	none		Allentown Formation
218	15	dark gray	coarse	massive blanket oolite, stylolite-bound contacts, circular algal colonies, up to 25.4 cm in diameter, found through entire oolite blanket, many	limestone	none		Allentown Formation

				algals filled with quartz and dolomite crystals, some pellets and pisoids				
219	609.5			Covered interval				Allentown Formation
220	53	medium gray	medium	completely stylolitized, lower 30.5 cm: pellets, pisoids, ooids, intraclasts, and intraformational conglomerates, upper 23 cm: largely ooids and pellets, no signs of grading, a little bit finer-grained up-section, small algal stromatolites	limestone	none		Allentown Formation
221	20	medium gray	fine	completely stylolitized throughout and at contacts, thickly bedded, lower contact hummocky, upper contact flat	limestone	none		Allentown Formation
222	23	medium gray	fine	lower 7.5: rip-ups clasts throughout, lower 12.7 cm: micrite, upper portion, mixed layers, non-graded ooids/pellets and intraclasts	limestone	none		Allentown Formation
223	33	medium gray	medium	oolite, scattered lenses of ooids, stylolitized throughout and at contacts, iron sulfides with stylolites	limestone	none		Allentown Formation
224	33	medium gray	coarse	oolite, scattered rip-up clasts, upper 10.2 cm: rip-up clasts and intraformational conglomerate, stylolite-bounded contacts, upper contacts, iron sulfides	limestone	none		Allentown Formation
225	30.5	dark gray	coarse	lower 13 cm: abundant rip-up clasts, upper 15 cm: graded ooids	limestone	none		Allentown Formation
226	13	medium gray	coarse	graded oolite, stylolite-bounded contacts	limestone	none		Allentown Formation
227	28	medium gray	medium	graded oolite, fining-upward sequence, arenaceous, especially lower 10 cm., on bottom of bed are rounded clay fragments that could be volcanic ash or glass	limestone	none		Allentown Formation
228	13	medium gray	coarse	non-graded oolite, coarsening-upward sequence	limestone	none		Allentown Formation
229	274			Covered interval				Allentown

								Formation
230	101.5	dark gray	coarse	occasionally graded, 4 fining-upward sequences, stylolite-bounded contacts	limestone	none		Allentown Formation
231	15	medium gray	coarse	oolite, intraclasts and intraformational conglomerates throughout unit	limestone	none		Allentown Formation
232	10	medium gray	medium	non-graded oolite	limestone	none		Allentown Formation
233	20	dark gray	medium-coarse	graded oolite, fining-upward sequence	limestone	none		Allentown Formation
234	15	medium gray	coarse	abundant rip-up clasts	limestone	none		Allentown Formation
235	10	dark gray	coarse	oolite, moldic porosity is extreme, abundant oncoids and algal fragments	limestone	none		Allentown Formation
236	18	charcoal gray	medium	graded oolite, fining-upward sequence, stylolite-bounded contacts	limestone	none		Allentown Formation
237	20	medium gray	medium	oolite, cauliflower algal stromatolites at base of unit, abundant rip-ups above algal, pellets, ooid fragments, ooid lenses	limestone	none		Allentown Formation
238	23	medium gray	coarse	algal laminated, abundant rip-up clasts throughout, layers of ooids, upper 5 cm: all intraformational conglomerate, abundant clay fragments, look like volcanic ash/glass	limestone	none		Allentown Formation
239	53	medium gray	coarse	algal laminated, lower 30.5 cm: abundant 2.5-5 cm diameter quartz and dolomite vugs, stylolite-bounded contacts, mid-unit: filled with oncoidal algal, upper 10 cm: all algal stromatolites, oncoids (0.64 cm diameter).	limestone	none		Allentown Formation
240	13	medium gray	coarse	hummocky base, uneven algal, oncoid colonies up to 61 cm in diameter, scoured by a blanket of very coarse ooids, tiny fining-upward cycles, very large fragments of ripped-up algal laminated micrite	limestone	none		Allentown Formation
241	10	medium gray	coarse	non-graded oolite, occasional rip-up clasts	limestone	none		Allentown Formation

				composed of other ooids				
242	10	medium gray	medium	algal laminated, occasional oncoids, strong stylolite-bounded contacts	limestone	none		Allentown Formation
243	25	medium gray	medium	very very fine-grained oolite	limestone	none		Allentown Formation
244	28	medium gray	coarse	graded ooid blanket, mid-unit: colonies of oncoids up to 15 cm diameter, colonies in contact, stylolite-bounded contacts	limestone	none		Allentown Formation
245	25	light gray	medium	algal laminated, occasional oncoids	limestone	none		Allentown Formation
246	305			Covered interval				Allentown Formation
247	20	variable	fine	lower 10 cm: dark charcoal gray, shaly, stylolite-bounded contacts, upper 10 cm: light gray, micrite, algal laminated, signs of dessication on surface	limestone	none		Allentown Formation
248	23	medium gray	coarse	graded oolite, occasional intraclasts, stylolite-bounded contacts	limestone	none		Allentown Formation
249	35.5	medium gray	coarse	oolite, occasional intraclasts and abundant oncoids (U.S. quarter in diameter).	limestone	none		Allentown Formation
250	25.5	variable	fine	lower 7.5 cm: light gray, micrite, finely algal laminated, very thinly bedded, mid-10 cm: extremely dark gray/charcoal, finely laminated, shaly, abundant quartz silt seams, upper 7.5 cm: light gray, fine-grained, algal laminated, some quartz silt.	limestone	none		Allentown Formation
251	25.5	medium gray	coarse	oolitic, occasional rip-up clasts and oncoids	limestone	none		Allentown Formation
252	20	medium gray	coarse	oolitic, occasional rip-up clasts and oncoids	limestone	none		Allentown Formation
253	10	medium gray	coarse	oolitic, occasional rip-up clasts and oncoids	limestone	none		Allentown Formation
254	23	medium gray	coarse	oolitic, occasional rip-up clasts and oncoids	limestone	none		Allentown Formation
255	7.5	light gray	micrite	algal laminated	limestone	none		Allentown Formation
256	7.5	medium gray	coarse	oolite	limestone	none		Allentown Formation
257	28	medium	micrite	abundant ooids,	limestone	none		Allentown

		gray		occasional oncoids, 1 cm quartz vugs along top				Formation

B.6 – HARMONYVALE SECTION

Harmonyvale Section, Sussex County, New Jersey								
Bed	**Thickness (cm)**	**Color**	**Grain Size**	**Bedding Description**	**Lithology**	**Chert**	**Member**	**Formation**
1	41	blue/gray	medium	uneven upper contact	dolomite	none		Allentown
2	30	blue/gray	medium	uneven upper contact	dolomite	none		Allentown
3	66	blue/gray	medium	lower 33 cm: evidence of cross-bedding, upper 33 cm: finely bedded, ooids, very even, sharp upper contact	dolomite	none		Allentown
4	71	variable	variable	lower 38 cm: blue/gray, medium-grained, thinly bedded, graded ooids, upper 33 cm: light gray, pelmicrite				Allentown
5	40	light gray	variable	lower 20 cm: medium-grained, middle 5 cm: coarse-grained, stylolite-bound upper surface, upper 15 cm: coarse-grained, sharp, uneven upper contact	dolomite	none		Allentown
6	18	light gray	very coarse	stylolite-bound contacts	dolomite	none		Allentown
7	38	medium gray	medium	alternating brown and gray beds (1 cm thick), contoured bedding structure, occasional quartz vugs	dolomite	none		Allentown
8	137	light gray	coarse	crystalline, uneven upper contact	dolomite	none		Allentown
9	30.5	medium gray	coarse	thrombolitic algal stromatolites, quartz vugs 2.5 cm diameter, intraclasts and rip-up clasts common	dolomite	none		Allentown
10	101	dark gray	medium		dolomite	none		Allentown
11	76	dark gray	coarse	transitional upper contact into a fine-grained sequence	dolomite	none		Allentown
12	43	light gray	fine	thinly bedded, concave upward and possibly algal controlled	dolomite	none		Allentown
13	25	light gray	fine	thinly bedded, concave upward and possibly algal controlled	dolomite	none		Allentown
14	18	ash gray	very fine		dolomite	none		Allentown
15	91	medium	micrite	thinly bedded, flaggy,	dolomite	none		Allentown

		gray		orange iron stains, some arenaceous shale on upper contact				
16	18	medium gray	very coarse	intermittent quartz sand lenses which are up to 8 cm thick, intraclasts and rip-up clasts are common in this unit	dolomite	middle 6 cm: thick dark gray to navy blue chert bed, opaque to translucent along edges, chert contains sand grains, in some places it is thinly bedded, in other places it occurs as wisps and clots; limited quarry activity along the face of the slope		Allentown
17	142	dark gray		highly sulfurous, scattered ooids, 13 cm thick beds, worm burrow mottling	dolomite	none		Allentown
18	41	dark gray	fine	thinly bedded, finely laminated, occasional 1 cm quartz vugs	dolomite	none		Allentown
19	71	dark gray	medium	crystalline, thickly bedded with 1 cm quartz vugs	dolomite	none		Allentown
20	157	medium gray	medium	scattered quartz vugs, upper surfaces uneven, stylolite surfaces, convex upward upper contact	dolomite	none		Allentown
21	107	medium gray	medium	scattered quartz vugs, upper surfaces uneven, stylolite surfaces, convex upward upper contact, algal	dolomite	none		Allentown

				controlled, thickly bedded, scattered quartz grains up to 25 cm in diameter.				
22	71	dark gray	micrite	interbedded and alternating with quartz sand and lenses up to 15 cm thick, uneven bed surfaces, possible thrust surface (although no evidence for thrust)	dolomite	none		Allentown
23	38	medium gray	micrite	small quartz vugs throughout, minor quartz sand lenses at top of unit	dolomite	none		Allentown
24	76	medium gray	medium	lower 10 cm: numerous quartz vugs, uneven upper contact	dolomite	none		Allentown
25	51	light gray	micrite		dolomite	none		Allentown
26	76	medium gray	coarse	oolitic, overturned algal stromatolites, few sand lenses, quartz vugs up to 2.5 cm in diameter (especially in lower part of unit)	dolomite	lower 45 cm: abundant ooids replaced by chert, wisps and bands of transluce nt, blue/gray , oolitic chert, chert lenses approxim ately 35 cm in length, pod shaped and convex upward, in other places chert replaces algal stromatol ites		Allentown
27	15	medium gray	coarse	finely laminated, shaly, quartz grains,	dolomite	rounded chert		Allentown

				ooids, rip-up clasts of micrite, shale unit above chert contains abundant quartz sand lenses with finely disseminated quartz sand grains (wisps).		fragments, charcoal gray, translucent on edges, in one location occur as 15 cm long pods of oolite replaced by chert with a 15 cm shale sequence just above it, chert may have been ripped up and overturned, but contains ooids and sand grains		
28	30	dark gray	medium	10 cm thick, finely laminated, convex up algal	dolomite	none		Allentown
29	20	dark gray	micrite	highly convex upper surfaces, algal control	dolomite	none		Allentown
30	46	dark gray	medium	highly sulfurous , lower 10 cm: laminated algal, upper suface uneven	dolomite	none		Allentown
31	30	medium gray	medium		dolomite	none		Allentown
32	40	medium gray	medium	finely laminated	dolomite	none		Allentown
33	30	medium light gray	fine	thinly bedded	dolomite	none		Allentown
34	23	medium gray	micrite		dolomite	none		Allentown
35	18	medium gray	micrite		dolomite	none		Allentown
36	41	light gray	micrite		dolomite	none		Allentown

37	25	medium light gray	micrite		dolomite	none		Allentown
38	41	medium gray	micrite		dolomite	none		Allentown
39	122	medium gray	medium		dolomite	none		Allentown
40	86	brown/gray	fine	very thinly bedded, algal laminations	dolomite	none		Allentown
41	30	medium gray	coarse	abundant quartz sand lenses, dolomite intraclasts, minor cross-bedding	dolomite	none		Allentown
42	51	dark gray	fine	lower 25 cm are alternating gray and brown algal laminate	dolomite	none		Allentown
43	46	medium gray	medium	occasional algal laminations	dolomite	none		Allentown
44	41	light gray	coarse	thinly bedded, flaggy, some sense of convex up laminate, especially near base of bed	dolomite	none		Allentown
45	64	medium dark gray	micrite	finely algal laminated, weathers orange-yellow	dolomite	none		Allentown
46	61	medium gray	fine	occasional algal laminations, sharp upper contact	dolomite	none		Allentown
47	41	medium gray	fine		dolomite	none		Allentown
48	30	medium gray	medium	occasional algal laminations	dolomite	none		Allentown
49	41	medium gray	fine	thinly bedded, flaggy, some algal partings, individual units are 2.5 cm thick	dolomite	none		Allentown
50	30	medium gray	medium	laminated	dolomite	none		Allentown
51	8	medium gray	medium	thinly bedded	dolomite	none		Allentown
52	20	medium gray	medium	thinly bedded, upper bed contacts are uneven but sharp	dolomite	none		Allentown
53	38	medium gray	fine	lower unit: 8 cm, mid-unit: 20 cm, upper unit 10 cm: has thin shale partings	dolomite	none		Allentown
54	25	medium gray	fine	thinly bedded, flaggy	dolomite	none		Allentown
55	10	medium gray	fine	thinly bedded, flaggy	dolomite	none		Allentown
56	15	light gray	fine	thin shale partings or stylolite surfaces, very	dolomite	none		Allentown

				flaggy				
57	122	light gray	fine	thinly bedded, flaggy, fine algal laminations, stylolite surfaces, possible shale particles	dolomite	none		Allentown
58	25	light gray	fine	thinly bedded, flaggy, fine algal laminations, stylolite surfaces, possible shale particles	dolomite	none		Allentown
59	42		coarse	quartzose	sandstone	none		Allentown
60	56	very light gray	very coarse	sulfurous with plentiful large closts of quartz crystals in circular vugs up to 10 cm in diameter	dolomite	none		Allentown/ Rickenbach
61	51	medium gray	medium	thinly bedded	dolomite	none		Allentown/ Rickenbach
62	15	very light gray	medium /coarse	flaggy with lenses of quartz sand	dolomite	none		Allentown/ Rickenbach
63	36	dark gray	coarse	fetid with wisps of sand grains	dolomite	none		Allentown/ Rickenbach
64	51	medium gray	medium	abundant large vugs filled with quartz (8-10 cm diameter)	dolomite	none		Allentown/ Rickenbach
65	71	medium gray	micrite	thinly bedded with algal laminations and occasional lenses of quartz	dolomite	shale partings wit intermitt ant seams of chert replacing sand lenses, chert has brecciate d masses of chert with sand grains		Allentown/ Rickenbach
66	64	medium gray	coarse	abundant quartz vugs, thickly bedded, Hope weathering pattern	dolomite	none	Hope	Rickenbach
67	102	light gray	coarse	sulfurous, abundant quartz vugs (6 inches in diameter)	dolomite	none	Hope	Rickenbach
South Traverse, Far Eastern Corner of Study Area								
68	30	medium/ dark gray	medium	sulfurous	dolomite	none	Hope	Rickenbach
69	24	light ash gray	medium	bedding surfaces are wavy and uneven	dolomite	none	Hope	Rickenbach
70	70	light	medium	scattered quartz vugs	dolomite	none	Hope	Rickenbach

		gray	/fine	up to 5 cm in diameter				
71	10	very light gray	medium /fine		dolomite	none	Hope	Rickenbach
72	9	very light gray	medium /fine		dolomite	none	Hope	Rickenbach
73	8	very light gray	medium /fine		dolomite	none	Hope	Rickenbach
74	24	light gray	micrite		dolomite	none	Hope	Rickenbach
75	17	light gray	medium		dolomite	none	Hope	Rickenbach
76	90	light gray	medium /coarse	sugary, quartz vugs 8 cm in diameter, highly sulfurous	dolomite	none	Hope	Rickenbach
77	28	medium gray	very coarse	sandy, upper contact sharp but uneven, cuspate in places	dolomite	none	Hope	Rickenbach
78	30	medium gray	coarse	sulfurous, billowy sequence, some beds up to 40 cm thick in places, 2.5 cm quartz vugs scattered throughout, upper 5 cm: white quartzite accumulating in sags atop uneven surface of dolomite, some evidence of cross-bedding and algal laminations	dolomite	none	Hope	Rickenbach
79	15	medium gray	micrite		dolomite	none	Hope	Rickenbach
80	14	light gray	micrite	2.5 cm sand lenses	dolomite	none	Hope	Rickenbach
81	9	brown	coarse	iron stained, quartzose	sandstone	none	Hope	Rickenbach
Moved 30 meters along strike								
82	42	very dark gray	very coarse	crystalline, cuspate upper surface	dolomite	chert occuring as pods and thin beds lining the upper surface, dark gray, transluce nt, brecciate d, tightly welded,	Hope	Rickenbach

						much like Rock Island section, up to 30 cm thick, found in convexities of upper surface		
83	40	dark gray	very coarse	crystalline, sulfurous, Crooked Swamp-like, already transitioning into Branchville Member	dolomite	none	Crooked Swamp	Rickenbach
84	40	very dark gray	medium	crystalline, rank swampy smell,finely laminated shale partings, orange weathering	dolomite	none	Branchville	Epler
85	60	medium gray	fine	finely laminated, argillic partings on bed surfaces, partings about 2.5 cm apart, quartz vugs 2.5 cm wide scattered sporadically	dolomite	at some locations : 3 to 5 beds (2.5 cm thick) of chert separated by 5 cm of dolomite, above 5 cherts is another surface that has a thicker chert bed (15 cm thick)	Branchville	Epler
86	22	dark gray	coarse	crystalline, yellow inclusions (sphalerite), abrupt upper contact	dolomite	none	Branchville	Epler
87	30	light gray	fine	divided into 3 beds; 6/4/20 cm: thinly bedded, laminated algal partings, slump structues common, scour and fill channels, uneven upper surface	dolomite	none	Branchville	Epler
88	25	very dark gray	very fine	thinly bedded, lower 10 cm: scour and fill composed of quartz	dolomite	none	Branchville	Epler

				sand, quartz sand diminishes up section				
89	12	dark gray	micrite	algal laminations common, concave/convex upper surface, sharp and uneven upper contact	dolomite	none	Branchville	Epler
90	12	dark gray	micrite	algal laminations common, concave/convex upper surface, sharp and uneven upper contact	dolomite	none	Branchville	Epler
91	28	dark gray	micrite	algal laminations common, concave/convex upper surface, sharp and uneven upper contact, argillic partings	dolomite	none	Branchville	Epler
92	38	dark gray	medium	finely laminated	dolomite	none	Branchville	Epler
93	13	dark gray	micrite	shale partings and algal laminations	dolomite	none	Branchville	Epler
94	8	dark gray	micrite	shale partings and algal laminations	dolomite	none	Branchville	Epler
95	30	dark gray	micrite	shale partings and algal laminations	dolomite	none	Branchville	Epler
Section 30 meters to North								
96	50	medium gray	very coarse	billowy beds, no sulfurous smell, much like Crooked Swamp	dolomite	none	Branchville	Epler
97	35	medium/light gray	very coarse	slightly sulfurous, thickly bedded, billowy	dolomite	none	Branchville	Epler
98	45	light gray	very coarse	thickly bedded	dolomite	none	Branchville	Epler
99	25	light gray	very coarse	small Epler workshop, Epler workshops along strike to the north	dolomite	chert?	Branchville	Epler
30 meters to South								
100	120	medium gray	very coarse	thickly bedded	dolomite	none	Branchville	Epler
101	17	very light gray	coarse		dolomite	two thinly developed beds of lavender to orchid and white chert	Branchville	Epler
102	20	light gray	very coarse		dolomite	none	Branchville	Epler
103	52	light gray	very coarse	very thickly bedded, no sulfurous smell	dolomite	none	Branchville	Epler

104	14	light gray	very coarse	very thickly bedded, no sulfurous smell	dolomite	none	Branchville	Epler
105	75	light gray	very coarse	very thickly bedded, no sulfurous smell	dolomite	none	Branchville	Epler
106	15	light gray	very coarse	very thickly bedded, no sulfurous smell	dolomite	none	Branchville	Epler
107	60	light gray	very coarse	very thickly bedded, although it looks like Crooked Swamp, it does not have a sulfurous smell, similar to cataclasite zone at the Aggregate Quarry	dolomite	none	Crooked Swamp	Rickenbach
30 meters to Southwest								
108	80	light gray	coarse	sulfurous like Crooked Swamp	dolomite	none	Crooked Swamp	Rickenbach
109	80	light gray	coarse	fetid, hummocky upper contact	dolomite	none	Branchville	Epler
110	30	light gray	coarse	fetid	dolomite	none	Branchville	Epler
111	25	light gray	coarse	thinly bedded, strongly fetid	dolomite	none	Branchville	Epler
112	15	medium gray	medium	thinly bedded, signs of cross-bedding	dolomite	base of unit contains a thin seam of chert, dark gray to blue gray to light gray to white, lavender and orchid in places, highly transluce nt	Big Springs	Epler
113	55	medium gray	medium		dolomite	thin laminatio ns bearing 4 distinct chert units: lower 2 units are 2.5 cm thick and separated	Big Springs	Epler

						by 2 to 20 cm, upper 2 units are 3 to 4 cm thick, chert is white, gray, orchid or lavender, translucent		
Large Twin Maple Section								
114	20	medium gray	medium	upper contact sharp and uneven	dolomite	none	Big Springs	Epler
115	7	medium gray	coarse	signs of cross-bedding	dolomite	none	Big Springs	Epler
116	28	light gray	fine	thinly bedded, algal laminated	dolomite	none	Big Springs	Epler
117	17	very dark gray	medium to fine		dolomite	none	Big Springs	Epler
118	15	light gray	very coarse	fetid	dolomite	none	Big Springs	Epler
119	8	light gray	coarse	fetid	dolomite	none	Big Springs	Epler
120	14	light gray	coarse	fetid	dolomite	none	Big Springs	Epler
121	13	medium gray	medium		dolomite	none	Big Springs	Epler
122	15	medium gray	medium		dolomite	none	Big Springs	Epler
123	22	medium gray	medium		dolomite	none	Big Springs	Epler
124	13	medium gray	medium		dolomite	none	Big Springs	Epler
75 meters North (Purple chert horizon, down section slightly)								
125	50	light gray	medium to fine		dolomite	chert occurs as thin beds or clots, purple chert clasts are angular, embedded in later generation of light colored chert, on strike with last purple	Big Springs	Epler

						chert occurrence.		
126	37	dark gray	micrite	very finely laminated, algal laminations abundant, rip-up clasts, abundant sand lenses, top of unit: green argillite partings	dolomite	angular fragments of chert	Big Springs	Epler
127	50	dark gray	micrite	algal laminated, occasional rip-up clasts, thickly bedded, shale partings along upper surface	dolomite	none	Big Springs	Epler
128	70	medium to dark gray	medium	crystalline, algal laminated, occasional floating sand grains, rip-up clasts and digitate algal, unit weathers orange	dolomite	lower 15 cm: porcellainous, gray, chert-replaced algal, entering red/green chert horizons	Big Springs	Epler
129	60	dark gray	medium to fine	continuing up section with red/green chert horizons at base of unit	dolomite	red/green chert at base	Big Springs	Epler
130	12	light gray	medium		dolomite	none	Big Springs	Epler
131	19	very dark gray	fine		dolomite	none	Big Springs	Epler
132	38	medium gray	medium		dolomite	none	Big Springs	Epler
133	60	dark gray	medium to fine	yellow and white clots on inside of unit, upper 20 cm, fine algal laminations	dolomite	none	Big Springs	Epler
134	80	light gray	fine	algal laminated, occasional rip-up clasts, weathers orange	dolomite	none	Big Springs	Epler
135	10	dark gray	micrite		dolomite	none	Big Springs	Epler
136	54	medium gray	medium	algal laminated	dolomite	none	Big Springs	Epler
137	35	medium gray	medium	algal laminated, similar to algal structures associated with gray porcelainous zone, fallen block detached from unit: 90 cm of dark gray, medium-grained, algal	dolomite	quarry activity area, on strike with red/greee n chert sequence	Big Springs	Epler

				laminated dolomite with conspicuous, contorted algal structres which appear dessicate in places		s		
138	40	light gray	micrite	algal laminated, weathers orange	dolomite	none	Big Springs	Epler
20 meters to south by 4 Beech trees								
139	70	medium gray	medium	algal laminated with some dessicated algal structues	dolomite	none	Big Springs	Epler
140	80	medium gray	medium	algal laminated with some dessicated algal structues	dolomite	none	Big Springs	Epler
141	60	medium gray	micrite	algal laminated with some dessicated algal structues	dolomite	none	Big Springs	Epler
142	5	dark gray	fine	finely laminated, arenaceous	dolomite	none	Big Springs	Epler
143	70	light gray	micrite	large brecciated clasts of dolomite incorporated into unit, may be paleokarst, 5 cm thick red punctate algal structures throughout	dolomite	none	Big Springs	Epler
144	80	light gray	micrite	interspersed with algal laminations, upper 20 cm: rip-up clasts and brecciated fragments	dolomite	none	Big Springs	Epler
145	50	ash gray	micrite	finely algal laminated with thin wisps of sand	dolomite	none	Big Springs	Epler
146	70	light ash gray	micrite	algal laminated,occasional sand lenses and wisps, rip-up clasts	dolomite	none	Big Springs	Epler
				75 meters south along strike, large purple chert quarry (dropped down in section a few feet), 200 feet further south along strike in Big Springs Member: large chert quarry under single Beech tree				
Parallel traverse going back down section, possibly as low as Crooked Swamp: 75 meters south of previous traverse line, beginning at large Black Walnut tree								
147	50	medium gray	very coarse	sharp uneven upper contact	dolomite	none	Crooked Swamp	Rickenbach
148	50	medium gray	very coarse	billowy, sharp but uneven upper contact	dolomite	none	Crooked Swamp	Rickenbach
149	26	medium	coarse	billowy upper contact	dolomite	none	Crooked	Rickenbach

		gray					Swamp	
150	30	medium gray	coarse	billowy upper contact	dolomite	none	Crooked Swamp	Rickenbach
151	30	medium gray	coarse	billowy upper contact, quartz sand lenses in depressions up to 40 cm in length	dolomite	none	Crooked Swamp	Rickenbach
152	30	dark gray	micrite	algal laminated, abundant cross bedding, 2.5 cm sand lenses, some thrombolitic algal stromatolites	dolomite	none	Crooked Swamp	Rickenbach
153	30	dark gray	micrite	algal laminated, abundant cross bedding, 2.5 cm sand lenses, some thrombolitic algal stromatolites	dolomite	none	Crooked Swamp	Rickenbach
154	20	dark gray	micrite	algal laminated, abundant cross bedding, 2.5 cm sand lenses, some thrombolitic algal stromatolites	dolomite	none	Crooked Swamp	Rickenbach
155	14	light gray	micrite	upper 7 cm: thick accumulations of sand lenses	dolomite	none	Crooked Swamp	Rickenbach
156	70	very dark gray	coarse	crystalline, fetid, hummocky but sharp upper contact (Rickenbach/Epler contact)	dolomite	5 cm thick brecciated chert horizon, gray blue with dark blue to black clasts, above chert horizon is argillic sequnce with 2 cm of shaly chert, chert increases in thickness laterally, becomes light blue/gray	Branchville	Epler

						in places, finely laminated/shaly in places		
157	25	medium gray	coarse	quartz sand lenses capped by shale units, upper contact is hummocky but sharp, sand lenses appear to be confined to sags in beds	dolomite	none	Branchville	Epler
158	70	medium gray	medium	algal laminated, 1 cm thick quartz sand lenses scattered throughout unit	dolomite	none	Branchville	Epler
159	15	dark gray	micrite	finely algal laminated, wisps of quartz sand and clots of quartz vugs up to 2 cm in diameter	dolomite	none	Branchville	Epler
160	40	dark gray	micrite	scattered quartz vugs up to 5 cm in diameter	dolomite	none	Branchville	Epler
161	20	light gray	coarse	crystalline, occasional sand grains	dolomite	none	Branchville	Epler
162	28	dark gray	micrite	occasional quartz clots	dolomite	none	Branchville	Epler
163	25	dark gray	medium	crystalline	dolomite	none	Branchville	Epler
164	30	dark gray	micrite	abundant stylolites	dolomite	none	Branchville	Epler
165	25	dark gray	micrite	algal laminated, stylolites present	dolomite	none	Branchville	Epler
Outcrop # 3								
166	70	dark gray	coarse	crystalline, fetid, hummocky and sharp upper surface	dolomite	none	Branchville	Epler
167	15	dark gray	medium	algal laminated	dolomite	none	Branchville	Epler
168	10	dark gray	medium	algal laminated	dolomite	none	Branchville	Epler
169	20	dark gray	medium	occasional wisps of sand	dolomite	none	Branchville	Epler
170	13	dark gray	medium to fine		dolomite	none	Branchville	Epler
171	10	very dark gray	micritic	floating sand grains, laminated algal and stylolites	dolomite	none	Branchville	Epler
172	34	dark gray	micritic	stylolite surfaces, occasional laminated algal, floating quartz grains	dolomite	none	Branchville	Epler
Continuation up section may begin here								
173	13	very dark gray	micritic	argillic partings	dolomite	mid-unit: 2 cm thick ash gray, finely	Big Springs	Epler

						laminated chert bed		
174	17	medium gray	medium	thinly bedded	dolomite	chert unit grades laterally into shale unit	Big Springs	Epler
175	40	ash gray	micritic	finely algal laminated, weathers orange	dolomite	none	Big Springs	Epler
176	18	very light gray	fine	algal laminated, weathers white	dolomite	none	Big Springs	Epler
177	28	medium gray	coarse		dolomite	none	Big Springs	Epler
178	60	medium gray	coarse	fetid	dolomite	none	Big Springs	Epler
179	60	medium gray	coarse	fetid	dolomite	none	Big Springs	Epler
180	24	medium gray	coarse		dolomite	none	Big Springs	Epler
181	40	medium gray	micritic	algal laminated, floating sand grains, stylolites	dolomite	none	Big Springs	Epler
182	78	medium gray	medium		dolomite	none	Big Springs	Epler
183	20	medium gray	coarse		dolomite	none	Big Springs	Epler
184	30	very dark gray/nearly black	fine	finely laminated	shaly dolomite	none	Big Springs	Epler
185	20	very dark gray	coarse	thinly bedded, scattered quartz sand grains	dolomite	none	Big Springs	Epler
186	20	medium/ dark gray	coarse		dolomite	none	Big Springs	Epler
187	10	dark gray	coarse	shale partings on bottom of bed	dolomite	none	Big Springs	Epler
188	17	medium gray	very coarse	fetid	dolomite	none	Big Springs	Epler
189	30	medium gray	coarse	fetid	dolomite	none	Big Springs	Epler
190	30	dark gray	medium		dolomite	none	Big Springs	Epler
191	28	dark gray	medium	rip-up clasts	dolomite	none	Big Springs	Epler
192	20	medium gray	medium	finely laminated	dolomite	none	Big Springs	Epler
193	60	variable	variable	lower 10 cm: dark grain, micrite; next 7 cm: light gray, coarse-grained, sandy; next 30 cm: light gray, medium to fine-	dolomite	at 13 cm: 2 cm thick purple chert beds,	Big Springs	Epler

				grained, algal laminated		each separted by 1 cm of quartz sand dolomite; at 23 cm: thinly bedded chert beds, 2 cm thick, separated by 1 cm of quartz sand dolomite		
194	50	light gray	coarse		dolomite	none	Big Springs	Epler
195	80	light medium gray	coarse	billowy	dolomite	none	Big Springs	Epler
196	35	medium gray	medium		dolomite	none	Big Springs	Epler
197	15	light gray	medium		dolomite	none	Big Springs	Epler
198	15	light gray	micrite		dolomite	none	Big Springs	Epler
199	30	light gray	micrite		dolomite	none	Big Springs	Epler
200	40	medium gray	medium		dolomite	none	Big Springs	Epler
201	16	light gray	micrite		dolomite	none	Big Springs	Epler
202	20	light gray	micrite		dolomite	none	Big Springs	Epler
203	40	light/medium gray	very coarse	billowy beds, convex upward, thinly laminated	dolomite	purple chert occurs as thin seams, wisps, and clots	Big Springs	Epler
204	8	light/medium gray	very coarse	billowy beds, convex upward, thinly laminated	dolomite	capped by purple, algal laminated chert	Big Springs	Epler
205	33	light gray	very coarse	convex upward, billowy beds	dolomite	top of unit: 3 thick algal laminate	Big Springs	Epler

						d purple chert		
Covered setion, as much as 2 meters								
206	32	medium gray	very coarse		dolomite	none	Big Springs	Epler
207	27	medium gray	coarse	thinly bedded	dolomite	none	Big Springs	Epler
208	37	medium gray	coarse	cross-bedded sands, cut-n-fill channels	dolomite	brecciated chert, bounded at top by 3 cm of gray, algal laminated chert	Big Springs	Epler
209	45	medium gray	very coarse	billowy, convex upward surfaces	dolomite	in adjacent concavity, 60 cm of brecciated chert, dark purple/gray, finely laminated, matrix: light gray, coarse-grained dolomite	Big Springs	Epler
210								
Top of hill, missing another 2 meters of section								
211	90	dark gray	micrite	thinly laminated	dolomite	none	Big Springs	Epler
212	80	dark gray	medium	fetid, looks like paleokarst block	dolomite	none	Big Springs	Epler
213	80	dark gray	coarse	crystalline, coul be paleokarst	dolomite	none	Big Springs	Epler
214	80	medium gray	micrite	weathers orange, occasional intraclasts, could be paleokarst, capped by dessicated algal mats, porous, punky	dolomite	none	Big Springs	Epler
Gigantic stand of twin beeches								
215	70	medium gray	coarse	upper contact sharp but uneven	dolomite	none	Big Springs	Epler
216	60	medium gray	very coarse		dolomite	none	Big Springs	Epler
217	90	very dark gray	fine	finely laminated with algal structures, sand	dolomite	none	Big Springs	Epler

				lenses, upper 20 cm: very coarse -grained, upper surface marked by argillic shale partings (quartz clots 2 cm diameter)				
218	36	medium gray	coarse	upper surface marked by shale or argillic unit approximately 3 cm thick	dolomite	none	Big Springs	Epler
219	30	medium gray	coarse	billowy	dolomite	none	Big Springs	Epler
220	20	medium gray	coarse		dolomite	none	Big Springs	Epler
221	40	medium gray	very coarse		dolomite	top of bed: occasional brecciated chert, light purple/gray clasts	Crooked Swamp	Rickenbach
222	60	light gray	very coarse		dolomite	none	Big Springs	Epler
223	38	medium gray	coarse	very fetid	dolomite	lower 10 cm: 7 brecciated very thin, purple chert beds, chert beds are less than 1 cm thick and are concave/convex, next 10 cm: very brecciated, algal laminated cherts, comprise one or two one cm. thick beds, another brecciated chert	Big Springs	Epler

						sequence, algal		
224	25	light gray	coarse	finely laminated	dolomite	upper 10 cm: remains of three 2 cm thick chert beds, now very brecciated	Big Springs	Epler
Outcrop 4A								
225	30	dark gray	medium		dolomite	none	Big Springs	Epler
226	35	medium gray	medium	upper 10 cm: dessicated algal structures	dolomite	none	Big Springs	Epler
227	58	medium gray	medium	minor argillite partings	dolomite	none	Big Springs	Epler
228	50	medium gray	micrite	scattered algal structures, intraclasts, overturned blocks, possible paleokarst	dolomite	plentiful brecciated chert fragments	Big Springs	Epler
Outcrop 4B								
229	40	medium gray	medium	fetid, unit may be sheared out	dolomite	none	Big Springs	Epler
230	25	dark gray	micrite		dolomite	none	Big Springs	Epler
231	25	light gray	micrite	algal laminated	dolomite	none	Big Springs	Epler
232	30	light gray	micrite	algal laminated	dolomite	none	Big Springs	Epler
233	50	medium gray	medium	stylolite surfaces	dolomite	none	Big Springs	Epler
234	70	medium gray	micrite	sharp upper contact	dolomite	none	Big Springs	Epler
235	30	medium gray	micrite	billowy surfaces, fine algal laminations	dolomite	none	Big Springs	Epler
236	38	medium gray	medium		dolomite	none	Big Springs	Epler
237	50	very dark gray	coarse	fetid, algal laminations, floating sand grains, stylolite surfaces, abundant intraclasts, rip-up clasts	dolomite	none	Big Springs	Epler
238	40	dark gray	coarse	fetid, stylolite surfaces, minor algal laminations	dolomite	none	Big Springs	Epler
239	50	medium gray	fine	algal laminated, stylolites, weathers orange	dolomite	none	Big Springs	Epler
West side of ravine, linear series of algal mound structures, crossed a number of Big Spring								

outcrops(look like supertidal micrites)								
240	75	medium gray	fine	algal laminated, some argillic parting surfaces	dolomite	none	Big Springs	Epler
241	40	medium gray	fine	algal laminated, upper 20 cm: much darker gray, some algal sructures, looks dessicated	dolomite	none	Big Springs	Epler
242	10	medium gray	medium	algal laminated	dolomite	none	Big Springs	Epler
243	20	light gray	medium	algal laminated	dolomite	none	Big Springs	Epler
244	50	medium gray	coarse	algal lamianted, algal become somewhat convex, some argillic shale partings, contorted beds	dolomite	none	Big Springs	Epler
245	40	medium gray	medium	finely laminated	dolomite	none	Big Springs	Epler
246	80	medium gray	medium	finely laminated, intraclasts and rip-up clasts toward upper half of unit	dolomite	none	Big Springs	Epler
West side of ravine								
247	45	medium/ dark gray	medium	algal laminated, bright red weathering	dolomite	none	Big Springs	Epler
248	50	dark gray	medium	thinly bedded, strongly fetid	dolomite	none	Big Springs	Epler
249	35	medium gray	micrite	thickly bedded	dolomite	none	Big Springs	Epler
250	20	medium gray	coarse	algal laminated, convex beds	dolomite	none	Big Springs	Epler
251	40	medium gray	medium	algal laminated, dessicated algal structures	dolomite	none	Big Springs	Epler
Eastern side of pond, outcrop parallel to stone wall which runs to pond								
252	50	dark gray	medium	algal laminated and stylolitized	dolomite	none	Big Springs	Epler
				Upsection along strike				
253	50	dark gray	medium	algal laminated and stylolitized	dolomite	none	Big Springs	Epler
254	20	very dark gray	micrite		dolomite	none	Big Springs	Epler
255	70	medium gray	medium	fetid	dolomite	none	Big Springs	Epler
25 meters to south, proceeding up-section								
256	?	medium gray	very coarse	massive	dolomite	chert breccia, black, transluce nt, somewha	Lafayette	Epler

						t oolitic		
257	30	dark gray	medium		dolomite	none	Lafayette	Epler
258	40	very dark gray	micrite		dolomite	none	Lafayette	Epler
259	30	medium gray	medium		dolomite	none	Lafayette	Epler
260	30	medium/ dark gray	medium	dark burrow structures (1 cm each)	dolomite	none	Lafayette	Epler
261	20	medium/ dark gray	medium	dark burrow structures (1 cm each)	dolomite	none	Lafayette	Epler
262	25	dark gray	coarse	crystalline, fetid	dolomite	none	Beaver Run	Ontelaunee
263	40	dark gray	medium		dolomite	none	Lafayette	Epler
264	10	dark gray	medium		dolomite	none	Lafayette	Epler
263	70	dark gray	coarse	algal laminations, orange weathering	dolomite	none	Lafayette	Epler
264	100	very dark gray	micrite	finely laminated, weathers orange, stylolite surfaces, argillic clay seams	dolomite	none	Lafayette	Epler
North along strike about 75 meters from transitional beds								
265	100	very dark gray	micrite	solution cleavage, stylolite surfaces	dolomite	chert at base, dark colored, rubbly, oolitic	Lafayette	Epler
266	55	very dark gray	micrite	fetid, upper 10 cm: quartz vugs up to 2 cm in diameter	dolomite	none	Lafayette	Epler
267	100	very dark gray	micrite	strong solution cleavage, some fine laminations	dolomite	none	Lafayette	Epler
268	110	very dark gray	very fine	laminated, solution cleavage, top of unit: 3 to 5 cm of desiccated algal structures	dolomite	top of unit: some algal structures replaced by alternating black and gray, laminated chert	Lafayette	Epler
Outcrop on south side of carriage path								
269	120	medium gray	medium	thinly bedded	dolomite	none	Lafayette	Epler
270	20	dark gray	very coarse		dolomite	none	Lafayette	Epler
271	25	medium gray	coarse	fetid, thinly algal laminated	dolomite	none	Lafayette	Epler
272	70	medium	coarse	hummocky, uneven	dolomite	none	Lafayette	Epler

		gray		surfaces				
273	50	medium gray	medium	thinly bedded, finely laminated, sharp and hummocky upper contacts	dolomite	none	Lafayette	Epler
274	30	dark gray	fine	thinly bedded, algal laminated, sharp and hummocky upper contacts	dolomite	none	Lafayette	Epler
275	50	very dark gray	micrite	thickly bedded, algal laminated, upper 10 cm: desiccated algal, sharp and hummocky upper contacts	dolomite	none	Lafayette	Epler
276	60	medium gray	medium	finely algal laminated	dolomite	none	Lafayette	Epler
277	45	medium gray	medium	finely algal laminated	dolomite	none	Lafayette	Epler
278	70	dark gray	fine	thickly bedded, fetid, hummocky, billowy beds	dolomite	none	Lafayette	Epler
279	50	dark gray	medium	fetid, finely algal laminated	dolomite	none	Lafayette	Epler
280	20	dark gray	medium	fetid, finely algal laminated	dolomite	none	Lafayette	Epler
281	50	dark gray	medium	fetid, thickly bedded	dolomite	none	Lafayette	Epler
282	80	very dark gray	fine	fetid	dolomite	none	Lafayette	Epler
283	50	medium gray	medium	thinly bedded	dolomite	none	Lafayette	Epler
284	70	dark gray	medium	finely algal laminated	dolomite	none	Lafayette	Epler
285	75	very dark gray	medium	finely algal laminated	dolomite	none	Lafayette	Epler
286	30	medium gray	medium	fetid	dolomite	none	Lafayette	Epler
287	40	dark gray	medium		dolomite	none	Lafayette	Epler
	1005							
				stopped at outcrop just east of western carriage path, on western edge of pond				
Fox's Lair: south of lair 100 feet, center of ravine, down-section from blue Lafayette chert								
288	130	medium gray	medium	strongly fetid, thinly bedded, each bed 7 cm thick, possibly paleokarst	dolomite	none	Big Springs	Epler
289	60	medium gray	medium	strongly fetid, thinly bedded, each bed 7 cm thick, possibly paleokarst, N54E 40 NW	dolomite	none	Big Springs	Epler
290	15	medium gray	fine	finely algal laminated, fetid	dolomite	none	Big Springs	Epler

291	120	medium gray	medium	finely algal laminated, very fetid, appears to be paleokarst	dolomite	none	Big Springs	Epler
50 feet north of Fox's Lair, 2 silver beeches								
292	240	dark gray	medium /coarse	thin beds, 5-7 cm thick, algal laminated, ruditic, calcarenite	dolomite	none	Big Springs	Epler
				to northwest of fox's lair may be a repeat of last section, now in a ravine				
293	90	dark gray	medium /coarse	algal laminated	dolomite	none	Big Springs	Epler
294	70	dark gray	fine	algal laminated, weathers to a light ash gray, signs of internal horizontal burrow structures	dolomite	none	Big Springs	Epler
295	80	variable	variable	lower 20 cm: light gray, coarse-grained, fetid, punky, next 20 cm: dark gray, micrite, thinly bedded, argillic sequences, ash gray remnants of algal laminations, next 30 cm: dark gray, fine-grained, fetid, thin-bedded, next 13 cm: dark gray, medium-grain	dolomite	chert throughout lower 20 cm	Big Springs	Epler
296	105	medium gray	very fine	thinly bedded, algal laminated, signs of hummocky cross-bedding	dolomitic limestone	none	Big Springs	Epler
297	100	medium gray	very fine	thinly bedded, algal laminated, signs of hummocky cross-bedding, some algal structures, convex upward	dolomite	in limestone: black chert units (N70E)	Big Springs	Epler
North of main path, below Shagback Hickory and Twin Maple, down-section								
298	80	medium gray	medium	some burrow structures, algal laminations	dolomitic limestone	none	Big Springs	Epler
299	70	medium gray	fine	algal laminated	dolomitic limestone	none	Big Springs	Epler
	150							
				brings us up to argillic unit				
300	120	medium/ dark gray	medium /fine	1 cm wide quartz vugs and rosettes, 60 cm up in section: two concentrations of algal	dolomitic limestone	none	Big Springs	Epler

				laminations				
301	65	medium/ dark gray	medium /fine	1 cm wide quartz vugs and rosettes, no distinct concentrations of algal	dolomitic limestone	none	Big Springs	Epler
302	145	very dark gray	fine	finely laminated	dolomitic limestone	none	Big Springs	Epler
303	65	very dark gray	fine	finely laminated, upper 10 cm: argillic, desiccated, silicified, punky, perforated, laminated argillic sequence	dolomitic limestone	algal sequence grades into laminate d, dark to light gray, blue chert of Lafayette Member	Lafayette	Epler
SW edge of pond, 50 feet from water, north of main path, small hummock above chert horizon								
304	68	medium gray	medium	thickly bedded, billowy, upper surface of bed is uneven but sharp, bedding may be controlled by algal, fetid	dolomite	none	Lafayette	Epler
305	60	medium gray	coarse	thickly bedded, algal laminated throughout, sporadic, slabby, thin-bedded algal structures	dolomite	none	Lafayette	Epler
306	80	dark gray	medium /fine	strongly fetid, algal laminated, burrow structures, lower 10 to 15 cm: thick accumulations of flaggy, convex algal	dolomite	none	Lafayette	Epler
307	38	dark gray	fine	algal laminated, lower 10 cm: thick convex, argillic algals	dolomite	none	Lafayette	Epler
308	155	very dark	micrite	algal laminated, upper 20 cm: thin-bedded, flaggy, possibly karst	dolomitic limestone	upper 10 cm: chert-replaced algal, blue/gray , punky, perforate d	Lafayette	Epler
309	100	very dark	micrite	algal laminated, upper 20 cm: thin-bedded, flaggy, possibly karst	dolomitic limestone	upper 10 cm: chert-replaced algal, blue/gray	Lafayette	Epler

						, punky, perforated		
310	40	very dark	micrite	algal laminated, upper 20 cm: thin-bedded, flaggy, possibly karst	dolomitic limestone	upper 10 cm: chert-replaced algal, blue/gray, punky, perforated	Lafayette	Epler
311	90	light gray	coarse	infrequent algal laminations	dolomitic limestone	none	Lafayette	Epler
312	120	dark gray	medium	crystalline, thinly algal laminated	dolomite	none	Lafayette	Epler
313	110	medium gray	medium	finely algal laminated, upper 20 cm: concentrations of argillic stromatolites, perforated, punky, lighter gray towards top	dolomite	none	Lafayette	Epler
314	40	light gray	medium /fine	paleokarst, broken overturned beds, 1 cm wide quartz vugs, upper 10 cm: argillic algal laminations	dolomitic limestone	none	Lafayette	Epler
Moved southward down-section, on western side of north/south carriage path, west side of pond								
315	100	light gray	medium to fine	finely laminated	dolomitic limestone	none	Lafayette	Epler
316	60	light gray	medium	thickly bedded, sporadic algal laminations	dolomitic limestone	none	Lafayette	Epler
317	125	medium ash gray	medium	interspersed quartz vugs concentrated at 50 cm mark	dolomitic limestone	none	Lafayette	Epler
318	120	medium gray	medium	lower 30 cm: concentrations of algal laminations, upper portion gets dark gray	dolomitic limestone	none	Lafayette	Epler
319	130	medium gray	medium	fetid	dolomite	none	Lafayette	Epler
320	90	medium gray	medium	upper 10 cm: laminated algal	dolomite	lower 20 cm: scattered chert nodules up to 10 cm in diameter, at 80 cm: dark gray chert	Lafayette	Epler

						replacing algal structures or breccia zone,		
321	55	medium gray	medium	1 to 5 cm wide quartz vugs, some evidence of rip-up clasts	dolomitic limestone	none	Lafayette	Epler
322	110	dark gray	medium /coarse	scattered 1 to 2 cm wide quartz vugs, upper 40 cm: billowy, thick beds of algal laminate, punky perforated	dolomitic limestone	chert replacig upper 40 cm of punky unit	Lafayette	Epler
				50 feet of section missed				
Very large Beaver Run quarry, far western side of lake, quarries at Hemlocks, may have transitional beds in them								
323	200	medium gray	coarse	thickly bedded, billowy, fetid	dolomite	upper surface has 5 cm thick, discontinuous chert replacing algal sequence, scattered clots of chert in series of beds	Beaver Run	Ontelaunee
324	180	medium gray	coarse	thickly bedded, algal laminated, upper surface of bed is castilated and uneven	dolomite	upper 40 cm: thick concentration of algal stromatolitic beds, porous, punky, perforated and replaced by chert	Beaver Run	Ontelaunee
325	120			algal laminated, upper unit: beds convex in places as if algal controlled	dolomite	20-30 cm: thick accumulation of chert-replaced algal,	Beaver Run	Ontelaunee

						porous, punky, next 20 cm: algal laminated dolomite with sporadic chert, remainder of unit: thick concentration of chert-replaced algal, top of unit: 15-20 cm thick homogeneous, black chert		
326	40			algal laminated	dolomite	chert replacing algal stromatolites, porous, punky, perforated	Beaver Run	Ontelaunee
327	15	medium gray	medium	algal laminated	dolomite	none	Beaver Run	Ontelaunee
328	80			algal laminated	dolomite	black chert replacing algal stromatolites, porous, punky, perforated, convex mounds	Beaver Run	Ontelaunee
329	35	medium gray	medium	algal stromatolitic	dolomite	sporadic chert replacement, upper 40 cm: punky,	Beaver Run	Ontelaunee

						homogeneous black chert, all are convex lobes, domal		
330	130	medium gray	medium /fine	very fetid, sporadic algal laminations	dolomite	some sporadic, clotty, chert replaced algal	Beaver Run	Ontelaunee
At first terrace above large quarry in transitional Harmonyvale beds								
331	120	blue/gray	micrite	solution cleavage, white weathering surfaces	dolomite	lighter blue gray to navy blue clots of chert	Harmonyvale	Ontelaunee
332	270	blue	micrite	thickly bedded, pervasive solution cleavage, highly fetid	dolomite	fine-grained chert clots up to 10 cm in diameter scattered throughout	Harmonyvale	Ontelaunee
333	140	medium gray	micrite		dolomite	chert occurs as thin clots and wisps up to 20 cm in diameter	Harmonyvale	Ontelaunee
334	150	medium gray	micrite	hummocky and uneven upper contact	dolomite	large shards and clasts of ripped-up chert beds	Harmonyvale	Ontelaunee
335	80		micrite	pervasive solution cleavage, beds may be boudins	dolomite	navy to robins-egg blue chert beds, lower 20 cm: brecciated chert,	Harmonyvale	Ontelaunee

						mid-unit: homogeneous beds, upper unit: finely laminated and brecciated, like a shear zone, boudinage, chert pods are 180-200 cm in diameter, grade laterally into micritic dolomite		
336	17					convex pods of chert (100 to 120 cm in diameter), brecciated throughout, dark clasts and light blue/gray matrix	Harmonyvale	Ontelaunee
337	40					dark blue to fine ash gray chert, laminated, brecciated in part, convex beds, grade laterally into dolomite	Harmonyvale	Ontelaunee
338	150	dark gray	micrite	weathers white,	dolomite	none	Harmonyva	Ontelaunee

				solution cleavage present, no signs of algal stromatolites			le	
339	70	very dark gray	micrite	solution cleavage, white weathering surfaces	dolomite	none	Harmonyva le	Ontelaunee
340	20	very dark gray	micrite	solution cleavage, white weathering surfaces	dolomite	none	Harmonyva le	Ontelaunee
341	50	very dark gray	micrite	solution cleavage, white weathering surfaces	dolomite	none	Harmonyva le	Ontelaunee
342	70	very dark blue/gray	micrite		dolomite	lower 30 cm: light blue/gray chert	Harmonyva le	Ontelaunee
At large Harmonyvale Quarry at hillside, may be repeat of last 2 chert units								
343	80					homogeneous chert, lower 40 cm: dark navy blue, brecciated	Harmonyva le	Ontelaunee
344	15					robins egg blue, laminated chert, ramainder is convex, billowy chert with brecciated upper surface, breccia clasts are dark blue	Harmonyva le	Ontelaunee
345	80	blue	micritic	lower 10 cm: thinly bedded, next 20 cm: thinly bedded, occasional algal laminations, upper 30 cm: algal laminated, upper surface is very sharp contact, solution cleavage at its best	dolomite	30-50 cm: irregular punky clots of brecciated blue/gray chert	Harmonyva le	Ontelaunee
346	15	blue	micritic	fine algal laminations, solution cleavage, upper contact is very sharp	dolomite	none	Harmonyva le	Ontelaunee

347	40	blue	micritic	thinly bedded, algal laminated	dolomite	algal concentrations in lower 10 cm and mid-unit contain irregular clots and masses of chet occuring as wisps and stringers	Harmonyvale	Ontelaunee
348	15	blue	micritic		dolomite	clots and masses of chert wisps and stringers, chert clots are 15 cm in diameter	Harmonyvale	Ontelaunee
349	15	blue	micritic	algal laminated, sharp bed contacts	dolomite	algal laminations replaced by light gray chert	Harmonyvale	Ontelaunee
350	13			upper and lower contacts are sharp		blue/gray to light blue/gray chert	Harmonyvale	Ontelaunee
351	20	blue	micritic	finely laminated	dolomite	chert replaces algal at 10 and 20 cm	Harmonyvale	Ontelaunee
352	5			algal laminated	dolomite	very punky, porous perforated chert replacing algal	Harmonyvale	Ontelaunee
353	10					robins ege blue, laminated chert	Harmonyvale	Ontelaunee
354	20	blue/gray	micritic	solution cleavage, sharp contacts, convex beds	dolomite	none	Harmonyvale	Ontelaunee

355	20					dark gray, translucent chert occurring as convex upward pods 130 cm in diameter, quartz vugs present	Harmonyvale	Ontelaunee
356	40	blue/gray	micritic	solution cleavage, sharp contacts, convex beds	dolomite	none	Harmonyvale	Ontelaunee
357	50	blue/gray	micritic	thinly bedded, algallmainated throughout	dolomite	chert partly replacing algal	Harmonyvale	Ontelaunee
358	40	blue/gray	micritic	thinly bedded, solution cleavage present	dolomite	upper 15 cm: clots of chert randomly oriented 2 to 3 cm in diameter	Harmonyvale	Ontelaunee
359	60	blue/gray	micritic	thinly bedded, solution cleavage present	dolomite	upper 15 cm: clots of chert randomly oriented 2 to 3 cm in diameter	Harmonyvale	Ontelaunee
360	25	blue	micritic	finely algal laminated	dolomite	partly replaced by chert	Harmonyvale	Ontelaunee
361	20	blue	micritic	solution cleavage, sharp contacts		1 cm of finely laminated chert at base	Harmonyvale	Ontelaunee
362	80	blue	micritic	solution cleavage, algal laminated, internally brecciated	dolomite	chert occurring as distinct algal stromatolites up to 15 cm in diameter at base,	Harmonyvale	Ontelaunee

						chert occurs as clots mid-unit, upper 30 cm: chert as irregular shards and clots		
363	60	blue	micritic	thinly bedded, solution cleavage, sharp contacts, thoroughly algal laminated	dolomite	chert as perfect replacement of algal laminations, some chert may occur as burrow infillings	Harmonyvale	Ontelaunee
364	20	blue	micritic	thinly bedded, solution cleavage, sporadic algal	dolomite	none	Harmonyvale	Ontelaunee
365	45	blue	micritic	some solution cleavage, sharp bedding contacts, sporadic algal stromatolites	dolomite	none	Harmonyvale	Ontelaunee
366	160	blue	micritic	finely algal laminated, some solution cleavage, sharp contacts	dolomite	none	Harmonyvale	Ontelaunee
367	60					dark navy blue, fairly homogeneous, somewhat porous chert, continuous beds which grade laterally into dolomite	Harmonyvale	Ontelaunee
368	60	dark gray	micritic	thinly bedded, occasional algal, abrupt and sharp contact, weathers dark	dolomite	none	Harmonyvale	Ontelaunee
369	25					dark	Harmonyva	Ontelaunee

						navy to robins egg blue to ash gray chert bed, extremely continuous, laminated, lower and upper surfaces are pale blue, mid-unit: dark navy blue and brecciated	le	
370	30	blue	micritic	finely algal laminated, solution cleavage, sharp contacts	dolomite	none	Harmonyvale	Ontelaunee
371	30	blue	micritic	sharp contacts, thinly bedded, occasional algal	dolomite	upper 15 cm: punky chert partially replacing algal, lower portions are fairly homogeneous and lack algal	Harmonyvale	Ontelaunee
372	80	blue	micritic	thinly bedded, solution cleavage	dolomite	lower 25 cm: abundant algal laminated, partially replaced by chert	Harmonyvale	Ontelaunee
373	30	blue/gray	micritic	occasional algal laminations	dolomite	chert nodules at base of unit, up to 10 cm	Harmonyvale	Ontelaunee

						in diameter, navy blue with light blue rims		
374	60	blue	micritic	occasional algal laminations, abundant finely disseminated algal	dolomite	none	Harmonyvale	Ontelaunee
375	30	blue	micritic	finely algal laminated	dolomite	none	Harmonyvale	Ontelaunee
376	25	blue	micritic	algal laminated, sharp contacts, solution cleavage	dolomite	none	Harmonyvale	Ontelaunee
377	20	blue	micritic	algal laminated, sharp contacts	dolomite	none	Harmonyvale	Ontelaunee
378	40	blue	micritic	algal laminated, sharp contacts	dolomite	none	Harmonyvale	Ontelaunee
379	20	blue	micritic	algal laminated, sharp contacts	dolomite	none	Harmonyvale	Ontelaunee
380	40	blue	micritic	occasional algal, sharp contacts	dolomite	none	Harmonyvale	Ontelaunee
381	90	blue	micritic	algal laminated, sharp contacts, thinly bedded	dolomite	none	Harmonyvale	Ontelaunee
382	35	blue	micritic	occasional algal, sharp contacts	dolomite	lower 10 cm: punky, perforated, gray, algal laminated, chert	Harmonyvale	Ontelaunee
383	50	blue	micritic	solution cleavage, occasional algal laminations, sharp contacts	dolomite	none	Harmonyvale	Ontelaunee
384	60	blue	micritic	abundant algal laminations, solution cleavage, sharp contacts	dolomite	none	Harmonyvale	Ontelaunee
385	25	blue	micritic	no algal, solution cleavage, sharp contacts	dolomite	none	Harmonyvale	Ontelaunee
386	40	blue	micritic	finely algal laminated, sharp contacts	dolomite	upper 5 cm: ash gray chert replacing algal stromatolites	Harmonyvale	Ontelaunee
387	15	blue	micritic	finely algal laminated, sharp contacts, some	dolomite	none	Harmonyvale	Ontelaunee

				pressure solution				
388	30	blue	micritic	solution cleavage, occasional algal laminations	dolomite	none	Harmonyvale	Ontelaunee
389	30	dark gray	micritic	solution cleavage	dolomite	abundant dark navy blue, very thin, chert beds, 1 cm thick, 10-15 cm wide	Harmonyvale	Ontelaunee
390	25	blue	micritic	abundant pressure solution, occasional algal	dolomite	none	Harmonyvale	Ontelaunee
391	25	blue	micritic	occasional algal, outstanding pressure solution, weathers white	dolomite	none	Harmonyvale	Ontelaunee

B.7 – ROCK ISLAND SECTION

Rock Island Section, Sussex County, New Jersey								
Bed	**Thickness (cm)**	**Color**	**Grain Size**	**Bedding Description**	**Lithology**	**Chert**	**Member**	**Formation**
Hemlock Grove Section (missing 150 feet of section)								
1	40	medium gray	medium	thinly bedded	dolomite	none		
2	30	medium gray	medium	thinly bedded, occasional stylolitized shards of chert, bedding surface covered with black shale	dolomite	none		
3	50	dark blue/ gray	micrite	thinly bedded (5-10 cm thick), shale partings at both contacts,argillite infillings in vertical joints and fractures, spider web structures, quartz vugs (10 cm diameter)	dolomite	chert replacing spider web structures		
4	70	dark blue/gray	micrite	thinly bedded (5-10 cm thick), shale partings at both contacts,argillite infillings in vertical joints and fractures, spider web structures, quartz vugs (10 cm diameter)	dolomite	chert replacing spider web structures		
5	70	dark blue/gray	micrite	thinly bedded (5-10 cm thick), shale partings at both contacts,argillite infillings in vertical joints and fractures, spider web structures, quartz vugs (10 cm diameter)	dolomite	chert replacing spider web structures		
6	70	dark blue/gray	micrite	thinly bedded (5-10 cm thick), shale partings at both contacts,argillite infillings in vertical joints and fractures, spider web structures, quartz vugs (10 cm diameter)	dolomite	chert replacing spider web structures		
7	100	dark blue/gray	micrite	thinly bedded (5-10 cm thick), shale partings at both contacts,argillite infillings in vertical joints and fractures, spider web structures, quartz vugs (10 cm diameter)	dolomite	chert replacing spider web structures		
30 feet to South								
1	20	medium gray	coarse	arenaceous, 10 cm thick quartz sand layer at bottom portion	dolomite	none		
2	40	medium gray	medium	thickly bedded, algal laminated	dolomite	at base: chert seam or		

						pod (3X15cm) in cut-n-fill channel, chert has floating sand grains		
3	120	medium gray	medium	algal laminated, some of algal convex upward, bedding planes capped by 2 cm black argillaceous shale, upper 10 cm of unit has floating sand grains	dolomite	none		
4	90	dark blue/gray	micrite	algal laminated and floating sand grains throughout, quartz vugs up to 40 cm in diameter, at some loactions along base, quartz vugs are stringers up to 20 cm wide, shale partings lace entire unit	dolomite	upper contact: thin porcellainous chert, could be algal replaced (3X30cm), convex downward		
5	50	dark gray	fine	algal laminated	dolomite	none	Crooked Swamp	Rickenbach
6	110	light gray	medium	fetid, sparse algal laminations, quartz as vugs and clots at base (5 cm thick), upper third of unit: more algal laminations and quartz seams (2X50cm)	dolomite	none		
7	50	light gray	medium	fetid, sparse algal laminations, quartz as vugs and clots at base (5 cm thick), upper third of unit: more algal laminations and quartz seams (2X50cm)	dolomite	none		
8	50	light gray	medium	fetid, sparse algal laminations, quartz as vugs and clots at base (5 cm thick), upper third of unit: more algal laminations and quartz seams (2X50cm)	dolomite	none		
9	25	dark gray	micrite	abundant shale partings at both contacts	dolomite	none		
10	85	medium/light gray	medium	shale partings at base, sparse algal	dolomite	none		
11	95	medium gray	medium/fine	thicker beds at upper portion of unit, sparse algal, severe	dolomite	none		

				solution cleavage				
12	40	medium gray	coarse	arenaceous	dolomite	mid unit: chert seam (50X5cm), discontinuous along strike		
13	60	dark gray	medium	thickly bedded	dolomite	none		
14	70	medium/dark gray	coarse	severe solution cleavage, strong recrystallization fabric, possible thrust fault, fracture/joint surfaces covered with black shale	dolomite	upper 20 cm: 2 continuous chert beds (3-4X15cm), cherts replacing algal laminations		
15	160		micrite	thickly bedded, occasional floating quartz sand grains, N40E (apparent strike of beds).	dolomite	none		
100 feet NE of previous section (along strike)								
1	300	medium gray	medium/coarse	shale partings throughout, some hints of algal, very contorted beds, possible thrust zone	dolomite	none		
				200 feet Ne of contorted section (Dead Tree Fall zone), northern zone of island				
1	80	medium gray	fine	fetid, floating sand grains, minor algal laminations throughout, horizontal stylolites	dolomite	occasional clots of chert		
2	50	medium gray	fine	fetid, minor algal structures	dolomite	none		
3	140	medium/dark gray			dolomite	none		
4	40	dark gray	very coarse	fetid, possibly Baby Swamp	dolomite	none		
5	50	dark gray	very coarse	fetid, looks like Crooked Swamp facies	dolomite	none		
6	20	medium gray	micrite	abundant quartz stringers and seams, upper 5 cm: continuous quartz sand lenses	dolomite	none		

7	95	light gray	medium /coarse	fetid, occasional quartz vugs thowards upper third of unit (N55E strike)	dolomite	none		
8	45	dark gray	medium /coarse	fetid	dolomite	none		
9	50	medium gray	coarse	fetid	dolomite	none		
10	55	dark gray	coarse	fetid, no sense of algal or any structures, maybe bioturbated, but that is it	dolomite	none		
11	50	dark gray	micrite	thinly bedded	dolomite	chert lenses and pods (2X10 cm).		
12	60	medium gray	variable	finely algal laminated, lower 20 cm are dark gray, fine-grained, becomes very coarse-grained towards top	dolomite	none		
13	170	variable	medium /coarse	fetid, quartz veining, quartz vugs, lower 40 cm: med gray, fetid, possible thrust zone, algal laminated, next 80 cm: dark gray, argillaceous infillings in horizontal and vertical joints, upper 35-40 cm: light gray, billowy, thickly-bedded	dolomite	from 25-40 cm: argillaceous infillings and algal structures replaced by chert, quartz vugs (5 cm diam) occur at base of infillings		
14	50	light gray	medium /coarse	strongly fetid, slabby, flaggy, like Baby Swamp, quartz vugs and stringers towards top of unit (up to 10 cm diameter), thin shale seam (1 cm thick)	dolomite	none		
15	40	light gray	medium /coarse	fetid, scattered quartz vugs throughout	dolomite	none		
16	120	medium gray	medium	fetid, lower 20 cm: abundant quartz vugs (2 cm diameter)	dolomite	none		
17	30	medium gray	micrite	thinly bedded, shale partings throughout, slightly convex upward, algal controlled, occasional floating sand	dolomite	none		
18	70	dark gray	micrite	fetid	dolomite	none		
19	35	light gray	micrite	5 cm thick beds of shale partings at both contacts	dolomite	none		

20	60	medium gray	micrite	algal laminated, shale partings, and sand stringers and lenses throughout unit, vertical dip	dolomite	none		
21	600			Missing Interval				
22	20	light gray	micrite	fetid, base of unit: large clots of quartz (10X10cm)	dolomite	top of unit: chert replacing alagal units (5 cm thick), discontinuous and continuous along strike		
23	40	light gray	micrite	fetid, base of unit: large clots of quartz (10X10cm)	dolomite	top of unit: chert replacing alagal units (5 cm thick), discontinuous and continuous along strike		
24	50	light gray	micrite	fetid, base of unit: large clots of quartz (10X10cm)	dolomite	top of unit: chert replacing alagal units (5 cm thick), discontinuous and continuous along strike		
25	40	medium gray	medium	strongly fetid, dips change from vertical to approximately 30 degrees	dolomite	none		
26	40	medium gray	medium	many shale partings	dolomite	none		
27	20	medium gray	medium /coarse		dolomite	none		
28	30	medium gray	medium	occasional shale partings	dolomite	none		
29	20	dark	micrite	numerous shale partings	dolomite	none		

		gray						
30	20	dark gray	coarse	fetid, occasional floating sand grains	dolomite	wisps and clots of black chert with floating sand grains		
31	20	medium gray	medium		dolomite	none		
32	40	medium /dark gray	coarse		dolomite	none		
33	50	light gray	coarse	fetid	dolomite	none		
34	25	medium gray	medium		dolomite	none		
35	55		micrite	fetid, thickly bedded	dolomite	upper 1 cm capped by thick shale turned to chert		
36	50	light gray	micrite	algal laminated, abundant quartz sand lenses and seams up to 1 cm thick	dolomite	none		
37	200		micrite	Covered interval: from floating blocks: algal laminated with abundant quartz sand layers (5X15 cm)	dolomite	black, highly transluce nt chert blocks in cut-n-fill channels, quartz grains floating in chert.		
38	30	light gray	medium	fetid, some signs of burrowing	dolomite	none		
39	50	light gray	coarse	fetid, 1cm thick quartz sand lens at base, expands laterally up to 10 cm, current indicators: cross-beds	dolomite	none		
40	25	light gray	medium	thickly bedded	dolomite	none		
41	30	light gray	medium	thickly bedded, upper 5 cm: quartz vugs	dolomite	none		
42	25	medium gray	fine	fetid	dolomite	none		

43	40	dark gray	micrite	fetid, abundant stylolites, lower 15 cm: looks burrowed and has sand lenses, upper 15 cm: abundant intraclasts and edgewise conglomerates	dolomite	mid-unit: sand becomes black, transluce nt chert pods, nodules and clots, has floating sand grains		
44	50	medium gray	micrite	slightly fetid, abundant floating sand grains and lenses, large zones of intraclasts, cut-n-fill channels	dolomite	none		
45	70	medium /light gray	medium	fetid, abundant rip-up clasts, occasional sand lenses	dolomite	none		
46	25	light gray	coarse	strongly fetid, large clots of quartz (10 cm diameter)	dolomite	none		
47	25	dark gray	medium	thickly bedded, abundant rip-up clasts and floating sand grains	dolomite	none		
48	300			Covered interval				
49	70	medium gray	medium /coarse		dolomite	none		
50	300			Covered interval				
51	70	medium gray	coarse	strongly fetid	dolomite	upper 10 cm: convex upward algal replaced by chert		
52	120	medium gray	medium /fine	slightly fetid, sand lenses-sand filling in joint spaces	dolomite	none		
53	50	light gray	medium	strongly fetid, dips change again to almost vertical	dolomite	none		
54	60	light gray	coarse	strongly fetid	dolomite	none		
55	45	light gray	medium /fine	upper 10 cm: abundant quartz sand lenses	dolomite	none		
56	55	very light gray	micrite	fetid	dolomite	none		
57	40	light blue/gra y	medium	fetid	dolomite	none		
58	40	light blue/gra y	medium	fetid	dolomite	none		

59	20	light gray	medium	shale partings and quartz sand lenses	dolomite	none		
60	70	dark gray	micrite	thickly bedded, abundant vertical quartz veins, thrust zone	dolomite	none		
61	10	dark gray	micrite	fetid	dolomite	none		
62	40	dark gray	micrite	fetid	dolomite	none		
63	15	dark gray	coarse	convex upward bedding	dolomite	laterally runs from dolomite to rugose, very porous chert lenses		
64	40	dark gray	fine	fetid, abundant shale partings, occasional quartz vugs (1 cm diameter), occasional floating quartz sand grains	dolomite	none		
65	30	medium gray	medium	slightly fetid	dolomite	none		
66	80	dark gray	fine	thinly bedded, abundant shale partings, occasional floating sand grains	dolomite	none		
67	25	medium gray	medium	thinly bedded, slightly fetid, signs of burrowing	dolomite	none		
68	30	medium gray	medium	shale partings, floating sand grains	dolomite	none		
69	30	dark gray	micrite	algal laminated, floating sand grains, shale partings, upper 5 cm: abundant quartz sand lenses	dolomite	none		
70	50	dark gray	micrite	finely algal laminated, occasional shale partings	dolomite	none		
71	40	dark gray	micrite	finely algal laminated, shale partings	dolomite	none		
72	35	dark gray	micrite	strongly fetid, abundant shale partings, abundant floating quartz sand, occasional quartz vugs (1 cm diameter).	dolomite	none		
73	30	dark gray	fine	fetid, algal laminated, convex upward bedding	dolomite	none		
74	40	dark gray	micrite	fetid, algal laminated	dolomite	none		
75	30	medium gray	fine	slightly fetid, occasional sand lenes and quartz vugs (1 cm diameter)	dolomite	none		

76	30	medium gray	very coarse	strongly fetid, Crooked Swamp-like	dolomite	none		
77	70	medium gray	very coarse	strongly fetid	dolomite	grades laterally into rugose chert: vuggy, highly porous, looks like an algal mound, ranges from 1 to 70 cm thick.		
Close to Garbage Dumps on N side of Island								
1	175	medium gray	micrite	thinly bedded, shale partings and wisps of sand lenses throughout, strong solution cleavage, unit becomes slightly more coarse-grained near cherts	dolomite	upper 40 cm: 12 chert beds (3X15cm), chert grades laterally into shale units.		
2	80	medium gray	fine	abundant shale partings throughout, occasional algal structures mid-unit	dolomite	upper portion of unit becomes a chert bed laterally		
3	85	medium gray	medium	thinly bedded, flaggy (5-10 cm beds), abundant thick shale partings, abundant quartz vugs (5 cm diameter).	dolomite	some of shale partings become chert laterally		
4	45	light gray	coarse	arenaceous with abundant quartz clots and vugs (up to 3 cm diameter)	dolomite	none		
Carriage Path: Dilation Breccia								
1	150	medium gray	very coarse	fine-grained in places, extremely fetid, algal laminated, thin wisps of algal laminations, convex upward, upper 50 cm: numerous quartz sand stringers, rip-up clasts occasioanlly toward upper	dolomite	lower 30 cm: chert as shards and angular fragment s in		

				part of unit, numerous vertical quartz veins		coarse-grained dolomite, at very base of unit: shale replaced by chert, convex upward, could be algal		
2	35	ash gray		finely laminated, replaced by secondary silica, occasional spaces between chert filled with Crooked Swamp-like dolomite	chert	dilation breccia chert: 190 cm wide, pod-like (as if boudined), angular to subrounded clasts of translucent Crooked Swamp-like chert, also angular to subrounded, opaque clasts of Hope chert		
3	30	dark gray	micrite	fetid, broken into angular fragments, recemented by coarse-grained, Crooked Swamp-like dolomite	dolomite	none		
4	60		micrite	slightly fetid, somewhat brecciated, thin quartz sand lenses, vertical stylolites, horizontal and vertical quartz shear veins, signs of cut-n-fill channels, almost a disconformity.`	dolomite	none		
5	80	medium /dark gray	micrite	strongly fetid, shale partings throughout, occasional quartz shear veins	dolomite	none		

6	80	medium /dark gray	micrite	strongly fetid, shale partings throughout, occasional quartz shear veins	dolomite	upper part of unit: siliceous chert unit coating a disconformity, chert is ash gray, in places dark gray, discontinuous (5X20cm)		
7	70	medium gray	medium	algal laminated, upper 15 cm: numerous shale partings, quartz veins	dolomite	upper 15 cm: shale lenses replaced by chert that have been subsequently broken up, may be disconformity		
8	10	dark gray	micrite	shear veins throughout	dolomite	throughout unit: discontinuous layers and clots of sheared out, very light ash gray chert		
9	40	medium gray	medium	algal laminated, numerous wisps of quartz sand grains, quartz shear veins, upper 15 cm: finely algal laminated.	dolomite	none		
10	80	medium gray	fine	algal laminated, veritcal stylolites and numerous quartz shears, throughout unit, abundant fragments of angular gray chert.	dolomite	mid-unit: large clots and masses of ash gray chert,		

						very irregular (10-15X15-20cm), quartz shear veins running right through cherts, cherts are convex upward		
11	70	dark gray	fine	fetid, sand lenses, finely algal laminated, quartz veins	dolomite	none		
12	40	dark gray	fine	fetid, sand lenses, finely algal laminated, quartz veins, strongly fetid	dolomite	none		
N 50 feet of previous section, another quarry face								
1	50	medium gray	medium /fine	slightly fetid, abundant quartz sand lenses towards upper part of unit, algal laminated, quartz shears, beds dipping about 70 degrees	dolomite	none		
2	90	medium /light	medium	no structure, at top of unit: cut-n-fill channels, two generations of quartz veins, sand units abundant	dolomite	upper 40 cm: dilation breccia chert, translucent, opaque, black, angular fragments tightly welded to light gray, second generation chert, chert contacts look very clay rich and finely laminated, numerou		

						s angular fragmens t of chert occur at top of unit.		
3	20	medium gray	fine	fetid, algal laminated, abundant quartz sand at base of unit, thoroughly quartz veined.	dolomite	none		
4	50	medium gray	fine	fetid, fine algal laminations, quartz sand stringers, two generations of quartz veins	dolomite	none		
5	50	dark gray	micrite	fetid, algal laminated, occasional sand lenses, thoroughly quartz veined.	dolomite	none		
6	90	medium /dark gray	micrite	fetid, abundant quartz veining, bedding dip about 60 degrees.	dolomite	none		
7	90	medium /dark gray	micrite	fetid, abundant quartz veining, bedding dip about 60 degrees.	dolomite	none		
8	90	medium gray	medium /fine	strongly fetid, slabby, thin-bedded, algal and sand laminations abundant towards top	dolomite	mid unit: (8X30cm) ash gray chert, slightly castilated on lower surface, convex at upper chert contact.		
9	50	medium gray	coarse	fetid, thinly bedded, Crooked Swamp-like characteristics	dolomite	none		
10	65	medium gray	coarse	highly fetid, lower 10 cm: thin quartz lenses, upper 20 cm: slightly more fine-grained	dolomite	lower 10 cm: angular fragment s of ash gray chert, up to 1 cm in diameter, ash gray chert lens mid-unit (1-2X20 cm).		

11	50	very dark gray	very fine	strongly fetid, very Hope like, but without weathering characteristics, some thin sand lenses, some signs of algal.	dolomite	none		
12	50	medium gray	medium /coarse	fetid, abundant quartz veining	dolomite	none		
Northernmost 50 feet to next quarry (Hemlock grove)								
1	60	dark blue gray	micrite	fetid, occasional sand lenses at top, occasional algal throughout, thoroughly quartz veined	dolomite	none		
2	60	blue gray	micrite	fetid, lower 10 and upper 20 cm: strongly algal laminated, occasional shale partings, quartz sand stringers along top, strong solution cleavage, lower 10 cm: algal rich	dolomite	none		
3	30	light gray	very coarse	Crooked Swamp, quartz veining very common upper 20 cm	dolomite	lower 10 cm: finely laminated, ash gray chert, dark gray, angular chert fragments embedded in ash gray chert, upper 20 cm: 1 cm wide fragments of light gray chert		
4	40	light gray	coarse	fetid	dolomite	lower 10 cm: dilation breccia chert, angular fragments of dark gray chert embedded in a		

						fine matrix, upper 20 cm: abundant angular chert fragments (5 cm diameter), chert replaced siliceous lenses, look like algal replaced by chert		
5	20	light gray	coarse	fetid, very Crooked Swamp-like, algal laminated	dolomite	upper surface contains siliceous infillings, algal replaced by chert, upper surface castilated.		
6	35				chert	dilation breccia chert, where chert occurs in sags (10X50cm), large, angular fragments of transulucent, gray chert in gray, laminated chert matrix, upper 20 cm: dark, angular fragments		

						embedded in finely laminated gray chert, lower surface castilated.		
7	60	dark gray	micrite	fetid, algal laminated, thoroughly quartz veined	dolomite	none		
8	30	dark gray	micrite	fetid, strongly algal laminated, thoroughly quartz veined, upper part of unit: shale partings and occasional quartz vugs up to 20 cm diameter.	dolomite	none		
9	25	dark gray	micrite	fetid	dolomite	none		
10	100	dark gray	micrite	fetid, algal laminated, thoroughly quartz veined, thinly bedded	dolomite	none		
11	200	dark gray	micrite	fetid, algal laminated, thoroughly quartz veined, thinly bedded, may be Hope	dolomite	none	Hope	Rickenbach
West side of Carriage Path								
1	120	dark gray	micrite	fetid, occasional lenses of coarse-grained, lighter gray, fetid dolomite, Upper Member Allentown weathering pattern, Hope facies characteristics	dolomite	none	Hope	Rickenbach
2	160	variable	variable	lower 130 cm: Hope-like, dark gray, micritic, thickly bedded, fetid, upper 30 cm: lighter gray, coarse-grained, thickly bedded, fetid	dolomite	none	Hope	Rickenbach
3	200			interbedded Hope and Crooked Swamp	dolomite	none	Hope/Crooked Swamp	Rickenbach
4	160			Branchville in swale, continues up-section into Big Springs mound	dolomite	none	Branchville/Big Springs	Epler
South Edge of Rock Island, above Dilation Breccia, west side of Carriage Path								
1	50	dark gray	micrite	occasional shale partings and quartz veining	dolomite	none	Hope	Rickenbach
2	80	dark gray	micrite	occasional shale partings and quartz veining	dolomite	none	Hope	Rickenbach
3	50	medium gray	medium	fetid, algal laminated, shale partings	dolomite	upper 2 cm: shale partings replaced	Hope	Rickenbach

						by chert		
4	40	medium gray	medium	thinly bedded, strongly fetid	dolomite	lower 15 cm: 6 chert nodule horizons (2X10cm) (Hope 7 cherts!!).	Hope	Rickenbach
5	60	medium gray	coarse	thinly bedded, slightly fetid, some quartz sand lenss, a lot of quartz veins	dolomite	none	Hope	Rickenbach
6	50	medium gray	coarse	strongly fetid, algal laminations	dolomite	none	Hope	Rickenbach
7	100	medium gray	medium	occasional algal laminations	dolomite	none	Hope	Rickenbach
8	60	medium gray	medium	occasional algal laminations, this seems to be the end of the Rickenbach	dolomite	none	Hope	Rickenbach
9	200			Covered interval: Rickenbach Formation	dolomite	none	Hope	Rickenbach
10	30			Sand interval	sandstone	none	Hope	Rickenbach
11	20	light gray	medium	finely algal laminated dolomite with quartz veining, looks like the end of the Upper Allentown	dolomite	none	Upper Allentown	Allentown
Southern Tip of Rock Island, Facing Ravine (stepped back in section to Rick: Work up section)								
1	200	dark gray	micrite	occasional algal partings, strong quartz veining	dolomite	none	Crooked Swamp	Rickenbach
2	70	very dark gray	fine	fetid, fine algal laminations	dolomite	none	Crooked Swamp	Rickenbach
3	25	light gray	medium	algal laminated, strongly fetid	dolomite	none	Crooked Swamp	Rickenbach
4	25	dark gray	medium	strongly fetid, algal laminated	dolomite	lower 10 cm: chert nodules (2-3X5cm), black to gray, contains some sand grains	Crooked Swamp	Rickenbach
5	70	medium gray	medium	slightly fetid, some algal laminations	dolomite	none	Crooked Swamp	Rickenbach
6	50	medium gray	medium	strongly fetid, occasional algal laminations	dolomite	none	Crooked Swamp	Rickenbach
7	40	medium gray	medium	strongly fetid, occasional algal laminations	dolomite	none	Crooked Swamp	Rickenbach

8	50	medium gray	coarse	strongly fetid	dolomite	none	Crooked Swamp	Rickenbach
9	40	medium gray	fine	fetid, some algal laminations	dolomite	none	Crooked Swamp	Rickenbach
10	40	medium gray	medium	stronlgy fetid, occasional shale partings	dolomite	none	Crooked Swamp	Rickenbach
11	30	medium /light gray	coarse	slightly fetid, some quartz veins	dolomite	none	Crooked Swamp	Rickenbach
50 feet to South, along nose, south end of Rock Island								
1	50	light gray	medium /fine	finely algal laminated	dolomite	none	Branchville	Epler
2	80	light gray	medium /fine	algal more concentrated	dolomite	upper 10 cm: thick concentration of algal converted to some concentration of argillite that is cherty	Branchville	Epler
3	110	dark gray	medium	algal laminated	dolomite	none	Branchville	Epler
4	50	medium /light gray	medium	algal laminated	dolomite	none	Branchville	Epler
5	160	medium /light gray	medium	algal laminated, quartz veins throughout, lower 50 cm: thick algal laminations that are desiccated and turned into some sort of argillite	dolomite	none	Branchville	Epler
6	120	medium gray	medium	very thinly bedded, algal laminated, lower 40 cm: desiccated algal laminations that have been replaced by argillite, intermittent sand lenses with argillic algals, sand lenses seem to fill in burrow structures, beds are nearly vertical and quartz veined	dolomite	none	Branchville	Epler
7	120	light gray	coarse	thinly bedded, slightly fetid, lower 30 cm: quartz lenses and argillic desiccated algal structures, looks like some kind of micritic cycle	dolomite	none	Branchville	Epler

8	120	light gray	coarse	slightly fetid, lower 20 cm: strong argillic algal mats, mid 70-80 cm: dispersed algal, upper 30-40 cm: dense concentration of argillite, desiccated algal and sand lenses (2-3cm thick), algal (30-40 cm long, but laminar).	dolomite	none	Branchville	Epler
9	110	medium /light gray	medium /coarse	algal laminated, interspersed with desiccated algal throughout section, sand lenses mid-unit	dolomite	Big Springs within this horizon that has purple chert	Big Springs	Epler
10	70	medium gray	medium	fetid, strongly algal laminated, algal in two distinct horizons, are castilated and occur 40 cm from base, upper half of unit: argillic algal (desiccated), with sand grains, sand filling in burrows.	dolomite	none	Big Springs	Epler
11	30		coarse	slightly fetid, algal laminated, lower 10 cm: convex upward algal and also have argillite variety.	dolomite	none	Big Springs	Epler
12	50		coarse	slightly fetid, algal laminated, lower 10 cm: convex upward algal and also have argillite variety.	dolomite	none	Big Springs	Epler
13	100	light gray	coarse	Covered interval: algal laminated, algal less abundant except at top	dolomite	none	Big Springs	Epler
14	140	medium gray	medium	thinly bedded, slightly fetid, algal laminated, occasional quartz sand lenses	dolomite	none	Big Springs	Epler
15	100	very light gray	medium /fine	finely algal laminated	dolomite	none	Big Springs	Epler
16	90	light gray	medium /coarse	algal laminated, dessicated algal throughout, occasional sand lenses, thrust fault zone	dolomite	none	Big Springs	Epler
17	70	medium /dark gray	coarse	fetid, occasional algal	dolomite	none	Big Springs	Epler
18	90	dark gray	medium /coarse	some algal laminations, occasional wisps of quartz sand, signs of horizontal burrowing	dolomite	none	Big Springs	Epler

19	80	light gray	coarse	thinly bedded, strongly fetid, few algal laminations	dolomite	none	Big Springs	Epler
20	80	dark gray	very fine	coming into Lafayette beds, some signs of paleokarst	dolomitic limestone	none	Lafayette	Epler
21	60	medium gray	coarse	slightly fetid, very slight effervescence, minor algal laminations	dolomite	none	Lafayette	Epler
22	60	medium gray	medium	slightly algal laminated, looks like Lafayette Member, roughly parallel to beding is a generation of quartz veins that runs through sequence	dolomitic limestone	blue/gray argillic infillings that have turned to chert, just like in Harmony vale section.	Lafayette	Epler
23	200	medium gray	medium	slightly algal laminated, looks like Lafayette Member, roughly parallel to beding is a generation of quartz veins that runs through sequence	dolomitic limestone	blue/gray argillic infillings that have turned to chert, just like in Harmony vale section.	Lafayette	Epler
Western slope of island, center of island, western side of quarry								
1	1760	dark gray	micrite	thinly bedded, algal laminated, occasional shale partings	dolomite	at 3900 cm: blue chert (5X15-20 cm), composed mostly of rip-up clasts, may mark unconformity, seems to mark transition into Beaver Run	Lafayette	Epler
2	600	dark gray	medium /coarse	transition into Beaver Run units at 600 cm, facies in and out.	dolomitic limestone	none	Beaver Run	Ontelaunee
3	300	dark gray	coarse		dolomitic limestone	at 300 cm:	Beaver Run	Ontelaunee

						appearance of a mound-like, rugose chert, may be first chert within the Beaver Run Member.		
4	400	medium /dark gray	coarse	fetid, at 300 cm: 50 cm of quartz vugs, 1 cm wide	dolomitic limestone	at 400 cm: another black chert horizon	Beaver Run	Ontelaunee
5	300	medium gray	coarse	at 300 cm: very fetid	dolomitic limestone	lower 200 cm: dark gray to black, rugose, gastropodal chert occurring in thin bands and intermittent lenses (5-10 cm thick), upper 50 cm: chert as possible burrow infill horizon.	Beaver Run	Ontelaunee
6	900	medium gray	coarse	fetid, at 300 cm: 50 cm of quartz vugs, 1 cm wide	dolomitic limestone	at 450 cm: chert bearing unit (200 cm thick): gastropodal chert, very vuggy with	Beaver Run	Ontelaunee

						chert crystals, some signs of algal laminations, seems to have layering, as if replacing algal, between 800-900 cm: chert horizon occurring sporadically as an algal lining on		
7	900	medium gray	very coarse		dolomitic limestone	upper 300 cm: entirely gastropodal chert, unit also contains chert beds: (1-10 cm thick), slightly convex upward, becomes homogenous in places, in others brecciated	Beaver Run	Ontelaunee
8	300	medium gray	coarse		dolomitic limestone	upper 100 cm: gastropodal chert	Beaver Run	Ontelaunee
9	300	light gray	coarse	very fetid	dolomite	dark gray to black chert, angular fragments, clots, and fracture	Beaver Run	Ontelaunee

						infillings throughout		
10	300	light gray	coarse	looks like Crooked Swamp facies	dolomitic limestone	gastropodal chert	Beaver Run	Ontelaunee
11	200	very dark gray	coarse	fetid, at 300 cm: 50 cm of quartz vugs, 1 cm wide	dolomitic limestone	gastropodal chert horizon (20 cm thick)	Beaver Run	Ontelaunee
12	80	medium gray	micrite	thickly bedded	dolomitic limestone	scattered chert clots in lower 20 cm (2 cm diameter), angular fragments may be burrow infillings	Beaver Run	Ontelaunee
13	260	medium gray	fine	weathering to a lighter color, entering Harmonyvale Member?	dolomitic limestone	walk along strike, upper 30 cm: gastropodal chert	Harmony vale	Ontelaunee
14	100	medium gray	medium	thickly bedded, strongly fetid, some algal laminations	dolomitic limestone	none	Harmony vale	Ontelaunee
15	100	medium /dark gray	medium	fetid, some signs of burrowing, algal laminations	dolomitic limestone	none	Harmony vale	Ontelaunee
Western slope of island, above dilation breccia units, top of island, facing western slope, transitional beds, facing Big Springs, definitely repeating section								
1	30	medium gray	micrite	beds dipping 65-70 degrees, algal laminated, occasional shale partings, looks paleokarst	dolomite	desiccated cherty algal	Lafayette	Epler
2	120	dark/medium gray	micrite	thinly bedded, finely algal laminated, occasional signs of horizontal burrows, may be edges of clasts	dolomite	none	Lafayette	Epler
3	100	medium gray	coarse	thinly bedded, fetid, algal laminated, great numbers of rip-up clasts throughout	dolomitic limestone	none	Lafayette	Epler
4	100	medium gray	medium	thinly bedded, algal laminated, numerous shale partings, occasional rip-up clasts	dolomitic limestone	none	Lafayette	Epler
5	100	medium gray	medium	thinly bedded, algal laminated, some signs of	dolomite	top of unit:	Lafayette	Epler

				burrowing, some signs of paleokarst		medium/ dark gray to ash gray chert (5X20cm), seems to be edge-wise conglom erate that is replaced by chert		
6	100	dark gray	medium	fetid, algal laminated, numerous layers of rip-up clasts, signs of channelization, blocks seem to be paleokarst	dolomitic limestone	none	Lafayette	Epler
7	100	medium gray	medium	algal laminated, upper unit contains rubble zones and possible paleokarst, solution-collapsed beds	dolomitic limestone	chert bed at base, dark gray, laminate d and contains fragment s of rip-up clasts	Lafayette	Epler
8	100	medium gray	medium /coarse	fetid, some algal laminations, occasional paleokarst, dessicated algal	dolomitic limestone	none	Lafayette	Epler
9	140	medium gray	medium	finely algal laminated	dolomitic limestone	some shale partings occasion al replaced by gray chert	Lafayette	Epler
10	120	medium /dark gray	medium /fine	slightly thicker-bedded, slightly fetid, occasional signs of paleokarst	dolomitic limestone	none	Lafayette	Epler
11	140	medium gray	medium	strongly fetid, algal laminated, occasional dessicated algal, periodic zones of rip-up clasts, argillic infillins on bed surface, argillite may be cave mud.	dolomitic limestone	none	Lafayette	Epler
12	140	medium gray	medium	bedding dips 75 to 80 degrees or steeper, thinly bedded, algal laminated, signs of rip-up clasts, signs	dolomitic limestone	none	Lafayette	Epler

				of dessicated algal and paleokarst (internally brecciated, clasts micritic and angular, crystalline matrix), fetid				
13	120	dark gray	micrite	bedding dipping at about 80 degrees, thinly bedded, algal laminated, no signs of paleokarst, though whole block may be paleokarst	dolomitic limestone	none	Lafayette	Epler
14	150	medium gray	medium	very thinly bedded, strongly fetid, occasional sand lenses, 70-80 cm: 10 cm thick band of dessicated algal, upper 20 cm: 1 cm thick sand lenses	dolomitic limestone	lower 20 cm: very concentrated area of dessicated algal mats, not cherts but silica rich, very bottom of unit, 1 cm thick dark gray chert	Lafayette	Epler
15	70	medium light gray	coarse	fetid, algal laminated	dolomitic limestone	none	Lafayette	Epler
16	45	medium gray	fine	bedding dip nearly vertical, very thinly bedded, finely algal laminated, paleokarst throughout	dolomite	none	Lafayette	Epler
17	80	medium gray	medium /coarse	algal laminated, some occasional dessicated algal units, signs of solution weathering	dolomitic limestone	none	Lafayette	Epler
18	60	medium dark gray	medium	thinly bedded, finely algal laminated, fetid, solution weathering, top of unit: argillic infillings	dolomitic limestone	none	Lafayette	Epler
19	100	dark gray	medium	slightly more thickly bedded, somewhat more algal laminated	limestone	none	Lafayette	Epler
20	200	medium gray	medium /fine	algal laminated, at base: numerous wisps of quartz sand grains, top of unit: wisps of argillic infillings and paleokarst: whole slope might be karstic, tough to find consistant strike lines, tumbled blocks, argillic infillings may be seams in paleokarst	dolomitic limestone	none	Lafayette	Epler

21	300	medium gray	medium /fine	thinly bedded, algal laminated, numerous sand lenses, controlled by algal laminations, occasional argillic infillings, looks like algal filament with quartz sand grains adhering to it.	dolomitic limestone	none	Lafayette	Epler
22	300	medium gray	medium /fine	very thinly bedded, strongly fetid, strong algal laminations throughout, a lot of paleokarst (200 cm in upper unit), upper 20 cm of dessicated algal	dolomitic limestone	none	Lafayette	Epler
23	70	medium gray	medium	finely algal laminated, between 40-50 cm and 60-70 cm are two dessicated algal units, occasional sand lenses.	dolomitic limestone	none	Lafayette	Epler
24	150	medium dark gray	medium	very thinly bedded, algal laminated, some signs of paleokarst, upper 20 cm: three dessicated algal sequences (4-5 cm thick), separated by limestone	dolomitic limestone	upper part of bed: 5 cm thick, battleship gray, laminated chert, contains rip-up clasts of other angular to subangular chert clasts.	Lafayette	Epler
25	300	medium dark gray	medium	fetid, very finely algal laminated, seems as if algal laminations are coated with sand and some argillic infilling, little solution weathering	dolomitic limestone	none	Lafayette	Epler
26	300	medium gray	medium /fine	thinly bedded, finely algal laminated, numerous and-lined algal, especially mid-unit, upper 30 cm: numerous rip-up clasts, edgewise conglomerates, quartz, sand-lined algal and cross-bedding	dolomitic limestone	none	Lafayette	Epler
27	170	medium gray	medum/ coarse	slightly fetid, strongly algal laminated, numerous quartz sand on algal, some black shale lenses	dolomite	none	Lafayette	Epler

28	200	medium gray	medium /coarse	thickly bedded, fetid, change in weathering pattern, absence of fine, Lafayette-type algal laminations	dolomite	upper 50 cm: numerous horizontal burrow structures or algal laminations replaced by chert, first Beaver Run-like unit: grades laterally into gastropodal chert, either burrows or algal structures (1X3-5 cm).	Beaver Run	Ontelaunee
29	80	dark gray	coarse	thickly bedded	dolomite	40 cm into unit: dark gray, laminated chert (5X20cm)	Beaver Run	Ontelaunee
30	90	medium gray	coarse	thickly bedded, strongly fetid	dolomite	upper 40 cm: strongly burrowed, burrows filled with chert	Beaver Run	Ontelaunee
31	70	medium gray	coarse	thickly bedded, strongly fetid	dolomitic limestone	none	Beaver Run	Ontelaunee
32	80	medium gray	coarse	lower 30 cm: thickly bedded, strongly fetid	dolomitic limestone	upper 50 cm: gastropodal chert, looks like large concave algal (120 cm wide):	Beaver Run	Ontelaunee

						burrowed through by gastropods, medium/dark gray, punky chert		
33	170	medium gray	coarse	thickly bedded, fetid	dolomitic limestone	10 cm from top: 2X5 cm chert bed, in places: second gastropodal chert (30 cm thick), seems to come and go in masses (about 150 cm diameter)	Beaver Run	Ontelaunee
34	170	medium gray	coarse	thickly bedded, strongly fetid	dolomitic limestone	upper 30 cm: gastropodal chert replacing chicken wire structures	Beaver Run	Ontelaunee
35	230	dark gray	coarse	Covered interval: thickly bedded, strongly fetid, no sign of algal, occasional chicken wire structures, widely disseminated quartz vugs	dolomitic limestone	none	Beaver Run	Ontelaunee
36	100	dark gray	coarse	thickly bedded, fetid	dolomite	finely disseminated chicken wire structures replaced by chert	Beaver Run	Ontelaunee

37	70	dark gray	coarse	flaggy, thin beds, strongly fetid	dolomite	lower 40 cm: chicken wire structures replaced by chert, upper 10 cm: shardy, nodular, irregular masses of chert (2-3X5-10cm), in places, bottoms of chert lined with quartz vugs, chert may replacing cut-n-fill channels or algal.	Beaver Run	Ontelaunee
38	90	medium gray	coarse	thickly bedded, strongly fetid, great concentrations of quartz vugs upper 25 cm	dolomitic limestone	upper 25 cm: chicken wire structures replaced by chert	Beaver Run	Ontelaunee
39	150	medium gray	coarse	thicky bedded, strongly fetid, upper45 cm: more chicken wire structures and scattered quartz vugs (2 cm diamter)	dolomitic limestone	upper 1 cm: angular fragments of shardy chert (2X5 cm) replacing algal	Beaver Run	Ontelaunee
40	50	medium gray	coarse	thickly bedded, strongly fetid	dolomitic limestone	upper 30 cm: chicken wire structures	Beaver Run	Ontelaunee

						replaced by chert		
41	130	medium gray	coarse	thickly bedded, strongly fetid	dolomitic limestone	70-85 cm: chicken wire replaced by chert, 105-120 cm: scattered clots and angular fragments of dark gray chert (5X10cm) scattered throughout upper part of unit and associated with quartz vugs up to 2 cm diameter, as many as a dozen algal beds present	Beaver Run	Ontelaunee
42	100	medium gray	coarse	thickly bedded, fetid	dolomitic limestone	upper 10 cm: shardy chert (5X10 cm)	Beaver Run	Ontelaunee
43	120	medium gray	coarse	thinly bedded, fetid	dolomitic limestone	halfway through unit: 20 cm thick chicken wire structres have gray chert caps (5X10 cm),	Beaver Run	Ontelaunee

						uppper 15 cm: gastropodal chert, algal sequence replaced by silic		
44	300	medium gray	coarse	Covered interval: thickly bedded, strongly fetid	dolomitic limestone	none	Beaver Run	Ontelaunee
45	240	medium gray	coarse	thickly bedded, strongly fetid	dolomitic limestone	mid-unit: (10X20-30 cm thick) chert unit that could be replacing algal, scattered quartz vugs and chicken wire structures replaced by chert throughout remainder of unit	Beaver Run	Ontelaunee
46	110	medium gray	coarse	thickly bedded, strongly fetid	dolomitic limestone	lower 40 cm: seems to be gastropod-bored algal stromatolites replaced by medium/light gray chert	Beaver Run	Ontelaunee
47	120	medium gray	coarse	thickly bedded, fetid	dolomitic limestone	none	Beaver Run	Ontelaunee
48	100	medium gray	coarse	strongly fetid	dolomite	incredibly thick gastropodal chert, algal mats bored by	Beaver Run	Ontelaunee

						gastropods or an evaporite sequence, in places becomes black chert		
49	300	medium gray	coarse	strongly fetid, infrequent number of algal beds (1-2X120cm)	dolomite	gastropodal chert	Beaver Run	Ontelaunee
50	300	medium gray	coarse	strongly fetid, occasional chicken wire structure	dolomite	none	Beaver Run	Ontelaunee
51	300	medium gray	coarse	flaggy, thinly bedded, rubbly	dolomitic limestone	upper 270 cm: gastropodal chert, in places chert becomes homogeneous beds, other locations, extremely punky and coarse, cherts lined with quartz crystals.	Beaver Run	Ontelaunee
52	300	medium gray	coarse	bedding nearly vertical, flaggy beds, not thick or thin	chert	entire 300 cm: gastropodal chert, lower 50 cm: homogeneous bed of chert	Beaver Run	Ontelaunee
53	300	medium gray	coarse	thin, flaggy, dolomite between gastropodal chert looks like off-reef flanking facies	dolomitic limestone	gastropodal chert, in places, cherts become homogeneous beds, especially upper	Harmony vale	Ontelaunee

						100 cm, however chert still contains geometric vacuoles.		
54	300	dark gray	coarse	thick and thin, plumose, uneven, hummocky, strongly fetid, rubbly,	dolomitic limestone	lower 100 cm: occasional chicken wire structures replaced by chert, upper 50 cm: gastropodal chert in some places, fairly homogeneous chert beds.	Harmony vale	Ontelaunee
55	300	medium gray	coarse	thicly bedded, strongly fetid, lower 150 cm: chicken wire structure, inside ravine that could be a fault, lime bed or prehistoric activity	dolomite	blue-gray chert at 900 cm	Harmony vale	Ontelaunee
56	300	medium gray	coarse	thickly bedded	dolomite	upper 70 cm: chicken wire structure capped with gastropodal chert	Harmony vale	Ontelaunee
57	300	medium gray	coarse	thickly bedded, strongly fetid, signs of algal laminations, almost hints of cross-bedding, some hints of horizontal burrows	dolomitic limestone	none	Harmony vale	Ontelaunee
58	200	medium gray	coarse	thickly bedded, algal laminations throughout	dolomitic limestone	none	Harmony vale	Ontelaunee
Far northwestern corner of island on western side of road								
1	1200	charcoal gray	micrite	thickly bedded, finely algal laminated, strong solution cleavage, no rubbles zones	dolomite	500-600 cm: zone of		

						chicken wire structures turned to chert		
2	750			red				Wantage
3	50			mottled red and green				Wantage
4	500			green				Wantage

B.8 – ROUTE 23S SECTION

Route 23 S Section, Sussex County, New Jersey								
Bed	**Thickness (cm)**	**Color**	**Grain Size**	**Bedding Description**	**Lithology**	**Chert**	**Member**	**Formation**
1	42	dark gray		thickly bedded	dolomite	none	Califon	Leithsville
2	15	dark gray		thickly bedded	dolomite	none	Califon	Leithsville
3	60			covered section		none	Califon	Leithsville
4	45	dark gray		thinly bedded, ruditic structures		none	Califon	Leithsville
				upper 15 cm: finely laminated				
5	32	dark gray		thickly bedded, occasional laminations	dolomite	none	Califon	Leithsville
6	23	dark gray		lower 10 cm: rip up clasts; upper 13 cm: fine laminations	dolomite	none	Califon	Leithsville
7	52	dark gray		very thinly bedded, fissile	shaly dolomite	none	Califon	Leithsville
8	13	medium gray	very fine	finely laminated	dolomite	none	Califon	Leithsville
9	65	medium gray	medium	thickly bedded	dolomite	none	Califon	Leithsville
10	120			covered section		none	Califon	Leithsville
11	60	medium gray	coarse	finely laminated, occasional quartz sand layers, shale seams, highly stylolitized, rubbly looking, possible burrows.	dolomite	none	Califon	Leithsville
12	51	medium gray	coarse	lower 33 cm: fine shaly laminations; middle 4 cm: very fissile calcareous shale; upper 14 cm: rip up clasts	dolomite	none	Califon	Leithsville
13	90	dark gray	fine	intermittent sand lenses, several generations of cleavage	dolomite	none	Califon	Leithsville
14	24	dark gray	fine	finely laminated, possible burrows	shaly dolomite	none	Califon	Leithsville

15	30	dark gray	fine	fissile, swamp or lagoon, extraordinary flow regime	calcareous shale	none	Califon	Leithsville
16	48	medium gray	medium	thinly bedded, numerous shale partings, quartz clasts	dolomite	none	Califon	Leithsville
17	31	medium gray	fine	shale partings, stromatolites, occasional quartz grains	dolomite	none	Califon	Leithsville
18	14	dark gray	very coarse	almost pure quartz sand in places	dolarenite	none	Califon	Leithsville
19	42	dark gray	fine	finely laminated, shale partings	dolomite	none	Califon	Leithsville
20	45	medium gray	medium	finely laminated, shale partings	dolomite	none	Califon	Leithsville
21	25	medium gray	very fine	finely laminated	dolomite	none	Califon	Leithsville
22	52	dark gray	fine	finely laminated, closely spaced shale partings, worm trails	dolomite	none	Califon	Leithsville
23	95	dark gray	fine	finely laminated, numerous shale partings	dolomite	none	Califon	Leithsville
24	90	dark gray	very coarse	finely laminated; upper 30 cm: extremely sandy	dolomite	none	Califon	Leithsville
25	45	medium gray	coarse	lower 27 cm: very sandy; upper 18 cm: shale partings	dolomite	none	Califon	Leithsville
26	60	medium gray	fine	finely laminated, very thick shale partings, quite flow regime, coming to close of cycle?	dolomite	none	Califon	Leithsville
27	95	medium gray	medium	very thick shale partings	dolomite	none	Califon	Leithsville
28	49	dark gray	very fine	lower 41 cm: finely laminated, numerous shale partings, stromatolites?	dolomite	none	Califon	Leithsville
		dark gray	coarse	upper 8 cm: rip up clasts, billowy	dolarenite			
29	43	dark gray	fine	finely laminated, ruditic rubbly texture,	dolomite	none	Califon	Leithsville

				stromatolite rich				
30	28	dark gray	medium	finely laminated	dolomite	none	Califon	Leithsville
31	40	drab olive	very coarse	thickly bedded, no cross-bedding	dolomite	none	Califon	Leithsville
32	25	dark gray	fine	finely laminated	dolomite	none	Califon	Leithsville
33	26	olive green	very coarse	rip up clasts at base	dolarenite	none	Califon	Leithsville
34	30	medium gray	fine	finely laminated	dolomite	none	Califon	Leithsville
35	22	olive	very coarse	drab, arenaceous	dolomite	none	Califon	Leithsville
36	20	dark gray	fine	finely laminated	dolomite	none	Califon	Leithsville
37	54	dark gray	very fine	laminated	dolomite	none	Califon	Leithsville
38	57	olive	coarse	drab, finely bedded, arenaceous layers	dolomite	none	Califon	Leithsville
39	90	dark gray	fine	finely laminated, very thinly bedded, numerous shale partings (2-3 cm thick)	dolomite	none	Califon	Leithsville
Leithsville Formation, Rte 23 N, Sussex County, New Jersey								
1	65	very dark gray	coarse	thickly bedded	dolomite	none	Califon	Leithsville
2	90	medium gray	coarse	very thickly bedded, discontinuous beds, abundant shale layers	dolomite	8-10 cm thick beds midway through unit	Califon	Leithsville
3	70	medium gray	medium	lower 20 cm: rubbly, thinly bedded, middle 25 cm: thickly bedded, rip up clasts, upper 25 cm: thinly bedded, shaly , finely laminated, algal possible	dolomite	none	Califon	Leithsville
4	14	very dark gray	very fine	thinly bedded, very fissile, shaly	shaly dolomite	none	Califon	Leithsville
5	13	medium gray	medium	thickly bedded	dolomite	none	Califon	Leithsville
6	20	medium gray	very fine	finely laminated, convex upward	dolomite	nodules	Hamburg	Leithsville

				beds				
7	40	dark gray	fine	laminated	dolomite	none	Hamburg	Leithsville
8	30	black	fine	lower 13 cm: fissile, calcareous shale, middle 10 cm: highly cleaved slate, upper 10 cm: fissile, calcareous shale	shale	none	Hamburg	Leithsville
9	65	dark gray	coarse	rubbly	dolomite	bottom and upper 10 cm: nodules	Hamburg	Leithsville
10	35	medium gray	medium	thinly bedded	dolomite	none	Hamburg	Leithsville
11	30	very dark gray	very fine	micritic	dolomite	none	Hamburg	Leithsville
12	40	black	very fine	fissile	shale	none	Hamburg	Leithsville
13	70	dark gray	medium	finely laminated, siliceous	dolomite	none	Hamburg	Leithsville
14	20	black	fine	very fissile	shale	none	Hamburg	Leithsville
15	17	dark gray	fine	finely laminated	dolomite	small wisps	Hamburg	Leithsville
16	75	medium gray	medium	thickly bedded, lower 25 cm: convex up bedding, maybe algal laminations	dolomite	25-40 cm: very thin chert layers	Hamburg	Leithsville
17	50	dark gray	medium	thin to thick bedded, small algal domes, laminated, upper 20 cm: 10 cm diameter algal domes	dolomite	none	Hamburg	Leithsville
18	40	dark gray	medium/coarse	rubbly bedding	dolomite	none	Hamburg	Leithsville
19	54	medium gray	medium	thickly bedded	dolomite	lower 10 cm: nodules	Hamburg	Leithsville
20	20	dark gray	coarse	very porous, thin bedding	dolomite	none	Hamburg	Leithsville
21	60	medium gray	medium	thick, rubbly bedding, lower 20 cm: siliceous	dolomite	none	Hamburg	Leithsville
22	140	dark gray	medium	thickly bedded, sulfides present	dolomite	none	Hamburg	Leithsville
23	55	dark gray	medium		dolomite	none	Hamburg	Leithsville
24	40	medium gray	coarse	rubbly bedding	dolomite	none	Hamburg	Leithsville

25	75	very dark gray	medium	thickly bedded, sulfide rich, very siliceous	dolomite	none	Hamburg	Leithsville
26	90	dark gray	medium	thickly bedded, disseminated sulfides	dolomite	none	Hamburg	Leithsville
27	110	dark gray	coarse	very thickly bedded, sulfide rich, stylolites, very porous, upper 50 cm: very rubbly	dolomite	none	Hamburg	Leithsville
28	40	dark gray	medium	very porous	dolomite	none	Hamburg	Leithsville
29	50	dark gray	medium	thickly bedded	dolomite	none	Hamburg	Leithsville
30	35	medium gray	medium	thickly bedded	dolomite	none	Hamburg	Leithsville
31	95	medium gray	medium	thickly bedded, very porous, sulfides present	dolomite	none	Hamburg	Leithsville
Leithsville Formation, Dump Site, Sussex County, New Jersey								
1	120	dark gray	medium	rubbly, thickly bedded	dolomite	none	Wallkill	Leithsville
2	200	very dark gray	coarse	very thickly bedded, very porous (looks like Or2), gnarled weathered surface, sulfide rich	dolomite	none	Wallkill	Leithsville
3	100	very dark gray	coarse	thickly bedded, sugary dolomite, uneven weathered surface, sulfide rich	dolomite	none	Wallkill	Leithsville
4	23	very dark gray	coarse	thickly bedded, sugary dolomite, uneven weathered surface, sulfide rich	dolomite	none	Wallkill	Leithsville
5	70	very dark gray	coarse	thickly bedded, sugary dolomite, uneven weathered surface, sulfide rich	dolomite	none	Wallkill	Leithsville
6	300	very dark gray	coarse	thickly bedded, sugary dolomite, uneven	dolomite	none	Wallkill	Leithsville

				weathered surface, sulfide rich				
7	210	dark gray	medium	rubbly, capping upper surface are 15-30 cm diameter stromatolites	dolomite	none	Wallkill	Leithsville
Leithsville Formation, Chase Farm, Sussex County, New Jersey								
1	100	medium gray	medium	algal rich, domal algal stromatolites (100 cm diameter X 25 cm height) at 40 to 50 cm, quartz vugs	dolomite	black, very vitreous nodules (20X15 cm avg, 30X20 cm. others) from 50 to 80 cm.	Wallkill	Leithsville
2	50	dark gray	coarse	algal stromatolites (100 X 40 cm) at 20 to 30 cm, rubble zones at 30 to 50 cm unconformity at 50 to 60 cm	dolomite	none	Wallkill	Leithsville
3	15	medium-dark gray	coarse	rubble zone	dolomite	chert wisps	Wallkill	Leithsville
4	90	dark gray	coarse	algal laminated, domal algal lower 50 cm, laminated upper 40 cm, intraformational conglomerate @ 30-40 cm, unconformity at 75 to 90 cm	dolomite	chert replacement at unconformities and domal algal sequences	Wallkill	Leithsville
5	70	dark gray	coarse	domal algal, unconformity at 15 cm.	dolomite	chert replacing algal at 10 to 15 cm	Wallkill	Leithsville
6	115	dark gray	coarse	algal laminated, sporadic quartz vugs	dolomite	none	Wallkill	Leithsville
7	60	dark gray	medium	very infrequently algal laminated, completely filled with quartz vugs, very sulfide rich, unconformity at base	dolomite	none	Wallkill	Leithsville
8	85	dark gray	medium	very infrequently algal laminated,	dolomite	none	Wallkill	Leithsville

				completely filled with quartz vugs, very sulfide rich				

B.9 – WILDCAT ROAD SECTION

Wildcat Road Section, Sussex County, New Jersey								
Bed #	**Thickness (cm)**	**Color**	**Grain Size**	**Bedding Description**	**Lithology**	**Chert**	**Member**	**Formation**
1	33	light gray	micrite	thinly bedded	dolomite	none	Hamburg	Leithsville
2	2.54	very dark gray	fine		shaly dolomite	none	Hamburg	Leithsville
3	10	light gray	micrite		dolomite	none	Hamburg	Leithsville
4	20	light gray/tan	micrite	thinly bedded, fetid, top of unit: sandy	dolomite	none	Hamburg	Leithsville
5	5	dark gray	micrite	effervesces slightly	shaly dolomite	none	Hamburg	Leithsville
6	10	medium gray	micrite		dolomite	none	Hamburg	Leithsville
7	18	dark olive gray	fine	very fissile, very phyllitic, very thinly bedded	shaly dolomite	none	Hamburg	Leithsville
8	15		coarse	pinch and swell, extremely quartz sand rich, limestone matrix	quartzite	none	Hamburg	Leithsville
9	28	weathers red	fine	very thinly bedded, fissile, cross bedded, possible current laminations, fetid, ferruginous	dolomite	none	Hamburg	Leithsville
10	56	red/olive	fine	alternating layers, occasional quartz sand layers, some signs of current ripples and algal laminations, upper 20 cm: alternating layers of red shale and olive dolomite, fining upward sequence, mud cracks	dolomite/shale	none	Hamburg	Leithsville
11	30	mauve/olive/maroon	fine	thick beds (5 cm), weathers red, floating sand grains	sandy dolomite	none	Hamburg	Leithsville
12	28	brown	fine	weathers red, very thinly bedded, finely laminated	shale	none	Hamburg	Leithsville
13	23		coarse	graded, cross bedded, argillite at top, contains ripples and mud cracks	quartz sandstone	none	Hamburg	Leithsville
14	10	olive/maroon	fine	alternating layers, finely laminated	sandy shale/dolomite	none	Hamburg	Leithsville
15	30	orange	fine	covered interval, finely laminated, ferruginous, may be weathered shale horizon	clay loam	none	Hamburg	Leithsville
16	10		coarse	arkosic, dolomite matrix,	dolomite/s	none	Hamburg	Leithsville

				mildly graded	andstone			
17	10	brown/taupe	coarse	arkosic, fetid, punky	sandstone	none	Hamburg	Leithsville
18	13		coarse	graded, quartz-rich arkose	sandstone	none	Hamburg	Leithsville
19	8	brown/red	fine	finely laminated, graded, shale cap on top	sandy shale/dolomite	none	Hamburg	Leithsville
20	18		coarse	graded, quartz-rich arkose	sandstone	none	Hamburg	Leithsville
21	8	mauve/olive	fine	finely laminated	sandy shale	none	Hamburg	Leithsville
22	10		coarse	quartz-rich arkose	sandy dolomite	none	Hamburg	Leithsville
23	10	mauve/olive	fine	sand-rich	shale	none	Hamburg	Leithsville
24	36	mauve/olive	fine	alternating, thin beds, finely graded, sandy, arkosic, rip-up clasts	sandy dolomite	none	Hamburg	Leithsville
25	10		coarse	finely laminated, quartz-rich arkose	sandy dolomite	none	Hamburg	Leithsville
26	8	brown/gray/taupe	coarse	sand-rich, upper unit: finely laminated shale, mudcracks	sandy dolomite	none	Hamburg	Leithsville
27	30	gray	coarse	very thinly bedded, fetid	sandy dolomite	none	Hamburg	Leithsville
28	10	brown/mauve	coarse	very fissile, occasional rip-up clasts	sandy shale	none	Hamburg	Leithsville
29	8	brown	coarse	thin and graded bedded	sandy dolomite	none	Hamburg	Leithsville
30	162	orange	fine	71 cm: thinly bedded, finely laminated, ferruginous	shale	none	Hamburg	Leithsville
			micrite	15 cm: very finely laminated, thinly bedded, fetid, slight deepening phase	dolomite	none	Hamburg	Leithsville
			fine	15 cm: finely laminated, thinly bedded, ferruginous	shale	none	Hamburg	Leithsville
			micrite	48 cm: finely laminated, lithographic	limestone	none	Hamburg	Leithsville
31	61		coarse	thickly bedded, 3 20cm beds, graded and cross bedding, scour surface at base, dolomite lenses within unit	quartzite	none	Hamburg	Leithsville
32	28	medium/dark gray	micrite	strongly fetid	dolomite	none	Hamburg	Leithsville
33	107		very coarse	quartz-rich, thickly bedded, upper 2.5 cm: shaly	quartzite	none	Hamburg	Leithsville

34	81	ash gray	micrite	fetid, divided into 4 beds, stylolite-bounded bed surfaces, occasional signs of algal laminations, pisoid grains at base of unit, top of unit, very fine-grained, ash gray	dolomite	none	Hamburg	Leithsville
35	130		coarse	thickly bedded, cross bedded, every 5 to 8 cm: lenses of micritic dolomite, rip-up clasts	quartz sandstone	none	Hamburg	Leithsville
36	81		coarse	thinly bedded, ferruginous, arkosic	sandstone	none	Hamburg	Leithsville
37	10	maroon	fine	very thinly bedded, finely laminated	sandy shale	none	Hamburg	Leithsville
38	18		coarse	thickly bedded, cut-n-fill surface at top of bed	sandstone	none	Hamburg	Leithsville
39	91	mauve/olive	coarse	alternating layers	sandy shale	none	Hamburg	Leithsville
40	41	ash gray	micrite	thickly bedded, finely laminated	dolomite	none	Hamburg	Leithsville
41	101	mauve/olive	coarse	thinly bedded, finely laminated	sandy shale	none	Hamburg	Leithsville
42	58	black	fine	fissile	dolomitic shale	none	Wallkill	Leithsville
43	20	medium gray	medium-coarse	fetid	dolomite	occasional clots of black/bray, opaque chert	Wallkill	Leithsville
44	28	dark gray	micrite	sparkly, upper 10 cm: algal laminated	dolomite	none	Wallkill	Leithsville
45	8	dark gray	fine	sparkly, algal laminated	dolomite	none	Wallkill	Leithsville
46	23	medium gray	coarse	fetid, algal laminated, laminations become cabbage heads	dolomite	upper 15 cm: large, spherical, dark gray, opaque chert in center of pod, light gray, mottled and transparent chert at edge of pod (17X15 cm)	Wallkill	Leithsville
47	10	medium gray	coarse	algal laminated, strongly fetid	dolomite	none	Wallkill	Leithsville
48	23	medium gray	coarse	sparkly, strongly fetid	dolomite	Rudinski pod at base of unit:	Wallkill	Leithsville

						13X10 cm: black (inside), gray (outside)		
49	23	medium gray	coarse	strongly fetid, very thinly bedded	shaly dolomite	none	Wallkill	Leithsville
50	30	dark gray	micrite	strongly fetid	dolomite	none	Wallkill	Leithsville
51	46	ash gray	micrite	Covered interval, thinly bedded,	dolomite	occasional wisps of dark gray chert toward top of unit	Wallkill	Leithsville
52	18	black	fine	dolomitic	shale	none	Wallkill	Leithsville
53	41	medium/ dark gray	fine	thickly bedded, lower 5 cm: finely algal laminated, punky smelling	dolomite	none	Wallkill	Leithsville
54	5	black	fine		shale	none	Wallkill	Leithsville
55	51	dark gray	medium	sparkly, very thinly bedded, slightly fetid	dolomite	none	Wallkill	Leithsville
56	51	dark gray	micrite	thickly bedded but becomes thin and flaggy along strike dolomite pods up to 91 cm long comprise entire thickness of bed, fetid, upper surface may be truncated	dolomite	chert pods (8X30 cm), convex upper and lower contacts as if controlled by algal, cherts become thin and smaller in flaggy dolomite beds	Wallkill	Leithsville
57	91	dark gray	medium -fine	thickly bedded, billowy, sparkly, strongly fetid, occasional pisoids, algal laminations, and rip-up clasts, middle 30 cm: convex upward algal structures, upper 15-`18 cm: light ash gray, coarse-grained dolomite	dolomite	lower 25 cm: large algal mound with black, opaque chert occurring at base and within algal structures	Wallkill	Leithsville
58	8	dark gray/blac k		strong fracture cleavage, algal laminated	chert	chert pods (8X30 cm), convex upper and lower	Wallkill	Leithsville

						contacts as if controlled by algal, cherts become thin and smaller in flaggy dolomite beds		
59	23	medium/ dark gray	medium	strongly fetid, algal laminated, upper surface hummocky	dolomite	none	Wallkill	Leithsville
60	46	dark gray/black	medium	very sparkly, strongly fetid, algal laminated	dolomite	none	Wallkill	Leithsville
61	18	black	medium	thinly bedded, strongly fetid, algal laminated	dolomite	chert replacing algal in places	Wallkill	Leithsville
62	8	dark gray	medium	algal laminated, pinches and swells	dolomite	none	Wallkill	Leithsville
63	30	dark gray	fine, almost micrite	thick bedding, fetid	dolomite	none	Wallkill	Leithsville
64	51	dark gray	medium-fine	sparkly	dolomite	none	Wallkill	Leithsville
65	18	very dark gray	medium-fine	barely sparkly, very small vugs filled with calcite	dolomite	none	Limeport	Allentown
66	61	dark gray	medium	sparkly	dolomite	none	Limeport	Allentown
67	43	medium gray	medium	thickly bedded	dolomite	none	Limeport	Allentown
68	46	medium gray	medium-coarse	thickly bedded, no structure	dolomite	none	Limeport	Allentown
69	46	medium gray	medium	slightly sparkly, non-fetid	dolomite	none	Limeport	Allentown
70	20	medium gray	medium	slightly sparkly, non-fetid	dolomite	none	Limeport	Allentown
71	33	medium gray	medium	thickly bedded	dolomite	none	Limeport	Allentown
72	56	medium gray	coarse		dolomite	none	Limeport	Allentown
73	10	medium	coarse		dolomite	none	Limeport	Allentown
74	10	light gray	coarse	coarsely crystalline (Or3, Baby Swamp like), strongly fetid	dolomite	none	Limeport	Allentown
75	53	light gray	coarse	coarsely crystalline, slightly fetid	dolomite	none	Limeport	Allentown
76	23	medium gray	medium	slightly fetid	dolomite	none	Limeport	Allentown
77	48	medium-	medium	slightly sparkly, fetid	dolomite	none	Limeport	Allentown

		dark gray						
78	66	very dark gray	medium	slightly fetid	dolomite	none	Limeport	Allentown
79	28	dark gray	medium -fine		dolomite	none	Limeport	Allentown
80	30	dark gray	medium	slightly fetid, punky, porous	dolomite	none	Limeport	Allentown
81	23	dark gray	medium -fine	slightly fetid	dolomite	none	Limeport	Allentown
82	53	medium-dark gray	medium	slightly fetid	dolomite	none	Limeport	Allentown
83	20	medium gray	medium		dolomite	none	Limeport	Allentown
84	13	dark gray	medium	slightly fetid	dolomite	none	Limeport	Allentown
85	13	dark gray	medium -fine		dolomite	none	Limeport	Allentown
86	15	dark gray	medium	slightly fetid, abundant algal laminations along base	dolomite	chert replacing algal in places	Limeport	Allentown
87	20	light gray	coarse	thinly bedded, strongly fetid, algal laminated	dolomite	none	Limeport	Allentown
88	36	very dark gray	medium -fine	some sign of algal control to bedding	dolomite	none	Limeport	Allentown
89	18	medium-light gray	coarse	slightly fetid, some algal laminations	dolomite	none	Limeport	Allentown
90	28	medium gray	coarse	coarsely crystalline, slightly fetid, punky, some algal laminations	dolomite	none	Limeport	Allentown
91	25.4	medium gray	coarse	slightly fetid, no signs of algal	dolomite	none	Limeport	Allentown
92	13	black	fine		shale	none	Limeport	Allentown
93	61	medium gray	medium	slightly fetid, signs of algal laminations in middle of unit	dolomite	none	Limeport	Allentown
94	38	medium gray	medium	fetid	dolomite	none	Limeport	Allentown
95	38	medium-light gray	medium	slightly fetid, algal laminated, at base, 2.5 cm thick quartz seam	dolomite	none	Limeport	Allentown
96	23	medium gray	medium	thinly bedded, algal laminated	dolomite	none	Limeport	Allentown
97	20	medium gray	medium	algal laminated	dolomite	none	Limeport	Allentown
98	13	olive gray/charcoal	fine		shale	none	Limeport	Allentown
99	38	nearly black		very thinly bedded, stylolite rich, algal laminated, occasional rip-up clasts	dolomite	none	Limeport	Allentown

100	30	dark gray	medium	slightly fetid, algal laminated	dolomite	upper 2.5-5cm: black, opaque chert bed: pinches and swells along strike, in places chert becomes thick and rounded like pod; strong stylolite surface at base of chert bed, at one location chert bed is 20 cm thick and continues along strike	Limeport	Allentown
101	28	medium gray	medium-fine	slightly fetid, some stylolite surfaces at base of bed, occasional algal seen on weathered surface	dolomite	none	Limeport	Allentown
102	13	dark gray	medium-coarse		dolomite	none	Limeport	Allentown
103	15	medium gray	medium-coarse	slightly algal laminated, upper 10 cm: rip-up clasts and intraformational conglomerate	dolomite	none	Limeport	Allentown
104	10	dark gray	medium	slightly fetid, upper surface is stylolite bounded	dolomite	none	Limeport	Allentown
105	15	medium gray	coarse	most of bed: rip-up clasts and intraformational conglomerates, disconformable	dolomite	none	Limeport	Allentown
106	15	medium gray	medium	lower 10 cm: oolitic, not graded, upper part of bed: finely algal laminated	dolomite	lower beds: chert pods (15X8cm), ooid and algal replacement	Limeport	Allentown
107	5	light gray	medium	algal laminated	dolomite	none	Limeport	Allentown

108	15	dark gray	micrite	algal laminated	dolomite	none	Limeport	Allentown
109	13	medium-dark gray	fine	fetid, finely algal laminated	dolomite	none	Limeport	Allentown
110	15	medium-dark gray	fine	fetid, finely algal laminated	dolomite	none	Limeport	Allentown
111	53	medium gray	fine	algal laminated	dolomite	none	Limeport	Allentown
112	23	light gray	medium	thin flaggy beds, oolitic, almost pisoid rich, some signs of cross bedding, plentiful algal, upper part of unit has rip-up clasts	dolomite	none	Limeport	Allentown
113	43	light gray	medium-coarse	algal laminated, pisoids, cross bedded, current laminations, rip-up clasts, fetid	dolomite	lower 20 cm: 2 chert-bearing zones: lower one, 4 cm thick, upper one, 5 cm thick, pinch and swell, homogenous, black, contains ooids, seems to be part of a network and forms a single bed at times	Limeport	Allentown
114	20	medium gray	fine	strongly fetid, between 2 chert-bearing sequences, dolomite is thin and flaggy, dark gray dolomite underneath first chert	dolomite	at base: chert about 36X8 cm: fairly continuous, contains rip-up clasts	Limeport	Allentown
115	74	dark gray	fine	thinly bedded, slightly fetid, some signs of algal laminations, no signs of any other structure	dolomite	none	Limeport	Allentown
116	81	medium gray	medium-fine	somewhat more thickly bedded, strongly algal laminated, shale partings at both contacts, upper 2.5 cm: fibrous quartz, looks as if deposited in a fault	dolomite	none	Limeport	Allentown
117	18	medium-	medium	algal laminated	dolomite	none	Limeport	Allentown

		dark gray	-fine					
118	20	medium gray	medium	algal laminated	dolomite	none	Limeport	Allentown
119	15	medium gray	medium	plentiful algal laminations, especially upper 15.2 cm	dolomite	none	Limeport	Allentown
120	30	medium-dark gray	medium	thickly bedded, slightly fetid, sparse algal laminations	dolomite	none	Limeport	Allentown
121	36	medium gray	medium-coarse	fetid	dolomite	none	Limeport	Allentown
122	18	dark gray	medium-coarse	fetid, slightly algal laminated	dolomite	none	Limeport	Allentown
123	36	light gray	medium	thickly bedded, fetid	dolomite	none	Limeport	Allentown
124	41	light gray	coarse	medium bedded, slightly fetid	dolomite	none	Limeport	Allentown
125	56	dark gray	medium-fine	slightly fetid	dolomite	none	Limeport	Allentown
126	36	dark gray	medium	slightly fetid	dolomite	none	Limeport	Allentown
127	30	dark gray	medium-fine		dolomite	none	Limeport	Allentown
128	43	medium-dark gray	medium-coarse		dolomite	none	Limeport	Allentown
129	58	dark gray	fine	slightly fetid	dolomite	none	Limeport	Allentown
130	56	dark gray	fine	slightly fetid	dolomite	none	Limeport	Allentown
131	51	dark gray	fine	slightly fetid	dolomite	none	Limeport	Allentown
132	51	dark gray	fine	4 beds, each 12 cm: strongly fetid, upper 12 cm: strongly algal laminated	dolomite	none	Limeport	Allentown
133	91	dark gray	fine	slightly fetid	dolomite	none	Limeport	Allentown
134	48	dark gray	medium	slightly fetid, possible burrow structures?, otherwise structureless	dolomite	none	Limeport	Allentown
135	61	light gray	medium	slightly fetid, punky, porous, holes filled with quartz, possible burrow structures?	dolomite	none	Limeport	Allentown
136	41	medium gray	medium	slightly fetid, burrow structures?	dolomite	none	Limeport	Allentown
137	38	medium gray	medium	slightly fetid, upper 10 cm: fine algal laminations, thickly bedded	dolomite	none	Limeport	Allentown
138	41	light gray	medium	thickly bedded	dolomite	none	Limeport	Allentown
139	46	medium gray	medium	massive, many bed boundaries ate stylolites	dolomite	none	Limeport	Allentown
140	112	medium gray	fine	lower 81 cm: finely algal laminated, upper	dolomite	none	Limeport	Allentown

				30 cm: light gray, coarse-grained				
141	51	light gray	medium	algal laminated	dolomite	none	Limeport	Allentown
142	10	medium gray	medium	finely algal laminated	dolomite	none	Limeport	Allentown
143	15	dark gray	micrite	finely algal laminated	dolomite	none	Limeport	Allentown
144	46	medium gray	fine	slightly algal laminated	dolomite	none	Limeport	Allentown
145	38	medium gray	fine	strongly fetid, punky, bioturbated, possible burrow structures?	dolomite	none	Limeport	Allentown
146	25	medium gray	coarse		dolomite	none	Limeport	Allentown
147	43	light gray	medium	upper and lower contacts are stylolite boundaries	dolomite	none	Limeport	Allentown
148	28	medium gray	medium		dolomite	none	Limeport	Allentown
149	36	medium gray	medium		dolomite	none	Limeport	Allentown
150	10	medium gray	coarse	slightly fetid	dolomite	none	Limeport	Allentown
151	86	light gray	fine		dolomite	none	Limeport	Allentown
152	33	light gray	fine	lower 10 cm	dolomite	none	Limeport	Allentown
				middle 15 cm	dolomite	none	Limeport	Allentown
				upper 8 cm: rubble zone	dolomite	none	Limeport	Allentown
153	25	medium gray	micrite	stylolite surfaces	dolomite	none	Limeport	Allentown
154	20	medium gray	medium	slightly fetid, shallowing upward sequence, rubbly, shaly, lumpy, ruditic, clay-rich, fault gouge: all sheared dolomite	dolomite	none	Limeport	Allentown
155	13	dark gray	fine	slightly fetid	dolomite	none	Limeport	Allentown
156	13	medium gray	medium	slightly fetid, rip-up clasts	dolomite	none	Limeport	Allentown
157	30	medium gray	medium	numerous rip-up clasts, strong stylolite surfaces, lower 8 cm: rubble zone, rugose, ruditic, fragmented, shaly, sheared out, uneven surface, entering a recess	dolomite	none	Limeport	Allentown
158	6	yellow/olive	fine		shaly dolomite	none	Limeport	Allentown
159	20	medium gray	fine	possible rip-up clasts, especially at base	dolomite	none	Limeport	Allentown
160	33	black	fine	thinly laminated, possible marker horizon	sandy shale	none	Limeport	Allentown

161	51	dark gray	fine	fetid, lower 33 cm: strongly algal laminated, possible flute casts, ripple marks, sole markings, upper 18 cm: rubbly, uneven beds, rip-up clasts, possible grainstone facies	dolomite	none	Limeport	Allentown
162	15	dark gray	fine	algal laminated, algals may be overturned, occasional rip-up clasts, intraformational conglomerates, possible grainstone	dolomite	none	Limeport	Allentown
163	15	dark gray	coarse	fetid, rubbly	dolomite	none	Limeport	Allentown
164	10	dark gray	coarse	slightly fetid, algal laminated, some rip-up clasts	dolomite	none	Limeport	Allentown
165	8	dark gray	coarse	rubbly, intraformational conglomerate	dolomite	none	Limeport	Allentown
166	20	light gray	medium	slightly fetid, algal laminated, thick-bedded	dolomite	none	Limeport	Allentown
167	36	dark gray	coarse	slightly fetid	dolomite	none	Limeport	Allentown
168	15	dark gray	coarse	very thinly bedded, algal laminated, stylolite boundaries	dolomite	none	Limeport	Allentown
169	8	dark gray	coarse	very thinly bedded, algal laminated, stylolite boundaries	dolomite	none	Limeport	Allentown
170	18	dark gray	coarse	very thinly bedded, algal laminated, stylolite boundaries	dolomite	none	Limeport	Allentown
171	10	dark gray	coarse	very thinly bedded, algal laminated, stylolite boundaries	dolomite	none	Limeport	Allentown
172	43	black/olive	fine	finely laminated	silty shale	none	Limeport	Allentown
173	91	dark gray	coarse	very thinly bedded, fissile, algal control, a lot of sand	shaly dolomite	none	Limeport	Allentown
174	68	dark gray	coarse	slightly effervescent, very thinly bedded, fissile, algal controlled, a lot of sand	shaly dolomite	none	Limeport	Allentown
175	25	very dark gray	micrite	some signs of algal	dolomite	none	Limeport	Allentown
176	18	very dark gray	micrite	some signs of algal	dolomite	none	Limeport	Allentown
177	30	medium gray	medium	fetid, algal laminations	sandy shale	none	Limeport	Allentown
178	36	dark gray	medium-fine	very thinly bedded, algal laminated, upper 13 cm: numerous rip-up clasts	dolomite	none	Limeport	Allentown

179	48	dark gray	micrite	algal laminated, occasional rip-up clasts toward top of unit	dolomite	none	Limeport	Allentown
180	46	black/olive	fine	thinly bedded, fissile, some signs of algal control	sandy shale	none	Limeport	Allentown
181	51	very dark gray	micrite	thinly bedded, sparse algal laminations, limey content	dolomite	none	Limeport	Allentown
182	48	olive/black	fine	extremely fissile,	silty shale	none	Limeport	Allentown
183	56	medium-dark gray	medium-coarse	slightly fetid, ripple marks, flute casts, occasional rip-up clasts at base, algal structures convex upward, upper 20 cm: remnants of current ripple marks, upper30 cm: abundant ooids, upper contact: current ripples	dolomitic limestone	none	Limeport	Allentown
184	13	medium gray	micrite	algal laminated towards top of unit, rip-up clasts common, shale partings at both contacts, numerous overturned algal, rip-up clasts, and conglomerate, ripple marks and current ripples present	dolomite	none	Limeport	Allentown
185	10	medium gray	micrite	algal laminated towards top of unit, rip-up clasts common, shale partings at both contacts, numerous overturned algal, rip-up clasts, and conglomerate, ripple marks and current ripples present	dolomite	none	Limeport	Allentown
186	61	dark gray	fine	thin flaggy, occasional thin units of black shale	interbedded silty dolomite and dolomitic limestone	none	Limeport	Allentown
187	66	very dark gray	micrite	4-5 beds: algal laminated, medium bedded	dolomite	none	Limeport	Allentown
188	10	dark gray,	medium	structureless	dolomite	none	Limeport	Allentown
189	56	very dark gray	fine	slightly fetid, moderately thin bedding (8-10cm), lower 15 cm: finely algal laminated, rest of	dolomite	none	Limeport	Allentown

				unit: contoured with algal, as if algal growing on old ripple surfaces, sulfide concentrations seem to be lining algal, rip-up clasts at top of unit				
190	41	dark gray	medium -coarse	slightly algal laminated, shale partings on both contacts, thinly bedded	dolomite	none	Limeport	Allentown
191	86	dark gray	micrite	fetid, strongly algal laminated, 8-10 cm thick beds, sulfides concentrated at algal structures, shale partings at bed intervals	dolomite	none	Limeport	Allentown

B.9 – Summary

Formation Name	Member Name	Dunham Classification	Thickness (cm)	Percent of Unit
Ontelaunee	Harmonyvale	Mudstone	4915	100
Ontelaunee	Beaver Run	Grainstone	5192	55
Ontelaunee	Beaver Run	Mudstone	580	6
Ontelaunee	Beaver Run	Packstone	3295	35
Ontelaunee	Beaver Run	Wackestone	318	4
Epler	Lafayette	Crystalline	25	1
Epler	Lafayette	Grainstone	245	4
Epler	Lafayette	Mudstone	4540	73
Epler	Lafayette	Packstone	1160	19
Epler	Lafayette	Wackestone	180	3
Epler	Big Springs	Crystalline	80	1
Epler	Big Springs	Grainstone	3079	36
Epler	Big Springs	Mudstone	1816	21
Epler	Big Springs	Packstone	3226	38
Epler	Big Springs	Wackestone	323	4
Epler	Branchville	Grainstone	395	27
Epler	Branchville	Mudstone	110	8
Epler	Branchville	Packstone	940	65
Rickenbach	Hope	Crystalline	139	5
Rickenbach	Hope	Grainstone	499	18
Rickenbach	Hope	Mudstone	1246	45
Rickenbach	Hope	Packstone	819	29
Rickenbach	Hope	Wackestone	90	4
Rickenbach	Lower	Grainstone	801	23
Rickenbach	Lower	Mudstone	1340	39
Rickenbach	Lower	Packstone	900	26
Rickenbach	Lower	Wackestone	425	12
Allentown	Upper	Grainstone	1929	18
Allentown	Upper	Mudstone	3671	34
Allentown	Upper	Packstone	4222	40
Allentown	Upper	Wackestone	855	8
Allentown	Limeport	Crystalline	91	1
Allentown	Limeport	Grainstone	5744	32
Allentown	Limeport	Mudstone	3036	17
Allentown	Limeport	Packstone	6053	33
Allentown	Limeport	Wackestone	3087	17
Leithsville	Wallkill	Grainstone	927	45
Leithsville	Wallkill	Mudstone	266	13
Leithsville	Wallkill	Packstone	806	39
Leithsville	Wallkill	Wackestone	49	3
Leithsville	Hamburg	Grainstone	609	20

Leithsville	Hamburg	Mudstone	522	17
Leithsville	Hamburg	Packstone	1787	60
Leithsville	Hamburg	Wackestone	67	3
Leithsville	Califon	Grainstone	577	25
Leithsville	Califon	Mudstone	482	20
Leithsville	Califon	Packstone	690	30
Leithsville	Califon	Wackestone	578	25

APPENDIX C – A MODEL FOR THE PREDICTION OF PREHISTORIC CHERT QUARRY LOCATIONS, CHERT EXTRACTION, QUARRY DEVELOPMENT AND TASK SUBDIVISION WITHIN PREHISTORIC QUARRIES (INTERIOR LAKES MODEL)

C.1 Introduction

This appendix addresses the archaeological potential of this dissertation on the geologic investigation of the Cambrian-Ordovician cherts of the Great Valley Sequence in the Wallkill River Valley, Sussex County, New Jersey and Orange County, New York. During detailed stratigraphic measurement at a scale of 1:98, the author observed fractures on chert beds that were of a different orientation and style than what usually associated with geologic fractures such as faults and joints. Also, these fractures were curvilinear and possessed a radial curvature that lent support to the hypothesis that percussion using hammerstones of a certain radius and elasticity may have been the cause of the scars that were restricted only to the chert beds in outcrop. Associated with these worked surfaces were modified glacial cobbles and boulders (interpreted as hammerstones), along slopes containing chert and dolomite debris (interpreted as mining debris). While mapping, the author mapped the occurrence of these prehistoric chert quarries at a scale of 1:24,000. Further substantiation of the prehistoric quarry hypothesis was found when the author observed Cambrian-Ordovician Wallkill chert in local archaeological collections.

In the archaeological literature, there is an obvious slant in how researchers are perceiving prehistoric quarries. Quarries typically are thought of in the following frameworks; as point sources for investigations of trade (Bement, 1999; Ingbar, 1994; Kelly, 1984; Mitchum, 1991; Odell, 1984; Perttula, 1984; Torrence, 1986; Winters,

1984), as workshops occurring near quarries (Roemer, 1991; Stoltman et al., 1984), and as reduction strategies after quarrying (Jelinek, 1991; Johnson, 1984) that fail in treating the actual extraction of the materials, or the remnant architecture of the quarries. The studies also fail to investigate the more detailed geologic controls of the ore/raw material, thus providing a weak foundation for quarry studies, as well as trade and exchange. In addition, these investigations fail to take into consideration the rich historical and modern mining/quarrying literature on prospecting (Hoover, 1909; Osborn, 1907; Peters, 1978; von Bernewitz, 1931), the mineral resources and mining engineering (Emmons, 1922; Flawn, 1966; Peele, 1941), and ore dressing (Pryor, 1965; Richards and Locke, 1940; Taggart, 1927). Historical mining literature starts with Georgius Agricola's *De Re Metalica* (Agricola, 1950[1556]), providing a foundation for the quarrying and working of stone and metal that had been pre-established for over 400 years. On this foundation, it was the intention of this investigation to provide model(s) accounting for the occurrence of prehistoric quarries, as well as the activities required for extraction of ore from the earth, using the framework geology imposes on quarrying as a hand-operated industry.

A brief presentation of previous quarry investigations is provided in this appendix and divided into: division of labor; mining habitation; boundaries and ownership; trade and exchange; and ritual and ideology. These divisions are addressed with ethnographic, historical, and archaeological investigations to provide a background on what can occur at quarries (ethnographic and historical), and what may be left in the archaeological record.

The quarry investigation discussion is followed by a brief synopsis of Native American mining of lead and copper. While lead and copper are raw materials with distinctly different geologic properties from chert, their mining is discusses in this appendix precisely because there have been extensive investigations on Great Lakes copper mining (Drier, 1961b; Du Temple, 1961; Holmes, 1919; Whittlesey, 1863). Additionally, this appendix provides a brief discussion of Native American lead mining in the nearby Shawangunks of Sullivan County, New York (Crawford, 1981; Eilertsen, 1950; Quinlan, 1873), including a direct observation of Native American lead mining.

Following the previous research, two new models are presented in this dissertation for the chert quarries of the Wallkill River Valley; specifically (1) a model for predicting the precise locations of Cambrian-Ordovician prehistoric chert quarries in the Wallkill River Valley; and (2) the typical quarry plan in a Cambrian-Ordovician prehistoric chert quarry in the Wallkill River Valley. Two alternate studies are also presented based on archaeological investigations conducted by this researcher in northeastern New York, as well as ethno-archaeological investigations at an extant limestone quarry near Talicoot, in the Bhima Basin of India. A brief discussion follows on the success of geological investigations in provenancing archaeological artifacts not only to lithologic formations and members, but to individual prehistoric quarries as well.

In addition to this brief treatment of on-going archaeological studies, copies of two papers on prehistoric quarries in the Wallkill River Valley are provided. "*Lithostratigraphic models and the geographic distribution of prehistoric chert quarries within the Cambro-Ordovician lithologies of the Great Valley Sequence, Sussex County, New Jersey*" (LaPorta, 1994) is the first publication of models to predict prehistoric

quarries. The second publication, "*Lithostratigraphy as a predictive tool for prehistoric quarry investigations:examples from the Dutchess Quarry site, Orange County, New York*" (LaPorta, 1996a), addresses the application to the medial Ordovician chert-bearing carbonates in the vicinity of the Dutchess Quarry prehistoric site, as well as addressing the "typical quarry plan." A third paper, which is an ethnographic study of hand-operated quarries in modern-day India, is included; specifically, "*A geologic model for the development of bedrock quarries, with an ethnoarchaeological application"* (LaPorta, 2005). This paper compares the models developed for the prehistoric quarries documented in the Wallkill River Valley to the ethnographic record and explains the similarities and discrepancies outlined in the comparison.

C.2 Anthropological Archaeology Issues in the Study of Mines and Quarries: A Brief Presentation of Previous Research

As Godoy (1985) pointed out, anthropologists "recently" discovered miners due to environmental and energy crises. Godoy (1985) notes that systematic anthropological studies have, as of 1985, not arrived. Many anthropological, sociological, and historical studies of mining and quarrying (Godoy, 1985; Knapp et al., 1998; Paul, 1970; Shinn, 1965[1884]; Temple, 1972) illustrate the connection to more modern mining and quarrying when treating economic aspects. These works almost exclusively deal with post-Industrial mining and quarrying but each carry sections on "pre-Roman" (Shinn, 1965[1884]; Temple, 1972), Roman (Shinn, 1965[1884]; Temple, 1972), and Medieval (Paul, 1970). Few studies (Burton, 1984; Hampton, 1999; Jones and White, 1988; LaPorta, 2004; Pétrequin and Pétrequin, 1993) provide ethnoarchaeological investigations on pre-Industrial methods of mining that are closer analogs to prehistoric chert quarrying in the Hudson Valley.

Based on other researchers (Godoy, 1985; Ericson, 1984; Torrence, 1986) archaeologists can divide the anthropological and archaeological study of mining, specifying on social aspect, into five basic sections: division of labor; mining habitation; boundaries and ownership; trade and exchange; and ritual and ideology.

C.2.1 Division of Labor. The division of labor, which creates the chain of operations, or *chaînes des opératoires*, can have a different connotation in terms of activity (LaPorta, 1994, 1996a, 2004; Parker, 1925), economy (Godoy, 1985), and gender (Brumbach and Weinstein, 1999; Childs, 1998; Lawrence, 1998; Rusco and Shelly, 1992).

Of the three connotations, activity is the most plausible connotation for archaeological reconstruction. Arthur C. Parker received authorization for one months worth of fieldwork by John Clarke of the Geological Survey of New York (Parker 1925). It was during this expedition that Parker observed the uneven clustered spatial distribution of hammerstones and associated chert quarry tailings. Based on the inferred spatial distribution of chert artifacts and associated hammerstones, Arthur C. Parker (1925) hypothesized six task subdivisions in the prehistoric quarries of Flint Mine Hill in Coxsackie, New York. The six subdivisions are summarized as: (1) extraction pit; (2) shale and coarse-grained flint dump; (3) chert sorting piles; (4) chipping quality station; (5) station for further chipping into bifaces; and (6) stations where bifaces were working into projectile points. The author independently observed anomalous concentrations of predominantly glacially derived, Silurian metaconglomerate, and other metamorphic rocks, as occurring both immediately in the vicinity of chert outcrops, as well as within neighboring stone walls. Archaeological fieldwork conducted for this dissertation

allowed for the discrimination of the glacially derived objects into morphological classes, as well as a further subdivision into petrological groups. This permitted the eventual delineation of distinct task subdivisions in the prehistoric chert quarries as they occurred in the Cambrian-Ordovician lithologies (LaPorta, 1994; 1996a; 2004). Discrete classes of quarry tailings were correlated to specific hammerstone function types. The result of this exercise was the development of the first quarry work plan, or model for task subdivision, for the chert quarries occurring within the Wallkill River Valley in northwestern New Jersey and southeastern New York by applying these typological constructs (see following sections and attached articles for the 'typical quarry model').

The economic aspect of quarrying requires a social context. Aside from the use of chert for the construction of subsistence related implements, the implication of a reciprocal based economy is explored further in the "trade and exchange" section. In more modern respects, Godoy (1985) places mining into the capitalist economic system.

Even A. Bernard Knapp (1998), who notes the gender-neutral (neutral = male) archaeological studies on mines, also notes the need for social context. While documentation may be available for historical activities (Lawrence, 1998), the social context is nowhere near as developed for prehistoric quarrying and mining. Brumbach and Weinstein (1999) reinforce Parker's (1925) activity assessment of Flint Mine Hill, but deconstruct his gender assumptions of only males working at the quarry.

C.2.2 Mining Habitation. Godoy (1985) notes that mineral locations in inaccessible areas give rise to "relatively self-contained communities," whether open or paternalistic. The size of associated habitation, or production, sites depends on the size

of the mine, or quarry. Ethnographic studies in Irian Jaya, Indonesia (Hampton, 1999; Pétrequin and Pétrequin, 1993) note that quarries are located nearby villages.

Historic studies on mining habitations (Bell, 1998; Douglass, 1998; Knapp, 1998; Rule, 1998; Shinn, 1965[1884]) support Godoy's (1985) statement about the remoteness of mining camps, villages, and towns. William Douglass (1998) stated that the mining camps and communities of the American West, Canada, and Alaska were fluid and cosmopolitan in nature and included a disparate collection of human beings. Camps like these were a collection of strangers (Bell, 1998; Douglass, 1998), as opposed to a community of kinsmen (Rule, 1998). When mining operation ceases, the buildings and remains are sold for scrap (Bell, 1998).

For archaeologists, evidence of earlier habitation may be eradicated by further quarry/mine expansion (Topping, 1997). In Egypt, Shaw (1994) characterizes Pharaonic quarrying and mining site components as containing: (1) traces of quarrying/mining activity; (2) remains of settlements and encampments; (3) facilities for provisions of water; (4) arteries of transport and communication; (5) evidence of processing and manufacturing activities; (6) textual and pictorial memorials of the expeditions; and (7) ritualistic and religious remains. Egyptian miners sometimes had minimal accommodations if they were close to permanent settlements (Shaw, 1994). Through the architecture and archaeological remains of low-level exploitation, Shaw (1994) differentiates between state-run and private mining/quarrying expeditions. Shaw concludes with eight prominent factors for settlement patterns: (1) nature and necessary quantities of material; (2) degree to which material is processed "*in-situ*;" (3) distance from sources of food and water; (4) perceived need for relatively constant supply; (5) risk

of attack; (6) stability of Egyptian socio-economic system; (7) skilled vs. unskilled composition of the work force; and (8) primary destination of material and its range of use.

C.2.3 Boundaries and Ownership. Boundaries are lines and frontiers are zones, or an uninhabited space between zones (Prescott, 1965). Frontiers are analogs for boundaries based on physical landscapes and superimposed boundaries (Prescott, 1965). Boundaries imply territorialism, and are separated into: (1) overt competition through restricted space, or resources; and (2) reciprocal altruism through restricted access (Cashdan, 1983; Hampton, 1999). Ecological studies on territoriality have noted qualitative aspects of resource availability, but have not measured the availability to produce quantitative aspects. Barth (1969) notes empirical investigations show that boundaries persist even with flow and stable social interactions across boundaries are based on dichotomized ethnic statuses.

Hampton (1999) notes that the river is the longitudinal boundary between individually owned quarry sites in the Langda area of Irian Jaya, Indonesia. Head quarrymen own the river quarries along the shores of only their hamlet (Hampton, 1999). Each hamlet has a head quarryman who inherits quarrying rights from his father, who was head quarryman and trained his son(s). The rights always belong to the quarry man and not the most influential person in the hamlet, or big man, unless they are one in the same (Hampton, 1999). In a contradictory note, Pétrequin and Pétrequin (1993) note that ownership does not exist among the Dani, but a right of passage is paid in the form of food to Wano hamlets that control mountain access.

A “stone quarry” in southeast Australia, at Mt. William near Lancefield, used to obtain material for manufacturing tomahawks, was a family proprietorship (Howitt, 1904). A condition of people coming to the quarry, for trade/exchange, was not to cause trouble (Howitt, 1904). Howitt (1904) also noted that fights would break out when people took stone without exchange, or outright stole rock. The ownership and need for permission is supported by the study of central Australian aborigines by Baldwin Spencer and F.J. Gillen (1899).

Wilfrid Jury (1949) references a Jesuit account (Fr. Jerome Lalemont, 1641) on the Attawandrian Indians in the peninsula of southwestern Ontario, bounded by Lake Ontario and Lake Huron. Lalemont relayed that the Attawandrians were known as “The Neutral Nation,” where tribes of Hurons and Iroquois, sworn enemies, were at peace as long as they were in villages (Jury, 1949). Jury (1949) posits a hypothesis, backed by Reverend Dean W.R. Harris in 1896, that the Attawandrians controlled chert resources that were a necessity to the Iroquois and Hurons. George Catlin noted that the red pipestone quarry in Minnesota was owned in common as a neutral group (Holmes, 1919). Possibly, the most important single hypothesis put forward by Jury (1949) relates to the extraction of rock at the chert quarries. Jury (1949) proposes that after blocks of chert are extracted from outcrops they are placed under large trees, between the extensions of the root systems. A large hand-hewn lever is then placed in a notch carved into the base of the tree (Jury, 1949). The lever is then lowered down over the chert block, which rests on a stone platform, until the chert breaks into pieces (Jury, 1949). If this process was correct, then it would serve to explain the enormous volume of chert debris visible around and within old tree and root systems. More importantly, as the tree grows and

dies, the resulting overturned tree would produce a depression that would be completely encircled by debris. This chert debris would eventually partially slump back-fill into the circular depressions. Furthermore, at some locations such as Pleasantdale, near Troy New York, entire ancient tree trunks have been plucked from the bottoms of old circular quarry pits (Charles Ellett, personal communication, 2007). The use of wooden levers would imply the working knowledge of the basic physics of the use of wedges as well as levers for breaking rock.

Ian Shaw (1994) notes the control over mineral resources as crucial to the emergence of the ancient Egyptian state, provided stability and prosperity in the late 2nd millennium, and provided survival of names for some rulers through the inscriptions commemorating quarrying or mining expeditions. The writer (LaPorta) has observed the inscriptions of quarry men at Cerrabitt Hathem the Early Kingdom Hathor temple and copper complex of the Sinai Peninsula. At this location, several thousand feet above sea level, hafted hammers are inscribed into the bedrock walls along the pathway to the various copper mines. Also, the writer discovered a massive basalt hammer blocking the front of a false door occurring along the base of the temple. The object weighed approximately 114 kg and, more importantly, there are no basalt sources occurring within the region.

C.2.4 Trade and Exchange. To successfully address trade and exchange of raw material, or non-metallic ores, one must realize the fundamental premise directly linking an artifact to a source. This is frequently presumed with a lack of methodology linking artifact to quarry (see discussion at the end of this appendix for the author's suggestion on how to remedy this problem).

Bud Hampton (1999) notes that small housing clusters of Dani along the Ey River (Irina Jaya Province, Indonesia) trade with hamlets that have head quarrymen and toolmakers (axes) since they do no have these specialized people. Pétrequin and Pétrequin (1993) elaborate on the ritualized aspects of trading among the Dani, where trade is not controlled by supply and demand, but by the rules of others. Tools are used by dowry by Yelme-Kembe warriors, but can do so only to belong to a traditional exchange relationship with the Wanos (Pétrequin and Pétrequin, 1993). The majority of axes are exchanged in a complex reciprocal gift exchange controlled by men and relate to the payment of dowries and manslaughter (Pétrequin and Pétrequin, 1993). Pétrequin and Pétrequin (1993) note that the value of the axes, in a relative sense, is less than pigs and cowries. Fragile green-schist axes are stones for exchange (*je-yao*), which are different from utilitarian axes. A pair of *je* axes are presented for copulation, with a "male" axe resting on a "female" axe (Pétrequin and Pétrequin, 1993).

The family owners of the "stone quarry" in southeast Australia, at Mt. William near Lancefield, exchanged goods when neighboring tribes wished for some stone (Howitt, 1904).

To tie artifacts to a point source and reconstruct trade and exchange is one of the more popular quarry related types of investigations (Bement, 1999; Torrence, 1986). Alternately, the trade or exchange may also represent mobility (Bement, 1999; Ingbar, 1994)

C.2.5 Ritual and Ideology. The more abstract ideas of ritualism and ideology are perhaps the most difficult to relate to an archaeological investigation. The relative lack of preservation eliminates a large part of perishable cultural material associated with

mining (Childs, 1998). Hampton (1999) provides ethnographic evidence of vegetable offerings to the Elgor, the spirit power owner of all rocks, in "special places" at Yeineri quarries in Irian Jaya. Historical accounts (Rule, 1998) of religion and injury/death dominate Cornish tin mining society, described as sometimes becoming an "epidemic."

Hampton (1999) elaborates further with the rituals for the Langda-Sela quarries in Irian Jaya prior to involvement with missionaries. Skulls of Una ancestors were believed to hold power to provide good stones for quarrying. Villagers would ask permission and directions to "find many stones" when a shaman would call a major ceremony, called *yowali*, every five years. After the ceremony, a massive quarry operation would take place, a major supply of stone was located, and biface blanks were stockpiled. Vegetable, and sometimes pig, offerings were made to the female spirit Alim Yongnum, who owned the land near the river (locations of quarries), and the male spirit Murbilik Kue, who owned the stones. Sacralized pig fat, saved from various sacrificial pig rituals throughout the year, is used to rub boulders selected for quarrying to make the stones beautiful and please the spirits in the stone (Hampton, 1999; Pétrequin and Pétrequin, 1993). Additionally, pig fat was sometimes rubbed on remaining quarry core rock so that good quality stones would be found on the next visit (Hampton, 1999). Lastly, Hampton (1999) mentions spirit sticks stuck in the river or ground by the edge of the river. These spirit sticks were to communicate to spirits that quarry operation was in progress.

Jean Nicollette, in his geological expedition in Minnesota between 1836-1843, noted that the red pipestone quarry of the Sissiton tribe (Sioux) was protected by the Great Spirit, who saluted them with lightning and thunder when they visited (Winchell, 1884). Nicollete and his camp, as he noted "coincidentally," met with a short-lived

severe thunderstorm, with high winds, as they approached the quarry to make their geological observations (Winchell, 1884). The storm soon passed and the sun showed, interpreted as the Great Spirit "reconciled to our presence" (Winchell, 1884).

In Mindanáo, Philipines, John Garver (1941) observed a religious procedure to gold mining in the Híbung River, its tributaries, the Wá-wa River, and the Taligaman district. The gold, panned in the rivers, is property of the gold spirit of the Manóbos (Garver, 1941). Miners come to the quarry with a white fowl (future meal for the gold spirit) and kill a white pig to honor the gold spirit. In addition, the miners present the spirit with leaf packages of boiled native rice before mining (Garver, 1941). Garver (1941) also comments that noise and merriment are forbidden while mining, since it is displeases the gold spirit, but further obligations of rice are made in that case so that additional gold is found.

Religious rituals for quarrying can also be a secretive aspect to the mining and quarrying experience (Jones and White, 1988). Jones and White (1988) note the Australian (eastern Arnherm Land) aboriginal myth of two Wawilak sisters coming from the far interior of the south (Ngilipitji area) with stone spears, as noted by Jones, White, and additional researchers. Approval to visit an extant quarry site, however, was granted with four conditions, one of which was that "'inside,' i.e. restricted names and associated ceremonial 'business' were not to be made public" (Jones and White, 1988).

The inference of burial at prehistoric quarry sites is more limited. In England, Peter Topping explores symbolism in English flint mines, specifically Grimes Graves (Barber et al., 1999; Topping, 1997). Topping (1997) noted the presence of a skull discovered above an ox bone, and wedged between floor stone chalk, similar to ones

found in Cissbury (England) and Spiennes (Belgium). An extended burial, facing galleries and an inferred mining victim, was noted in a shaft at Cissbury (Topping, 1997). Based on the presence of a skull, antlers, axe marks, a polished axe, and bird remains, Topping (1997) infers possible totemism, linking clan or kinship rights to mines at the Greenwell pit in Grimes Graves.

C.3 A Brief Treatment of Mining and Quarrying of Lead and Copper by Native Americans

Due to the large scope of Native American mining and quarrying (Ball, 1941), only additional instances of Native American mining of metals, specifically copper and lead, are presented. Copper represents some of the earliest and most extensive archaeological treatment of prehistoric mining and quarrying. Lead was chosen due to the proximity of the study area (Wallkill River Valley) and the early observation of Native American mining. More specifically, the mining of metals in North America is largely restricted to accounts of copper, lead, silver and gold mining. The former copper includes an impressive volume of literature (Drier, 1961b; Du Temple, 1961; Holmes, 1919; Whittlesey, 1863) which is largely, but not entirely, restricted to copper extraction occurring along the Great Lakes Region. The extraction of lead is found in a broad band of quarries stretching across the Midwest, just below the Great Lakes, and overlaps with the present-day distribution of historic period lead-zinc, barite-fluorite production areas. The occurrence of silver mines usually co-occurs with the much more common turquoise extraction locations of the American southwest, and gold mining operations are even more isolated occurrences (Ball, 1940). Noteworthy, is the use of the term “mine” when referring to the extraction of metals, and “quarry” when referring to the extraction of non-metal raw materials. In some instances the architectural elements aid in determining the

broad classification; however, more commonly, term distinction is decided by the type of ore itself. For example, in many cases, the Lake Superior copper mines are simply circular depressions or elongate trenches, oriented along the trend of the copper bearing bedrock and excavated down to bedrock (Drier, 1961b; Du Temple, 1961; Holmes, 1919; Whittlesey, 1863). Conversely, in some occurrences, the zone of extraction is a well-defined shaft with adits and drifts, and associated backfill piles. Therefore the term mine is appropriate. The same is true of the lead occurrences of the upper Midwest. Many of the prehistoric lead occurrences are relatively simple excavations into unconsolidated overburden, downward to the bedrock surface. One of the exceptions is the elongate trench where silver was extracted in western Kentucky (Ball, 1940). The ancient silver mines at Cerillos (New Mexico) are described as mines and indeed include underground galleries and shaftways (Ball, 1940). However, the co-occurring turquoise quarries and pits, which occur over a much greater expanse of terrain, are referred to simply as pits (Ball, 1940; Holmes, 1919; Pogue 1973[1915]).

The transition between mine and quarry is most evident where the ore is of the commodity type. The first example, salt, which is non-metallic is referred to as being mined at locations in Kentucky, Virginia, Arkansas, and Arizona, and never quarried (Early, 1993; Morris, 1928). Oddly, in most occurrences, the salt is actually dried in flat pans once hand excavated from shallow depressions (Early, 1993). In fact, dessication areas, and not mines or quarries, are the rule for North American salt extraction occurrences. A second example includes obsidian locations, which are referred to as both mines as well as quarries (Holmes, 1919). At many locations near Pachuca, obsidian is hoisted from deep shafts and falls downward to stable platforms along well organized

spillways (Holmes, 1919). The extraction at Pachuca are truly mines; however, the landscape also contains walled excavations as well as numerous circular depressions excavated down to bedrock (Holmes, 1919). The obsidian locations at Hemes, in New Mexico, are open cast excavations into volcanic tuff. The multitudes of obsidian locations found in the Mineral Mountains, in southwest Utah, are predominantly open excavations into softer ash and tuff (personal observation by the author in during Prehistoric Quarries and Early Mines Interest Group field trip at 2006 annual SAA meeting). In many instances, with regards to the Mineral Mountains, the mines and quarries are in fact vast expanses of open terrain where dislodged masses of obsidian have been comminuted, leaving behind an enormous volume of tailings. The examples of commodity-type ore deposits which straddle the system includes red ochre pits (quarries and mines); mica (mines), graphite pits (quarries), turquoise pits (quarries and mines), pipestone quarries, as well as quartz crystal localities. Obviously, within this group of ores are a range of extraction styles, which includes architectured mines, quarries, as well as simpler pits. However, in most cases, regardless of the commodity type, they are all relatively simple pits excavated into unconsolidated overburden or bedrock.

The next group includes raw material types that border on the classification of groundstone (Murrell, 2007; Schneider and Altschul, 2000). These include steatite, andesite, basalt, sandstone, gypsum and travertine. Regardless of the degree of architectural design, or the length and organization of the chain of operation necessary to mill or process these ores, the extraction is referred to as a quarry or a pit and not a mine. In many instances, the locations that prove to sustain extraction and production over

considerable lengths of time, or those workings which produce great numbers of similar objects, are referred to as factories or workshops (Schneider and Altschul, 2000). Such of course is the case with adze and axe production sites at locations such as New Guinea (Clark, 1989), Iri Injara (Hampton, 1999; Pétrequin and Pétrequin, 1993), Hawaii (Lass, 1994), Australia (Clark, 1989), and even Great Britian (Clark, 1989).

This of course raises the question, how are chert and flint extraction locations treated? The most extreme examples would include the lavish chalk-flint galleries of western and central Europe (Barber et al., 1999; Topping, 1997). They represent some of the finest architectural remnants cherished within the prehistoric record. The vertical mine shafts, expansive galleries, with associated pillars and columns are the finest examples of prehistoric mining activity. However, separate from the chalk-flint galleries, the focus of this work is the much greater number of chert locations occurring in North America. The number of chert extraction sites is exhaustive and they are represented throughout the prehistoric cultural continuum. Chert extraction sites exist in all 50 states, they occur within the full spectrum of geological terrains from Proterozoic to Pliocene, they are so vast that they can be detected by satellite yet they are all, with few exceptions, miraculously fit into the one category of extraction- the quarry.

C.3.1 Native American Copper Mining

A majority of the early Native mining, especially some of the earliest recognized mining, comes from the copper mining on Isle Royale in Lake Superior (Drier, 1961b; Du Temple, 1961; Holmes, 1919; Whittlesey, 1863). Early mention of Native American copper use in the region comes from the records in the 1500s (Early Historical Accounts of the Lake Superior Copper District, 1961). The first mention of copper mines was in

1636 by Lagarde (Du Temple, 1961), who mentioned that there were mines of copper 80-100 leagues from the Huron. In 1640, Pierre Boucher noted that there was a "great island which is 50 leagues in circuit, in which there is a very beautiful mine of copper" (Du Temple, 1961). The "great island," Isle Royale, was known by the natives as "Minong." Local tribes ascribed divinity to the lake (Lake Superior), was noted by Jesuits, as providing them with fish for nourishing and 10-20 pound native copper under the water as signs of good fortune (Du Temple, 1961). By the 1660s, notations became more explicit and Lake Superior features began to appear on European maps (Early Historical Accounts of the Lake Superior Copper District, 1961).

Due to historic mining (Whittlesey, 1863), much of the Native American mines were destroyed, but evidence of ancient mining was not obliterated (Holmes, 1901). Drier (1961a) and Holmes (1901) suggests native inhabitants used fire, stone hammers, copper wedges, chisels, and gouges to mine veins that resulted in the removal of rock from shafts as deep as 50 feet and from trenches as long as 100 feet. So prevalent were stone tools in the area that a historic mining engineer estimated in 1871 that nearly 1,000 tons (200,000 to 300,000 hammerstones) existed in the Minong Mining area of Isle Royale (Drier 1961a). Holmes (1901) notes that they are constantly present and bruised and battered remnants literally fill mining debris. Drier (1961a, 1961b) classified the hammers as mauls, grooved (rare) and not grooved. Charles Whittlesey (1863) notes that worn wooden shovels, made from white cedar, were discovered by Dr. Blake at the Waterbury mine and a Mr. Hill at the Copper Falls location.

The Native American's methods of working the copper at Isle Royale were noted by William Henry Holmes (1901). Holmes (1901) remarks about the pitted and battered

surfaces, as well as the method of beating up the copper into ridges and points for easier removal. An in-situ work was noted by J.H. Lathrop (1961[1901]) as a 5,720-ton piece of native copper resting in a trench 30 feet below the surface. The large mass was discovered by prospector Albert Hughes in 1846 and described by Samuel Knapp of the Minnesota mine (Lathrop, 1961[1901]). The large mass was 18 feet below the surface and was discovered resting up five feet on billets and sleepers of oak, along with densely packed earth (Lathrop, 1961[1901]).

C.3.2 Native American Mining of Lead and Galena

The Native American mining of lead, and its natural occurrence of galena, was also known from an early time (Ball, 1941). The largest notation of this is in the Wisconsin-Iowa-Illinois lead district (Ball, 1941; Kuhm, 1951). The presence of galena was noted in prehistoric mounds of the upper Mississippi River Valley, which was attributed to the Great Spirit placing lead in the ground so that the Native American tribes could still exist (Ball, 1941). Colonel Smith and Mr. Moorehead purchased the Wisconsin-Iowa-Illinois lead district from Augustus Choutou in 1810 (Ball, 1941). Additional mines referenced by Ball (1941) include a 300-foot long trench, also 12 feet deep, in Kentucky that was sunk on a galena-barite vein. In addition there is mention of a New Mexico site in Cook's Peak, where an old stope, in galena-bearing rock, was observed along with stone tools (Ball, 1941). Ethnographic evidence is offered by the observation of Eskimos using galena pebbles to blacken skins (Ball, 1941).

Native Americans mined lead in the Devonian age Shawangunk sandstone north of Wurtsboro, Sullivan County, New York (Crawford, 1981; Eilertsen, 1950; Quinlan, 1873). Gerhamn and his sister Norachaneanon transferred ownership of the areas, part of

the Warwarsing Deed in 1684 (Crawford, 1981). Natives refused to show where they found lead, in the form of galena (Crawford, 1981), and a European-American hunter followed them to a location (Quinlan, 1873). The earliest development by white settlers was in 1820 (Crawford, 1981).

C.4 Model Building and its Application to Quarries

The anthropological, and more specifically archaeological, studies of mines and quarries all too often fail due to their lack of a sound foundation. Young et al. (1994) noticed the same problem with archaeological studies attempting to reconstruct the organization and dynamics of prehistoric societies, citing weak methods. In an attempt to clarify model building, Bonnichsen (1977) and Young et al. (1994) reintroduced Fleibeman's *Theory of Integrative Levels* along with seven proposals: (1) each level organizes the level(s) below, providing a cumulative upward; (2) complexity increases upwards; (3) higher levels depend on lower levels; (4) lower levels direct the higher; (5) for any level, its mechanism lies in the level below and its purpose lies in the level above; (6) disturbance introduced to any level reverberates at all levels; and (7) the higher the level, the smaller its population of instances. This dissertation is suggesting that prehistoric quarries be treated in a similar fashion; except that the various levels are represented with the integrated levels of geological understanding. In ascending order, the foundation of the quarry study should be rooted in tectonics, and the tectonic history of the terrain. Once the tectonic setting is understood, it should be overlain by a structural interpretation. The structural history, should be in turn, be overprinted by the detailed petrofabric analysis of the rocks, under investigation. At this juncture in the study, the tectonics, structure and petrofabric analyses should be integrated and cross-

checked so that they harmonize. Next, the stratigraphic history of the rocks should be determined, focusing on the stratigraphic nature of the ore target, in this case the chert beds. Overlying the stratigraphy is the bio-stratigraphy, sedimentology, and diagenesis of the sediments. The biostratigraphy, sedimentology, and diagenesis should also be integrated into a second harmonizing succession of interpretive understanding. Lastly, the geomorphological history should be elucidated in order to better understand the site formation processes ongoing at the quarry. From this research design, the archaeological research questions can be organized. This approach is necessary because the salient aspects of each quarry may vary considerably, and some quarries offer insight into only a few research questions. Therefore, before archaeology is to be performed, the entire quarry complex should be treated as a geological problem, not an archaeological one. Ultimately, this level of treatment focuses all research questions towards a low-range analysis, and the author feels that most fundamental quarry issues are of the low range type.

Binford (1978) advocated the middle-range theory approach to archaeology. Low-range theory addresses artifact(s) specific relationships (Young et al., 1994). Middle-range theory focuses on "understanding the organization and operational dynamics on past cultural systems" (Young et al., 1994). High-range theory draws on statements from middle-range theory to construct extra-societal questions (Young et al., 1994). The geological study presented in this dissertation provides, for the purpose of archaeological investigations, a much needed, low-range analysis of the Wallkill River Valley, Cambrian-Ordovician cherts to serve as a baseline for the identification of a fixed resource.

C.4.1 The Wallkill River Quarry Models

The earliest recorded manufacturing of chert in the dissertation study area is for the use of flint in gun manufacture; as noted in the letters of Colonel Henry Wisner, operator a gunpowder mill (1775-1776) in Phillipsburg, New York (Orange County) that contained a trip hammer for manufacturing gunflints (Burdge, 1918; Kinne, 1977; Wisner 1918). Additionally, a 1776 letter from Susquehanna Indians to Henry Wisner exists; the Susquehanna thank Wisner for powder and the Susquehanna indicate that they wish to trade for more powder and gunflints in the future (Kinne, 1977; Wisner, 1918). The source of the flint was European ship ballast off loaded at the harbor in Peekskill, NY and was brought over by land from the Hudson River (Kinne, 1977).

Based on geologic data collected for this dissertation (battered chert outcrops, modified glacial cobbles, and chert debris), two prehistoric quarry models were generated. The first model allows for the prediction of prehistoric chert quarries in the Cambrian-Ordovician cherts of the Wallkill River Valley. The second model is for the spatial behavioral activities at quarries in Cambrian-Ordovician chert in the Wallkill Valley, referred to as the "typical quarry plan."

A Model for the Prediction of Prehistoric Cambrian-Ordovician Chert Quarries in the Wallkill River Valley

The great number of chert quarries that occur in the Wallkill valley (LaPorta, 1994) result from the combination and overprinting of unique geological circumstances, which have been described in this dissertation. Sea-level curve data (Chapter 4), combined with facies relations (Chapter 4), stratigraphic (Chapters 3 and 4, Appendices A and B), and structural data (Chapter 5) combine to form a powerful predictive model for detecting quarries (LaPorta, 1996a, 2004; LaPorta et al., 2000). As the quarries were

discovered during field work conducted for this dissertation, they were divided into their respective formations, members, and individual chert horizons (Chapter 3 and Appendices A and B) occurring along stratigraphic strike. The quarries, upon structural analysis and interpretation, are also able to be placed into their structural settings such as those occurring within normal and reverse faulted sections, as well as in back thrusts, half synclines and syncline pairs (Chapter 5).

Development of the Wallkill River quarries is based upon eight factors (LaPorta, 2004; LaPorta et al., 2000):

1. the general inclination, or dip, of the beds into the subsurface (attitude),
2. the thickness of the surrounding limestone, dolomite, or shale beds,
3. the presence of well defined bedding planes,
4. the thickness of the chert beds, or pods, within the limestone or dolomite,
5. the proximity of two or more closely spaced chert beds,
6. the presence of stratigraphic, or structural, nuances which may serve to impede or terminate quarry activity,
7. the contact relations between the chert and associated dolomite or limestone (sharp or gradational contact),
8. the development of joint surfaces, particularly conjugate joints, and/or fracture cleavage,
9. the presence of a stable platform below the zone of extraction,
10. the availability of glacial till in the form of boulders of high-rank metamorphic rocks, preferably quartzites.

What follows is a hierarchy (LaPorta, 2004) of prehistoric chert quarries based on terms used in modern quarrying/mining operations (personal observation by the author in granite quarries of Bar Harbor, Maine). An aspect of mining or prospecting is referred to as an *expression*. Successful expressions evolve into *motions*. Successful motions expand into full-scale quarries *movements*, i.e. a successful repeated orchestration of rock from the earth. Expressions, motions, and movements located along *strike* within a series of geologically related formations are referred to as *trends*. Linear trends occurring within one outcrop belt are *slices* and structural *fensters* or windows contain *inliers* and *outliers*. Spatially clustered trends bound within a geological province are referred to as a *district*. Districts comprise a *metallogenic province*.

The arrangement of prehistoric quarries into these categories allows analysis of what role, if any, the various classes of macro-scale geological constraints play in determining the presence or absence of quarries. The model has served to elucidate the precise whereabouts of the greater than 800 prehistoric quarry complexes discovered to date as occurring within the Wallkill River Valley. On the New York recess (Chapters 2 and 5), the model can predict not just the geographic location of quarries on the landscape, but in what formation(s) the quarries can occur, in which facies the chert quarries can co-occur, the average rock attitude in which quarries can occur (a corollary allows determination of which attitudes support certain types of quarry architecture, if any at all), and the degree to which quarries can develop (expression, motion, movement). In many cases, the model will predict even the chert facies, the overall tenor of the ore, and even what types of products are produced at the various quarries.

Ultimately, the geographic distribution of the vast array of quarries serves to define the boundaries of a prehistoric chert quarry province, constrained by large-scale structural lineaments (Table 1). This province includes several quarry districts defined by thrust blocks, trends, fold slices, and zones of inliers and outliers. All of these discrete quarry subdivisions comprise a vast province of Native American chert quarries (Table 1), superimposed on what has been identified as the Franklin-Ogdensburg Metallogenic District (Sohl and LaPorta, 2002) (Figure C.1).

Fm/Mbr	**Structural Feature**	**Attitude**	**Wallkill Valley Placement**	**Regression / Transgression**	**Chert Type**	**Quarry Types**
Cl_{1-3}	NF	0-14%	east	Regression	SR, WR, PS	EXP, MOT, MVT
Ca_1	F	4-17%	central-east	Transgression/ Regression	SR, WR, PS	EXP, MOT, MVT
Ca_2	F ∏ R	21-45%	central-west	Transgression	VF	EXP
Or_1	LR	21-45%	central-west	Transgression	VF	EXP
Or_2	MR	21-45%	central-west	Transgression	SR	EXP, MOT
Or_3	MR	21-45%	central-west	Transgression/ Regression	SR, WR	EXP, MOT, MVT
Oe_1	UR	21-45%	central-west	Transgression	SR, WR	EXP
Oe_2	UR	21-45%	central-west	Regression	SR, WR, PS	EXP, MOT, MVT
Oe_3	UR	21-45%	central-west	Transgression/ Regression	SR	EXP
Oo_1	UR	24-60%	west	Regression	SR, WR, PS	EXP, MOT, MVT
Oo_2	UR	24-60%	far west	Regression	SR, WR, PS	EXP, MOT, MVT

STRUCTURAL FEATURES: NF=normal fault; F=flat; R=ramp; LR=lower ramp; MR=mid ramp; UP=upper ramp
CHERT TYPES: WR=wholesale replacement; VF=void filling; SR=selective replacement; PS=pressure solution
QUARRY TYPES: EXP=expression; MOT=motion; MVT=movement

Table 1. Prehistoric quarry predictive model for Cambrian-Ordovician cherts in the Wallkill River Valley.

A Typical Prehistoric Chert Quarry in the Wallkill River Valley

The validity of the quarry hierarchy presented above rests in the ability to not only identify prehistoric quarries, but to identify activities in prehistoric quarries as a means of distinguishing between different types of quarries (expression, motion, and movement). Building on this, criteria presented in the previous model will dictate the activities that directly and indirectly occur/co-occur with quarrying.

The nature of the extraction process can now be explored with a focus towards understanding how the extraction technology was organized, and how it varied within and between different geological settings. The fine-scale of quarry anatomy is revealed, along with the associated assemblages of quarry instruments (Figures C.2 and C.3). The instruments were mapped in the field, and arranged into morphological types; which was in turn followed by the analysis of their petrological and mechanical attributes. The results suggest that the quarry worker possessed an empirical understanding of the physical properties of the rock type selected for each aspect of the extraction process, and that specific petrological rock types were chosen for certain tasks. Furthermore, that the petrology, and associated mechanical attributes of the rock, could be contoured or shaped to meet specific or changing needs at the quarry. Therefore a quarry-tool assemblage may illustrate some degree of correlation between petrological groupings and morphological types. Also, these distinctive types and forms should be repeatedly associated with similar parts of the quarry anatomy, for example the zone of extraction. The zone of extraction bears a great concentration of large metaconglomerate boulders, which have similar flake-scar patterns. Spatially, they are found in close proximity to the locations where chert is extracted from the outcrops. The objects possess similar

petrological, as well as morphological, characteristics. The spatial distribution of the instruments (Figure C.4) often outlines the chain of operation, or sequencing of mining events (Figures C.5-C.7). Therefore, the precise instrument mapping, and associated petrological and morphological analyses, suggests the presence of an ordered subdivision of quarry extraction and refinement tasks. What serves to mask the orderliness of the chain of operation is 1) the often times premature rupture of quarry tools, usually along joints or relict bedding planes, 2) the fact that many objects are re-shaped and re-sharpened to a point dysfunction, and eventual discard, and finally, 3) the objects which break are often re-cycled into utilizable quarry tools for application at other zones of the quarry.

The original model for chert extraction is a three component model. The components include an area where chert is extracted, followed by an area where the chert is freed up from the matrix, and finally a location where the chert is manufactured into objects. However, the geological baseline investigations launched in the Wallkill valley amassed enough data to forward a generalized four-step model which includes an intermediate step known as beneficiation. This intermediate step may include as many as two additional phases of lithic refinement. Ultimately, a four part general model (Figure C.3) applied to task subdivision in quarries is introduced along with several derivative types (LaPorta, 1996a, 2004; LaPorta et al, 2000). The model includes a zone of extraction (Zone I), a zone of ore milling (Zone II), a zone of ore processing (Zone III), and a zone of ore refinement (Zone IV). Accentuated joints (Figures C.6 and C.7), battered surfaces (Figure C.8), plug-and-feather surfaces (Figure C.9), and conchoidal scars (Figure C.10) characterize a zone of extraction (Zone I). A stable platform directly

below the zone of extraction (Figure C.11) is necessary for the development of the quarry. Frequently, milling (Zone II) and beneficiation (Zone III) are performed below the zone of extraction (Zone I), and are thus frequently observed as artifacts in scree (Figures C.12 and C.13). The area of beneficiation occurs between zones II and III, and may represent one or two more discrete zones of lithic refinement. Refinement (Zone IV) occurs above extraction (Zone I), milling (Zone II), and beneficiation (Zone III). A smaller class of chert debris (Figure C.14) and smaller instruments (Figure C.14) characterizes the zones of refinement.

Certainly, if the quarry extraction technology were organized, then it would stand to reason that the mine tailings must reflect this very organized production sequence. Therefore, this appendix adds yet another critical dimension to the general quarry model, by associating discrete classes of excavated mine tailings, with the quarry tools that produced them. Occurring with the quarry instruments are great quantities of chert tailings (Figures C.12 and C-14), the by-product of lithic manufacture, which preserve much of the internal fabric of the rock. These objects, once sequenced together with the quarry tools, represent an elaborate chain of operation towards the production of finished stone tools.

The various zones of the quarry are each associated with characteristic macro-scale, meso-scale, as well as micro-scale scarification which serves as testimony to the type of extraction ongoing at that particular part of the quarry. The zone of extraction reveals accentuated joints, as well as impact scars illustrating horizontal trajectories of impact objects. At many locations, the trace of the impact marks follows a sealed joint surface, and serves to score the surface. In places, plug-and-feather joints mark chert

blocks which are being pried apart. Many of the chert surfaces in this zone are also burned. At locations where technology fails, the chert surface takes on a castellated outline which often matches the circumference of the impactor. The castellations, which serve as part of the architecture of the quarry, index the termination of the episode of extraction. The base of the stable platform below the zone of extraction is covered with ore blocks, as well as dislodged blocks of carbonate country rock. The milling stations include fragments of impactors and failed anvils; however, the diagnostic milling tool is an elongate rectangular sandstone, or orthoquartzite, with high-clay content. The milling areas are associated with small wedges which can be fashioned from quartzite, however softer rock types do occur. The petrology of this group of tools is arkosic in large part, but also includes more elastic hammers as well. The lower and upper edges of the elongate hammers are usually battered. The rubble and backfill of the mill is composed of irregular masses of failed ore blocks, large masses of tailings, lean ore, as well as exhausted instruments (especially wedges) which occur in great numbers at this zone. Occasionally, blocks of dressed ore are also found in the backfill. The ore processing stations contain a variety of smaller, highly elastic hammers; many of which are circular in outline and flattened in cross section. Large anvils of metaquartzite are present at this zone of the quarry. The backfill piles contain a great variety of equant rhombic, or rectangular fragments of chert which is now free of matrix rock. Close inspection shows that the edges of the blocks are often rubbed, crushed, or even flaked. Occasionally, caches of rhombic blocks of chert are discovered at these locations. A very small class of chisels accompanies this zone (many only the size of a marble) which contains completely battered surfaces. The workshops, or zones of ore refinement, often occur

above the quarry face and are indexed by the presence of non-portable anvils. The anvils are usually fashioned from metaconglomerates which are free of internal flaws. In many cases the anvils, as well as the impactors, are similar in outline prior to repeated use and recycling. Generally, the anvils are surrounded and covered by an apron of flake debris, failed bifaces, and cores. The hammerstones are small, circular, highly elastic metaquartzites, orthoquartzites, and occasionally softer rock types such as sandstone.

The twenty-four to thirty-six steps elucidated in the chain of operation illustrate how the petrofabric constraints of the chert were managed by artisans in order to design stone tools from this highly tectonized rock. The analysis is complimented by a number of controlled replication studies. This chain of operation connects the mine tailings excavated from the quarries to various petrological and morphological classes of instruments, and finally to the four zones of task subdivision, and the overall quarry architecture.

Cursory examination of considerable quantities of diagnostic stone tools fashioned from Cambrian-Ordovician cherts revealed that subtle aspects of the petrofabric character of the chert were still visible within end products, fashioned from quarry sources. Therefore, what role if any, does petrofabric play in setting constraints for the manufacture of stone tools? Can the fine-scale geological constraints be measured as existing within the stone tool forms, and do they aid in defining templates for stone tool construction? How do the measurable aspects of the fabric such as fracture cleavage, and pressure solution fabric, aid in determining the types of half product produced at quarries?

C.4.2 Testing the Models: Archaeological and Ethnographic work in New York and India

Success of a model is in prediction. Paradoxically, models by their very nature must be redefined when new datasets are encountered. The author conducted archaeological fieldwork in New York (LaPorta et al., 2000) and India (LaPorta, 2004) to assess the validity of the model outside the Wallkill River Valley.

The predictive quarry model, and the associated hierarchical classification, was field tested by applying it to coeval Cambrian-Ordovician, chert-bearing strata cropping out within the Quebec salient (LaPorta et al., 2000). The study area is in Washington County, New York, east of the Champlain Canal. Geological and archaeological field surveys identified prehistoric quarries in five different bedrock units along different trends. Gentle inclination of the beds produced high numbers of expressions, whereas the more steeply dipping beds produced larger motions and movements. Investigations are currently in the process of advanced investigations at specific quarries with the study area.

Ethnographic analogies are important when addressing the past, since little exists as a proxy. These analogies provide tentative explanations for material relationships found in the archaeological record (Gibbon, 1984). For this, the workings of modern open-cast limestone quarries were observed by this author in Tallicoot, southern India (LaPorta, 2004). Similarities were found in the layout of the modern day quarries, in the types of hand operated tools used to extract the rock from the quarry and as such, interpretations can be made in how behavior in modern-day, hand operated quarries might be similar to prehistoric behavior, from extraction, to maintenance, to re-use.

Discussion: The Potential for Provenance Application on Archaeological Artifacts

The author contends that a sample of archaeological objects is analyzed for the purpose testing the usefulness of the provenance application. The results suggest that the database of physical and chemical characteristics is indeed very useful in determining the source quarries for this group of cherts.

A fine scale atlas, including SEM, diagenetic, stratigraphic and structural data permits the development of a unique provenance tool developed for archaeological investigations. The regional structural controls described in Chapter 2 elucidate a Native American mining, or "folk geology" (James Moore, personal communication, 1988), concept (LaPorta, 1993, 1996b). The analysis incorporates the results of the entire research design, which is referred to as the design pyramid in order to analyze and provenance stone tools from archaeological sites back to precise quarry sources. This includes a broad foundation of field and outcrop measurements, slab and thin section data, SEM and EDAX data, as well as X-Ray fluorescence data. The analysis of recovered artifacts may then be plotted spatially in order to discern patterns of raw material distribution emanating from quarry districts.

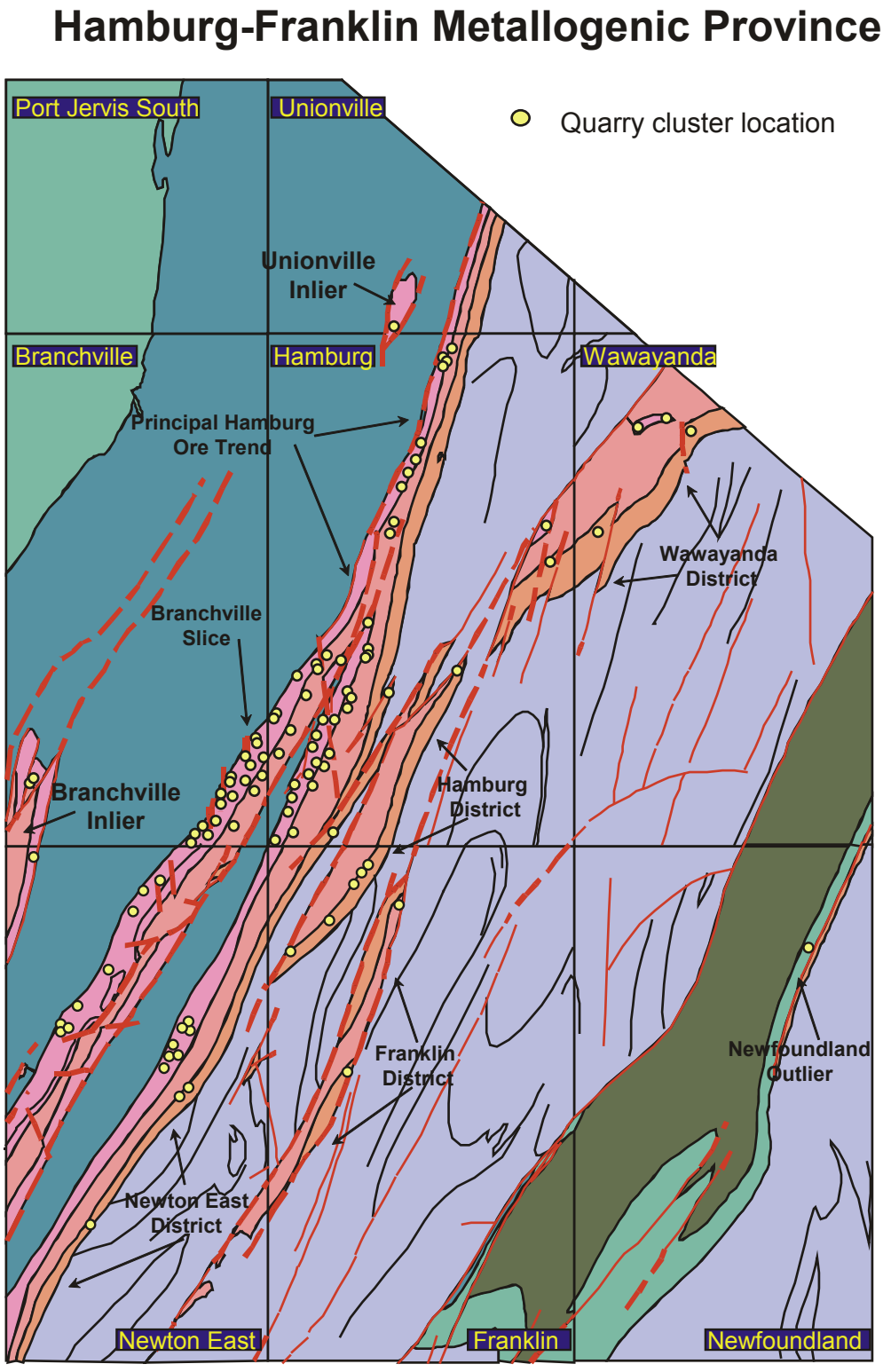


Figure C.1: Hamburg-Franklin Metallogenic Province with districts, outliers, and quarry clusters (yellow circles with black borders).

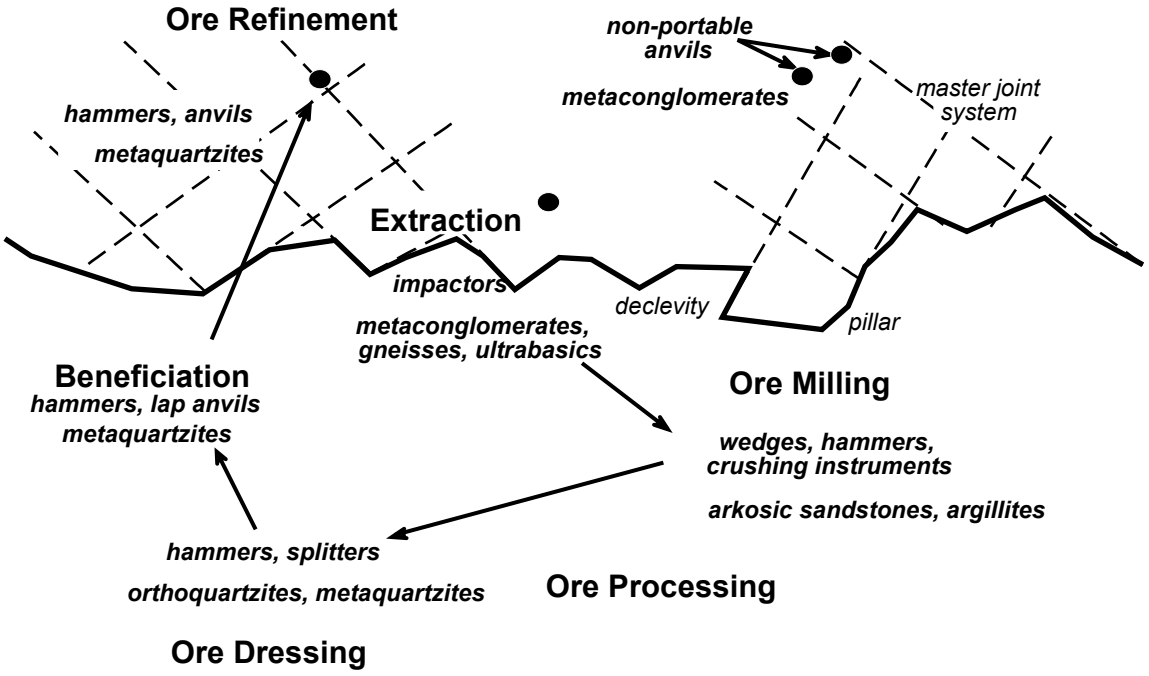


Figure C.2: Schematic 2-D view of the typical quarry plan (LaPorta, 2004), as elucidated from the Walkill River Valley study, depicting associated mining instruments and their petrologies.

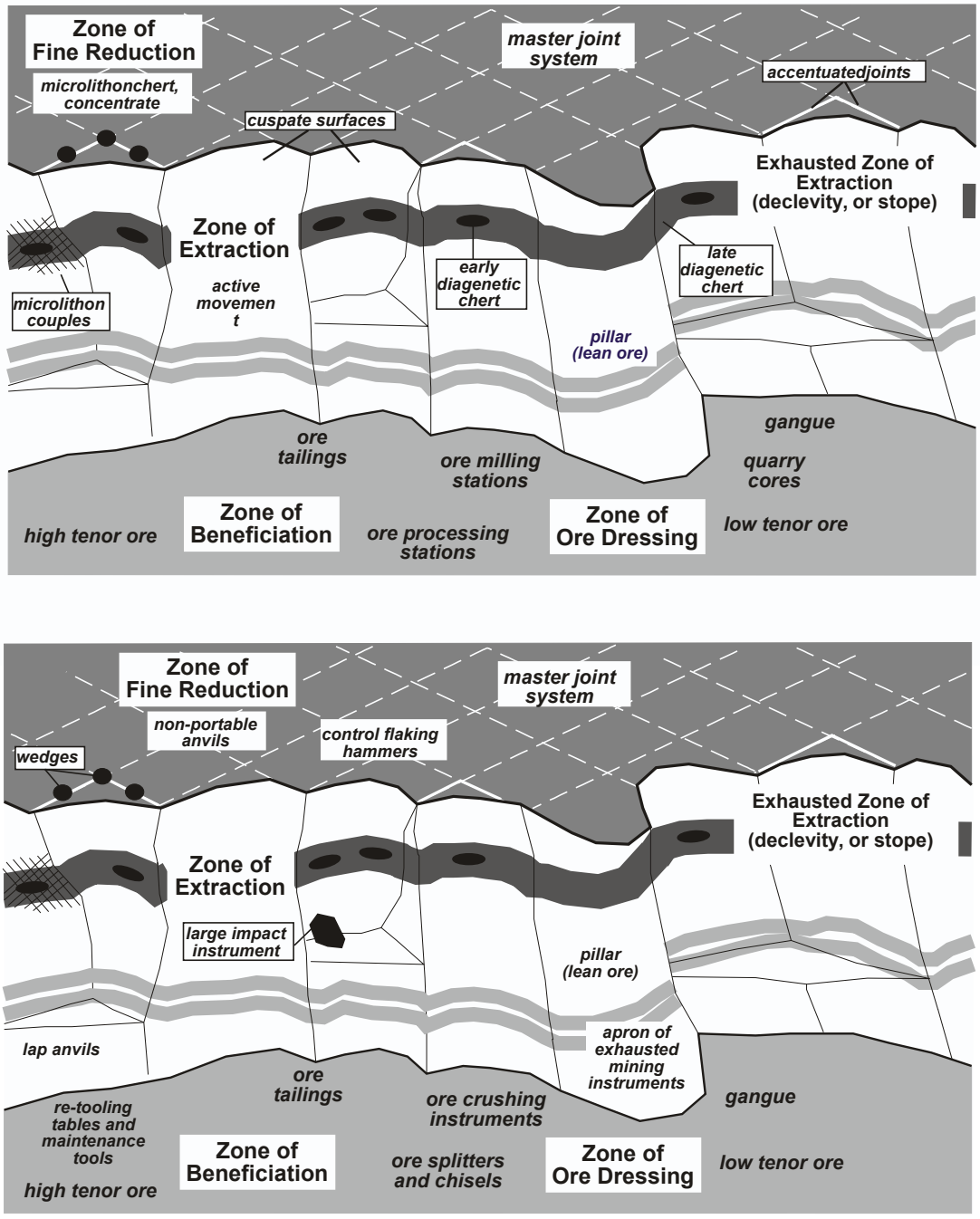


Figure C.3: Schematic view of the typical quarry plan, as elucidated from the Walkill River Valley study . Plan A depicts the labor subdivisions, while plan B includes the associated mining instruments.



Figure C.4: Cache of hammerstones at the Beaver Run Standard Section.



Figure C.5: Spalled hammerstone in a prehistoric quarry trench at the Beaver Run Standard Section.



Figure C.6: Instrument in an accentuated joint, zone of extraction (Zone I), Harmonyvale Member chert, Harmonyvale Section.

Figure C.7: Small instrument lodged in an accentuated joint, zone of extraction (Zone I), Harmonyvale Member, Harmonyvale Section.





Figure C.8: Heavy surface battering and plug-and-feather (by finger) on Beaver Run Member chert, Harmonyvale Section.

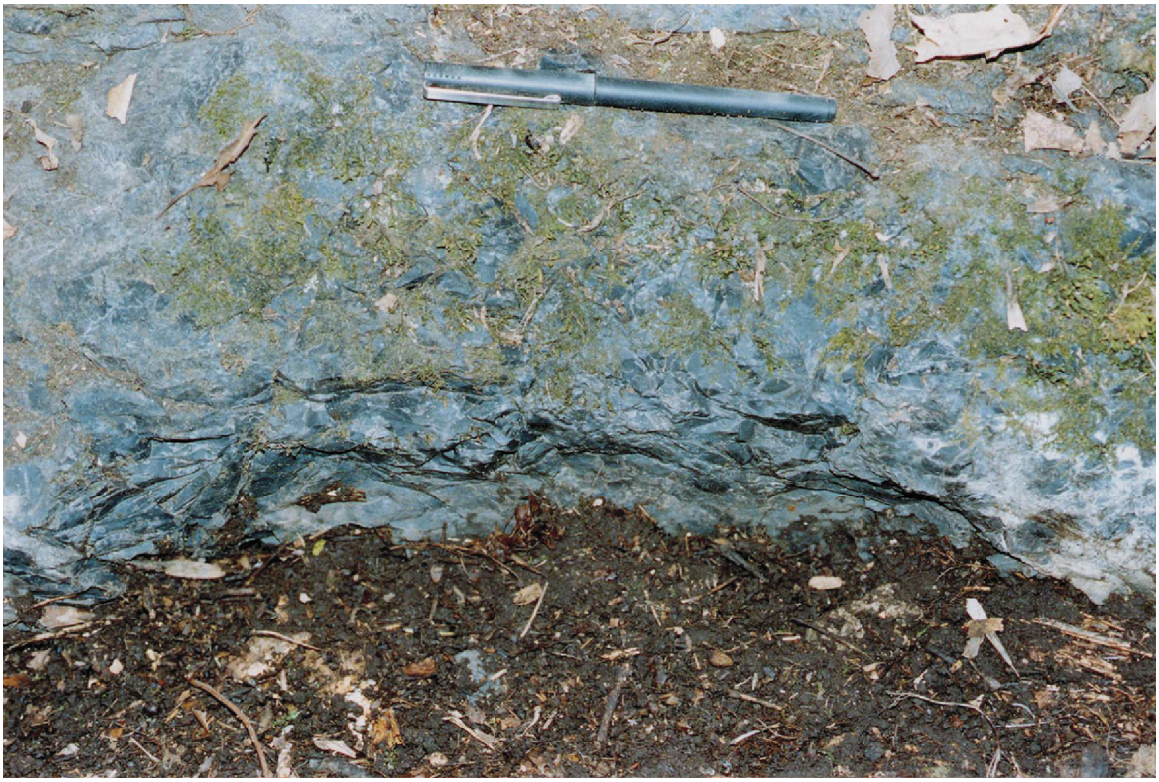


Figure C.9: Cuspate and castellated surface, Harmonyvale Member, Beaver Run Standard Section.



Figure C.10: Concoidal scars on weathered surface of Big Springs Member chert, Harmonyvale Section.



Figure C.11: Stable platform directly in front of a Zone of Extraction, Harmonyvale Member chert, Beaver Run Standard Section.



Figure C.12: Scree of Beaver Run Member chert middling blocks, Harmonyvale Section.

Figure C.13: Middling debris and three conglomerate instruments, Beaver Run Section.





Figure C.14: Chert debris, flakes, and small instruments; Harmonyvale Member chert, Harmonyvale Section.

REFERENCES CITED

Agricola, G., 1950[1556], De Re Metallica: Dover Books, New York. Translated by Herbert C. Hoover and Lou H. Hoover.

Ball, S.H., 1941, The Mining of Gems and Ornamental Stones by American Indians. Anthropological Papers, No. 13. Smithsonina Institution, Bureau of American Ethnology. Washington, D.C.: Government Printing Office.

Barber, M., Field, D., and Topping, P., 1999, The Neolithic Flint Mines of England, English Heritage, Swindon.

Barth, F., 1969, Introduction, *in* Barth, F., ed., Ethnic Groups and Boundaries: Little Brown and Company, Boston, p. 9-39.

Bell, P., 1998, The fabric and structure of Australian mining settlements, *in* Knapp, A., Bernard, P., Vincent C., and Herbert, E.W., eds, Social Approaches to an Industrial Past: The Archaeology and Anthropology of Mining: Routledge, New York, p. 27-38.

Bement, L., 1999, Bison Hunting at the Cooper Site: Where Lightning Bolts drew Thundering Herds: University of Oklahoma Press, Norman.

Binford, L., 1978, Dimensional analysis of behavior and site structure: Learning from an Eskimo hunting stand: American Antiquity, v. 43, p. 330-361.

Bonnichsen, R., 1977, Models for Deriving Cultural Information from Stone Tools: National Museum of Man, Mercury Series, Archaeological Survey of Canada, Paper No. 60.

Brumbach, H., and Weinstein, J., 1999, Material selection, rejection, and failure at Flint Mine Hill: an eastern New York State chert quarry: Northeast Anthropology, v. 58, p. 1-25.

Burdge, F., 1918, A memorial of Henry Wisner, the only New Yorker who voted for the Declaration of Independence, *in* Wisner, G., The Wisners of America: Published Privately, Baltimore, p. 32-40.

Burton, J., 1984, Quarrying in tribal society: World Archaeology, v.16, no. 2, p.234-247.

Cashdan, E., 1983, Territoriality among human foragers: Ecological models and applications to four Bushman groups: Current Anthropology, v. 24, p. 47-66.

Childs, S., 1998, 'Find the ekijunjumira:' Iron mine discovery, ownership and power among the Toro, *in* Knapp, A. Bernard, P., Vincent C., and Herbert, E.W., eds, Social Approaches to an Industrial Past: The Archaeology and Anthropology of Mining: Routledge, New York, p. 123-137.

Clark, G., 1989, Traffic in stone axe and adze blades, *in* Clark, Grahame, ed., Economic Prehistory: Papers on Archaeology by Grahame Clark: Cambridge University Press, Cambridge, p. 169-198.

Crawford, M., 1981, Geology and Lead-Zinc Mineralization of the Sandstone-Hosted Shawangunk Mine, New York, as Compared to Other Lead-Zinc Sandstone Deposits. M.A. Thesis submitted to University of Toronto, Toronto, Canada, 184 p.

Douglass, W., 1998, The mining camp as community, *in* Knapp, A., Pigott, V., and Herbert, E. W., eds, Social Approaches to an Industrial Past: The Archaeology and Anthropology of Mining: Routledge, New York, p. 97-108.

Drier, R., 1961a, Michigan's most ancient history is America's prehistoric copper mine, *in* Drier, R.W., and Du Templ, O.J., eds., Prehistoric Copper Mining in the Lake Superior Region: Published privately by the editors, p. 19-25.

___ 1961b, Pre-Historic mining in the copper country, *in* Drier, R.W., and Du Templ, O.J., eds., Prehistoric Copper Mining in the Lake Superior Region: Published privately by the editors, p. 27-31.

Du Temple, O.J., 1961, First account of copper country published in France in the year 1636, , *in* Drier, R.W., and Du Templ, O.J., eds., Prehistoric Copper Mining in the Lake Superior Region, Published privately by the editors, 37 p.

Early, A., 1993, Hardman and Coddoan salt making, *in* Early, A.M., ed., Caddoan Saltmakers in the Ouachita Valley: The Hardman Site: Arkansas Archaeological Survey Research Series No. 43. Fayetteville: Arkansas Archaeological Survey, p.223-234.

Eilertsen, N.A., 1950, Investigation of Shawangunk Mine Zinc-Lead Deposit, Near Summitville, Sullivan County, New York: United States Department of the Interior, Bureau of Mines, Report of Investigations 4675, 41 p.

Emmons, W., 1922, General Economic Geology: McGraw-Hill, New York, 516 p.

Ericson, J., 1984, Toward the analysis of lithic production systems, *in* Ericson, J.E., and Purdy, B.A., eds., Prehistoric Quarries and Lithic Production: Cambridge University Press, Cambridge, pp.1-9.

Flawn, P., 1966, Mineral Resources: Rand McNally & Co., New York, 406 p.

Garvan, J., 1941, The Manóbos of Mindanáo, Memoirs of the National Academy of Sciences, Volume 23, First Memoir: Government Printing Office, Washington, D.C.

Gibbon, G., 1984, Anthropological archaeology: Columbia University Press, New York.

Godoy, R., 1985, Mining: anthropological perspectives: Annual Review of Anthropology v. 14, p. 199-217.

Hampton, O., 1999, Culture of Stone: Sacred and Profane Uses of Stone among the Denali: Texas A&M University Press, College Station.

Early Historical Accounts of the Lake Superior Copper District, 1961. Lake Superior Copper and the Indians: Miscellaneous Studies of Great Lakes Prehistory, *in* Griffin, J., ed., Anthropological Papers No.17, Museum of Anthropology: University of Michigan, Ann Arbor, p. 32-45.

Holmes, W., 1901, Aboriginal copper mines of Isle Royale, Lake Superior: American Anthropologist, v. 3, p. 684-696.

___ 1919, Handbook of Aboriginal Antiquities: Smithsonian Institution, Bureau of Ethnology, Bulletin No. 60, Washington, Government Printing Office.

Hoover, H., 1909, Principles of Mining: Valuation, Organization, and Administration: McGraw-Hill, New York, 199 p.

Howitt, A., 1904, The Native Tribes of South-East Australia: MacMillan and Co., New York.

Ingbar, E., 1994, Lithic material selection and technological organization, *in* Card, P.J., ed., The Organization of North American Prehistoric Chipped Stone Tool Technologies: International Monographs in Prehistory, Archaeological Series 7, Ann Arbor, Michigan, p. 45-56.

Jelinek, A., 1991, Observations on Reduction Patterns and Raw Materials in Some Middle Paleolithic Industries in the Perigord, *in* Montet-White, A., and Holen, S., eds., Raw Material Economies Among Prehistoric Hunter-Gatherers: University of Kansas Publications in Anthropology, v. 19. Lawrence, Kansas, p.7-32.

Johnson, J., 1984, Measuring Prehistoric Quarry Site Activity in Northern Mississippi, *in* Butler, B.M., and May, E.E., Prehistoric Chert Exploitation: Studies from the Midcontinent: Center for Archaeological Investigations, Occasional Paper 2. Carbondale: Southern Illinois University, p. 225-235.

Jones, R., and White, N.,1988, Point blank: Stone tool manufacture at the Ngilipitji Quarry, Arnhem Land, 1981, *in* Meehan, B., and Jones, R., eds., Archaeology with Ethnography: An Australian Perspective, Canberra: Department of Prehistory, Research School of Pacific Studies, Australian National University, p.51-87.

Jury, W., 1949, Report on Prehistoric Flint Workshops at Port Franks, Ontario. Museum Bulletin No. 8, Museum of Indian Archaeology, The University of Western Ontario. London, Ontario: Museum of Indian Archaeology.

Kelly, J., 1984, Late Bluff Chert Utilization on the Mettell Tract, Cahokia, *in* Butler, B.M., and May, E.E., Prehistoric Chert Exploitation: Studies from the Midcontinent: Center for Archaeological Investigations, Occasional Paper 2. Carbondale: Southern Illinois University, p. 23-44.

Kinne, E., 1977, Bloomingburg grist mill, long a landmark, razed, *in* Jonas, H.J., ed, The 1825 Census of the Wallkill Precinct and Old Mills: The Historical Society of Middletown and the Wallkill Precinct, Middletown: Prior King Press, p. 36-39.

Knapp, A., 1998, Social approaches to the archaeology and anthropology of mining, *in* Knapp, A. B., Pigott, V.C., and Herbert, E.W., eds, Social Approaches to an Industrial Past: The Archaeology and Anthropology of Mining: Routledge, New York, p.1-23.

Knapp, A., Pigott, V., and Herbert, E.,1998, Social Approaches to an Industrial Past: The Archaeology and Anthropology of Mining: Routledge, New York.

Kuhm, H.W., 1951, The mining and use of lead by the Wisconsin Indians. The Wisconisn Archaeologist, v. 32, p. 25-38.

Lathrop, J., 1961 [1901], Prehistoric mines of Lake Superior, *in* Drier, R.W., and Du Templ, O. J., eds., Prehistoric Copper Mining in the Lake Superior Region: Published privately by the editors, pp.119-126. Originally in *The American Antiquarian and Oriental Journal*, vol. 23.

LaPorta, P., 1993, The application of cognitive models for lithic resource exploitation: Folk geology within the Wallkill River Valley [abs.]: New York State Archaeological Association, Annual Meeting Program and Abstracts, p. 11.

___1994, Lithostratigraphic models and the geographic distribution of prehistoric chert quarries within the Cambro-Ordovician lithologies of the Great Valley Sequence, Sussex County, New Jersey, *in* Bergman, C.A. and Doershuk, J.F., eds., Recent Research into the Prehistory of the Delaware Valley, Journal of Middle Atlantic Archaeology, v. 10, p. 47-66.

___ 1996a, Lithostratigraphy as a predictive tool for prehistoric quarry investigations: Examples from the Dutchess Quarry Site, Orange County, New York, in Lindner, C., ed., A Golden Chronograph for Robert E. Funk: Occasional Papers in Northeastern Anthropology No. 15: Bethlehem, Connecticut, Archaeological Services, p. 73-84.

____1996b, The quarry is a place [abs.]: Presented at the First Appalachian Integrated Highland Conference, Albany, New York.

___ 2004, A geological model for the development of bedrock quarries, with an ethnoarchaeological perspective, in Topping, P., and Lynott, M., eds., The Cultural Landscape of Prehistoric Mines: Oxbow Books, U.K., p. 123-139.

LaPorta, P., Brewer, M., and Sohl, L., 2000, Phase 1B Cultural Resources Survey-Supplement, Characterization of Prehistoric Quarry Development, Smiths Basin Mine Site, Washington County, New York, OPRHP Review No. 96PRO303: Submitted to Spectra Environmental Group Inc., Latham, New York.

Lass, B., 1994, Hawaiian Adze Production and Distribution, Institute of Archaeology, Monograph 37: Institute of Archaeology, University of California, at Los Angeles.

Lawrence, S., 1998, Gender and community structure on Australian colonial gold fields, *in* Knapp, A., Pigott, V., and Herbert, E., eds., Social Approaches to an Industrial Past: The Archaeology and Anthropology of Mining: Routledge, New York, p. 39-58.

Mitchum, B., 1991, Lithic Artifacts from Cerros, Belize: Production, Consumption, and Trade, *in* Hester, Thomas R., and Shafer, Harry J., eds., Maya Stone Tools: Selected Papers from the Maya Lithic Conference: Monographs in World Archaeology No. 1., Prehistory Press, Madison, Wisconsin, p. 45-54.

Morris, E., 1928, An Aboriginal Salt Mine at Camp Verde, Arizona, Anthropological Papers of the Museum of American History, v. 30, part 3: The American Museum of Natural History, New York.

Murrell, J., 2007, Differentiating Persistence of Variation in Prehistoric Milling Tools from the Middle Rio Puerco Valley, New Mexico, BAR International Series 1594: Archaeopress, Oxford.

Odell, G., 1984, Chert Resource Availability in the Lower Illinois Valley: A Transect Sample, *in* Butler, B.M., and May, E.E., eds., Prehistoric Chert Exploitation: Studies from the Midcontinent: Center for Archaeological Investigations, Occasional Paper 2: Southern Illinois University, Carbondale, p. 45-67.

Osborn, H., 1907, Field-Book and Guide in the Search for and the Easy Determination of Ores and Other Useful Minerals: Henry Carey Baird & Co. 7th Edition, Philadelphia, 355 p.

Parker, A., 1925, The great Algonkin flint mines at Coxsackie, Researches and Transactions of the New York State Archaeological Society: Lewis H. Morgan Chapter, Vol. LV, No.4.

Paul, W., 1970 Mining Lore, Portland, Oregon: Morris Printing.

Peele, R., 1941 Mining Engineers' Handbook, New York: John Wiley & Sons.

Perttula, T., 1984, Patterns of Prehistoric Lithic Raw Material Utilization in the Caddoan Area: The Western Gulf Coastal Plain, *in* Butler, B.M., and May, E.E., eds., Prehistoric Chert Exploitation: Studies from the Midcontinent: Center for Archaeological Investigations, Occasional Paper 2, Southern Illinois University, Carbondale, p. 129-148.

Peters, W., 1978, Exploration and Mining Geology: John Wiley & Sons, New York, 696 p.

Pétrequin, P., and Pétrequin, A., 1993, From polished stone tool to sacred axe: The axes of the Danis of Irian Jaya, Indonesia, *in* Barthelet, A., and Chavaillon, J., eds., The Use of Tools by Human and Non-Human Primates: Oxford University Press, Oxford, P. 360-377.

Pogue, J., 1973[1915], Turquoise, Memoirs of the National Academy of Sciences, v. XII, part II, Glorietta, New Mexico: The Rio Grande Press.

Prescott, J.R.V., 1965, The Geography of Frontiers and Boundaries, Chicago: Aldine Publishing.

Pryor, E. J., 1965, Mineral Processing, 3rd edition: Elsevier, New York, 844 p.

Quinlan, J.E., 1873, The History of Sullivan County, New York: G.M. Beebe & W.T. Morgan, New York.

Richards, R., and Locke, C., 1940, Textbook of Ore Dressing, 3rd edition: McGraw-Hill, 608 p.

Roemer, E., 1991, A Late Classic Workshop at Colha, Belize, *in* Hester, T., and Shafer, H., eds., Maya Stone Tools: Selected Papers from the Maya Lithic Conference, Monographs in World Archaeology No. 1: Prehistory Press, Madison, p. 55-66.

Rule, J., 1998, A risky business: death, injury, and religion in Cornish mining c. 1780 1870, *in* Knapp, A., Pigott, V., and Herbert, E., eds, Social Approaches to an Industrial Past: The Archaeology and Anthropology of Mining: Routledge, New York, p.155-173.

Rusco, M., and Raven, S., 1992, Background Study for Consultation with Native Americans on Proposed Mining Development with the Traditional *Tosawihi* ('White Knife') Quarry North of Battle Mountain, Nevada in the traditional Land of the *Tosawihi*, Eastern Shoshone Nation: Prepared by Archaeological Research Services, Inc., Virginia City, Nevada, 52 p.

Schneider, J., and Altschul, J., 2000, Of Stone and Spirits: Pursuing the Past of Antelope Hill, Statistical Research Technical Series 76, Tucson: Statistical Research, Inc.

Shaw, I., 1994, Pharaonic quarrying and mining: Settlement and procurement in Egypt's marginal regions: Antiquity, v. 68, p. 108-119.

Shinn, C., 1956[1884], Mining Camps: A Study in American Frontier Government, New York: Harper and Row.

Sohl, L., and LaPorta, P., 2002, The prehistoric quarry landscape in contemporary mine settings [abs.]: Society for American Archaeology, Annual Meeting Abstracts, v. 67, p. 271.

Spencer, B., and Spencer, F.,1899, The Native Tribes of Central Australia. New York: MacMillan and Co.

Stoltman, J., Behm, J., and Palmer, H., 1984, The Bass Site: A Hardin Quarry/Workshop in Southern Wisconsin, *in* Butler, B.M., and May, E.E., eds., Prehistoric Chert Exploitation: Studies from the Midcontinent, Center for Archaeological Investigations, Occasional Paper 2: Southern Illinois University, Carbondale, p.197-224.

Taggart, A., 1927, Handbook of Ore Dressing, New York: John Wiley & Sons, 1679 p.

Temple, J., 1972 Mining: An international History, Praeger Publishers, New York.

Topping, P., 1997, Structured deposition, symbolism and the English flint mines, in Schild, R., and Sulgostowska, Z., eds., Man and Flint: Proceedings of the VIIth International Flint Symposium: Institute of Archaeology and Ethnology, Polish Academy of Sciences, Warszawa, p.127-132.

Torrence, R., 1984, Monopoly or direct access? Industrial organization at the Melos obsidian quarries, in Ericson, J.E., and Purdy, B.A., eds., Prehistoric Quarries and Lithic Production: Cambridge University Press, Cambridge, p.49-64.

___ 1986, Production and exchange in Stone Tools: Prehistoric Obsidian in the Aegean: Cambridge University Press, Cambridge.

Von Bernewitz, M., 1931 Handbook for Prospectors: McGraw-Hill, New York, 359 p.

Whittlesey, C., 1863, Ancient Mining on the Shores of Lake Superior, Smithsonian Contribution to Knowledge, No. 155: D. Appleton & Co., New York.

Winchell, N., 1884, The Geology of Minnesota, Volume I of the Final Report: Johnson, Smith, and Harrison, Minneapolis.

Winters, H., 1984, The Significance of Chert Procurement and Exchange in the Middle Woodland Traditions of the Illinois Area, *in* Butler, B.M., and May, E.E., eds., Prehistoric Chert Exploitation: Studies from the Midcontinent, Center for Archaeological Investigations, Occasional Paper 2: Southern Illinois University, Carbondale, p. 3-21.

Wisner, G., 1918, The Wisners of America: Published Privately, Baltimore.

Young, D.E., Bonnichsen, R., Douglas, D., McMahon, J., and Swartz, L., 1994, Low range theory and lithic technology: Exploring the cognitive approach, *in* Bonnichsen, R., and Steele, D.G., eds., Method and Theory for Investigating the Peopling of the Americas: Oregon State University Press, Corvallis, p. 209-238.

LITHOSTRATIGRAPHIC MODELS AND THE GEOGRAPHIC DISTRIBUTION OF PREHISTORIC CHERT QUARRIES WITHIN THE CAMBRO-ORDOVICIAN LITHOLOGIES OF THE GREAT VALLEY SEQUENCE, SUSSEX COUNTY, NEW JERSEY.

PHILLIP LaPORTA
DEPARTMENT OF GEOLOGY AND GEOGRAPHY
HUNTER COLLEGE OF THE CITY UNIVERSITY OF NEW YORK

ABSTRACT

Nodular chert occurs within all 13 members of the Cambro-Ordovician Kittatinny Supergroup of northern New Jersey, yet very little is known about their origin and history. Research studies in the Wallkill Valley of New Jersey indicate that the cherts form by pore-filling, dissolution, and replacement mechanisms. Because laterally persistent chert sequences can be utilized as marker horizons, detailed stratigraphy could be worked out on the basis of formation-to-formation variations in megascopic and mesoscopic texture and structure. The primary goal has been to use textures to develop models of the origin and diagenetic history of nodular cherts. A second goal has been to create geological models which accurately predict the locations of prehistoric chert quarries. A third goal has been to correlate the physical and chemical properties of prehistoric chert artifacts with specific chert horizons and even to one of the more than 300 chert quarries that have been located in northern New Jersey and southern New York.

INTRODUCTION

More than 300 prehistoric chert quarries have been documented as occurring within the northeast-southwest trending axis of the Wallkill River Valley of Sussex County, New Jersey, and neighboring Orange County, New York (LaPorta 1989). Many of these quarries were located over the past 15 years during a period of geological mapping within the Cambro-Ordovician lithologies of the Great Valley Sequence (LaPorta 1989).

The central theme of this report is to describe the methods by which this researcher has been successful in locating the precise whereabouts of several hundred prehistoric chert quarries located within this the first tectonic cycle of the Appalachians. The models which have been developed during a decade and a half of geologic mapping are structural, stratigraphic, as well as sedimentological. The interplay among the three has been resolved into a number of working models which can predict the precise locations of prehistoric chert quarries within this, as well as other tectonic provinces.

Geological base maps and structure cross sections have been assembled for the Hamburg quadrangle, as well as for portions of the Branchville, Newton East, Franklin, Wawayanda, and Unionville quadrangles, Sussex County, New Jersey. In Orange County, New York, geological mapping is ongoing within the Pine Island and Goshen quadrangles. Accompanying the geological maps and structure cross sections are roughly 4000 ft of detailed stratigraphic sections. These include specific locations of unconformities, algal stromatolitic sequences, oolitic zones, supratidal micrites, storm deposits, paleokarst and lead-zinc bearing horizons, as well as the precise stratigraphic positions of chert-bearing lithologies.

Application of these models has been successful in locating chert quarries

in the Siluro-Devonian lithologies of the second tectonic cycle, to the west and north of the study area (LaPorte 1971). We are currently experimenting with models concerning Mississippian cherts, as well as with cherts occurring within the coal cycles of Pennsylvanian age. Strikingly different models have recently been developed which focus their capabilities towards discovering quarries in terrains which include deep water radiolarite cherts and associated volcanics in the New England provinces. These models have been field tested throughout the Appalachian-Ouachita orocline with formidable success.

We have summarized for the reader a layer cake stratigraphic sequence, accompanied by the textural properties of the cherts, or chert stratigraphy, and briefly summarize (Table 1; LaPorta n.d.) the structural and sedimentological aspects of the research. The following is a brief account of the construction of these models which has lead to the discovery of a great number of prehistoric quarries in a region which possesses no prior documentation of their existence.

Chert occurs as nodules in the Paleozoic carbonates of northwestern New Jersey. Cherts are more resistant to weathering than carbonates and stand out in bold relief in areas where the carbonates are poorly exposed. In many places, they are a convenient stratigraphic guide in the identification of the particular formation in which they occur. Cherts of individual horizons are easily distinguished from cherts of other horizons, a fact that is of considerable importance to the field geologist (Woodward 1931; Markewicz and Dalton 1977). This distinguishability appears to be especially useful in the case of the Cambro-Ordovician carbonates of the Kittatinny Supergroup where the host carbonate members differ so slightly from each other that any assistance in their stratigraphic recognition is of special importance (Woodward 1931).

The research has been at three levels of analysis: megascopic (base maps, major structure, and stratigraphy); macroscopic (outcrop to outcrop hand samples, color, texture, sedimentary, and structural features); and microscopic (thin sections and scanning electron microscope (SEM) analysis). An atlas of physical and chemical properties has served as a much needed mapping tool for the field geologist in this area. Furthermore, the research has provided information on the relationships between the physical and chemical characteristics of each chert type and the origin and subsequent diagenetic and structural history of the cherts and surrounding carbonate sequence.

TECTONICS AND STRUCTURE

The break apart of the PreCambrian supercontinent occurred along a series of ridge axes and transform faults whose progressive extension allowed for the development of the Iapetic seaway, during the beginning of the Cambrian period, roughly 600 million years ago. The orthogonal configuration of ridge axes and transform faults led to the development of a jigsaw-like pattern of attenuated PreCambrian crustal blocks along what is now the eastern seaboard of North America (Rance, personal communication 1988). The ridge axes roughly conform or lead to the development of embayed regions referred to as reentrants, while the transform faults bound seaward projections of land known as promontories. Greater accumulations of carbonate sediment are found in reentrants, as opposed to promontories. Later, during the structural evolution of the eastern margin of North America, reentrants would evolve into salients, while promontories would become recesses (Thomas 1977). This is largely due to the fact that compressive stress can be propagated greater distances through thicker packages of sedimentary strata.

Decollements or low angle thrust faults are propagated nearly horizontally

TABLE 1. TEXTURAL PROPERTIES OF CHERTS AND THEIR STRATIGRAPHY

	Formation Name Used on New Jersey Geologic Map	Formations Recognized by H.B. Kummel & Others	Formations Recognized by A.A. Drake & F.J. Markewicz	Current Stratigraphy As used by F.J. Markewicz & R.F. Dalton			Chert Stratigraphy	Lithostratigraphy
LOWER ORDOVICIAN	KITTATINNY LIMESTONE	Beekmantown	Epler	Ontelaunee Formation (Oo)	Harmonyvale Mbr (Oo_2)		light blue, blue/grey, thin & thick, laminated beds	light blue micritic, extremely massive, finely laminated dol.
					Beaver Run Mbr (Oo_1)		thick black massive beds, stromatolitic, brecciated	black, coarsely crystalline, sulfide-rich, laminated dolomite
				Epler Formation (Oe)	Lafayette Mbr (Oe_3)		steel blue/grey pods & beds, laminated sequences	black, sparkly, thick-bedded dolomite
					Big Springs Mbr (Oe_2)		lavendar, orchid, white, laminated beds (red & green in karst)	massive iron-stained, highly siliceous dolomite
					Branchville Mbr (Oe_1)		black, opaque, brecciated, thin & thick bedded, porcelain grey beds	sulfide zone, black, coarsely crystalline, thinly-bedded dolomite
			Rickenbach	Rickenbach Formation (Or)	Hope Mbr (Or_2)	Crooked Swamp Dolomite Facies (Or_3)	Or_3--highly translucent, light blue/grey, algal sequences	extremely coarse-grained, sulfide-rich, light blue/grey dol.
							Or_2--convex pods, continuous beds, dark blue/grey to blue, replacing evaporites	massive five-grained, dark blue, thinly-bedded dolomite
					Lower Mbr (Or_1)		Or_1--brecciated massive blue/grey matrix with black clasts	discontinuous sandy dolomite
CAMBRIAN		Allentown	Allentown	Allentown Formation (Ca)	Upper Mbr (Ca_2)		algal, oolitic, black, homogenuous, thin beds, silcrete	massive, thick-bedded, coarse-grained to micritic dolomite
					Limeport Mbr (Ca_1)		oolitic, cryptalgal, stylolitic, black	shallowing upward cycles, algal, oolitic dolomite
		Tomstown	Leithsville	Leithsville Formation (Cl)	Wallkill Mbr (Cl_3)		translucent blue/grey pods	coarse-grained, sparkly stromatolite-rich dol.
					Hamburg Mbr (Cl_2)		black, sparkly, vuggy, thin beds	cyclic, pink, green, grey dolomites, sulfides
					Califon Mbr (Cl_1)		black to dark grey pods & colloform masses	black shale, tidal flat dol., mud cracks, ripple marks, skolithos

through the PreCambrian crystalline rock and lower most Cambrian strata of Hardyston and Leithsville age. The thrust faults, step upward through Cambrian strata of the Limeport and Upper Allentown formations and ramp or incline themselves sharply upward through the lower Ordovician Beekmantown Group, including the Rickenbach, Epler, and Ontelaunee formations, which are referred to as the carbonate stiff layer (Geiser 1988). Ramping is said to be due to the rheologic properties of the carbonate strata and more specifically, to the deforming characteristics of calcite. Eventually, within the thicker sequences of strata occurring within reentrants, the ramp faults will flatten within the foreland basin sediments of the middle Ordovician Jacksonburg Limestone and Martinsburg Slate. In essence, the PreCambrian and lower most Cambrian strata behave in a brittle fashion during deformation and transmit stress waves horizontally. The progressive diminution of compressive stress westward causes the thrust fault to step upwards through Cambrian strata, until it enters the Rickenbach, Epler, and Ontelaunee formations of the lower Ordovician. The Beekmantown Group carbonates behave as a stiff layer of resistance allowing stress waves to become more inclined upwards. The intersection of steeply inclined ramp thrusts within lower Ordovician lithologies creates ramp folds, thrust faults, and repetition of strata within the Beekmantown Group. The above lying middle Ordovician Jacksonburg Limestone and Martinsburg Slate are much more ductile, and therefore stress waves flatten within this sequence. In vertical profile, the low angle thrusts appear nearly Z-shaped; the horizontal and stratigraphically lowest sole thrusts step upward into a ramp, which flattens once again in younger lithologies, where it is referred to as a roof thrust. Therefore, sole thrusts penetrate PreCambrian and Cambrian lithologies, ramp faults are inclined through the lower Ordovician strata, and roof thrusts flatten horizontally in the middle Ordovician lithologies. Appalachian structural history is partially determined by stratigraphy, that is, tectonism takes advantage of weaker lithologies. Also, thicker as opposed to thinner stratigraphic packages behave differently under compressive stress. The thicker accumulations of carbonate strata within reentrants as opposed to promontories permits the development of a greater number of thrust surfaces and therefore strata can be propagated farther westward as the embayment evolves into a salient feature. The accumulation of chert-bearing sediments is greater in reentrants than in promontories. Within promontories, sedimentary accumulations are thinner, therefore allowing for the development of less numbers of thrust faults hindering rock from westward transport and allowing promontories to evolve into recesses. The thicknesses and internal properties, largely determine the subsequent architecture of resulting folds; as well as, the stratigraphic positions of low angle thrust faults which transport the rock landward. Many of these thrust faults occur within chert-bearing lithologies in the study area, some of which may have originally been evaporite sequences. The resulting spatial distribution of repeated thrust slices of chert-bearing sequences is largely determined by the behavior of chert beds during periods of tectonism. Greater sedimentary accumulations occur within reentrants as opposed to promontories, therefore the likelihood of the occurrence of repeated thrust slices of chert-bearing strata are greater within the resulting salients as opposed to recesses. The S-shaped configuration of the Appalachian-Ouachita orocline is largely the result of the structural evolution that takes place within this tectonic setting.

Geologic setting and depositional environments

Cambro-Ordovician post-rift thermal subsidence permitted the accumulation of a shallow marine shelf sequence along the east-facing ramp of a laterally extensive miogeocline along the eastern margin of North America (Bond, Nickelson, and Kominz 1984). The study area within the Wallkill River Valley of Sussex

County, New Jersey is composed mostly of carbonates which represent a shallow depositional environment (predominantly proximal facies), that was periodically emergent (Braun and Friedman 1969; Mazzullo and Friedman 1975; Bova and Read 1987). Subsequently, the carbonates were folded and thrust into their present position representing an Alpine-like duplex thrust upon the Martinsburg Shales of Middle Ordovician age. Cherts occur in nearly every member of each formation (Markewicz and Dalton 1973, 1977; LaPorta, 1989).

The chert also preserves very delicate sedimentary features whose fragile structures would otherwise be eradicated by diagenesis (particularly dolomitization) and tectonism. These preserved features make it possible to infer depositional settings, sedimentary facies, and other features of the host carbonates (LaPorte 1971). Where macro-invertebrate fossils are present, they too are commonly preserved in chert. This preservation of uncommon fossils may be critical in determining more precise age relations of the various formation members in the future. Also, the chert has preserved a full spectrum of algal stromatolite forms throughout the Cambrian and lower Ordovician section (Aitken 1967).

The following chert stratigraphy has aided in unravelling the rather complicated structural style of deformation within the Hamburg and contiguous quadrangles. The varieties of chert unique to each formation member allowed the mapping of successive thrust slices which are barely discernable without the aid of the chert, and this mapping has lead to the proposal that the terrain was deformed as an Alpine-type duplex system (LaPorta n.d.).

THE ORIGIN OF NODULAR CHERTS

Nodular cherts should not be confused with bedded cherts that form by the lithification of oozes composed of siliceous organisms such as diatoms (diatomites) and radiolaria (radiolarian cherts). Nodular cherts occur as lenticular- to irregularly-shaped masses or as layers within a host sediment such as phosphatic shales, limestones, or dolomites. There are currently many models to explain the origin of nodular chert (Durney 1972; Knauth 1979; Clayton 1986; Maliva and Siever 1988a; Maliva 1989a, 1989b), but no single model appears to explain all nodular cherts. There are three general problems with nodular chert formation: the source of the silica; the chemical environments that cause the silica to dissolve, migrate, and finally precipitate; and the mode of growth of the silica nodules. The textural study that is the focus of this research is designed to address all three questions.

The textures of the cherts of the 13 members of the Kittatinny Supergroup are extremely variable and suggest that each chert horizon formed under unique conditions. Nevertheless, there appear to be three general mechanisms of chertification; void-filling, dissolution, and replacement. Void-fill cherts form, or at least start to form, within pre-existing spaces such as along fractures, between bedding planes, between breccia fragments, and between shell fragments in coquinas. They tend to form where the host sediment has a pronounced porosity such as along paleokarst horizons, within reef or mound structures, paleo-aquifers, unconformities, or within oolitic sequences. Dissolution cherts form during the solution and removal of the host sediment and are associated with distinct dissolution features such as stylolites, solution cleavage, and solution seams (Durney 1972; deBoer 1977). Replacement cherts appear to require a molecule-by-molecule replacement of carbonate with silica because the process leaves intact such delicate primary features as oolites, casts of evaporites, and fossils (such as stromatolites).

Most of the features described above are the result of investigations of out-

crops, hand samples, polished slabs, and microscopic thin sections. The further study of these diverse chert textures on an SEM scale has resulted in an increased understanding of chert formation. The application of the EDAX (Energy dispersive X-ray) has provided a semi-quantitative chemical fingerprint of the cherts, which has been useful in elucidating the diagenesis of the chert as well as providing a chemical framework for provenancing stone tools. Textural information derived from the SEM has proved to be critical in understanding the origin of many of the cherts.

Models for the Diagenesis and Sedimentology of Chert

Currently, we are working with approximately 18 models for the development of nodular cherts. Some of the variables of each model appear to be applicable to the myriad of chert types present within the Wallkill Valley. However, four or five models can account for some of the greatest accumulations of silica present within the research area. Interestingly, some chertification mechanisms, which are considered rare, are ubiquitous to the Cambro-Ordovician lithologies. These include the precipitation of chert from the dissolution of marine transgressive quartz sands and chertification through the development of silcretes. Also, the results of our study clearly suggest that pressure solution cherts and early diagenetic cherts are more prevalent than the literature indicates. The following is a brief description of the most common models for chertification applicable to the lithologies which are the focus of this study.

Silica of Continental Derivation:

Silica derived from cratonic sources plays a key role in the chert forming processes preserved in the rocks of the Wallkill River Valley. During the chemical weathering of continental rock, minerals of igneous, metamorphic, and sedimentary origin are converted to illite clay (Siever and Woodford 1973). If near-tropical environmental conditions are prevalent, the chemical weathering process could proceed, and illite would be further decomposed to kaolinite (Siever and Scott 1961). The process of kaolinitization requires that silica be expulsed from the clay lattice structure as potassium and aluminum are absorbed by the clay (Williams *et al.* 1985; Williams and Crerar 1985). The expulsed silica, along with calcium and organic compounds, can travel in meteoric water for great distances and be deposited along brackish water shorelines (Knauth 1979). In tidal flat settings, where slightly acidic meteoric waters mix with alkaline marine waters, the fluctuations of both eH and pH allow for the reprecipitation of silica as chert. The process could be enhanced, or speeded along, if grains of silica are already present along the shoreline to act as sites of nucleation. The zones of nucleation may occur as shoals containing vast quantities of sponge spicules, or more commonly, transgressive quartz beach sands.

Microscope petrography and SEM analysis suggest that the silica source is cratonic clay, and sponge spicules comprise only a minor component in the chert forming process. Other factors play a role in the reprecipitation of silica, such as the presence of organics and the degree of alkalinity of marine waters. Desilicated clays of cratonic origin are the most likely source of silica for the cherts within the study area. Furthermore, SEM analysis suggests that sponge spicules are only present in the Upper Lower Ordovician Ontelaunee Formation and therefore could not account for the great volume of chert which occurs in the lower formations.

Most of the Cambro-Ordovician formations occurring within the study area, are near shoreline facies (Harris 1973). The cherts within all formation members

contain high proportions of clay, and many bear quartz sand grains which possess etched outer surfaces when examined under the SEM. The dissolution of quartz sand grains in alkaline waters could provide an additional silica source for cherts occurring within the Cambrian-lower Ordovician lithologies. This is particularly true of the cherts associated with quartzite beds at the top of the upper Allentown formation. The complement of quartz sand grains, sponge spicules, and cratonic clays represent the sources of silica which account for the great volume of chert present within the research area. The mechanisms which concentrate silica as chert include the development of pressure solution halos (Durney 1972), environments of restricted replacement (Clayton 1986), mixing zones along coastal environments (Knauth 1979), and organic replacements (Siever and Scott 1961). The sites of chertification include surfaces of unconformities (LaPorta 1989), paleokarst horizons (Mustard and Donaldson 1990; Roberts 1966), zones of stylolitization, dilation breccias, organic structures such as sponge mounds, and stromatolite horizons, silcretes, and oolitic zones (LaPorta n.d.).

Early diagenetic cherts

For many years it was thought that the chertification process was very slow; and that the transformation from opal A to opal CT to stable quartz required 35 to 40 million years. Unfortunately most of the models developed were based upon studies of deep water radiolarites and diatomites as opposed to nodular cherts. Studies (Meyers 1977) of the Mississippian Lake Valley Formation in New Mexico suggest that the chertification process could be less that the assumed time period. Within the Wallkill River Valley, early diagenetic cherts appear to have formed within the Big Springs Member of the Epler Formation, as well as within the Hope Member of the Rickenbach Formation. Evidence for this is in the form of intraformational conglomerate lenses comprised of chert clasts occurring within each formation member.

Solution transfer model

The solution transfer model requires that silica be present, dissolved and reprecipitated, and the underlying mechanism is predominantly mechanical rather than chemical (Durney 1972). The solution transfer model applies to cherts that have been involved in severe deformation, compaction due to stylolitization, volume loss, and the development of progressive pressure solution features. Cherts which suffer boudinage, as well as dilation breccias are likely candidates for the pressure solution model. Thrust loading of sediments during tectonism would initiate the development of pressure solution features in deeply buried rock of Cambro-Ordovician age. Silica could be dissolved along pressure solution surfaces in the Cambro-Ordovician carbonates and be reprecipitated within the unconformities layered in the rock which were developed during periods of emergence and subaerial weathering of the miogeocline. Excellent examples of unconformity bounded cherts occur in all members of the Leithsville, Limeport, Allentown, Rickenbach, Epler, and Ontelaunee formations. Cherts which may be genetically related to the development of pressure solution features include the cherts of the Califon Member of the Leithsville Formation, and especially the oolitic cherts of the Limeport Formation. Here, volume loss associated with the progressive development of stylolites is associated with the growth and development of nodular and bedded chert. In some cases, the chert beds themselves, may actually represent stylolite surfaces. Some of the thickly bedded cherts within the Harmonyvale Member of the Ontelaunee Formation are intimately associated with solution cleavage and stylolite surfaces.

Cherts of organic replacement

Cherts of organic replacement rely on the presence of a vacuole or a pore space between grains (Siever 1962). The presence of organic structures allows for localized changes in pH which are extremely sharp and nongradational. Generally the pH conditions between the carbonate and the organic rich vacuole are sharply bounded. These sharply defined redox conditions allow for silica to be dissolved from host carbonate rock and then reprecipitated in the organic rich vacuole, which usually has a very low pH (Clayton 1982, 1986). The localized acidic conditions permit the complete molecule by molecule replacement of the host carbonate by silica. Algal stromatolites in the Leithsville, Limeport, Upper Allentown, Rickenbach, and Epler formations may be partially or completely replaced by chert. There is evidence for chert replaced bryozoan mounds and sponge reefs in the Ontelaunee Formation.

Mixing zone cherts

Chertification within mixing zones (Knauth 1979), requires the following conditions. The presence of a meteoric ground water table, which will carry silica in solution oceanward. Secondly, the presence of a silica source from which to dissolve silica. Thirdly, the presence of alkaline marine conditions which are depositing carbonate; and fourthly, short periods of transgression and regression which pucker the ground water table oceanward. If all these conditions are met, silica travelling in solution could be reprecipitated as chert as pH conditions change, where alkaline sea waters meet acidic meteoric waters. These conditions are optimal and all requirements are met during deposition of the Cambro-Ordovician carbonates within the study area. There is much evidence to suggest that the broad flat miogeoclinal carbonate planes, which deposited the Rickenbach and Epler formations and Harmonyvale Member of the Ontelaunee Formation met all the requirements for chertification within the ground water tables (Harris 1973). The results yield a series of thin and thick wispy beds of chert, which can be traced along stratigraphic strike for tens of kilometers. The chert beds are subsequently stretched, disconnected, and deformed into boudins during tectonic events. The boudins appear as lenticular beds which grade laterally into dolomite along stratigraphic strike.

SYNTHESIS

All of the chertification models require a silica source, a transportation mechanism, and a site of deposition. Certainly, the most likely sites for the reprecipitation of silica as chert include those environments or sedimentary facies that are transitional between marine and meteoric conditions. That is, the tidal flat environments, including the lower supratidal, upper intertidal, and shallow subtidal facies of a sabkha-like setting serve as the most likely sites for chert precipitation within Cambro-Ordovician lithologies (LaPorta n.d.). These are also the regions where regression and transgression are strictly recorded and chertification in mixing zones is common.

The starved margins of regressive sequences are also recorded as surfaces of unconformities. The eroded, sometimes uneven, hummocky surfaces of unconformities later serve as the porous zones or voids where dissolved silica can be reprecipitated as chert. This is especially true of the upper surface of the Upper Allentown Formation, where chert marks a succession of unconformities. Fluctuating eH and pH conditions in brackish water environments permit the formation of the necessary redox conditions which will allow chertification to proceed. The results of all the tested models clearly point to the shoreline facies as the

principal target for the thickest accumulations of chert and cratonic clay as the primary source of silica. It must be kept in mind that shoreline facies are rarely, if ever, evenly contoured in terms of sediment type, and therefore, along any one particular shoreline, chert-bearing horizons may wax and wane. Shaly, mud-bearing lagoonal facies may carry silica to the shallow and deeper subtidal sections of the depositional environment, therefore one might expect cherts in these environments to be bedded, but discontinuous along stratigraphic strike. The thickest accumulations and most persistent chert-bearing horizons occurring along stratigraphic strike would occur within the near-shoreline facies of the Beekmantown Group; including the Rickenbach, Epler, and Ontelaunee formations.

Cherts occurring on surfaces of unconformities are found within the Big Springs Member of the Epler Formation, the Hamburg Member of the Leithsville Formation, the Harmonyvale Member of the Ontelaunee Formation, and especially within the Upper Allentown Formation. The Big Springs Member of the Epler Formation also includes pervasive chertification within the vadose zone cave features of a paleokarst horizon incised during the development of the Sauk unconformity. The zone of paleokarstification is evident within the Hamburg, Branchville, and Newton East quadrangles where roughly 30 quarries occur scattered along stratigraphic strike. The distribution of chert-bearing horizons within the Beaver Run Member of the Ontelaunee Formation may represent the spatial distribution of bryozoan mounds or sponge reefs facing the middle Ordovician foreland basin. Lastly, the discontinuous nature of the Harmonyvale Member may result from extreme erosion of this lithology during the incisement of the Sauk unconformity. This same erosional event forms the cave filling cherts within the Big Springs Member of the Epler Formation (LaPorta n.d.).

CHERT STRATIGRAPHY

Hardyston Formation

The first sediments to accumulate along the rifted margin include a predominance of clastics derived from the weathering of the PreCambrian craton. In the study area, the basal Cambrian Hardyston Formation occurs as a residuum within sags and structural lows incised within PreCambrian rock. In many locations, the boundary between the PreCambrian and the Hardyston Formation is non-discernable as the PreCambrian is so thoroughly weathered that the Hardyston Formation occurs as a saprolite overlying igneous and metamorphic rocks. In Sussex County, the Hardyston may be 10 - 100 ft thick and consists of alternating layers of arkosic sandstone, argillic claystone, and conglomeritic sandstone (Aaron 1969). Although jasper or ferruginous cherts are known to be associated with the Hardyston Formation elsewhere (see Hatch, this volume) chert has not yet been documented within the Hardyston Formation within the immediate study area. It should be noted, that to the south in Warren County, near Califon, New Jersey, a residuum of chert is known to overlie the Hardyston Formation, and much of that chert is brown and yellow. Elsewhere to the north, in Litchfield County, Connecticut, near the town of Washington, ferruginous chert is associated with the Denton Formation, which is roughly coeval with the Hardyston of New Jersey, and the chert-bearing Hardyston Formation of southeastern Pennsylvania. The Hardyston Formation is not included in Table 1 because it is largely clastic as opposed to carbonate and non-chert-bearing within the immediate research area. However, the Hardyston Formation is included within the stratigraphic units of the Cambro-Ordovician in northwestern New Jersey (Berg *et al.* 1983).

Leithsville Formation

The Leithsville Formation may be as much as 700 ft thick in this study area and has been divided into three members, the Lower Califon, Hamburg, and Upper Wallkill members. All three are chert-bearing and represent the accumulation of transgressive carbonates on the rapidly subsiding continental margin.

Califon Member: The Califon Member is largely a basin axis filling shale and dolomite. Chert occurs as large and small pods up to a meter in length and their form may be the result of a type of structural deformation known as boudinage. Other varieties show concentric banding which may be diagenetic and suggest an organic origin. Califon chert is largely opaque, translucent along thin edges, contains much pyrite and emits a rank, fetid hydrogen sulfide odor when struck. Colors range from dark gray to light gray within the study area and light gray to blue gray varieties have been found within the Easton, Pennsylvania quadrangle (LaPorta 1986). Near Califon, New Jersey, alternating gray and yellow-orange varieties occur, and this variety has also been found at Macungie, Pennsylvania. When found in situ, the base of Califon pods often bear an open coxcomb structure, unsealed fractures intersect the outer portions of the pods, and a dusky, yellow iron oxide coating occurs on weathered outcrop surfaces as well as on artifacts. Stress tests performed upon Califon pods suggest that the outer shells of Califon pods are brittle, glassy, and break rather easily, while the internal portions of the pods are fibrous, waxy to dull, and exhibit extreme resistance to breakage when struck.

Hamburg Member: The Hamburg Member dolomite is a light gray, cyclic, pink to gray, thinly bedded dolarenite with shale partings, occasional algal stromatolites, and sulfide horizons. The chert within the Hamburg Member occurs in two stratigraphic positions. The lower chert occurs as thin beds up to 3 in thick, 20 - 30 ft in length, and pinches out into stringers and nodules. The chert is dark, charcoal gray. and weathered surfaces bear a blue cast. Freshly broken surfaces are saccharoidal, pyrite is visible while fractures are widely spaced and usually sealed, and euhedral microcrystals of quartz and pisoids may be present. Vugs, a few millimeters in diameter, are either filled with concentric chalcedonic quartz or with microcrystallites of euhedral quartz. The range of colors and textures of the lower Hamburg chert are very limited, as are the number of chert-bearing outcrops occurring along stratigraphic strike. Prehistoric quarries occurring in Amity, New York, and to the south 10 miles in Hamburg, New Jersey, yield similar textural fingerprints. The upper chert occurs along the crest of the Hamburg Member, as thick and thin beds which are ash gray to charcoal gray to brown. The ash gray zones are dull and matted, while the charcoal areas are extremely glassy. Close inspection of the ash gray portions indicate the presence of small angular fragments of what may be fossil debris, possibly graptolite fragments, or some type of shardy material. Blocks with widely spaced fractures are common.

Wallkill Member: The Wallkill Member occurs as a thickly bedded, coarsely crystallized, light gray dolarenite. Outcrops of the Wallkill Member are difficult to find, as they usually occur as structural terraces or benches above streams. Chert occurs as nodules and pods from less than an inch to greater than 20 in.; the larger variety being common at only one location in the Unionville quadrangle. The internal portions of the nodules reveal concentric banding which is associated with extreme variations in the texture of the chert. Some layers will be fibrous and waxy, while others are extremely glassy and highly translucent. The color and textural banding conforms to the outline of the pods, and the colors range from light gray to deep blue gray. Unsealed fractures intersect the

pods, and their centers sometimes contain a claystone or ankeritic concretion. Iron pyrite is commonly finely dispersed through the nodules.

Limeport Formation

The Limeport Formation, which is 400 - 700 ft thick in northern New Jersey (Markewicz and Dalton 1977) is a thickly bedded dolomite of peritidal origin, which consists of oolitic beds, biostromal reefs, and shale-bearing lagoonal sequences (Zadnick and Carozzi 1963). Algal stromatolites proliferate during this period of sea level rise, and several varieties of chert occur. At the bases of many of the algal stromatolitic sequences is often times a charcoal gray to black, highly translucent, oolitic chert which occurs as thin to thick beds and stringers. Closely spaced joint surfaces within the chert are resealed with microcrystalline quartz. Oolitic cherts are the most common variety within this formation, and petrographic thin sections indicate that the oolites are oftentimes deformed. At Wildcat Road in Franklin, New Jersey, in the Franklin quadrangle, a second variety of chert occurs as a burrow filling which contains the remains of fossil fragments, pisoids, and fecal pellets. The third type of chert is an organic replacement chert which is found as silica replaced algal stromatolites. This variety often contains alternating layers of chert and dolomite. Most of the chert-bearing facies are associated with strata which have been interpreted as lagoonal sequences.

Upper Allentown Formation

The Upper Allentown Formation is a very thickly bedded dolomite of subtidal origin which attains a thickness of just greater than 1000 ft in the Hamburg quadrangle. The deposition of this dolomite marks the maximum of marine transgression upon the land surface, and the formation is capped by a pronounced unconformity which punctuates sea level rise and terminates the deposition of Cambrian strata. Chert occurs sporadically within this formation as thin beds and nodules. At the top of the sequence there is a series of wispy beds which outline a succession of chert lined disconformities. The chert is black, highly lustrous and translucent along the edges. Associated with these cherts are silicified algal stromatolites, which are of a domal nature, and whose dimensions do not exceed a meter in width. Chert in this form is black, opaque, and bears alternating lighter colored layers, which mark the trace of the stromatolites. Thin and thick beds of quartzite mark the termination of the Upper Allentown.

Rickenbach Formation

The Rickenbach Formation is roughly 500 ft thick, subdivided into three members and is chert-bearing throughout. The members are, in ascending order; the lower unnamed member, the middle Hope Member, and the upper Crooked Swamp Facies. Due to the interplay of tectonics and sedimentation during this geological interval, the facies mosaic of these three members can occur in almost any order, and the most normal occurrence is described here (LaPorta n.d.: Figure 2).

The lower unnamed member: The lower unnamed member contains numerous quartz sand lenses throughout its base, as well as chert replaced algal stromatolites. Chert, where it is common, occurs as thin pods and beds which are slightly convex upwards. Beds are rarely greater than an inch or two in thickness, and close inspection reveals an abundance of floating quartz sand grains occurring within the chert. The chert is black to blue gray and translucent along the edges.

The Hope member: The Hope Member contains chert which may be in the form of an algal replacement. The chert occurs as thin, convex upward beds which are rarely more than a few inches thick, and as much as 3 - 4m in length. The black to dark blue-black, mildly translucent chert layers are common throughout this member. Chert replaced oolitic sequences are also common here. At one stratigraphic position within the Hope Member, several chert layers occur closely spaced, creating a distinctive marker horizon which can be traced from Orange County, New York, through Sussex and Warren Counties, New Jersey, into the Easton quadrangle in Pennsylvania. This distinctive chert-bearing horizon has been employed as a mapping tool and stratigraphic aid due to its lateral persistence (Markewicz and Dalton 1977).

The Crooked Swamp Facies: The coarse grained, thickly bedded, saccharoidal dolomite of the Crooked Swamp Facies may be fairly thin and discontinuous within the upper Rickenbach. The member bears chert as nodules, elongate pods, and algal replacements. The chert is deep blue gray to blue-black, highly translucent and delicately varved with finely dispersed organic filaments. Fractures within Crooked Swamp chert are usually bounded by smooth surfaces, are usually unsealed, and are visible in artifact form. The uppermost strata of the Crooked Swamp Member bear a very distinctive chert which has been interpreted (LaPorta, 1989) as a dilation breccia (Roehl 1981; Roberts 1966). The brecciated chert sequence is thick, distinctive, and occurs at the interface between the Crooked Swamp and the lower Branchville Member of the Epler Formation, wherever the two members are visible. The chert can be up to one meter in thickness and pinch and swell up to distances of several hundred meters along stratigraphic strike. Close inspection reveals angular fragments of dark, translucent Crooked Swamp chert embedded within a matrix of a second generation lighter colored chert which is usually ash gray to pale blue-gray. At some locations, such as Rock Island in the Hamburg quadrangle, the chert clasts and matrix are thoroughly welded together, so that the contact between clast and matrix is only discernable in microscopic thin section. The dilation breccia is common throughout Orange County, New York, in the Goshen and Pine Island quadrangles, where it outlines a series of imbricate thrust surfaces, as well as farther south within the Hamburg and Branchville quadrangles in Sussex County, New Jersey.

Epler Formation

The Epler Formation is 600 ft thick and divided into three members; the lower Branchville, middle Big Springs, and upper Lafayette, all of which are chert-bearing (LaPorta n.d.:Figures 2 and 3).

Branchville Member: The Branchville Member shares the dilation breccia (Roehl 1981) with the upper portion of the Crooked Swamp Facies of the Rickenbach Formation, therefore, the base of the Epler Formation is cherty (Markewicz 1974). But several other varieties of chert occur in minor amounts throughout the member. Stratigraphically lowest is a series of finely dispersed, thin lenses, and beds of oolitic chert. The oolites are much larger than those present either within the Rickenbach or Limeport formations. The chert is distinctively charcoal gray to black and translucent only along the thinnest edges. The second variety of chert occurs as a highly lustrous, thinly bedded, black chert with a purple cast. The chert is highly translucent, bounded by sharp unsealed fractures, and forms thin convex upward beds around large algal stromatolites. The third variety of chert is closely associated with oolitic sequences and coarse sand-bearing horizons. It occurs as a purple to lavender to orchid color, thinly bedded, highly lustrous to waxy chert, which contains finely interspersed sand grains. Occasionally this

chert is seen to replace or underlie algal stromatolite features within this member.

Big Springs Member: The Big Springs Member is a thickly bedded series of unconformity bounded sequences containing a myriad of chert types (LaPorta 1987). The base of the member contains a thin to thick bed of ash gray, porcellainous chert (Markewicz and Dalton 1977). The chert is punky to matted, dull to waxy, and contains the remains of rhombic vacuoles where dolomite euhedra have been pitted by solution. Above this marker horizon is a zone of chertification, which includes intraformational conglomerates composed of chert clasts and paleokarst features, which are filled with collapsed chert breccias (Mustard and Donaldson 1990). The paleokarst features include fallen and eroded blocks of purple chert recemented in a matrix of a second generation of chert which occurs as gray to white to milk white highly translucent infillings within the paleokarst features. Average hand samples of this material yield welded masses of angular pieces of purple chert cemented into a matrix of white chert. Rhombic vacuoles are common in the white phase. At one location within the Branchville quadrangle, the white chert is translucent enough to appear chalcedonic. At the same location near Harmonyvale in the Branchville quadrangle, silicified cave infillings within the Big Springs occur as maroon to bright red chert sequences associated with gray to jade green chert sequences, all occurring within the same horizon. Rhombic vacuoles are prevalent within all the cave filling cherts, an index of their replacive nature. Low to intermediate level SEM analysis has revealed a triple point novaculitic structure present within some samples of the white chert.

Lafayette Member: The Lafayette Member is similar in appearance to the Branchville Member, but contains more shale and less sulfides. Chert occurs as black, opaque, thinly developed beds which pinch and swell, and are continuous for only a few meters along stratigraphic strike. More characteristically, Lafayette chert occurs as steel blue nodules and thin beds, which are translucent only along the thinnest edges. Fracture sets occurring within Lafayette chert pods are usually lighter colored than the surrounding chert and contain a carbonate cement. Chert replaced oolitic sequences are also present.

Ontelaunee Formation

The Ontelaunee Formation is approximately 400 feet thick and represents the uppermost formation of the lower Ordovician. It is divided into two members: the lower Beaver Run and the upper Harmonyvale Member (Markewicz 1976; LaPorta n.d.:Figures 4 and 5).

Beaver Run Member: The lower Beaver Run Member begins at an unconformity at the top of the Lafayette Member of the Epler Formation. It occurs as a thin to thickly bedded, dark sulfide rich dolomite and chert appears approximately 40 ft up into the section. The thickest chert accumulations occur approximately 60 - 70 ft up in the section, where the chert occur as beds which reach a thickness of 8 - 10 ft and pinch and swell along stratigraphic strike. The anastomosing cherts may be laterally extensive ranging from 100 - 200m and in cross section appear as large boudins. The chert accumulations may represent silicified bryozoans and sponge mounds. The chert may be black to charcoal gray, opaque to highly translucent, and often times contains floating sand grains. Brecciated and algal stromatolitic forms are common and weathered surfaces patinate nearly white. Low level SEM images reveal the presence of sponge spicules within this chert. Stratigraphically upsection, the dolomite becomes lighter, as does the associated chert, and strata which are transitional between Beaver Run and

Harmonyvale contain varieties of chert which are black to navy blue to blue gray. Several unconformities are present within the upper portion of the Beaver Run Member.

Harmonyvale Member: The Harmonyvale Member is a very thickly bedded, massive, micritic dolomite which contains abundant solution cleavage and weathered surfaces are white. The chert within the Harmonyvale Member occurs as beds up to a foot thick and greater than 100 ft in length and are usually bounded on their upper surfaces by a centimeter or so of illitic clay. The chert occurs as robin's egg blue, laminated to massive beds which grade to gray and almost white in the upper portion of the member. In general outline, the beds appear to be somewhat convex upwards and may represent large scale boudins. Internal cracking or brecciation is common within Harmonyvale chert, as are sealed and unsealed fractures. Acid etched slabs reveal intraformational conglomerates within the Harmonyvale beds suggesting the presence of hidden unconformities. Where the transition between the Beaver Run and Harmonyvale Members is abrupt, as at the Lower Road Quarry, near Unionville, New York, Orange County, the chert may grade from black to robin's egg blue within a single hand sample. Elsewhere, the chert can be highly lustrous and glassy, as at the Phillip's Quarry, within the Hamburg quadrangle, Sussex County.

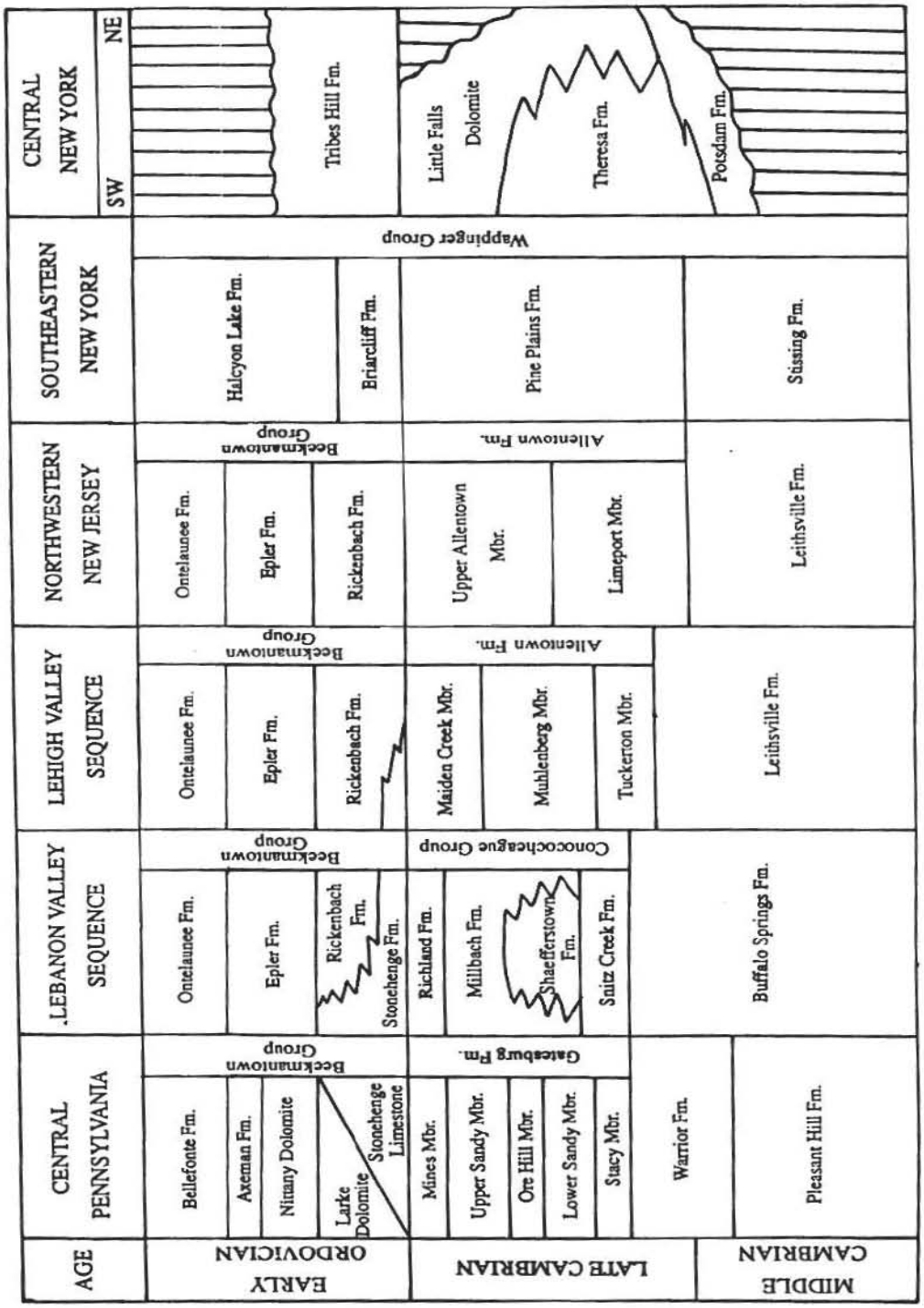
STATEWIDE CORRELATIONS

Field work in the tri-state New York, New Jersey, Pennsylvania region has disclosed a considerable number of general correlations between chert-bearing strata within Cambrian and Ordovician rocks (Table 2). Employing the stratigraphic sections from northwestern New Jersey, we found the following relationships. In ascending order, within the lower Cambrian Leithsville Formation, the unconformity bounded chert within the Hamburg Member could be easily traced into Orange County, New York. In Duchess County, New York, the distinctive cherts of the Hamburg Member have been described at Stissing Mountain (Knoph 1962). Califon and Wallkill members and their associated cherts were not present to the north of the study area. To the south, in the Easton quadrangle, cherts representative of the Califon Member were present. It is worth noting that in Virginia Woodward (1931) described several varieties of bedded and nodular cherts within the Shady and Elbrook formations, which are strikingly similar to those occurring with the Hamburg and Wallkill members of the Leithsville Formation (LaPorta n.d.).

The oolitic cherts of the Limeport Formation are present throughout Orange County, New York, as well as within the Lehigh Valley sequence of Pennsylvania. The coeval Clarendon Springs Formation of the Champlain Valley has many of the same characteristics as the Limeport Formation in northwestern New Jersey (Twenhofel 1954). The Little Falls dolomite of central New York and the Mines Formation of central Pennsylvania are roughly equivalent in age to the Upper Allentown, yet all three associated cherts are very different in their appearance.

The Rickenbach Formation of upper most Cambrian, lower Ordovician age is the oldest formation within the Beekmantown Group. The lower member cannot be traced to the north or south of the study area without great difficulty. Conversely, the Hope member is visible in Orange County, New York, Sussex and Warren Counties, New Jersey, and is present and chert-bearing within the Lehigh and Lebanon Valley sequences of east-central Pennsylvania. The distinctive marker horizon within the Hope Member can be traced from Orange County, New York to just south of the Easton quadrangle in eastern Pennsylvania. The

TABLE 2. CORRELATION OF STRATIGRAPHIES



Crooked Swamp Facies is visible in Orange County, but the Rickenbach Formation in general is thinly developed in this area. When chert occurs, its textural characteristics are identical to those of the Crooked Swamp Facies in Sussex and Warren Counties, New Jersey. The lower member of the Rickenbach is not present in Orange County, and the Briarcliff Formation is then roughly equivalent to the Hope member of the Rickenbach (Offield 1967). In New York State, the Crooked Swamp Facies is placed stratigraphically within the base of the Halcyon Lake Formation, which is actually a group.

The Halcyon Lake Group includes the Crooked Swamp Facies of the Rickenbach Formation, all three members of the Epler Formation, as well as the entire Ontelaunee formation. The grouping of all three formations into one has masked the resolution of five chert-bearing members. The Epler Formation, which is included in the middle of Halcyon Lake is also cherty in Orange County, New York, but the paleokarst horizons are absent. Instead, at the base of the Big Springs Member, there is an ash gray, porcelain-like chert which can be traced to Fishkill, New York, greater than 100 miles north of the immediate study area. What is more striking, is that stratigraphically upsection from this gray chert horizon occurs a series of lavender to purple, poorly developed chert beds, which are identical to those occurring in the Big Springs Member of the Epler Formation at the type section in Sussex County, New Jersey. The white and lavender brecciated cherts of the paleokarst horizons present in Sussex County, as well as their associated green and red cave in-filling cherts occur as a restricted zone within Sussex County. The massive black chert beds of the lower Beaver Run Member of the Ontelaunee Formation are also present in southeastern New York State, within the Halcyon Lake Formation. The black chert beds pinch out north of Maybrook, New York, where they are replaced by a series of algal stromatolites. To the south, near Unionville, New York, blue gray chert beds of the Harmonyvale Member of the Ontelaunee overlie black cherts of the Beaver Run Member at the top of the Halcyon Lake Formation. To the south in the Lehigh Valley Sequence and in Lebanon Valley, both the Epler and Ontelaunee formations are chert-bearing (Hobson 1963; LaPorta n.d:table 2). Farther west in central Pennsylvania, the Epler equivalents in the Nittany and Axeman Dolomites are also chert-bearing. The Ontelaunee equivalent in central Pennsylvania, the Bellefonte Formation, contains chert as nodules which bear only a minor resemblance to the cherts of the Ontelaunee Formation in New Jersey.

Farther to the south in the Tennessee salient, the Mascot and Kingsport formations possess strikingly similar characteristics to the Epler and Ontelaunee formations in New Jersey, including the presence of the characteristic varieties of chert and paleokarst features (Markewicz and Dalton 1977). In Virginia, the Jonesboro, Nittany, and lower Stones River formations, which are Beekmantown equivalents, are also chert-bearing.

THE SPATIAL DISTRIBUTION OF QUARRIES WITHIN THE STUDY AREA

The present study has shed some light on the controls that stratigraphy have over the development of structure, and this is especially true of the Cambro-Ordovician carbonates. On a refined scale, the sedimentology of the carbonates, the shallow inclination of the miogeoclinal ramp, and the periodic emergence of that ramp lead to the development of a great number of closely spaced chert-bearing horizons. The greatest number of chert rich facies and the broadest variety of chert types occur within the lower Ordovician Beekmantown Group; whose sedimentary facies mosaics are highly complex. This is largely due to the interplay between eustasy and tectonics, which determine the character and

duration of transgression and regression on the carbonate ramp. On a slightly broader scale, the chert-bearing carbonates of the Beekmantown Group behave differently under compressive stress than do the underlying Cambrian and overlying middle Ordovician lithologies. The variations in rheologic properties of the three sedimentary packages permit the development of sole thrusts, ramps, and roof thrusts. The upper and lower lithostratigraphic units transmit stress horizontally, while the intermediate unit refracts stress waves upwards, generating a series of complicated folds and thrusts within the lower Ordovician units. This process permits the development of repeated exposures of chert-bearing strata across stratigraphic strike. On a more regional scale, greater accumulations of chert-bearing carbonates form within reentrants. The carbonate sequences forming within reentrants contain greater concentrations of chert due to factors of sedimentology, stratigraphy, and paleoslope of the miogeocline. As the reentrants evolve into salients the chert-bearing strata are folded and thrusted repeatedly. The structural evolution occurring in the salients promotes the development of pressure solution cherts within these embayments. Thinner sedimentary accumulations, within promontories, hinder the westward migration of stresses propagated as thrust faults. Variations in sedimentology and stratigraphy, as well as differences in structural evolution limit the development of chert-bearing strata within the resulting recess. Field evidence indicates that the Cambrian cherts are fairly continuous between salients and recesses, but cherts occurring within the lower Ordovician lithologies are best developed in salients and poorly developed along recesses. These observations indicate that the Cambrian paleogeography was fairly uniform within both reentrants and promontories. This is largely due to the fact that the Cambrian sequence was deposited during a period of rifting and uniform thermal subsidence of the continental margin (LaPorta n.d.). Heterogeneities within the paleolandscape were created during several episodes of Ordovician tectonism. Despite the disruption caused by tectonics, the lower Ordovician carbonate sedimentary facies are remarkably persistent along stratigraphic strike. This suggests that the lower Ordovician lithologies were probably formed in direct response to regional tectonics, are similar to each other within salients, and exhibit marked facies changes within recesses. The striking similarity between the Mascot and Kingsport formations occurring within the Tennessee salient and the Epler and Ontelaunee formations of the Pennsylvania salient are confirmation of this hypothesis (LaPorta n.d.).

The spatial distribution of prehistoric quarries within the immediate study area is largely the result of the interplay between stratigraphy and structure on these three levels. The heterogeneities present within the carbonates lead to archaeological considerations on three levels. Firstly, the lower Ordovician Rickenbach, Epler, and Ontelaunee formations are folded and thrusted into a relatively narrow band trending northeast-southwest along the axis of the Wallkill River Valley. The steeply dipping chert beds and repeated thrust slices occurring along chert-bearing sequences are exposed in a narrow zone of the valley. Prehistoric quarries occurring within all eight members of the three formations are often in close proximity to each other. Extensive quarry operations have been discovered within both members of the Ontelaunee Formation. Quarries have been developed in the lower Beaver Run Member and where erosion has not removed the upper Harmonyvale Member, both are mined together. Quarries of this type frequently range from 100 - 200m in length. The steeply dipping beds offer excellent access to chert-bearing horizons. Chert quarries within this formation occur along the western side of the Wallkill River Valley, adjacent to the Jacksonburg Limestone and the Martinsburg Slate. The linear distribution of Beaver Run quarries found along strike may represent the ecological zonation of lower Ordovician sponge reefs or bryozoan mounds. The distribution of Harmony-

vale quarries is largely dependent upon the degree of middle Ordovician erosion. The extensive prehistoric quarries developed within the Ontelaunee Formation are always associated with a highly organized quartzite mining technology. Beaver Run quarries occur in a trend from Orange County, New York through Sussex, Warren and Hunterdon counties, New Jersey, as well as in eastern Pennsylvania.

Prehistoric quarries developed within the Epler Formation are generally smaller than those occurring within the Ontelaunee. Quarries discovered within the Big Springs Member of the Epler Formation occur in a narrow, linear band outcropping within three quadrangles. The quarries are small, less than 75m in length, and sporadically developed due to the brecciated nature of the karst-filling chert. The outlines of the quarries are generally determined by the dimensions of the paleokarst features and also by the number of associated chert-bearing horizons. Quarries developed within the Big Springs Member will also include the chert-bearing upper Lafayette Member, as well as the porcelain chert which occurs at the base of the Big Springs Member. Occasionally, cherts within the Branchville Member are exploited in the same operations. Although the brecciated cherts occur in a restricted zone, the porcelain gray chert within the base of the member has been traced for 100 miles to the northeast where prehistoric quarries are found in Fishkill, New York.

An extensive zone of brecciated chert occurs at the interface between the Branchville Member of the Epler Formation and the Crooked Swamp Member of the Rickenbach Formation. The chert has been classified as a dilation breccia (LaPorta n.d.) and occurs as a single thick chert bed which follows along strike. Prehistoric quarries in the form of trenches and conical pits occur along the length of the chert-bearing outcrops. In Orange County, New York, the dilation breccia marks the surfaces of several repeated thrust slices occurring within the Halcyon Lake Group. The elucidation of the complicated style of structural deformation within the area of the Pine Island and Goshen quadrangles (LaPorta n.d.) has led to the discovery of more than 20 prehistoric quarries within this chert-bearing horizon (Jack Webster, personal communication 1991-1994).

Chert quarries developed within the Rickenbach Formation represent the smallest class of prehistoric quarries within the Beekmantown Group. Although chert occurs within all three members, it is generally scattered as thin beds and nodules and rarely occurs as an extensive concentration. Stone tool inventories suggest that all three members were mined, but to date, quarries discovered within this formation are numerous, but small, usually less than 25m in length. The Rickenbach Formation is the stratigraphically lowest formation within the Beekmantown Group, and this important fact may have determined the limitations of its use as a prehistoric lithic resource. Due to its low stratigraphic position, ramp faults developed within the Beekmantown Group often place the Rickenbach Formation in a footwall relationship with limited surface exposure. The beds may occur along steep-sided east-facing walls, which renders them difficult to mine, regardless of their angle of inclination.

The Hardyston, Leithsville, Limeport, and Upper Allentown formations occur within the zone of the sole thrust in the study area. They are often bounded to the east by allochthanous masses of PreCambrian crystalline rock and in general comprise the lower elevations of the valley along the eastern side of the Wallkill River. Their low relief and mild topographic expression is further masked by a thick veneer of glacial drift which covers the valley floor. Outcrops of steeply dipping Cambrian strata are most common when they are in close association with PreCambrian rocks. Prehistoric quarries occurring within these formations are generally widely scattered and poorly developed. Rarely are beds inclined steeply enough to afford easy access. Most quarries are developed as small conical pits and outcrop quarries. Oftentimes, Califon, Hamburg, and Wallkill member cherts

are gathered from pits excavated into the residuum which forms above the outcrop. In southeastern Pennsylvania, Califon chert occurs intimately associated with ferruginous chert or yellow jasper of the Hardyston Formation.

Prehistoric quarries developed within the Limeport and Upper Allentown formations are more numerous than those occurring within the Leithsville Formation. This is due to the proximity of these formations to the ramp thrusts of the Beekmantown Group. The sole thrust occurring within the floor of the valley, steps upward through the Limeport and Upper Allentown formations, creating a series of footwall relationships scattered across the valley floor. The washboard effect formed by the sole thrust during its westward migratory transition into a ramp creates a variety of steeply inclined exposed surfaces, which when chert-bearing are suitable for mining. To the south in the Paulins Kill Valley, structural complications result in excellent exposures of the Limeport Formation, and as a result it was extensively mined in prehistoric times. Lastly, our research has suggested that prehistoric quarries occurring within the Cambro-Ordovician carbonates are most common within salient features which evolve from the structural deformation of reentrants. Quarries are less common along promontories which accumulate thin packages of sedimentary strata and evolve into recesses.

SUMMARY

Chert is present in all 13 formation members within the Cambro-Ordovician lithologies of the Great Valley Sequence in Sussex and Warren counties, New Jersey. The cherts appear to be restricted to tidal flat or supratidal facies, and associated intertidal sequences. Cherts are present as early diagenetic, late replacive, dissolution, paleokarst, and pressure solution cherts. Cherts are nearly absent in the deeper subtidal Upper Allentown Formation. The textures of the cherts, and their associated dolomite are laterally persistent for tens to hundreds of kilometers to the north and south of the study area (Table 2). Similar cherts are found at even greater distances, within coeval strata, within the Champlain embayment and the Tennessee salient. The replacive nature of the chert, as well as its stratigraphic position marking unconformities of regional extent allows for easy correlation on a statewide basis. The cherts appear to be time stratigraphic along stratigraphic strike, and only mildly time transgressive between various carbonate basins. The evenness of the Cambro-Ordovician miogeoclinal ramp is most likely responsible for the lateral persistence of the sedimentary carbonate facies. If most of the cherts are carbonate replacements, then it can only be concluded that the chert marker horizons could be employed as mapping aids on a statewide basis.

The mixing zone model (Knauth 1979), which is applicable to the chertification process within shoreline facies, engenders the growth and development of continuous chert sequences within the Rickenbach, Epler, and Ontelaunee formations. Chert occurring on local unconformities, within paleokarst horizons and as organic replacements will be geographically restricted, as will early diagenetic cherts. Cherts occurring within the paleokarst horizons of the Big Springs Member of the Epler Formation are the most localized. Cherts lining unconformities within the Hamburg Member of the Leithsville Formation and at the crest of the Upper Allentown Formation may be of regional significance, but are difficult to trace northward into Orange County. Although sponge spicules are present under SEM within the Beaver Run and Harmonyvale members of the Ontelaunee Formation, they cannot account for the vast volume of chert present within the study area. Several other sources including cratonic silica, the dissolution of transgressive marine quartz sands, and the development of pressure solution cherts pro-

vide the necessary mechanisms and models to account for the great quantity of chert within these lithologies.

The structural, stratigraphic, and sedimentological models lead to the following archaeological considerations. Quarries occurring within the Leithsville, Limeport, and Upper Allentown formations are usually associated with sole thrusts and occur as small, spatially widespread, lithic resources. In the Hamburg and contiguous quadrangles, the Cambrian lithologies underlie topographically low lying regions. Many of the small scattered quarries occur in steeply inclined strata juxtaposed to allochthanous Precambrian sequences. The Precambrian and Cambrian lithologies are located geographically within the eastern portion of the Hamburg quadrangle.

Quarries occurring within the Rickenbach, Epler, and Ontelaunee formations occur within the carbonate stiff layer and their fault bounded folded nature compresses these formations into a narrow band, trending northeast-southwest through the study area. Most outcrops occur along the western side of the Wallkill River Valley in the Hamburg and Branchville quadrangles. Thrust faulting, in some areas, causes a repetition of chert-bearing outcrops, the thinly developed shoreline facies present narrow outcrop patterns, which implies that a great number of chert-bearing horizons representing different formation members could be exposed over a geographically narrow distance. The greatest concentration of prehistoric chert quarries occurs within the lower Ordovician Beekmantown Group, whose three formations, and eight chert-bearing members of shallow, intertidal origin, comprise a narrow belt of dolomite which trends northeast-southwest along the western limb of the axis of the Wallkill River Valley. Complications of folding and thrusting within the carbonate stiff layer reveals a great number of repetitive thrust slices whose outcrop patterns are the traces of chert beds. The greatest concentration of prehistoric chert quarries occurs within the Beekmantown Group, in a restricted area, coinciding with the trace of the thrust faults, in these narrowly restricted zones of folded and thrusted strata a great variety of cherts can be easily acquired. The roof thrust within the Jacksonburg Limestone and Martinsburg Slate occurs along the western portion of the valley and is not chert-bearing, but contains minable quantities of metamorphosed slates and argillites.

Reprinted with permission.
LaPorta, Philip C., 1996, Lithostratigraphic models and the geographic distribution of prehistoric chert quarries within the Cambro-Ordovician lithologies of the Great Valley Sequence, Sussex County, New Jersey, *in* Bergman, C.A., and Doershuk, J.F., Recent Research into the Prehistory of the Delaware Valley: Journal of Middle Atlantic Archaeology, v. 10, p. 47-66.

LITHOSTRATIGRAPHY AS A PREDICTIVE TOOL FOR PREHISTORIC QUARRY INVESTIGATIONS: EXAMPLES FROM THE DUTCHESS QUARRY SITE, ORANGE COUNTY, NEW YORK

PHILIP C. LA PORTA
CITY UNIVERSITY OF NEW YORK

ABSTRACT

Detailed geological mapping in the Goshen and Pine Island quadrangles has led to a reinterpretation of the structural geology of that area. Complicated thrust faulting has brought repeated slices of chert-bearing lithologies to the surface. The application of a chert stratigraphy for Cambrian and Ordovician rocks served as a mapping aid that elucidated the complicated structural style. The intersection of thrust faults defines a trend along which a great number of prehistoric quarries has been located. Most of these quarries occur within the Lower Ordovician Halcyon Lake Group. This lithological suite consists of the Crooked Swamp Member of the Rickenbach Formation, the Branchville, Big Springs, and Lafayette members of the Epler Formation, as well as the Beaver Run and Harmonyvale members of the Ontelaunee Formation. All six members bear distinctive varieties of chert.

BACKGROUND

Lookout Mountain (Dutchess Quarry) occurs within the Ontelaunee Formation. Subtle evidences of prehistoric mining have been discovered at this location. Several larger prehistoric quarries occurring within this formation have been discovered in the vicinity. Associated with the quarries are the full complement of prehistoric mining instruments fashioned from quartzite. The spatial distribution of quartzite instruments within the quarries outlines various aspects of the extraction and reduction process. The mining technology is present elsewhere in the Wallkill River Valley and is suggestive of a "folk geology" practice.

My quarry investigations in the Wallkill River Valley suggest the presence of a "folk geology" operative during the entire Archaic period. The practice includes following marker horizons across the landscape and the development of large and small scale quarry operations through an acquired knowledge of the physical characteristics of the rock. This knowledge is reflected in the preferences visible in excavated stone tool assemblages. Also shared is a mining technology that includes quarry instruments fashioned from metaconglomerate, arkose, and quartzites. This article provides a summary description from observations to be documented elsewhere.

STRATIGRAPHY OF THE DUTCHESS QUARRY AREA

The lithologies cropping out within the vicinity of the Dutchess Quarry area are those of the Halcyon Lake Formation. The Halcyon Lake Formation was first described by Knopf (1946) at the Halcyon Lake type section in Dutchess County, New York. The formation was described as Canadian in age, which is Lower Ordovician (505 - 475 Ma) and roughly equivalent to the Beekmantown Group rocks occurring to the north and south of the study area. A Middle Ordovician unconformity caps the Halcyon Lake Formation and is subsequently overlain by the Rochdale and Balmville limestones and Mt. Marino

shale. Compressed within the Halcyon Lake Formation is much of the Beekmantown Group (Figure 1), which is represented to the south in New Jersey by three formations, divisible into eight distinct, chert-bearing members. The formation occurring stratigraphically lowest in New Jersey, and equivalent to the base of the Halcyon Lake, is the Rickenbach Formation (Figure 2). The uppermost member of the Rickenbach Formation is the Crooked Swamp, which contains a highly translucent, black to blue-gray chert occurring as nodules and replacements of algal stromatolites that may appear as finely laminated, chert pods which occasionally retain their original rounded form. The procurement locus I have named New Quarry #2 occurs approximately one mile to the east of Lookout Mountain and is developed within the Crooked Swamp facies. Above this is the Epler Formation, which contains the Branchville, Big Springs, and Lafayette members, all of which are chert-bearing. The Epler Formation is roughly equivalent to the middle portion of the Halcyon Lake Formation. Infrequently is the Epler Formation exposed in this region. Owing to structural complexities, it usually occurs deep in the subsurface. Potential quarries within the Epler Formation crop out along a thrust fault at a reservoir several miles to the north of Lookout Mountain.

The Ontelaunee Formation comprises the upper portion of the Halcyon Lake Formation in New Jersey. It was recognized in New Jersey by Markewicz and Dalton (1974, 1976). The Ontelaunee Formation contains two members: the lower Beaver Run member, which is 150 - 200 ft thick, and the upper Harmonyvale Member, which is in excess of 220 ft thick. At many locations, the Harmonyvale has been completely eroded away, and the Jacksonburg Limestone (Balmville equivalent) is deposited directly on the Beaver Run. An exception to this is the Lower Road quarry, where abrupt facies changes bring the Beaver Run and Harmonyvale members in close contact. The Beaver Run member contains three distinct units, the lowest of which is a coarsely-crystalline, fetid or sulfurous dolomite approximately 40 ft thick. This unit would occur below the base of Lookout Mountain at Dutchess Quarry and would be only infrequently visible as outcrop. New Quarry #1 is located at the top of this facies. Above this is a 50 - 100 ft thick massive dolomite, which contains individual chert beds up to 10 ft thick. The top of this unit occurs at the 520-foot contour interval and is exposed along the western base of Lookout Mountain. Extensive chert beds within this unit house the prehistoric quarries at Houston Road and Lower Road, among others. The upper portion of this member, which can be 50 ft thick, is medium-grained, black to gray dolomite with intermittent chert beds and pods of lighter gray color. It is the upper unit which comprises the walls of Lookout Mountain, the caves, and the chert quarries occurring at the top of the mountain.

The Halcyon Lake Formation is a condensed section, and possibly an entire formation group, as it comprises most of the Beekmantown Group lithologies. The Crooked Swamp Member of the Rickenbach Formation, the Branchville, Big Springs, and Lafayette members of the Epler Formation, and the Beaver Run and Harmonyvale members of the Ontelaunee Formation are all roughly equivalent to the Halcyon Lake Formation.

CRITERIA FOR QUARRY DEVELOPMENT

The traditional view of prehistoric quarries and chert exploitation relies heavily upon the assumption that quarries are found where chert is highly concentrated. More recent studies (e.g., La Porta 1989, 1994) have presented strong arguments to suggest that the structural history of the rock determines the spatial distribution of quarry areas and associated reduction sequences more often than does the simple presence of chert. Unlike other areas of the world, chert occurring in the Paleozoic rocks of the Appalachians oftentimes occurs as thin beds, deformed boudins (sausage-shaped structures), and strata-bound layers of nodules embedded in a great volume of surrounding country rock. The development of a quarry (or motion [La Porta n.d.]) depends largely upon the following criteria:

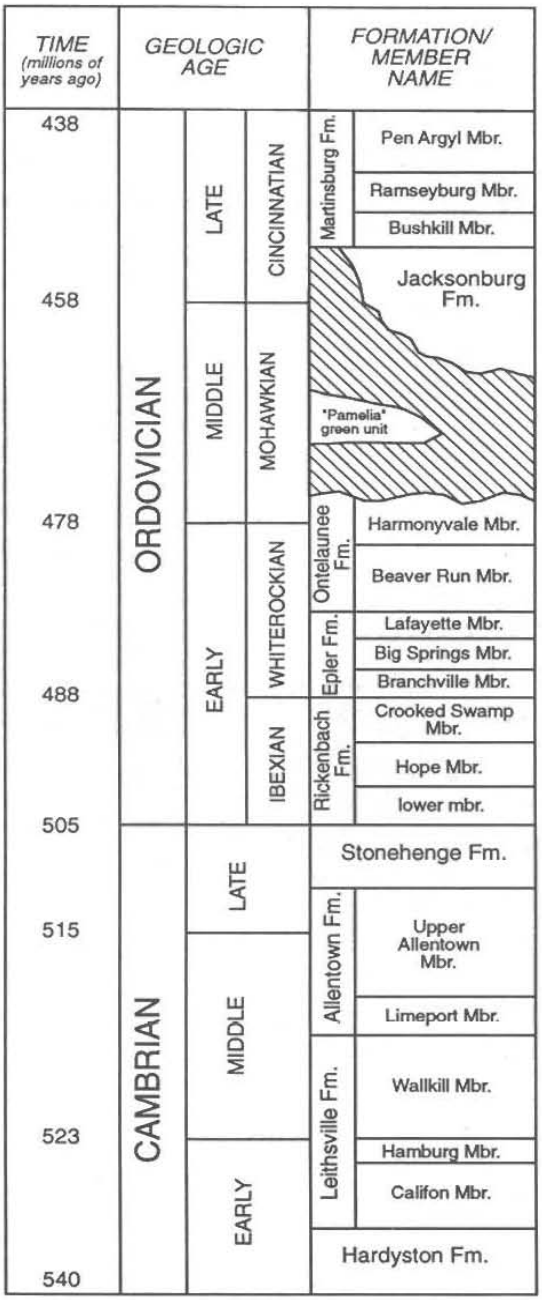


Figure 1. Stratigraphic units of northeastern New Jersey. The formations comprising the Beekmantown Group, Upper Cambrian to Middle Ordovician, are roughly equivalent to the Halcyon Lake Formation, which is Canadian in age, found in New York State.

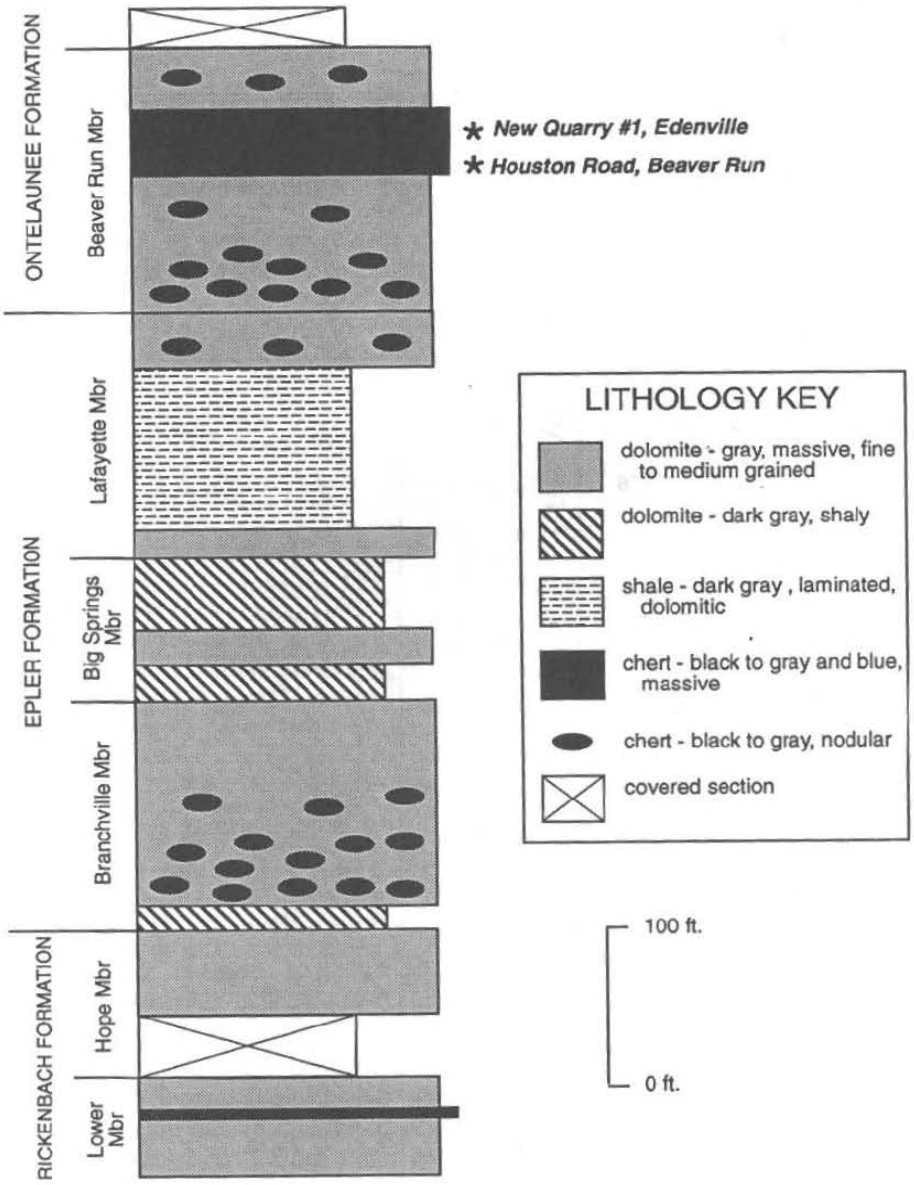


Figure 2. Allentown to Ontelaunee. This stratigraphic section clearly illustrates the three formations of the Beekmantown Group present in New Jersey which are equivalent to the Halcyon Lake Formation in New York State. This section also illustrates the stratigraphic position of quarries occurring within the first 100 - 150 ft of the Beaver Run Member. (Note: The 525-foot contour interval occurring along the western base of Mt. Lookout is equivalent to this stratigraphic horizon.)

1. Angle of inclination of the beds or the dip angle with respect to horizontal.
2. Presence of joint surfaces.
3. Presence of well-defined bedding planes.
4. Development of fracture cleavage.
5. Concentration of chert-bearing units.

Dolomite beds which range from being steeply to gently inclined lend themselves to chert extraction by levers or wedges. Where chert occurs in horizontal beds, the extraction process involves the removal of great quantities of overburden rock or surrounding country rock (gangue) to reach the chert-rich horizons. The process often involves the development of a vertical shaft or conical pit, such as those discovered at Dutchess Quarry site Locus 2 (Costello *et al.* 1992). This type of extraction process, which has been referred to as a prospect, usually fails owing to the difficulty in removing the chert (ore). Horizontal beds are most easily mined along cliff faces, or where the horizontal beds are interrupted by an erosional break in slope in the local topography, such as at Dutchess Quarry Locus 3 (in scree).

Joints are open fracture spaces in rock that form as a result of warping or folding of strata. They often occur in intersecting pairs, and the accentuation of jointing by groundwater activity leads to the development of karst ("sinkhole") topography. The Ontelaunee Formation exhibits all these traits. Because the Ontelaunee was multiply deformed during the Alleghenian mountain-building event, the jointing has been refolded. Despite this fact, excellent examples of well-integrated master joint systems are present within this Ordovician formation. The joint surfaces permit the use of mining tools such as levers and wedges to further accentuate the openings in the rock, increasing the ease of ore extraction.

Where bedding planes exhibit a contrast in grain size, the weaknesses therein developed may be exploited to break rock in a direction perpendicular to the joint surface. At many locations, where chert comprises a distinct unit between beds of dolomite, a force applied directly at the interface between the chert and dolomite will serve to dislodge the chert from the country rock.

During the development of regional folds, cleavage develops as a fabric within the rock, especially fine-grained rock. Cleavage is a preferred orientation of grains which appears as closely-spaced flat planes in microscopic thin section and hand sample. Although cleavage appears to be best developed in shales and slates, the fabric is ubiquitous in all deformed rocks. Because of the differences in rheology (style of deformation) between chert and dolomite, closely-spaced cleavage planes refract and widen as they penetrate chert nodules and beds. The spaces between fracture cleavage surfaces in chert vary from less than a millimeter to several centimeters in width, and the cleavage surface itself appears as a smooth, flat plane, much like that developed in a slate. Between fracture cleavages, the homogeneous chert is referred to as the microlithon and represents the template upon which the stone tool technologist begins lithic reduction.

The association of several closely-spaced, chert-rich beds presents an attractive target for mining activity. These beds are often left undisturbed, however, if they are not inclined or do not face an abutment.

QUARRY TYPES

During the past several years of quarry research, I have documented a number of different quarry types. These include conical pits developed in soil or regolith, inclined shafts cut through rock, terraced mines, screes, dip-slope mines, and declivities in horizontal strata. In the immediate study area, the prehistoric quarries are of the dip-slope variety. In this quarry type, the exposed limbs of gently-dipping folds are cut by more steeply dipping erosional faces, so that a succession of chert-bearing beds are exposed along a single slope. Joint blocks containing ore may then be easily removed without the development of a vertical shaft.

QUARRY INSTRUMENTS

The zones of extraction, or declivities, require the largest mining instruments. These are generally fashioned from metaconglomerates and less commonly from arkosic sandstones, gneisses, and quartzites. They usually display at least one wedge-shaped surface bearing large flake scars from battering. They range in size up to 100 pounds or more and are typically found in close association with the zones of extraction.

A second class of instruments includes milling and concentrating tools that weigh about half as much as the extraction tools. They are usually composed of arkosic sandstone and, to a lesser degree, quartzites. They are rectangular in shape and often display signs of crushing or battering along one or more edges. These tools are employed to free chert from its dolomite country rock, separate high and low tenor ore, and free chert along the microlithon surface.

The third class of instruments includes smaller hammerstones, which are roughly circular in outline and may possess a flattened upper surface. This class of tools is usually associated with non-portable anvils and reduction sequence debitage, related to the production of bifaces and cores, that is found on flat terraces above the quarry surface. The hammerstones are almost always made of quartzite.

MODEL FOR THE DEVELOPMENT OF A TYPICAL QUARRY: THE HOUSTON ROAD QUARRY

Steeply to moderately dipping strata are best suited to the extraction process. Gently dipping or horizontal strata are usually bypassed because they require the excavation of vertical, conical pits through the country rock to penetrate the chert-bearing strata. Conical pits in bedrock must be widened in all directions, and the floor of the pit must be constantly maintained. Beneficiation or upgrading the tenor of the chert is therefore difficult because the quantity of country rock so greatly exceeds the volume of chert extracted by this type of process. Horizontal beds are usually mined where they are exposed along a steep cliff face, where joint surfaces can be accentuated by lever methods.

The extent or dimensions of a potential quarry face, or declivity, are determined by the development of joint surfaces and the spacing between joints in the chert-bearing strata. The Cambro-Ordovician lithologies under investigation have undergone several episodes of tectonism and structural deformation that have led to the generation of multiple sets of joints, fractures, and cleavages that intersect at differing angles. This creates irregularities within the chert, rendering the mining practice more difficult.

The development of a quarry face or declivity, such as the ones created at Houston Road, begins with the accentuation of joint surfaces by the use of levers. The joint surfaces themselves may project through several beds of chert-bearing rock or may terminate randomly at any one bed surface. Accentuation of the joint surface proceeds by hammering wooden wedges into the open spaces. (At several locations within the Wallkill River Valley, expended quartzite hammerstones and anvils have been found wedged between joint blocks). This wedging procedure would generally take place in the autumn, allowing winter snow and ice to freeze in joint surfaces. The expansion and contraction of joints due to freeze-thaw then ruptured the rock along the joint surface. Quarrying activity is accelerated during the spring months when weakened joint-faced blocks are loosened by the use of levers, and the blocks of ore are transported to a position below the quarry face. This procedure of accentuating joint surfaces will continue until the joint surfaces connect from different directions, thereby creating a vertical notch projecting into the quarry wall, which is then bounded on its lower surface by a flat bedding plane. The bedding plane serves as a stable platform for quarry operations.

Extensive exploitation of the joint surfaces over a prolonged period of time results in the development of a stepped surface within the v-shaped notch (which has been referred to as a declivity; the controlling joint surfaces from which chert is extracted are referred to as the master joint system). Generally, declivities are abandoned when the volume of country rock on the stepped floor of the quarry so greatly

exceeds the volume of ore to be extracted that further extraction of the ore is not economically viable. Usually, the declivity is abandoned for an adjacent area of easier extraction. Thus, as declivities are developed along vertical faces in inclined strata, the profile of the quarry takes on a saw-toothed form, bearing a series of both active and depleted and abandoned declivities. Historically this process is called stoping. The extraction process leaves behind pedestals or pillars of ore. In fully developed quarry surfaces, widely-spaced declivities are bounded by projections of undisturbed pedestal rock. The convergence of two declivities results in the formation of a v-shaped projection which, being ore-rich, is vulnerable to mining from both sides of adjacent declivities. Where the lateral distribution of chert occurs as boudins or disconnected pods, the pedestals are usually chert-free and left standing between declivities, as was the case in the Wallkill River Valley within the Cambro-Ordovician lithologies.

At the Houston Road quarry, close inspection of the declivity surface reveals the presence of cuspate surfaces and v-shaped notches. The cuspate surfaces are essentially carved into the exposed chert, although the upper edges have been pounded into a white, saccharoidal external rind. The dimensions of the cuspate surfaces precisely match the outline of the outer edge of the metaconglomerate extraction tools. Where the castellated surfaces are not present, a small v-shaped notch penetrates the chert along the wall. The v-shaped notches represent an area in which crushing was successful in removing chert along intersecting fracture cleavage surfaces. Thus the presence of the cuspate surfaces suggests a failed attempt to extract chert. The block removed from the wall is bounded on two sides by intersecting fracture cleavage surfaces, and the upper face of the chert bears battering marks and the remnants of a partially developed cusp surface.

ORE PROCESSING STATIONS

Even within historic mines, ore is never hoisted above the mine surface. It is instead dropped below to a stable area where it is concentrated before removal from the mine. The same is true in prehistoric quarries. The extracted fracture-faced blocks are dropped below the quarry face to a stable platform which serves as an ore processing station. Several activities take place in the ore processing station, of which the most important is referred to simply as ore dressing.

Ore Dressing

The ore dressing process involves the separation of the dolomite or limestone from the chert. The limestone and dolomite blocks form a tailings pile of little or no value. The dressed ore, bounded by numerous close-spaced fracture surfaces, is now free of gangue. Observations at Houston Road indicate that the ore was transported manually to either side of the tailings pile, but generally not any farther below it.

Ore Grading, or Further Beneficiation

At some position to either side of the tailings, ore of all qualities or tenor is placed into piles for inspection. Here blocks of chert bounded by fractures are placed on large anvils and further reduced to rectangular and wedge-shaped blocks by crushing the upper surfaces with quartzite wedges and splitters. The anvils are generally large blocks of extracted, low tenor ore or country rock, which serve as temporary stable areas along a steep slope. At these locations, ragged edges are removed from the joint blocks, and the chert is cleaned of highly fractured material. Low tenor ore in the form of large blocks and shatter is discarded along slopes at these positions. High tenor ore, or chert bounded by even fracture surfaces and bearing highly translucent phases of silica, is further separated from the ore and transported to a surface above the quarry. An intermediate type of ore, one which bears both high and low tenor chert, is found abundantly at these locations. Large blocks of low tenor chert may contain small patches of high tenor ore that are suitable for stone tool manufacture. These blocks will be further split and broken along fracture cleavage surfaces to release the desirable chert. During this process, the fracture cleavage and joint

surfaces of the block are removed. The result is a quarry core, which serves as a source of small quantities of high tenor chert, but itself never leaves the quarry surface.

The Reduction Sequences

The finer reduction of the chert, i.e., the production of stage one bifaces and cores, is conducted above the quarry face. My research in the Wallkill River Valley clearly indicates that the finest scale of reduction that takes place in the quarry occurs above the zones of extraction. High tenor ore is transported from the processing stations to a stable area above the declivity. Non-portable anvils that serve as stable work stations for skilled technicians are usually found here and are generally fashioned from quartzite glacial erratics. The glacial erratics are typically surrounded by an apron of fine flaking debris produced as the fracture-bounded blocks of ore are flaked into bifaces and cores. Organized clusters or piles of small pieces of chert are common at these locations, as are discarded pieces of chert which do not pass final inspection.

CONCLUSION

I recently discovered several extensive prehistoric quarries developed within both the Beaver Run and Harmonyvale members of the Ontelaunee Formation in the vicinity of the Dutchess Quarry site. The most extensive of the quarries, Houston Road, is a series of declivities located within the middle chert-bearing unit of the Beaver Run Member. Rapid facies changes between the upper unit of the Beaver Run and the Harmonyvale member permit the development of a second large quarry, the Lower Road Quarry in Unionville, New York. Quarries developed within the lower unit of the Beaver Run Member represent unsuccessful attempts at quarrying (New Quarry #1). Where the Crooked Swamp Member of the Rickenbach Formation is exposed at a thrust surface one mile to the east of Lookout Mountain, a successful quarry operation is established.

Lookout Mountain, above the Dutchess Quarry caves, contains a series of vertical prospect pits (Locus 2), three failed declivities in gently inclined strata (Locus 5), and the successful quarry operation developed within a scree (Locus 3) (Figure 3). Traditionally, the chert-bearing sequences are associated with chert-bearing horizons in the Ontelaunee Formation. Exposed along the southwest face of Lookout Mountain, within the same stratigraphic horizon as the caves, is a series of algal stromatolite zones bearing chert. The uppermost of these zones is made visible by these biogenic structures in the base of the prospect pits of Locus 2 (Figure 4). A second, lower marker horizon is exposed at Locus 3 and Locus 5. Stromatolites are also abundant at the Houston Road Quarry, where they serve as a useful stratigraphic guide in locating both the Beaver Run Member and chert-bearing units. The spatial distribution of the various quarry activities at Lookout Mountain suggests that the algal marker horizon and associated chert-bearing units were mined out systematically where they were exposed. This could have been accomplished by traversing perpendicular to stratigraphic strike until the chert and associated stromatolites are encountered, and then following the outcrop pattern along stratigraphic strike.

The integrated quarry activities atop Lookout Mountain are minor, largely due to the fact that the upper unit of the Beaver Run Member of the Ontelaunee Formation is largely chert-deficient. A natural beneficiation of the ore takes place where the gently inclined beds are intersected by an equilibrium slope, creating the scree at Locus 3. Here chert could be easily removed where the beds jutted out along a moderate slope. The presence of cuspate surfaces on chert blocks also suggests that the chert was worked from beds that were in place along the quarry wall by a procedure very similar to that employed at Houston Road. Large metaconglomerate extraction instruments were located at the base of the scree, and quartzite impact spalls were discovered mixed in with the tailings along the face of the scree. The spatial distribution of the various quartzite instruments discovered in and around Locus 3 strongly resembles the distribution reflecting task subdivision at Houston Road.

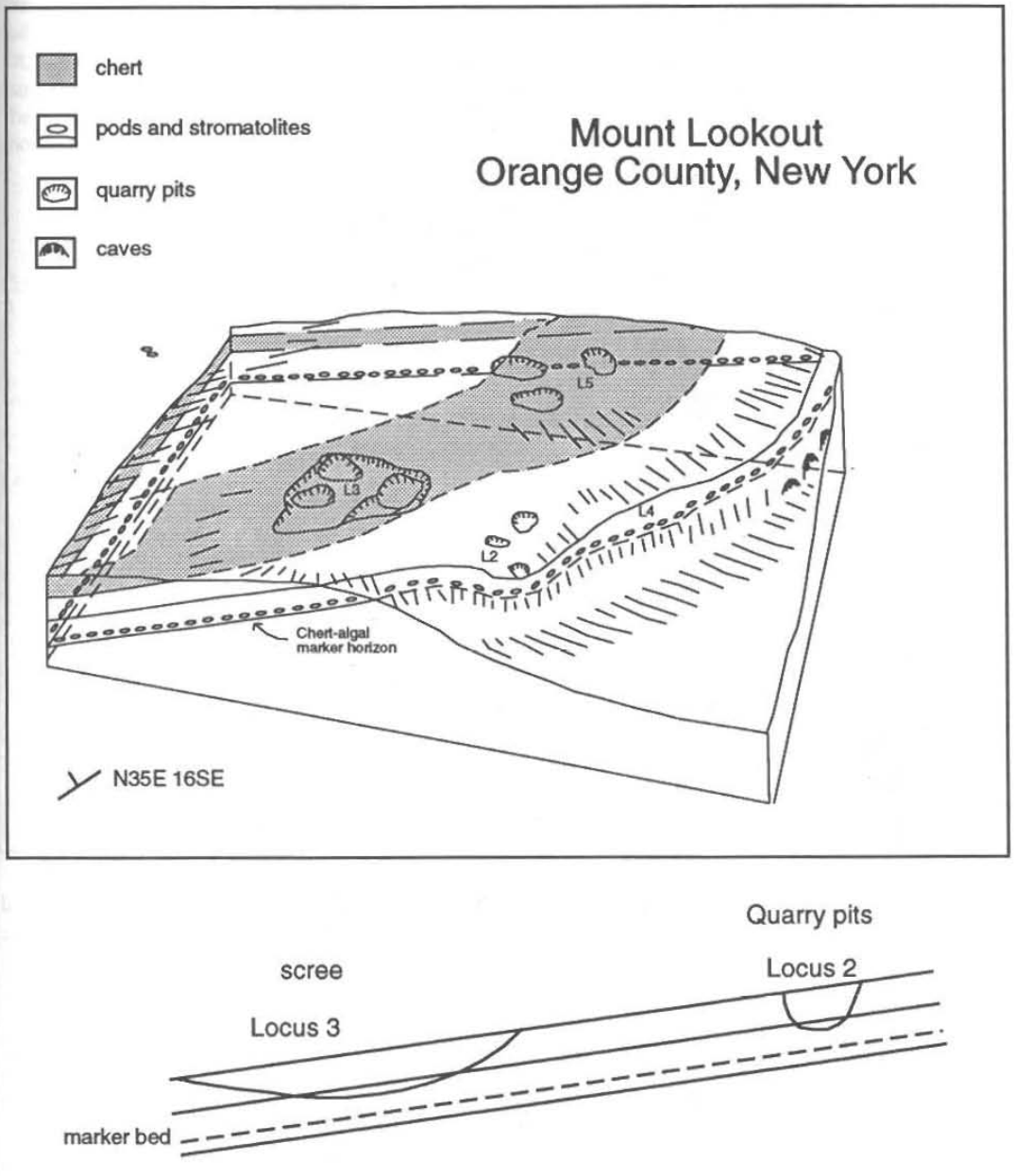


Figure 3. Block diagram of the lithology of the prehistoric quarry at Mt. Lookout. This schematic clearly illustrates three chert-bearing marker horizons, of which the upper two intersect Locus 3. The beds are inclined 15-20 degrees to the southeast and the lowest marker horizon projects out from the western wall of Mt. Lookout.

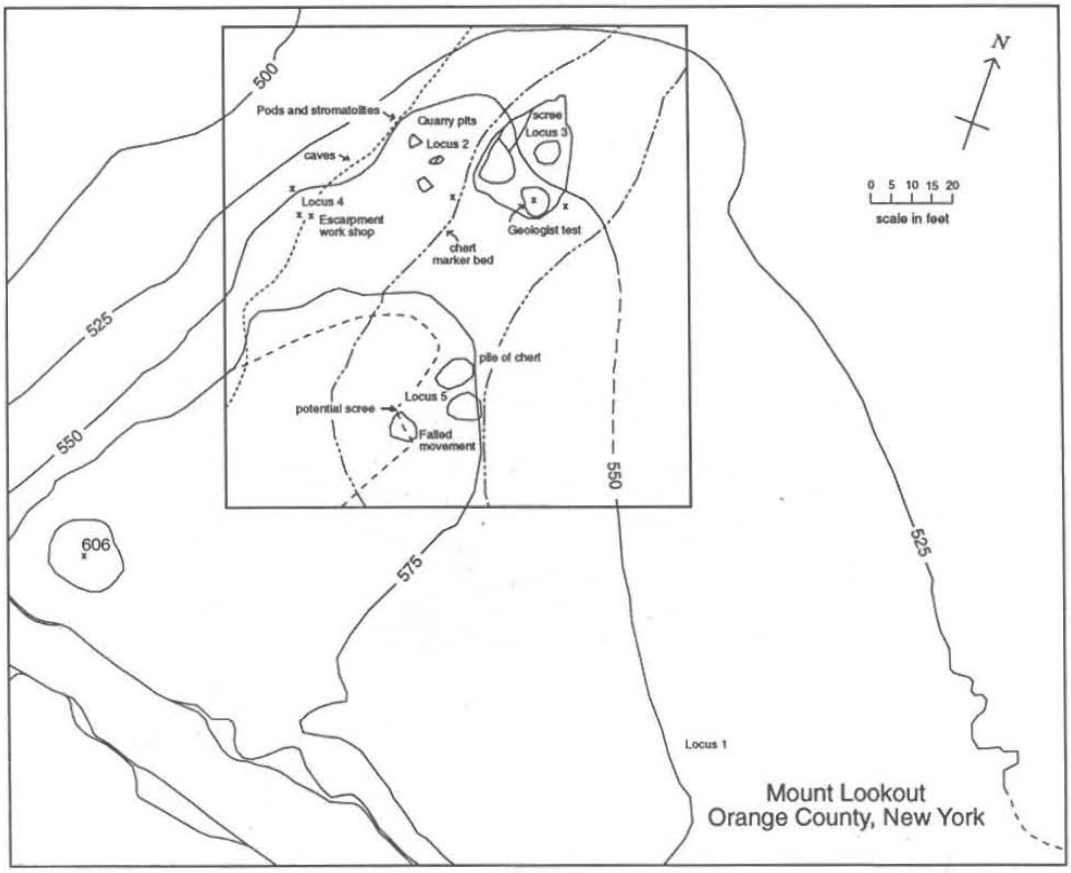


Figure 4. Prehistoric quarry features -- Mt. Lookout. This contour map illustrates with dotted and dashed lines the surface distribution of the chert-bearing horizons and chert marker beds. The prehistoric features (Locus 1 through Locus 5) are outlined on the map.

The remains of quarry activities at Lookout Mountain suggest failed attempts at "folk mining" activity. Only the scree at Locus 3 represents a development of a declivity that was successful for some period of time. Certainly, the quarry activities at Houston and Lower Roads were more successful because they were located stratigraphically within the chert-bearing portions of the Ontelaunee Formation. It is important to note that the technology at all these locations was apparently shared. Both the quarry extraction process and "tool kit" are similar at each location.

Furthermore, examination of diagnostic Orient Fishtail projectile points and associated bifaces recovered from Locus 1 along the eastern side of the mountain yield the following information. The scanning electron microscope (SEM) characterization of the chert employed to fashion the Orient Fishtails matches the Crooked Swamp chert located at New Quarry #1, located one mile to the east. The large, pale gray-blue bifaces and biface thinning and reduction flakes suggest provenance in the upper unit within the Harmonyvale Member at the Lower Road Quarry, seven miles to the west. The association of both Lamoka and Orient Fishtail projectile points, fashioned from Crooked Swamp chert and found with large

bifaces of Harmonyvale chert, is common in the upper watersheds of the Wallkill River Valley. Tests on both varieties of chert suggest that the clay-deficient Crooked Swamp chert is extremely brittle and does not thin or resharpen well, rendering it useful for projectile points as impact instruments. On the other hand, the Harmonyvale chert has a high illite clay content that is amenable to resharpening in biface form. The association of these two cherts in artifact form originating from two specific quarries suggests shared knowledge of the characteristics of the chert and the whereabouts of suitable outcrops.

REFERENCES CITED

Costello, M.A., R.C. LaFleur, K.S. Hartgen, J.W. Bouchard, A. Krievs, and P.C. La Porta
1992 Dutchess Quarry & Supply Company, Inc. Cultural Resources Survey Stages 1 and 2, Goshen Quarry Future Mining Area, Town of Goshen, Orange County, New York: Report prepared by Dunn Corporation and Hartgen Archaeological Associates.

Knopf, E. B.
1946 Stratigraphy of the Lower Paleozoic Rocks Surrounding Stissing Mountain, Dutchess County, New York. *Abstracts of Geological Society of America Bulletin* 57:1211.

La Porta, P. C.
1989 The Stratigraphic Relevance and Archaeological Potential of the Chert-Bearing Carbonates Within the Kittatinny Supergroup. 61st Annual Meeting of the New York State Geological Association *Field Trip Guidebook For 1989* pp. 240-269. Middletown, New York.
1994 Lithostratigraphic Models and the Geographic Distribution of Prehistoric Chert Quarries Within the Cambro-Ordovician Lithologies of the Great Valley Sequence, Sussex County, New Jersey, In Recent Research into the Prehistory of the Delaware Valley, edited by C.A. Bergman and J.F. Doershuk, *Journal of Middle Atlantic Archaeology* 10: 47-66.
n.d. *The Cambrian and Ordovician Carbonates of the Wallkill River Valley: The Nature of the Diagenesis of Chert and its Archaeological Behavior*. Ph.D. dissertation in progress, Queens College of the City University of New York, New York City.

Markewiecz, F. J. and R. Dalton
1974 Subdivision of the Lower Ordovician Epler Formation in New Jersey. *Geological Society of America Abstracts with Programs* 6(1):52.
1976 The Lower Ordovician Ontelaunee Formation in New Jersey. *Geological Society of America Abstracts with Programs* 8(2):225-226.

Reprinted with Permission.
LaPorta, Philip C., 1996, Lithostratigraphy as a Predictive Tool for Prehistoric Quarry Investigations: Examples from the Dutchess Quarry Site, Orange County, New York, *in* Lindner, C., and Curtin, E.V., A Golden Chronograph for Robert E. Funk: Occasional Publications in Northeastern Anthropology, no. 15, p. 73-84.

8

A Geologic Model for the Development of Bedrock Quarries, with an Ethnoarchaeological Application

Philip C. LaPorta

Introduction

A long-term field study of the distribution of prehistoric bedrock quarries and quarry-related activities in the Central Appalachians, U.S.A., has revealed strong relationships between the stratigraphy and structural deformation of bedrock, the surface expression of the bedrock on the landscape and the ease to which the bedrock may be quarried for the raw materials sought after by prehistoric peoples (LaPorta 1989, 1994). Local variations in bedrock stratigraphy (*i.e.*, facies changes) and the type of structural deformation have an impact on the style and extent of quarrying activity. However the physical constraints introduced by bedrock stratigraphy and structural deformation ensure that there are common elements not only in the development and layout of quarries but also in the size of the tools that can be manufactured and the tool kit that is required, regardless of geographic setting. The repeated, successful extraction of raw materials across the landscape suggests that these physical geological constraints were recognized in prehistory, yielding a kind of 'folk geology' knowledge. The application of such knowledge belies the commonly held view that raw material extraction in prehistory was largely an expedient affair with relatively little forethought.

This paper presents a conceptual framework for investigating prehistoric bedrock quarries. It discusses the factors that influence prehistoric bedrock quarry development and introduces a hierarchical classification scheme to distinguish between varying levels of mining effort, towards a folk geology concept. Modern mining terminology is employed to describe the chain of operation (Godoy 1985) within a typical quarry, and the tool kit associated with each task. The universal impact of physical geologic constraints on bedrock quarry development is then illustrated by ethnographic analogy to modern hard-hammer, hand-mining methods in southern India.

General Model for Bedrock Quarry Development

Traditional archaeological investigations of lithic artifacts infrequently address the importance of quarries, usually relegating the subject. Researchers are led to believe

prehistoric lithic technologists happened upon a utilizable piece of raw material, from which diagnostic pieces such as bifaces and cores were fashioned. This view, however, fails to account for earlier steps in extracting the raw material, or the cultural information before the 'blank'.

More recent studies (*e.g.*, LaPorta 1989, 1994) have argued that the structural history of the rock determines the spatial distribution of quarry areas and associated reduction sequences (refinement centers) more often than does the simple presence of chert. Field observations of the distribution of prehistoric bedrock quarries and quarry-related activities in the Wallkill Valley of New Jersey-New York (1988 to 1995) revealed strong relationships between stratigraphy and structural deformation of the Cambrian-Ordovician carbonate rocks, the surface expression of these rocks on the landscape and the ease to which the bedrock may be quarried for the chert raw material sought after by prehistoric peoples (LaPorta 1989, 1994, 1996). The complexly deformed and fractured cherts tend to be somewhat difficult to extract; access to jointing and bedding surfaces is much more difficult since these surfaces are no longer relatively smooth and even and the ore units are generally rather small in size. These chert targets thus pose a challenge to the ingenuity of the prehistoric miner.

Subsequent field studies into raw material sources derived from other geologic formations and in other structural settings (*e.g.* Raemsch & LaPorta 2001) indicate that similar physical constraints also control raw material extraction, with some modifications appropriate to the specifics of each setting. For example, cherts found in the Silurian and Devonian strata of Pennsylvania and New York State have experienced less deformation overall, providing easier access to joint planes and bedding surfaces and permitting the extraction of larger ore units. These individual cases have provided the basis for the development of a general model for bedrock quarry development.

General Criteria for Bedrock Quarry Development

The development of a quarry, and the type of extraction processes employed, depends upon several factors:

1. Concentration of raw material-bearing units
   The association of several closely-spaced raw material beds (*e.g.*, chert beds) presents an attractive target for mining. The close spatial proximity of two or more raw material units increases the ore value (*i.e.*, the tenor of the ore).
2. General inclination, or dip, of the raw material-bearing rocks into the subsurface (bedding attitude)
   Levers and wedges can be used to extract chert from beds dipping 10° or more. Raw material extraction from horizontal, or sub-horizontal beds, usually involves the removal of great quantities of overburden, unless the beds are exposed along the face of a cliff.
3. Thickness of the surrounding rocks
4. Thickness of the ore within a bed
   Criteria 3 and 4 go hand in hand, as they involve an assessment of the worthiness of the mining effort. The ore may be very high grade, but if the surrounding rocks are too thick the effort expended may be too great to make quarrying worthwhile. Alternately, the ore

may not be the best grade of material, but if the surrounding rock is relatively easy to remove, or if a number of low-grade ore beds are closely spaced, the ore value is increased and the lower-grade ore may become the preferred target.

5. Presence of well-defined bedding planes
   Where bedding plane surfaces exhibit a contrast in grain size, the weakness therein developed may be exploited to break rock. At many locations, where chert comprises a distinct unit between beds of dolomite, a force applied directly to the interface between the chert and dolomite is sufficient to dislodge the chert.
6. Presence and orientation of joint surfaces
   This is particularly important with regard to conjugate joints (intersecting joint sets) and/or fracture cleavage; the domains of the cleavage and joints serve as the focal point for wedge and lever work. The volume of chert between the cleavage domains (microlithon) is the ore of varying grade to be mined.
7. Presence of a stable platform below the zone of extraction
   The stable platform in front of or below the zone of extraction aids in providing access to strata from a position above, on the side, or below the quarry face.
8. Availability of glacial till which includes boulders of high-rank metamorphic rocks (preferably quartzites), or else another minable formation of suitable material as a source for hammerstones
   The full-scale development of a quarry relies upon the prevalence of hammerstones of varying degrees of elasticity. Glacial till near the Wallkill Valley bearing Silurian-age metaconglomerates, quartzites, arkosic sandstones and argillites provides the mining tool kit necessary for the development of a quarry that includes the full range of task subdivisions.

Since the above criteria are typically met to varying degrees at any one location, the extent of quarrying activity may also vary. As a means of classifying the level of quarry activity in a given location or over a particular region, we have developed a hierarchical classification scheme based upon terms used in modern quarry/mining operations. Any aspect of mining or prospecting is referred to as an *expression.* Successful expressions evolve into *motions.* Successful motions may then expand to become a full-scale quarry *movement*, *i.e.*, a successful quarry or the successful orchestration of rock from the earth. All quarries located along strike, within a particular series of geologically related formations, are referred to as a *trend.* All trends that are spatially clustered and bound within one geological province are referred to as a *district.* Expressions, motions, and movements can be incorporated into regional mining trends and districts, with accompanying inliers and outliers. All districts comprise a *metallogenic province.*

Chain of Operation within a Quarry

Where all stratigraphic and structural criteria are met, a *zone of extraction (Zone 1)* is created (Fig. 8.1). The actual quarry face, or mine surface, is the zone of extraction. Evacuated or abandoned quarry faces are referred to as *declevities*, V-shaped depressions cut into the vertical face of an outcrop by accentuating the master joint system. (This activity is a form of stoping). Below the face of the declevity is a scree slope bearing a conical apron of quarry debris that includes the ore, country rock and abandoned

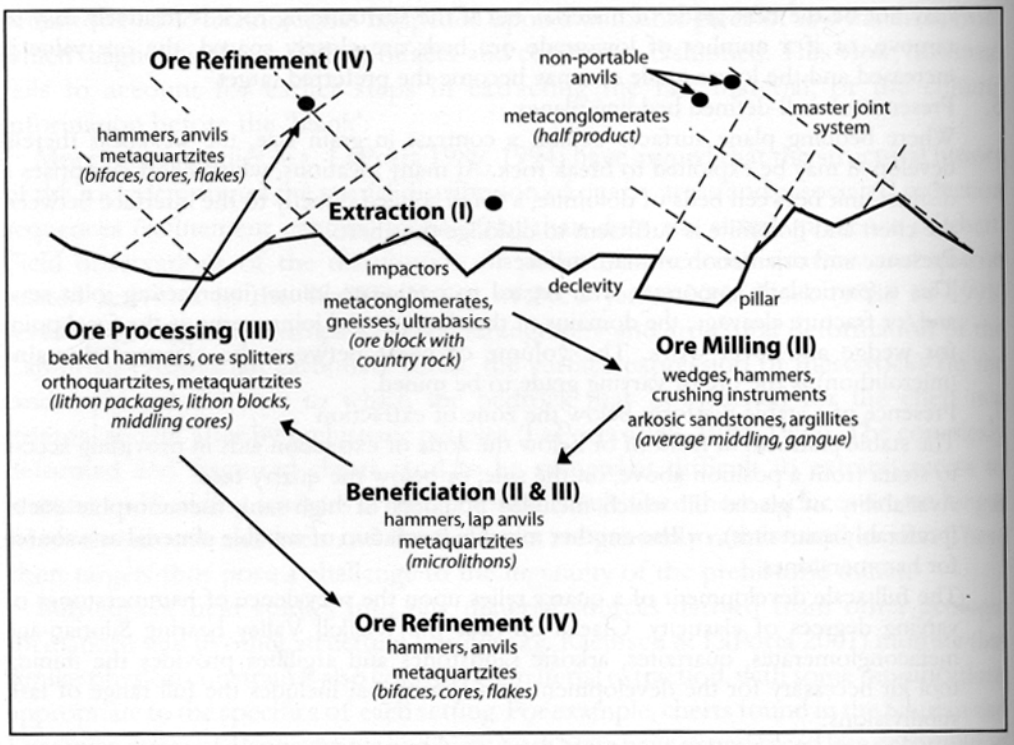


Fig. 8.1. Schematic plan view of a typical quarry, showing the spatial relationship between task areas in each zone of the mine (bold type), the diagnostic quarry instruments for each task (normal type), and their associated class of mining debris (italics). The zone of extraction (zone I) is part of the active quarry face itself. Ore milling, beneficiation and processing (zones II and III) take place on a stable platform in front of the quarry face. Ore refinement (zone IV) may occur either on the stable platform or above the active quarry face

mining instruments. Located on either side of the zone of extraction is a stable platform supporting the vital working areas associated with the prehistoric mine; *zones of milling* associated with freeing the ore from the gangue (Zone II).

The separated raw material is then transported to *ore processing stations* (Zone III) where the ore is crushed along open joint surfaces in order to free homogeneous pieces. The varying physical properties of the raw material are generally appraised, winnowed and concentrated into small isolated areas in Zone III. The milling and concentrating processes are referred to as *ore beneficiation*. During ore milling and processing, hammers of various lithologies and specific weight classes are employed to crush the ore along the fracture cleavage planes mentioned earlier, eventually removing all remaining open fractures and separating grades of ore based on diagenetic properties, and to select pieces based on domainal spacing. As a result, mill areas are designated by the presence of large, angular fragments of broken country rock with associated low grade ore adhering to the surface, and abundant angular fragments of

low grade ore split along the surfaces of domainal cleavage and close-spaced joints.

From the processing station, high-tenor ore may travel in two possible directions. The ore is generally brought above the quarry surface to an elevated flat area overlooking the quarry, where it is flaked into bifaces and cores employing large non-portable anvils (Zone IV). At some quarry locations, however, the ore is further removed from the quarry face to flat low-lying areas, usually where quarry support sites occur in close association to the quarry extraction zone. Here workshops and factories bearing half-product (bifaces, cores, and flakes) occur in association with finer classes of lithic debris, or tailings.

Tool Kits and Task Subdivision

Partial confirmation for the existence of organized quarry task subdivision comes in the form of an organized mining technology, often fashioned from high rank metamorphic rocks (Fig. 8.1). The zone of extraction is usually associated with the presence of large boulders that may weigh anywhere from 20 kilograms to several hundred. Hammers of this weight class are necessary to free the blocks along the master joints, and may have been manipulated with the help of wooden levers or trusses. Zones of ore processing are indicated by a class of smaller hammerstones (typically 5kg to 21kg). Owing to the precision required for crushing the ore along fracture cleavages, hammerstones found in concentrating areas tend to be at the lower end of the weight spectrum for this class. Refinement stations located above the quarry face are associated with the smallest hammerstones (less than 1kg to 2kg) in close proximity to non-portable anvils. These small hammerstones are commonly found in nested clusters that may represent organized tool kits designed for specific types of lithic refinement.

Modern Bedrock Quarry Development: An Example from Tallicoot, Southern India

The general model for bedrock quarry development described above is hypothesised as being applicable to any hand-excavated quarry location, during any time period, since the mechanics of the raw material source and its exposure upon the landscape are largely independent of cultural issues. Bedrock quarries may be developed as long as the local people are cognizant of the physical constraints on their activities.

Here a modern ethnographic example is discussed that illustrates this type of cognition (folk geology). In the southern Indian state of Karnataka there is a district of open-cast limestone quarries near the town of Tallicoot, located at the northern edge of the Bhima basin (Fig. 8.2). These hard-hammer, hand-operated quarries are operated by miners from Tallicoot and neighboring villages. Although there have been modern influences on some specific aspects of stone extraction and subsequent transport, such as the use of steel railroad spikes as chisels, many of the criteria for bedrock quarry development – established through the examination of prehistoric quarries –

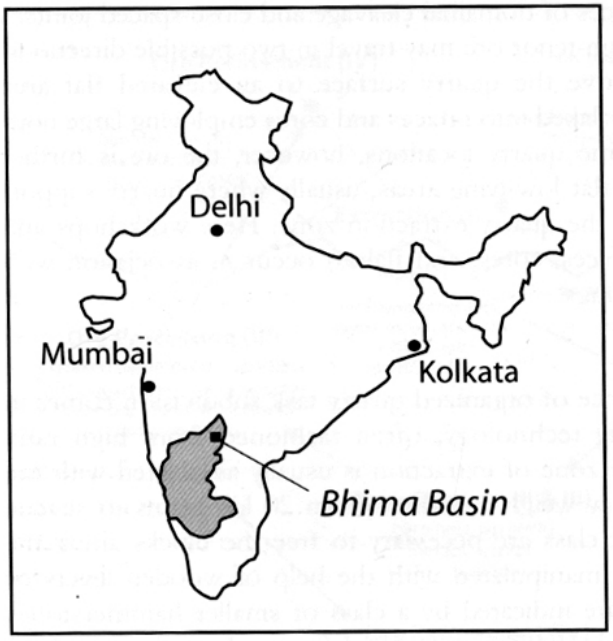


Fig. 8.2. Map highlighting the state of Karnataka (shaded gray) in relation to major Indian cities. The quarries of Tallicoot are located within the Bhima basin in northeastern Karnataka

are applicable in Tallicoot as well.

The geologic setting and potential influences on quarry development will be briefly described, and a description of the activities that have been observed will be provided. The utility of ethnographic studies in understanding the archaeological record will be discussed.

Geology of the Tallicoot Region, India

The Bhima basin is one of several in India (collectively referred to as the Purana basins; Kale & Phansalkar 1991) in which the rocks are more than 545 million years old. Located in the southwestern Indian state of Karnataka (Fig. 8.2), the Bhima basin has an areal extent of approximately 5,200 square kilometres, with a maximum width of nearly 40km (Radhakrishna & Vaidyanadhan 1994). The thickest lithostratigraphic unit in the basin, and also the most economically important, is the limestone of the Shahabad Formation. The blue-gray limestone is fine-grained and dense, has a waxy luster and breaks with a conchoidal fracture. One variety of this limestone has a tendency to break along bedding planes into thin slabs suitable for paving and polished facing stone; a blockier variety is suitable for cement production. Both varieties are extensively quarries by the Tallicoot miners (Radhakrishna & Vaidyanadhan 1994). A distinctive feature common to all the Purana basins in India is their relative lack of structural deformation, despite their ages. The Bhima basin is no exception; limestone and sandstone beds dip at very low angles, often just a few degrees. There is, however, a strongly expressed set of conjugate master joints which intersect at nearly right angles.

Along the northern edge of the Bhima basin (and partially obscuring it) are the extensive basaltic lava flows of the Deccan Traps. Approximately 2 km thick, and covering an area of approximately 500,000 square kilometres, the lava flows were deposited over the course of approximately 2 million years, about 65 million years ago (Radhakrishna & Vaidyanadhan 1994). A number of flow units have been identified through geochemical analyses, but the bulk petrological composition is fairly uniform. The basalts are gray-green to green-black, fine- to coarse-crystalline (in the interior of

the flow) to glassy (along the margins of the flow, where the lava cooled quickly to form larger crystals). The tops of the basal flows are vesicular (pockets created by escaping gases that were subsequently filled by secondary minerals). The primary economic use of the Deccan basalts today is as road metal or railway ballast, although some of the secondary minerals have value as semi-precious stones or as filtering materials in industry (Radhakrishna & Vaidyanadhan 1994).

Quarry Activity at Tallicoot

Many of the limestone quarries are shafts that are 3m × 3m to 4m × 5m on the surface, plunging vertically to a depth of 2m to 8m and terminating near the basal limestone-shale contact. Along the sides of the shafts are numerous smaller prospects. The surface outcrops of the prospects are pried upwards and the landscape bristles with dislodged and overturned limestone beds. The prospects range in size from 1m × 2m to 5m × 5 m. Lying in direct contrast to the vertical shafts, and overturned prospect limestone beds, are a series of more expansive quarry operations. These expansive undertakings are fewer in number but comprise the upper echelon of mines in the district. These quarry types are approximately 100m to 200m in length, less than 50m to 75m in width, and are elongate, or pod-shaped, in outline.

Quarry Expressions

Small prospects cover the entire landscape, and in some cases, may be found even in dry riverbeds (Figs. 8.3 and 8.4). The prospects range in size from 1m × 2m to 5m × 5m and are characterized by disrupted, dislodged, and/or overturned limestone beds. The limestone beds are flaked and battered along their edges and upper surfaces. The quarry workers were observed mining the prospects by hammering the beds from above, raising the ruptured bed upwards with hands and or pry bars, then placing failed and exhausted mining hammers underneath the upturned beds (Fig. 8.4). From this position, the hammerstone is employed to snap the bed by directing a blow from the top, driving the bed downward. Beds broken in this fashion have irregular edges, although their upper and lower surfaces are flat bedding planes.

Dolerite hammerstones at the quarry prospects were observed being lodged by quarry workers in between beds of limestone (Fig. 8.4). The weight of the hammerstones ranges from 2kg to 8kg each. Hammerstone morphology varies from circular, to ovate, to crescentic. The upper edges are always battered, or faceted, and projections, beaks and castellations are visible on and along the outer edges of the hammers. The quarry workers did not haft the hammerstone, but the hammers, as well as the quarry technician's hands, were occasionally wrapped in cloth, while the hammers were being employed. As the hammerstones diminished in size and weight though use, the quarry workers would employ the hammers as levers, wedges and pry bars. Hammerstones that split along relict joint surfaces, or broke prematurely along mechanically weak slickenside surfaces, were wedged by quarry technicians between limestone beds, or employed to balance a nearly horizontal slab.

8.3 8.4



Figs. 8.3 and 8.4. A two-member quarry gang exploits (develops) an expression within a dry riverbed. The horizontal limestone units are raised, and steel railroad spikes fashioned into chisels are placed underneath the beds (Fig. 8.3). A beaked and cuspate dolerite hammer may be placed underneath the pried-up beds as a wedge for further splitting (Fig. 8.4)

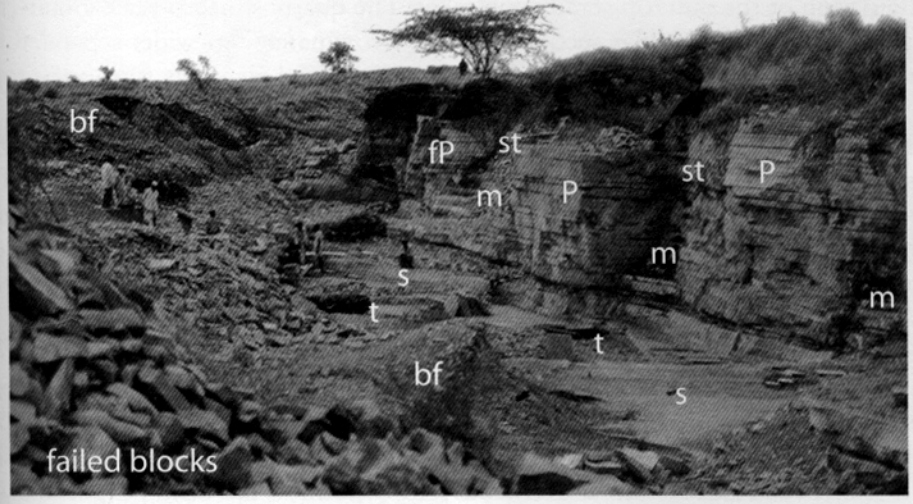
The lack of a discrete zone of extraction, the small areal dimensions of the prospects and the abundant geographic distribution of the prospects across the landscape infers that these quarry elements are *expressions* of mining (LaPorta 1990). The prospects represent reconnaissance for ore economically suitable for mining.

Quarry Motion

An intermediate class of quarries are vertical shafts which occur in lesser numbers than the above-discussed prospects, an abundance ratio of approximately 1:4. The intermediate quarries were not in operation at the time of the field investigation; however, measurements were taken of the quarry exposures (Figs. 8.5 and 8.6). All of the shafts are vertical, attaining a depth of 3m to 10m. The areal extent of the quarries is approximately 3m × 3m to 5m × 5m, with disrupted and overturned limestone beds that radiate away from the vertical axis of the shaft. The overturned beds represent large back fill piles, with dolerite hammerstones and hammerstone fragments comprising a small percentage of the back-fill-lithic population. The walls of the mine shaft are vertical joint surfaces. Unlike the smaller class of prospects (expressions), which are accessed through weakened bedding planes, the shafts are developed through the accentuation of tightly sealed joint spaces. Overburden and backfill piles radiate outwards from the lip of the shaft and slumping has caused some of the tailings to fill in the empty shaftways. In a few examples, the shaft walls widen significantly with depth, imparting a bell-shape to the shaft morphology. This is particularly the case when the limestone beds are nearly horizontal. The shafts attain a diameter that is twice as wide at its base than at its lip or entrance. The widening of the shaft is interpreted as a form of stoping. Evidence indicating the method employed to

8.5





8.6

Figs. 8.5 and 8.6. View of a Tallicoot quarry. Note the locations of the taskmaster (beneath the tree at top of quarry), the quarry technician (on the stable platform) and the quarry gang (at left) (Fig. 8.5). Salient features of a quarry: P = pillar, fP = failed pillar; st = stope; m = motion; s = stable platform; t = trench; bf = backfill (Fig. 8.6)

haul rock to the surface was lacking. During the initial reconnaissance there was no evidence suggesting that any of the shafts were connected in the subsurface. In most cases, subsurface connections were difficult to determine because most of the vertical shafts were partially or completely filled with refuse.

The presence of a shaft (rudimentary extraction zone) and backfill pile, the increased areal dimensions of the shaft proper, and the decrease in shaft population across the landscape (with respect to expression distribution) is evidence that these quarry structures are *motions* (LaPorta 1990).

Quarry Movements

The third class of quarries is the largest occurring within the district, attaining dimensions ranging from 100m to 200m in length by 50m to 75m in width. The limestone beds are horizontal and the quarries are aligned in a north-south trend direction (there may be stratigraphic or structural reasons for this preferred alignment, or it may involve aspect). These are the locations where the open-cast quarries reach their acme of development. This class of quarries does not include shaft development, but instead relies upon the presence of erosional topographic remnants projecting upwards from the quarry floor; although it is very possible that all expressions and motions were consumed and assimilated into this, the larger orchestration of rock. The dimensions of the quarries therefore are partially pre-determined by the configuration of the outcrop standing in relief. The quarry's macro-scale architectural elements include seven pillar sections, each approximately 9m wide; separated by a stope approximately 4m to 5m in width. All architectural elements run to the top of the quarry (Figs. 8.5 & 8.6). Infill material also includes failed quarry blocks and exhausted mining instruments. The pillar sections are roughly rectangular, slightly longer in the vertical direction, and bear smooth surfaces. The outer surfaces of the stope sections oftentimes bear flaked surfaces, while the pillar face is a smooth sweeping surface bounded by vertical joints. The stope and pillar sections serve dual purposes; rock extraction, but also widening the base of the quarry floor. The zone of extraction is present in the advancing quarry floor. In these quarries the principal ore is the flat-lying allochemical limestone, therefore the preparation of a stable platform at the base of the stope and pillar section is the most important aspect of the quarry, as the rock is exhumed from the base of the quarry.

The large size, restricted aerial distribution, and presence of an extraction zone indicate that these types of quarries are movements. The hypothesis has been proposed that all expression and motions were consumed and assimilated into the movement; however, it is not currently known or understood if the expressions or motions represent the progression in thought towards the development of the movement. It is possible now to postulate that the stopes may represent older motions, which have been intentionally intersected during the development of the movement. This hypothesis is supported by the observation of older backfill piles present in intersected slopes.

Ethnoarchaeological Observations

A quarry gang consists of five to seven individuals, plus a task master or quarry gang boss. Each member of the quarry gang was interviewed by the author during the field season about individual task responsibility, group task responsibility, and acquisition of quarry knowledge. The gang boss spends much of the day under an acacia tree above the quarry face, and from this vantage point, all orders are given and all business conducted (Fig. 8.5). The day starts shortly after sunrise, with careful hygienic maintenance of the quarry floor. All backfill and tailings remaining from the previous episode of mining are brushed and swept into new conical-shaped backfill piles near the back end of the quarry (Fig. 8.7). The quarry floor is then brushed clean of even small flakes until it is remarkably smooth. At this time the master joints are brushed clean and the quarry is staged for the next episode of extraction.

8.7



8.8





8.9



8.10

Figs. 8.7–8.10. Removal of limestone slabs from the quarry. A quarry gang member clears the floor of the stable platform before extracting the next slab (Fig. 8.7). The joint surfaces are brushed clean prior to extraction of the slab (Fig. 8.8). The extracted blocks are dressed and stacked for subsequent removal (Fig. 8.9). Quarry gang members transport the slab to a waiting truck outside the quarry limits as a quarry technician (far right) looks on (Fig. 8.10)

In the zone of extraction, on the stable platform, the quarry gang is led by a technician who possesses an intimate understanding of the limestone's mechanical properties. The gang of five workers rolls a large circular dolerite hammerstone out from the edge of the pillar section and it is left at the foot of the technician. The technician rolls the hammerstone along the bedding surface to a position over a sealed joint surface, where it is held stationary under the technician's foot. The hammer (30kg) is then raised by the technician, between his legs approximately 30cms to 40cms, and then dropped abruptly on the vertical joint. The hammer is then rolled with the hands or feet approximately 10cms and the process is repeated along the entire joint surface. When the technician reaches the point where the work began, the process is initiated over again until the joint is crushed everywhere around the circumference of the block. At any time during this process, the technician might ask for assistance or relief from one of the members of the quarry gang. Measurement shows that the block edges are crushed for a depth of 10cms on either side of the joint surface. Subsequent to this, the crushed limestone is brushed out from between the bocks, leaving a clean channel running between the limestone blocks, where the sealed joint used to be (Fig. 8.8). The flakes of crushed limestone are conchoidal to sub-conchoidal splinters, which are as long as the block is thick, and approximately twice as wide. The crushing action of the hammerstone fractures the limestone block along the bedding plane. However, the blocks are still attached at the base of the limestone platform (Fig. 8.9). An eight–sided pry bar is wedged at the intersection of the vertical joint and the stationary limestone platform. Gentle prying along the edges releases the block along the bedding plane. Once the joint-bounded blocks are severed away from the platform, they are stacked en-echelon towards the back of the quarry. The ore remains at that location until the arrival of a truck, which will bring the quarry blocks into town for sale as building stone. When the truck arrives, all members of the quarry gang carry each block of limestone to the back end of the truck, where they are loaded onto a flat bed (Fig. 8.10). Although it may only require two or three members of the gang to carry each quarry block to the truck, all members of the gang insist on touching the limestone block as it is loaded onto the truck. No mechanized vehicles are permitted into the quarry proper.

Prior to the initiation of the development of the movement, workers walk several kilometers into the laterite soils outside Tallicoot, where they use pry bars to exhume the spheroidally weathered boulders of Deccan basalt (Fig. 8.11). The boulders are both rolled and trucked to the site of the new quarry, while quarry gang members exercise ritual prayer and song. The core stones of the dolerite boulders are employed as hammerstones in the limestone quarries, while the vesicular and fine-grained chill zone basalts are transported into the community centers where they are fashioned into manos and metates in the village square. The dolerite hammerstones lie poised at the base of the pillar sections of the quarry, and no one is permitted to move them until it is time to crush the conjugate joint surfaces on the stable platform (Fig. 8.12).

The quarry possesses seven stable platform areas, which serve as the zones of

8.11





8.12

Figs. 8.11 and 8.12. Laterite soils thinly overlying the edge of the Bhima basin are the source of spheroidally-weathered dolerite hammers, which are recovered from pits several kilometers from the actual quarry (Fig. 8.11). Coarsely-grained dolerite hammerstone used for crushing joint surfaces, weighing approximately 30kg (Fig. 8.12)

extraction (Fig. 8.6). Each pillar section supports two platforms. The pillars are regularly maintenanced and are all the same height above the quarry floor. The trough excavated between each platform is filled with backfill material. The troughs, which are geologically defined by master joint sets, are the entrance points for the construction of platforms. The most important aspect of the trench configuration is that it allows the quarry operators to gain leverage over the horizontal limestone beds. Working from a trench, the technician can gain access to the master joint horizontally, rather than from a vertical position. Also, from this vantage point, the technician can appraise the depth of the limestone units. From that appraisal, the technician can estimate how continuous the ore is and more importantly, what structural or stratigraphic complications might arise during extraction. The construction of the trenches and the platforms, as well as their maintenance, is to be the responsibility of the technician.

Backfill piles, which line the back wall of the quarry, are roughly circular in form and are approximately as high as they are wide during their early stages of development. The backfill piles begin to coalesce after several episodes of extraction because the tailings are incorporated into one area of backfill (Fig. 8.6). The entire extraction episode is observable in the back-fill pile, even though several back filling episodes have been incorporated into one area. The separate back fill events do not loose their integrity and the extraction episodes can be differentiated. Also in cross-section, the en-echelon back fill layers representing episodes of mining lay li-par-li over each other. Occasionally, but not commonly, exhausted and/or failed hammerstones are incorporated into the backfill. However, more commonly, hammerstone flake spalls and granulated fragments are present. During the extraction process, members of the quarry gang will occasionally retrieve hammer fragments from the old backfill piles or tear apart a back-fill pile looking for hammer fragments to wedge under pried open beds of limestone.

Ethnoarchaeological Observations at the Tallipoor Living Quarries

The extraction of cultural information from archaeological sites usually entails addressing the functions of artifacts and features. While archaeologists are infrequently left with preservation, such as that seen in Pompeii, they can reconstruct past behavior. To do this, archaeologists create analogs through experiments, ethnographic analogies, or modern day inferences (Coles 1973, 1979). Archaeologists using ethnographic analogies, a process commonly termed ethnoarchaeology, study material relationships in contemporary societies to provide tentative explanations for material relationships found in the archaeological record (Gibbon 1984, 420).

Prehistoric archaeologists able to view extant traditions can collect much detailed data useful for interpreting archaeological remains by analogy (Watson *et al.* 1984, 261). When encountering old cultural continuity of a particular type, analogies of such archaeological data are considered advantageous. However, Watson et al. provide two

basic criticisms on ethnographic use in archaeology: (1) such use will bias and distort ethnographic research, and (2) too much attention is paid to particularistic data for rather narrow problems of archaeological interpretation. The first criticism is hard to defend since archaeological interpretation is in some way based on observations of modern occurrences. The second criticism is research dependent, since particularistic or generalized data depends on the research questions at hand.

Binford (1972, 60) notes that the ethnographic analogy provides a postulate that the behavioral context was the same in both circumstances, necessitating testable hypotheses to be formulated and tested. The model developed by the author compares a proposed interpretation, the model derived from Wallkill prehistoric quarries, with well-confirmed interpretations of the same general type, the quarry in India. While this is not meant to substitute testing of the model, it is used for checking and modifying the proposed model.

Discussion

Ethnoarchaeological research is critical in the search for constants or universals, the commonalities, of all quarries and mines. If the common factors involved are understood, then the inconsistencies and quarry nuances are also understandable. This understanding is a step towards developing the basic principles of prehistoric quarry development.

The application of the terms expression, motion, and movement explicitly point to a progression of thinking in the prehistoric mind, or the development of cognition of the landscape and its resources. Movements, motions and expressions are a red thread of prehistoric thinking, representing logical and linear thought progression in the mind of a miner. This logical and linear thought progression is the prehistoric practice of a 'folk geology' by prehistoric miners. The expression is the first contact with the rock, after the recognition that the ore exists or some useful mineral assemblage is present; it is the benchmark of the discovery. Expressions lead to the development of full-scale motions, which may fail due to stratigraphic or structural nuances or changes in the ore-bearing unit. Movements represent the development of large-scale architectural forms and transformation of thinking in the mind of the prehistoric miner. The movement (a repeated exercise) represents, for the first time, a point on a map, a political reference, possibly one associated with topographic features, specific soils, a unique drainage and even a specialized vegetation growth. It converts a featureless landscape into one with political references, boundaries and frontiers. Moreover, the movement is an architectural remnant which bears the imprint or signature of the quarry gang, an individual, or possibly a gifted technician. Ultimately the miner, the individual, leaves with a collection of experiences and memories which can be related to others and serves to collect as an oral history. The collected experiences of the miners embody the fabric of the folk geology concept. Only through the understanding of the hierarchy of quarry types can a miner arise at the 'folk geology' concept because

again it is the linear and logical progression of prehistoric thought. The thought process of the prehistoric miner is in essence 'fossilized in the rock'.

Ethnoarchaeological work, a time capsule of human behavior, it is a fleshing out of the rock extraction experience in a landscape usually parched by rock; lacking bone, written records, wood, material, human skeletal remains. Quarries are usually bleak experiences. The ethnoarchaeological exercise adds a new dimension, a narrative approach towards understanding the extraction of rock through the application of the basic principles of mechanics: the use of levers, wedges, fulcrums and accumulated knowledge. A sense of cognition is at work. These are the elements missing from eastern North American prehistoric quarries and other prehistoric quarries worldwide. It is not so much a question of what is similar in living quarries *vs.* prehistoric quarries; but more importantly, what elements are missing from the archaeological record that are visible in the ethnoarchaeological record. These are the critical questions.

Acknowledgements

Field research in the northeastern U. S. and the development of the bedrock quarry model was supported in part by a Dissertation Fellowship from the City University of New York and LaPorta & Associates, LLC. The ethnographic observations were made during a 1997 visit to Karnataka, India, supported by grants to M. Petraglia from the Office of International Relations, Smithsonian Institution; the Human Origins Program, National Museum of Natural History; the Leakey Foundation; and the Boise Foundation. The author thanks K. Paddayya of Deccan College (Pune) for his cordial hospitality and assistance in India; P. Topping for editorial assistance above and beyond the call of duty; and S. A. Minchak, L. E. Sohl and M. C. Brewer for assistance during the preparation of this manuscript.

References

Binford, L. R. (1972). *An archaeological perspective*. New York. Seminar Press.

Coles, J. (1973). *Archaeology by experiment*. New York. Charles Scribner's & Sons.

Coles, J. (1979). *Experimental archaeology*. New York. Academic Press.

Kale, V. S. and Phansalkar, V. G. (1991). Purana basins of peninsular India: a review. *Basin Research* 3, 1–36.

Gibbon, G. (1984). *Anthropological archaeology*. New York. Columbia University Press.

Godoy, R. (1985). Mining: anthropological perspectives. *Annual Review of Anthropology* 14, 199–219.

LaPorta, P. C. (1989). The stratigraphic relevance and archaeological potential of the chert-bearing carbonates within the Kittatinny Supergroup. *New York State Geological Association Field Trip Guidebook*, 61st Annual Meeting, Middletown, New York.

LaPorta, P. C. (1990). *The Stratigraphic Relevance and Archaeological Potential of the Cambro-Ordovician Kittatinny Supergroup of the Wallkill River Valley of Northern New Jersey*. MA Thesis, Queens College of the City University of New York.

LaPorta, P. C. (1994). Lithostratigraphic models and the geographic distribution of prehistoric chert quarries within the Cambro-Ordovician lithologies of the Great Valley Sequence, Sussex County, New Jersey. *Journal of Middle Atlantic Archaeology* 10, 47–66.

LaPorta, P. C. (1996). 'Lithostratigraphy as a predictive tool for prehistoric quarry investigations: examples from the Dutchess Quarry Site, Orange County, New York'. In C. Lindner (ed.) *A Golden Chronograph for Robert E. Funk*. Bethlehem, Connecticut. Archaeological Services. 73–84.

Radhakrishna, B. P. and Vaidyanadhan, R. (1994). *Geology of Karnataka*. Bangalore. Geological Society of India.

Raemsch, C. A. and LaPorta, P. C. (2001). Geological constraints on stone stool and debitage morphology at the Sage's Crossing Site. Unadilla Valley, New York [abs]. *Society of American Archaeology, 66th Annual Meeting Abstracts*, 57.

Rich, J. L. (1934). Mechanics of low-angle overthrust faulting as illustrated by Cumberland thrust block, Virginia, Kentucky, and Tennessee. *American Association of Petroleum Geologists Bulletin* 47, 1527–1536.

Watson, P. J., LeBlanc, S. A. and Redman C. L. (1984). *Archaeological explanation: the scientific method in archaeology*. New York. Columbia University Press.

Reprinted with Permission.
LaPorta, Philip C., 2004, A Geological Development for the Development of Quarries, with an Ethnoarchaeological Application, *in* Topping, P., and Lynott, M., eds., The Cultural Landscape of Prehistoric Mines: Oxbow Books, Oxford, p. 123-139.

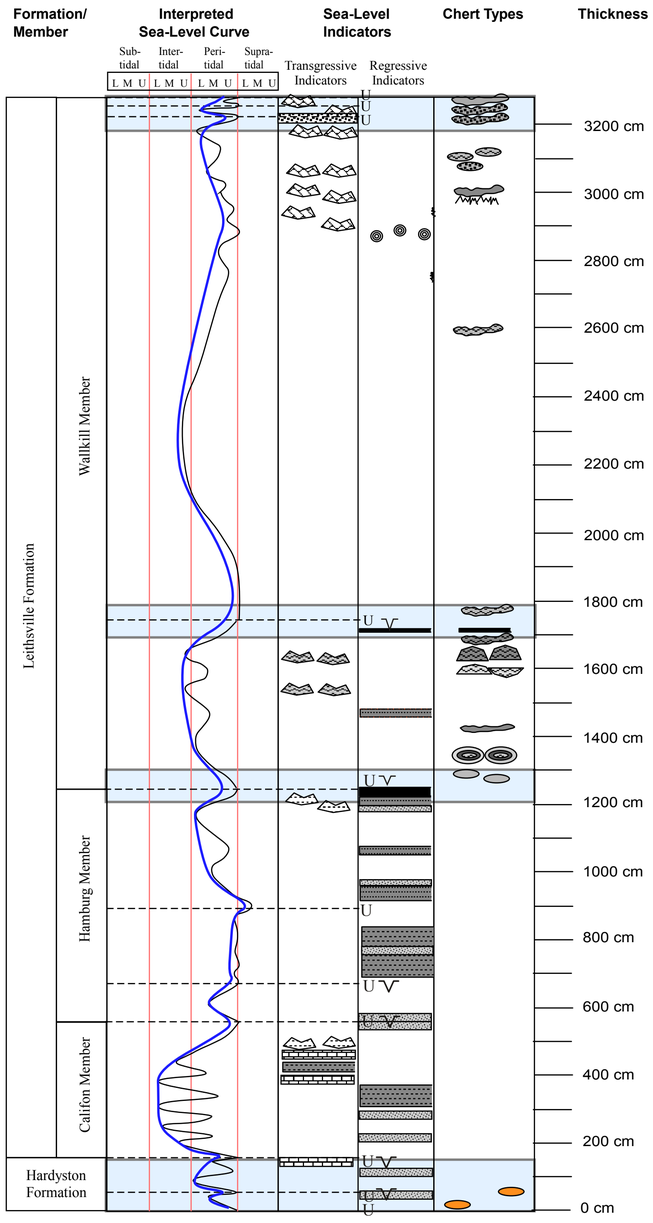
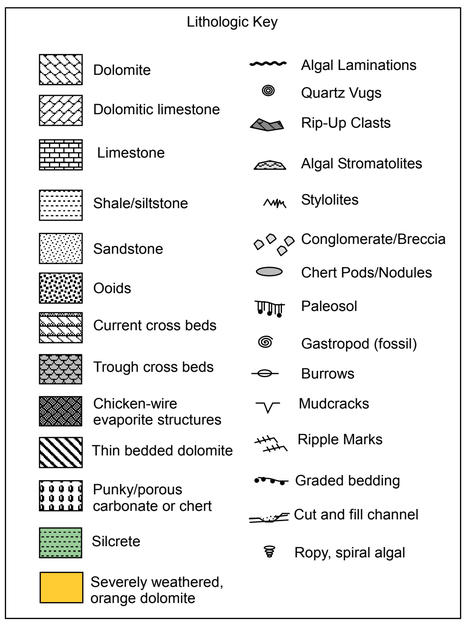


Plate 4.1 : Sea-level indicator for the Cambrian Hardyston and Leithsville Formations (scale 1:98).



Key for stratigraphic sections and sea-level curves of the Kittatinny Supergroup, New Jersey-New York.

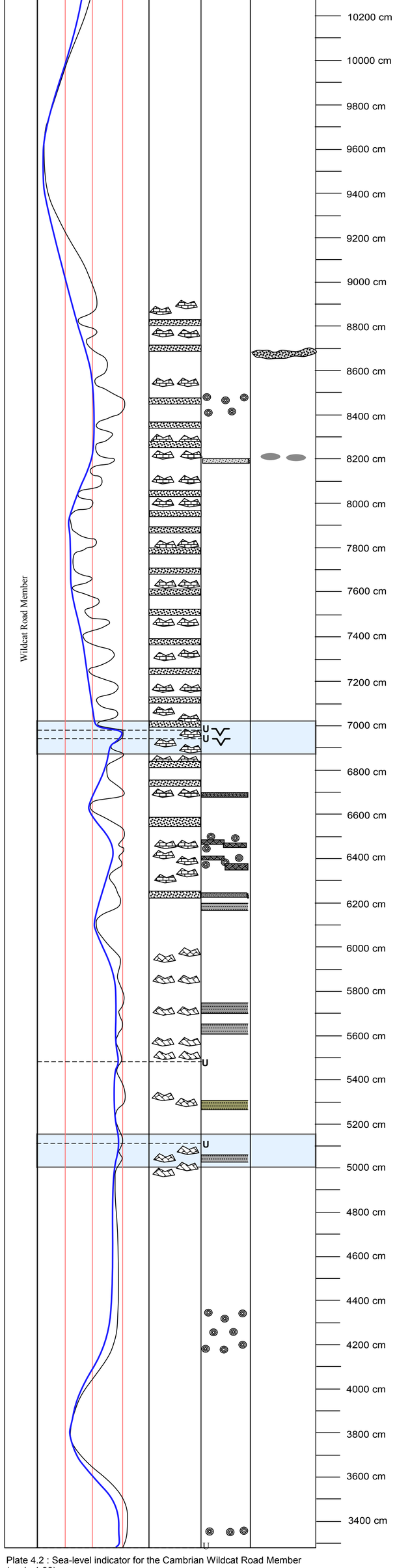


Plate 4.2 : Sea-level indicator for the Cambrian Wildcat Road Member (scale 1:98).

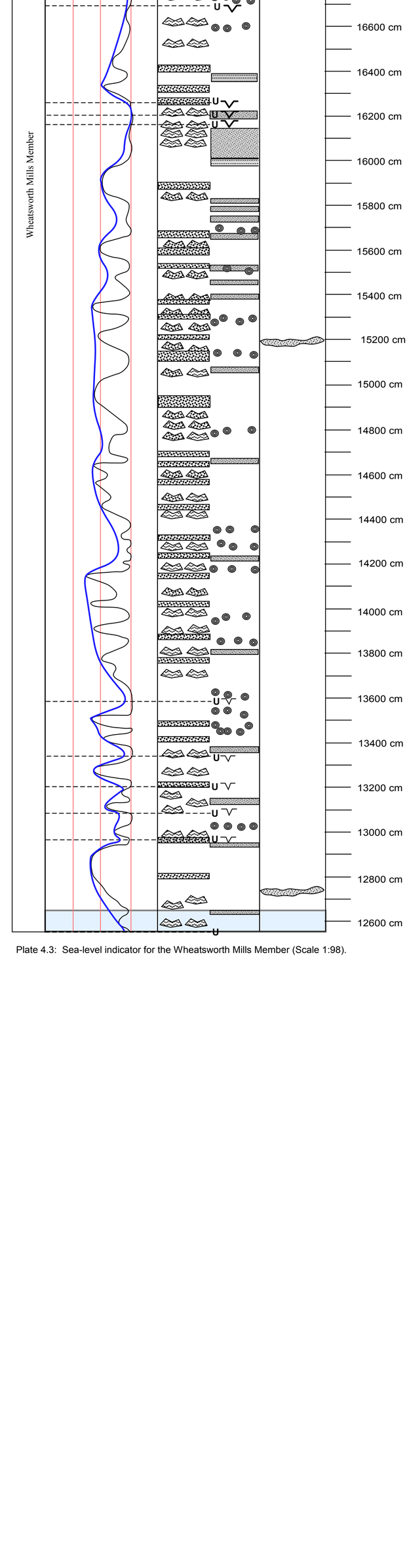


Plate 4.3: Sea-level indicator for the Wheatsworth Mills Member (Scale 1:98).

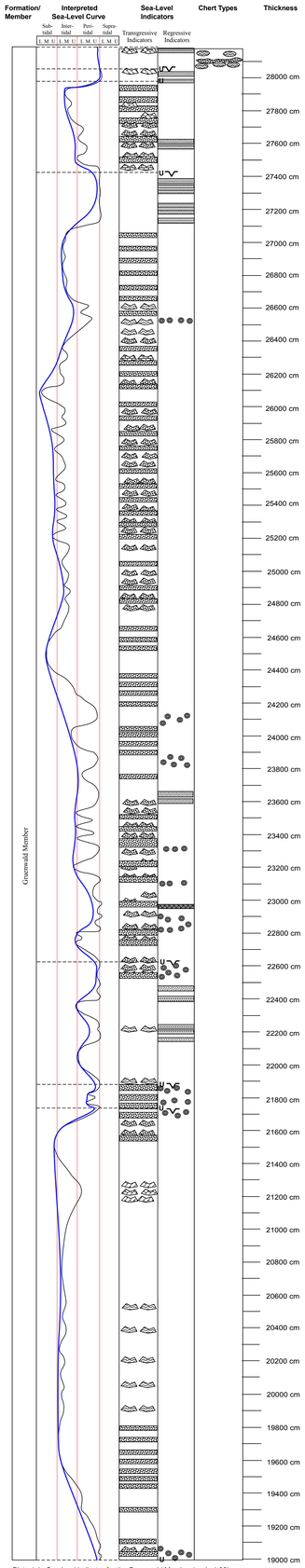


Plate 4.4 : Sea-level indicator for the Gruenwald Member (scale 1:98).

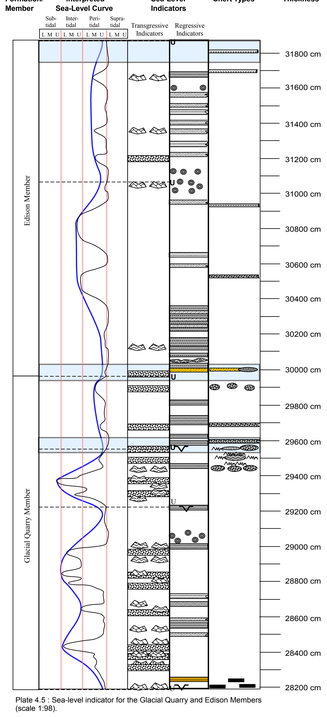


Plate 4.5 : Sea-level indicator for the Glacial Quarry and Edison Members (scale 1:98).

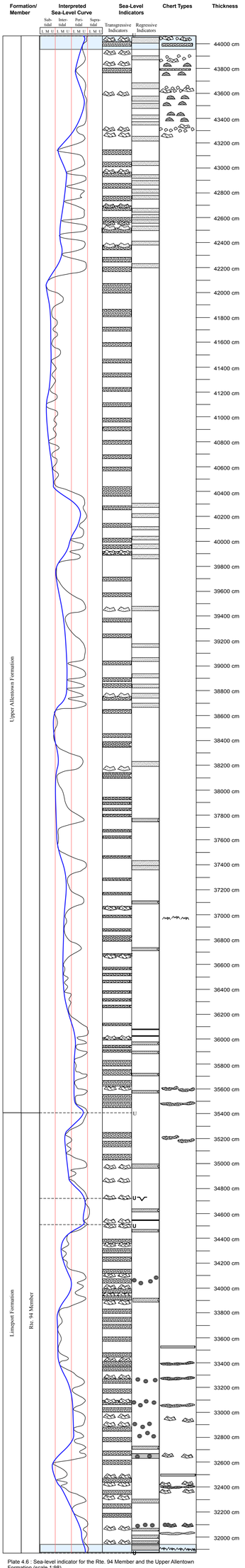


Plate 4.6 : Sea-level indicator for the Rte. 94 Member and the Upper Allentown Formation (scale 1:98).

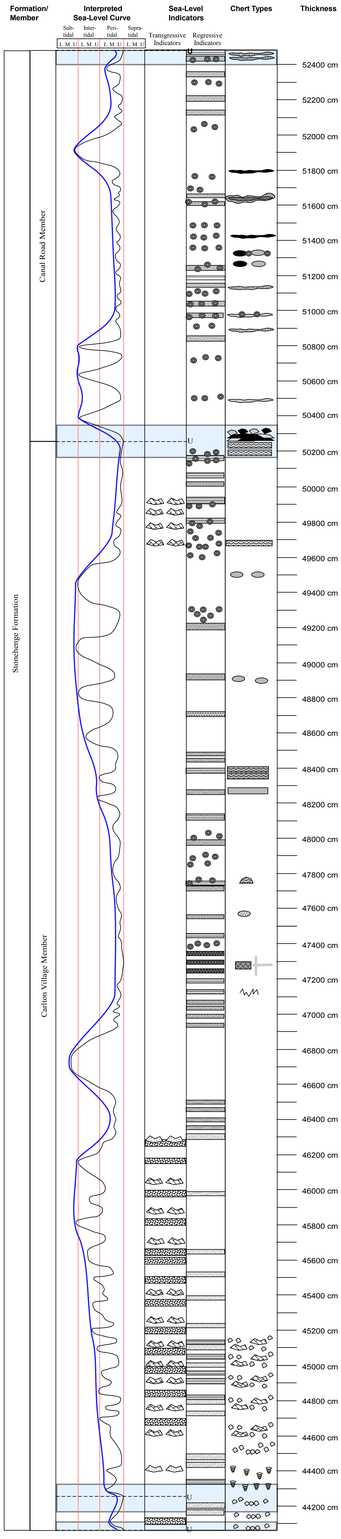
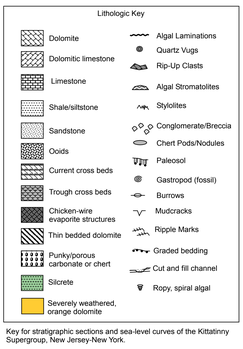


Plate 4.7 : Sea-level indicator for the Stonehenge Formation (scale 1:98).



Key for stratigraphic sections and sea-level curves of the Kittatinny Supergroup, New Jersey-New York.

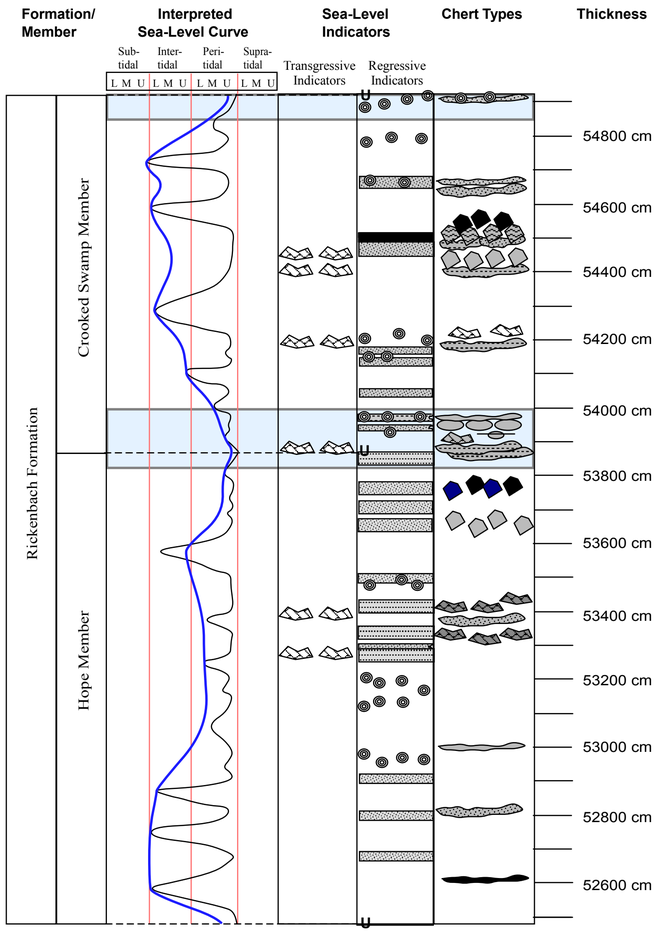


Plate 4.8 : Sea-level indicator for the Rickenbach Formation (scale 1:98).

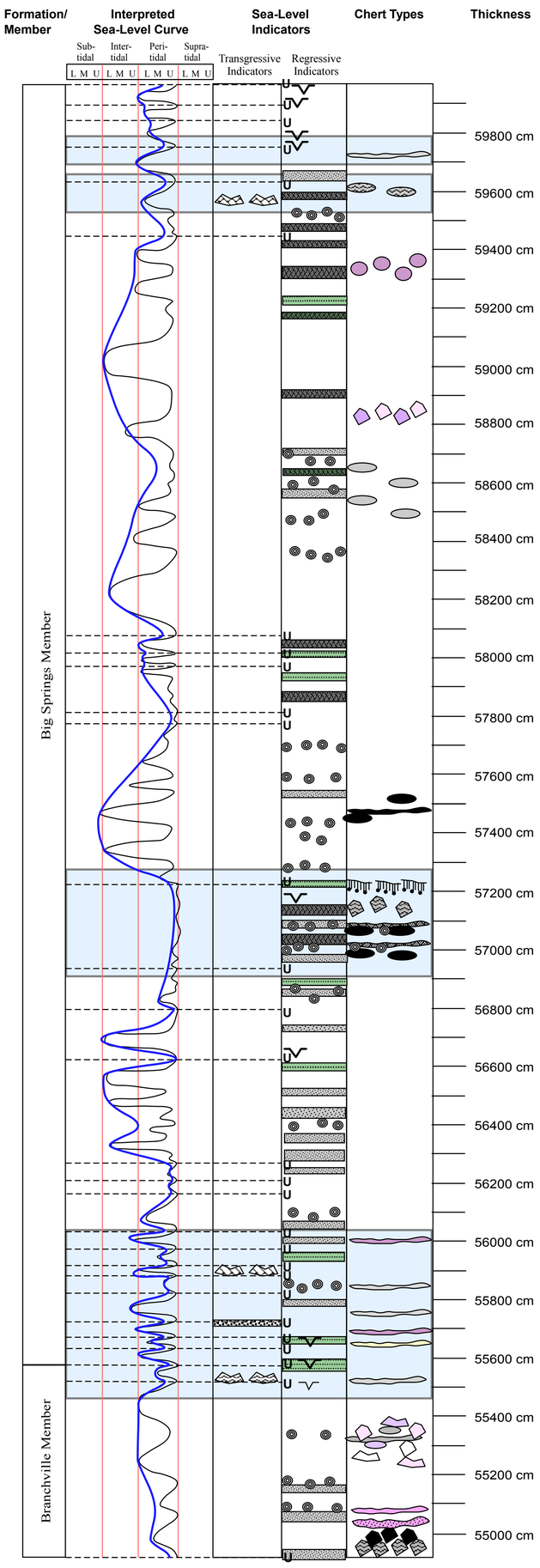


Plate 4.9 : Sea-level indicator for the Branchville and Big Springs Members (scale 1:98).

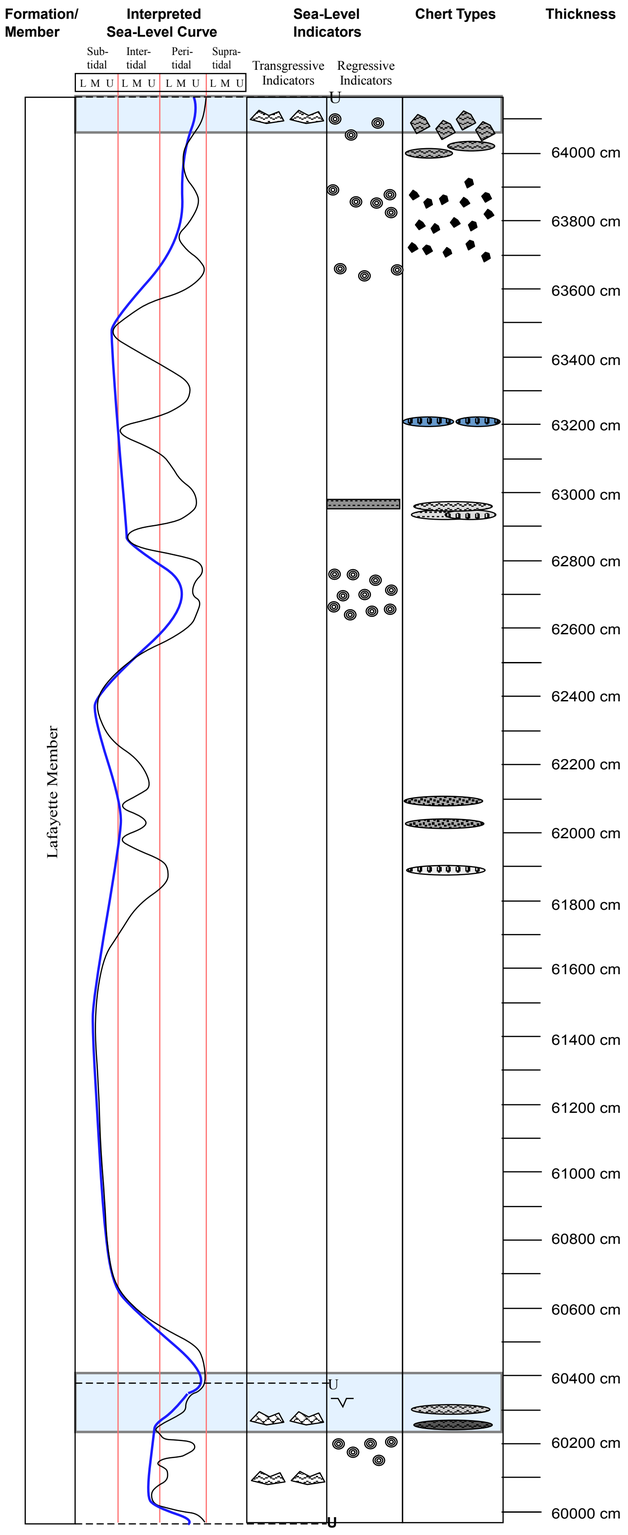
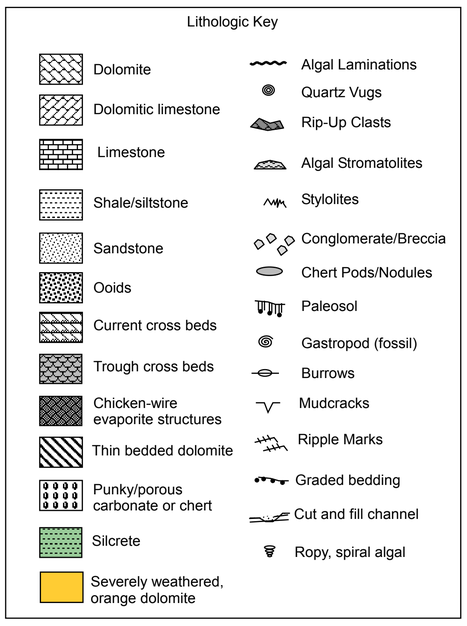


Plate 4.10 : Sea-level indicator for the Lafayette Member (scale 1:98).



Key for stratigraphic sections and sea-level curves of the Kittatinny Supergroup, New Jersey-New York.

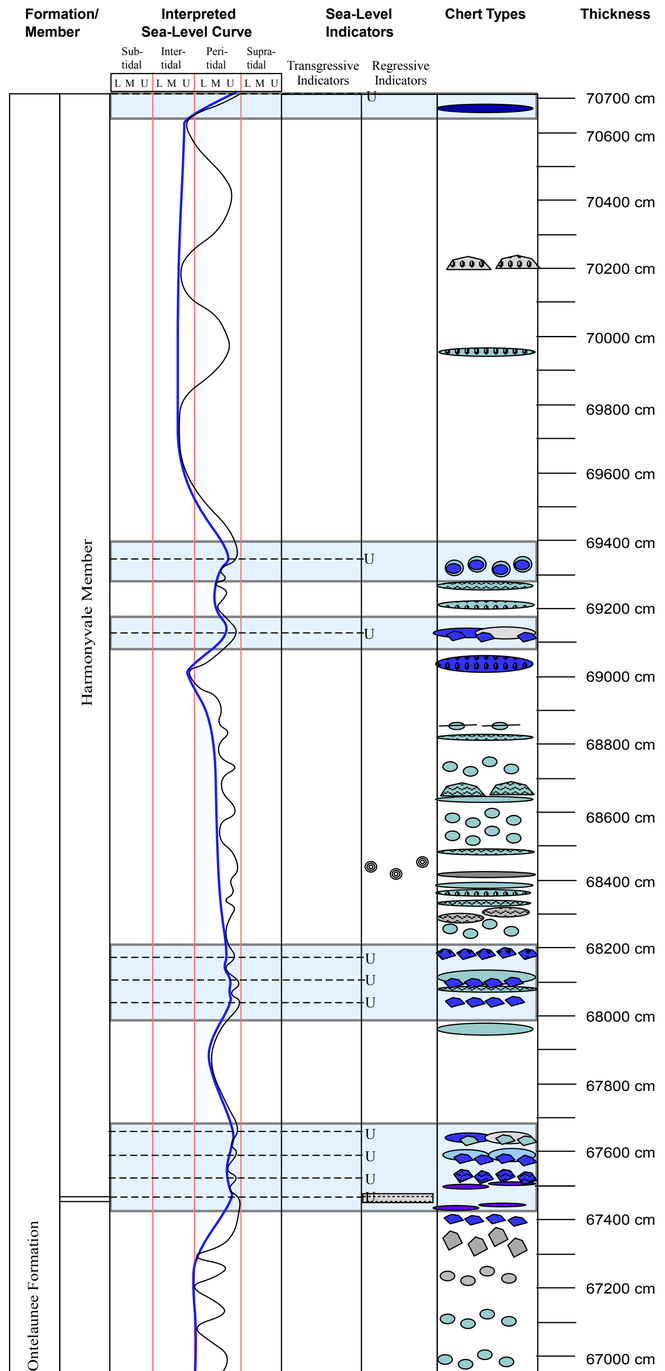
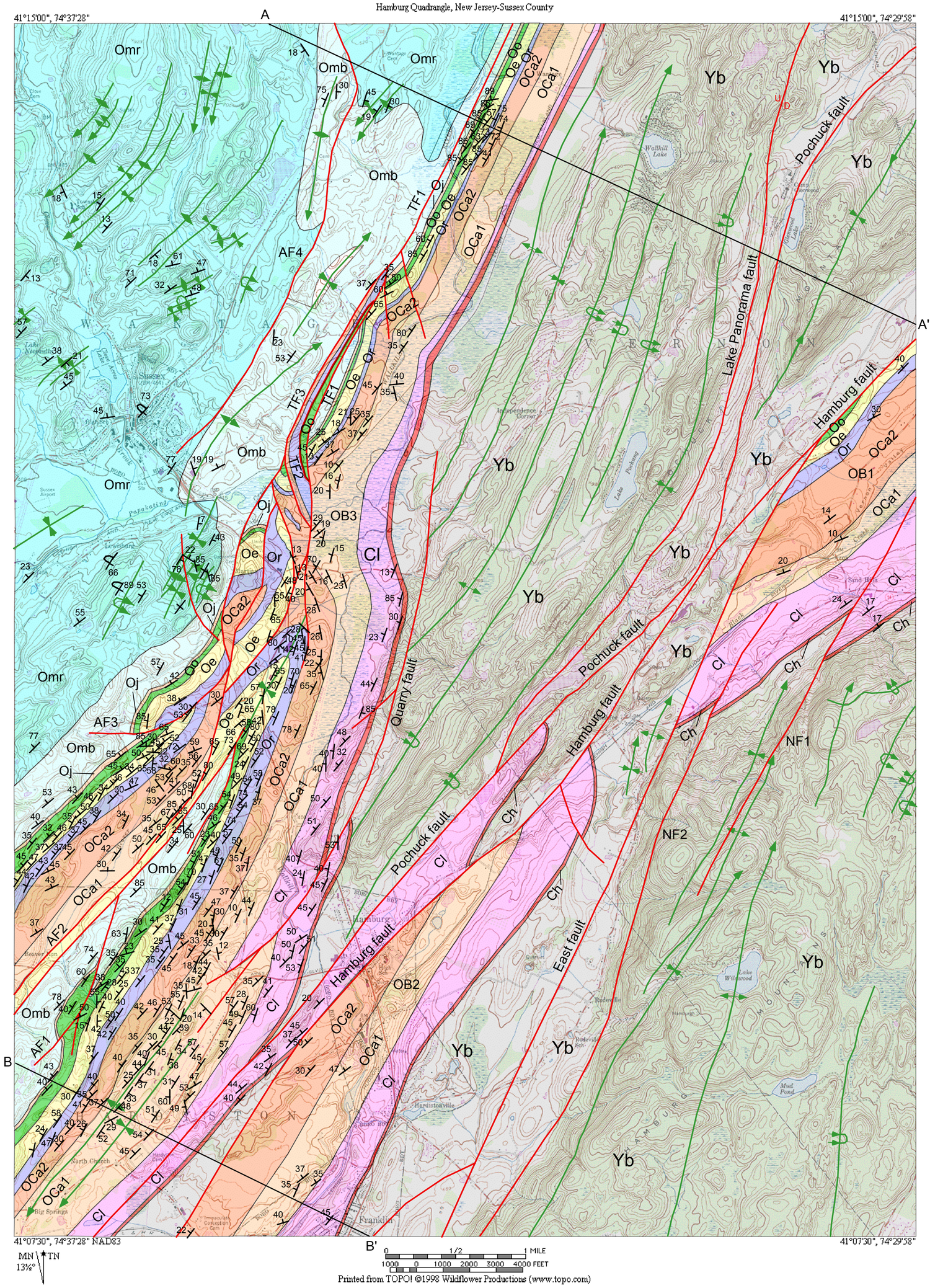


Plate 4.11 : Sea-level indicator for the Beaver Run and Harmonyvale Members (scale 1:98).



Explanation

Valley and Ridge
Kittatinny Valley Sequence

Ordovician

- Omr — Martinsburg Formation (Ranseyburg Member)
- Omb — Martinsburg Formation (Bushkill Member)
- Oj — Jacksonburg Limestone

Beekmantown Sequence

- Oo — Ontelaunee Formation
- Oe — Epler Formation
- Or — Rickenbach Formation
- OCa_2 — Upper Allentown Formation

Cambrian

- OCa_1 — Limeport Formation
- Cl — Leithsville Formation
- Ch — Hardyston Formation

Proterozoic

New Jersey Highlands

- Yb — Proterozoic Igneous and Metamorphic Basement Complex (Undifferentiated)

23 — Strike and Dip of Bedding

Fault Trace

NF — Normal Fault Interpretation

AF — Antithetic Fault Interpretation

TF — Thrust Fault Interpretation

Antiform Interpretation

Synform Interpretation

Overturned Synform Interpretation

Overturned Antiform Interpretation

Plunging Fold Interpretation

A — A' Completed Cross Section

D — D' Cross Section in Progress

Plate 5.1: Composite geologic map of the Hamburg 7.5' Quadrangle (Scale 1:24,000).

Contribution responsibility:
Proterozoic basement and Ordovician Martinsburg Formation: Richard F. Dalton, Robert J. Canace, Richard A. Volkert, Donald H. Monteverde and Gregory C. Herman (NJ Geological Survey).

Cambrian-Ordovician carbonates (including Martinsburg Formation within carbonate belt): Philip C. LaPorta, Jr. (Queens College, CUNY)

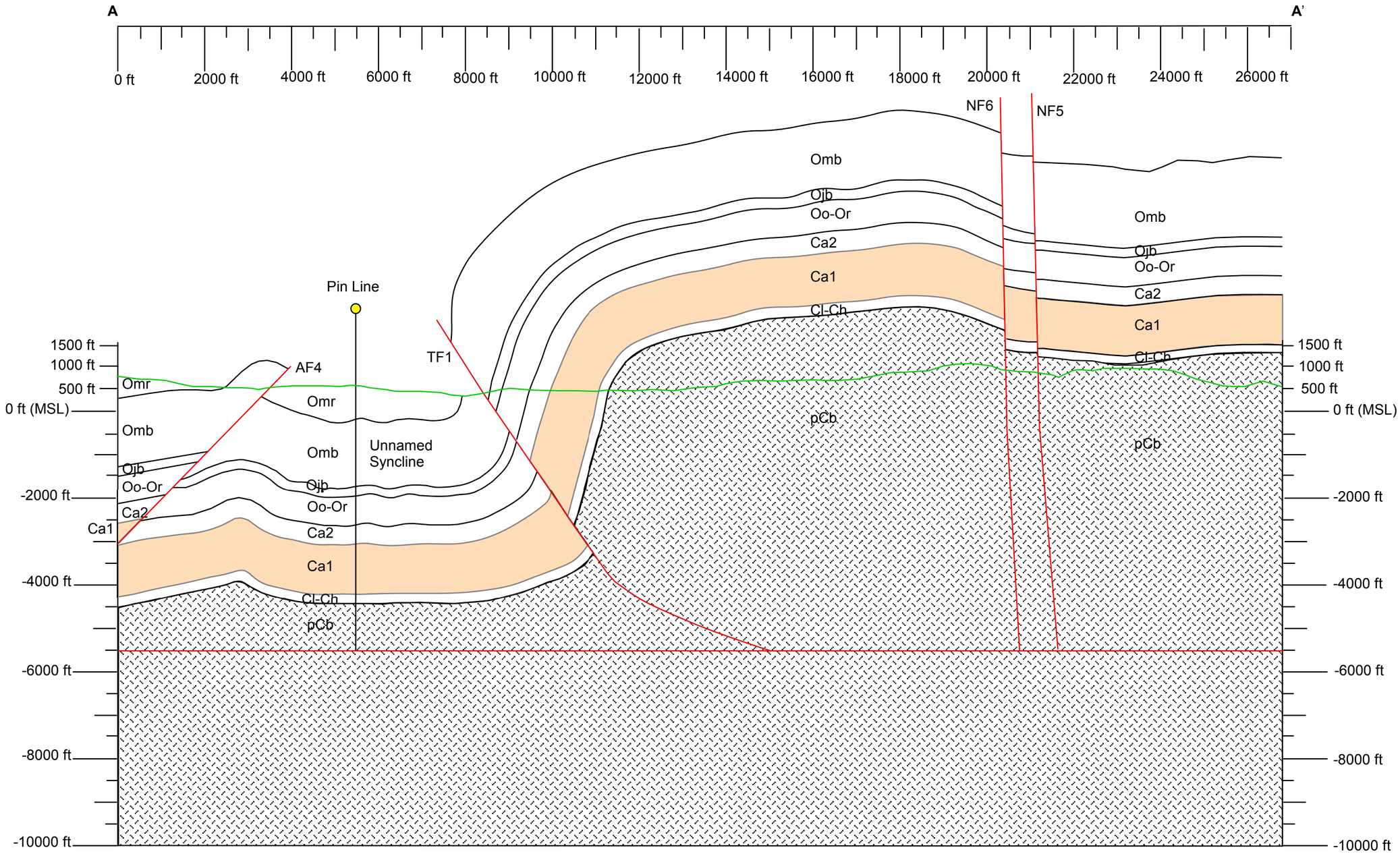


Plate 5.2A: Deformed state cross section of part of the Hamburg 7.5' Quadrangle (pCb= Precambrian basement; Cl-Ch = Cambrian Hardyston-Leithsville Formations; Ca1 = Cambrian Limeport Formation; Ca2 = Cambrian Upper Allentown Formation; Oo-Or = Ordovician Rickenbach to Ontelaunee Formation; Omb = Ordovician Bushkill Member of the Martinsburg Formation; Omr = Ordovician Ramseyburg Member of the Martinsburg Formation).

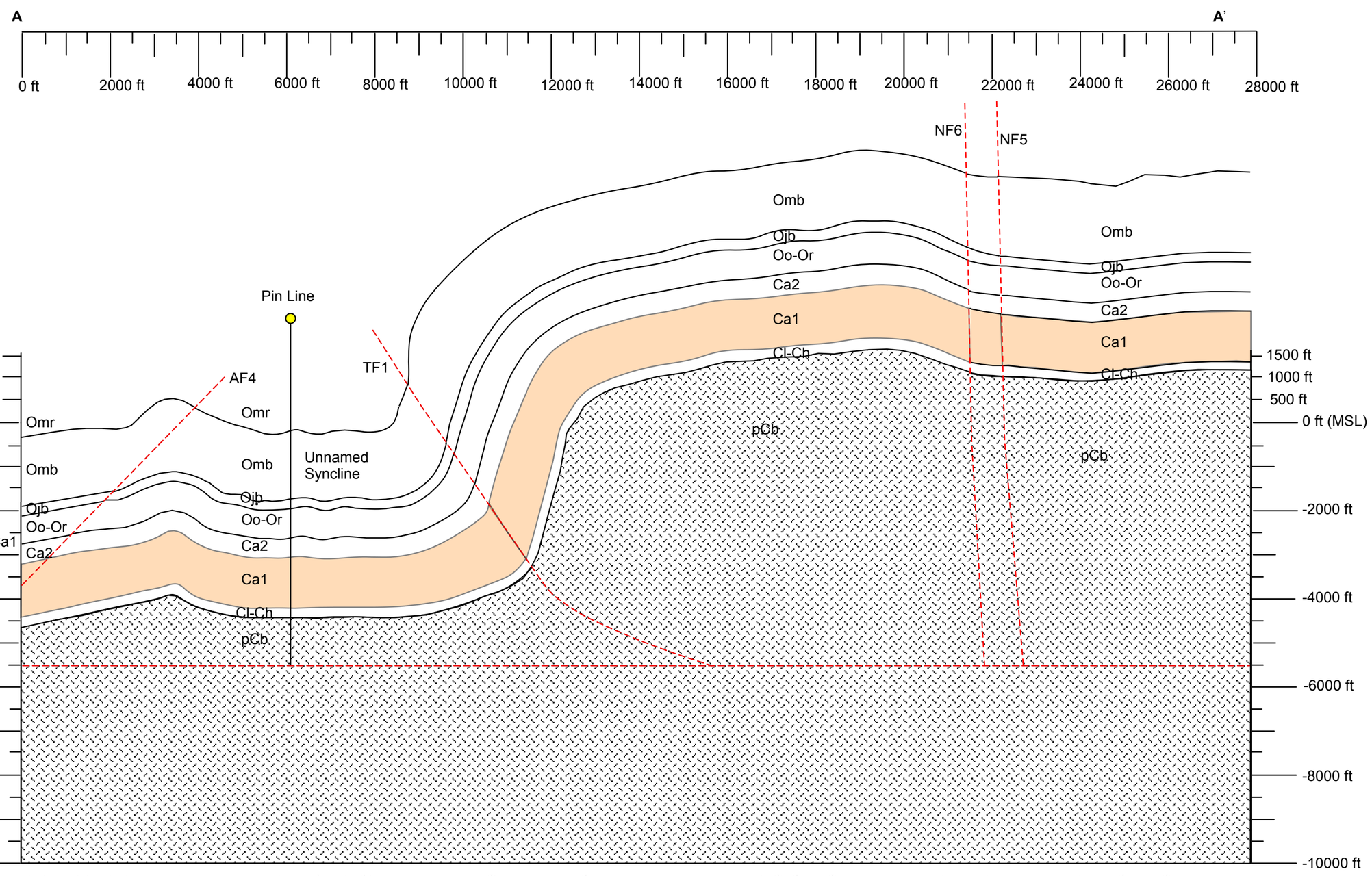


Plate 5.2B: Partially restored cross section of part of the Hamburg 7.5' Quadrangle (pCb= Precambrian basement; Cl-Ch = Cambrian Hardyston-Leithsville Formations; Ca1 = Cambrian Limeport Formation; Ca2 = Cambrian Upper Allentown Formation; Oo-Or = Ordovician Rickenbach to Ontelaunee Formation; Omb = Ordovician Bushkill Member of the Martinsburg Formation; Omr = Ordovician Ramseyburg Member of the Martinsburg Formation).

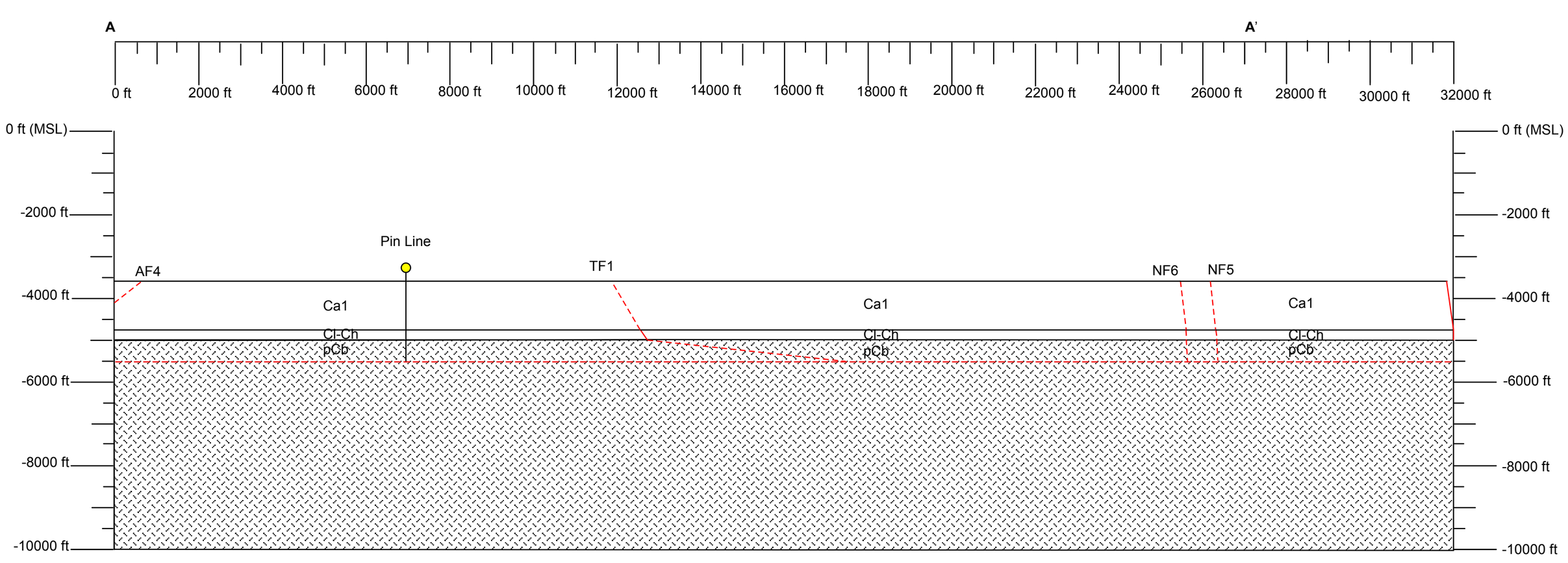


Plate 5.2C: Palinspastically restored cross section of part of the Hamburg 7.5' Quadrangle (pCb= Precambrian basement; Cl-Ch = Cambrian Hardyston-Leithsville Formations; Ca1 = Cambrian Limeport Formation; Ca2 = Cambrian Upper Allentown Formation; Oo-Or = Ordovician Rickenbach to Ontelaunee Formation; Omb = Ordovician Bushkill Member of the Martinsburg Formation; Omr = Ordovician Ramseyburg Member of the Martinsburg Formation).

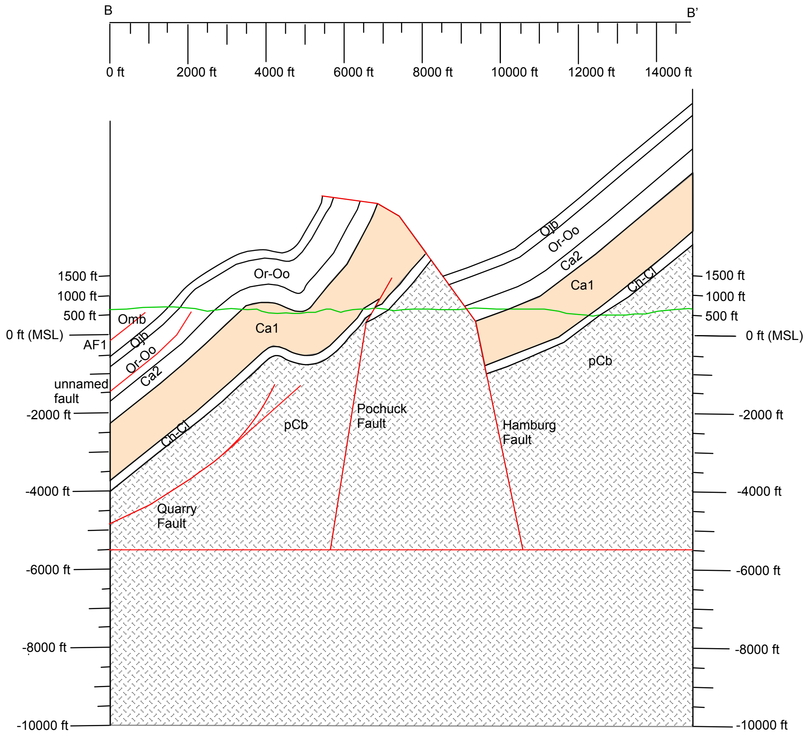


Plate 5.3A: Deformed state cross section of a part of the Hamburg 7.5' Qudrangle (pCb = Precambrian basement; Ch-Cl = Cambrian Hardyston-Leithsville Formations; Ca1 = Cambrian Limeport Formation; Ca2 = Cambrian Upper Allentown Formation; Or-Oo = Ordovician Rickenbach to Ontelaunee Formation; Ojb = Ordovician Jacksonburg Limestone; Omb = Ordovician Bushkill Member of the Martinsburg Formation).

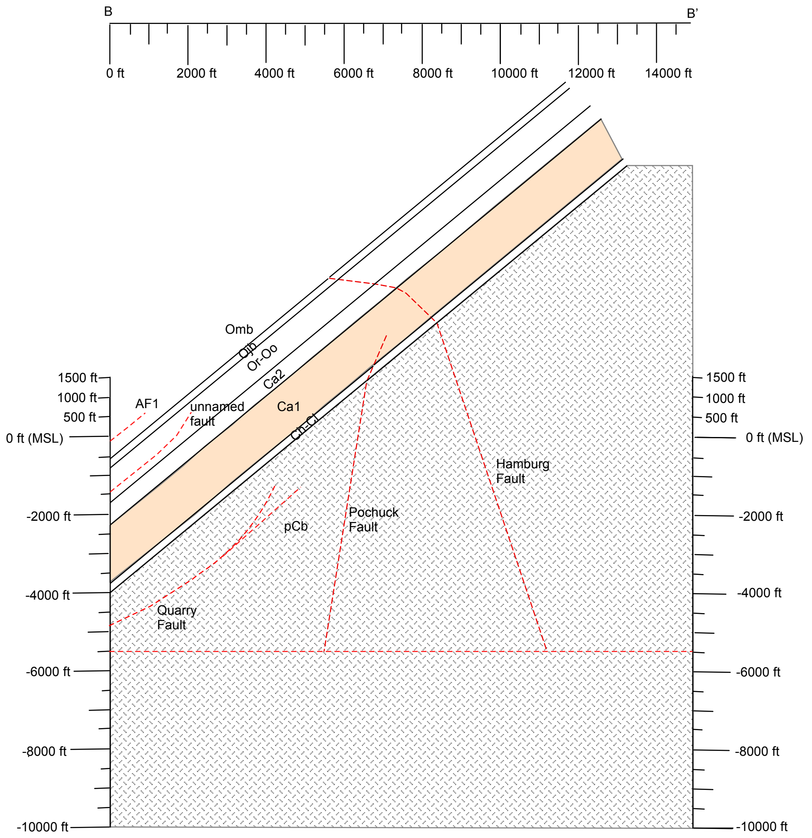


Plate 5.3B: Partially retrodeformed cross section of a part of the Hamburg 7.5' Qudrangle (pCb = Precambrian basement; Ch-Cl = Cambrian Hardyston-Leithsville Formations; Ca1 = Cambrian Limeport Formation; Ca2 = Cambrian Upper Allentown Formation; Or-Oo = Ordovician Rickenbach to Ontelaunee Formation; Ojb = Ordovician Jacksonburg Limestone; Omb = Ordovician Bushkill Member of the Martinsburg Formation).

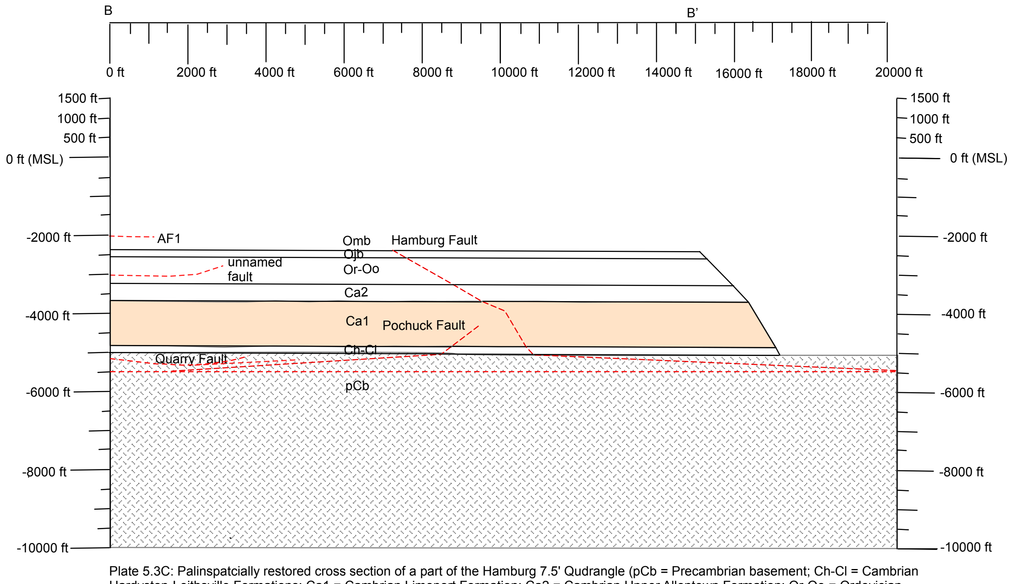


Plate 5.3C: Palinspatcially restored cross section of a part of the Hamburg 7.5' Qudrangle (pCb = Precambrian basement; Ch-Cl = Cambrian Hardyston-Leithsville Formations; Ca1 = Cambrian Limeport Formation; Ca2 = Cambrian Upper Allentown Formation; Or-Oo = Ordovician Rickenbach to Ontelaunee Formation; Ojb = Ordovician Jacksonburg Limestone; Omb = Ordovician Bushkill Member of the Martinsburg Formation).

Cambrian Hardyston Formation
Type Stratigraphic Section
Vernon, New Jersey
Wawayanda 7.5' Quadrangle

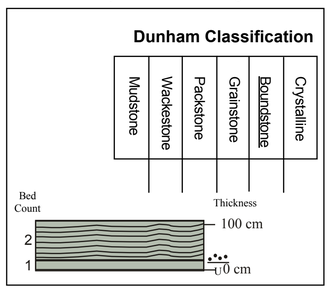


Plate A.1: Type stratigraphic section for the Cambrian Hardyston Formation.

Cambrian Califon Member of the Leithsville Formation
Type Stratigraphic Section
Harmonyvale, New Jersey
Branchville 7.5' Quadrangle

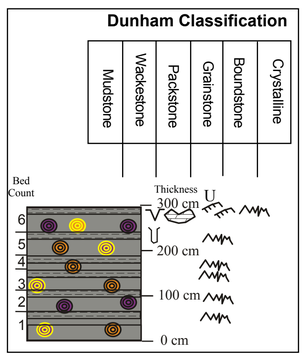


Plate A.2: Type stratigraphic section for the Cambrian Califon Member of the Leithsville Formation.

Cambrian Hamburg Member of the Leithsville Formation
Type Stratigraphic Section
Vernon, New Jersey
Wawayanda 7.5' Quadrangle

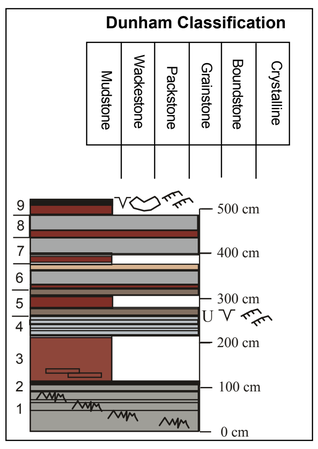


Plate A.3: Type stratigraphic section for the Cambrian Hamburg Member of the Leithsville Formation.

Cambrian Wallkill Member of the Leithsville Formation
Type Stratigraphic section
Franklin, New Jersey
Franklin 7.5' Quadrangle

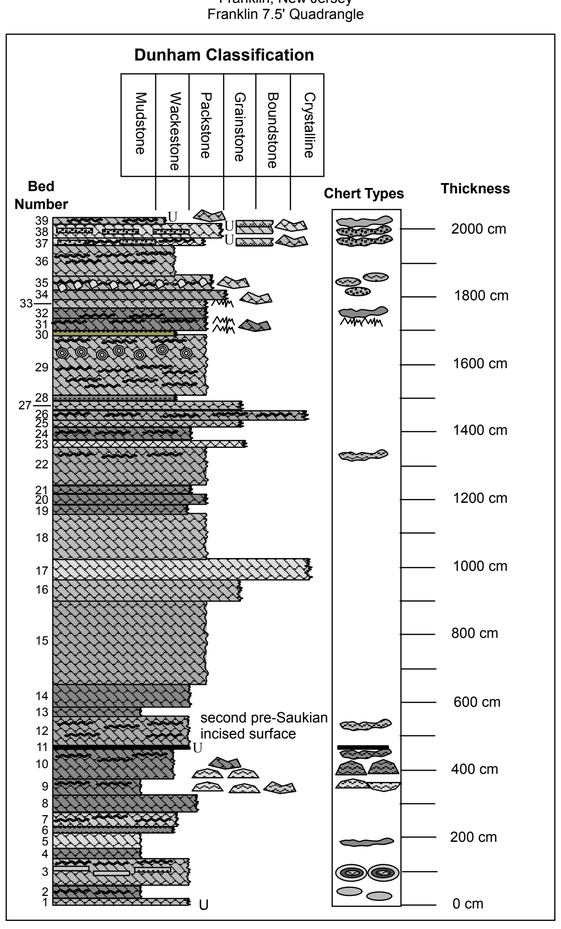
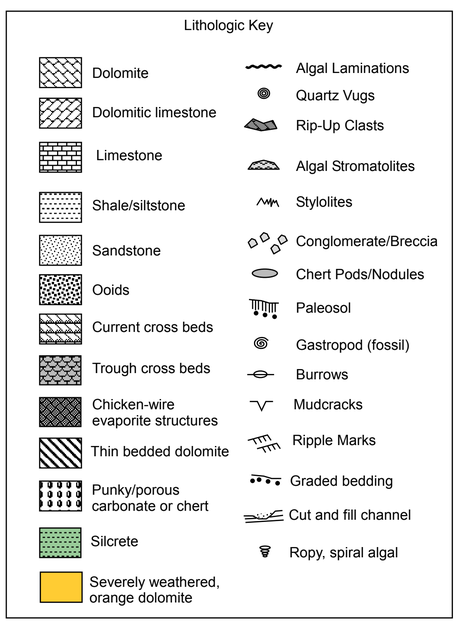


Plate A.4: Type stratigraphic section for the Cambrian Wallkill Member of the Leithsville Formation.



Key for stratigraphic columns.

Cambrian Wildcat Road Member of the Limeport Formation
Type Stratigraphic Section
Franklin, New Jersey
Franklin 7.5' Quadrangle

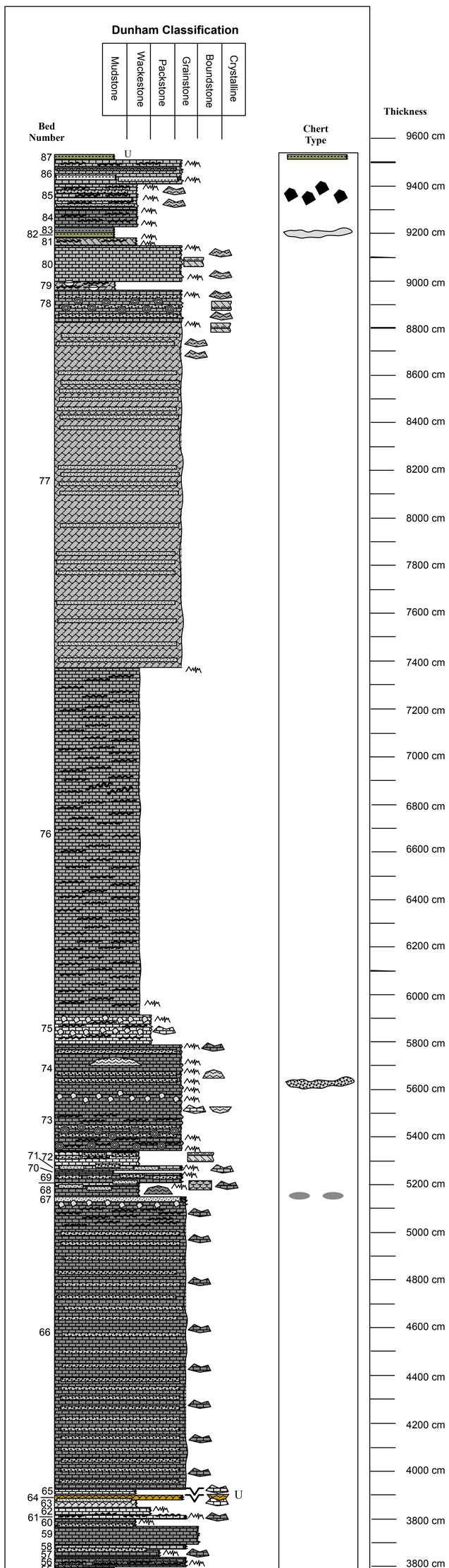


Plate A.5: Type stratigraphic section for the Cambrian Wildcat Road Member of the Limeport Formation.

Cambrian Wheatsworth Mills Member of the Limeport Formation
Type Stratigraphic Section
Wildcat Road, Franklin, New Jersey
Franklin 7.5' Quadrangle

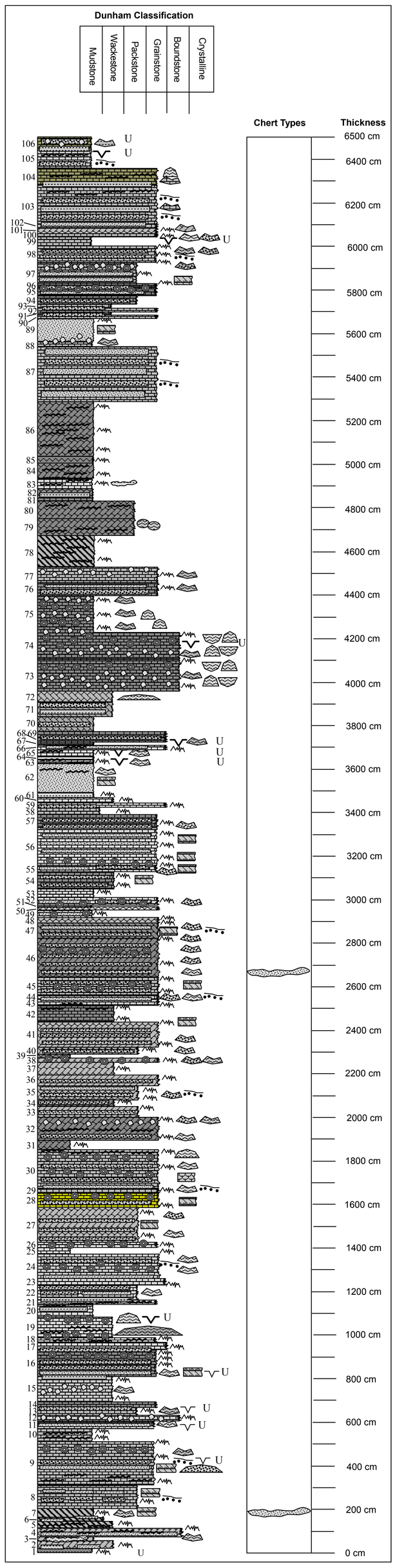


Plate A.6: Type stratigraphic section for the Cambrian Wheatsworth Mills Member of the Leithsville Formation.

Cambrian Gruenwald Member of the Limeport Formation
Type Stratigraphic section
Hamburg, New Jersey
Hamburg 7.5' Quadrangle

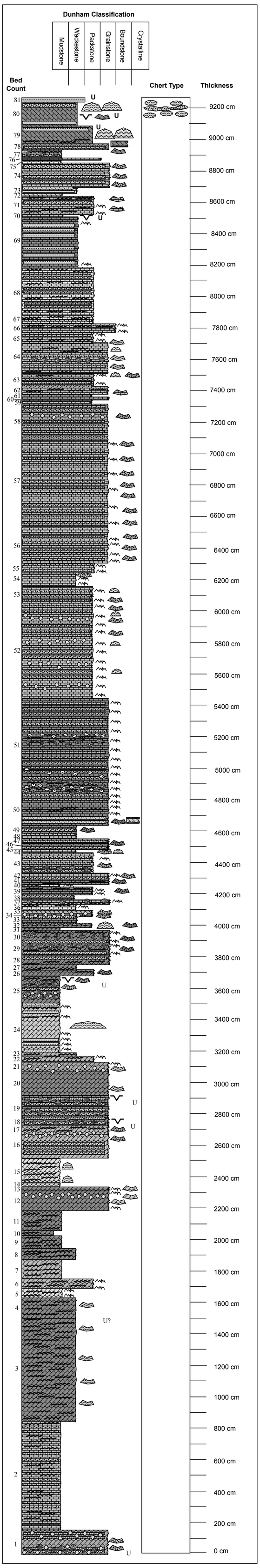


Plate A.7: Type stratigraphic section for the Cambrian Gruenwald Member of the Limeport Formation.

Cambrian Glacial Quarry Member of the Limeport Formation
Type Stratigraphic Section
Hamburg, New Jersey
Hamburg 7.5' Quadrangle

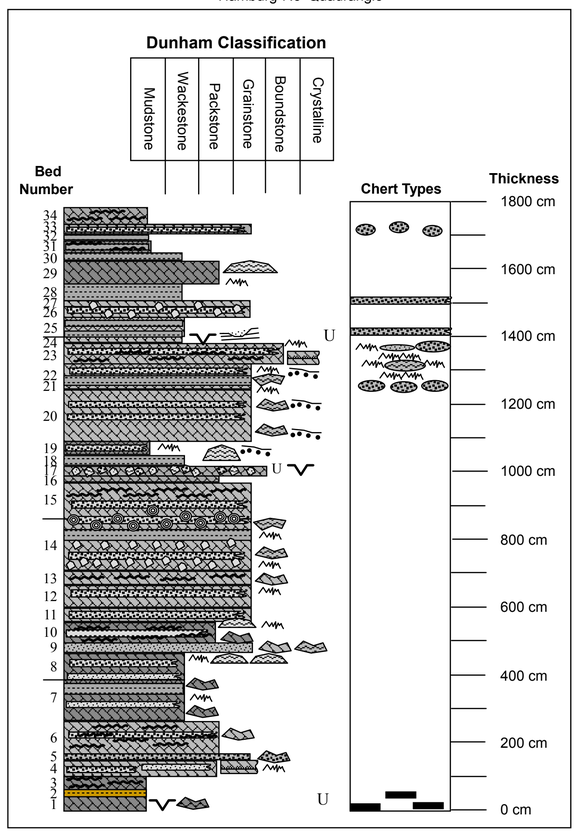


Plate A.8: Type stratigraphic section for the Cambrian Glacial Quarry Member of the Leithsville Formation.

Cambrian Edison Member of the Limeport Formation
Type Stratigraphic section
Hamburg, New Jersey
Hamburg 7.5' Quadrangle

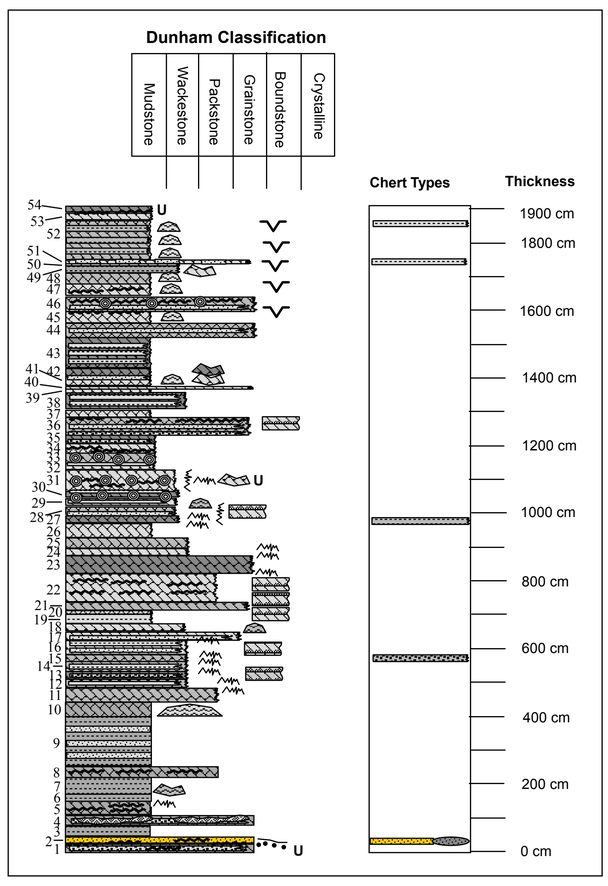


Plate A.9: Type stratigraphic section for the Cambrian Edison Member of the Limeport Formation.

Cambrian Rte. 94 Member of the Limeport Formation
Type Stratigraphic section
Hamburg, New Jersey
Hamburg 7.5' Quadrangle

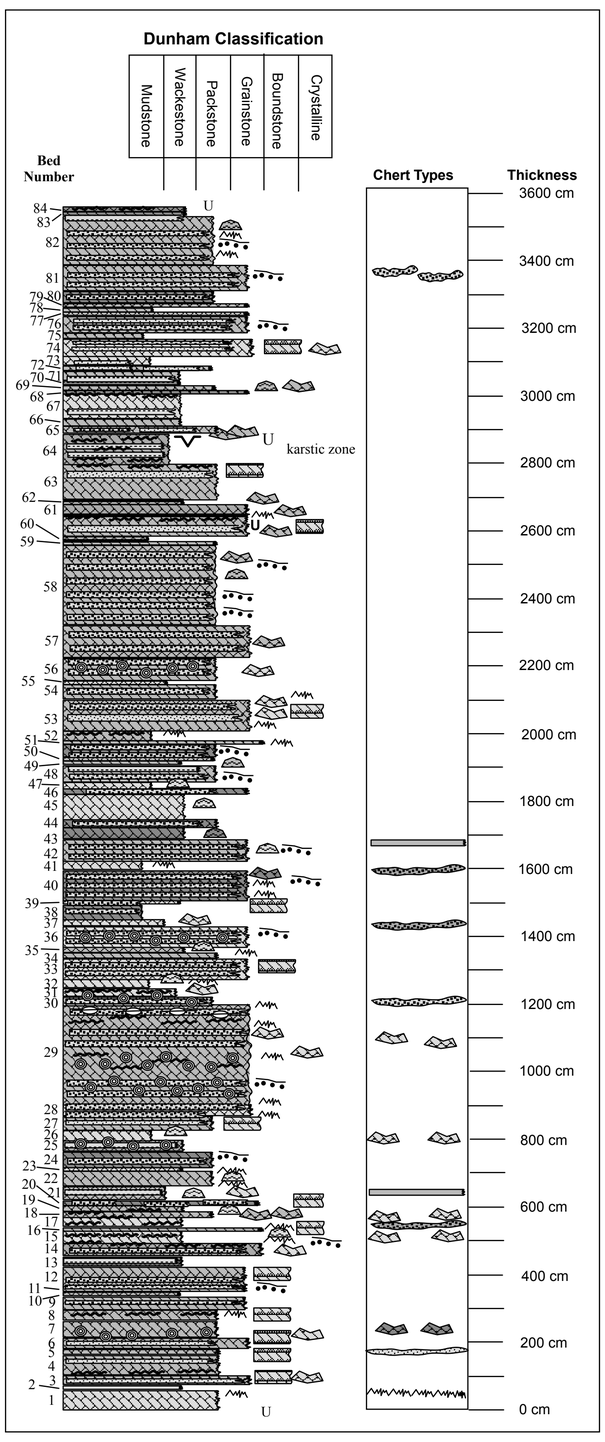


Plate A.10: Type stratigraphic section for the Cambrian Rte. 94 Member of the Limeport Formation.

Cambrian Upper Allentown Formation
Type Stratigraphic section
Hamburg, New Jersey
Hamburg 7.5' Quadrangle

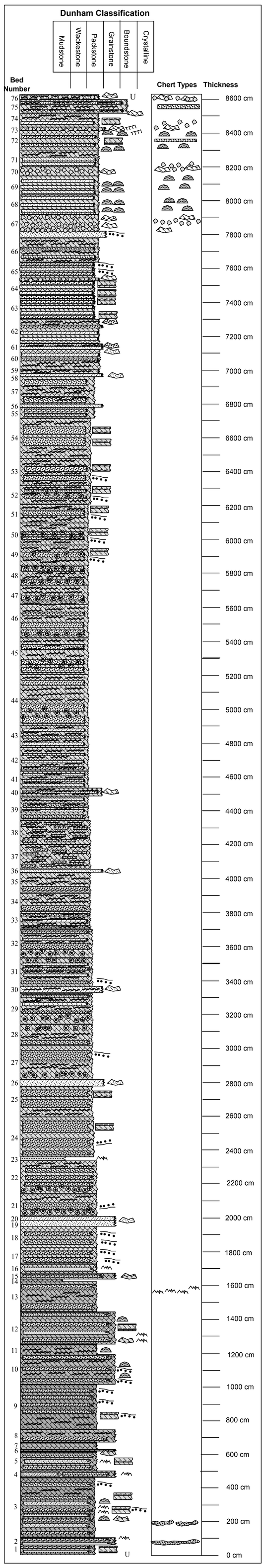


Plate A.11: Type stratigraphic section for the Cambrian Upper Allentown Formation.

Key for stratigraphic columns.

Cambrian Carlton Village Member of the Stonehenge Formation
Type Stratigraphic Section
Hamburg, New Jersey
Hamburg 7.5' Quadrangle

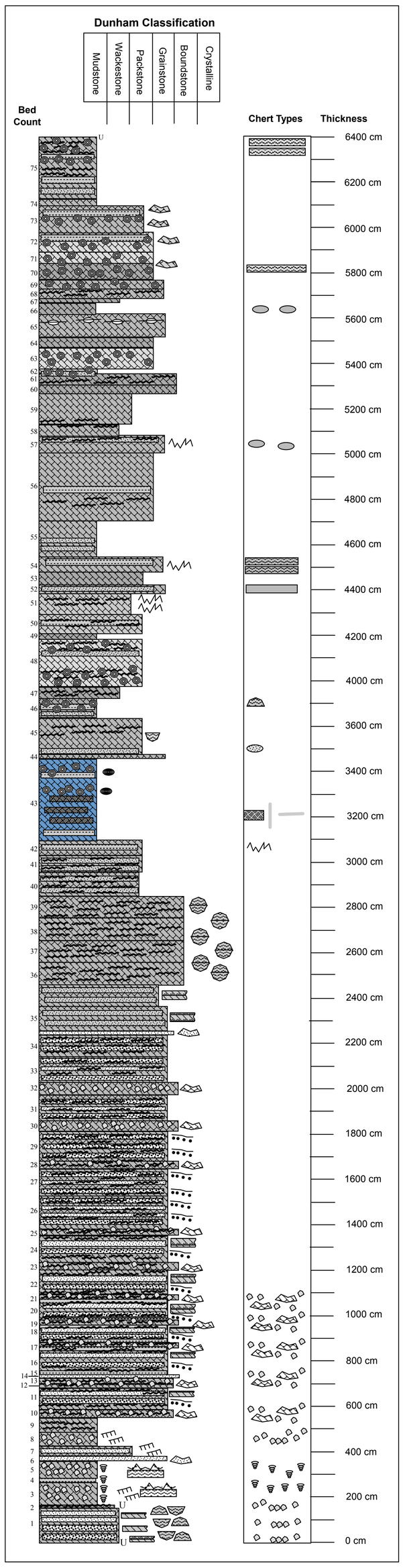
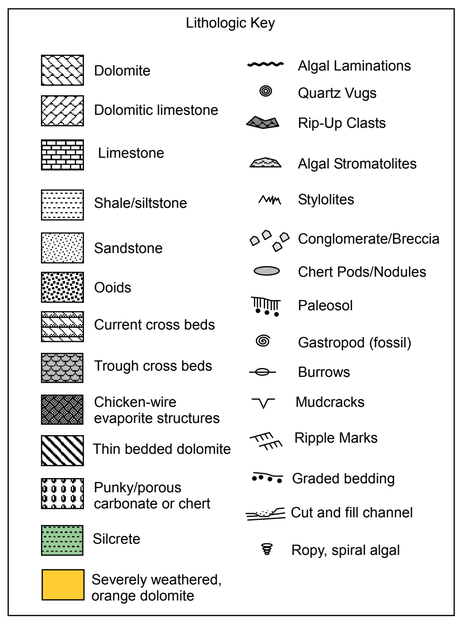


Plate A.12: Type stratigraphic section for the Cambrian Carlton Village Member of the Stonehenge Formation.



Key to Stratigraphic Columns.

Ordovician Canal Road Member of the Stonehenge Formation
Type Stratigraphic Section
Vernon, New Jersey
Wawayanda 7.5' Quadrangle

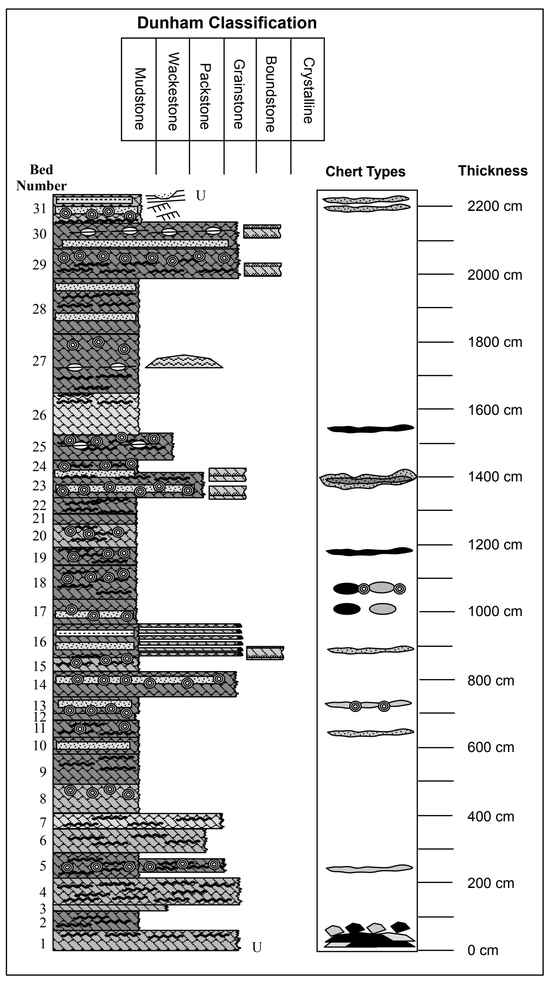


Plate A.13: Type stratigraphic section for the Ordovician Canal Road Member of the Stonehenge Formation.

Ordovician Hope Member of the Rickenbach Formation
Type Stratigraphic Section
Vernon, New Jersey
Wawayanda 7.5' Quadrangle

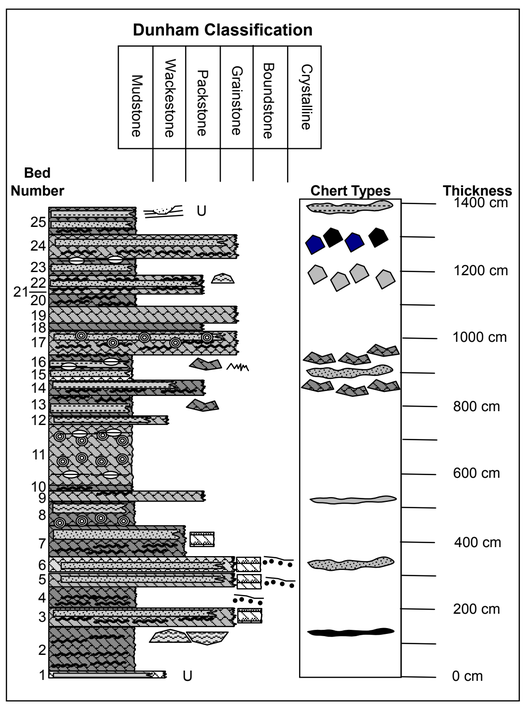


Plate A.14: Type stratigraphic section for the Ordovician Hope Member of the Rickenbach Formation.

Ordovician Crooked Swamp Member of the Rickenbach Formation
Type Stratigraphic Section
Vernon, New Jersey
Wawayanda 7.5' Quadrangle

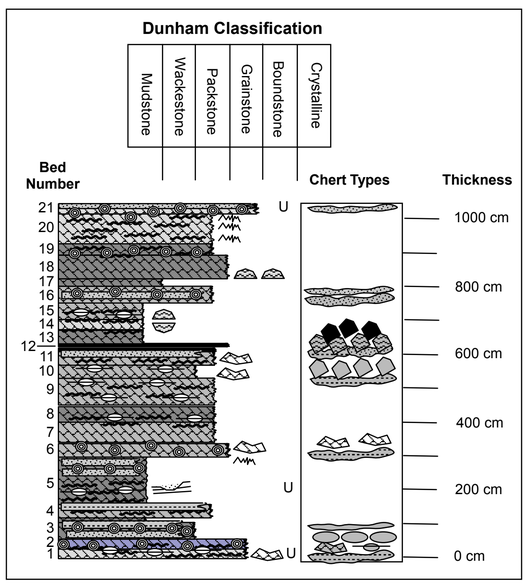


Plate A.15: Type stratigraphic section for the Ordovician Crooked Swamp Member of the Rickenbach Formation.

Ordovician Branchville Member of the Epler Formation
Type Stratigraphic section
Vernon, New Jersey
Wawayanda 7.5' Quadrangle

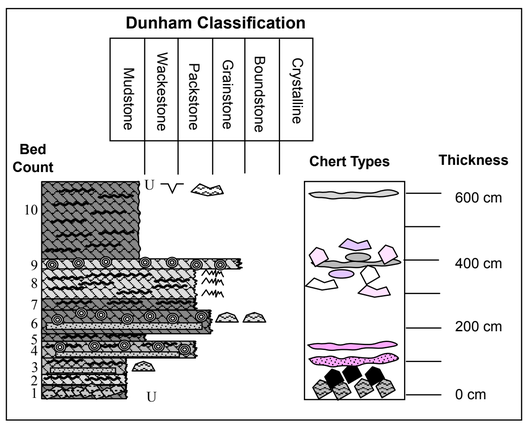


Plate A.16: Type stratigraphic section for the Ordovician Branchville Member of the Epler. Formation.

Ordovician Big Springs Member of the Epler Formation
Type Stratigraphic section
Hamburg, New Jersey
Hamburg 7.5' Quadrangle

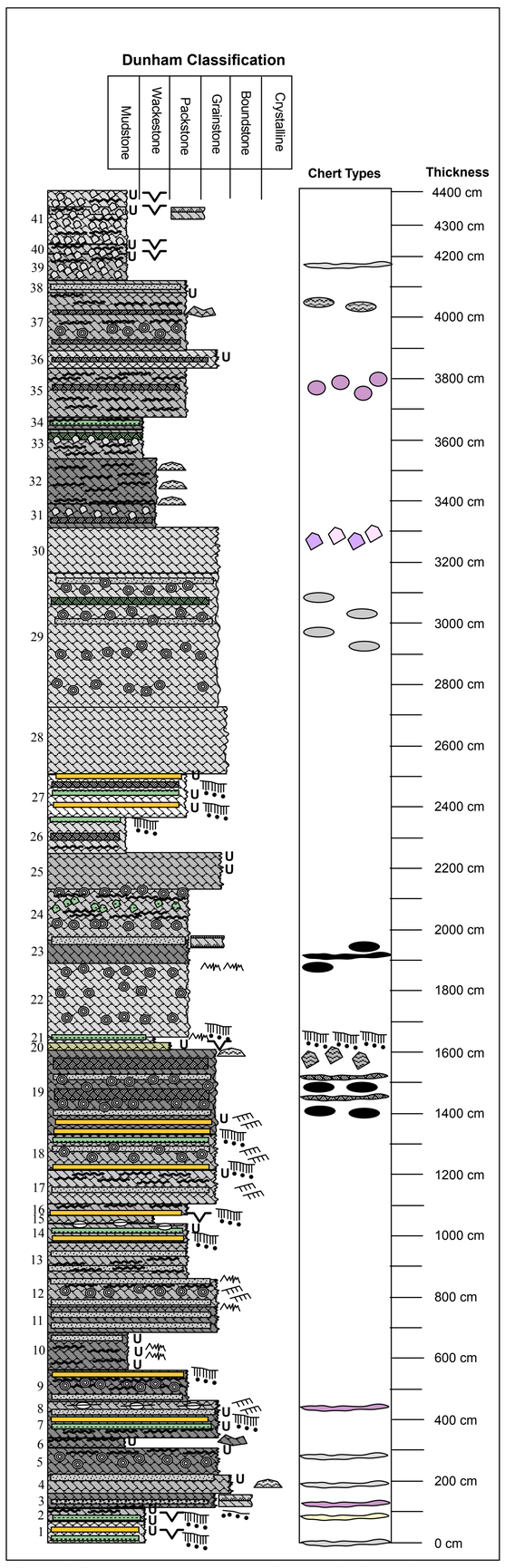


Plate A.17: Type stratigraphic section for the Ordovician Big Springs Member of the Epler Formation.

Ordovician Lafayette Member of the Epler Formation
Type Stratigraphic Section
Harmonyvale, New Jersey
Branchville 7.5' Quadrangle

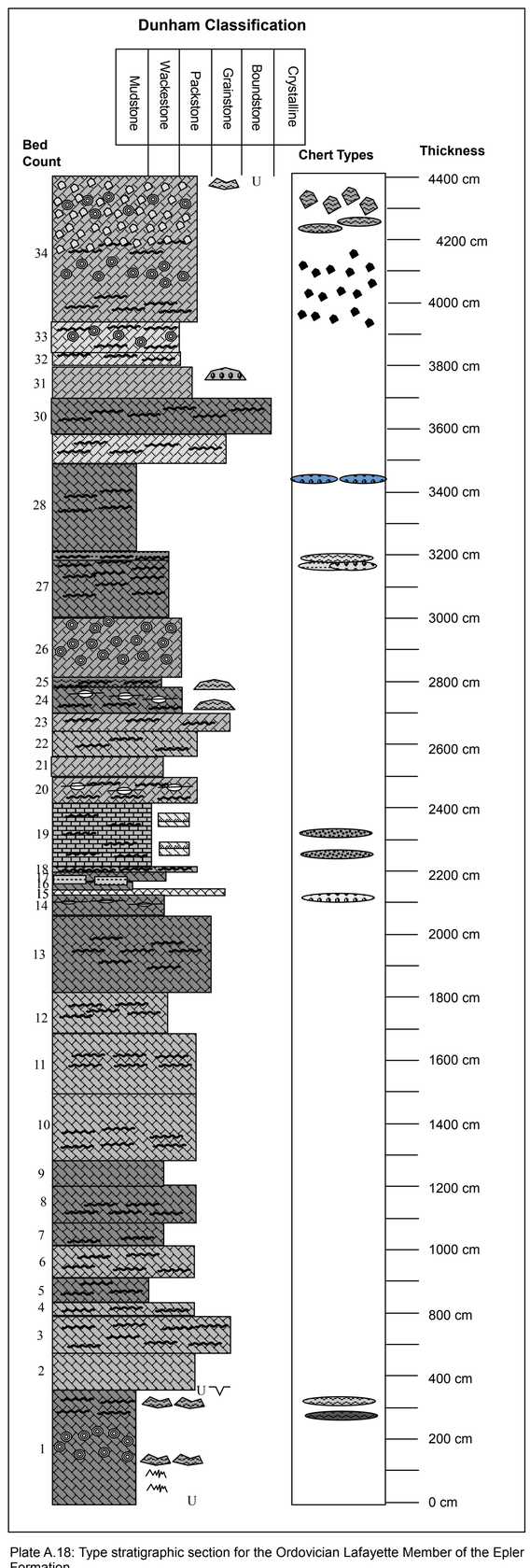


Plate A.18: Type stratigraphic section for the Ordovician Lafayette Member of the Epler Formation.

Ordovician Beaver Run Member of the Ontelaunee Formation
Type Stratigraphic Section
Harmonyvale, New Jersey
Branchville 7.5' Quadrangle

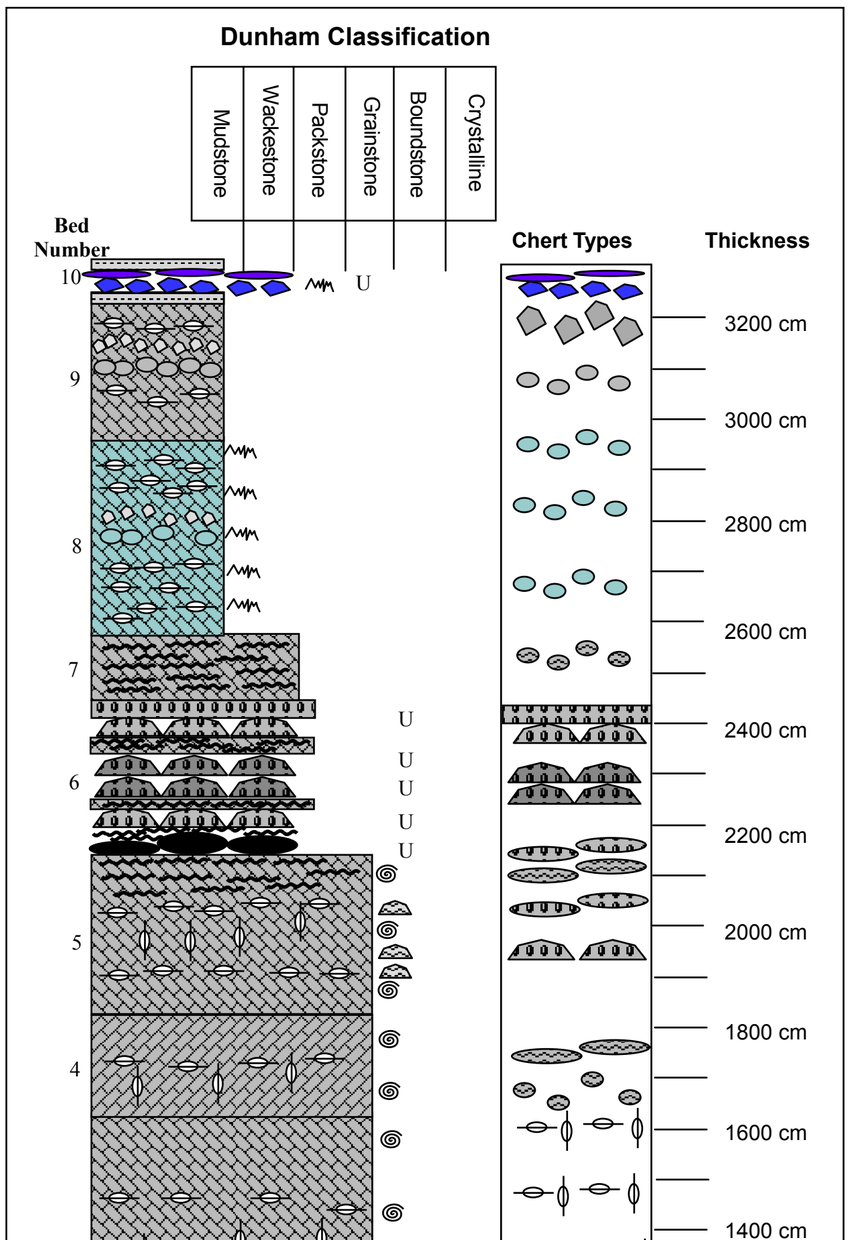


Plate A.19: Type stratigraphic section for the Ordovician Beaver Run Member of the Ontelaunee Formation.

Ordovician Harmonyvale Member of the Ontelaunee Formation
Type Stratigraphic Section
Harmonyvale, New Jersey
Branchville 7.5' Quadrangle

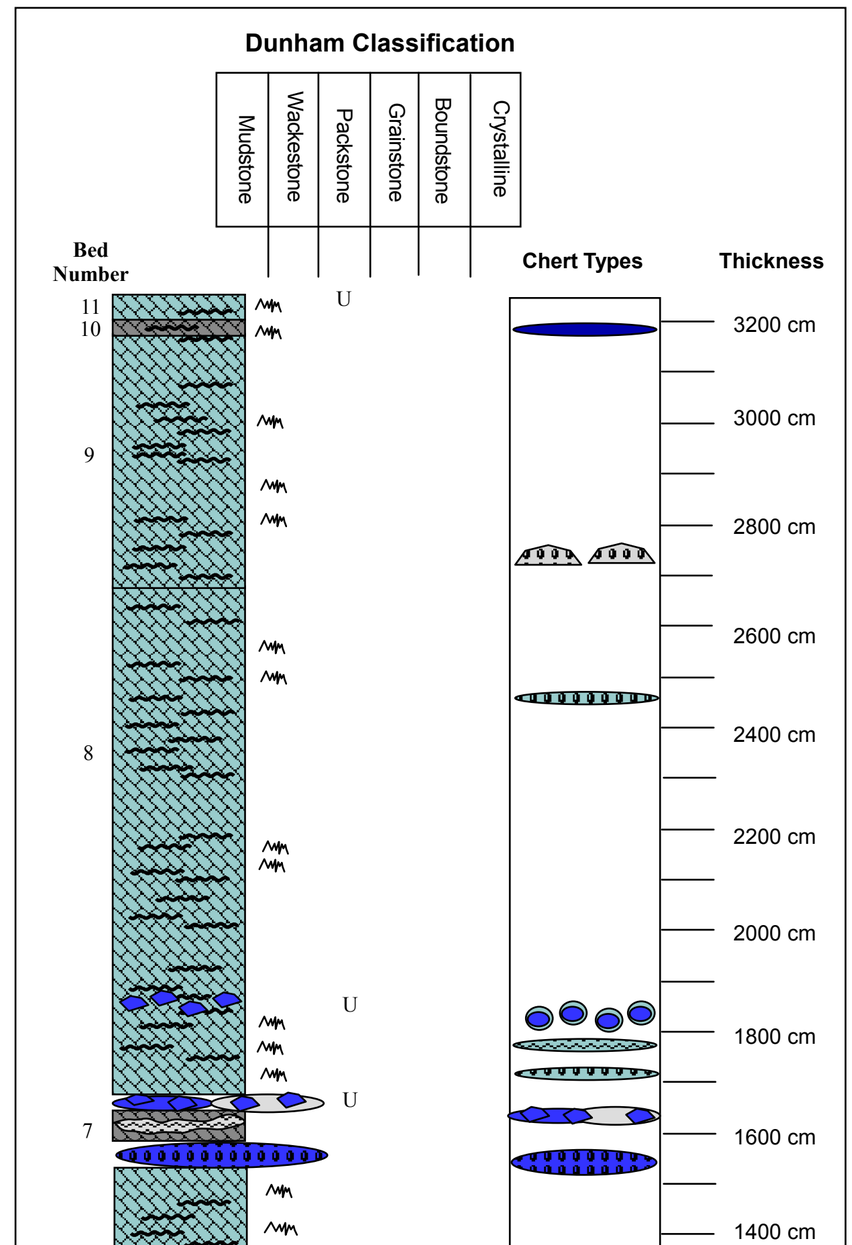
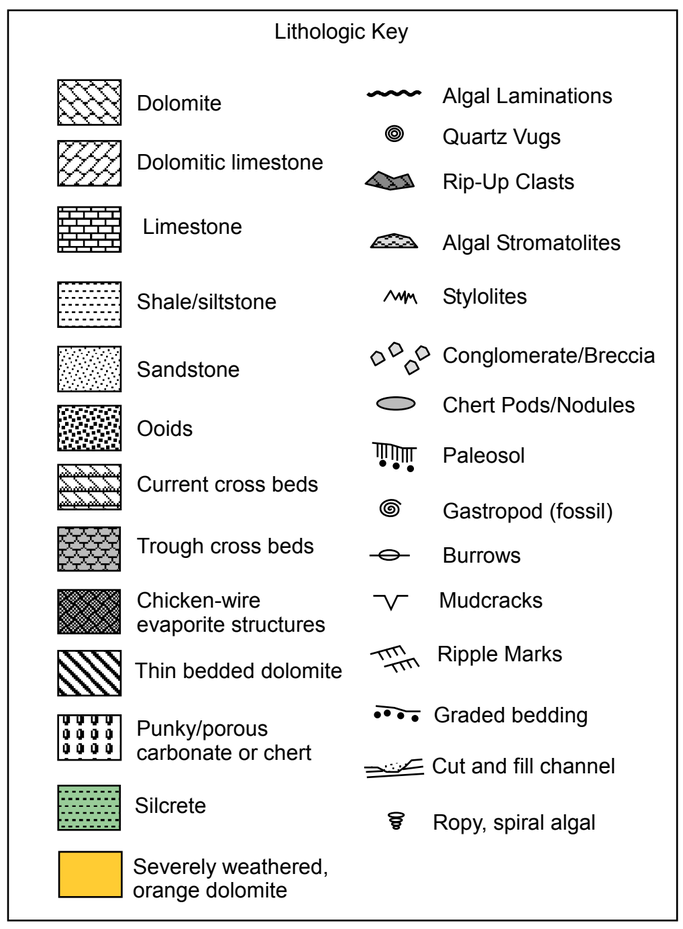


Plate A.20: Type stratigraphic section for the Ordovician Harmonyvale Member of the Ontelaunee Formation.



Key for Stratigraphic Columns